The Rise of Conjugated Poly-ynes and Poly(Metalla-ynes): From Design Through Synthesis to Structure-Property Relationships and Applications

Ashanul Haque,[†] Rayya A. Al-Balushi,[†] Idris Juma Al-Busaidi,[†] Muhammad S. Khan,[†*] Paul R. Raithby*[§]

[†]Department of Chemistry, Sultan Qaboos University, P.O. Box 36, Al-Khod 123, Sultanate of Oman.
*E-mail: msk@squ.edu.om

[§]Department of Chemistry, University of Bath, Claverton Down, Bath BA2 7AY, UK.
E-mail: p.r.raithby@bath.ac.uk

Abstract

Conjugated poly-ynes and poly(metalla-ynes) constitute an important class of new materials with potential application in various domains of science. The key factors responsible for the diverse usage of these materials is their intriguing and tunable chemical and photo-physical properties. This review highlights fascinating advances made in the field of conjugated organic poly-ynes and poly(metalla-ynes) incorporating group 4-11 metals. This includes several important aspects of conjugated poly-ynes *viz*. synthetic protocols, bonding, electronic structure, and nature of luminescence, structure-property relationships, diverse applications, and concluding remarks. Furthermore, we delineated the future directions and challenges in this particular area of research.

Keywords: Conjugated poly-ynes, Poly(metalla-ynes), Electronic structure, Bonding, Luminescence, Applications.

Table of Contents

TOC graphic

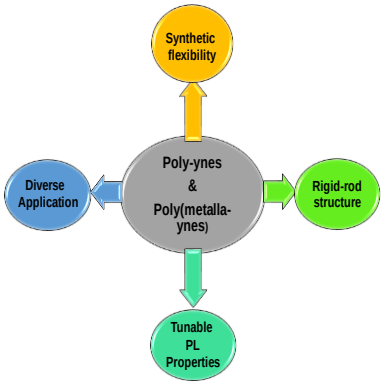

(5 cm x 5 cm)

1. Introduction

The 2016 Nobel Prize in Chemistry was awarded to Jean-Pierre Sauvage, Fraser Stoddart and Ben Feringa for their pioneering work on the design and development of small functional molecular machines.[1] The award in this particular area of research (miniaturization of the electronic devices and equipment) reflects the quest for micro- to nano-sized smart materials for real-life applications. A plethora of research has been conducted in academic and industrial laboratories around the globe in n the last few decades to develop smart devices based on organic, inorganic and hybrid materials.[2,3] In particular, for opto-electronic (O-E) applications, chemists have developed various π-conjugated systems and among them, oligo-ynes, poly-ynes and poly(metalla-ynes) have emerged as one of the archetypical candidates.[4-6] Low cost, light-weight, suitability for large area applications, possibility to process at low temperatures, mechanical flexibility, tunable photo-physical and physico-chemical properties, and unique capability to retain electronic and chemical properties of organic and metal frameworks are some of the intriguing features offered by this class of materials. These features make them suitable for application in nano-scale molecular wires, molecular magnets, optical filters, logic gates, liquid crystal displays, light emitting diodes (LEDs), sensors, photovoltaic devices (PVs), field-effect transistors (FETs), sensing, catalysis, medicine, etc.[7-10] The occurrence of oligo- and poly-ynes in flora and founa[11,12] as well as in interstellar materials[13] richly justifies their unique and broad verstality. Moreover, they are regarded as model compounds of carbyne, a controversial allotropic form of carbon.[14-16]

Figure 1 depicts the general chemical formula of a π-conjugated organic poly-yne and poly(metalla-yne) backbone. The term π-conjugated poly-yne is used for structures containing alternating and repeating -C≡C- units. It may also contain a carbocyclic or heterocyclic π-conjugated spacer (Ar). An organic poly-yne may be classified as homo- or hetero-/co-poly-yne depending upon the type/nature of spacer incorporated. The property and the application of the organic poly-yne significantly depends on the extent of π-conjugation as well as the type of spacer used.[17] On the other hand, metalla-ynes and poly(metalla-ynes) contain one or more transition metal(s) (or in some cases non-transition metal) along the polymer backbone or at the termini of oligomers surrounded by auxiliary ligands (π-backbonding or σ-donating auxiliaries). The overall physico-chemical properties of the conjugated system are dependent on the level of conjugation (number of C≡C bonds), the type of spacers, the transition metal ions and the auxiliary ligands present.[18-20]

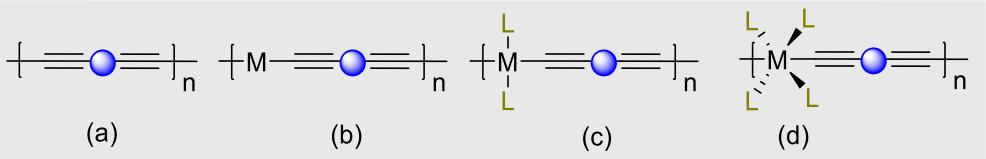

Figure 1. (a) General chemical formula of an organic co-poly-yne, (b-d) linear (M = Ag(I), Au(I), Hg(II) etc.), square planar (M = Ni(II), Pd(II), Pt(II) etc), or octahedral (M = Cr(III), Rh(I)/(III) etc.) poly(metalla-yne) backbone. L = Mono- or bindentate π-backbonding or σ-donating auxiliary ligands. Circles in blue shows spacers, M = group 4-12 metal ions.

Over the past few decades, comprehensive research has been conducted on conjugated poly-yne materials with or without metal ions. Figure 2 depicts histograms generated by the Web of Science when searched for the term "*acetylide*" during 2000-2018. A total of 2345 articles have been published since the beginning of 21st century, giving an average of ~ 123 articles per year, and this number is still on the rise. Citations related to this topic have also grown enormously.

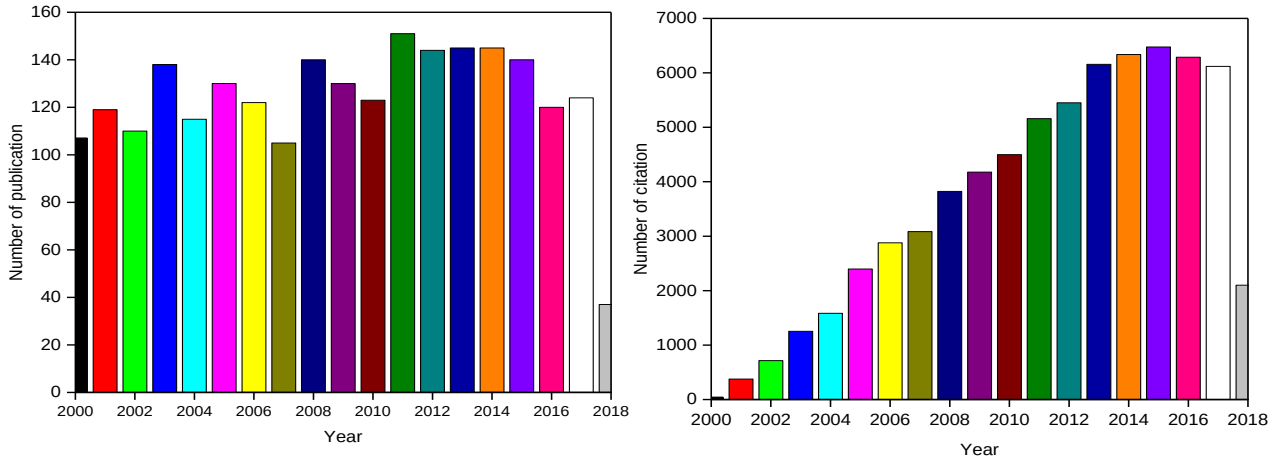

Figure 2. Histogram showing the annual number of publications and citations. (Data searched from Web of Science on June 04, 2018. The period was 2000-2018 for the keyword "*acetylide*". Certain data included herein are derived from Clarivate Analytics Web of ScienceTM.

Several reviews and books on the linear, starred, branched and dendritic form of this class of materials exist (Table 1).[4,7,10,21-27] In this review we focus on the synthesis, properties and application of linear organic and organometallic oligo- and poly-ynes. Because of the large number of variants in this class of materials, we have restricted ourselves to linear (a) organic oligo- and poly-ynes, (b) organometallic oligo- and poly-ynes containing at least one M-C σ-bond with *trans*-alkynyl configuration around the metal center, (few examples of *cis*-complexes have also been discussed). This review consists of six sections. Following this introductory section, synthetic protocols for conjugated oligo-ynes, poly-ynes and poly(metalla-ynes) will be presented in section 2. Structure-property relationships of organic and organometallic systems incorporating group 4-11 metals will be discussed in section 3. In the same section, there is a brief discussion on bonding, electronic structure and role of co-ligands. The topic will be further sub-divided into the number of C≡C bonds (di-ynes, oligo-ynes and poly-ynes) and the type of transition metals used (Group 4-11). Section 4 of this review will focus on the applications of selected and representative examples of conjugated oligo-ynes, poly-ynes and poly(metalla-ynes) in various fields. In section 5, we will outline the future directions of research in this fascinating area of new materials. Concluding remarks will be presented in section 6.

Table 1. Some Important Reviews Published in This Area

S. No.	Title	Number of citations[a]	ref.
1.	Multifunctional polymetallaynes: properties, functions and applications	23	Ho, C. –L.; Yu, Z. Q.; Wong, W. Y. *Chem. Soc. Rev.* **2016**, *45*, 5264-5295.
2.	Organometallic photovoltaics: a new and versatile approach for harvesting solar energy using conjugated polymetallaynes	301	Wong, W. Y.; Ho, C.-L. *Acc. Chem. Res.* **2010**, *43*, 1246.
3.	Acetylenic Polymers: Syntheses, Structures, and Functions	659	Liu, J.; Lam, J. W. Y.; Tang, B. Z. *Chem. Rev.* **2009**, *109*, 5799.
4.	Synthesis of Conjugated Polymers for Organic Solar Cell Applications	2449	Cheng, Y. –J.; Yang, S. –H.; Hsu, C.–S. *Chem. Rev.* **2009**, *109*, 5868.
5.	Metal Alkynyl σ Complexes: Synthesis and Materials	538	Long, N. J.; Williams, C. K.; *Angew. Chemie.* **2003**, *42*, 2586.
6.	Molecular electronics. Synthesis and testing of components	1152	Tour, J. M. *Acc. Chem. Res.* **2000**, *33*, 791.
7.	Poly(aryleneethynylene)s: Syntheses, Properties, Structures, and Applications	1460	Bunz, U. H. F. *Chem. Rev.* **2000**, *100*, 1605.
8.	Organometallic Polymers with Transition Metals in the Main Chain	728	Nguyen, P.; Gómez-Elipe, P.; Manners, I.; *Chem Rev.* **1999**, *99*, 1515.

[a]As per Web of Science on October 29, 2017.

2. Synthesis

With increasing interest in the development of novel materials with fascinating photo-physical properties and applications, much attention has been drawn toward the synthesis of small, medium and large π-conjugated acetylenic materials. Following the revolutionary discovery by Glaser[28], a plethora of homo- and cross-coupling reaction methodologies have been developed and are being used to realize di-, oligo, and poly-ynes with pre-defined architecture and chemical composition. Herein, we discuss some important methodologies (classical as well as modern) used to synthesize linear organic and metal-containing di-ynes through oligo-ynes to poly-ynes. For a detailed discussion on the synthesis of acetylenic materials, interested readers are referred to the recent reviews by Shi and Lei,[29] and Sindhu et al.[30,31]

2.1. Synthesis of organic mono-, oligo- and poly-ynes

A wide variety of classical as well as new approaches for incorporating alkynyl moieties into organic framework (formation of $Csp-Csp$, Csp^2-Csp^2, Csp^2-Csp^3, and Csp^3-Csp^3 $C_{sp}-C_{sp}$, $C_{sp}-C_{sp^2}$ or $C_{sp}-C_{sp^3}$ bonds) have appeared in the literature.[32] This includes, but is not limited to, Hay,[33,34] Eglinton-Galbraith,[35] Cadiot-Chodkiewicz, Sonogashira,[36] Stille,[37] Negishi,[38] Kumada,[39] Grignard,[40] Fritsch-Buttenberg-Wiechell (FBW) rearrangement,[41] and others.[42-53][54] Scheme 1 depicts some well-known protocols developed for the synthesis of symmetrical and asymmetrical alkynyl compounds starting from terminal alkynes. Classically, to introduce ethynyl moieties as substituents onto an aliphatic chain/aromatic ring and to synthesize a polymeric material, a sequence of metal-catalyzed Sonogashira, Stille, Hagihara, Negishi or Kumada

coupling reactions are used. In most cases, a transition metal-based catalyst is utilized in a basic solvent.[51,55-58] The reaction times and the yield of the products critically depend on the condition (anaerobic), nature and number of leaving groups (halide, triflate, or boronic acid) and the nature of functional groups present over coupling partners. For example, Sonogashira coupling is more successful with aryl iodides while Negishi alkynylation is more successful with aryl bromides.[59] Despite these advantages and disadvantages, the lack of chemo-selectivity, high price of the catalysts, waste generation, catalytic contamination of the final product and the requirement of high temperature impose substantial hurdles on these reactions. In general, undesired alkyne homo-coupling is the main problem associated with any direct C−H alkynylation. To develop a direct alkyne cross-coupling, homo-coupling of both alkynes must be suppressed to a minimum level, which is a big challenge for Cu(I) and Pd(II) catalysed systems. Gong and Liu[60] found that the deprotection of a Sonogashira product in NaOH/MeOH mixture gives the homo-coupled product instead of the deprotected one. Furthermore, this methodology also suffers from difficulties with respect to the introduction of alkyl groups into the C≡C bond for the synthesis of terminal alkyl alkynes. Similarly, in a typical Glaser-Hay cross-coupling method, one of the alkynes is used in large excess leading to the formation of homo-coupled by-products, while in the Cadiot-Chodkiewicz method, pre-functionalized halogenated alkynes are required, which are generally unstable.[61]

Scheme 1. Synthesis of Symmetrical and Unsymmetrical Di-ynes *via* Classical and Modified Methods

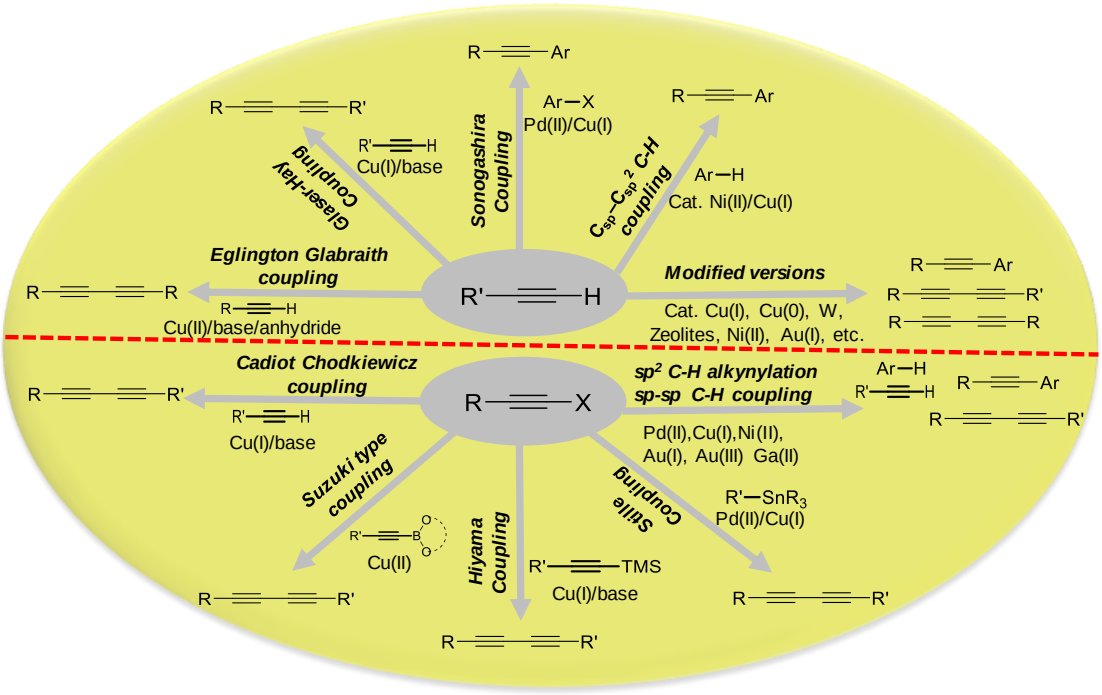

To circumvent these issues, several newly modified versions have been reported. For example, Zhou and co-workers[62] recently reported a Pd(II)-catalyzed Sonogashira-type cross-coupling reaction (Scheme 2). Under acid- and base-free condition, the reaction between arylsulfonyl hydrazides (**1**) and aryl/alkyl/

heteroaryl alkynes (**2**) progressed *via* Ar(C)–S bond cleavage to yield mixed alkynes (**3**). Since several functionalized arylsulfonyl hydrazides such as *p*-tolylsulfonyl hydrazide, *p*-bromosulfonyl hydrazide, naphthalene-2-sulfonohydrazide etc. can be used as the substrate, the reported methodology offers a unique strategy to accomplish 1,2-disubstituted internal alkynes (47 examples) in good to excellent yields (up to 92%).

Scheme 2. **Sonogashira-Type Cross-Coupling Reaction Between Arylsulfonyl Hydrazides and Terminal Alkynes**[62]

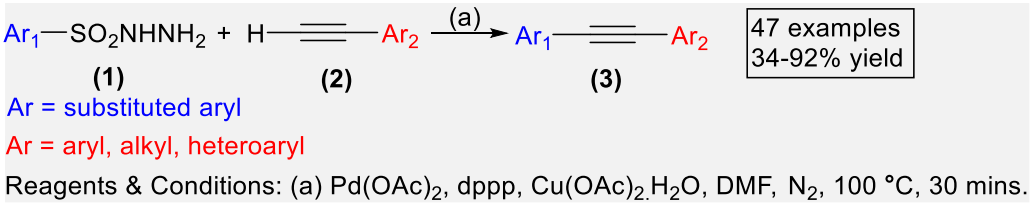

Fraile and co-workers[63-65] reported anti-Michael addition of organomagnesium (**5**) and organolithium reagents (**6**) to arylsulfonyl acetylenes (**4**) to produce Csp^2–Csp^2 (aryl–aryl alkynes), Csp^2–Csp^3 (aryl–alkyl alkynes), and Csp^3–Csp^3 (alkyl–alkyl alkynes) coupled products (**7a** & **b**, Scheme 3). The organomagnesium reagent was found to be more versatile and the reaction proceeds under very mild conditions, without using low temperatures and an extremely dry atmosphere. Using these two protocols, a broad range of symmetric and asymmetric alkynes could be achieved in excellent yields within a short period of time. Prior to this report, Ye et al.[66] reported a double elimination protocol for the synthesis of unsymmetrical oligo-ynes using substituted benzylic or propargylic sulfones as starting compounds.

Scheme 3. Anti-Michael Addition of Organolithium and Organomagnesium Reagents to Arylsulfonyl Acetylenes[63-65]

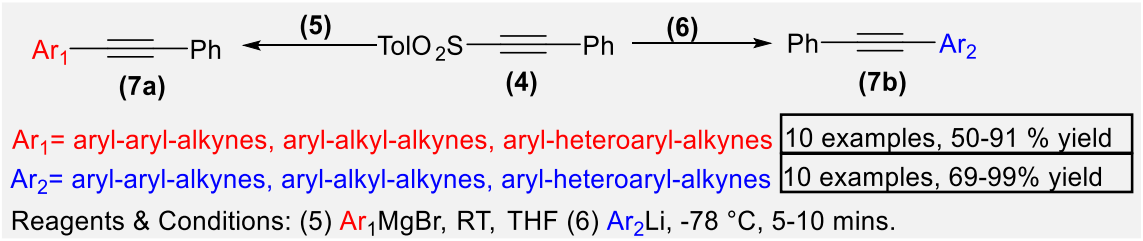

Several other Sonogashira-type cross-coupling reactions have also been developed.[67] Sagadevan and Hwang[68] reported a Cu(I)-catalyzed, "Pd-free," Sonogashira reaction (Scheme 4). This visible light mediated reaction between phenyl acetylene (**8**) and 2/3/4-substituted aryl bromide or iodide (**9**) proceeds at RT in the presence of inexpensive Cu(I)-catalyst without using any exogenous photosensitizers. Furthermore, the reaction proceeds successfully with both iodo and bromo precursors to yield Sonogashira products (**10**) quantitatively. The overall yield with the iodo precursors were higher than with the bromo counterparts. Compared to other photo-induced reactions, this method offers a great scope of reactants without generating any photo-degraded side products, which is a common challenge in photo-induced reactions.

Scheme 4. Hwang's Photo-induced Cu(I)-catalyzed, ''Pd-free,'' Sonogashira Reaction[68]

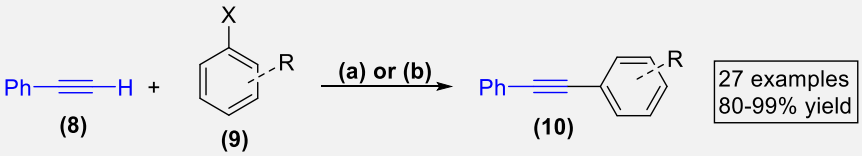

(8) (9) (10)

X = Br/I
R= electron-donating/accepting functionality at 2/3/4-position

Reagents & Conditions: (a) For Br-precursors: 2/3/4-substituted aryl bromide, CuCl, AgOTf, KOAC, MeOH, N_2, Blue LED. (b) For I-precursors: 2/3/4-substituted aryl iodide, CuCl, K_2CO_3, MeCN-MeOH, RT, THF, Blue LED.

Apart from the new synthetic methodologies for the synthesis of mono-ynes, an array of efficient metal catalyzed and metal-free methods has also been developed to achieve symmetrical and unsymmetrical 1,3-diynes, which are important building blocks for pharmaceuticals, O-E materials, and polymers.[69,70] There is a long-held belief that the Glaser−Hay reaction, which is an efficient method for di-ynes, favors the formation of the homo-coupled product and has less scope for cross-coupling. To overcome this barrier, several modifications have been attempted. For instance, solid-supported chemo-selective modified version of the Glaser-Hay method under microwave conditions has been developed, which produced di-ynes in moderate to good yields.[44] This newly developed method was very fast (20 mins.) compared to the thermal reaction.[48] Despite the fact that the microwave method[44] produces chemo-selective products and is energy-efficient, the thermal method[48] has ability to produce a library of compounds. Recently, Su et al.[71] reported a Glaser-Hay-type reaction in which cross-coupling of terminal alkynes was achieved in excellent yields under ambient condition. Undoubtedly, this work disproved the belief that homo-couplings are exclusively favored in the Glaser−Hay reaction. The authors noted that cross-coupling between two asymmetric alkynes (**11** and **12**) proceeds with high selectivity in the presence of Cu(0)-powder and the bidentate ligand (N^1,N^1,N^2,N^2-tetramethylethylene diamine, TMEDA) in chloroform/dioxane solvent yields mono- and oligo-ynes **13**-**15** (Scheme 5). High yield, wide range of substrates, (47 examples, upto 91% yield), outstanding functional group tolerance and products including tetra-ynes are main features of this method. It was reported that Cu(II) catalyst (Figure 3) "*distinguishes*" two different alkynes based on their differences in intrinsic reactivity and steric hindrance, resulting in selective hetero-coupling. However, the reaction was found to be sensitive to temperature (both high and low temperatures) leading to the formation of homo-coupled product. A similar type of reaction using a Ni(II) catalyst was also reported for the synthesis of unsymmetrical 1,3-di-ynes, which was the first of its kind.[72]

Scheme 5. Cu(0)-Catalyzed Glaser-Hay Hetero-coupling of Terminal Alkynes[71]

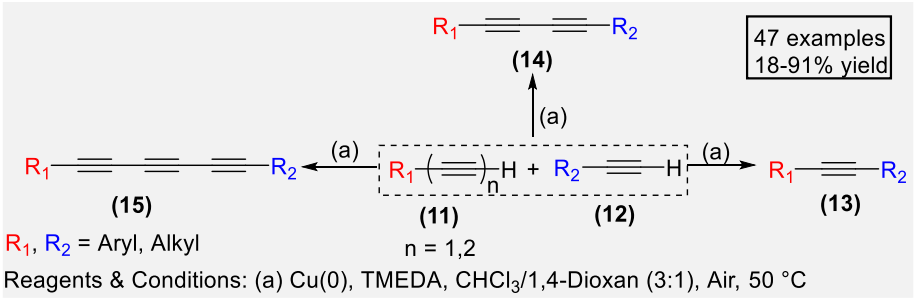

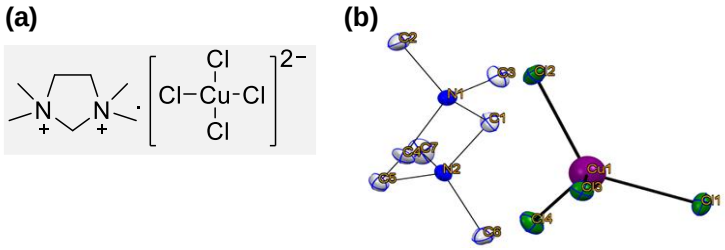

Figure 3. X-ray Crystal Structure of an Active Cu(II) Catalyst Generated *In-situ*. Reprinted with permission from ref [71]. Copyright 2016 American Chemical Society.

The group led by Togni[73] reported the Glaser-type alkyne coupling using recyclable Au nanoparticles (d = 0.8 ± 0.2 nm) homogeneously dispersed on amino-functionalized silica catalyst. The group of Shi[61] for the first time, developed the Au(I)/(III)-catalyzed oxidative cross-coupling of alkynes **16** and **17** to produce unsymmetrical 1,3-di-ynes **18** utilizing stoichiometric amounts of bidentate ligand (1,10-Phen) and external oxidant ($PhI(OAc)_2$) (Scheme 6A). Using the method, the desired cross-coupled conjugated di-ynes with excellent hetero-selectivity (>10:1), good to excellent yields, and with large substrate tolerability were achieved. Since this new approach did not require excess of one of the coupling partners or pre-functionalization of the alkynes (**16/17**), it offers a unique strategy to afford unsymmetrical 1,3-diynes. Improving this methodology, Banerjee and Patil[74] reported that unsymmetrical 1,3-diynes **21** could also be achieved by reacting an alkyne **19** with ethynylbenziodoxolones (EBXs, **20**) without using any external oxidants (Scheme 6B). They found that EBXs serve dual roles: as oxidants as well as alkyne transfer agents during Au(I)-catalyzed synthesis of unsymmetrical 1,3-diynes. Using this protocol too, a number of di-ynes could be obtained including those bearing polar functional moieties (such as NH, OH and $B(OH)_2$). The same group also reported the very first example of a Ni(II)/Ag(I) catalysed Glaser-Hay type cross-coupling reaction to produce unsymmetrical 1,3-diynes.[75] The method is highly selective and works under mild and aerobic conditions without employing any base, ligand or additives. In addition, a modified version of Cadiot–Chodkiewicz-type cross-coupling reaction was also reported recently to obtain unsymmetrical 1,3-diynes.[76,77] Chinta and Baire[51] reported a cross-coupling methodology to synthesize 1,3-diynes. The new reaction conditions provide operational simplicity, high selectivity for hetero-coupling (>97%), use of water, and low basicity of the reaction medium compared to commonly used highly basic conditions, i.e., 30–70% amine in water or 100% piperidine.

Scheme 6. Au(I)/(III)-Catalyzed Csp –Csp Cross-Coupling Reactions[61,74]

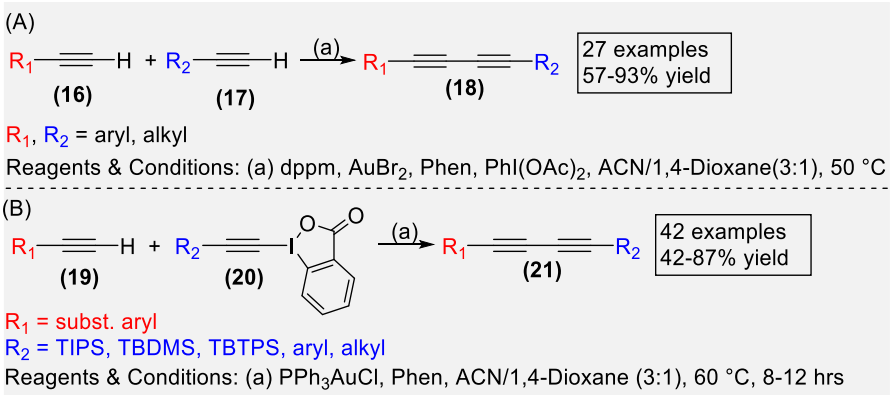

One of the main challenges in the synthesis of long chain oligo- and poly-ynes is their low stability, making them potentially reactive. This led to the decomposition of the product, and in the worst situation, explosion may occur (even under inert conditions). To circumvent this issue, one must protect/end-cap the terminal alkynes using an aryl or a bulky substituent. For example, to realize oligo-ynes (n = 2–6) from acetylene or dihaloacetylene[78] as the main precursor, end-capping groups such as phenylacetylene,[79] 1-naphthyl acetylene,[80] or biphenyl[81] were found to be useful. The chemo-selective synthesis of asymmetric oligo-ynes can be achieved *via* solid phase[46,82] and solution[43] methods. In a typical solid-phase method, a solid-supported alkyne **25** or **26** is obtained by stirring a mixture of propargyl alcohol (**23**) or 4-ethynylbenzyl alcohol (**24**) with 1% cross-linked trityl chloride derivatized polystyrene resin **22** in dichloromethane/ triethylamine (DCM/TEA) followed by trifluoroacetic acid (TFA)-induced cleavage (Scheme 7).[46] Upon reacting with appropriate alkynes, oligo-ynes (**27** or **28**, n = 1-4) could be obtained in good to moderate yields. Yield was found to be better in solid-phase method compared to solution-phase reaction (~ 30%).[48]

Scheme 7. Synthesis of Asymmetric Oligo-ynes Using Immobilized Resin[46]

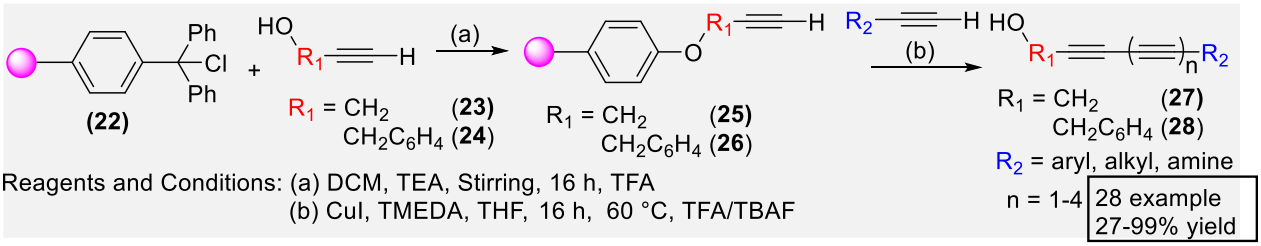

For the synthesis of oligo-ynes incorporating odd and even number of C≡C units, iterative iodination/Stille coupling has been reported (Scheme 8).[83] The starting precursor, i.e. TMS-protected scaffold could be realized by several methods.[84] For example, an alkali metal hydroxide catalyzed method has been recently developed by Grubbs and co-workers.[85] The *bis*-TMS-capped alkynes **29** after conversion to di-iodo alkyne precursors **30** react with end-capped Sn-acetylides (TMS, TIPS, and PhC≡CSnMe$_3$) to produce oligo-ynes **31** with 4-7 C≡C units. To produce oligo-ynes with an even number of C≡C bonds, *bis*(trimethylsilyl) butadiyne as starting precursor was used while for odd number of C≡C bonds *bis*(trimethylsilyl)hexatriyne was employed. Although most of the reactions were performed at 0 °C, hepta-yne was obtained at – 25 °C

while penta-yne having TIPS moieties at both ends was obtained at RT. Thus, the reaction yield (10-77%) was governed by the method and condition employed. One of the advantages of this methodology was the easy removal of side products (vacuum sublimation/ recrystallization rather than chromatographic separation). Despite these advantages, use of tin (a toxic metal) is the major concern.

Scheme 8. General Scheme for The Synthesis of Symmetric Poly-ynes With Odd and Even Number of C≡C Units[83]

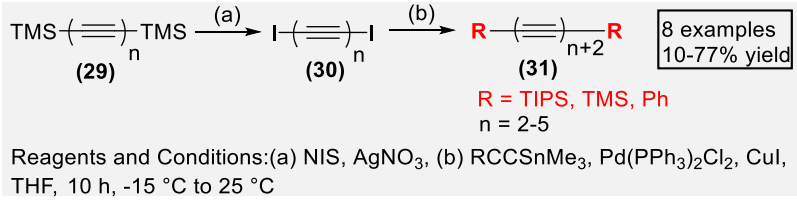

Another interesting approach to synthesize oligo-ynes involves "*masked alkyne equivalent*" (MAE), in which a masking group is used to protect the alkyne from undesired coupling and degradation.[86-89] In 1994, one of us reported the masking and unmaksing strategy of tetracobalt complexes of tetraynes with the dicobalt tetracarbonyldiphenylphosphinomethane ($Co_2(CO)_4$dppm).[90] Several other reports are also available for synthesizing oligo-ynes employing Co(0)-based masking agents; however, most of them suffer from challenging demasking step.[91-93] Recently, it has been demonstrated that TIPS end-capped oligo-ynes e.g. **38** (Scheme 9) could be achieved in good yields from its corresponding MAE *via* swift removal of the $Co_2(CO)_4$dppm mask.[94] The method started from the synthesis of dicobalt-masked building block **33** from TIPS,TMS-protected triyne **32**. Selective deprotection followed by chain-extension *via* Glaser coupling with TMS-acetylene afforded the dicobalt complex **36**, which undergoes oxidative homocoupling under Eglinton condition to produce tetracobalt complex **37**. Finally, smooth demasking of tetracobalt ($Co_2(CO)_4$dppm) complex **37** using molecular iodine in THF produced oligo-yne **38**. The novelty of this method includes swift removal of the mask, short reaction time, synthesis of long-chain oligo-ynes, easy handling, etc.

Chalifoux and Tykwinski[95] proposed that the stability issue could be circumvented by installing bulky sterically demanding substituents such as *tris*(3,5-di-^{t}butylphenyl)methyl (Tr). Using the Tr end-group, they synthesized and characterized oligo-ynes with 4-22 C≡C units.[95] The important features of this modified Eglinton-Galbraith coupling (Scheme 10) include *in-situ* removal of the TMS group and the use of 2,6-lutidine as the base instead of toxic pyridine. The oligo-ynes were achieved through a chain-extension sequence by reacting terminal oligo-ynes **39** and different end-capped oligo-ynes **40** to produce unsymmetrical oligo-ynes **41**. Subsequently, desilylation followed by oxidative dimerization of **41** yielded oligo-yne **42**, composed of alternating C–C and C≡C bonds with 44 carbon atoms. Despite these pros, the main con of this methodology is, of course, numerous synthetic steps. In addition, Tr end-capping strategy was also found to be unsuitable for the synthesis of long oligo-ynes at preparative scale when acetylene was used as the starting material.[96]

Scheme 9. Synthesis of Symmetric TIPS Endcapped Oligo-ynes Using "*Masked Alkyne Equivalent*" (MAE)[94]

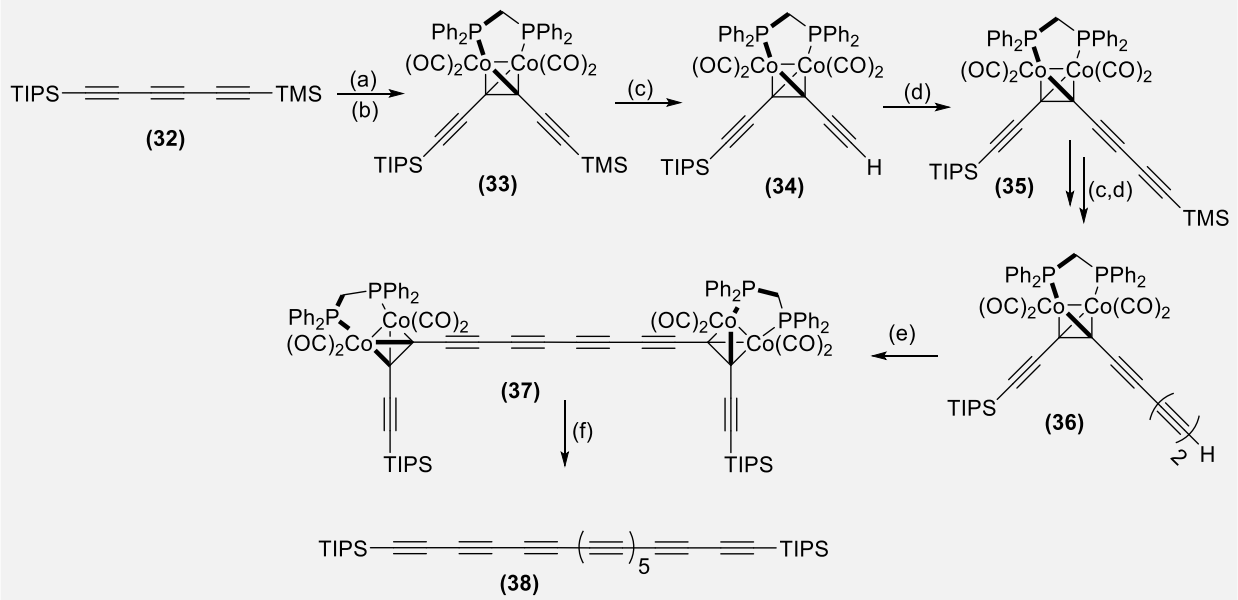

Reagents & conditions: (a) Co_2CO_8, Hexane, 25 °C, 12 h (b) dppm, Toluene, 110 °C, 20 min. (c) K_2CO_3, THF/MeOH 25 °C, 30 min. (d) TMSA, CuCl, TMEDA, DCM, 25 °C, 2 h (e) $Cu(OAc)_2$, Pyridine, 25 °C (f) I_2, THF, 25 °C, 3 h

Scheme 10. Synthesis of Symmetric Oligo-ynes[95]

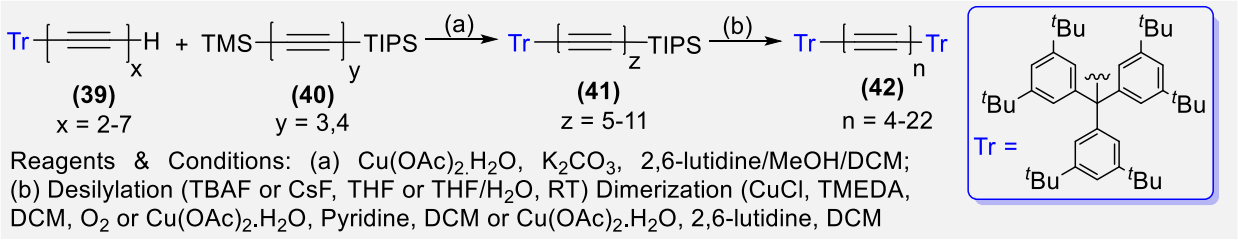

Reagents & Conditions: (a) $Cu(OAc)_2.H_2O$, K_2CO_3, 2,6-lutidine/MeOH/DCM; (b) Desilylation (TBAF or CsF, THF or THF/H_2O, RT) Dimerization (CuCl, TMEDA, DCM, O_2 or $Cu(OAc)_2.H_2O$, Pyridine, DCM or $Cu(OAc)_2.H_2O$, 2,6-lutidine, DCM

Oligo-ynes bearing terminal halogens constitute a rare class of compounds that exhibit several fascinating properties and act as precursors for higher poly-ynes. Several methods including halogenation of acetylenes or metal acetylides, decarboxylation/desilylation followed by halogenation, multi-step homologation/ iodination etc. are available to realize 1-haloalkynes.[97] Recently, Srujana et al.[98] developed a new *Green* synthetic protocol for 1-iodoalkynes (**44**) starting from terminal alkynes **43**. The method worked under metal-free, aqueous conditions catalyzed by tetrabutyl ammonium iodide and oxone. (Scheme 10) Simple reaction conditions, use of low-cost commercial reagents as well as readily available, non-toxic and universal solvent (water) makes this approach eco-friendly and economically viable. Limited work has been reported for the synthesis of symmetric 1-halo(oligo-ynes) (n ≥ 2).[99] To fill this gap, a general synthetic route has been suggested by Szafert and co-workers.[99] The method involves an iterative procedure using Cadiot-Chodkiewicz cross-coupling and halogenation and *in-situ* deprotection to yield labile, asymmetric and 1-halo(oligo-ynes, **46** and **47**, Scheme 11).[99] Using the protocol, oligo-ynes up to n = 5 could be achieved in moderate to good yield. They also reported Pd- and iodine end-capped oligo-ynes,

which were the first of their kind. In another work, the same group developed metal-free synthesis of oligo-yne substituted pyrroles.[100] These precursors were then used to synthesize hexatri- and octatetraynyl substituted 4,5,6,7-tetrahydro-1*H*-indole, its N-substituted derivatives and 2-phenylpyrroles, ester and phenyl end-capped 1-halobutadiynes (including chlorides, bromides and iodides) as well as push-pull type substituted thiophenes.[101,102] These methods paved a new way to a variety of substrates for organic synthesis including syntheses of pharmaceuticals.

Scheme 11. Synthesis of Iodine End-capped Poly-ynes[98,99]

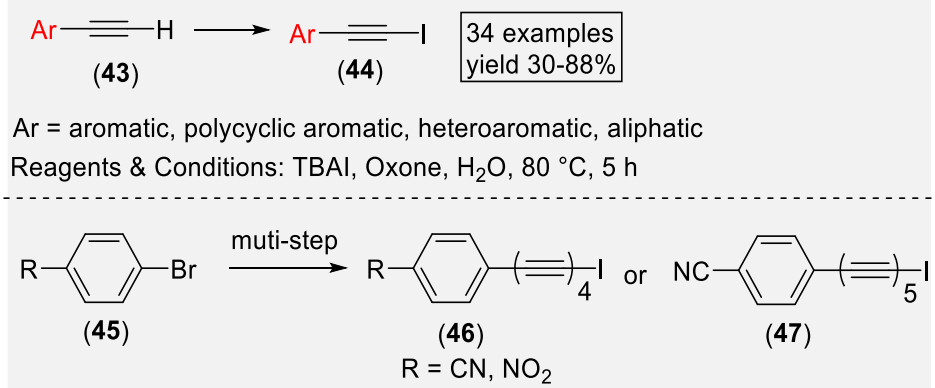

In addition to aforementioned methods, a significant volume of work has also been reported for the synthesis of oligo-ynes bearing conjugated spacers at alternate positions. For example, oligo-ynes, which may function as "*molecular wires*"[14,21,103,104] can be synthesized *via* divergent and convergent methods developed in 1990s by Tour and co-workers.[105-108] The group developed novel solution-phase iterative divergent/convergent (IDC) doubling strategy. This approach produces molecules having chain lengths twice the length of the molecule generated in the previous step. Several examples for the synthesis of conjugated oligo-ynes incorporating carbocyclic and heterocyclic spacers *via* this protocol are available.[105,107,109-113] Scheme 12 depicts a typical example of the IDC approach for the synthesis of oligo(thioarylene ethynylene)s.[21,107] In this method, 3-ethyl-2-[(TMS)-ethynyl] thiophene **48** is divided into two portions: one is iodinated at 5-position to yield **49** (93% yield) while the other portion is proto-desilylated to yield the alkynyl end **50** (99% yield). Pd(II)/Cu(I) catalyzed coupling of **49** & **50** led to the formation of dimer **51** (12 Å), with an overall yield of 90% and the length doubled compared to **48** (12 Å *vs* 6 Å). Through iterating the protocol, *i.e.* proto-desilylation, iodination and coupling, synthesis of 16-mer **52** of length 100 Å was obtained in good yield. Overall, *in-situ* desilylation/coupling, fast and easy separation are the main advantages of this method.[21,107] In the IDC method, the chain length increases from one side only. Furthermore, isolation of air unstable terminal alkyne or *bis*(terminal alkyne) is also necessary, which is often a tedious job. To circumvent this problem, step-wise biredirectional methodology was introduced,[113] which involved *in-situ* deprotection and coupling leading to chain growth from both sides. (Scheme 13)[113] The synthetic protocol starts with the alkynylation of 1,4-diiodo-2,5-didodecylbenzene (**53**) with TMSA to yield **54** followed by Sonogashira cross-coupling with 1-bromo-4-iodobenzene to generate **55** in 89% yield. Further alkynylation at both ends followed by *in-situ* desilylation and coupling yield the final product **57** (23% yield). Though the method is suitable for the synthesis of short length (n = 8) oligo-ynes, the generation of

insoluble materials (produced due to undesired oligomerization *via* alkyne/bromide coupling) was the major concern.

Scheme 12. Synthesis of Oligo(2,5-Thienylene ethynylene)s by The IDC Doubling Approach[21,107]

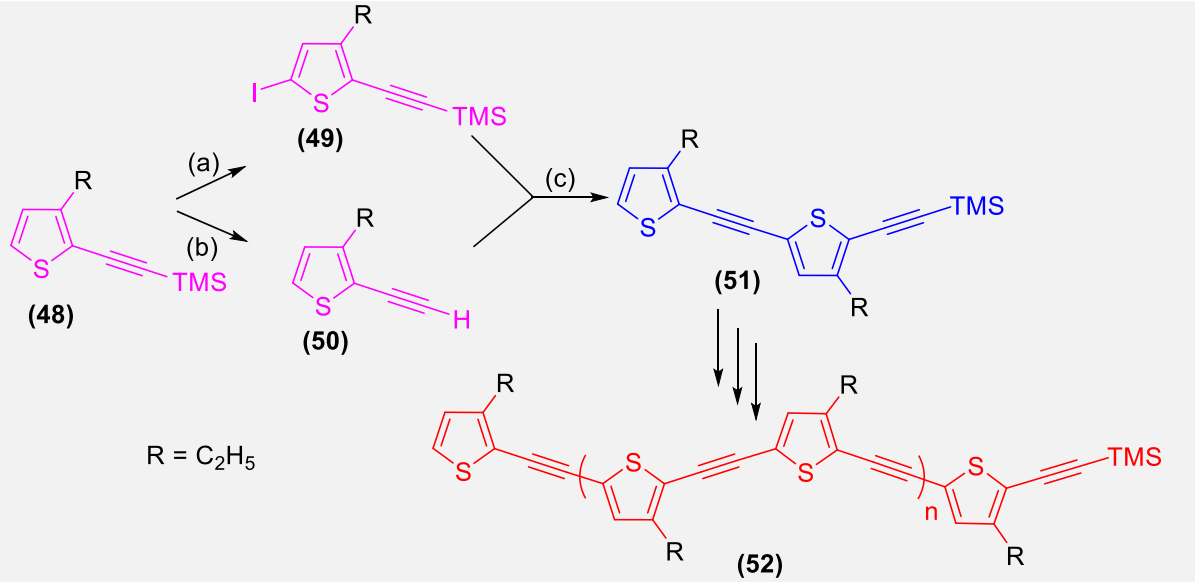

Reagents and Conditions: (a) LDA, Et_2O, -78 °C to 0 °C then I_2, -78 °C; (b) K_2CO_3, MeOH, 23 °C; (c) $Pd(PPh_3)_2Cl_2$, CuI, THF, $^iPr_2NH$, 23 °C.

In a recent study, a similar type of methodology has been adopted to synthesize 2,5-bis(alkoxy)phenylene ethynylene oligo- and polymers.[114,115] For the synthesis of oligo(1,4-phenylene ethynylenes) (n = 16), Schumm and Tour[116] reported IDC methodology using Merrifield's resin. Huang and Tour[112] using the same method successfully synthesized a 120-Å long 17-mer of oligo(1,4-phenylene ethynylenes). Main features of the developed method included aryl iodide masking/unmasking step-free procedure and a 3-fold increase in molecular length at every iteration. Good yields (20%) with no polymerized side products were additional advantages of this method. Regardless of these features, conformational flexibility of the Merrifield resin was the main issue as it obstructs the isolation of intermediate compounds.

For the synthesis of mono-disperse oligo[(1,4-phenylene ethynylene)-*alt*-(2,5-thienylene ethynylene)]s, both IDC and solid phase synthesis were found to be equally efficient (Scheme 14).[109] In a typical solid-phase method, the resin-supported terminal acetylene **59** obtained from the deprotection of **58** is coupled to 5-iodo-3-butyl-2-[(trimethylsilyl)ethynyl]thiophene **60** using Pd(II)/Cu(I) catalytic system to yield **61** (86%), which acts as '*starting monomer'* for the IDC doubling strategy. Further desilylation and iodination of **61** produces **62** and **63** (77%), respectively, which were then cross-coupled to afford **64** (85%) yield. The same procedure was followed to obtain **65-68** in moderate to good yields.

Scheme 13. Synthesis of Oligo-(1,4-Phenylene ethynylenes) Using Bidirectional Growth Approach[113]

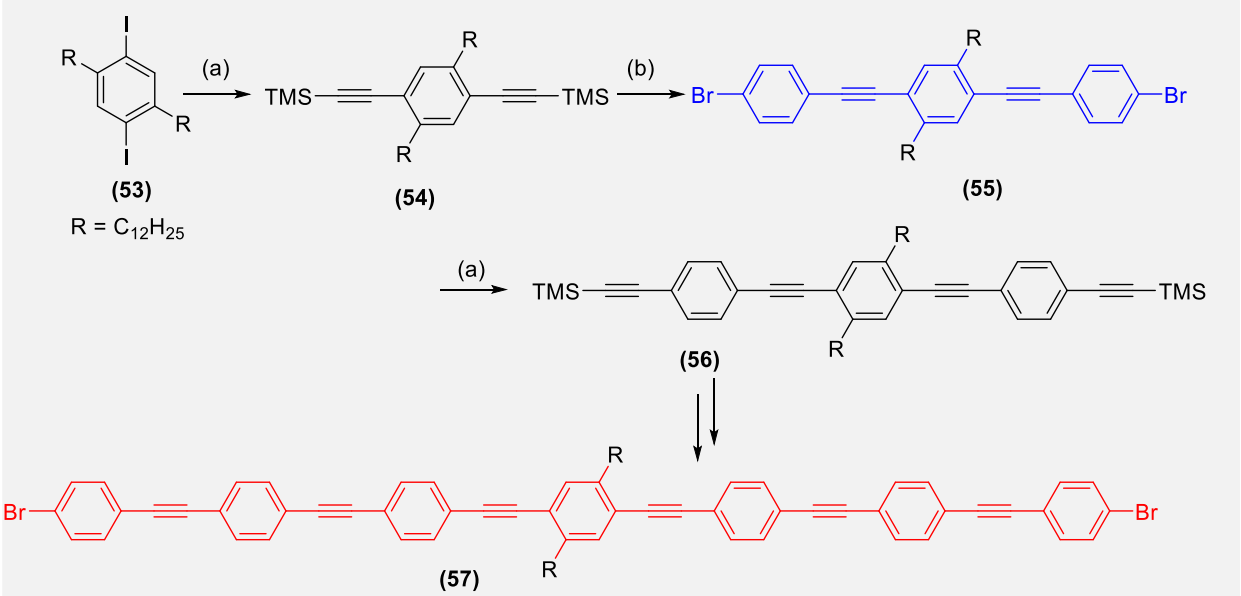

Reagents and Conditions: (a) TMSA, $Pd(PPh_3)_2Cl_2$, CuI, PPh_3, Et_3N, THF; (b) 1-bromo-4-iodobenzene, $Pd(dba)_2$, CuI, PPh_3, K_2CO_3, MeOH, THF.

Further elongation of the chain, i.e. synthesis of poly-ynes can be achieved by Hagihara-Sonogashira coupling of diethynylarylenes and dihaloarylenes or transition metal-catalysed metathesis of diy-nes.[4] For the polymerization of substituted acetylenes, transition metals,[117-122] post-transition metals[123] and MOF-catalysed[124] methods have also been reported. Thermal or light assisted metal-surface mediated C-H activation has also attracted the attention of chemists to realize carbon-based scaffolds and two-dimensional materials with a high degree of structural control.[125,126] For this purpose, metals with low-miller index surfaces are utilized.[127-129] Among non-chemical methods, the generation of oligo-ynes has also been reported using fs and ns lasers.[130,131] Kitaura et al.[132] reported the formation poly-ynes (up to 50 carbon atoms) within the narrow space of double wall carbon nanotubes (DWCNTs). They found that, under high temperature and under reduced pressure, oligo-yne $C_{10}H_2$ fuses together within the nanospace of DWCNTs to produce long chain poly-ynes. Though at its infancy, the method has opened a new route for the synthesis of structurally controlled poly-ynes.

Scheme 14. Synthesis of Oligo[(1,4-Phenylene ethynylene)-*alt*-(2,5-Thienylene ethynylene)]s Co-poly-yne on Merrifield Resin[109]

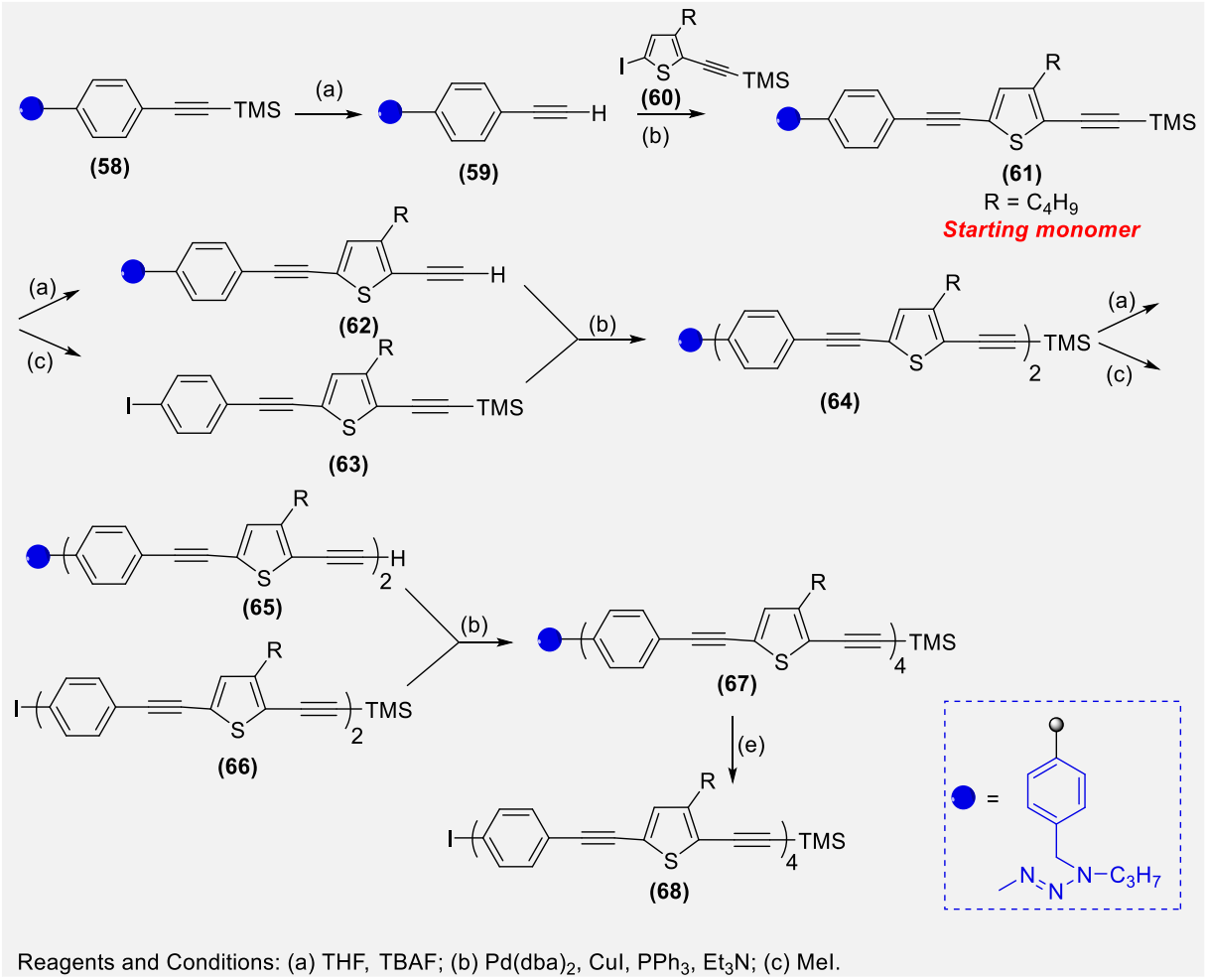

Reagents and Conditions: (a) THF, TBAF; (b) $Pd(dba)_2$, CuI, PPh_3, Et_3N; (c) MeI.

Further elongation of the chain, i.e. synthesis of poly-ynes can be achieved by Hagihara-Sonogashira coupling of diethynylarylenes and dihaloarylenes or transition metal-catalysed metathesis of diy-nes.[4] For the polymerization of substituted acetylenes, transition metals,[117-122] post-transition metals[123] and MOF-catalysed[124] methods have also been reported. Thermal or light assisted metal-surface mediated C-H activation has also attracted the attention of chemists to realize carbon-based scaffolds and two-dimensional materials with a high degree of structural control.[125,126] For this purpose, metals with low-miller index surfaces are utilized.[127-129] Among non-chemical methods, the generation of oligo-ynes has also been reported using fs and ns lasers.[130,131] Kitaura et al.[132] reported the formation poly-ynes (up to 50 carbon atoms) within the narrow space of double wall carbon nanotubes (DWCNTs). They found that, under high temperature and under reduced pressure, oligo-yne $C_{10}H_2$ fuses together within the nanospace of DWCNTs to produce long chain poly-ynes. Though at its infancy, the method has opened a new route for the synthesis of structurally controlled poly-ynes.

2.2. Synthesis of metalla(di-, oligo- and poly-ynes)

Oligo- and poly-ynes containing one or more metal ions are generally synthesized by Sonogashira dehydro-halogenation condensation, oxidative coupling, ethynyl ligand exchange, trans-metalation/ metathesis, vinylidene methods, C–H activation reactions, etc. All these methods have their own merits and demerits, which have been comprehensively reviewed earlier.[4,26,133] In this sub-section, we shall highlight some of the classical and modern methods employed for the synthesis of di-, oligo-and poly-ynes incorporating transition-metal ions in the main chain. Additional methodology for the synthesis of mono, di- or poly-nuclear σ-acetylide complexes could be extracted from sections **3** & **4**, where we discuss bonding, photophysical properties and applications of Group 4-11 metalla-ynes.

The very first synthesis of "*rigid-rod*" metalla-ynes incorporating transition metal ion was reported by Hagihara and co-workers[134-136] *via* dehydro-halogenation reaction. Despite the fact that the methodology has ability to produce an array of soluble metalla-ynes, the use of amine solvent was a major drawback as metal (other than those of Group 10) phosphine precursors are unstable in amine. This is because, for the earlier transition metal complexes, such as systems containing Ru-C bonds (or even Ru-P bonds) the formation of Ru-N(amine) bonds is energetically favorable as, in general, Ru-N bonds are stronger than Ru-C bonds or Ru-P bonds, and the kinetics are fast enough to facilitate the reaction. Therefore, when most complexes of metal phosphines or organometallic species are placed in amine solvent, the phosphine or carbon donor ligands will simply be replaced by the amine, to give the Ru hexaammine complexes. It is just group 10 where the M-N bond has a more similar energy to the M-C or M-P bonds that the replacement of the P- or C-donor ligand by the N-donor ligand does not occur. Also, in the case of Pt the kinetics are very slow and ligand substitution with amines does not readily occur. Essentially, in terms of hard/soft acids and bases, it needs a very soft metal centre (eg. platinum) for the formation of a bond with a hard base (amine) not to be favoured over bond formation or retention of a soft metal/soft base bond.[137]

Oxidative coupling is employed to synthesize terminal alkynes, while the alkynyl ligand exchange reaction is effective for the synthesis of Ni(II)-containing poly-ynes. Using this method, Hagihara and co-workers[138] reported the synthesis of α,ω-*bis*-nickel derivatives of butadi-yne and octatetra-yne. To overcome the limitations associated with Hagihara method, and inspired by the work of Lappert,[139,140] Lewis et al.[141] developed a more general and high yielding protocol for the synthesis of metalla-diynes, oligo-ynes and poly-ynes. This method has the ability to produce poly-ynes of higher molecular weight than previously reported by Hagihara.[135] In this method *bis*-trimethylstannyl(ethynyl) **69** offered an excellent precursor for synthesizing metalla-ynes. When *trans*-$M(PBu_3)_2Cl_2$ (M = Ni(II), Pd(II), Pt(II) was treated with 1.0 equiv. of **69**, the metalla-yne **70** was produced in respectable yields (Scheme 15). Similarly, treatment of 2.0 equiv. of **69** with 1.0 equiv. of *trans*-$Pt(PBu_3)_2Cl_2$ afforded **71** having one Pt(II) ion ligated by two *trans*-disposed acetylide groups and trimethylstannyl acetylide moieties. An *in-situ* reaction of **71** with excess of *trans*-$Pt(PBu_3)_2Cl_2$ gave **72**, with three Pt(II) ions linked together by two di-acetylide units. Using the method, metalla di-, oligo- and poly-ynes containing Ni(II), Pd(II) and Pt(II) and Rh(I) (**74**, **75, 77-78**, Scheme 15) in high yields (> 96%) and purity can be produced. However, the neurotoxic nature of trimethyl tin chloride

(Me_3SnCl) is the major concern[142] Similarly, Sonogashira cross-coupling reaction is useful method to obtain di-ynes and poly-ynes, but it does not always work. For example, when the protocol is applied to Pd(II) complexes, it failed. However, the same complex can be obtained by treating dibromo N-heterocyclic carbene (NHC) complex with Li-acetylide at -78 °C.[143]

Scheme 15. Synthetic Pathway for Ni(II), Pd(II), Pt(II) and Rh(I) di-ynes and poly-ynes by Lewis et al[141]

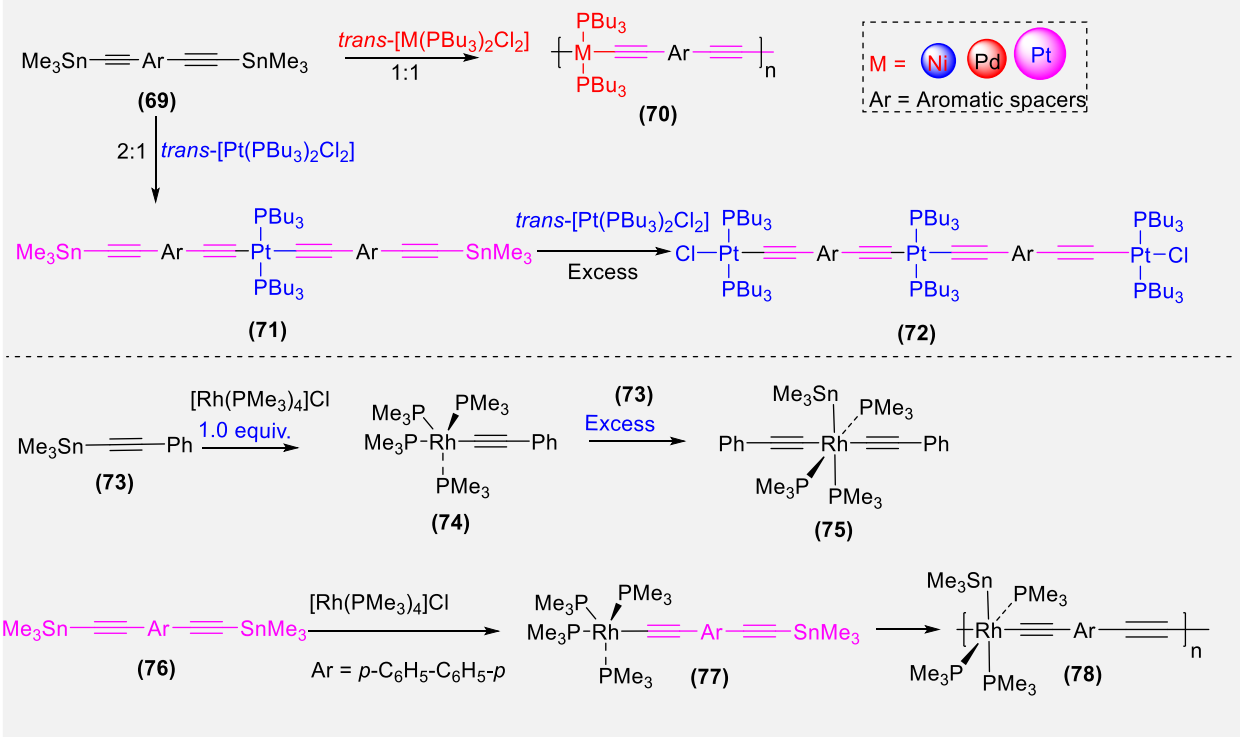

For the synthesis of metalla-ynes incorporating Rh(III) in the main chain/termini, Marder et al.[144] reported reductive coupling and C-H activation methods. Depending upon the stoichiometry of metal and the ethynyl core, mono- and poly-nuclear Rh(III) complexes **79-83** (Chart 1) can be obtained in high-yield along with CH_4 and PR_3 as by-products. Dixneuf et al.[145] reported a C-H activation method for the syntheses of Ru(II) vinylidene and acetylide complexes. They found that the metal precursor *cis*-[$(dppm)_2RuCl_2$] readily activates terminal alkynes (acetylene, propyne and ^{t}butyl acetylene) to produce stable *trans*-chloro vinylidene intermediate compound, which undergoes deprotonation to produce the corresponding metalla-ynes. Other C-H activation methods are also known such as pressure-assisted synthesis of unsymmetrical Fe(II) di-ynes.[146]

Chart 1.

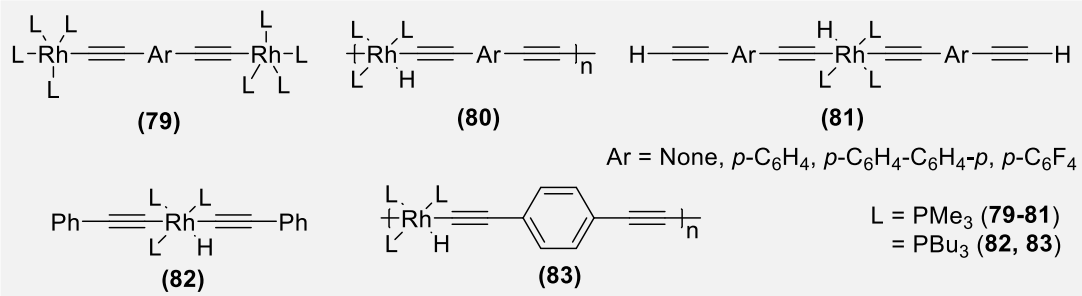

C-H activation methods have also been found equally effective for the synthesis other Group 9 metal acetylides. Goldmann and co-workers[147] reported oxidative addition of an alkyne C-H bond to the square planar pincer complex (PCP)Ir(CO) in the presence of a Brønsted acid (**84** → **85**, Scheme 16). The method was found to be highly dependent on the presence of acid as no reaction occurred upon heating (125 °C) even for a longer period of time (half year). In an improved version of the method, Kumar et al.[148] reported oxidative addition of a C-H bond to pincer complex without using any additive (**84** → **86**, Scheme 16). They concluded that metal-ligand cooperation (MLC) through the aromatization-dearomatization of the lutidine-based ligand backbone plays a crucial role in the reaction. In addition to this, using the concept of cooperativity, Group 10 metal (Ni(II), Pd(II)) complexes have also been reported.[149,150]

Scheme 16. Synthesis of Ir-complexes.[147,148]

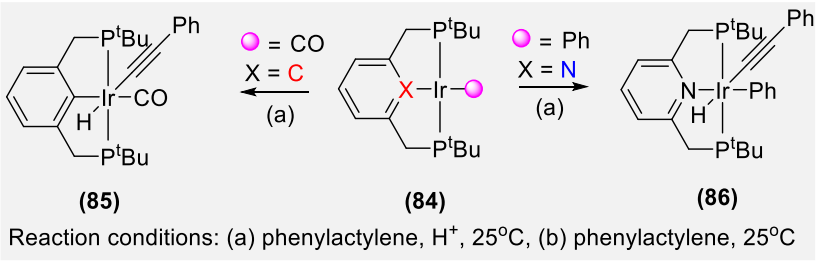

Long and co-workers[151] reported the synthesis of Ru(II)/Os(II) mono-acetylide using *trans*-[(dppe)$_2$RuCl$_2$]. Products containing both electron acceptor and donor functional groups were reported *via* vinylidene approach. Using the *trans*-[(dppe)$_2$RuCl$_2$], one can selectively obtain mono-acetylides in high yield. When a metal-acetylide **87** was treated with trimethylstannyl acetylides **88**, a series of symmetrical/unsymmetrical *bis*-acetylides **89**, containing Ru/Os were obtained (Scheme 17**)**. To synthesize Ru-acetylide, a similar type of reaction has been reported by Low and co-workers .[152]

Scheme 17. Synthesis of Unsymmetrical Ru(II)/Os(II) Bis-Acetylides[151]

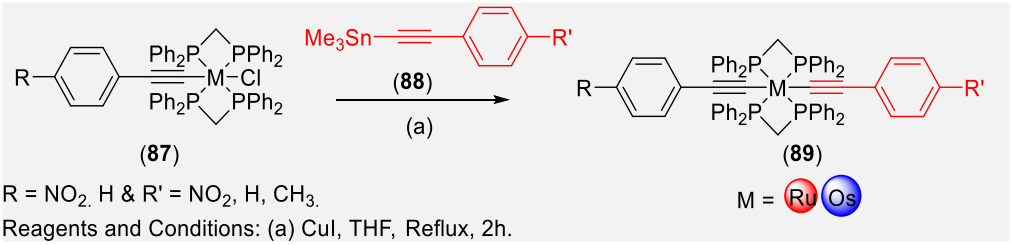

Ren and co-workers[153] reported a new synthetic method to synthesize Co(III) cyclam *bis*-alkynyls (cyclam = 1,4,8,11-tetraazacyclotetradecane) under aerobic and weakly basic conditions. The symmetrical **91(OTf)** (OTf = trifluoromethanesulfonate, Scheme 18) and unsymmetrical **92(OTf)** (Scheme 18) *bis*-alkynyl Co(III) cyclam complex were realized in high-yield from judiciously selected doubly charged solvento intermediate **90(OTf)$_2$**. These intermediate complexes were found to be more active and efficient in producing bis-alkynyl complexes than *trans*-[Co(cyclam)(alkyne)Cl]Cl counterpart. Overall, mild reaction condition (anaerobic or anhydrous environments) and stable nature of complexes were the salient features of this work. In addition to this work, the same group also reported several other monomeric and dimeric oligo-ynyl complexes.[154,155]

Scheme 18. Synthesis of symmetric and asymmetric Co(II) *bis*-acetylides[153]

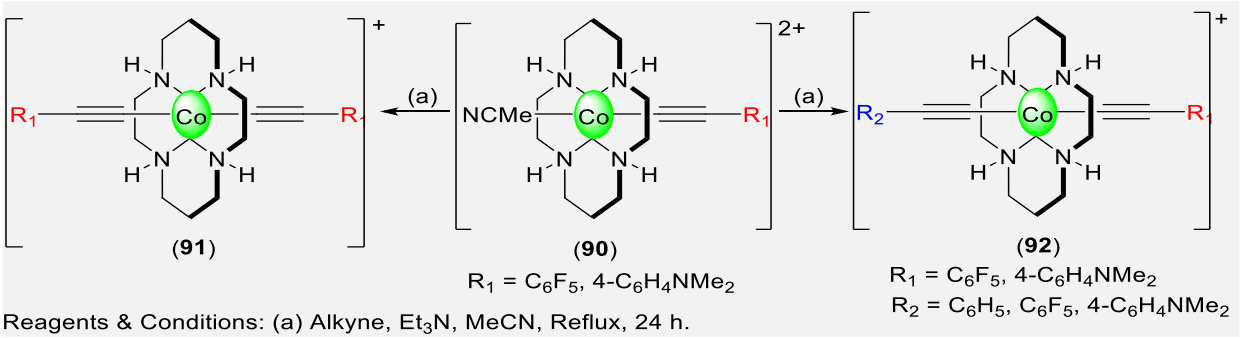

Field *et al*.[156] recently reported a facile synthetic protocol for a series of mono-, di- and trinuclear ethynyl-bridged Ru(II) complexes *via* the asymmetrically substituted Ru(II) di-yne complexes (Scheme 19**)**. The methyl acetylide Ru(II) complexes **93** upon treatment with diethynyl benzene in toluene/methanol produce mono-nuclear Ru(II) complexes **94** with a free alkyne unit. The presence of methanol is crucial for the conversion of **93** → **94**. Using **94** as precursor, symmetrical and unsymmetrical binuclear acetylide-bridged Ru(II) complexes **95** were obtained by adding excess of **93** followed by addition of methanol. Major advantages of the developed route were the controlled reactions at ambient temperature and pressure coupled with step-wise synthesis and isolation of complexes in high yield and purity with minimal workup. The same group also reported the formation of Fe(II) acetylide complexes starting from complexes of molecular hydrogen.[157]

Recently, Low et al.[158] reported Sonogashira type cross-coupling reactions to prepare Ru(II)-buta-1,3-diynyl complexes starting from a common Ru(C≡CC≡CH)-(PPh$_3$)$_2$Cp platform **97**, which was obtained from desilylation of the readily available complex Ru(C≡CC≡C SiMe$_3$)(PPh$_3$)$_2$Cp (**96**) (Scheme 20). This strategy obviates the need to prepare different di-yne ligands for each complex, providing rapid access to a range of complexes with various aryl buta-1,3-diynyl ligands (such as buta-1,3-diynyl complexes with electron-withdrawing (C$_6$H$_4$CN), electro-neutral (C$_6$H$_4$Me), electron-donating (C$_6$H$_4$OMe), or metal surface contacting (2,3-dihydrobenzo[b]thiophene) substituents). Reaction of **97** with the aryl iodides in basic medium produced substituted buta-1,3-diynyl complexes Ru(C≡CC≡CAr)(PPh$_3$)$_2$Cp **98** in moderate yield. Furthemore, the process is also suitable for the preparation of *bis*(diynyl) complexes such as **99** and **100**. Overall, these examples illustrate the versatility of the "*chemistry-on-complex*" strategy.

Scheme 19. Controlled Syntheses of Binuclear Ru(II) Complexes[156]

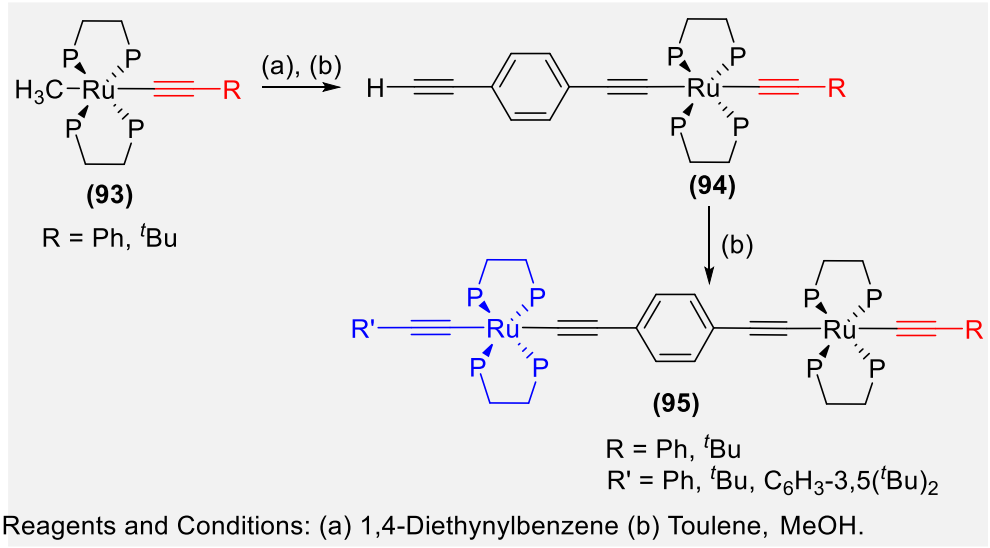

Scheme 20. Sonogashira Type Reaction For The Synthesis of Ru(II) Buta-1,3-Diynyl Complexes[158]

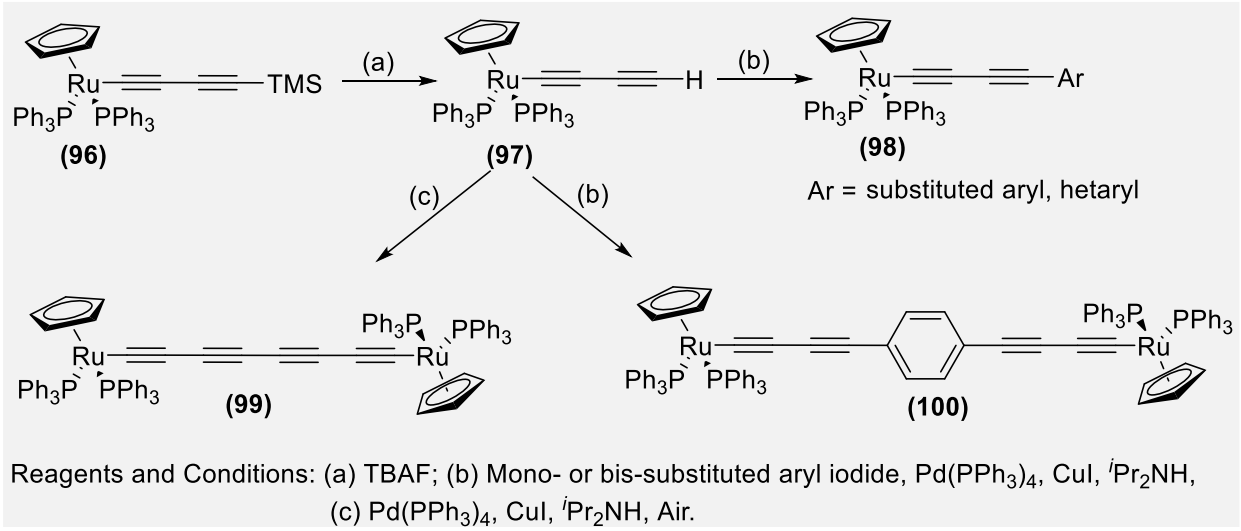

Szafert et al.[159] reported a highly atom economic preparation of new Pd(II) end-capped oligo-ynes (up to hexatriyne, **102**) using 1-halopoly-ynes (**101**) (Scheme 21), which were obtained from Sonogashira coupling followed by halogenation and chain elongation.[160] In the reported work, Pd(0) underwent an oxidative addition to yield Pd(II) complexes in good to excellent yields. They also reported the first X-ray crystal structure of Pd(II) end-capped hexatri-yne (Figure 4).

Scheme 21. Synthesis of Pd(II)-End-Capped Di-, Tetra- and Hexa-ynes[159]

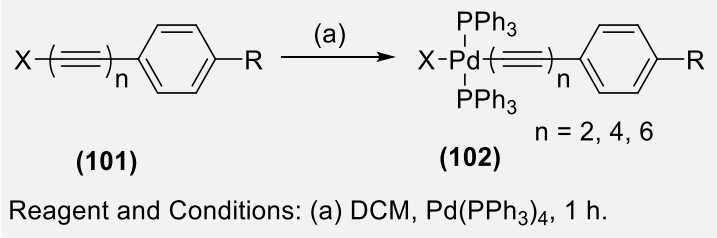

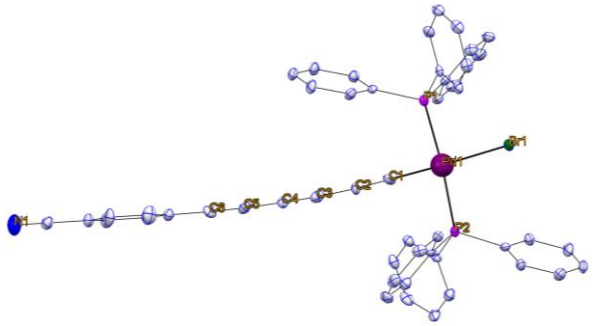

Figure 4. The First X-Ray Crystal Structure of Pd(II) End-Capped Hexatri-yne **102** (R = CN, X = Br, n = 3). Reprinted with permission from ref.[159] Copyright 2015 American Chemical Society.

Synthesis of long-chain metalla-yne is a challenging job due to the stability constraints. However, some leading researchers in the field, using state-of-the-art techniques and smart selection of reagents, successfully synthesized interesting long-chain metalla-ynes.[161] For example, Schanze et al.[162] reported the synthesis of mono-dispersed Pt(II) oligo-ynes of precise length using an iterative convergent approach. Oligo-ynes having different number of Pt(II) ions (**103**, Chart 2) were obtained by following a sequence of reactions between terminal acetylenes and *cis*-/*trans*-Pt(II) salts as the starting materials. Gladysz and co-workers[163,164] synthesized and structurally characterized several Pt(II) oligo-ynes **104** (Chart 2) in which the metal was separated by upto 28 carbon atoms.

Chart 2.

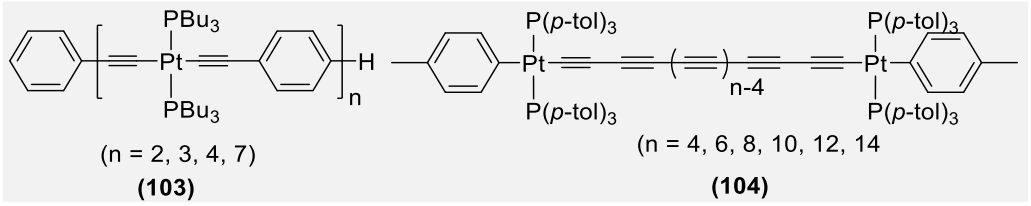

3. Structure-property relationships

Given the range and scope of synthetic routes for di-, oligo- and poly-ynes with or without a metallic core, it is necessary to understand the factors affecting the properties and applications of such materials. Keeping this in mind, we shall discuss structure-property relationship of organic and metalla di-, oligo- and poly-ynes in the following sections and sub-sections. The effect of varying the conjugation length, main chain or side

chain functionalization, metal insertion, auxiliary ligands, etc. on the photo-physical properties will be discussed.

3.1. Organic di-, oligo- and poly-ynes

Due to the intriguing properties and applications of π-conjugated organic materials *viz*. oligo(*p*-phenylene vinylene)s (OPVs) and oligo(*p*-phenylene ethynylene)s (OPEs), an extensive research has been carried out on the structure and photo-physical properties of these compounds. Although OPVs have some *natural* edge over OPEs in optical properties,[165] (**Figure 5a**) it has been demonstrated that the photo-physical properties of OPEs can be fine-tuned by modifying electronics of the molecular skeleton.[166] For example, Yamaguchi et al.[167] demonstrated that a minor change in OPE's structure significantly affects its luminescence efficiency (**Figure 5b**). Very recently, the same group realized a series of whole-rainbow fluorophores (WRFs) realized by installing different donor (D) or acceptor (A) functionalities on the main chain or terminal aromatic rings.[168] (*vide-infra*) Humbert-Droz, Piguet and Wesolowski[169] calculation further confirm that the fluorescence quantum yield (Φ_F) shows a global S-shape dependence on the magnitude of the charge separation.

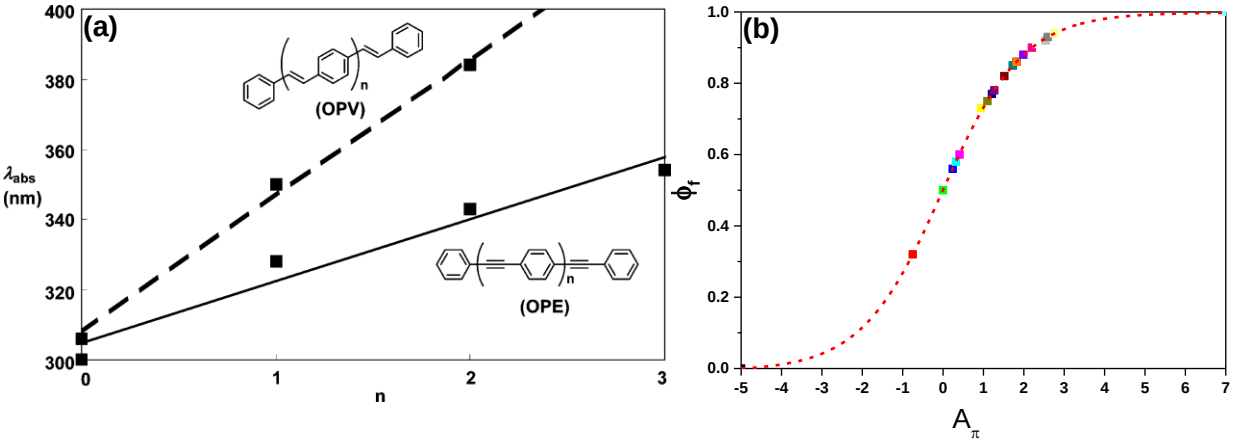

Figure 5. (a) Relationship of $\lambda_{max.}$ with π-conjugation length (n) in OPE and OPV systems. Reprinted with permission from ref [168]. Copyright 2015 American Chemical Society. (b) Variation of Φ_F with effective conjugation length (A_π) in the S_1 state of π-conjugated oligo-ynes. Adapted with permission from ref [167]. Copyright 2008 American Chemical Society.

Several groups including ours have investigated the photo-physical, photo-chemical properties and applications of di-, oligo- and poly-ynes with and without spacer groups.[4,21] Table 2 lists the $\lambda_{max.}^{em.}$ of selected compounds reported in Chart 3. We have shown that in small molecular architecture, ethynyl moieties are the defining synthons and serve as hydrogen bond donor hydrogen bond acceptor fragment.[170] The incorporation of aromatic spacers improves the emission profile (luminescence lifetime and quantum yield) of the systems.[171] Furthermore, substituents attached to the spacer group significantly controls the stability, optical properties (absorption/emission) and radiative and non-radiative processes.[172,173] Marder et al.[171] reported the synthesis and optical properties of 1,4-*bis*(4-carbomethoxy phenylethynyl)benzene (**105a**), 1,4-bis(4-carbomethoxy phenylethynyl)tetrafluorobenzene (**105b**) and 9,10-bis(4-carbomethoxy phenylethynyl)anthracene (**105c**) and a butadiyne (**106a**, Chart 3) system in different solvents (Table 2).

These di-ynes showed good to moderate Φ_F (up to 0.9) and intense UV absorption (except for **105c** and **106a)**. Compound **105c** having an anthracene core exhibited both absorption and emission in visible region, a smaller Stokes shift, a slightly lower Φ_F, and a shorter fluorescence lifetime (τ_F upto 2.7 ns) in comparison to the phenyl counterpart **105a**. Di-yne **106a** with no central spacers showed markedly lower Φ_F (1%) and a very short fluorescence lifetime (τ_F = 70 ps), indicative of high non-radiative deactivation processes. In contrast to this study, the fluorescence properties of a series of butadiyne fluorophores **106b-d** were reported by Gharpure and co-workers.[174] The replacement of phenyl from one of the termini in phenyl-phenyl derivatives by pyrene resulted in blue shift of absorption and emission spectra due to the formation of π-π stacking. Furthermore, the pyrene derivative also showed thermal/mechanical force induced fluorescence switching in the solid state. Similar mechanical, thermal and chemical controlled photo-physical properties have been reported for 1,3,6,8-tetra kis(trimethysilyl)ethynyl)pyrene.[175] The introduction of four trimethysilylethynyl groups resulted in four modes of molecular packing.

When the carbomethoxy group of **105a** ($\lambda_{max.}^{abs.}$ = 332 nm in MeCN and 335 nm in benzene and DCM) was replaced by H (**107a**, $\lambda_{max.}^{abs.}$= 322 nm), Me (**107b**, $\lambda_{max.}^{abs.}$ = 326 nm), OMe (**107c,** $\lambda_{max.}^{abs.}$= 334 nm) and CF_3 (**107h,** $\lambda_{max.}^{abs.}$ = 326 nm), the UV absorption band shows blue shift while it undergoes red shift when substituted with MeS (**107d,** $\lambda_{max.}^{abs.}$ = 346 nm), NO_2 (**107f,** $\lambda_{max.}^{abs.}$ = 356 nm), CN (**107e,** $\lambda_{max.}^{abs.}$ = 336 nm) and NMe_2 (**107g**, $\lambda_{max.}^{abs.}$ = 366 nm) (Chart 3).[176] Despite the fact that these data lacked a trend in absorption properties with different electron donor and acceptor groups, the roles of the coreand the peripheral groups in deactivation of the excited states have been recently established.[177] This study, indicated temperature and solvent dependent photo-physical properties in D-A di-ynes bearing anthracene or fluorene as the core with peripheral electron-withdrawing group. Marder and co-workers[178] reported a series of fluorinated and non-fluorinated di-ynes based on the 4-ethynylpyridyine (**108-112**, Chart 3). These compounds (**108-111**) absorb in the 314–320 nm range and their extinction coefficient (ε) increase with the degree of fluorination. When the central core of **108** was changed from phenyl to anthracenyl (**112**), the absorption of the resulting di-yne moved to the visible region ($\lambda_{max.}^{abs.}$ = 436 nm in MeCN) with improved emission profile due to extended conjugation. Interestingly, absorption and emission spectra of protonated species undergo a blue shift, which was more pronounced for non-fluorinated than fluorinated species. The substitution of terminal pyridyl moieties in **112** by different functionalized phenylene units produced a range of highly fluorescent di-ynes **113(a-h**) (Chart 3).[172] These fluorescent 9,10-*bis*(*p*-phenylethynyl)anthracene chromophores having functional groups such as Me (**113b)**, OMe (**113c)**, SMe (**113d)**, NMe_2 (**113e)**, CF_3 (**113f)**, CN (**113g)** and NO_2 (**113h)** showed Φ_F between 0.15-0.82, absorption between 438-490 nm (THF) and emission between 480-520 nm.

Table 2. Emission Maxima of Selected Compounds Reported in Chart 3.

Entry	$\lambda_{max.}^{em.}$ (nm)	Medium	ref.	Entry	$\lambda_{max.}^{em.}$ (nm)	Medium	ref.
105a	364	MeCN	[171]	112	634	MeCN	[178]
105b	360	MeCN	[171]	113a	480, 502	THF	[172]
105c	483	MeCN	[171]	113b	483, 511	THF	[172]
106a	351	MeCN	[171]	113c	492, 519	THF	[172]
106b	425, 450	Solid state	[174]	113d	500, 526	THF	[172]
106c	410, 425	Solid state	[174]	113e	556	THF	[172]
106d	490, 525	Solid state	[174]	113f	480, 508	THF	[172]
107a	351, 365	Toluene	[176]	113g	495, 516	THF	[172]
107b	354, 369	Toluene	[176]	113h	520	THF	[172]
107c	365, 380	Toluene	[176]	114a	382	Toluene	[173]
107d	382, 399	Toluene	[176]	114b	386	Toluene	[173]
107e	364, 385	Toluene	[176]	114c	394	Toluene	[173]
107f	406, 426	Toluene	[176]	114d	387	Toluene	[173]
107g	410, 430	Toluene	[176]	114e	434	Toluene	[173]
107h	356, 370	Toluene	[176]	114f	435	Toluene	[173]
108	424	MeCN	[178]	114g	401	Toluene	[173]
109	486	MeCN	[178]	114h	402	Toluene	[173]
110	473	MeCN	[178]	115	382	Toluene	[173]

Chart 3.

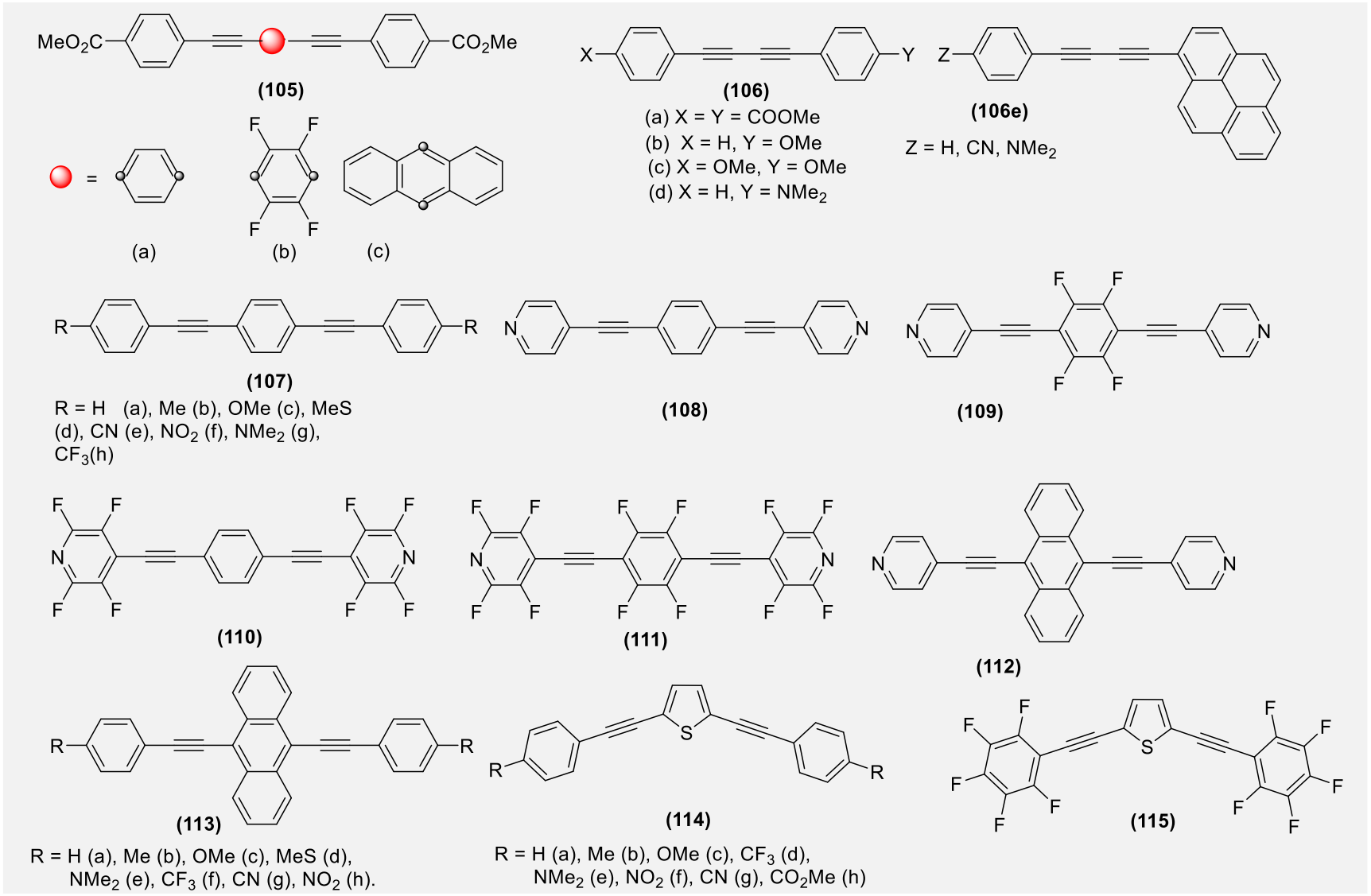
MeO2C
CO2Me
(105)
= (a)
F F F F (b)
(c)
X Y
(106)
(a) X = Y = COOMe
(b) X = H, Y = OMe
(c) X = OMe, Y = OMe
(d) X = H, Y = NMe2
Z
(106e)
Z = H, CN, NMe2
R R
(107)
R = H (a), Me (b), OMe (c), MeS (d), CN (e), NO2 (f), NMe2 (g), CF3(h)
N N
(108)
F F F F N N
(109)
F F F F N N F F F F
(110)
F F F F F F N N F F F F F F
(111)
N N
(112)
R R
(113)
R = H (a), Me (b), OMe (c), MeS (d), NMe2 (e), CF3 (f), CN (g), NO2 (h).
S R R
(114)
R = H (a), Me (b), OMe (c), CF3 (d), NMe2 (e), NO2 (f), CN (g), CO2Me (h)
F F F F F F S F F F F F
(115)

Marder and co-workers[173] extended their studies on organic di-ynes in which thienyl ring was inserted into the center and end-capped with substituted phenyl and pentafluorophenyl rings (**114, 115**, Chart 3). Contrary to the phenylene system, both electron donating and withdrawing *para*-substituents on the terminal phenyl rings (**114)** shifted the $\lambda_{max.}^{abs.}$ and $\lambda_{max.}^{em.}$ to lower energies. The shift was more pronounced with electron acceptor groups than with electron donors. Shorter excited state lifetimes and lower quantum yields compared to the related 4-*bis*(phenylethynyl)benzenes and 9,10-*bis*(phenylethynyl)anthracene systems, were the indication of $S_1 \rightarrow T_1$ conversion and attributed to the heavy atom effect by S-atom, enhancing the SOC. Furthermore, di-ynes having nitro groups at the end were found to cause non-radiative deactivation of the excited state and hence were the least fluorescent.

In OPEs, one important factor which determines the properties of materials is the coplanarity of aryl rings along the main chain. Due to the low rotational barriers about the arylene–alkyne bonds (< 1 kcal mol^{-1}), several conformations can be adopted by the molecules. Therefore, by capturing conformation, effective conjugation length dependent properties of the materials can be modulated. For this purpose, several strategies *viz*. induction of steric hindrance, H-bond formation, non-covalent interactions between the side and the main chains, inclusion of charged rings, etc. have been attempted. Furthermore, it has been demonstrated that the photo-physical properties of the oligo- and polymers can be significantly tuned by tailoring side chains and main chains of oligo-ynes. Chart 4 depicts some examples of di-ynes that show side-chain and main-chain interaction dependent spectral features. Thomas and co-workers[179] demonstrated that specific and non-covalent interactions between aromatic rings on the side-chains and the main-chains in **116** (Chart 4) control the O-E properties of conjugated materials (**Figure 6a,b**). The competition between these and other forces has potential for the design of responsive mechanochromic luminescent materials. Using fluorinated OPEs, Sharber et. al.[180] showed that the non-covalent interactions between the side-chain (fluorinated benzyl esters) and the main-chain (terminal arenes) in **117** (Chart 4) play a significant role in the determination of conformations and electronic structures. They showed that in solids and in solution, the optical properties are significantly controlled by the nature of pendant groups. Besides, the absorption/emission profile are also modulated by cofacial ArF−ArH interactions between the fluorinated aromatic pendants and terminal rings of the oligo-yne backbones as well as the nature of substituent present. Moigne et al.[181] found that the ether (an electron donor) and ester (an electron acceptor) side-chain groups (not formally part of the conjugated network) not only enhance the solubility but also modulates the electronic property of the oligo- and poly-ynes. Similar phenomena on the bandgaps of conjugated systems have also been shown using oligo-ynes with benzylated/fluorinated side chains.[182] The absorption and emission spectra of oligomers containing benzylated or fluorinated esters showed blue shifts compared to their ether counterparts. Schanze and co-workers[183,184] reported water-soluble cationic di-ynes having tertiary amine substituent at the core and ester or carboxyl groups at terminal aromatic rings. Interestingly, all the symmetrical molecules showed similar two-band absorption spectra and a relatively broad structureless single fluorescence transition with maxima in the 397-472 nm range in both water and methanol. The quantum efficiency of these molecules varied between 0.02 to 0.8. Although these

compounds showed strong fluorescence in methanol, the fluorescence yields were variable and substituent-dependent in water. Such type of interesting systems could find application in biological applications due low molecular weight, high solubility and $\lambda_{em.}$ in the visible region.

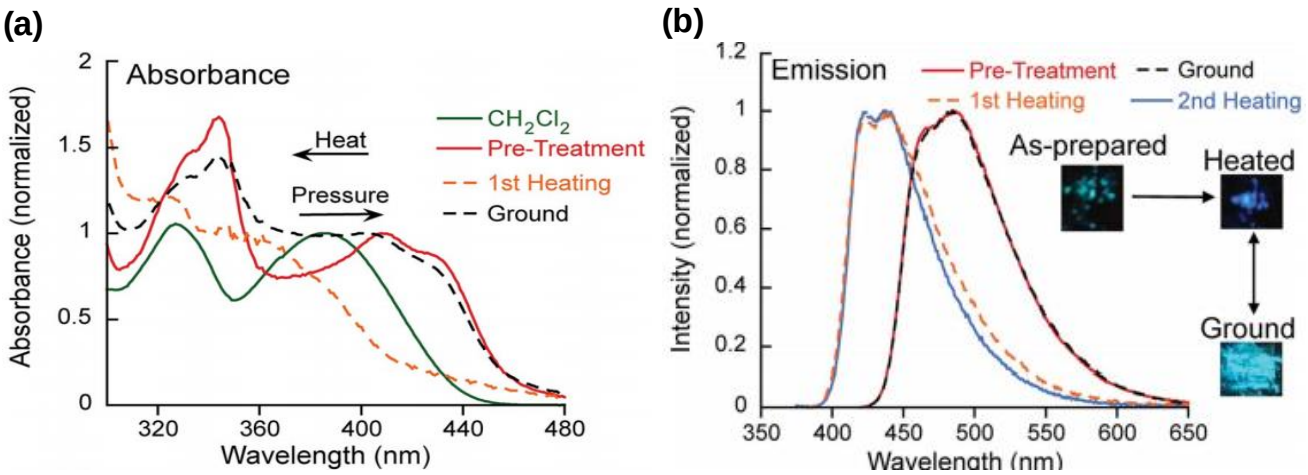

Figure 6. (a) Absorption and (b) emission spectra of **116** (R_1 = OC_8H_{17}, R_2 = H, X= F_5Ph), drop cast from DCM with heating and grinding cycles, Reprinted with permission from ref.[179]. Copyright 2014 Royal Society of Chemistry.

Chart 4.

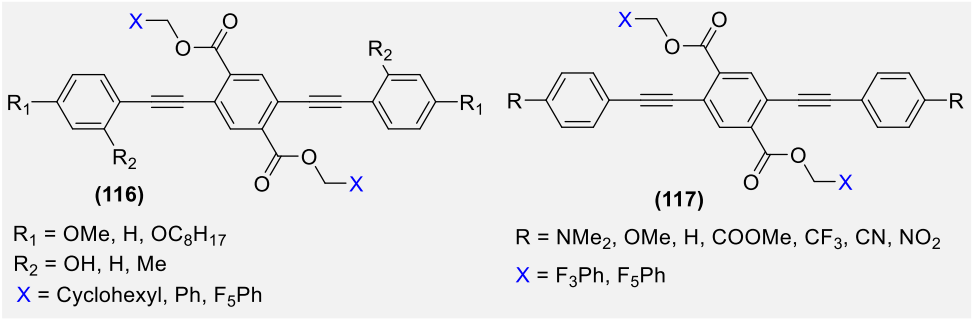

For O-E and bioimaging applications, strong light-emitting fluorophores with large Stokes shifts, small $\Delta\lambda_{em}$ (difference of emission maximum wavelength of two different fluorophores having the same core skeleton), and intense emission with high absolute quantum yield are highly demanding.[168,185] Especially, fluorophores covering whole visible spectrum with small $\Delta\lambda_{em}$ offer unique selectivity and exquisite control over colour. Therefore, fluorophores with small $\Delta\lambda_{em}$ have potential for the development of full-colour emitting devices while maintaining similar beautiful emissive characteristics, physical properties, and processability.[186] OPVs are well-known full colour chromophores with a large Stokes shift; however, their large value of $\Delta\lambda_{em}$ (> 30-40 nm) poses a big challenge.[186,187] It has already been demonstrated that installation of cyano (CN) functionality over a rod-shaped π-conjugated systems creates strong D-A interaction leading to significant improvement in emission properties of the fluorophores.[188-190] Motivated by this notion and earlier works, Yamaguchi and co-workers[168] prepared a series of WRFs (**118-124**, Chart 5) having excellent emission properties along with high absorptivity (log ε > 4.5), small value of $\Delta\lambda_{em}$ (Table 3) and mechano-fluoro-

chromic properties. Polymer (PS) doped with di-ynes emit light in the whole visible region and have $\Delta\lambda_{em}$ values < 20 nm and high Φ_f values (> 0.6, Figure 7). These properties were further improved upon extending the functionality (**123**-**124**), judicious installation of different donors (OMe, SMe, NMe_2, and NPh_2) and one or more cyano group as an acceptor over OPE backbone was the main reason behind this exceptional and improved PL properties.

Table 3. Selected Photo-Physical Data[a] for Compounds Reported in Chart 5[168]

Entry	Φ_f	log ε	$\lambda_{max.}^{em.}$ (nm)	Entry	Φ_f	log ε	$\lambda_{max.}^{em.}$ (nm)
118a	0.86	4.69	409	121b	0.92	4.62	488
118b	0.82	4.67	429	121c	0.50	4.61	594
118c	0.78	4.61	506	121d	0.73	4.54	609
118d	0.86	4.63	518	122a	0.91	4.48	473
119a	0.90	4.72	444	122b	0.88	4.55	506
119b	0.85	4.69	460	122c	0.32	4.61	624
119c	0.60	4.79	569	122d	0.56	4.54	639
119d	0.77	4.61	565	123a	1.00	4.53	525
120a	0.94	4.60	449	123b	0.01	4.50	721
120b	0.85	4.66	468	124a	0.26	4.53	671
120c	0.58	4.57	579	124b	0.76	4.56	611
120d	0.75	4.58	586	124c	0.03	4.47	732
121a	0.93	4.63	459				

[a]*Data collected in Chloroform solution at 298 K in chloroform.*

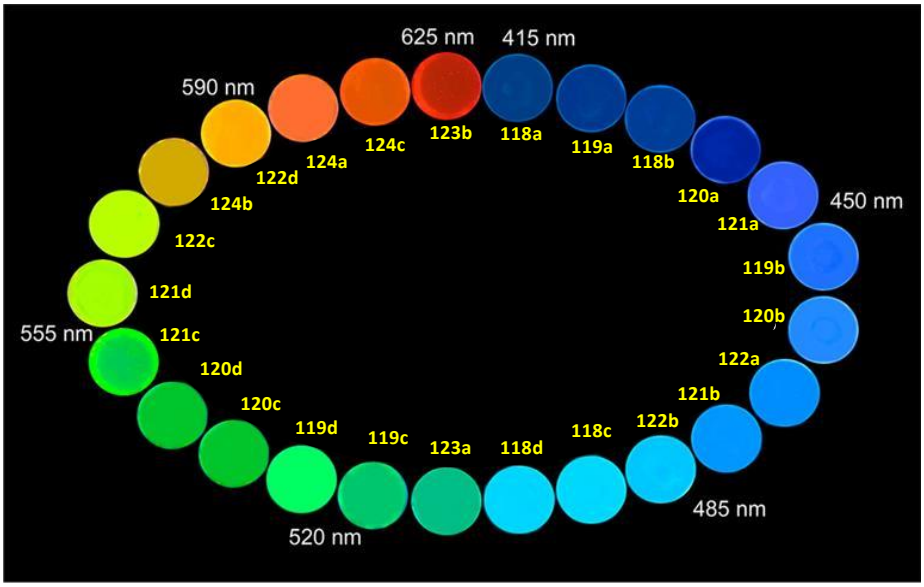

Figure 7. Emission color of **118-124** dispersed in PS film under irradiation at 254 nm. Reprinted with permission from ref [168]. Copyright 2015 American Chemical Society.

In Chart 6, we have shown some examples of oligo-ynes that possess improved optical properties over their alkenic counterparts. Frank et al.[191] synthesized and compared the photophysical and nonlinear absorption (NLA) properties of D-A systems (**125**, Chart 6) composed of *N,N*-dimethylaniline (DMA) or *N,N*-dihexylaniline (DHA) as donors and dicyanovinyl as acceptor with their alkene counterparts. For both the alkene and alkyne series, the optical (E_g^{op}) and electrochemical (E_g^{ec}) band gaps were almost identical up

to six carbon atoms and after that, no effect of chain length was seen (saturation point). Oligo-ynes **126** (n = 0-5, Chart 6)[192] having the same D-A system with higher number of acceptor groupS featured a broad, LE transition band due to intramolecular charge transfer (ICT) transition. This ICT transition resulted from the donor present at the termini to the acceptor. The energy of the charge transfer (CT) band was found to decrease with increasing chain length. As the flexibility of the ethynyl spacer in solution increased with increasing length, it resulted into broadening of the CT band at the longer wavelength. The inclusion of heteroatoms like phosphorus also produces significant changes in photophysical properties. It has been demonstrated that in oligo-ynes with phospha-alkene termini and different aromatic bridging units (**127a-d**, Chart 6) electronic communication between the termini increases with increasing aromaticity of the *para* linked central core[193] Depending upon the communication, color of the compounds changes too. The color of the compounds changed from light yellow through yellow to red on moving from **127a** → **127d**, indicating mixing of orbitals of phospha alkene-based fragment to ethynylarene frameworks leading to decreased E_g gaps.

Though the construction of a D–A architecture and extension of π-conjugation are common strategies to shift the absorption/emission to the red region, challenges researchers often face are π–π interactions and twisted intra-molecular charge transfer (TICT)-induced emission quenching. To circumvent these issues, aggregation-induced emission (AIE), the reverse of aggregation-caused quenching (ACQ),[185,194,195] emerged as a potential phenomenon with multi-dimensional applications.[196-204] AIE luminogens (AIEgens) produce efficient and bright luminescence due to restricted intra-molecular motion and the lack of π-π stacking interactions.[185] A number of organic and organometallic alkynyl-based AIEgens have been reported recently.[202,205] Tang and co-workers[206] reported AIEgen **128** (Chart 6) in which the incorporation of ethynyl linker not only served as a *rigid-rod* electron acceptor core for efficient ICT, but also inhibited the emission quenching arising from π-π interactions (Figure 8). A large difference in Φ_F (0.5% *vs* 7%) and τ_F (0.23 ns *vs* 0.52 ns) of **128** in dilute THF solutions and in the solid state strongly indicated the presence of AIE. Furthermore, rise in the radiative decay rate constant ($k_{r,soln}$ = 0.22 × 10^8 s^{-1}, 1.3 × 10^8 s^{-1}) and fall in the non-radiative decay constant ($k_{nr,soln}$ = 43.3 × 10^8 s^{-1}, $k_{nr,solid}$ = 17.9 × 10^8 s^{-1}) further confirm the presence of AIE. Using the same AIEgen **128**, aptamer-decorated self-assembled organic dots have been prepared and used as targeted imaging probe.[207]

Chart 5.

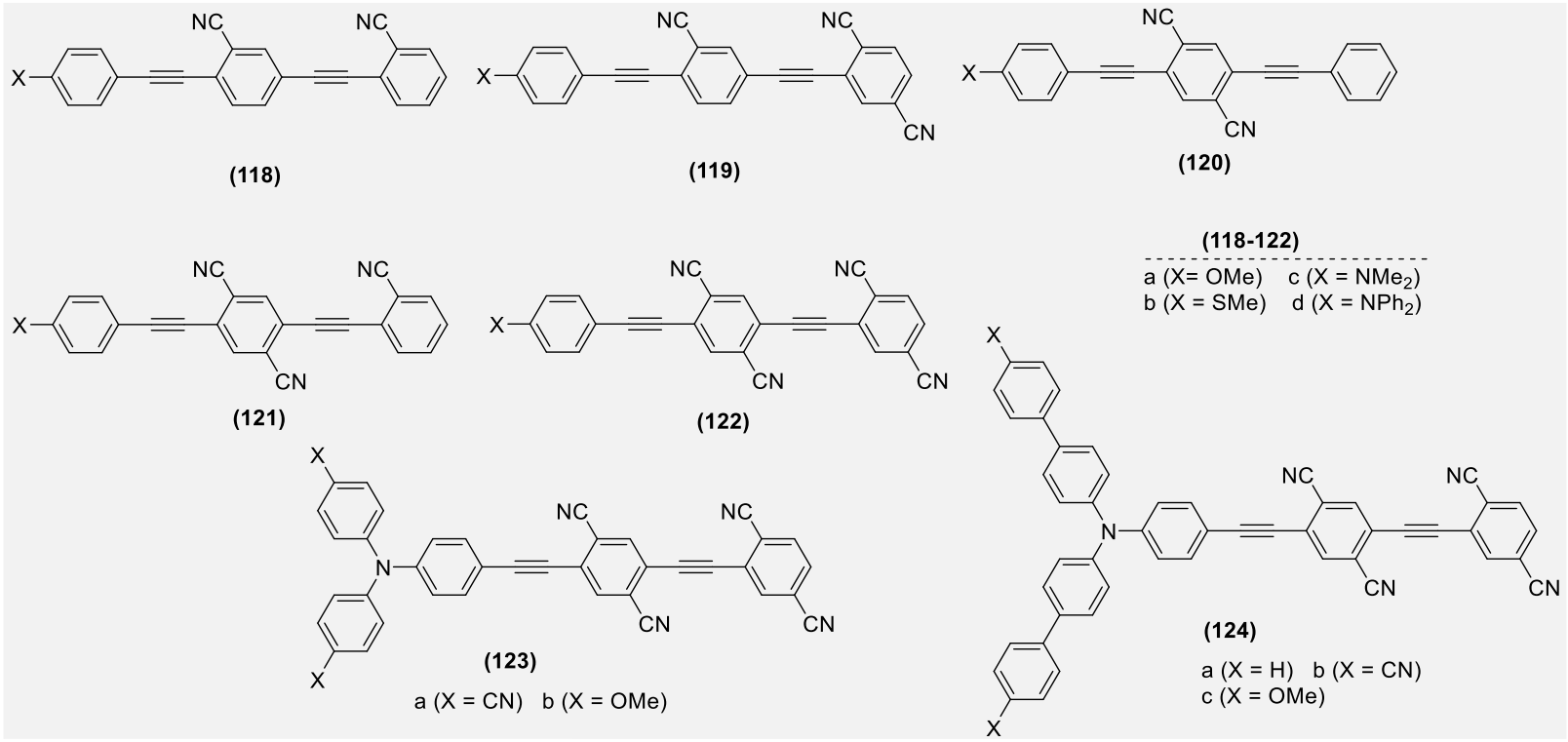
(118)
(119)
(120)
(118-122)
a (X= OMe) c (X = NMe2)
b (X = SMe) d (X = NPh2)
(121)
(122)
(123)
a (X = CN) b (X = OMe)
(124)
a (X = H) b (X = CN)
c (X = OMe)

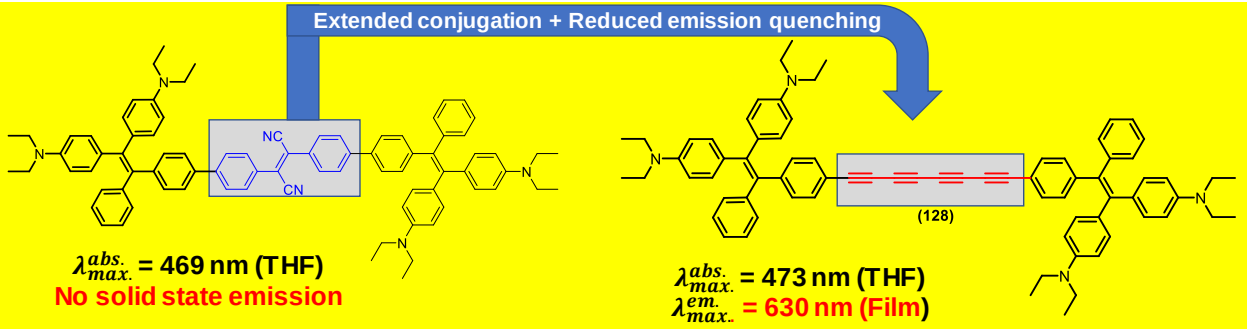

Figure 8. Impact of alkynylation in D-A based chromophores.

Chart 6.

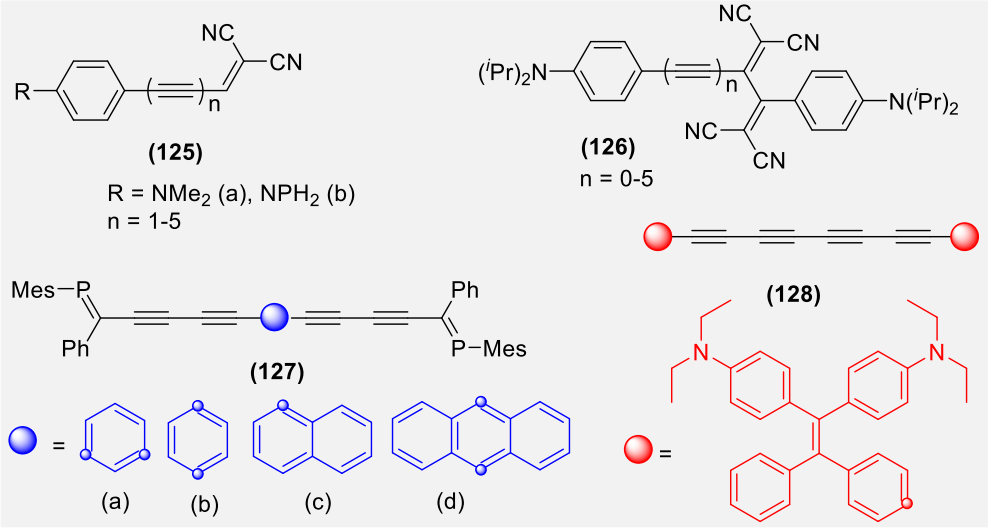

Iptycenes are a class of aromatic compounds with arene units fused to the [2.2.2]bicyclooctatriene bridgehead system. Their unique structures have attracted the attention of several researchers.[208] The incorporation of rigid iptycene scaffold (*viz*. triptycene and pentiptycene) to a rigid-rod oligo- or poly-yne modifies the oligo/polymer backbone, which ultimately affects its properties.[209] For example, the incorporation of iptycene enhances the solubility of the polymer, which is attributed to the "*internal free volume*" (IFV) possessed by iptycenes. Further, they also shield the molecular backbone, which is an important factor in O-E industries.[210] The group of Swager and others reported several triptycene-based di- and oligo-ynes as liquid crystalline materials, self-assembled microporous materials, molecular motors/rotors etc.[210-212] However, there is a minor effect of bridging π systems to iptycenes on photo-induced CT (as transport occurs mainly through the σ system). A recent work demonstrated that when a pentiptycene unit is connected at the termini of anthracene di-ynes[213], it produces multicolor fluorescence. Using such fluorophores, luminescence switching can be achieved by applying either external (*viz*. pH, ultrasound, temperature, light, thermal, magnetic forces, mechanical stress, etc.) or internal stimuli (*viz*. enzyme concentrations, inter and intracellular pH difference, biomolecules, etc.).[174,214-221] The externally/ internally applied stimuli cause rearrangement in the molecular architecture (ordered-to-disorder or *vice*

versa) at the supramolecular level leading to change in the luminescence. For example, the green-fluorescent di-yne **129** (Chart 7) showed a change in color (yellow to red) and fluorescence quenching (a change to black) upon treatment with aniline-derivatives and benzoquinone, respectively.[214] Furthermore, materials based on **129** showed mechano-fluoro-chromism and a memory of the resulting color (Figure 9a). Fluorescence switching behavior has also been reported in oligopyridine-decorated[219,222] (*vide-infra*) and pentiptycene-containing Pt(II) acetylide complexes[223] as well as in perylene monoimides end-capped oligo-ynes.[224] Amphiphile **130** (Chart 7) displayed two distinct emission colors (cyan from PPE and red from perylene) and the relative emission intensity depends on the surface pressure applied on the Langmuir monolayers.[224] The aqueous solution of lyotropic liquid crystals (LLC) based on **130** was found to be clear and highly emissive with varying colors from cyan to red (Figure 9b,c). In summary, luminescence switching makes the fluorophores suitable candidates for multi-disciplinary applications.[174,214-221]

Chart 7.

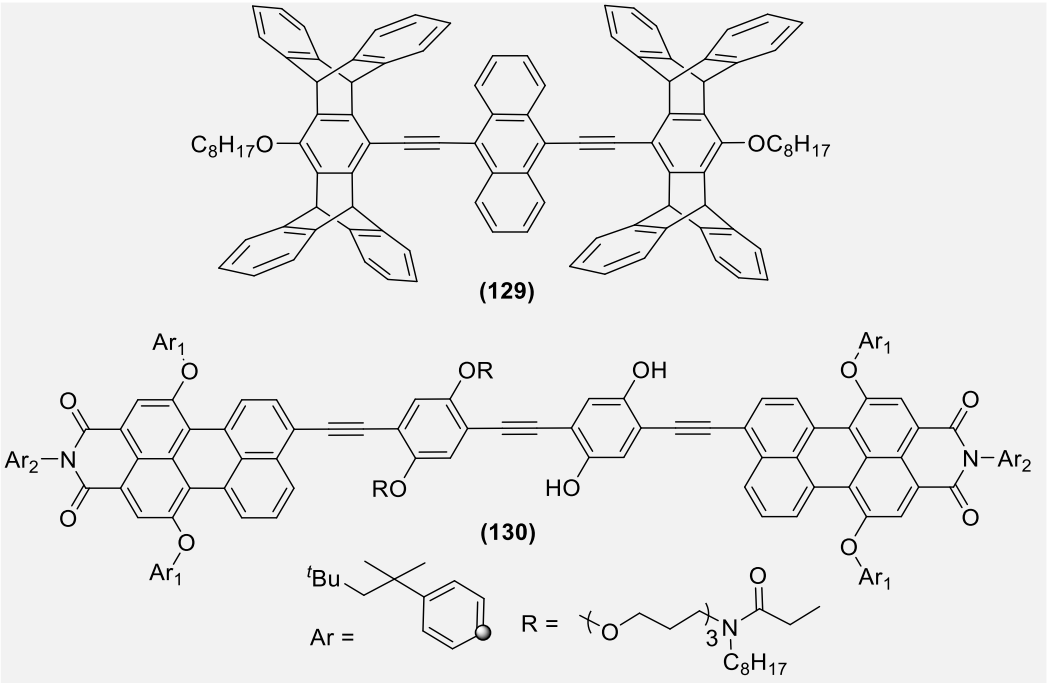

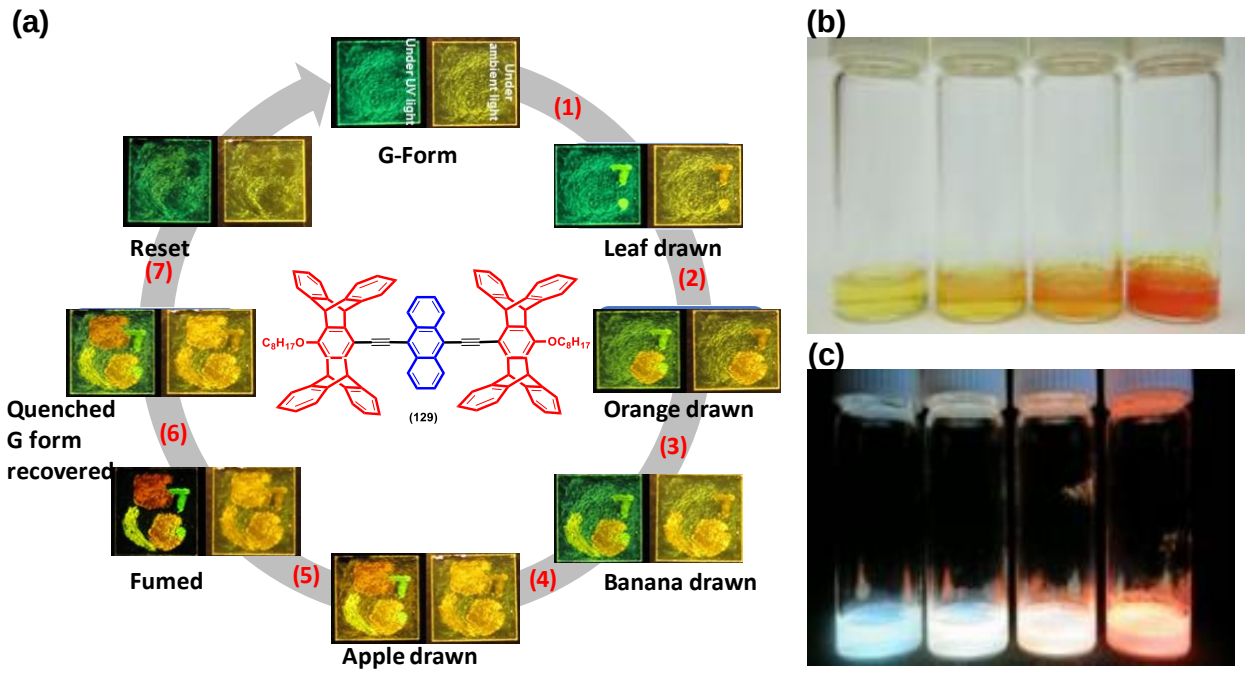

Figure 9. (a) Photographs of multicolor fluorescence drawing on a glass plate using **113** ((1) = Drawing, (2) = dimethylaniline fuming then drawing, (3) = 3,4-difluoro-*N,N*-dimethylaniline fuming then drawing, (4) = 4-Methyl-*N,N*-dimethylaniline fuming then drawing, (5) = Benzoquinone fuming, (6) = Air-blowing, and (7) = dichloromethane fuming). Reproduced with permission from ref [214]. Copyright 2015 John Wiley and Sons. (b) the transparent solution, and (c) Varying color fluorescence from LLC solution based on **130**. Reprinted with permission from ref [224]. Copyright 2017 American Chemical Society.

In addition to the conjugation length and type of spacers used, electronic properties of oligo-yne can also be modulated by backbone planarity.[209,214,225] For example, in an alternating OPE, when the ethynyl and phenylene rings lie in twisted forms, it gives enhanced π-π interactions, while perpendicular arrangements led to the enhanced conjugation.[209] The interchange of these two states depends on several factors including solvent, nature of the functional group, etc. Chart 8 shows oligo-ynes in which optical property is controlled by arrangement of alkyne/spacer (twisted or perpendicular) and extent of H-bonding. In OPE **131a-c** (Chart 8), having $\lambda_{max.}^{abs.}$ in 382-471 nm range, the two states were controlled by the presence or absence of intra-molecular H-bonds formed between carboxylate and amido substituents present on alternating position.[226] In contrast, compounds **132a-d** (Chart 8) retaining a similar number of C≡C bonds (n = 4) with benzene, anthracene or thiophene as the spacer and hydrogen as the terminal atom shows spacer dependent conjugation.[227]

Chart 8.

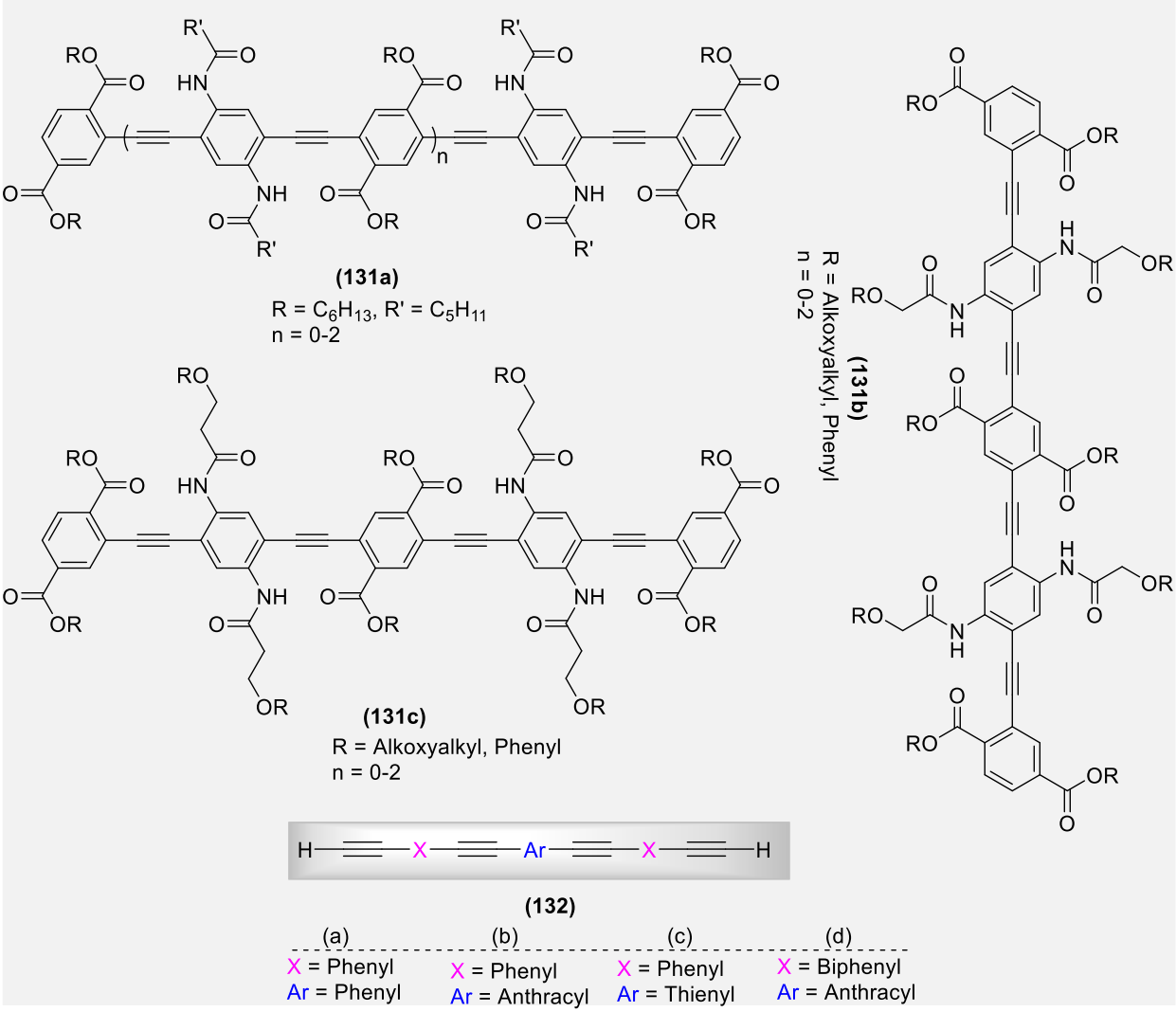

In a landmark study, Li et al.[228] introduced a new concept for designing luminescent oligomers. They found that when a non-planar polycyclic aromatic hydrocarbon, corannulene, and a planar aromatic unit, thiophene are connected through an ethynyl linkage, (**133a-d**, Chart 9) π-effects vary as a function of the oligomer length. They showed that the extended π-effects in conjugated discrete oligomers (**133a-c**) initially increase and then attenuate (**133c** and **133d**). Unexpectedly, longer oligomers showed unique nonlinear optical (NLO) properties i.e. a large two-photon absorption cross section and two-photon-excited bright luminescence. This is a unique finding as corannulene and its derivatives are, so far, not known to exhibit non-linear optical (properties. The oligomer with three corannulene and two thiophene units exhibits a two-photon absorption cross section of 600 GM and two-photon-excited intense green luminescence.

Chart 9.

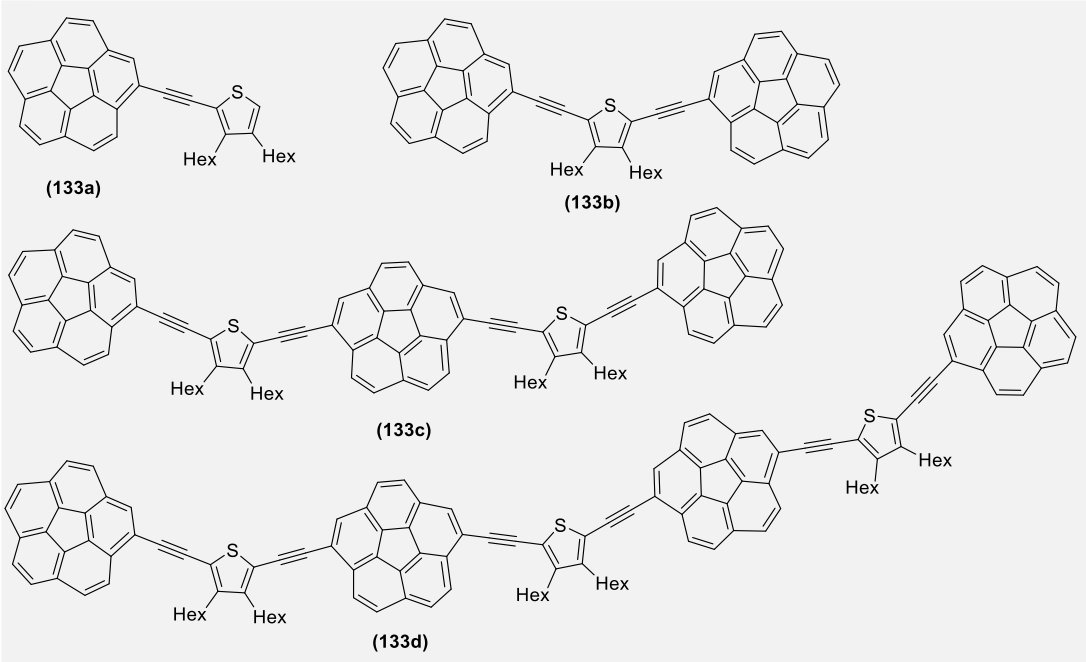

Several other studies detailing photo-physical properties and applications of poly-ynes/co-poly-ynes and their corresponding model compounds are available in the literature.[229-232] We have discussed a few key poly-ynes here while few others will be discussed in the application section (Section 4, *vide-infra*). Chemical structures and emission value of representative poly-ynes materials are summarized in Chart 10 and Table 4. From all the arguments developed before, it is clear that the optical properties of oligo-ynes vary in the same way as their model compounds. For example, the nature of the side-chain on the terephthalate ring in polymers **134-137** (Chart 10) control their optical properties (Table 4).[182] Moreover, these side-chains also give shape/conformation to the resulting poly-ynes. For instance, poly-yne containing hydrophilic side-chains and rigid-rod hydrophobic main-chains force the polymers to adopt an optically active helical conformation.[233-235] Due to the hydrophobic exterior (alkyl groups and phenylene ethynylene main chain) and hydrophilic interior (hydroxy groups) structure of these helices, these materials may find application in chiral separation as well removal of organic and inorganic pollutants from water. Both polar and non-polar interactions arising due to the chirality play important role in helix formation. Sanda et al.[236] reported co-poly-ynes bearing various arylene units (**138a-d**, Chart 10) that can adopt a one handed helical structures predominantly in THF. The photo-physical properties, temperature and solvent-responses of the polymers were found to be dependent upon the spacer (phenylene, naphthylene and pyrenylene) and their linking positions. 1,4-Naphthylene and 1,6-pyrenylene units in the polymeric chain were found to extend the conjugation length more compared to phenylene unit, while it was shortened in the case of 2,7-naphthylene. Polymers emitted blue, purplish blue, green and yellow fluorescence, depending upon the chirality and spacers used. In a similar work, the same group reported optically active blue emitting poly(m-phenylene ethynylene−arylene ethynylene)s bearing hydroxy groups with various arylene units (**139**, Chart 10).[237]

While some polymers formed predominantly one-handed helical structures in THF, others showed no evidence of chirality. Tube-like structures with diameters around 5 nm were observed, together with occasional periodic stripe patterns. Recently, Cheng and co-workers[238] reported chiral BINOL-based polymers (**140**, Chart 10). Interestingly, only polymers emitted circularly polarized luminescence (CPL) signals, which was attributed to the chirality transfer of the BINOL moiety *via* the rigid π-conjugated chain backbone structure system. CPL with chiral amplification has also been reported in π-conjugated ternary helical polymers **141** (Chart 10) containing a chiral and an achiral biphenyl units.[239]

Table 4. Emission Maxima of The Polymers Reported in Chart 10.

Entry	$\lambda_{max.}^{em.}$ (nm)	Solvent	ref.
134	498	DCM	[182]
135	505	DCM	[182]
136	509	DCM	[182]
137	523	DCM	[182]
138a	446	THF	[236]
138b	408	THF	[236]
138c	504	THF	[236]
138d	535	THF	[236]
139	412-446	THF	[237]
140	448	THF	[238]
141	~ 450-500	MeCN/$CHCl_3$ (70/30, v/v)	[240]

Chart 10.

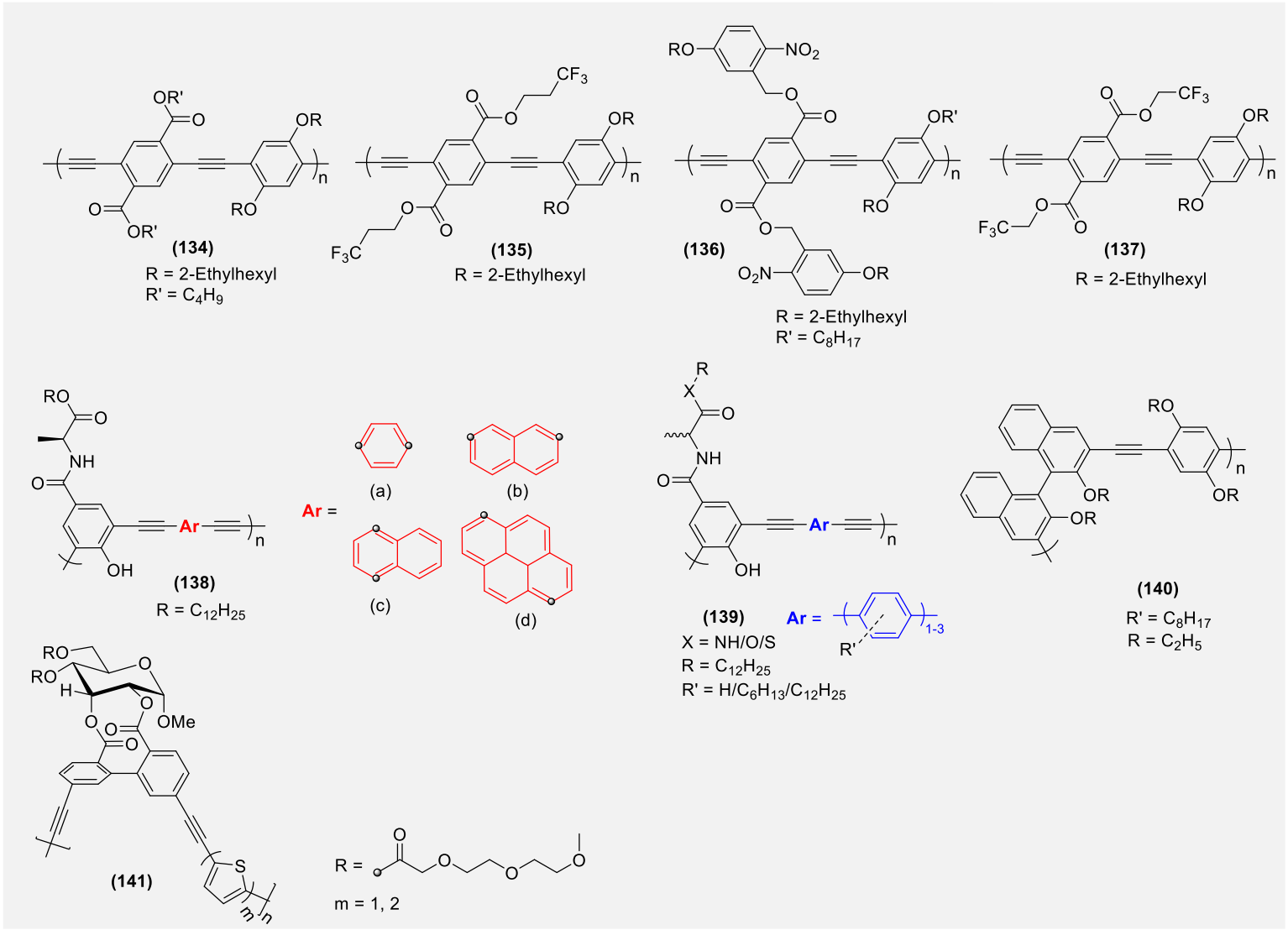
(134)
R = 2-Ethylhexyl
R' = C4H9
(135)
R = 2-Ethylhexyl
(136)
R = 2-Ethylhexyl
R' = C8H17
(137)
R = 2-Ethylhexyl
(138)
R = C12H25
Ar =
(a)
(b)
(c)
(d)
(139)
X = NH/O/S
R = C12H25
R' = H/C6H13/C12H25
(140)
R' = C8H17
R = C2H5
(141)
R =
m = 1, 2

3.2. Metalla(di-, oligo- and poly-ynes)

Since the pioneering work of Nast and Hagihara,[241] transition-metal acetylide complexes and polymers have attracted immense interest of academic and industrial researchers.[7,242,243] The inclusion of the metallic core in the organic framework dramatically improves the physico-chemical, photo-physical and O-E properties and endows the resulting materials with unique capabilities to resolve many challenges at the supramolecular level.[244,245] For example, the spin statistical probabilities for singlet (S_n) and triplet (T_n) excitons for organic poly-ynes are 25% and 75% and they lack a "*spin-flip*" mechanism, which is responsible for the intersystem crossing (ISC) between S_n and T_n states to produce phosphorescence.[246] The introduction of heavy metal ions, especially Pd(II) and Pt(II) into the polymer backbone causes "*spin-orbit coupling*" (SOC), allowing an efficient ISC leading to a huge yield in T_n-excitons (theoretically 100%).[247-250] Furthermore, compared to organic systems, metalla-ynes have a greater number of tunable components to tailor their properties. An organometallic monomer, dimer or polymer of general formula $(L)_n$-M-C≡C-Ar, $(L)_n$-M-C≡C-Ar-C≡C-M-$(L)_n$ and [-M$(L)_n$-C≡C-Ar-C≡C-]$_\infty$, respectively, can be modified by changing the metal (M), auxiliary (L) and organic spacer (Ar). In the following sub-sections, we shall briefly review the bonding and electronic structure of metalla-ynes followed by structural, electrochemical and photo-physical properties of mono and mixed metalla-ynes containing Group 4-11 metals.

3.2.1. Bonding and electronic structure in metalla-ynes: an overview

Alkynes are versatile ligands capable of interacting with transition metal through various coordination modes (η^1-σ-alkynyl and η^2-π-alkyne ligands to transition metal) to form mononuclear σ-acetylides and π-alkyne-metal complexes (Figure 10).[251] The type of coordination mode is determined by the metal and its oxidation state, the nature of auxiliary, and the group (Ar) attached to on the alkyne unit. In a prototype, a metal center is attached to one or more ethynyl units, which in turn, connect to carbocylic/heterocyclic/mixed spacer (Ar) or same/different metal ion(s). Depending upon the metal, the coordination sphere of the metal is satisfied by π-backbonding (PR_3/AsR_3) or σ-donating (*viz*. NHC) auxiliary ligands. Ethynyl ($HC{\equiv}C^-$) is a strong field ligand, acts as a good σ donor, a π acceptor[25,241] and raises the energy of metal centered d-d states, thereby offering a pathway for non-radiative decay of the excited state.[252-254]

In a σ-acetylide complex containing metal with a d^8 configuration such as Pt(II), the metal center has four doubly filled d-orbitals (d_{xz}, d_{xy}, d_{yz} and d_{z^2}) and one vacant $d_{x^2-y^2}$ orbital. The empty $d_{x^2-y^2}$ orbital is located along the plane of the σ-bond axis and can accept charge from the ligand fragment. Hence, both the metal and ethynyl functionalities lie in the same plane. The pure σ-bond nature of M-C bond in metal acetylides was first described by Kostic and Fenske using Fe acetylide.[255] Later, this work was experimentally supported by photo electron spectroscopy (PES) measurements as well as by theoretical calculations.[256-258] Both theoretical and experimental studies indicated an overlap of dπ-orbital of the metal and pπ-orbital of the ethynyl system. Due to this dπ-pπ interactions and some ionic character of the M-C bond, metal-acetylide bonds are thermally stable (for third row transition metals, > 100 kJ mol^{-1}).[256] Frapper and Kertesz[259] performed a detailed systematic study of the electronic structures of mono, oligo- and poly-metalla-ynes containing different transition metals (Mo(II), Fe(II), Ru(II), Co(III), Rh(III), Ni(II), Pd(II), Pt(II),

etc.) and auxiliary ligands (PBu_3, PMe_3, $AsBu_3$, Cl, SCN, CO, H, etc.). They concluded that there is a mixing of ligand and metal orbitals leading to extended conjugation through the metal sites. They also showed that a band gap difference (ΔE_g) of 0.3-0.7 eV exists between the square planar Pt(II) poly-ynes and corresponding model complexes.[247,249] Lichtenberger and co-workers[260] carried out ultra-weak photon emission (UPE) spectroscopic studies to understand the electronic interactions between Ru(II) and alkynyl ligands. They found that in these complexes too, metal-alkynyl π electronic structure is mainly dominated by the interaction between the filled metal-*d*π and filled alkynyl-π orbitals. A strong electronic communication between the metal centers in RpC≡CRp [Rp = $(\eta^5\text{-}C_5H_5)Ru(CO)_2$] supported this fact. The π-backbonding capacity of the alkynyl ligands were considerably lower compared to the CO ligand.

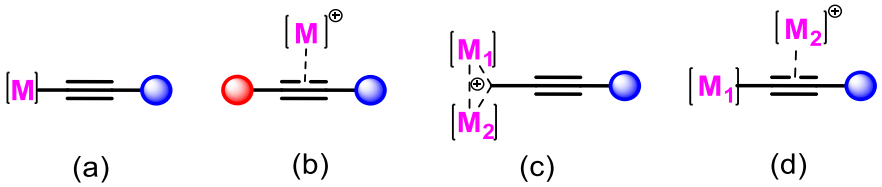

Figure 10. Coordination modes of acetylide to one or more metal ions *via* σ-and π- linkage. Circles in red and blue indicates spacers, M_1 & M_2 = group 4-12 metal ions.

3.2.2. Effect of auxiliary ligands

Apart from the metal, the alkynyl ligands and the conjugation length, the auxiliary ligands bonded to the metal also, directly or indirectly, affect the properties of oligo- or poly(metalla-ynes). As discussed, the coordination sphere of a metal in metalla-yne can be satisfied by π-backbonding (PR_3/AsR_3) or σ-donating auxiliary ligands (*viz*. NHC) in *trans*-complexes while cyclic diphosphines/diimines/cyclometallated ligands serve as auxiliaries in *cis*-analogues. In Chart 11, we have collected examples of some *cis*- and *trans*-metal acetylides with different auxiliaries.

Like CO, the phosphine ligands contribute two electrons to the metal center. Due to the "*innocent*" nature of phosphines, they do not participate directly in the reaction but profoundly modulate the electronic properties of the metal center to which they are bound.[261] For example, it has been reported that metals bearing strong π-acceptor auxiliary ligands (e.g. CO) display less electron CT to the alkynyl ligands than those bearing strong auxiliary ligands (*viz*. PR_3), which increases or decreases the π-conjugation in the backbone. Table 5 lists the influence of different phosphine ligands on the lowest energy band and the metal–carbon stretching frequency (ν_{M-C}) of a prototypical Ni(II) di-yne $NiL_2(C{\equiv}CC_6H_4\,C{\equiv}CH)_2$. As can be noted, without much affecting the ν_{M-C} stretching frequency, $\lambda_{max.}^{abs.}$ of the lowest energy band undergoes a significant red shift.[262] However, Vacher et al.[261] reported very little effect of the auxiliary ligand or the isomerism on the frequency of the $\nu_{C\equiv C}$ stretching vibration in Pt(II)-acetylides. Prior to this, Lewis et al.[263] noted that the attachment of PBu_3 to a Ru-metal fragment shifts the ν_{M-C} stretching frequency to the higher values compared to complex containing PH_3. Furthermore, the replacement of a group 10 (d^8) metal or by a group 8 (d^6) metal lowers the stretching frequency. Absorption studies of complex **142a** (Chart 11) bearing phosphine auxiliaries of varying σ-donor strength (PCy_3, PBu_3, PPh_3, $P(OEt)_3$, $P(OPh)_3$) indicated that the

the weak *σ*-donor/strong *π*-acceptor ligands lowers the energy of electronic transition, while strong *σ*-donor/weak *π*-acceptor has the opposite effect.[264] In the pastPt(II) acetylide dimers and polymers with pendant ferrocenyl groups were also studied.[265,266] Meisel et al.[266] showed that the σ-donor ability of ferrocene-containing auxiliary ligands decreases as the number of ferrocenyl groups increases on the P-atom. Furthermore, the phosphine ligands also influence the interactions between the ethynylferrocenyl units.

Lara, Lalinde and Moreno[267] observed that the presence of an electron acceptor ligand (CN^-) over Pt(II) imparts negative solvatochromic behaviour to **142b** (Chart 11), attributed to solvent-to-cyanide hydrogen bonding and increased solvent dipolarity–polarizability. Another study demonstrated that the replacement of the phosphine group by CN^- produces a stabilization of the Pt-alkynyl-based HOMO Pt(dπ)/π(C≡CR), giving rise to a significant blue shift in both the absorption and emission wavelengths.[268] Recently, P-chirogenic conjugated metalla-ynes have been reported, and a comparative study carried out with their achiral counterparts (**143a,b**, Chart 11).[18] The chiral complexes were found to be thermally more stable than the achiral counterparts. In addition, circular dichroism (CD) results indicated that the chiral environment of the phosphine ligands was felt by the aryl moieties. The effect of chirality was also reflected in the ^{31}P-^{195}Pt coupling constants, suggesting the influence of auxiliaries on the electronic environment of the metal. In the case of di-ynes, separated by arene groups, and having *t*butyl substituents on the P atom, the value of ^{31}P-^{195}Pt coupling constant was 2357 Hz, while *R*-/*S*- enantiomers showed a higher value (2521 Hz). The same pattern was observed in the corresponding poly-ynes.

Table 5. Effect of Phosphine Ligands on the Ni–C Stretching Vibration and Lowest Energy Band of $NiL_2(C{\equiv}CC_6H_4C{\equiv}CH)_2$.[262]

Ligand (L)	ν_{M-C} **(cm^{-1})**	$\lambda_{max.}^{em.}$ **(nm)**
$(PPh_3)_2$	539	371
$(PBu_3)_2$	542	353
dppe	540	355

In addition to the above discussed examples, intense research activities have also been undertaken to develop neutral as well charged *cis*- and *trans* σ-alkynyl complexes supported by mono-, di- or triimine ligands, cyclometallated complexes with di- (C^N, C^C) or tridentate (C^N^N, N^C^N, or C^C^N) cyclometalating or NHC auxiliaries (**144a**-**e**, Chart 11). Like phosphines, these ligands also impart a significant influence on the electronic structure. Researchers argued that diimine auxiliary ligands act as electron sinks in redox processes and the replacement of phosphines by functionlized diimine imparts NLO properies to the materials.[269,270] Eisenberg and co-workers[271] demonstrated that in Pt(II) diimine acetylide complexes the variation of the diimine ligands affects the energy of the LUMO while variation of the arylacetylide ligands produces only minor changes in the HOMO level. Since the emission properties of metalla-ynes are of mixed nature (^{3}MLCT, ^{3}LLCT), the electronic properties of the complexes significantly modulate upon the incorporation of such co-ligands.[272] For example, it has been demonstrated that the

strategic functionalization of auxiliary pyridinyl lowers the energy of the MLCT excited state leading to the attenuation of deactivation pathways.[273]

Similarly, σ-donating neutral NHCs are well-known electron donors and have ability to coordinate to the metal center more sturdily than their phosphine counterparts. NHC auxiliaries are, therefore, more effective in separating the non-radiative d−d states from the radiative states and in destabilizing the LUMO level.[274-276] The replacement of phoshines by exceptionally strong σ-bonding and readily tunable NHC ligands improves Φ_P and τ_P.[277-279] Recently, Zhang et al.[280] demonstrated that Φ_P, τ_P, and k_r/k_{nr} can be perturbed by the ligand, methylation, and the Pt-coordination environment. Furthermore, the solubility of the complexes, which is the biggest advantage with phosphine-based complexes, can be also be tuned by functionlizing NHC cores.

3.2.3. Group 4-7 metalla-ynes

Limited literature is available on monometallic Group 4 metal acetylides.[281-284] For example, Titanium (Ti)[285] and Zirconium (Zr)[286] containing π-conjugated systems were reported around two decades ago, but limited solubility of the materials was a major concern. To circumvent such challenges, complexes with one or more types of metal (mixed metalla-ynes) with simple or modified auxiliaries have been investigated.[287-294] In such complexes the possibility of metal-to-metal-charge transfer (MMCT) is quite high, which is a crucial factor for application in O-Es. Recently, a D-A type complex with ferrocene as donor and Ti(IV) as acceptor has been reported.[287] The introduction of ferrocene served dual benefits: it acts as electron reservoir and imparts stability to the complexes against photolysis. These complexes showed LE band in the visible region, while it was absent in analogus complex having phenyl groups attached to Ti(IV).[288] Both theoretical and experimental results indicate that the intense absorption band arises due to Fe(II)→Ti(IV) CT, which is the same as that observed in blue minerals such as sapphire and blue kyanite. Considering the strong electron accepting nature of Ti(IV), ferrocene was replaced by more electron donating groups (arylamines, triphenylamine and N,N-dimethylaniline).[288] These complexes, like previous example, showed strong LE band between 520-560 nm ascribed to LMCT. The replacement of ferrocene by these aromatic donors substantially enhanced (3x) the molar absorptivity of the complex. Despite this, photo-stability was main issue due to labile Ti-acetylide bond. To circumvent this, researchers prepared a new scaffold in which the donor group was attached to Cp ring instead of metal. The resulting complex showed high stability giving opportunity for further substitution, but lower absorptivity and weaker D-A coupling remain as the main challenges. Berben and co-workers[295] synthesized high-spin (HS) and redox-active tetrahedral V(III) complex **145** (Chart 12) using 2,6-bis(trimethylsilyl)phenylacetylene as ligand (Figure 11a). The use of this bulky ligand reduced the coordination number of the metal ion to four. Furthermore, structural analysis of complex indicated the pure alkynyl nature of C≡C bonds (and not the cumulenic). In addition to this, Fe(III) and Mn(III) complexes were also synthesized, which showed interesting redox properties such as the presence of multiple reduction peaks. The very first structurally characterized Cr(III) acetylide **146** (Chart 12) was reported only around one and half decade ago.[296] The air stable orange colored Cr(III) *tris*(acetylide) octahedral complex was reported with $\lambda_{max.}^{abs.}$ = 368 and 454 nm.

Chart 11.

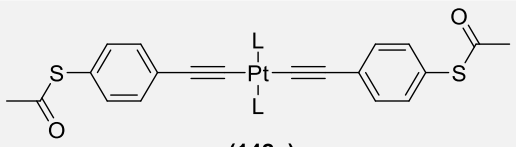

(142a)

L = PCy_3, PBu_3, PPh_3, $P(OEt)_3$, $P(OPh)_3$

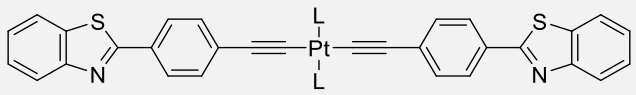

(142b)

L = PEt_3, PPh_3, PTA, CN

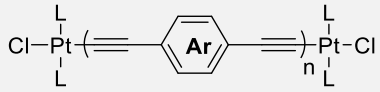

143a, Ar = Phenyl

143b, Ar = Benzothiadiazole

L = (*R/S*)-P(Ph)(^{i}Pr)($C_{17}H_{35}$)

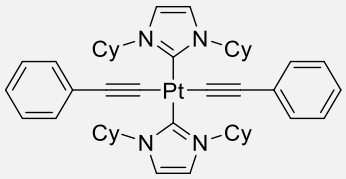

(144a)

Cy = Cyclohexyl

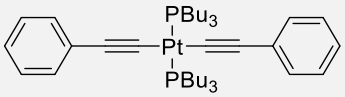

(144b)

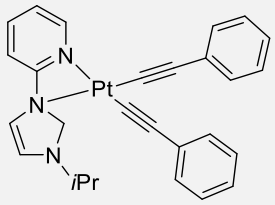

(144c)

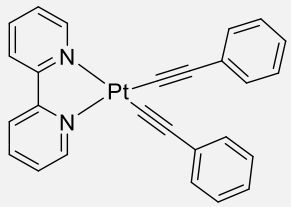

(144d)

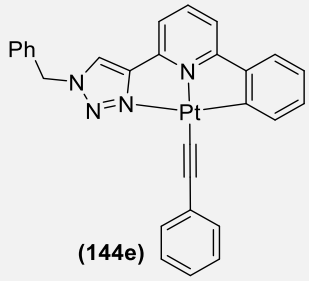

(144e)

The main features of the complex were its linear Cr−C≡C bond angle, C≡C bond distances identical to the corresponding distance in acetylene, unique cation-dependent sandwiched-type crystallization (Figure 11b,c) and weak antiferromagnetic properties.

Molecular communication, which is often observed in molecules with same/different redox centers separated by a small to medium spacer, is an important criterion for several important applications in molecular electronics.[297] The metal containing redox-active molecules are expected to possess low work functions and stronger dπ-pπ interactions than their organic counterparts.[298,299] These features make metal-containing polymeric materials suitable building blocks for "*molecular wire*". Using cyclam as the ligand, *cis*- and *trans*-Cr(III) as well as Rh(III) acetylide complexes **147** (Chart 12) with OTf as counterion were reported.[300] Some of the complexes show long-range electronic communication between metal centers when connected through arylalkynyl ligands. The *trans*-complexes have higher yield and good solubility, which are advantageous for molecular electronics processing. A clear and strong CT transition band in Cr(III) complexes indicated intensity stealing from a proximal CT band assisted by aryl ring and supporting the electronic communication between Cr(III) and the alkynyl ligand. The reported complexes showed long-lived, structureless, MC emissions in visible region with moderate lifetimes 240-327 μs for Cr(III) and 4-21 μs for Rh(III). Furthermore, the excited state relaxation process in the complexes were dependent on NH vibration. Prior to this work, similar types of Cr(III) complexes having phenyl and thiophene as aromatic spacer (**147a & i**, Chart 12) and $[Ni(mdt)_2]^-$ (mdt = 1,3-dithiole-4,5-dithiolate) as counterion were reported.[301] Several other complexes of Cr(III) bearing different substituents and separated by acetylide units have also been reported along with their magnetic properties (*vide-infra*). Berben and Kozimor[302] reported an interesting and unusual low valent and stable Cr(I) complex containing two Cr(I) ions bridged by a neutral N_2 moiety, i.e. *trans*,*trans*-$[(Me_3SiC{\equiv}C)(dmpe)_2Cr]_2(\mu\text{-}N_2)$ **148** (Chart 12). The complex underwent electrochemical oxidation to produce Cr(II) complex. Recently, the group led by Tong Ren[303] reported both *cis*- and *trans* macrocyclic Cr(III) *bis*(acetylide) complexes These complexes offer the possibility to tune electronic excited states through selectively exciting vibrational modes observed in the UV-Vis spectra.

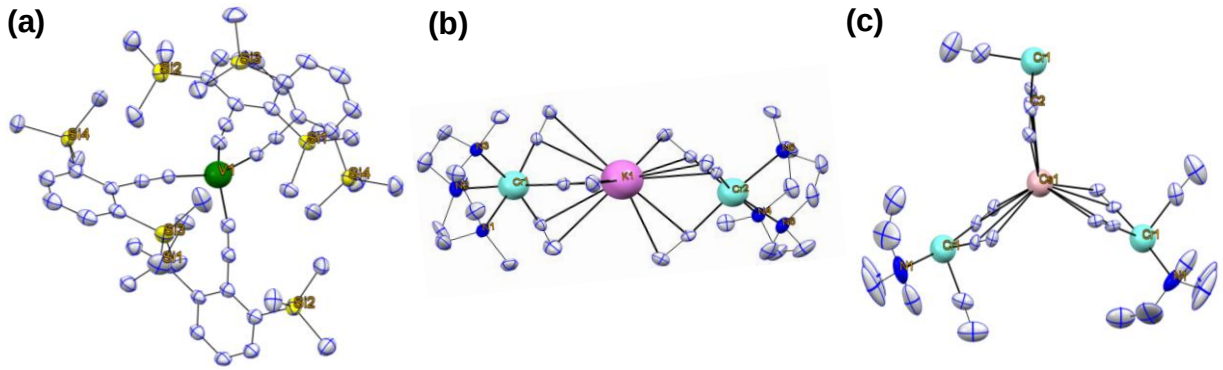

Figure 11. (a) Solid state structure of **145**. Reprinted with permission from ref [295]. Copyright 2011 Royal Society of Chemistry. Sandwiched structure formed by **146** with (b) K^+ and (c) Cs^+ ions. Reprinted with permission from ref [296]. Copyright 2002 American Chemical Society.

Chart 12.

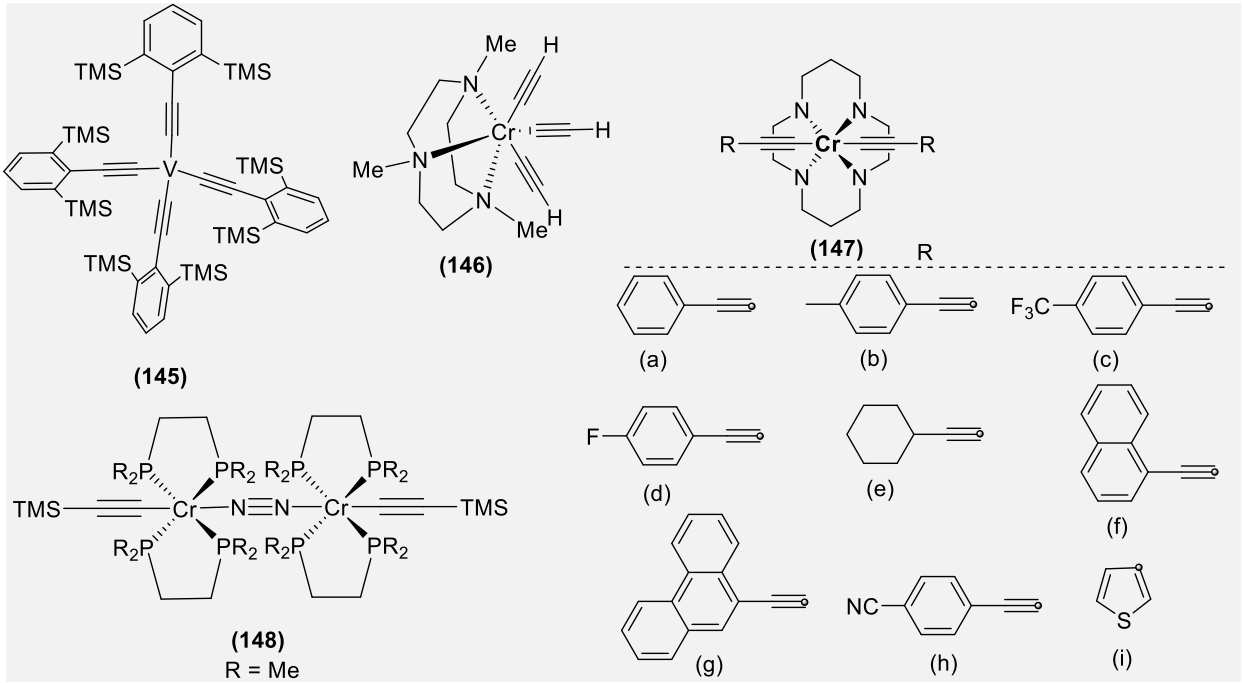

Moving to Group 6, a few papers recently reported spectro-electrochemical properties of molybdenum (Mo) and tungsten (W)-based oligo-ynes.[290,291,293,294] Whiteley and co-workers[291,292] demonstrated that the electrochemical and spectroscopic properties of Mo acetylide complexes (**149**, Chart 13) resemble Fe complexes more than their Ru-counterparts (**Table 6**). The same group[290] studied detailed electronic structure of di-ynes and tri-ynes incorporating Mo-complexes with different co-ligands (**150-151**, Chart 13). These 17 e^- complexes bearing bipyridyl (Bpy) auxiliary were more stable than the dppe counterparts. Crystal structure analyses of the complexes showed some interesting features such as the shortening of Mo-C_α bond length and bending of the chain (distortion in the linearity). These were attributed to the charge separation, hyperconjugation and other factors.[290] Furthermore, DFT calculations revealed metal localized frontier orbitals in these Mo-complexes.

A recent study showed the existence of molecular communication between two redox-active termini in a 24 Å mixed metal cylindrical shaped “Fe-W-W-Fe” complex **152** (Chart 13, Figure 12a,b).[298]). This long, linear complex containing two different metals (W at center and Fe at termini) showed a number of interesting features like high stability, fast electron transfer, reversible oxidation of all four metal centers (Figure 12c) and the presence of terminal reactive sites for further functionalization and the suitability for surface attachment. Furthermore, spectro-electrochemical study of the mixed valent complex **152**[PF_6] revealed absorption in the near infrared (NIR) region (λ_{max} ~ 1185 nm, Figure 12d) This *all in one* feature makes it an attractive candidate for metal-based molecular wires and organometallic dπ-pπ conjugated materials.

Table 6. Selected spectro-electrochemical infrared spectroscopic data ($\nu_{C\equiv C}$, cm^{-1}) for the alkynyl complexes of type $[M(C\equiv CR)(L)(\eta\text{-}C_7H_7)]^{n+}$ (M = Mo, Fe or Ru, L= dppe/Bpy).[290-292]

Spacer (R)	L	Metal					
		Mo		Fe		Ru	
		n = 0	n = 1	n = 0	n = 1	n = 0	n = 1
149 (R = C_6H_4-4)	dppe	2045	2032	2053	2021 1988	2072	1930
149 (R = C_6H_4Me-4)	dppe	2050	2017	2056	1994	2073	1928
149 (R = C_6H_4OMe-4)	dppe	2055	2011	2058	1988	2074	1929
149 (R = $C_6H_4NH_2$-4)	dppe	2055	1996	2060	1988 1962	2075 2050	1940
149 (n = 1, R = H)	bpy	2151 2111 1991	2158 2117 1998	–	–	–	–
150 (n = 1, R = ^{t}Bu)	bpy	2151 2110 1987	215 2116 1999	–	–	–	–
150 (n = 2, R = H)	bpy	2131 2106 1967	2146 1965	–	–	–	–
151 (n = 1, R = TMS)	dppe	2153 2105 2090 2063 1976	2151 2110 2095 1970	–	–	–	–
151 (n = 2, R = TMS)	dppe	2121 2092 1949	2138 2114 2103 1934	–	–	–	–
151 (n = 1, R = H)	dppe	2098 1956	1952	–	–	–	–

Chart 13.

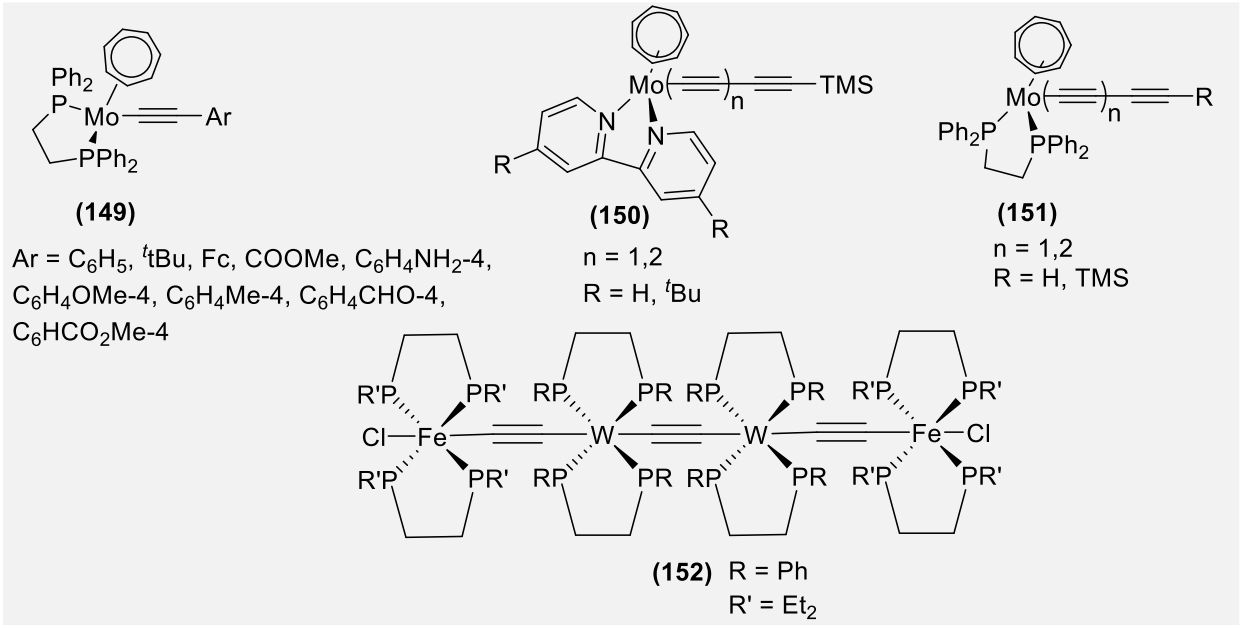

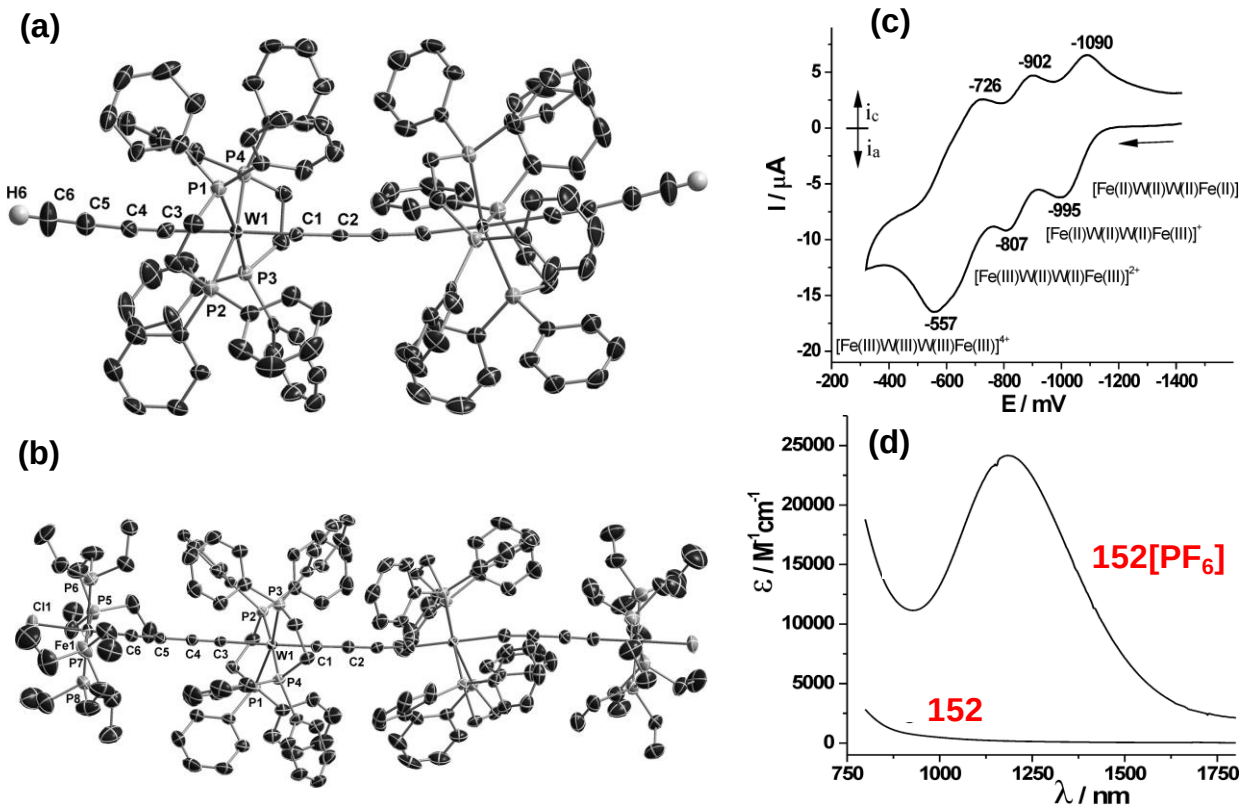

Figure 12. (a, b) Crystal structure of Fe-W mixed metalla-ynes, (b) CV of **152**, and (d) NIR spectrum of **152** and **152**[PF_6] in DCM solution. Measurement conditions: 0.1 M [$^nBu_4N$][PF_6] (Au electrode; E vs $Fc^{0/+}$; scan rate)100 mV/s; 20 °C; CH_2Cl_2). Reproduced with permission from ref [298]. Copyright 2010 American Chemical Society.

Since phosphine supported metal ion have the potential to act as redox-active end-groups with low energy work functions, several researchers have investigated the electronic communication in Manganese (Mn^{II}/Mn^{III}) complexes too.[304-310] Venkateshan et al.[311] reviewed the potential of a number of dinuclear Mn(II) complexes as molecular wires. Like other examples, interchange between the cumulenic and *bis*-carbyne resonance forms with a C–C single bond plays a significant role in the chemistry as well as in application. They demonstrated that the end-group attached to Mn(II) play subtle role in electronic communication between the metals, while it has marked effect on the reactivity and solubility of the complexes. Similarly, the substituents on the phosphorus atom have an effect on the redox properties of the complexes. An emerging interest in Re(I)-based material is due to its rich and intriguing electronic properties (such as electro-switchable PL).[312] The research on Re(I) acetylide systems started in late 1960s with the discovery of [$Re(CO)_5(C{\equiv}C{-}R)$] (R = Ph or C_6F_5).[313] Following this, several other Re(I)-based mono-, di- and poly-ynes have been reported.[314,315] Yam et al. exhaustively reviewed the mono- and multinuclear Re(I)-based acetylides reported in the last decade of the twentieth century[316] Therefore, only representative examples have been discussed herein (Chart 14), while some others are discussed in application sections.

In a breakthrough work, synthesis and detailed studies of oligo-ynes 1**53** incorporating Re(I) with 2-20 carbon atoms (Chart 14) supported the fact that optical properties in these complexes varies as the function of carbon chain length (Figure 13).[317] Yam and co-workers[318,319] reported alkynyl Re(I) tricarbonyl diimine complexes **154a-e** (Chart 14) with benzaldehyde, fused thiophene and cyanoacrylic acid moieties. Complex **154a** having benzaldehyde at the terminal ring showed absorption bands between 268-354 nm with a shoulder in visible region. On the other hand, complex **154b-e** showed a HE intense band between 270–320 nm and LE bands depending upon the nature of the diimine ligands (398-452 nm for **154b-e** and 270-420 **nm** for **154d-e**). Due to the long-lived charge separated state, they also studied the potential of complex **154d-e** as dye in DSSCs. Prior to this report, the same group[320] studied the efficiency of a Re(I) complex **155** (Chart 14) as OLED emitters in which the conjugation was extended by increasing the number of aromatic rings. These complexes, too, showed almost similar photophysical properties. Despite these limitations, the presence of functionalities (-C≡C-H, CHO) provides a reactive site to allow further derivatization to prepare novel materials with extended conjugation and properties.

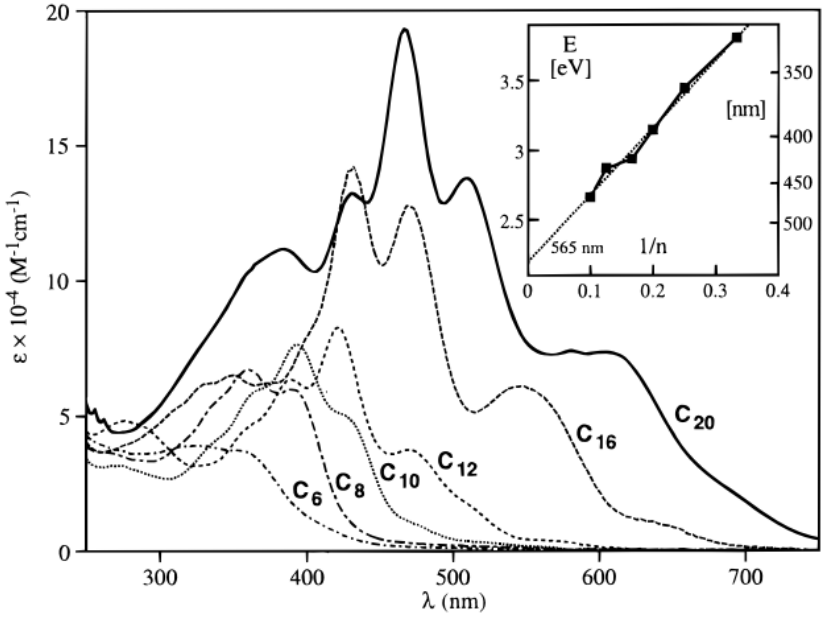

Figure 13. UV-visible spectra of polyynediyl complexes **153** (DCM) and (inset) relationship between λ_{max} (eV) and 1/n (n = number of alkynyl units). Reprinted with permission from ref [317]. Copyright 2000 American Chemical Society.

Chart 14.

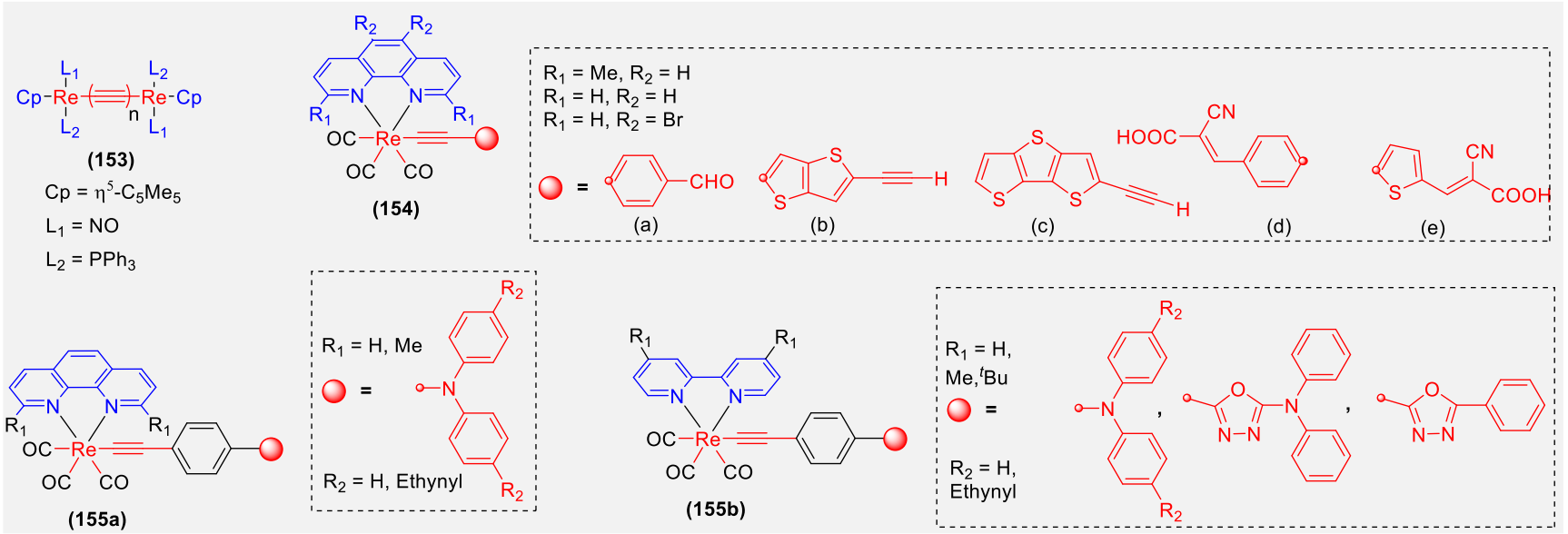
(153)
Cp = η5-C5Me5
L1 = NO
L2 = PPh3
(154)
R1 = Me, R2 = H
R1 = H, R2 = H
R1 = H, R2 = Br
(a)
(b)
(c)
(d)
(e)
(155a)
R1 = H, Me
R2 = H, Ethynyl
(155b)
R1 = H, Me, tBu
R2 = H, Ethynyl

3.2.4. Group 8 metalla-ynes

Though most of the metalla-ynes reported in the literature use d^8 or d^{10} metals (Pt(II), Pd(II), Ni(II), Au(I) etc.), interest is expanding to include other transition metal ions as well. Following the work on Pt(II), Group 8 metal-based homo- and hetero-metallic oligo-ynes and poly-ynes, especially those based on Ru(II) and Fe(II) complexes are frequently reported due to their direct and potential application as electronic wire and NLO materials.[321,322] To understand the impact of the nature and length of the spacer on interfacial electron-exchange process and their reactivity toward the photochemical grafting reaction, redox-active Fe(II) arylethynyl complexes and their radical cations with pendant 1,4- and 1,3-linked phenylene ethynylene spacers **156** have been reported.[323] These newly developed complexes possess better stability than the earlier reported similar complexes.[324] Oxidation state independent conjugation between the organo iron center and the terminal ethynyl group was found in these complexes (1,3-linked complexes less conjugated than 1,4-linked counterpart). Absorption studies of Fe(II) species showed orange colored MLCT absorption in the blue edge region (from 264 nm up to 500 nm), while dark brown-colored LMCT absorption (~700 nm) for Fe(III) species. However, for both Fe(II)/(III) complexes, only a slight impact of chain extension on electronic species was seen with weak electronic interaction between the carbon centers. DFT calculation showed π-character of HOMO of all the complexes localized mainly over metal, its adjacent ethynyl group and, to a lesser extent, on the next phenyl ring (Figure 14). On the other hand, substituents dependent LUMO was localized on the Fe(κ^2-dppe)(η^5-C_5Me_5) moiety or the carbon chain. Metalla-yne having phosphine (dppe) ligand at the terminal (**157**) has been found to dimerize upon oxidation of the Fe(II) center **158** to generate a dication **159**.[325] However, this dimerization could be seized by oxidizing the phosphine group (Scheme 22).[326] Interestingly, the metallophosphine oxide species **160** could be used to achieve monomeric cation **161**, with improved photo-physical properties.

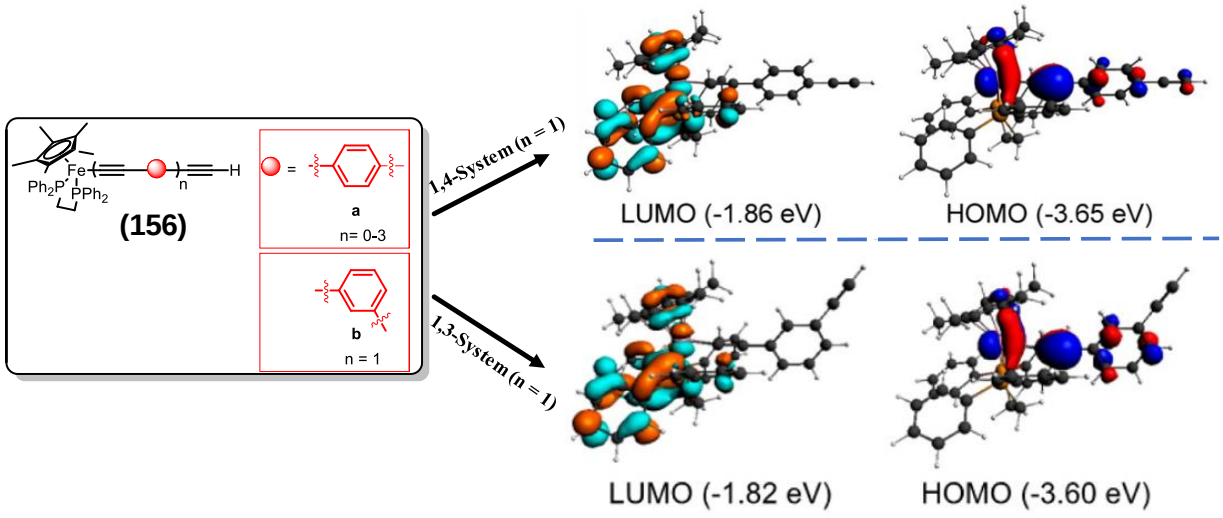

Figure 14. HOMO and LUMO plots redox-active Fe(II) arylethynyl complexes incorporating pendant 1,4- and 1,3-linked phenyleneethynylene spacer. Reprinted with permission from ref [323]. Copyright 2013 American Chemical Society.

Scheme 22. Dimerization of metallophosphine. Reprinted with permission from ref [326]. Copyright 2014 Royal Society of Chemistry.

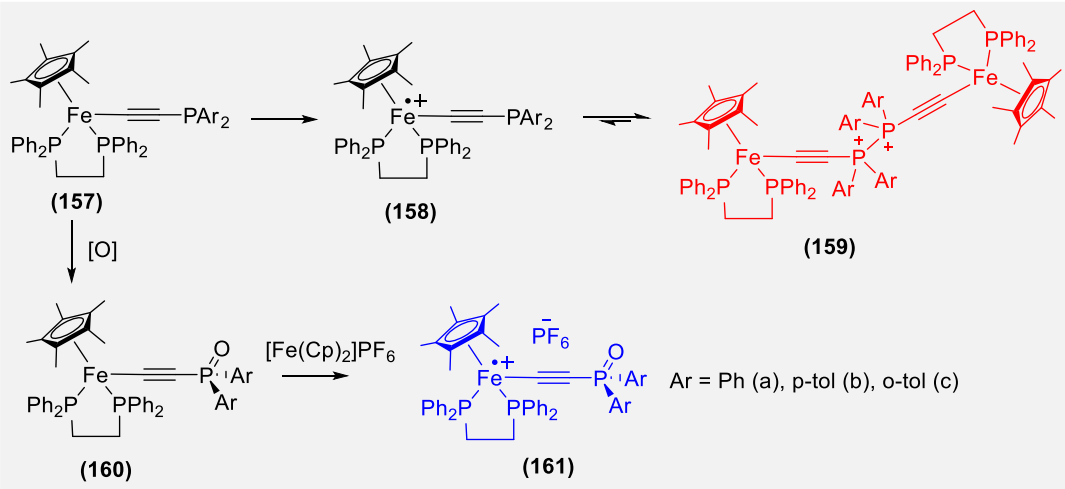

Despite the spectacular advances made in the synthesis of Fe(II) containing metalla-ynes, the first ever synthesis of redox-active Fe(III) *bis*-alkynyl compounds **162** (Chart 15) has been achieved recently.[327,328] The complexes were obtained by reacting *cis*-/*trans*-[Fe(cyclam)$(OTf)_2$]OTf with Li/Na acetylides. The high value of magnetic moment for intermediate complexes (5.32 μ_B without alkynyl moieties) than the final complexes **162** (1.89-1.96 μB with alkynyl) indicated strong field nature of alkynyl ligands which stabilized a low-spin Fe(III) center. Both theoretical and experimental studies indicated strong dπ-π(C≡C) interactions and acetylide unit dependent formal potential of the $Fe^{(+3/+2)}$ couple. Optical studies of the complexes revealed visible absorbing nature of the complexes with a high extinction co-efficient (Figure 15). The extrapolation of lowest electron excitation energy for *trans*-[Fe(cyclam) $(C_{2n}R)_2]^+$ gives a value of 1.44 eV as $n \rightarrow \infty$. Berke and co-workers[329] found that the E_g and chemical hardness of redox-active acetylide complexes could be modified by changing the sp/sp^2 bridging ligand. They reported several new intrinsically functional and redox-active complexes with iodo and isothiocyanate as terminal groups (**163**, Chart 15), which are especially suitable for the electronics industry. However, some issues such as stability and charge delocalization need further attention. Like **152**, a first tetranuclear homometallic Fe(II) centers incorporated symmetrical rigid-rod butadiyne based 5,10,15,20-tetraferratetra cosa-1,3,6,8,11,13, 16,18,21,23-decayne (**164**, Chart 15), along with their structural and photophysical characterization has also been reported.[330]

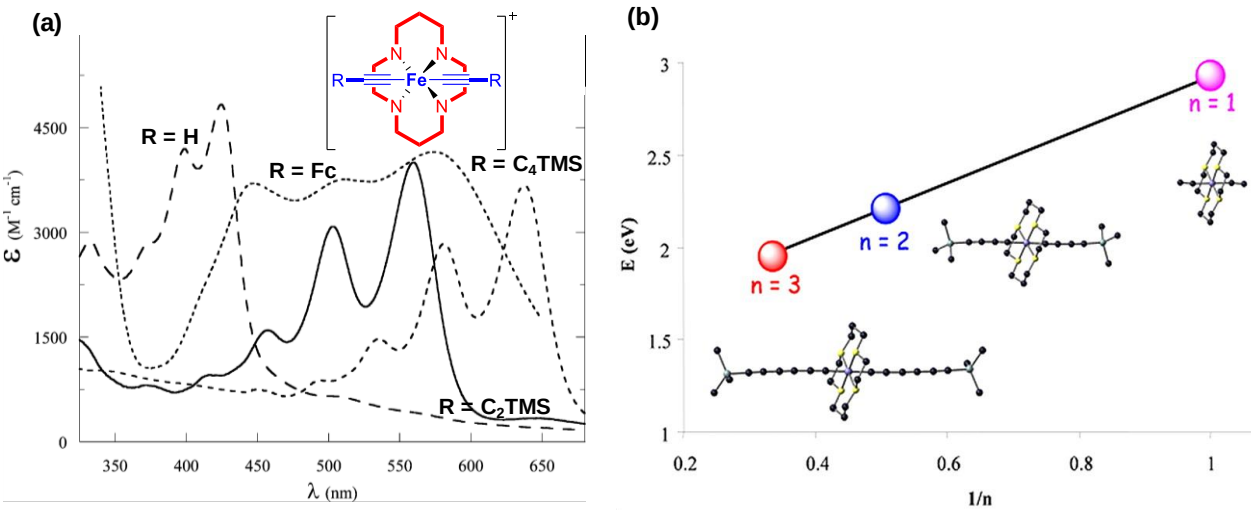

Figure 15. (a) Structured UV spectra of Fe(III) *bis*-alkynyl complex **162** (inset) in MeCN, and (b) variation of lowest energy absorption maxima with the number of C≡C units. Inset: Chemical structure of **162**. Reprinted with permission from ref [328]. Copyright 2012 American Chemical Society.

As we discussed in section 3.1, the planarity of the central spacer plays an important role in electron transfer. Lapinte and co-workers[331] studied the effect of steric hindrance on the chemical and physical properties of the binuclear complexes separated by *o*-, *m*- and *p*-benzene *bis* acetylide complexes **165(a-c**, Chart 15**)**. Paul and co-workers[332] investigated detailed electronic coupling and NLO properties of redox switchable complexes **165(d-f)** in both Fe(II)/(III) states having fluorene, phenyl or biphenyl spacers. The electronic communication between the metal centers *via* alkynyl units was reported to be more in complexes with planar spacer (fluorene > biphenyl). However, the luminescence was quenched in fluorene-containing complexes, it showed enhanced TPA than its organic counterparts, attributed to electron-rich organometallic end group.

While most of the studies have been concentrated on the homo-metallic systems, there is an increasing interest in the development of hetero-metallic species too. This is attributed to the electronic influence and synergistic effect of the second metal center on overall functional properties of the resulting hybrid materials. Recently, Lang and co-workers[333] reported a series of Fe(II) and Ru(III) half-sandwich alkynyl complexes bearing a thiophene or furan as π-conjugated connectivity and extensively studied the influence of metals and the heterocyclic bridge on the electronic interactions (**166-d**, Chart 16). Mono-cationic mixed-valence (MV) species (**166a,c**$^+$ and **166b,d**$^+$) exhibit high thermodynamic stability (K_c = 6.87 × 10^4 to 9.33 × 10^5) with intense, narrow, and non-solvatochromic π(dπ)→π*(dπ) absorptions in the NIR region with a HE shoulder (Figure 16). It was concluded that the combination of metal-metal interactions and five-membered heterocycles is a useful strategy to design new materials for intra-molecular electron transfer processes. This fact was further supported by the results of Fe-Ru hetero-binuclear complex which showed better properties than the homo-metallic Fe/Fe analogues.[334] Complex **167** (Chart 16), in which the metal core was separated by C_6 chain, showed large and chain dependent electronic coupling between the metals. Lapinte and co-workers[335] reported homo- and hetero-bimetallic redox-active systems based on

group 8 metals (Fe, Ru, Os) **168** (Chart 16). Basically, these complexes were tetrametallic MV complexes and belong to class II compounds as defined by Robin and Day.

Chart 15.

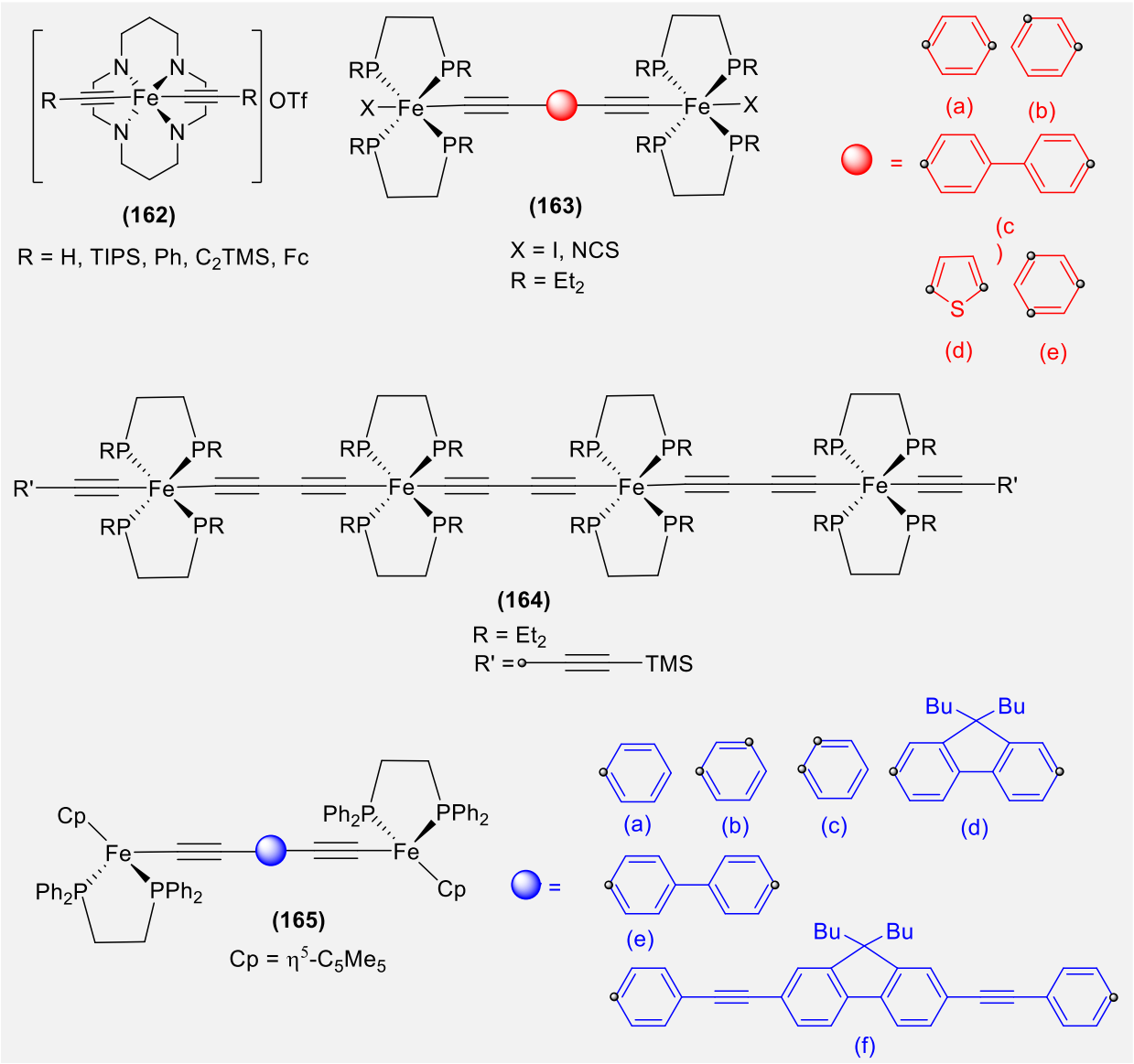

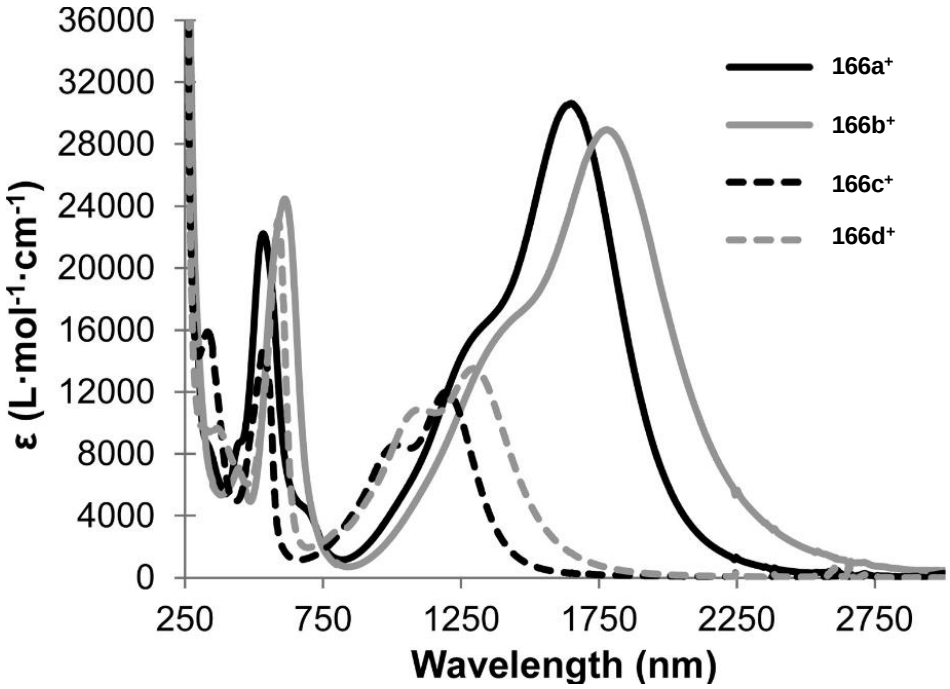

Figure 16. Comparison of the UV-Vis./NIR spectra of **166a⁺,c⁺** and **166b⁺,d⁺**. Measurement conditions: 2.0 mM analyte, 25 °C, DCM, 0.1 mol·L^{-1} [^{n}Bu$_4$N][B(C$_6$F$_5$)$_4$] as supporting electrolyte. Reprinted with permission from ref.[333]. Copyright 2015 American Chemical Society.

Chart 16.

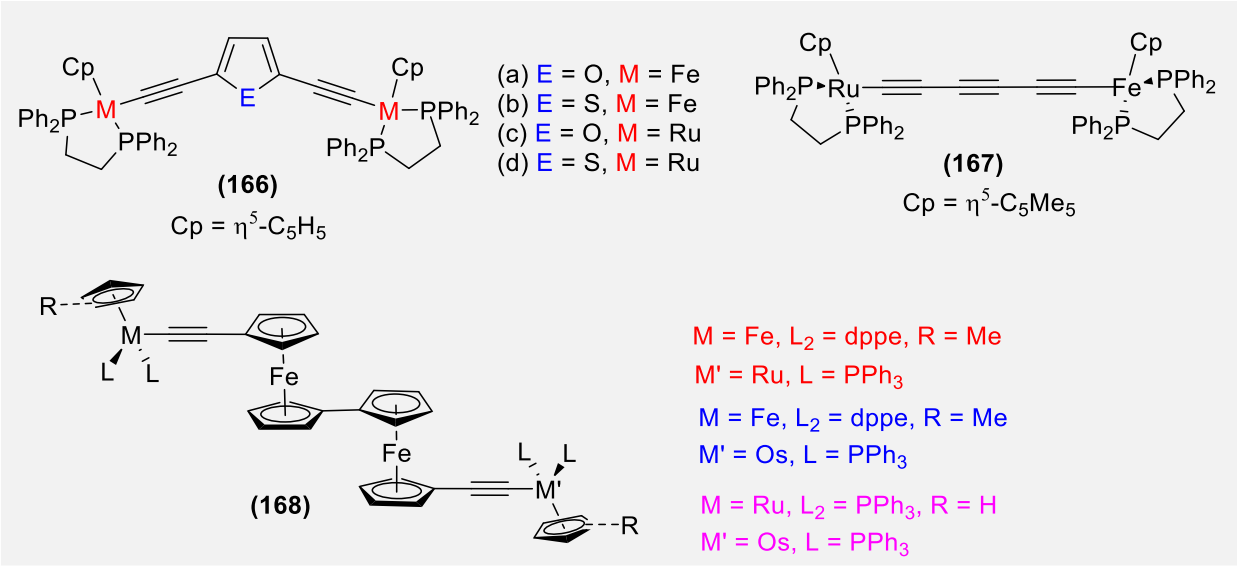

Zhang et al.[336] reported neutral and cationic mixed **(169a-c**, Chart 17**)** and monometallic acetylide complexes **(170a-c**, Chart 17) which showed interesting redox behavior and electronic communication. For example, in **170b** one-electron oxidation takes place at the Fe(II) center first. This affords moderate electron delocalization along the Ru(II)-C≡C-Cp$_2$Fe(III) backbone. On the other hand, **170c** having biphenyl-4-yl-ethynyl ferrocene, Ru(II) was oxidized first to give a corresponding MV cationic complex leading to total

electronic isolation between the Ru(III) and Fe(II) centers. Theoretical and experimental studies on **170b-d** indicated the "*redox-non-innocent*" nature of π-conjugated aromatic diynyl spacers involved in the one electron oxidation process. As the π-conjugated bridging systems expanded, the aromatic diethynyl ligands were more and more involved in electron delocalization (order of delocalization: benzene < naphthalene < anthracene). The effect of π-conjugated bridging ligands on redox processes was also observed in binuclear Ru(II) complexes separated by polyaromatic (biphenyl, fluorene, phenanthrene, and pyrene) alkynyl ligands **171a-d** (Chart 17**)**.[337] The specific evolution of the UV/Vis/NIR absorption upon step-wise 1e−oxidation demonstrates the significant contribution of the bridging ligands. Bridge localized oxidation of the complexes was enhanced upon increased conjugation. Similarly, a notable impact on the stability and absorption characteristics of the oxidized complexes have been reported when linear (**171e**-**f**) or bent (**171g**-**h**) benzodithiophene-based bridging spacers (Chart 17) were used.[338] For example, linear spacer-based complexes formed stable cationic complex whereas bent spacer-based cations were unstable. Here, like the previous example, the oxidation was largely localized on the bridging ligands, with a dominant contribution from the benzodithiophene core.[338] Similar types of [3,3]metaparacyclophanes bridged bimetallic Ru-complexes have been reported showing intra-molecular edge-to-face interactions, both in solutions and in the solid state.[339] In addition to the above discussed examples, numerous other redox-active Ru-based complexes are reported in literature with unique properties and applications. Researchers studied the impact of inclusion of organo phosphonate substituent at the termini[340] or electro-active tetrathia-fulvalene[341] on the electronic communication and also reported distance-dependent electronic coupling in *wire-like* poly-yne-diyls.[342]

Chart 17.

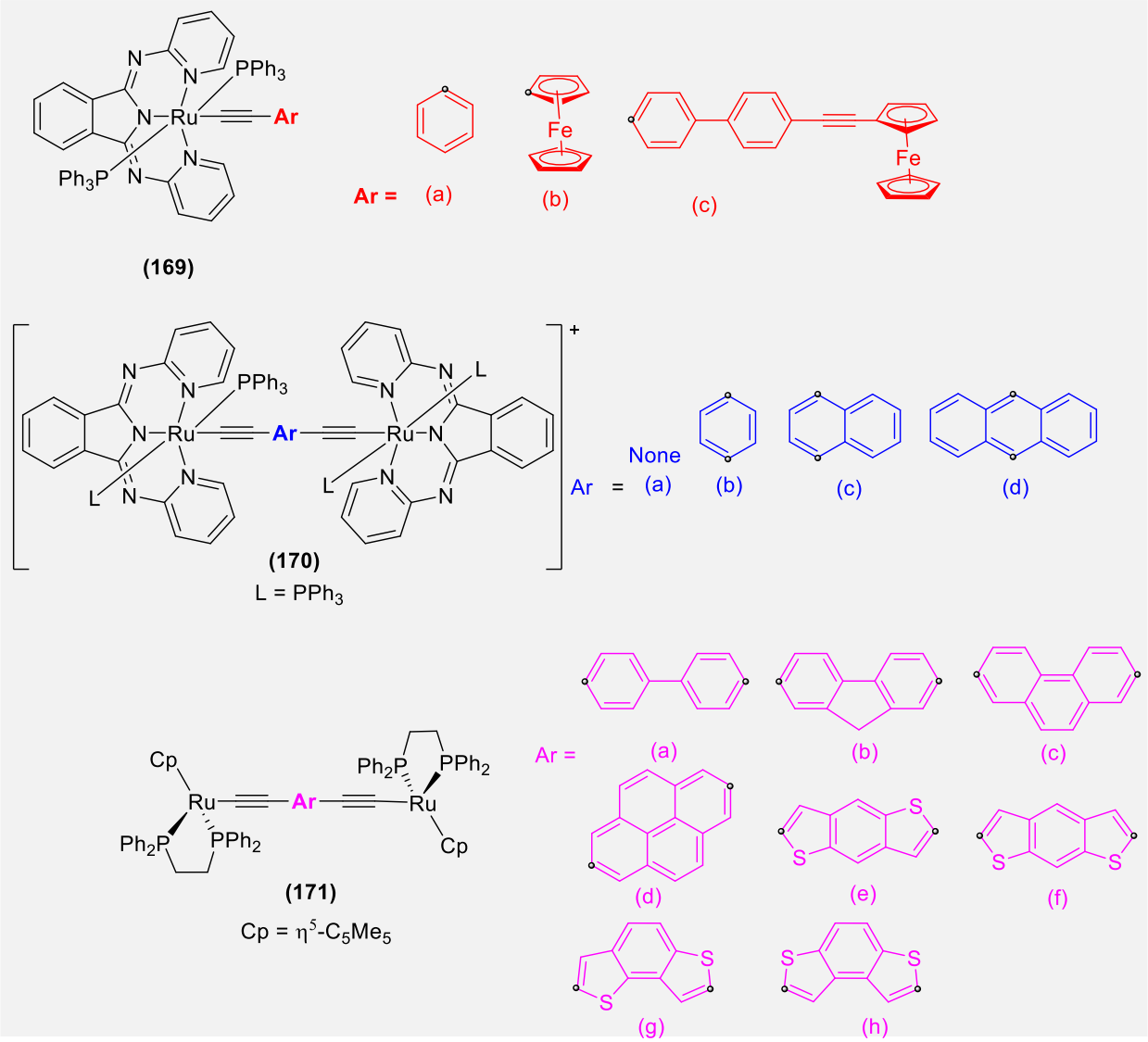

3.2.5. Group 9 metalla-ynes

The last decade of 20th century witnessed the synthesis of several group 9 metalla-ynes.[343,344] However, limited photo-physical studies of the materials were reported.[345] Unlike the group 10 metals, elements of group 9 show unique photochemical properties. For example, in organometallic poly-ynes, it is a well-known fact that the inclusion of a heavy metal ion greatly influences and controls the luminescence properties of the organic moiety. However, this is not always true, at least for this group of elements. A recent study shows that they behave differently from other organometallic oligo-ynes and poly-ynes. Cook et al.[346] synthesized *trans-bis(*acetylide) complex of Co(III)(cyclam) (**172-173**, Chart 18**)** bearing two different ethynyl ligands (**172**) and the first all-carbon-bridged binuclear Co species **173**. Electrochemical studies of **173** revealed its Robin-Day class I nature, wherein the two Co centers display minimal electronic coupling. This behavior was attributed to the absence of substantial pπ-dπ interactions between the bridge and metal centers. The surprising lack of coupling in this Co-C_4-Co species highlighted the importance of the choice

of both the metal centers and auxiliary ligands for mediating CT. The same group reported cyclam-based Co(III) mono-acetylide (**174**, Chart 18) and bis-acetylide (**175**, Chart 18) cationic complexes endowed with typical three Co-based couples (an irreversible $1e^-$ oxidation, and $2e^-$ reductions).[347] A weak and poly-yne length dependent Co-Co interaction through the bridge has been reported in polyynediyl complexes **176** (n = 2-6).[348,349] This behavior is in contrast to that of $[Co(cyclam)(C_2Ph)_2(\mu\text{-}C_4)]Cl_2$ which lacked observable Co−Co coupling, highlighting the sensitivity of $M-C_{2n}-M$ systems to the nature of ligands *trans* to the polyynediyl. The presence of labile chloride end groups allows facile incorporation into larger systems, so that the moiety can serve as an attenuator of conductivity or simply as a rigid linear linker. Mono-, di-, and poly-nuclear star-shaped Co(III)-cyclam complexes bearing a mixture of ethynylbenzene and chloride ligands at the axial coordination sites were also reported.[350] Thakker et al.[351] performed a comparative spectroscopic and electrochemical studies *trans*-$[M(cyclam)(C{\equiv}CR)_2]OTf$, (M = Cr(III), Co(III), and Rh(III)) **177** (Chart 18) and reported some unusual features of these complexes. For instance, arylalkynyl ligands act as π-donors in Cr(III) complexes, but not in Co(III) complexes (except trifluoropropynyl, which behaves as a π-acceptor). Similarly, a weak π-interaction was found between the arylalkynyl ligands and Co(III) coupled with lack of electronic communication through the organometallic backbone in complexes with ferrocene termini. A detailed electrochemical studies indicated that more electron withdrawing alkynyl ligands become π-acceptors toward the reduced form of Co.[351] Prior to this work, Sun et al.[352] performed detailed investigation on *trans*-$[M(cyclam)(C{\equiv}CCF_3)_2]^-OTf$ **178** (Chart 18) and compared them with cyano bearing complexes, i.e. $[M(cyclam)(CN)]OTf_2$ and $[M(cyclam)(C{\equiv}CCF_3)_2]$ (where M = Cr(III), Co(III), and Rh(III). They noted that both $M(cyclam)(CN)^{2+}$ and $[M(cyclam)(C{\equiv}CCF_3)_2]$ possess similar optical and electrochemical features, but the absorption spectra of alkynyl bearing complex have some bathochromic shift. This led them to conclude that the trifluoropropynyl is a slightly weaker field ligand than cyanide ion. Other notable observation was the naked eye visible metal centered phosphorescence at RT in aqueous solution for Rh(III) complex. The complex showed a $\Phi_P = 0.12$ and a $\tau_P = 73$ μs, nearly 10 times higher than those of its dicyano analogues.

Chart 18.

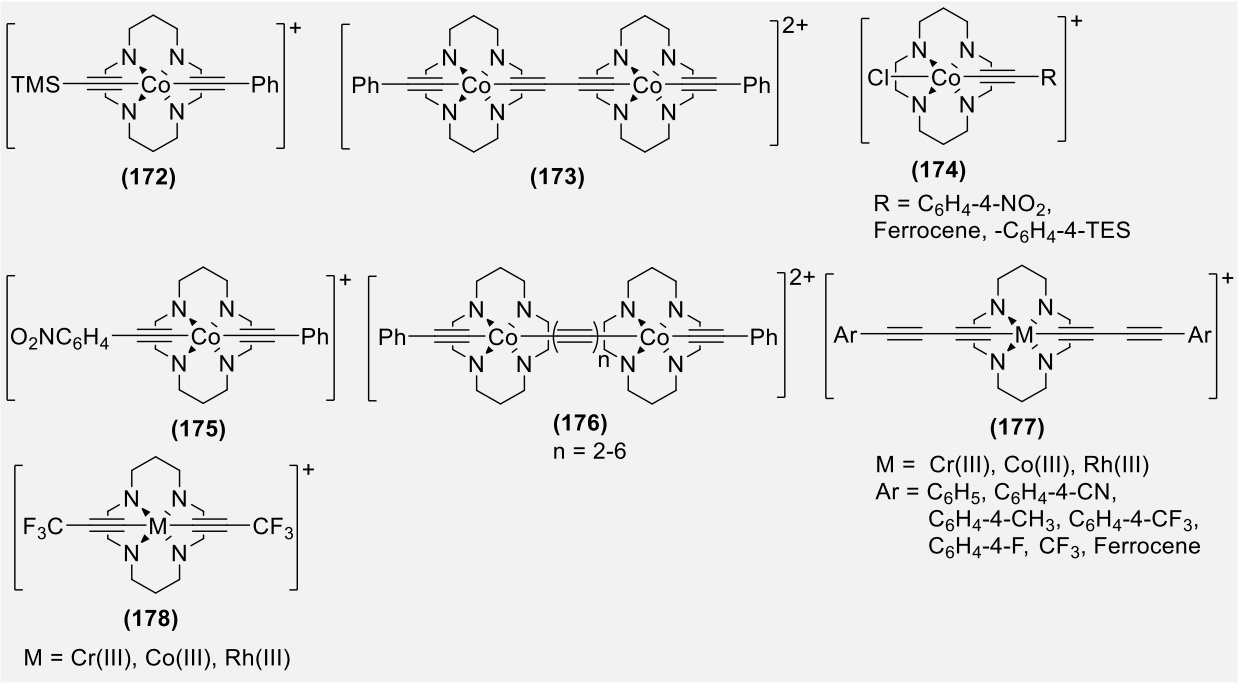

To utilize the *heavy atom effect*, researchers often incorporate one or more transition metals into the organic framework, sometime without getting the desired result. In some cases, the heavy atom plays a subtler role in controlling the photo-physical behavior than is commonly appreciated. Generally, Rh-based complexes facilitate ISC within femto (fs)- to picoseconds (ps) range and show phosphorescence from the T_1 state. However, recently an unusual property of Rh-acetylide has been explored. Marder et al.[353] reported the first example of a slow ISC process in octahedral complex 2,5-*bis*(arylethynyl)rhodacyclopenta-2,4-dienes (**179**, Chart 19). The luminescence studies revealed the absence of phosphorescence (even at low temperature) with the value of Φ_F upto = 0.69. Their study confirmed the slow formation of the T_1 state (ns scale instead of fs or ps) as expected for octahedral complexes.[354] The same group reported 2,5-*bis*(arylethynyl) rhodacyclopenta-2,4-dienes (**179**, Chart 19**)** in which the organic π-chromophore, not the metal ion, controlled the photo-chemical properties.[355] Such systems display unusual intense fluorescence from the S_1 excited state but no phosphorescence and k_{ISC} in the range of 10^8 s^{-1}. The photo-physical behavior of these octahedral complexes did not change even upon substitution of the other ligands at the Rh center or upon substitution of metals (Rh → Ir). Steffen et al.[345] reported a regiospecific reductively coupled product 2,5-*bis*(arylethynyl)rhodacyclopentadienes having unusual optical properties (**180-181**, Chart 19). These complexes exhibited, exclusively, fluorescence between 500-800 nm originating from the S_1 state in low to moderate quantum yields (Φ_{PL} = 0.01-0.22), but no observable phosphorescence. Like the previous examples, they also noted slow formation of the T_1 state on the ns timescale (Φ_{ISC} = 0.57). In these complexes, organic π-chromophore neglected the presence of the heavy Rh atom and the emitting state was assigned to unperturbed ^{1}IL(π–π*) state. Such behavior has also been reported in a Au(I) complex.[356] Overall, these studies highlighted a new class of luminescent materials that deserve further attention.

Although several papers reported the PL properties and application of cluster-type Ir-complexes on ethynyl platform,[357,358] limited literature is available on pure Ir–acetylide σ-coordination complexes.[359,360] This is mainly attributed to the low stability of σ- acetylide complexes. Based on the notion that the incorporation of phosphine auxiliaries stabilizes the resulting complexes,[361] Chen et al.[360] reported seven new highly stable cyclometallated Ir(III) acetylide complexes (**182**, Chart 19). They found that the substitution of chloride in precursor $Ir(ppy)_2(PPh_3)Cl$ (ppy = 2-phenylpyridine) by a strong field ethynyl ligand shifted emission to the red and enhanced luminescence efficiency. In 2013, Rio et al.[362] reported a highly stable, diamagnetic Ir-chains linked to acetylide moieties including tetranuclear Ir chain $[Ir_4–C≡CPhC≡C–Ir_4]^{2+}$ of length around 30 Å. (Figure 17) Interestingly, in such oligomers, an average oxidation state of 1.5 for the metals has been assigned. An extensive σ-delocalization between metals and linkers as well as strong electronic coupling between the metals was also noted in such systems.

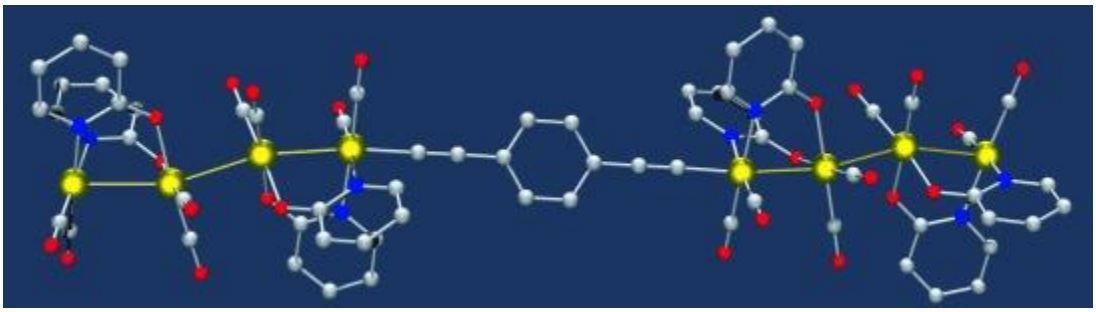

Figure 17. Tetrametallic iridium chain. Reprinted with permission from ref.[362] Copyright 2013 John Wiley and Sons.

Chart 19.

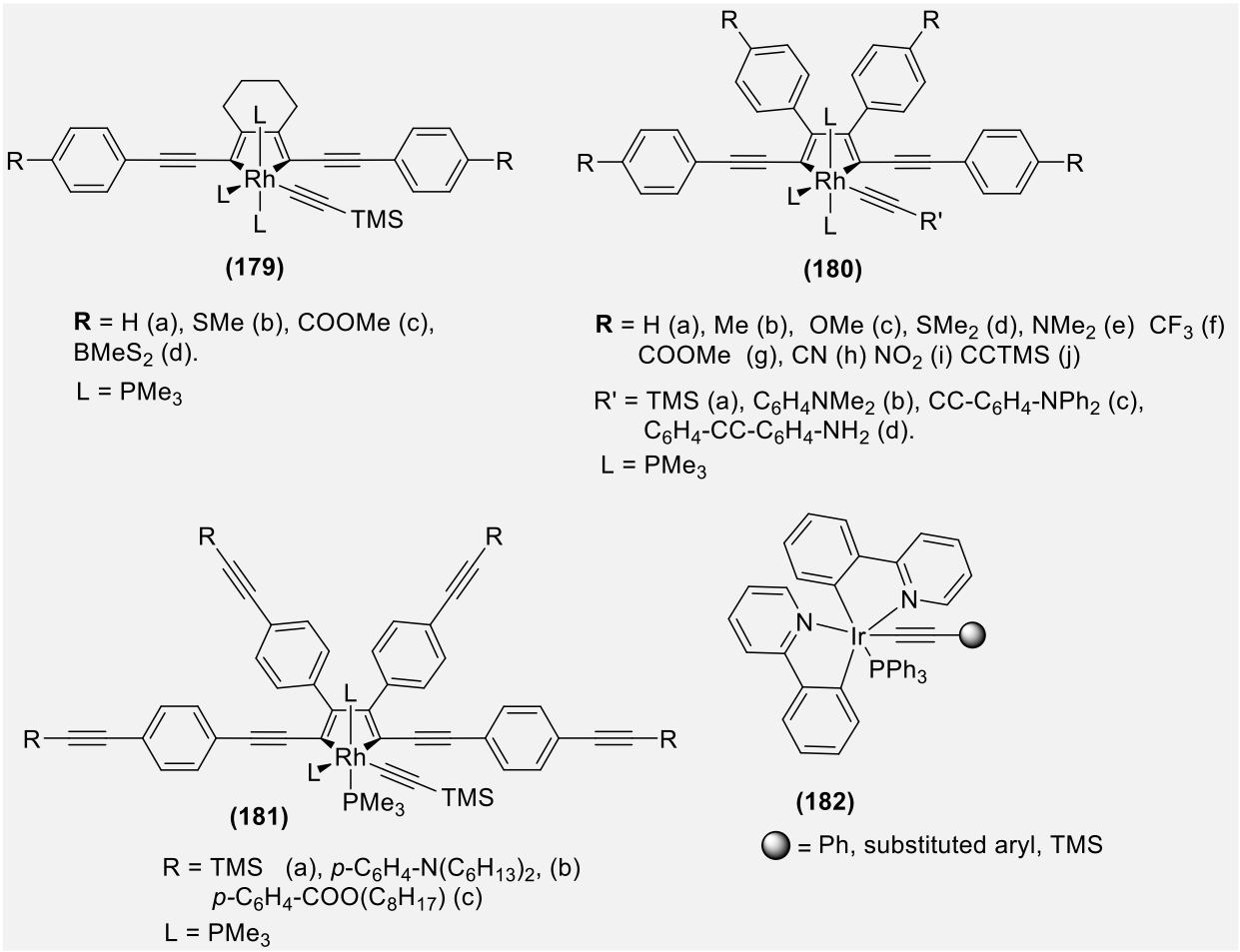

3.2.6. Group 10 metalla-ynes

3.2.6.1. Complexes bearing *trans*- auxiliaries

Unarguably, Group 10 metalla-ynes are the most studied class of metal-containing di-, oligo-, and poly-ynes materials. To date, a broad range of group 10 metalla-ynes have been reported to underpin the structural and photo-physical properties as well for different applications. (*vide-infra*, section 4) In fact, the first synthetic protocol developed for metalla-ynes involved metals from this group.[134] Among group 10 metalla-ynes, platinum is the most popular metal among chemists, followed by palladium and nickel.[5] This could be attributed to challenging synthesis, low stability of Ni(II) and Pd(II) complexes as well ability of Pt(II) in inducing the *heavy atom effect* more effectively than the other two.[133,363,364] In the past, several mono-, oligo- and poly-ynes incorporating Ni(II) and Pd(II) have been reported.[143,314,365-367] However, due to the stability issue and limited photo-physical properties, researchers shifted their research interest to other transition metals. Despite the fact that the modern literature on Ni(II) and Pd(II) containing metalla-yne is limited (Chart 20), they offer some intriguing properties and advantages. For example, Ni(II) acetylides can be used as precursors for the synthesis of cationic Ni allenylidene complexes.[368] Absorption

extended into the visible region has already reported for α,ω-*bis*-Ni-acetylide complexes.[138] Recently, some novel tetramethyl-1,4,8,11-tetraaza cyclotetradecane (TMC) appended complexes **183** (Chart 20) (Figure 18a) have been reported that show absorption extended to visible region (upto 800 nm, Figure 18b).[369] The monoacetylide complexes, which was prepared from the reaction between [Ni(TMC)Cl]Cl and the appropriate lithium acetylide, adopted a distorted square pyramidal geometry, with the acetylide ligand occupying the apical position.

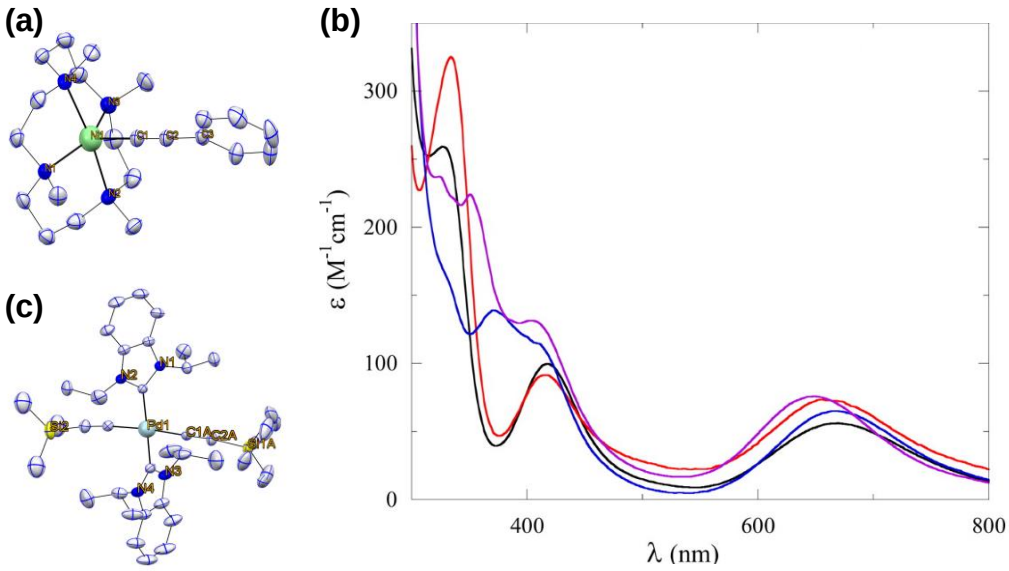

Figure 18. X-ray crystal structures of (a) [**183**]$^{+}$ (R = Ph), (b) UV-Vis- spectra of [**183**]$^{+}$ in DCM. Reprinted with permission from ref [369]. Copyright 2015 American Chemical Society. (c) **184** (R = TMS). Reproduced with permission from ref [143]. Copyright 2012 Elsevier Ltd.

Considering the unique properties associated with σ-donating neutral NHC, Koch et al.[143] reported the first example of *trans*-disposed NHC supported Pd(II) complexes **184** (Chart 20). Due to the steric constraints imposed by NHC ligands, Pd(II) complexes adopted slightly distorted square planar geometry (Figure 18c) at the Pd(II) centre and lack metallophilic interaction. All the complexes showed absorption in visible region. Compared to the phosphorescent Pt(II) complexes,[370] the corresponding Pd(II) complexes **184** show only fluorescence, even at 77 K, indicating that the heavy atom effect is less pronounced in the Pd(II) systems. There are a couple of reports on Pd(II) complexes with the emphasis more on structural studies rather than photo-physical properties.[365] For example, Braddock-Wilking reported some *cis*- and *trans*-Pd(II) and Pt(II) complexes bearing 1,3,5-triaza-7-phosphaadamantane and 3,7-diacetyl-1,3,7-triaza-5-phospha bicyclo [3.3.1]nonane **185** (Chart 20) as auxiliaries.[371] The impact of bulkier auxiliary was clearly observed in the geometry as well as in the bond angles in molecular structure of complexes (Figure 19a). For instance, whereas Pt(II) complex adopted square planar geometry, Pd(II) complex had slightly distorted square planar geometry. One notable feature of this study was the solubility of *cis*-isomers in water. Though an extensive structural characterization was performed, no absorption/emission study was reported, possibly due to the stability issue of complexes in solution. Smeyanov et al.[372] reported the first Pd(II) complexes

186 (Chart 20) bearing pyridinium- and quinolinium-3-acetylides. Since quinolinium-3-acetylide can be represented by resonance forms of a mesomeric betaine, allenylidenes, and a betaine-stabilized carbene, the determination of the final structure of the complex was quite challenging. However, using both theoretical and experimental approaches, they showed that Pd(II) complex preferred the structure of alkynyl palladium rather than allenylidene. This result was in contrast to the work of Asay et al.[373] who reported the formation of allenylidene complexes with Ru(II), Pd(II) and Ag(I). Like the previous example, no absorption/ emission study was reported.

The synthesis of discrete homometallic rigid rod-type Pd(II)-complexes was first reported three decades ago.[367] Despite this, binuclear palladium rods are comparatively scarce.[365] In a recent work, discrete binuclear [PdCl(PEt_3)$_2$] bridged by shorter and longer phenylene ethynylene rods **187a,b** (Chart 20) have been reported. Like the previous reports, the complexation with Pd(II) led to marked decrease in both the emission intensity and the Φ_F values compared to their ligands, attributed to LMCT.[374] However, the absorption of the starting ligand and the resulting complex were very similar. This work also reported the X-ray crystal structure of dinuclear rod **187b**, which is the first of its kind (Figure 19b). A marked impact of conjugation length, side-chains, and metal was observed on the properties of complexes. For instance, increasing the length of π-bridge led to an increase in oxidation potential, whereas introduction of alkoxy side-chains reduced the oxidation potential of complexes. Similarly, the lifetime of the complexes varies proportionally with the chain length. Prior to this work, Yam and co-workers[375] reported various Pd(II) and Pt(II) alkynyl complexes incorporating 3,6-substituted carbazole spacer. As expected, both Pd (**187c)** and corresponding Pt(II) complexes showed luminescence in the solid state (τ_0 = 2.9 μs at 77 K). Contrary to this, in solution, the Pd(II) complex was non-emissive while Pt(II) analogue showed a quenched luminescence (τ_0 < 0.1 μs). A significant increment in the intensity and lifetime was also observed for glass samples (77 K, EtOH–MeOH 4:1, v/v). The relatively large Stokes shifts, together with the emission lifetimes in the μs range suggested their triplet parentage. Another carbazole incorporated Pd(II) and Pt(II) di-ynes **188** (Chart 20) were studied by Ho and Wong.[376] In this work, they attached the metal through *N*-site of carbazole and systematically studied the impact of different metal centres (M) as well as co-ligands (R) on the optical absorption and PL properties. A very slight difference was noted in the solid state and solution (DCM) absorption spectra of Pd(II) and Pt(II) complexes. They also remained insensitive to the nature of phosphine auxiliaries. The same observation was made for the luminescence at 290 K (DCM). Due to the presence of a break junction (methylene next to acetylene), no major shift was observed upon metalation. Both Φ_F (290 K) and τ_F (290 K) of Pt(II) complex were lower than that of Pd(II) complex. At lower temperature (77 K), all the complexes showed large Stokes shifts and emission lifetimes in the microsecond range (τ_P = 3.67-4.54 μs), suggesting emission from T_1 state. In line with other studies, the ISC efficiency in the complexes indicated that Pt(II) has more pronounced effect on the optical properties of the complexes compared to the Pd(II) congeners. Other Pd(II) di- and oligo-ynes have also been reported incorporating ligands with different topologies. For example, Yam and co-workers[377,378] reported 1,3,5-triethynylbenzene-

based trinuclear Pd(II) complexes. Furthermore, Pd(II)-containing helical hetero-bimetallic complexes have also been studied.[379,380] All these systems shared PL features similar to related materials.

Chart 20.

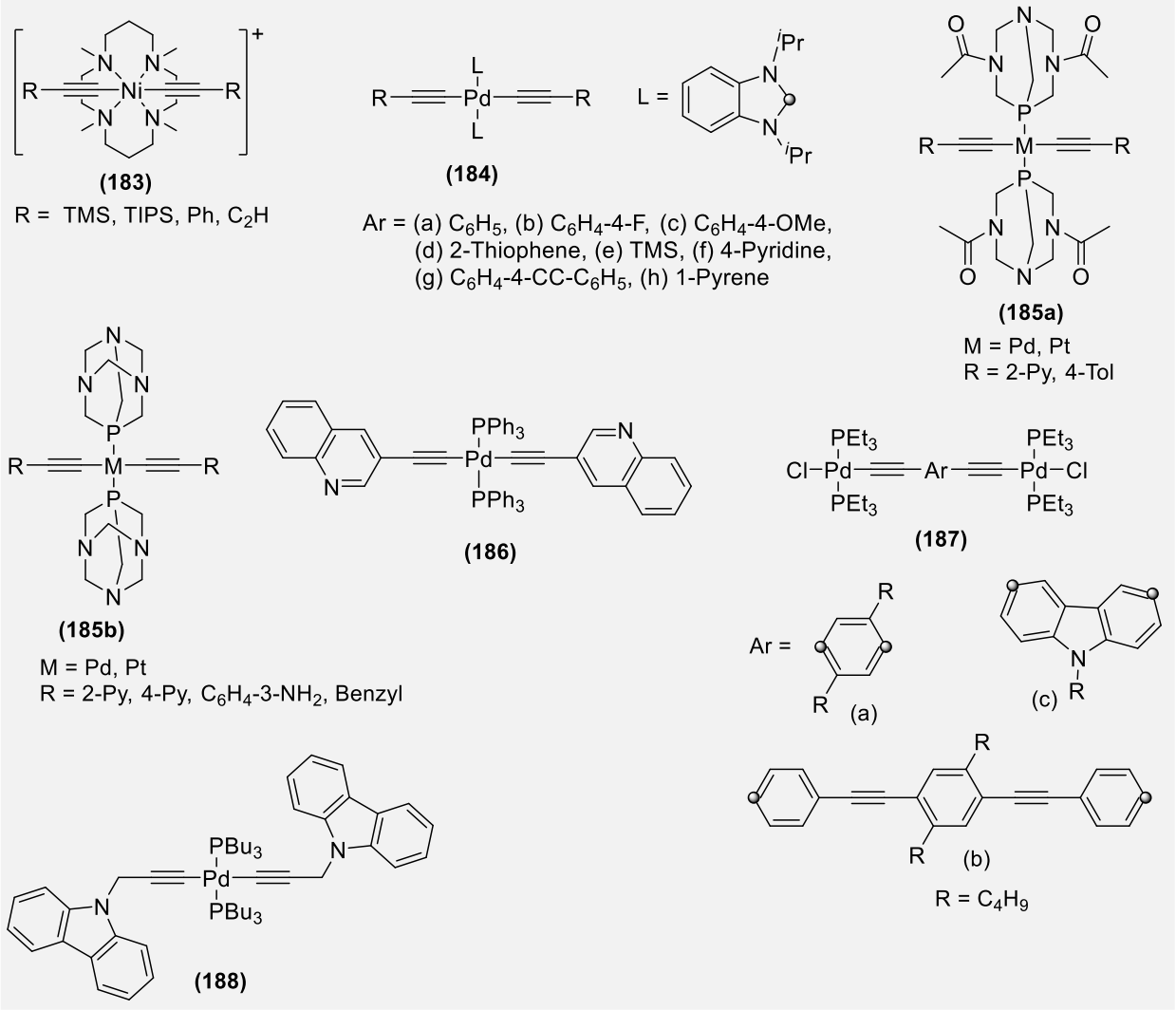

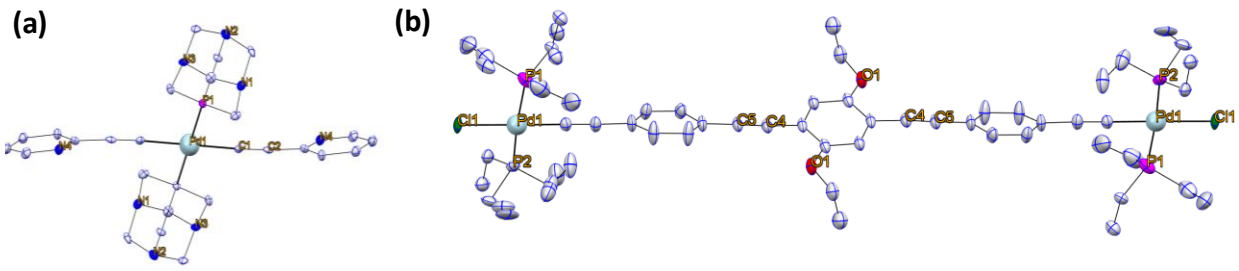

Figure 19. X-ray crystal structures of (a) **185b** (M = Pd, R = 2-py). Reproduced with permission from ref [371]. Copyright 2014 Elsevier Ltd, (b) X-ray crystal structures of **187b**. Figure reproduced with permission from ref [374], which is licensed under a Creative Commons Attribution 3.0 Unported License. Published by The Royal Society of Chemistry.

Since Pt(II)-based complexes are more stable and capable of emitting across a broad range of the spectrum (UV-Vis-NIR region) with high quantum yields and long excited state lifetimes, the majority of research has been carried out on this metal.[5,22,24] In the case of Pt(II) oligo-ynes having no spacer in the backbone (**189-192**, Chart 21), a red shift in $E_{0\text{-}0}$ bands was observed on moving from **189** (λ_{em} = 585 nm) to **190** and **191** (λ_{em} = 595 nm, Figure 20a). This, along with other experimental results, suggested a localized triplet state on a chromophore between the −[(C≡C)$_4$–Pt(PR$_3$)$_2$)]– repeat units.[381,382] **192** Having *p*-tolyl as terminal substituents showed moderate phosphorescence, while oligo-ynes with chloro terminal groups showed intense and narrow phosphorescence bands.[382] A phosphorescence decay kinetics study in Me-THF at different temperatures indicated that the emission lifetimes of **189-191** decreases with increasing temperature. Moreover, longer chain lengths give rise to higher emission lifetimes (Figure 20b). When a phenylene ring is introduced in the backbone of oligo-ynes (**193**), it showed $\lambda_{max.}^{em.}$ at 519 nm with Φ_P = ≈ 5%.[383] Di-yne incorporating a phenylene spacer and Pt(PEt$_3$)$_2$ at the termini possesses both singlet and triplet bands along with high E_g (3.4 eV), indicating weak electron withdrawing nature of the phenylene ring.[384] We, in the past, showed that the functionalization of phenylene ring shifts the absorption to the red, although minor, and enhances the phosphorescence intensity; however, the energy gap between singlet and triplet state ($\Delta E_{S1\text{-}T1}$) remains constant.[170,385] For example, a small shift (0.15 eV) was noted in the onset of absorption for the dinuclear Pt(II) complex **194** and its corresponding ethynyl ligand.[247,386] The introduction of electron-rich spacers such as naphthalene and anthracene **(195** and **196**, Chart 21) are known to create a relatively strong D-A interaction.[384] The lowering of absorption wavelength as well as E_g on moving from benzene through naphthalene to anthracene supports this fact very well **(195** and **196**, Chart 21). PL results indicated that di-yne incorporating naphthalene **195** has low phosphorescence yield compared to its poly-yne. Furthermore, di-yne incorporating anthracene **196** and its corresponding poly-ynes lacks T_1 state. These two observations were attributed to the exponential increment of k_{nr} with decreasing T_1 energy.[248,387] Almost similar photo-physical properties have been reported for *meta*- and *para*-substituted poly-ynes incorporating benzene, naphthalene and anthracene spacers.[388] A minor change in the auxiliary in **196** and the extension of conjugation length endowed the metalla-yne with some unique features.[389] In Pt(II) oligo-ynes (**197** and **198**, Chart 21), the Pt(II) acetylide segment acts as sensitizer to populate the T-state of the anthracene segment (acts as energy trap) *via* intra-molecular T-T energy transfer. **197** Showed only fluorescence emission arising from the anthracene segment (Φ_F = 0.96), while **198** showed Φ_F = 0.014 from the anthracene segment followed by slow phosphorescence decay from the Pt(II) acetylide segment. All these observations indicate a rare S → T energy transfer from the anthracene segment to the Pt(II) acetylide followed by T-T energy transfer from the Pt(II) acetylide to the anthracene segment (Figure 20c).

Chart 21.

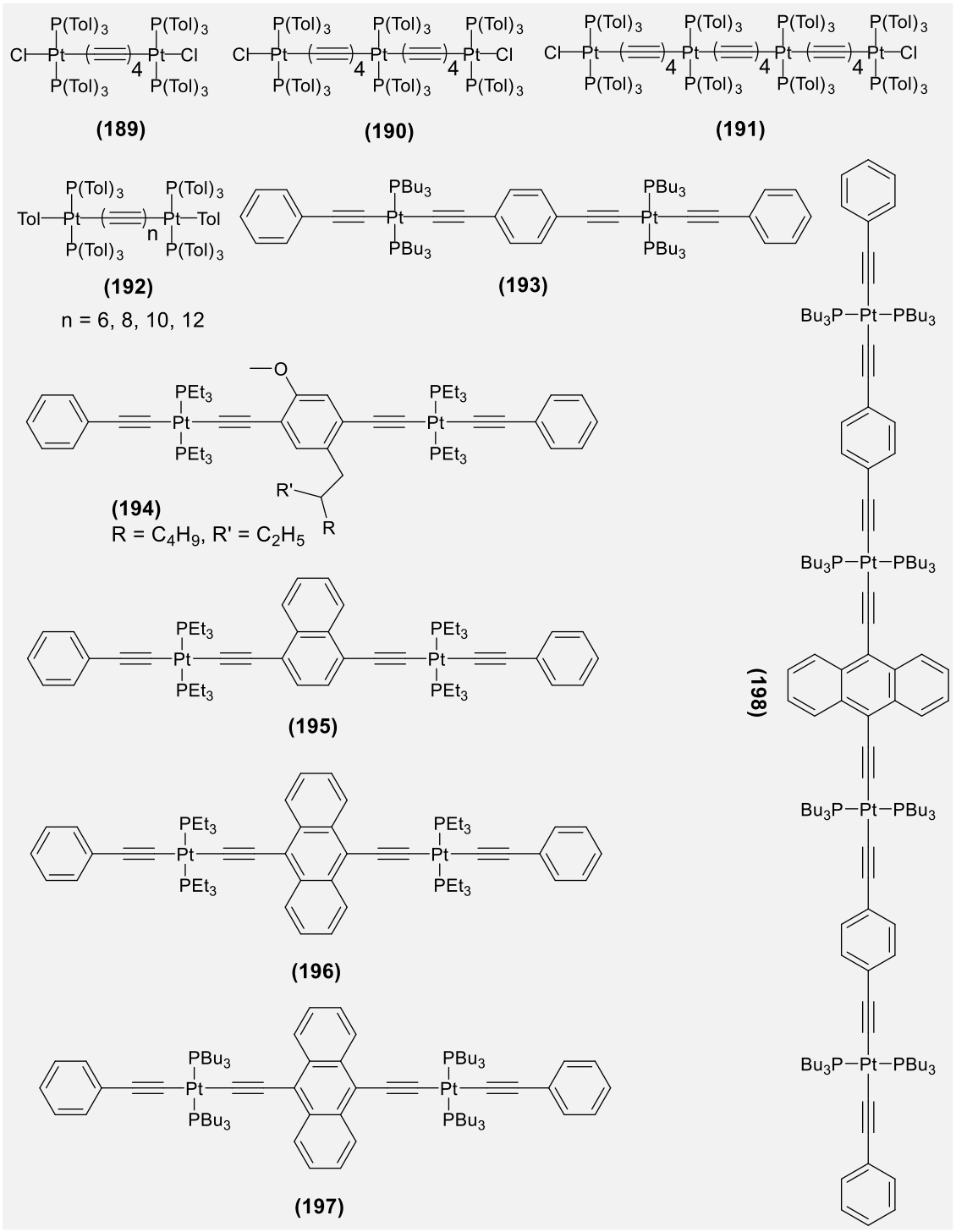

In another interesting study, Schanze and co-workers[390] reported an unexpected trend in the variation of Φ_F and τ_F. They noted that in Pt(II) oligo-ynes **199** (Chart 22), as the strength of the acceptor unit increases the excited state localizes on the acceptor unit, which is away from the metal. Furthermore, ISC rate was reported to vary inversely with the CT. The same group demonstrated the impact of varying conjugation

length in oligomer **200**-**202** (Chart 22) and the corresponding polymer on their T-excited state.[391] Through in-depth and extensive photo-physical studies, they concluded that the excite states (S and T) are mainly localized on D-A-D unit and the ISC rate increases with the chain length.

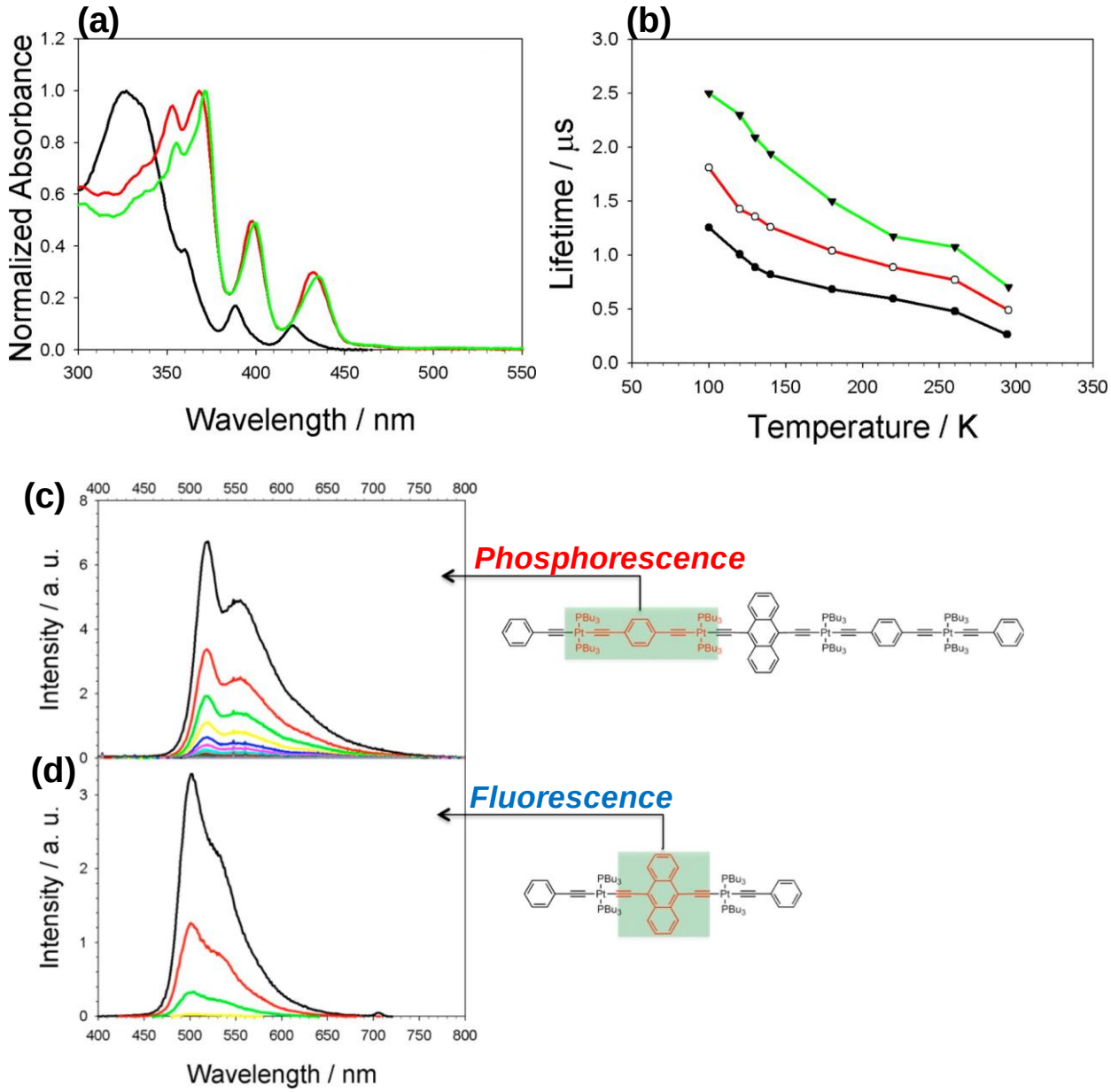

Figure 20. (a) Absorption spectra and (b) temperature dependence of photoluminescence lifetimes of **189** (black), **190** (red) and **191** (green) in deoxygenated Me-THF solution. Reprinted with permission from ref [381]. Copyright 2014 American Chemical Society. (c and d) Time resolved emission spectra in deoxygenated THF solution of **197** and **198**. Reprinted with permission from ref [389]. Copyright 2013 American Chemical Society.

Chart 22.

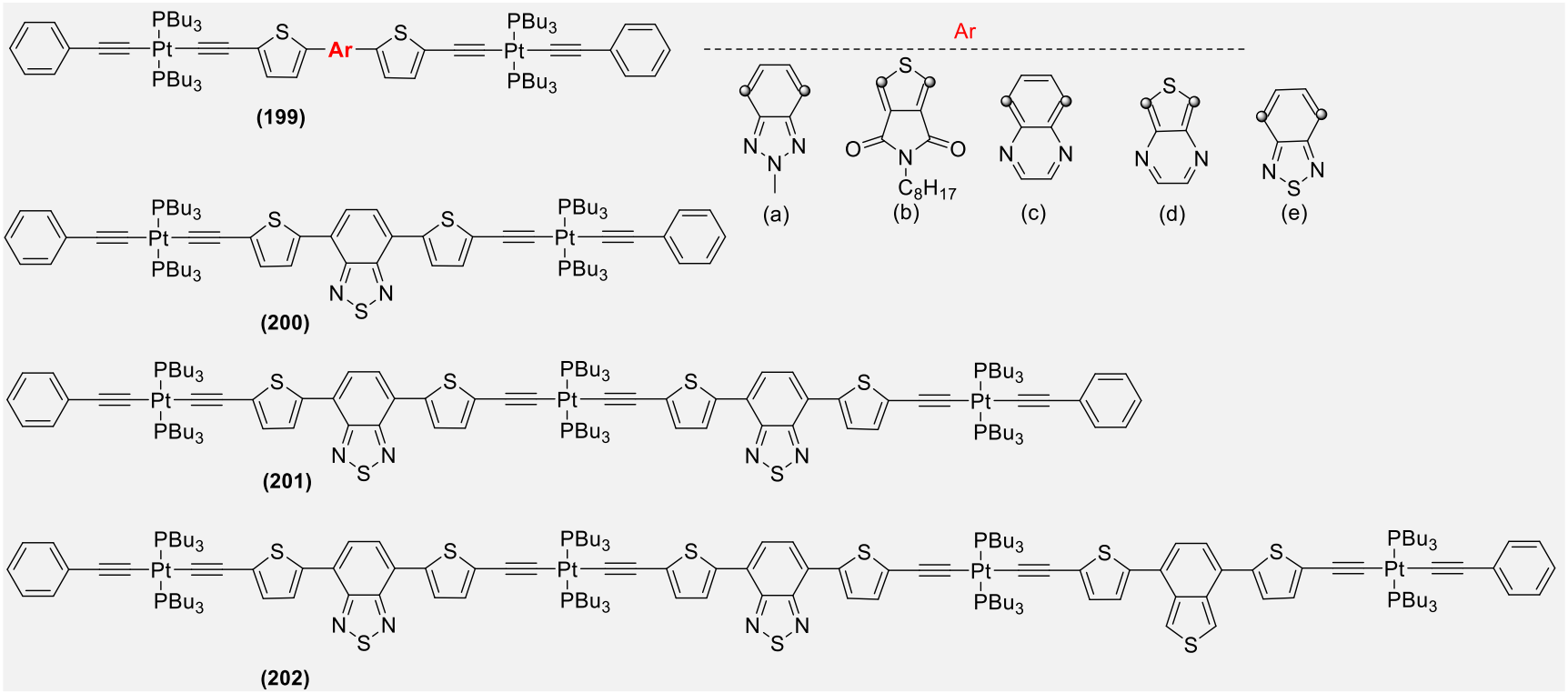

Acenes, with more than three fused aromatic rings, possess high electron density and are potential candidates for OLED, FET, PV, etc.[392]. In acenes, the energy required for $S_0 \rightarrow S_1$ transition decreases with increase in the number of aromatic rings.[393] Furthermore, the introduction ethynyl group enhances the stability of acenes against oxidation and decomposition.[394] In addition, higher electron affinity and oxidation potential could also be achieved by simply installing one or more heterocyclic atoms into the acene core. Several hetero-atom based acenes with ethynyl group have been reported with absorption/emission in NIR region and with low E_g.[395,396] To understand how Pt(II) perturbs the electronic structures of acenes, Nguyen et al.[397] reported a series of dinuclear tetracene complexes **203** (Chart 23) bearing different auxiliary ligands. Compared to 5,12-*bis*-(triisopropylsilylethynyl)tetracene, these complexes exhibited red-shifted absorption and fluorescence bands. The extent of shift was more pronounced in the neutral complexes with π-donor auxiliaries than the cationic complexes with π-acceptor auxiliaries (Figure 21a,b). The Φ_F value of these complexes ranged from 0.13-0.97 with τ_F in the range of 2.0 to 9.3 ns. Based on their small Stokes shifts (290-800 cm^{-1}) and nanosecond lifetimes, the emissions were assigned to metal-perturbed $S_1 \rightarrow S_0$. Low ISC rate resulting from a large extended π conjugation of the ligand surpassed the effect of Pt(II), and thus, the complexes did not show any phosphorescence. The extent of perturbation was dependent on the energies of the dπ orbital of the metal fragments.

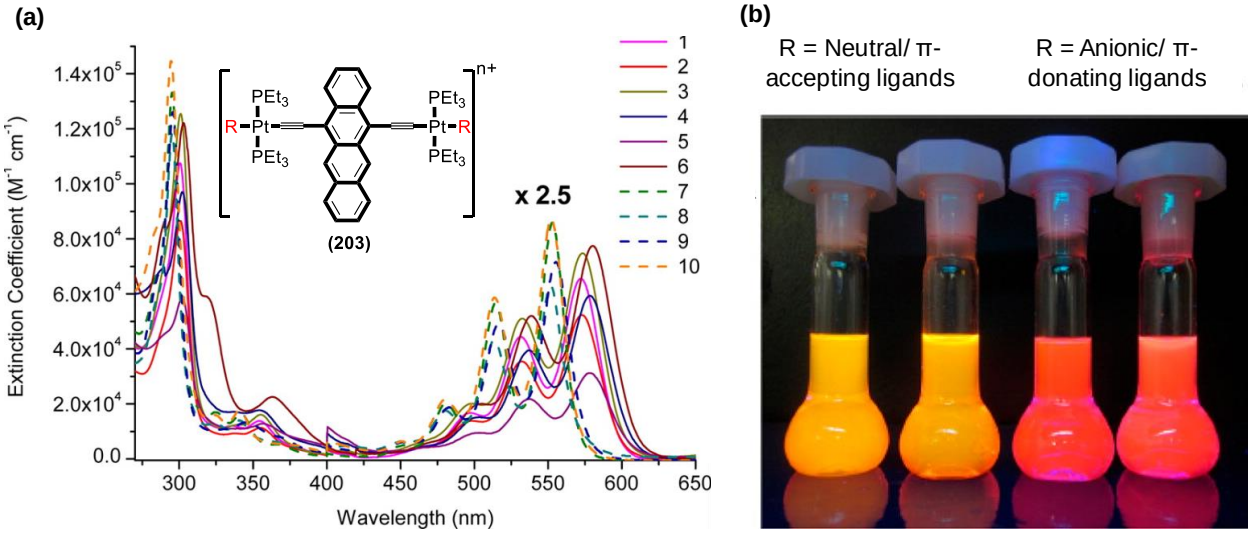

Figure 21. (a) Absorption spectra of **203** (R = -I (1), -Br (2), -Cl (3), -SPh (4), -SePh (5), -C≡C-Ph (6), (solid lines) and PPh_3 (7), Et_3P (8), C_5H_5N (9) and $C_6H_3(CH_3)_2NC$) (10) (dashed lines) in CH_2Cl_2 at RT. For the sake of clarity, the visible absorption bands (400-650 nm) are magnified 2.5 times. (b) Image showing the effect of different ligands on emission colors of metallated tetracenes **203**. Reprinted with permission from ref [397]. Copyright 2013 American Chemical Society.

Another series of anionic and neutral pentacene-based dinuclear Pt(II) acetylide complexes with different auxiliaries (**204-205**, Chart 23**)** was reported by the same group.[398] Solid state structure analysis revelaed that **204f** adopted 2D-Herringbone pattern (Figure 22a). Furthermore, optical absorption of **204** and **205** in DCM solution exhibited four bands (I-IV, Figure 22b) (HOMO (S_0) → LUMO (S_1), HOMO-1→LUMO+1

transition and two weak shoulders attributed to "*minus*" and "*plus*" states, respectively). It is worth noting that when Pt(II) was connected to the π-donor anionic ligand pentacenyl-6,13-diacetylide, it moved the fluorescence emission of the organic chromophore to the NIR region (λ_{em} = 710-726 nm) and lowered the HOMO-LUMO gap by 0.34 eV. Lifetimes in the ns range (2.7-8.9 ns) and small Stokes shifts were the indication of fluorescence. It was also noted that energy of the complexes with anionic, π-donor ligands was lower compared to complexes with neutral, π-acceptor ligands.

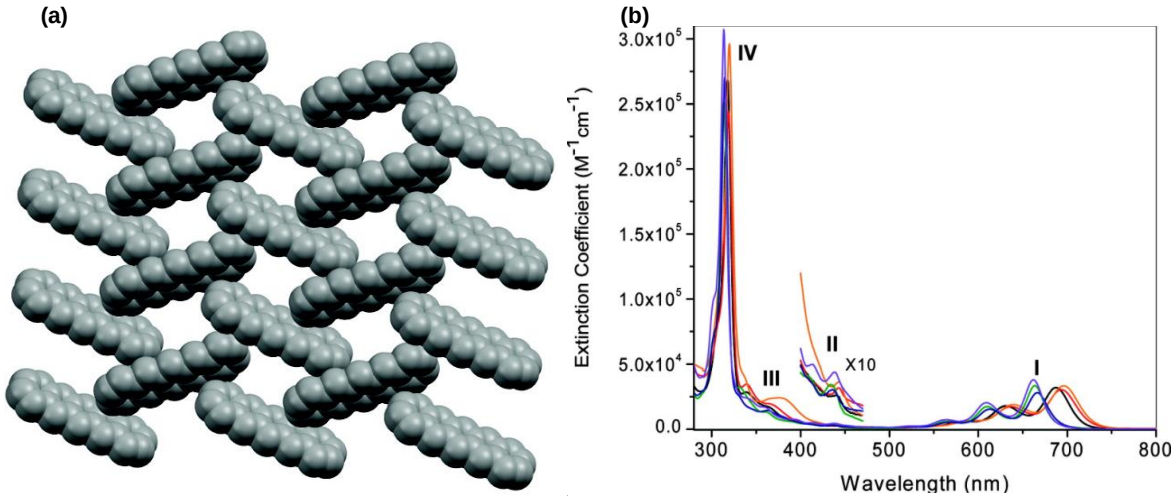

Figure 22. (a) Herringbone pattern of the pentacenyl rings of **204f**, (b) UV-vis. absorption spectra of **204b** (red), and **205** (black), **204c** (orange), **204d** (gree), **204e** (blue), and **204f** (violet) in DCM solutions. Reprinted with permission from ref [398]. Copyright 2011 American Chemical Society.

Chart 23.

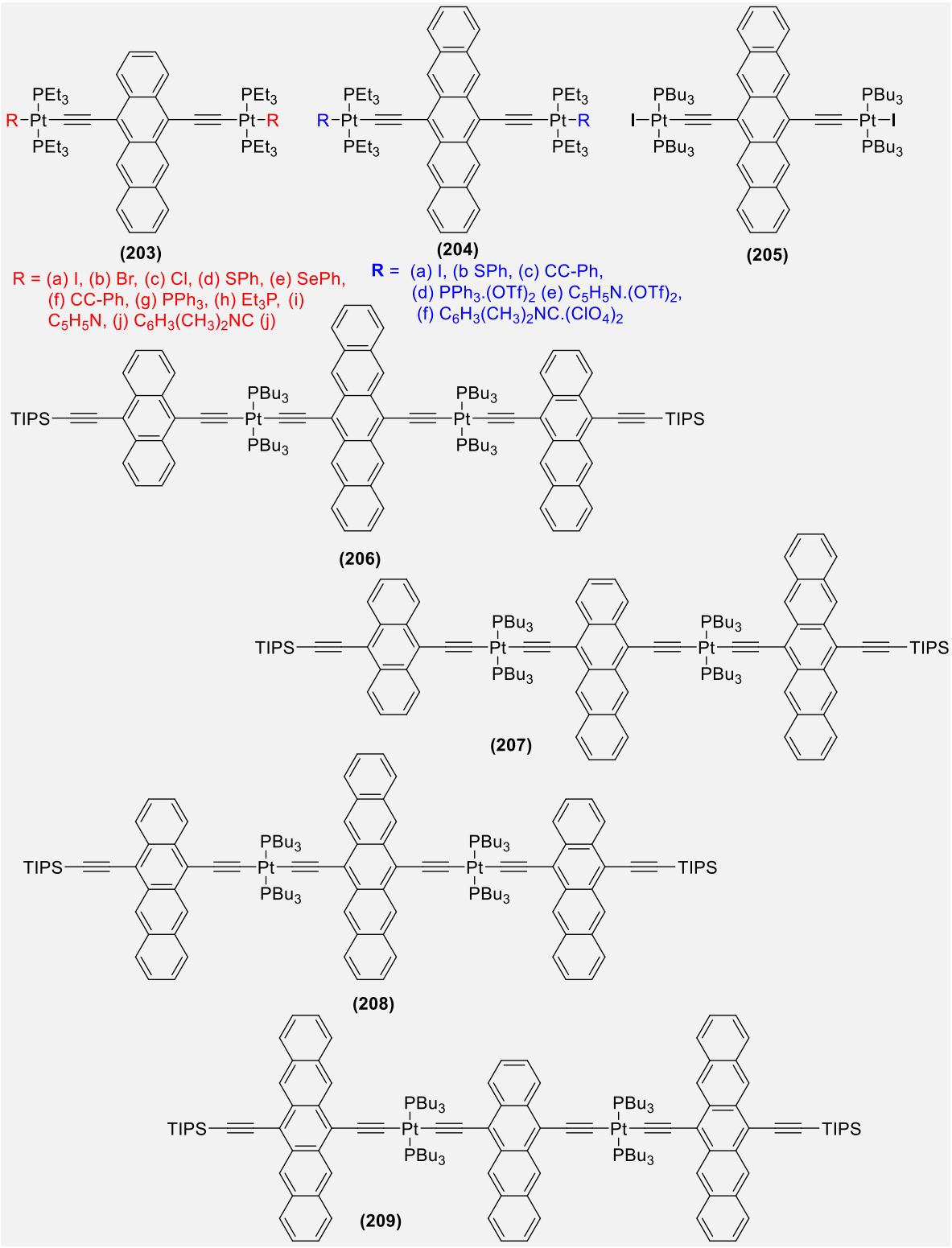

Extending their study, they prepared acene-based Pt(II) oligo-ynes having different combination of chromophores like T-P-T, A-P-T, A-T-P, and P-T-P (A = anthracenyl, T = tetracenyl and P = pentacenyl) (**206-209**, Chart 23).[393] These purple, blue and brown colored Pt(II) oligo-ynes or "*black chromophores*"

absorb strongly across the entire visible region ($\lambda_{max.}^{abs.}$= 278-700 nm, $S_0 \rightarrow S_1$). Figure 23 depicts a typical emission and excitation spectra of the triads **207**. The triad contained three visible and NIR emission bands for $S_1 \rightarrow S_0$ transition of each constituents (A, T and P). The comparison of excitation at 400 and 490 nm indicated the energy transfer process from the S_1(A) → S_1(T), S_1(A) → S_1(P) and S_1(T) → S_1(P). These complexes having Φ_F in the range of 0.6-7.7 x 10^{-3} in the NIR region, showed no phosphorescence even in the presence of Pt(II) center. The lack of SOC effect was attributed to the characteristic large S_1−T_1 gap, resulting into a barrier for $S_1 \rightarrow T_1$ ISC.

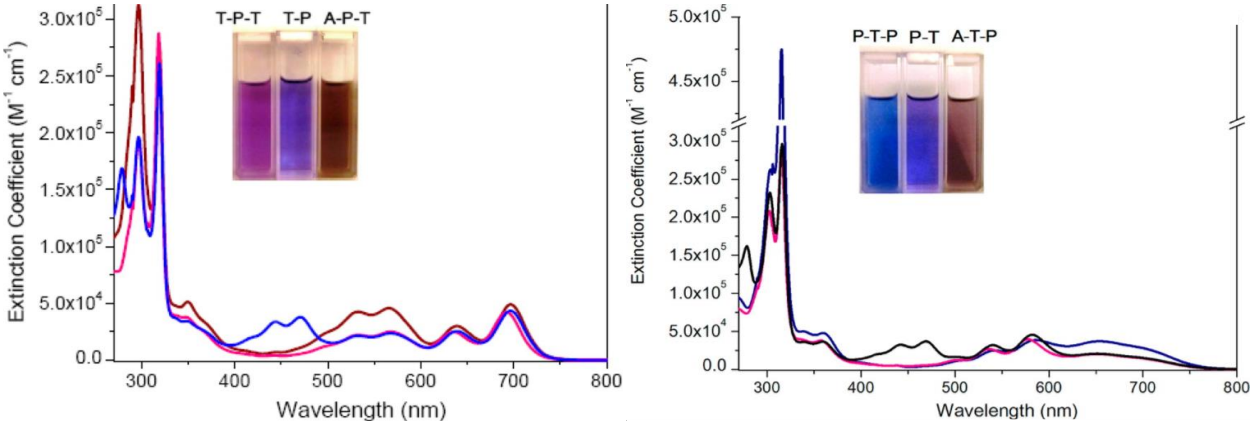

Figure 23. UV–vis absorption spectra and colors of DCM solutions of T-P-T (brown), T-P (pink), and A-P-T (blue), P-T-P(green), P-T (red), and A-T-P (black) at room temperature. Reprinted with permission from ref [393]. Copyright 2013 American Chemical Society.

Considering the advantages offered by rigid iptycene scaffolds (Section 3.1, *vide-supra*), Lin et al.[399] investigated the impact of incorporating iptycene into the Pt(II)-oligo-yne backbone (**210-213**, Chart 24) on their photo-physical properties. Interestingly, the introduction of pentiptycene groups around $Pt(PBu_3)_2$ center yielded dually emissive materials with long-lived triplet excitons (90-202 μs). For these oligo-ynes, $\lambda_{max.}^{em.}$ values ranged between 398-402 nm with Φ_f between 0.001-0.01. Furthermore, a direct impact of the relative backbone planarity on T_1 was also observed. They concluded that the twisting and steric shielding of the π-conjugated backbone around the Pt(II) center reduced the extent of SOC. Recently, we investigated the level of conjugation in isomeric carbazole-based Pt(II) mono-, di- and poly-ynes.[400] Although 2- and 3-carbazole-based systems are expected to have similar level of conjugation, we found that 2- and 2,7-carbazole based Pt(II) mono-, di- and poly-ynes (**214-219**, Chart 25) are more efficient in electron transport than 3- and 3,6-carbazole analogs, attributed to the presence of "*break junction*" in the latter. Similar observations, i.e. shorter $\lambda_{max.}^{abs.}$ and $\lambda_{max.}^{em.}$ of *m*-phenylene ethynylene-linked polymers compared to those of the *p*-phenylene ethynylene-linked counterparts have also been reported.[401] These results clearly indicate that the emission properties are directly related to the topology of the systems.

Chart 24.

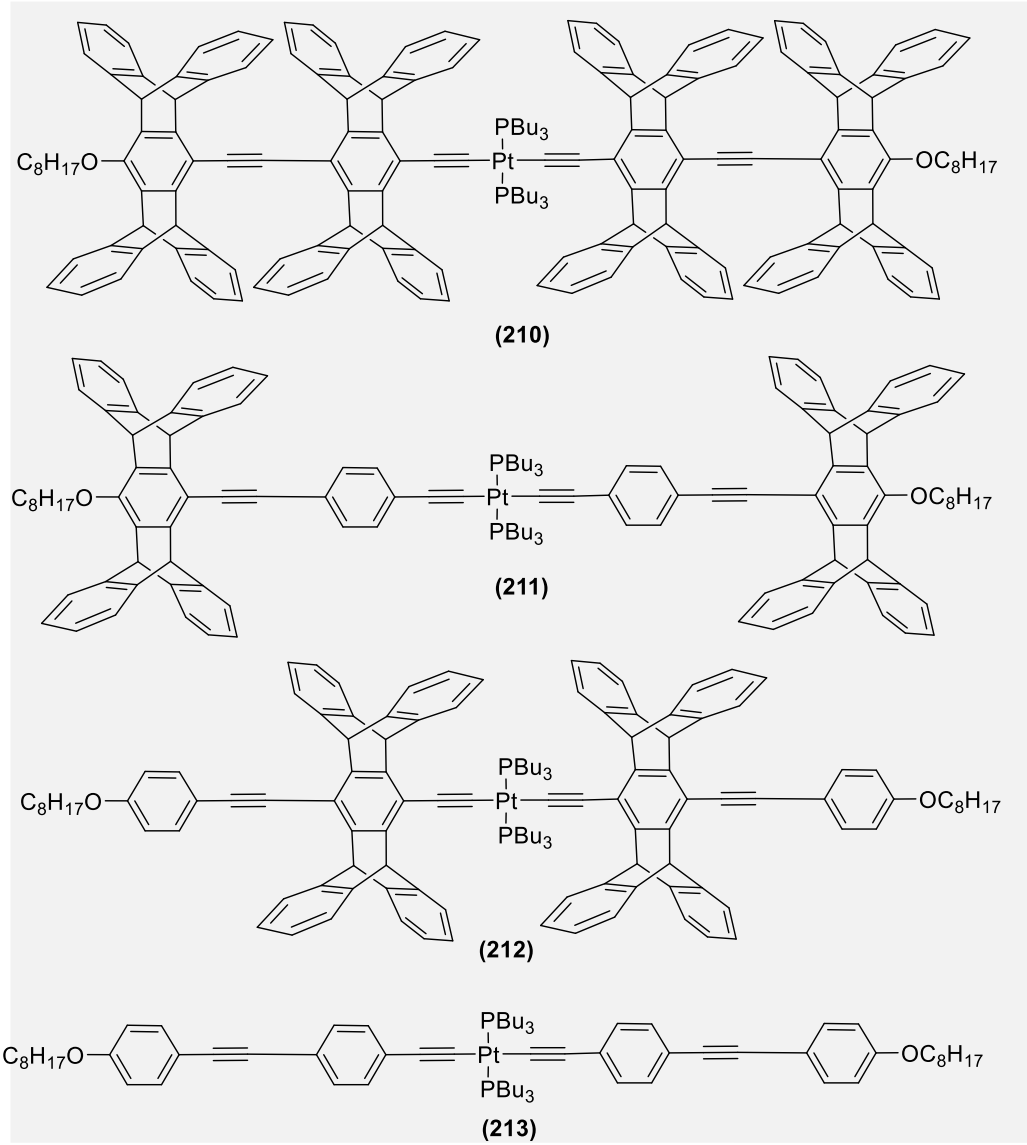

Cook and co-workers[280] reported that the Pt(II) acetylide complexes **220-223** (Chart 25) with terminal pyridyl moieties have a metallo-cumulene resonance structure, for which the contribution depends on the position of the *N*-atom, auxiliary ligand (L), and methylation. Like the carbazole systems, they found that the use of a 4-ethynylpyridine ligand, as opposed to a 3-ethynylpyridine, stabilizes the metallo-cumulene resonance structure more due to the presence of N-atoms at *para* position. The stabilization of a metallo-cumulene resonance form leads to increase in Φ_P *via* reduction in k_{nr} values. (Table 7) The alkylation of pyridinium nitrogen has synergistic effect on the metallo-cumulene structure leading to enhanced PL properties.

Table 7. Quantum yield, lifetimes, radiative, and non-radiative rate constants of isomeric Pt-alkynyl complexes **220-223**. (Reprinted with permission from Ref [280]. Copyright 2017 Royal Society of Chemistry)

	220		221		222		223	
	L = 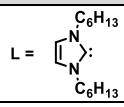	PEt_3	L = 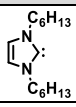	PEt_3	L = 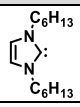	PEt_3	L = 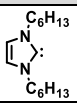	PEt_3
Φ_p	0.008	< 0.001	0.394	0.001	0.099	< 0.001	0.054	0.014
τ_p (μs)	0.375	0.0139	21.2	0.0210	17.6	0.0508	30.8	4.23
k_r ($\times 10^4\ s^{-1}$)	2.1	< 7.2	1.9	4.8	0.56	< 2.0	0.18	0.33
k_{nr} ($\times 10^4\ s^{-1}$)	260	> 7200	2.9	4800	5.1	> 2000	0.34	23

Fused and non-fused thiophenes have been employed for the synthesis of photochromic materials, which have diverse application in molecular wires, sensors, molecular logics and devices.[402,403] In Chart 26, we have collected some photo-responsive Pt(II) acetylides. Yam and co-workers[404] reported fused and non-fused thiophene-based photo-switchable functional materials **224-226** (Chart 26), which adopted a *closed* or *open* form depending on the wavelength of irradiated light. Due to these two forms, a significant change in the color of materials was noted. For example, when the material was photo-excited in UV region (320 nm for ligands and 370 nm for complexes), it turned purple with the emergence of LE absorption bands at about 560 nm, attributed to the closed form of the 8a,8b-dimethyl-1,8-thia-as-indacene moiety. Further irradiation at about 470-600 nm regenerated the open form of the product. In these systems, the closed form was also thermally stable. Compared to other reported complexes, these systems showed higher percentage conversion, which was attributed to the absence of labile chlorine atom. Recently, Chen and co-workers[405] reported *bis*-DTE Pt(II) acetylide complexes **227-230** (Chart 26) which could adopt four states and showed four color photochromic (asymmetric ring-open/closed (oc and co) and dually ring-closed species (cc). These states showed distinct colours through a selective photochemical cyclo-reversion process upon irradiation at appropriate wavelengths (Figure 24). Similar ring-opening and closure in the solid state, solvents of different polarity as well as in thin films of Pt(II) di-yne ligated with DTE (**231)** (Chart 26) was reported by one of us.[406] The process of photo-isomerization was further confirmed by single crystal X-ray structure analysis.[406] Remarkably, the photocyclization of **231** occurred under both the UV and visible light, which are normally not absorbed by the non-metalated DTE core by itself. This property was attributed to the presence of a CT transition and a Pt(II) ion in **231**, which promotes ISC and facilitates a $S_0 \rightarrow T_1$ transition, giving rise to the absorption extended in the visible region. Azobenzene is another extensively studied photo- and thermo-responsive spacer which undergoes light or heat induced *cis-trans* isomerization. Contrary to DTE, where the incorporation of Pt(II) ions induces synergistic effect, azobenzene shows somewhat unusual behavior. Recently, we reported the synthesis and characterization of *meta*- and *para*-substituted azobenzene based Pt(II) di-ynes **232-233** (Chart 26) and their corresponding polymers.[407] All these dimers were solid and stable at room temperature. On assessing the photo-physical properties of these dimers in DCM, we found that the incorporation of Pt(II)-acetylide fragment to the azobenzene units shifted absorption maxima to the red, which is expected due to the enhanced conjugation and SOC. However, the incorporation of the metal acetylide framework led to a reduced isomerization process.

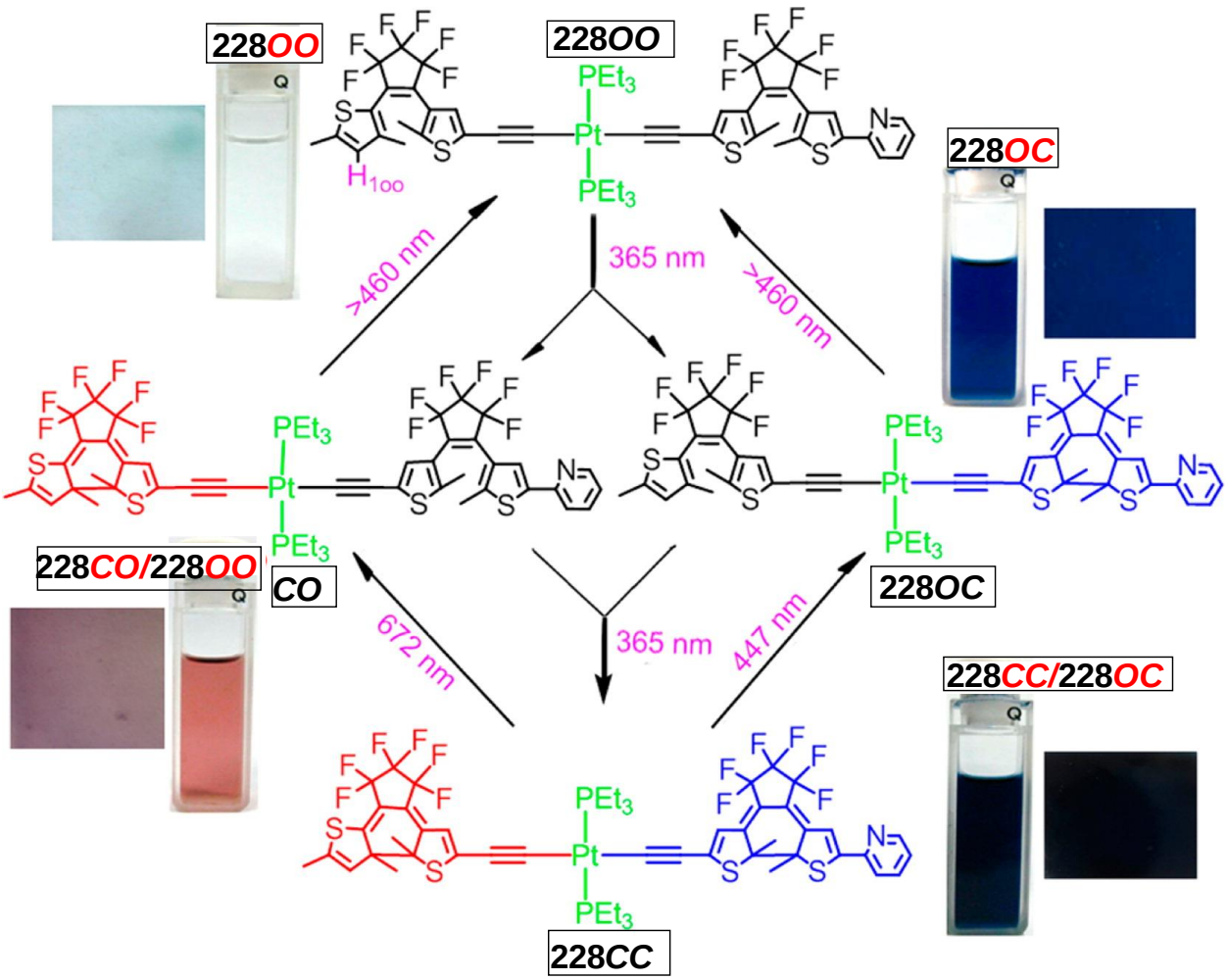

Figure 24. Step-wise and selective photochromic processes and color conversions in **228** in DCM solutions and PMMA film (25%). Reprinted with permission from ref [405]. Copyright 2015 American Chemical Society.

Like the previous example, the level of conjugation and isomerization was affected by topology of the ligands. A similar type of photo-physical behavior was noted in **234** (Chart 26).[408] However, due to the presence of extra amido-acetylene moieties at termini, an extensive H-bonding took place leading to the gelation of the complexes. Though the dilute DCM solution of **234** undergoes *cis-trans* isomerization, the organometallic gels did not show any major change. Moreover, the reported Pt(II) acetylides also adopted beautiful honeycomb-like structures (Figure 25). Prior to these studies, Schanze and co-workers[409] investigated the photophysics of stilbene-incorporated Pt(II) acetylides. They demonstrated that the extent of delocalization and π-conjugation through the metal is greatest when stilbene ligands are coordinated to the Pt(II) center in *trans*-disposition. Furthemore, the organic chromophore (stilbene) played important role in governing the photo-physics in Pt(II) acetylides systems.

Pt(II) acetylides with two peripheral coordinated BODIPY ligands and a centrally coordinated BODIPY ligands (**235-236**, Chart 27) give broadband absorption of visible light (ε up to 1.85 x 10^5 $M^{-1}cm^{-1}$ in the

region of 450-700 nm) with long-lived triplet excited states.[410] (τ_T = 63.13 µs for **235** and τ_T = 94.18 µs for **236a**). In these complexes, different BODIPY units are connected to Pt(II) fragment (either at the 2-position or the *meso* position of the BODIPY unit), resulting into different absorption wavelengths and T_1 state energy levels. The authors found that the triplet-excited state of **235** is delocalized over three BODIPY ligands, due to degenerate T_1 and T_2 states, whereas in **236a** the triplet-excited state is exclusively confined to one BODIPY ligand. These complexes showed high singlet oxygen ($^1O_2$) quantum yields (Φ_Δ = 76.0%) with delayed fluorescence (τ_{DF} = 43.8 µs for **235** and 111.0 µs for **236a**), which is unusal for transition metal complexes.

Chart 25.

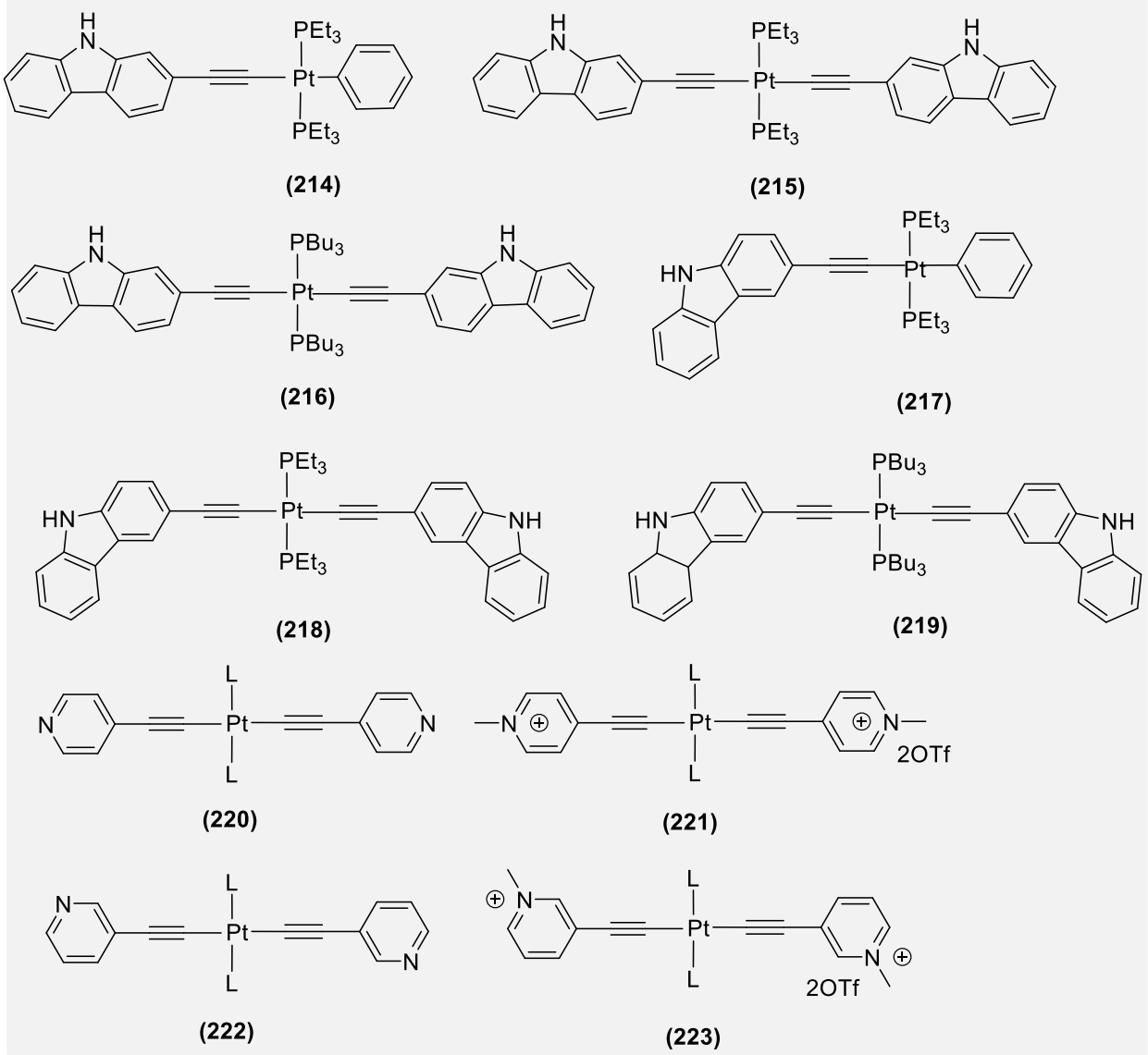

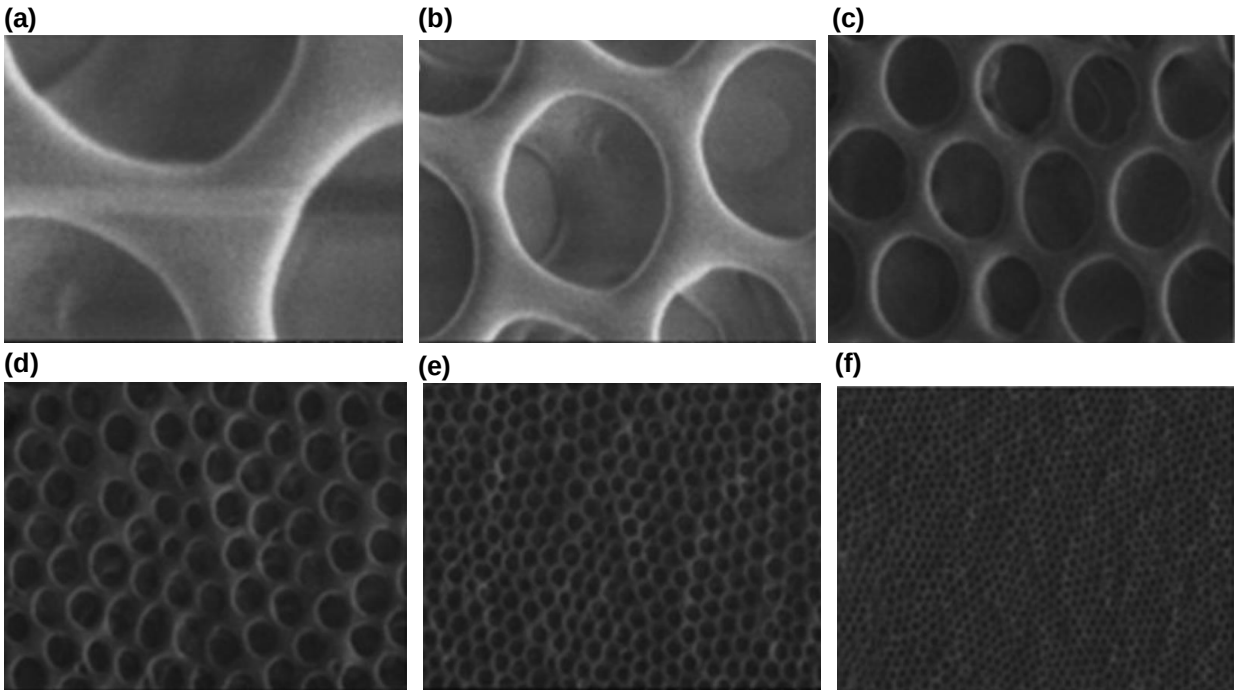

Figure 25. (a–f) SEM images of the xerogels formed by **234** in cyclohexane at different magnifications. Reprinted with permission from ref [408]. Copyright 2012 John Wiley and Sons.

Chart 26:

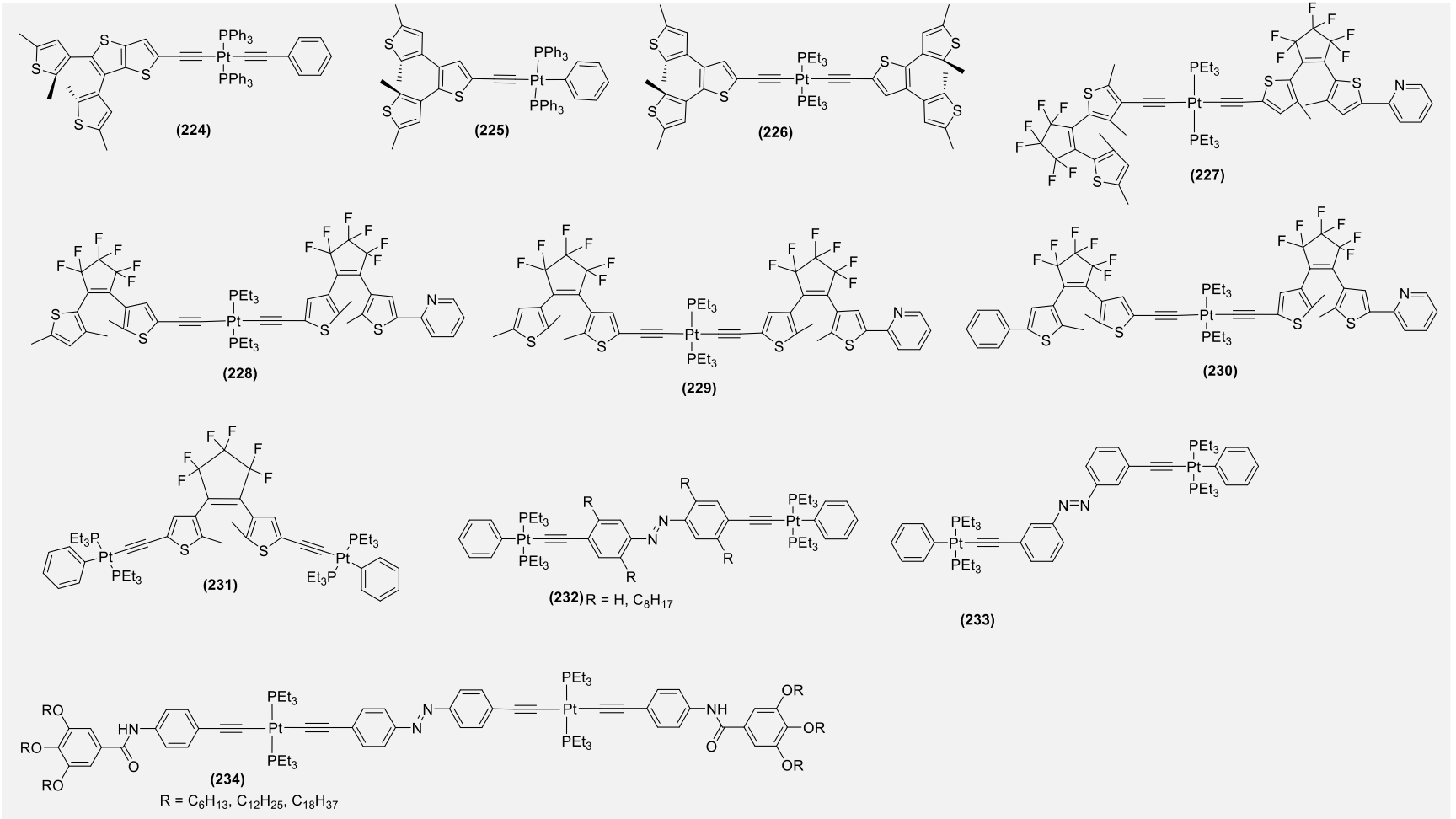
(224)
(225)
(226)
(227)
(228)
(229)
(230)
(231)
(232) R = H, C_8H_{17}
(233)
(234)
R = C_6H_{13}, $C_{12}H_{25}$, $C_{18}H_{37}$

Yang and co-workers[411] reported a similar dinuclear *trans*-Pt(II) *bis*(acetylide) complex **236b** (Chart 27) having styryl BODIPY at the center.[411] Unlike **235**, no phosphorescence was seen in **236b**; however, the complex showed a rare dual fluorescence at 518 and 754 nm. The incorporation of styryl moiety shifted the absorption band further to red and showed strong broadband absorption in both visible (503 nm, ε = 14 × 10^5 $M^{-1}cm^{-1}$) and NIR (731 nm, ε = 9.7 × 104 $M^{-1}cm^{-1}$) regions. Furthermore, ultrafast singlet-energy transfer *via* the through-bond energy-transfer (TBET) was also proposed in **236b** (Φ_{EnT} = 50%). Contrarily, **237** incorporating two different types of BODIPY ligands showed absorption in the visible region (450−650 nm, ε is up to 1.04 × 10^5 M^{-1} cm^{-1}).[412] The complex showed ultrafast intramolecular singlet/triplet energy transfer with triplet excited state confined to one of the ligands and lifetime of 54.1 μs. Furthermore, high triplet formation quantum yields in **237** (Φ_T = 69%) were also reported. When two different dyes were attached to Pt(II) center **238-239** (Chart 27), interesting structural and photo-physical properties were noted.[413] The reported complexes showed dual emission (fluorescence and phosphorescence) with Φ_p = 41%, which is one of the highest values at RT for such type of dye (**Figure 26**). In addition to the above discussed intriguing small oligo-ynes, fullerene and perylenediimides (PDI) based Pt(II) acetylides have also been reported.[414] Due to the n-type nature of these spacers, the resulting complexes possess good stability, absorption extended to visible region and high Φ_F.[415] Llewellyn et al.[416] compared the photo-physical properties of Pt(II)-diyne incorporating PDI with its organic counterpart and found, as expected, formation of an oxygen-sensitive T-state. Furthermore, fullerene incorporated Pt(II) acetylide has been reported that showed photo-induced electron transfer and generation of T-charged separated (CS) states with long lifetimes.[417] This type of system could find application in artificial photosynthesis and PV devices. In a recent work, Stang and co-workers[418] demonstrated that radiative excimers with longer-lived triplet excited states can exist in concentrated solution, due to the formation of triplet excimer. They noted a concentration-dependednt conversion of triplet excited-state absorption (TESA) to triplet excited-state emission (TESE) in a fullerene-functionalized Pt(II) metallacycle.

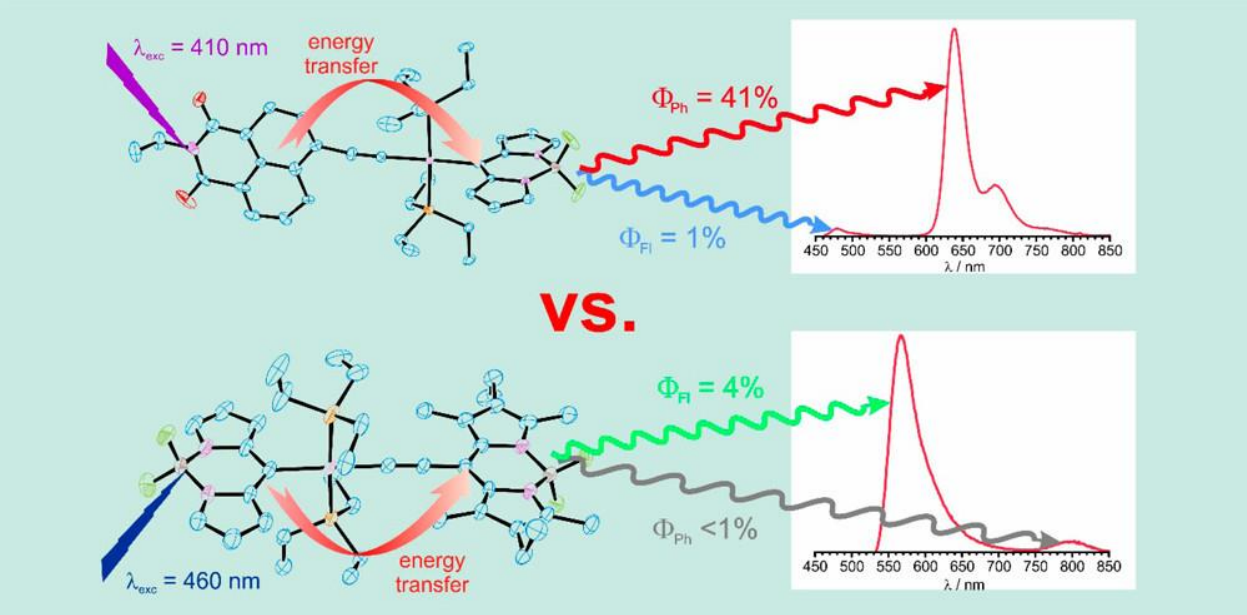

Figure 26. Energy transfer in Pt(II)-acetylides bearing BODIPY and naphthalimide chromophores **238**. Reprinted with permission from ref [413]. Copyright 2017 American Chemical Society.

Chart 27.

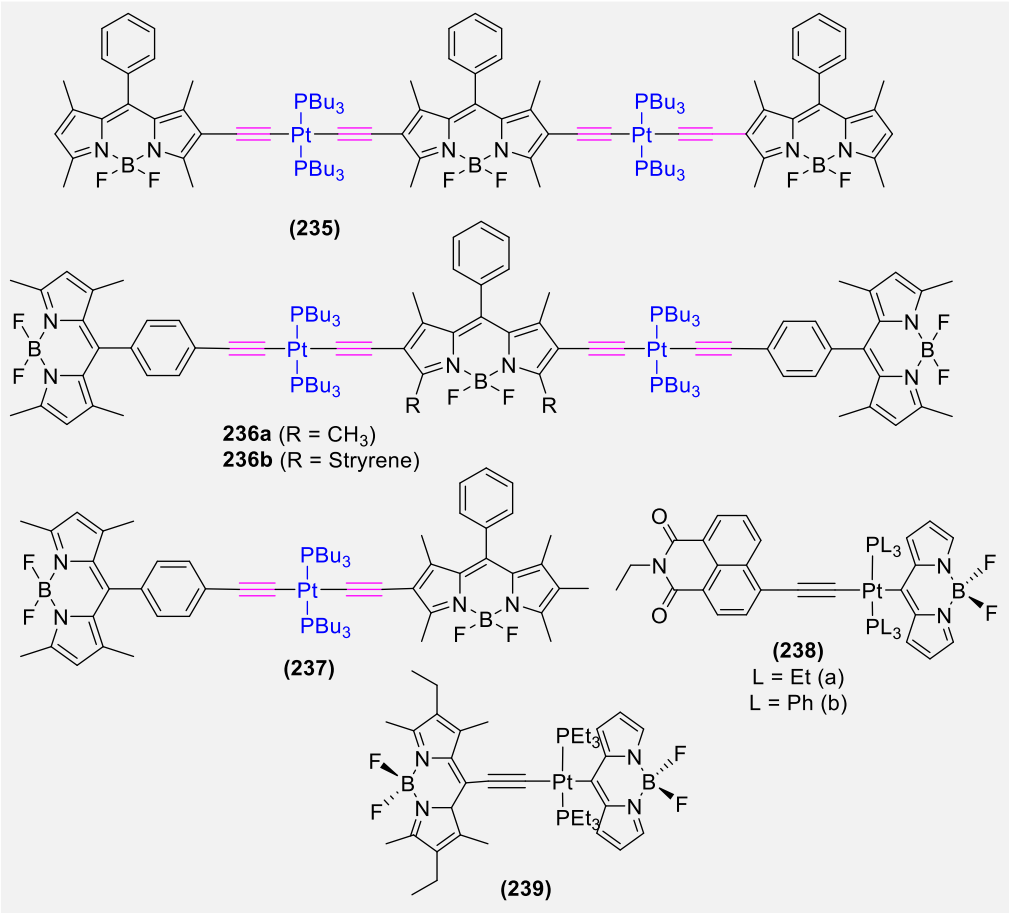

In the upcoming paragraphs, we shall briefly discuss the effect of increasing conjugation and Pt(II) fragments on the photo-physcical properties of oligo- and poly-ynes shown in Chart 28. Table 8 compares the photo-physical properties of several Pt(II) poly-ynes. It has been reported that upon increasing the number of C≡C units in simple oligo-ynes bearing phenylene spacer, $\lambda_{max.}^{abs.}$ and $\lambda_{max.}^{em.}$ shifts to the red and saturate between 5-7 units, indicating effective conjugation up to six repeat units.[162] The value of Φ_p for such oligo-ynes ranged between 5.2-7.1% with a localized T_1-state and a delocalized S_1-state. When the terminal ends of oligo-ynes is end-capped by 1,4,5,8-naphthalene diimide (NDI) units, a dramatic quenching of quantum yield ($\Phi_P \approx 0.1$-0.2%) was observed.[383] The lack of strong phosphorescence was attributed to the non-radiative pathway that effectively quenched the T-excitons. When alkoxyalkyl benzenes were used as core ligands and compared with their counterparts with and without the Pt(II) center, the one with metal showed red shifted absorption, due to the generation of D-A interaction.[419]. To establish a relation between chemical structures and optical characteristics, Frattodi and co-workers[419] synthesized a series of OPEs bearing Pt(II) oligo-ynes and determined the impact of chain length, number of metal units, type of auxiliaries, and end groups etc. on chemical and photo-physiocal properties. As expected, the optical and

luminescence properties were function of Pt(II) centers. Similar shifts of absorption/emission bands and modulation of PL characteristics have been reported on going from oligomer to polymer. For example, in fluorene-based di-ynes and poly-ynes **240a** (R = butyl), fluorescence wavelength was shifted by up to 30 nm.[420] Compared to poly-yne **240a** (R = butyl), monomer and dimer with 9,9'-dioctylfluorene **240a** (R = octyl) were non-fluorescent; however, the polymer showed temperature-dependent PL spectra.[421] This was attributed to the thermally activated diffusion of T-excitons along the polymer chain, which led to T-T annihilation or increased sampling of dissociation sites or non-radiative sites. Pt(II) oligo-ynes and poly-ynes incorporating 9,9-dihexylfluorene[422] **240a** (R = hexyl), Chart 28) showed lower T-energy, quantum yield and lifetime. The poly-yne had an E_g of 2.87 (Φ_F = 0.002), while the oligo-yne, having two C≡C units on each side of fluorene showed a E_g of 2.98 eV (Φ_F = 0.038). With diphenylfluorene as spacer, Pt(II) poly-yne showed better photo-physical properties over other metal ions.[423] In the case of diphenylfluorene (**240b**, Chart 28), the E_g for poly-yne was 3.38 eV (Φ_F = 0.003) while for di-yne, it was 3.60 eV (Φ_F = 0.022). However, in the absence of Pt(II) metal, the E_g value for the di-yne reached 3.92 eV.

Carbazole, an analogue of fluorene is known to have interesting photo-physical properties including a low S_1-T_1 gap. Due to its excellent PL and CT properties, several groups have investigated the isomeric carbazole (2-, 2,7- and 3-, 3,6-) based di-, oligo- and poly-ynes (**240c-l**).[400,420,424,425] Köhler et al.[424] studied the impact of topology on the PL properties (*viz*. S_1-T_1 splitting) using 2,7 and 3,6-substituted cabazole based Pt(II) di-ynes and poly-ynes (**240c-e**, Chart 28). They found that the S_1-T_1 splitting is more in *para*-linked di-ynes than their *meta*-linked counterpart. When the N-atom of the carbazole unit is replaced by S,S'-dioxide, it shows phosphorescence at room temperature.[426] With such a spacer, the di-yne showed E_g of 3.27 eV, while it was 3.14 eV for poly-ynes. Aly et al.[420,425] reported a conjugated backbone consisting of fluorene, carbazole as well as their hybrids (**240f**, **240g** and **240i-l**, Chart 28). They showed that emission profile of the isomeric 2,7- and 3,6-carbazole-based oligomer and polymers are controlled by the of the polymer. The detailed PL and computaional studies indicated that intramolecular singlet electron and triplet energy transfers from the carbazole chromophore to the fluorene moiety. For example, at 77K, both dimer and polymers incorporating 2,7-carbazole shows almost similar τ_F (0.32 and 0.26 ns for dimer and polymer, respectively) while the value of τ_P was higher for dimer (398 *vs* 112 µs at 77K). In addition, organic localized phosphorescence emission with spacer **240h** was found to be enhanced upon the metalation (Pt(II), Au(I) and Hg(II). Poly-ynes in which the conjugation length was increased by extending the number of thiophene rings (**240m -240o**, Chart 28) showed interesting photo-physical properties.[427,428] The $\lambda_{max.}^{abs.}$ values shifted to the red on going from thiophene (~ 406 nm) through bithiophene (~ 406 nm) to terthiophene (~ 458 nm) containing poly-ynes.[428] A similar trend was found in the E_g (2.80, 2.55 and 2.40 eV), indicating the impact of increased conjugation. Poly-ynes containing these three units showed emission from the S-excited state (fluorescence) between ~ 435-544 nm. Additionally, the ISC from S-excited state to the T-excited state reduced, while the S-T energy gap remains unaltered, indicating an extended T_1 excited state over multiple thiophene rings. Recently, some rare examples of main-group and transition metal-containing polymers **240p** (Chart 28) have been reported.[429] In these polymers, heavy-atom substitution causes a red-shift in

the values of $\lambda_{max.}^{abs.}$ and $\lambda_{max.}^{em.}$. Furthermore, a decrease in the phosphorescence intensity was noted on moving down the group (S → Se → Te, Figure 27a,b). In addition to these, long range coupling between the phosphorus and the chalcogenophene proton through the Pt(II) center was also observed. Similar variation in photo-physical properties have been reported in di-ynes with furan (O), thiophene (S) and selenophene (Se) spacers.[430] Our group[431] compared the electronic structure of Pt(II) poly-ynes containing fused and non-fused oligothiophene spacers. (**240 m-o and 240q-r**, Chart 28) In both fused and non-fused thiophene containing systems, which lacks π-π interactions in their molecular structure,[432,433] the energy was shifted from ligand through monomer to polymer indicating D-A interaction and moderate degree of conjugation. The energies of the S_1, T_1 and T_n excited states shifted to blue compared to the non-fused systems. This was attributed to the difference in the number of double bonds and S-atom. The introduction of ethylene 1,2-dioxy group over thiophene unit increases the electron density of the ring. It was observed that 3,4-ethylenedioxythiophene (EDOT) spacers **(240s** and **240t**, Chart 28) between the metal centers create a stronger D-A system than the non-fused and fused oligothiophene spacers do.[434] Among EDOT and *bis*-EDOT linker units, the E_g^{op} of the latter was found to be lower, due to more delocalized π electrons through the *bis*-EDOT spacer. The E_g^{op} of EDOT-diyne was 3.0 eV which reduced to 2.70 eV in *bis*-EDOT spacer. The E_g^{op} values of Pt(II) poly-ynes incorporating these two spacers was 2.70 and 2.50, respectively.[434]

Apart from S- based spacers, we also studied the impact of substitution position and number of rings on the electronic properties in oligo-pyridine based Pt(II) di-ynes and poly-ynes.[435,436] (**240u-y**, Chart 28) Poly-yne incorporating 2,5-disubstiuted pyridine showed E_g of 3.0 eV, while 5,5'- and 6,6'-disubstituted-2,2'-bipyridine containing poly-yne showed E_g of 2.90 and 3.30 eV, respectively. Terpyridine based poly-yne showed an E_g of 3.30 eV. Due to the presence of ethynyl moiety at different positions (2,5; 5,5'; 6,6'; 2,2':6',2'') of pyridine backbone, different level and extent of conjugation was reflected from the absorption spectra (**240v** based systems were fully conjugated while rest have hindered conjugation). For example, compared to monopyridine counterpart (**240u**), there was a red shift in poly-ynes containing **240v** while rest of the monomers and polymers underwent blue shift. This fact was further strengthened by the presence of fluorescence and phosphorescence in polymer with linear spacer **240v**, while phosphorescence was absent in di-ynes and poly-ynes with kinked spacers (**240w-y**, Chart 28). Similarly, model complexes with **240z-240aa** spacer show both S_1 and T_1 emissions, while complex with the spacer **240ab** generated only S-state.[247,386] Furthermore, with such spacers, an inverse relation between electronegativity and energy of excited states was reported.

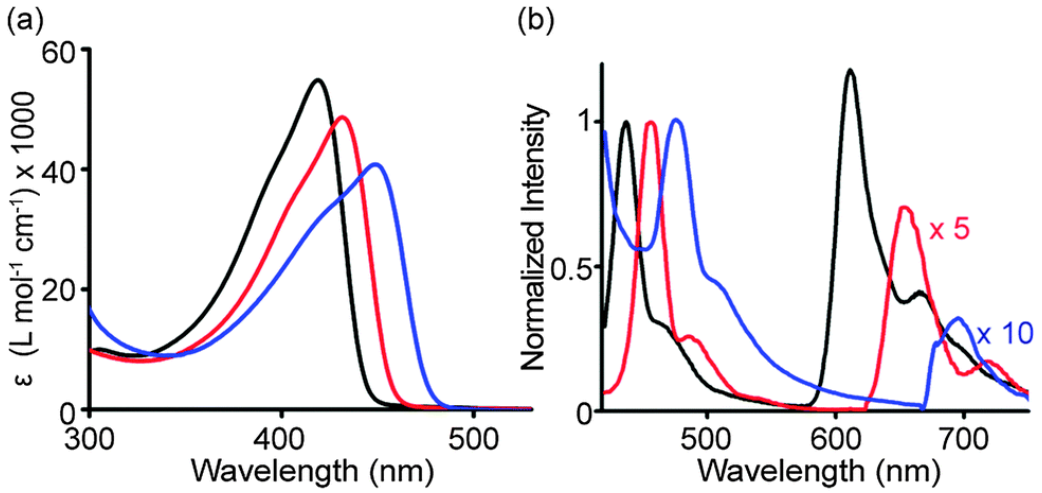

Figure 27. (a) Absorption spectra of polymers **240p**–s (black), –Se (red) and Te (blue) in chloroform solution at RT. (b) Emission spectra of **240p**–s (black), Se (red) and Te (blue) in degassed 2-MeTHF solution at 77 K normalized to the fluorescence band maxima. Reprinted with permission from ref [429]. Copyright 2014 Royal Society of Chemistry.

Thiophene is electron rich while pyridine is capable of modulating excited states; we studied the impact of conjugation extension by coupling these two heterocyclic moieties on the electronic structure.[437] (**240ac-240ae**, Chart 28**)** Poly(metalla-ynes) incorporating hybrid spacers **240ac** and **240ad** showed Eg of 2.67 eV and 2.55 eV, respectively. These values are essentially higher in energy compared to the poly-ynes bearing bithiophene and terthiophene spacers.[428] We also found that by adding thiophene units, the value of E_g drops. However, the magnitude of reduction was not the same upon the introduction of an additional thiophene ring, attributed to molecular twist and unwanted intramolecular interactions in the molecule. Overall, low S_1-S_0 gap (0.14 eV), S_1-T_1 gaps in the range of phenylene/thiophene based systems and blue shifted S-state were the main features of this system.[437] When a diphenylpyrazine unit is placed over the thiophene unit, the resulting thieno[3,4-*b*]pyrazine (**240af**, Chart 28) acts as an acceptor while Pt(II) or alkoxy-substituted phenylene unit acts as a donor. This combination creates a strong D-A system, which was reflected in the significant reduction of E_{gap}, CT type transition, the lowering of S_0-S_1 transition in Pt(II) poly-ynes and organic co- poly-ynes.[385,427,438] This phenomenon was ascribed to the large thieno[3,4-*b*] pyrazine spacer being orthogonal to the chain and being capable of pulling charge out of the main chain. Schanze et al.[439] reported Pt(II) poly-yne and oligo-ynes incorporating 2,1,3-benzothiadiazole moiety flanked on either side by 2,5-thienyl or EDOT donor units (**240ag** and **240ah**, **Chart 28)**. Both di-yne and poly-yne demonstrated absorption in the visible region and possessed an efficient ISC. Electrochemical investigation of the complexes showed the presence of a single reversible reduction peak at negative potentials and two oxidation peaks at positive potentials; attributed to oxidation/reduction of the electrophores concentrated on the π-conjugated segments that contain the three heterocyclic rings. The influence of the EDOT donor moiety in the cyclic voltammetry was clearly observed, in which reduction of the benzothiadiazole-thienyl materials occurred at a potential approximately 100 mV less negative

compared to that for the benzothiadiazole-EDOT donor materials. E_g of the di-ynes of **240ah** and **240ai** were 2.03 and 1.89 eV, respectively. On the other hand, it was 2.02 and 1.84 eV for their corresponding polymers. However, for Pt(II) poly-yne incorporating spacer **240ag**, E_g of 1.85 eV was reported by Wong et al.[440] All these values were less than the electron-rich bithienyl (2.55 eV)[428] or electron-deficient benzothiadiazole (2.20 eV) linked counterpart.[247,386] The spectral studies of both the model compound and the poly-yne of **240ag** indicated the presence of a confined S-state to a single repeating unit. PL studies and some other photo-physical experiments on the same molecule indicated CT nature of the transition, precluding the T-excited state as emitting state. Recently, Schanze and co-workers[391] studied the effect of chain length of oligomers on photophysical properties using **240ag** (Chart 28). They observed delocalization of LUMO throughout the π-conjugation with increasing chain length, leading to more efficient ISC. The spectral studies on poly-yne **204ah** suggested the presence of interchain interactions in polymer. Strong structureless peak in the NIR region (720 nm for poly-yne and 732 nm for di-yne) along with emission life time in ns (2.51 and 2.27 ns for poly-yne and di-yne, respectively) indicated fluorescence.[441] Another low and tunable E_g of 1.49 to 1.97 eV was reported for polymers incorporating 2,5-thienylene as donor and pyrido[3,4-*b*]pyrazine, 2,1,3-benzothiadiazole and thieno[3,4-*b*]pyrazine as acceptor.[442] Poly-ynes with at least one or two acceptor units in their backbone (**240ag** and **240ai-al**, Chart 28**)** showed strong ICT, broad absorption bands (extended to the NIR region), and ambipolar redox properties including small ionization potentials (4.82-5.23 eV). The absorption studies indicated that ICT strength increased with acceptor strength. Similar observation (improvement in ICT with increasing number of thienyl ring) has been made in Pt(II) poly-yne with side-chain-tethered phenanthrenylimidazole as acceptor.[443] (**240am**, Chart 28) Somewhat similar results ($\lambda_{abs.}$ = 346-554 nm and short life time) was also noted for poly-ynes incorporating bithiazole-oligothienyl D-A system (**240an**, Chart 28).[324,444] In this polymer, with different number of thienyl rings, E_g value ranged from 2.40 to 2.06 eV and the highly extended heteroaryl rings effectively reduced the heavy atom effect, viz. ISC and phosphorescence.[444] No change in Eg was even seen upon changing the length of alkyl group (**240ao**) on the bithiazole ring.[445] Polymer **240ap** is a red emitting, thermally stable and a visible absorbing polymer with 2,1,3-benzothiadiazole/triphenylamine groups as acceptor and thienyl as donor functionalities.[446] The extended π-conjugated system lowered the excited state energy so that the material can emit red to NIR fluorescence.[324] The E_g of the fluorescent red di-ynes were 2.09 and 1.86 eV, while for the poly-ynes, it was 2.06 and 1.85 eV. The solvatochromic effect and low E_g values of the materials were ascribed to ICT through the involvement of strong D-A structural motif in the polymer chain. Liu et al.[447] studied the effect of thienyl chain length on PV performance in poly-yne with 9,9-dioctylfluorene flanked by 0-3 thienyl rings (**240aq**, Chart 28). Though the conjugative interaction along the oligothienyl-fluorene unit was remarkably enhanced, the extent of red shift was not much affected by the extension of π-conjugation length. This kind of extended π-electron delocalized Pt(II) poly-ynes showed absorption in the visible region (399-457 nm with E_g between 2.93 to 2.33 eV), strong fluorescence (439–515 nm) and thienyl dependent PV efficiency. Compared to this, poly-yne **240ar-240as** composed of weak donor (9,9-hexylfluorene and strong acceptors (Benzo[1,2-c;4,5-c′]Bis[1,2,5]Thiadiazole) and Dibenzo[*a*,*c*][1,2,5]

thiadiazolo[3,4-i]phenazine) showed absorbance in the NIR region with moderate E_g^{op}(1.54 and 1.65 eV) and NIR fluorescence emission with no emission from the T-state (even at lower temperature).[448] Interestingly, the polymers showed the HOMO at -5.50 eV which assisted in attaining good solar cell performance. The relative strength of the acceptor units was reflected from the red shift in going from **240ar** to **240as**.

Even though most of the poly-ynes show intriguing electronic properties, achieving solid-state phosphorescence is still a challenging job. However, it has been recently suggested that it could be achieved if the thermal fluctuation in polymer is controlled *via* shielding the polymer backbone by rigid structures (*viz*. iptycene or cyclodextrin etc).[449] Terao and co-workers[449] reported the first example of unimolecular phosphorescence from highly-dense solid material composed of a polymer **241**. They achieved this goal by integrating the features of phosphorescence and rotaxane structure in one system, i.e. shielding the polymeric backbone through cyclodextrin. They observed that the 3D-cyclic insulation protected the polymer chain from (a) interactions with other Pt(II) and alkynyl units, and (b) oxygen molecules leading to enhanced phosphorescence intensity in both the solution and solid states (Figure 28). Following this remarkable finding, the same group designed a new PM α-CD insulated π-conjugated polymer incorporating Bpy units.[450] In addition to enhanced luminescence properties in both solution and in the solid states, the presence of Bpy unit offered sensing site for metals.

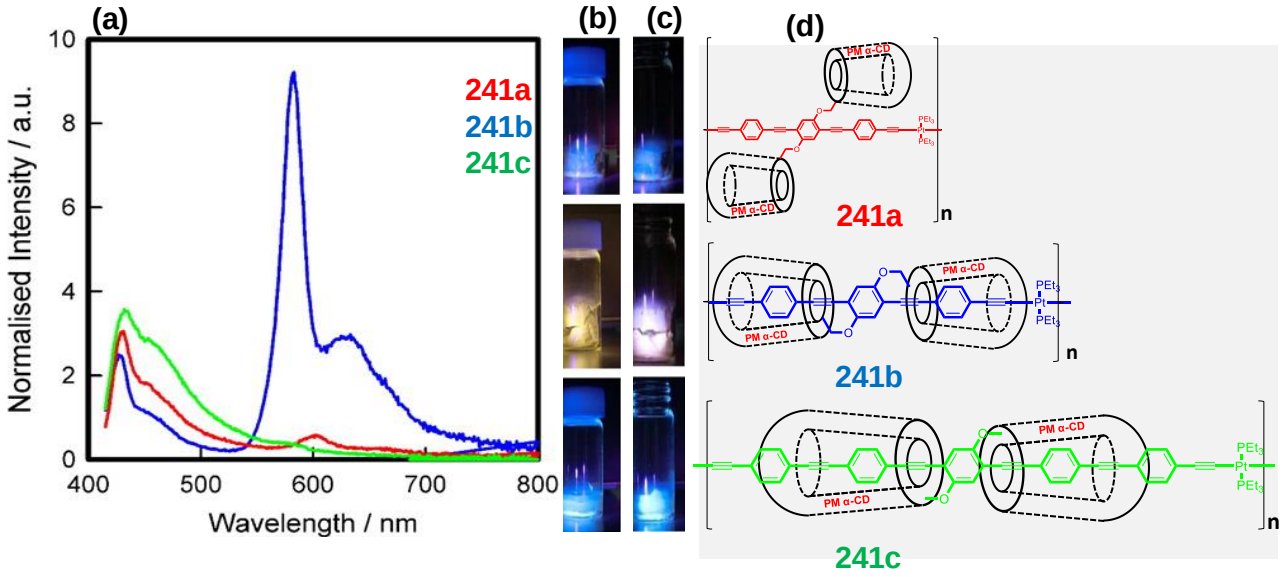

Figure 28. (a) Emission spectra of polymer solids of **241a** (red), **241b** blue), and **241c** (green) under degassed conditions (excitation: 405 nm). Emission behaviour of Pt(II)−acetylide polymer solids of **241a-c** (b) under N_2, and (c) under air (excitation: 380–425 nm). (d) Chemical structures of **241a-c**.
Reprinted with permission from ref [449]. Copyright 2014 American Chemical Society.

Chart 28:

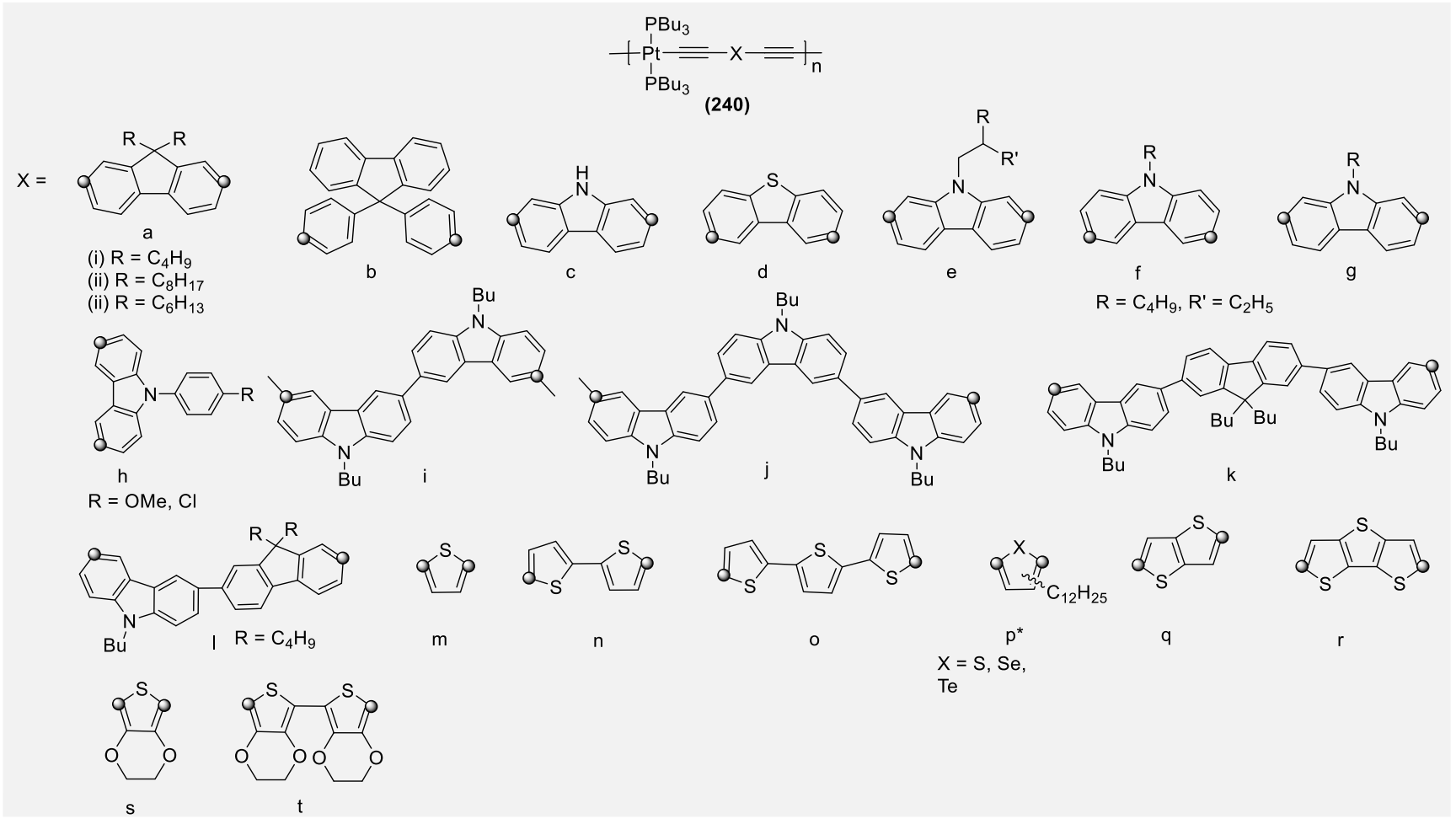

*.*Denotes PEt_3 as auxiliary ligand and # indicateS their di-ynes.*

continued…

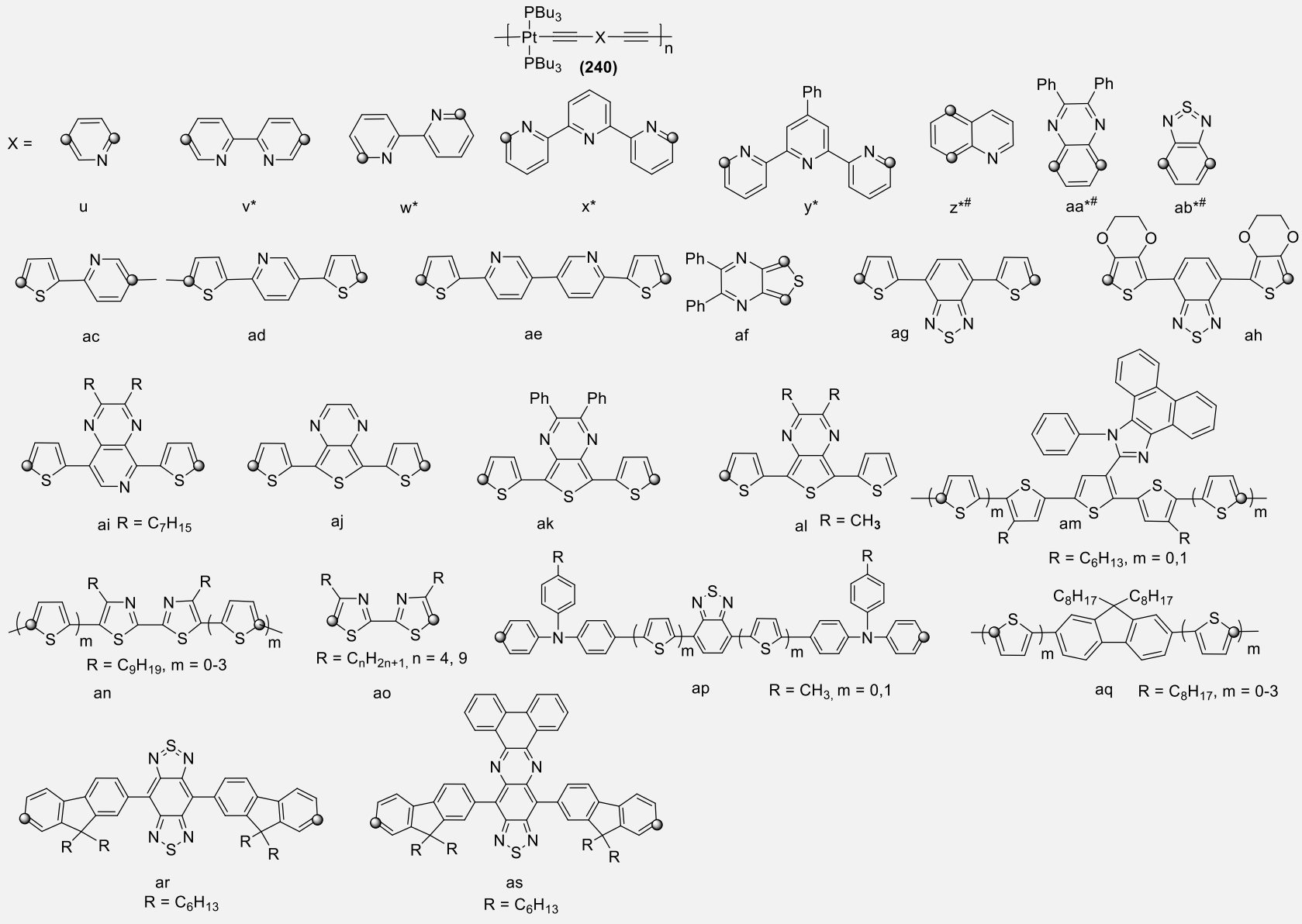
PBu3
Pt
X
n
PBu3
(240)
X =
u
v*
w*
x*
y*
z*#
aa*#
ab*#
ac
ad
ae
af
ag
ah
ai R = C7H15
aj
ak
al R = CH3
am
R = C6H13, m = 0,1
an
R = C9H19, m = 0-3
ao
R = CnH2n+1, n = 4, 9
ap
R = CH3, m = 0,1
aq
R = C8H17, m = 0-3
ar
R = C6H13
as
R = C6H13

Table 8. Photo-Physical Properties of Pt(II)-Poly-ynes Incorporating Carbocyclic and Heterocyclic Spacers.

Entry	GPC data				Photo-physical data					Electrochemical band-gap	
					Absorption (nm)	Emission (nm)					
	$\bar{M}_w$ (g/mol)	$\bar{M}_n$(g/mol)	PD	DP	$\lambda_{max.}^{abs.}$	$\lambda_{max.}^{fl.}$	$\lambda_{max.}^{ph.}$	Φ_P (%)	τ_P (µs)	E_g^{ec} (eV)	ref.
240a	74560	31780	2.35	–	310, 392	409, 431	550[a]	0.028	19.4± 0.7	–	[420]
240b	45700	43410	1.05	–	267, 291, 331, 342	369, 419, 456, 509[b]	455, 486, 501, 542	0.30[k]	24.6±0.6[c]	3.38	[451]
240c	40500	25500	1.6	–	376	413	528[f]	–	–	2.12-2.20	[424]
240d	30500	17900	1.37	–	344[h]	-	458[c]	–	2.6	1.7-2.0	[426]
240e	72000	40000	1.80	–	376	413	528	–	–	2.8-2.9	[424]
240f	10700	8590	1.25	–	284, 292, 326, 346, 360, 370[l]	395, 422[l]	455, 477, 490, 504, 525[l]	0.49	61± 1	3.19	[420,425]
240g	–	–	–	–	264, 390[l]	409[a]	526[a]	0.0025	55.3± 0.3	–	[420,425]
240h	13950 (OMe) 6660 (Cl)	13060 (OMe) 5550 (Cl)	1.1-1.2	16 (OMe) 8 (Cl)	248, 298,345[a] 249, 300, 344	369, 399, 418 370, 402, 419[b]	452-502	–	56.4 (OMe) 40.1 (Cl)	3.21 3.23	[452]
240i	10700	8590	1.25	–	324, 348, 370[l]	395, 420[l]	458, 483, 505, 540[l], 525[c]	0.47	0.280 ± 0.020	3.19	[425]
240j	45930	34410	1.33	–	258, 320, 350[a]	380, 400, 420[a]	458, 483, 505, 540[c]	0.47±10[c]	66 ± 1[c]	3.19	[425]
240k	21190	15 890	1.33	–	250, 294, 348[a]	404, 420[a]	454, 530, 570, 615[c]	0.14[c]	52 ± 2[c]	3.12	[425]
240l	20650	16900	1.22	–	272, 288, 374[a]	400, 422[a]	545[a]	315 ± 5[c]	0.016	–	[420]
240m	–	–	–	–	225-407[d]	–	606	–	–	2.80[d]	[453]
240n	181900	56180	3.24	–	457	–	744	–	–	2.55[d]	[453]
240o	82860	64560	1.28	–	470	–	812	–	–	2.40[d]	[453]
240p	25800 (S) 30900 (Se) 13900 (Te)	48200 (S) 64400 (Se) 51300 (Te)	1.87 2.08 3.69	–	418 431 448	438-460	617-671[a]	–	–	–	[429]
240q	401800	223200	1.8	–	447[e]	–	–	–	–	2.76	[454]

240r	422400	222300	1.9	–	464[e]	–	–	–	–	2.68	454
240s	52008	30500	1.7	–	428	–	–	–	–	2.70	434
240t	40836	29556	1.4	–	469	–	–	–	–	2.50	434
240v	89570	68900	1.3	–	311, 355-414[a]	426[f]	569[f]	–	–	2.9	455
240w	102170	60100	1.7	–	264, 296, 336-355[a]	-	462[f]	–	–	3.3	455
240x	129780	72100	1.8	–	288, 336[a]	-	462[f]	–	–	3.3	455
240y	156240	86800	1.8	–	256, 289, 345	-	462[f]	–	–	3.3	455
240ac	85420	–	–	–	430[h]	450-600[f]	646[f]	–	–	2.67	437
240ad	141467	–	–	–	453 [h] (430, 405)[d]	450-600[f]	691[f]	–	–	2.55	437
240af	14006	–	–	–	627[h]	715, 775	–	–	–	1.77[d]	385,427,438
240ag	41800	22 000	1.9	–	378, 563	683	–	–	1.1	2.07[i]	439
240ah	52800	33000	1.6	–	408, 621	717	–	–	1.2	1.93[i]	439
240ai	58200	23300	2.50	–	543-680	644[h]	–	–	–	1.97	442
240aj	7800	4000	1.95	–	543-680	-	–	–	–	1.54	442
240ak	9000	5000	1.80	–	543-680	-	–	–	–	1.49	442
240al	11100	5800	1.91	–	543-680	740[h]	–	–	–	1.66	442
240am	76280 (m=0) 58370 (m=1)	35430 (m=0) 20910 (m = 1)	2.15 (m=0), 2.79 (m=1)	26 (m = 0), 14 (m = 1)	259, 466 (m=0) 259, 459 (m = 1)[h]	531, 552 (m = 0), 560 (m = 1)	–	–	–	2.34 (m = 0), 2.28 (m = 1)	443
240an	28740-67930	15700-35570	1.83-1.91	10-34	452-481 [h]	497-603[h]	–	–	–	2.06-2.40	456
240ao	19790 (n=4), 67930 (n=9)	11 570 (n=4), 35 570 (n=9)	1.71 (n=4), 1.91 (n=9)	–	452-474[h]	496 (n = 4), 497 (n = 9)[h]	–	–	–	2.4	445
240ap	9550 (m = 0), 10690 (m = 1)	6840 (m=0), 6540 (m=1)	1.4 (m=0), 1.63 (m=1)	–	363, 484 (m = 0), 380, 539 (m = 1)[j]	665 (m = 0), 716 (m = 1)	–	–	–	2.06 (m = 0), 1.85 (m = 1)	446
240aq	14390-81440	7660-19340	1.9-4.3	5-19	307, 399 420, 439, 446, 463, 457[h]	439-549[h]	–	–	–	-	447
240ar	–	22620-5120	1.91	14	380, 666[h]	810	–	–	–	1.54	448
240as	–	22620-15120	1.71	9	372, 637[h]	776	–	–	–	1.65	448

[a]2-MeTHF at 29 8K, [b]at 290K in DCM, [c]at 77 K, [d]in solid state, [e]onset of absorption, [f]at 10 k, [g]16-18K, [h]at 298 K in DCM, [i]in THF, [j]at 293 K in DCM, [k]at 20 K, [l]2-MeTHF at 77 K

3.2.6.2. Complexes bearing *cis*-auxiliaries

3.2.6.2.1. Complexes bearing oligopyridyl auxiliaries

In the preceeding sub-section, we reviewed Group 10 metals-based oligo- and poly-ynes bearing phosphine auxiliaries. *Cis*- and *trans*-platina-ynes bearing mono- and oligo-pyridyl auxiliaries with fascinating structures, properties and applications are also reported.[270,272,279,322,457-461] Like phosphines, mono- di- and terpyridine impart intriguing chemical, optical and electrochemical properties, and stability to platina-ynes.[462] Furthermore, oligo-pyridiyl auxiliaries gives good opportunity to modulate the optical properties *via* aromatic ring functionalization. Although *N*-donor ligands greatly modulate electronic properties, solubility of the resulting materials is a major issue. The very first example of soluble Pt(II) di-ynes and poly-ynes incorporating alkylated *N*-donor auxiliaries in the *trans* geometry (**242**, Chart 29) was reported by one of us.[463] Using bulkier alkylated pyridine, Qu et al.[270] synthesized two new Pt(II) di-ynes flanked by D-A chromophores (**243a-b**, Chart 29). Both complexes showed absorption in visible region with emission in blue–green (**243a**) and orange-red (**243b**) region. They noted that Pt(II) diimine acts as weak donor and raises the HOMO levels upon coordination. Lalinde et al.[272] synthesised and assessed the properties of unusual mononuclear tris(alkynyl) complexes **244a-c** (Chart 29) bearing phenylquinoline ligand along with their binuclear cyclometallated derivatives. They found that when a brigded binuclear precursor [Pt(pq)(μ-Cl)]$_2$ (pq = Phenylquinoline) is treated with excess (8 eq.) lithiated arylacetylene followed by treatment with TBAB, it forms rare monoanionic complexes (NBu$_4$)[Pt(CCR)$_3$(Hpq)] (R = Tol **244a**, C$_6$H$_4$OMe-3 **244b**, C$_6$H$_4$CF$_3$-4 **244c**). However, when the stoichiometry is changed (3.0 equiv. of precursor), it formed cyclometallated dimeric compounds. Complexes **244a-c** showed excellent yellow-orange emission profile in the solid state with moderate PL parameters, the emission was attributed to an admixture of alkynyl−metal to pq ^{3}[(L′ + M)LCT] excited states.

Chart 29.

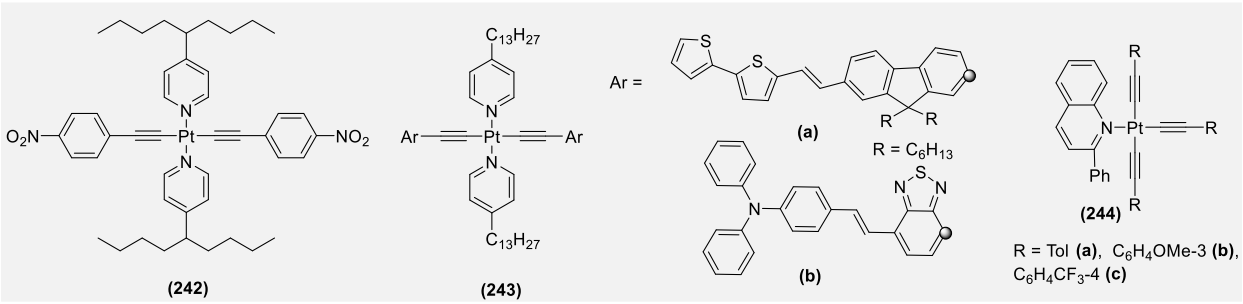

Pt(II) diimine (bis)acetylide chromophores have been a subject of intense research, owing to the presence of a ML/LLCT excited state with a relatively long lifetime. It has been demonstrated in several studies that the Pt(II) acetylide complexes bearing Bpy ligands possess luminescent properties (green to red) with bright emission and long lifetime.[460,464-468] Besides, the presence of metallophilic interaction in such complexes is advantageous and has significant impact on PL properties.[219] Several studies indicated that due to different extent of Pt–Pt interactions, planar *cis*-Pt(II) complexes exhibit remarkable vapochromism,[469-471] thermochromism,[472] and mechanochromism.[473-475] Moreover, due to the presence of two different modification sites (diiimine and acetylide units), the electron transport phenomena can be significantly

modulated.[476] In 1997, James et al.[477] published an initial study on the synthesis and characterization of Bpy supported *cis*-Pt(II) acetylide complexes. They noticed that the complexes were highly stable (even in the absence of supporting phosphine ligand). Later, the same group reported structural, photophysical and computational details of Bpy supported *cis*-Pt(II) acetylide complexes **245** (R = H, NO_2-4 and Me-4, Chart 30).[**478**] Depending the functionality, the complexes showed different absorption and electrochemical properties. For instance, solvatochromic Pt(II) → Bpy metal-to-ligand charge transfer (^{3}MLCT) bands in absorption spectra with HOMO localized on metal centre and LUMO on Bipy ligand were noted. Hua and co-workers[467] found that the complex **245** (R = H) in DCM emits at 560 nm with a quantum yield of 0.34 and a luminescence life-time of 1.36 μs.[467] Castellano and co-workers[479] demonstrated that σ-donor strength of the ethynyl ligands significantly affects the energy of excited state. They[467] and others[480] showed that PL properties of **245** (R = H) can be significantly improved *via* cyclization of the acetylide units. They found that **246 (**Chart 30), a cyclized analogue of **245** (R = H) has PL quantum yield and excited-state lifetime of 0.52 and 2.56 μs, respectively, at RT. They also noticed red PL with relatively long lifetime at RT (48.5 μs) in Pt(II) complexes when the phenyl ring was replaced by a pyrene unit **247a (**Chart 30).[481] Sun et al.[269] found that the insertion of 2-(benzothiazol-2'-yl)-9,9-diethylfluorene **247b (**Chart 30) fragment imparts solvatochromism and switches its excited state (acetylide ligand localized ^{3}π,π* → ^{3}MLCT on moving from more polar to less polar solvents). More interestingly, complex **247b** exhibited very broad and strong NLA behavior. Other researchers have also noted solvent dependent energy level and emission wavelength variation in Bpy complexes.[482,483]

The impact of the auxiliaries on the electronic and physicochemical properties in *cis*- or *trans*-Pt(II) acetylide complexes was investigated by Vacher et al.[261] Theyy judiciously attached redox-active ligand (tetrathiafulvalene, TTF) *via* acetylide linker and found that simple Bpy-based complex showed poor solubility compared to ^{t}Bu decorated Bpy **247c (**Chart 30) and other phosphine analogues. Due to the presence of TTF, they noted some unique optical and PL behaviour. For example, absorption spectra of complex **247c** in DCM showed four peaks spanning both UV and visible regions: at 229 and 294 (attributed to ^{1}π–π* transitions localized on the ^{t}Bu$_2$Bpy and the alkynyl-TTF fragments), at 380 nm (attributed to the superimposition of the absorption bands centered on the TTFs and Pt → ^{t}Bu$_2$Bpy ^{1}MLCT transition), and at 483 nm (attributed to (^{1}LL'CT) between the alkynylTTF and the Bpy fragments. These assignments differ remarkably from *cis*- and *trans*- phosphine-supported complexes. Furthermore, unlike other diimine Pt(II) acetylide complexes,[467] **247c** did not show any luminescence (even upon the addition of oxidants)**.** This quenching of luminescence was attributed to photo-induced electron transfer from the TTF unit toward the excited states localized on the Pt(II)–diimine fragments. Indeed, concentration-dependent self-quenching in Pt(II) acetylide complexes is well-known.[271,484] A similar solvent-dependent electron transfer quenching of the ^{3}MLCT excited state has been reported in phenothiazine (PTZ)-based Pt(II)-acetylide systems.[252] However, the replacement of electro-active units (PTZ or TTF) by a planar system gives opposite effects. For example, a very first report on RT phosphorescence (RTP) in square planar chromophore was reported by Castellano and co-workers.[279] They showed that naphthalimide based Pt(II) acetylide complex **247d**

(Chart 30) shows organic chromophore-based RTP with impressive lifetime (τ_p = 124 μs), high-quantum-efficiency (Φ_p = 0.215) at 621 nm in Me-THF. The first study on the effect of MLCT excitation on the vibrational frequency of an acetylide ligand was carried out by Schanze and co-workers.[485] By carrying out a detailed photo-physical investigation on a series of eight Pt(II)−diimine bis-acetylide complexes, they showed that Pt → Bipy MLCT excited state can be varied (up to 4000 cm^{-1} or 0.5 eV) by changing the substituents present on the 4,4'- and/or the 5,5'-positions of the Bpy ligand, which is much higher than other N,N-ligand based complexes.[466] However, majority of the complexes displayed energetically low-lying Pt → Bpy ^{3}MLCT state, some of them also featured transitions between π- and π*-type orbitals localized largely on the aryl acetylide ligands, i.e. transition from low-lying intra-ligand (IL) ^{3}π, π* excited state. Functionalization of diimine unit or acetylide-linked fragments is a common approach to modulate PL properties. In addition, it has been shown that the introduction of chirality on Bpy unit makes a significant impact on the PL properties. Zhang et al.[219] noted that when a chiral pinene unit is installed at 4,5-positions of Bpy core **248** (Chart 30), the resulting Pt(II) acetylide complexes show naked eye visible reversible mechanochromism (yellow to orange) and mechanoluminscence (orange to red). The lifetimes and quantum yield of complexes decrease upon mechanical grinding, attributed to the formation of Pt···Pt and/or π−π contact assisted aggregate formation.

Chart 30.

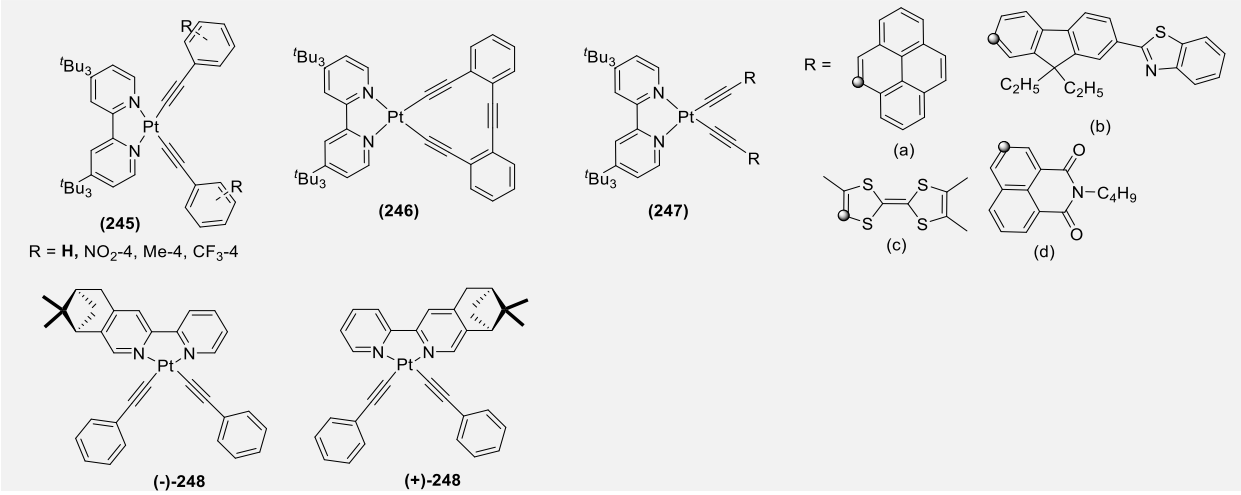

The first phenanthroline (Phen) ligand based *cis*-Pt(II) acetylide complex **249** (Chart 31) was reported by Che and co-workers.[486] They proposed that the excited-state energy of **249** lies between those of the di(cyanide) and the dithiolate complexes and shows ^{3}MLCT emission. To probe the effect of ligand variation on the nature of the excited state, Eisenberg and co-workers[466] carried out a comparative PL study of substituted Bpy and Phen-based Pt(II) acetylide complexes **250** (Chart 31). As discussed, these complexes too exhibited functional group dependent Pt d → $\pi^*_{diimine}$ CT transition and MLCT emission. It is worth noting that the lifetime of MLCT excited state is too short[487] even when an acceptor unit is attached to diimine ligand coordinated to $PtCl_2$. However, the attachment of a donor fragment like PTZ *via* an alkynyl linkage to the metal motif ($PtCl_2$) enhances the lifetime of excited state.[252,412,476,488] To find out the time-scale and

energy involved in such phenomenon, Sazanovich et al.[489] carried out a comprehensive study using Pt(II) acceptor–chromophore–donor frameworks (NDI attached to Phen as acceptor and PTZ as donor to metal). In addition to HE bands (330–400 nm) related to intra-NDI transitions, Complex **251** (Chart 31) showed a shoulder band at 480 nm assigned to MLL′CT (mixed MLCT/LL'CT) transitions. Combined combination of time-resolved infrared (TRIR) and femtosecond electronic transient absorption (TA) spectroscopic spectral results showed that the energy of ^{1}MLL'CT state was 2.6 eV while they assumed the energy of ^{3}MLL'CT as 2.5 eV. Results of electrochemical study showed that the energy of the charge-separated state (composed of reduced NDI and oxidised Phen–Pt–acetylide) was at ~ 1.5 eV while ~ 1.2 eV for final charge-separated state [NDI^{-}–Pt–PTZ^{+}]. They also showed a step-wise formation of the full charge-separated state on the picosecond time scale (~ 15 ps) while charge recombination *via* tunnelling occurs with two distinct time constants (36 ns and 107 ns), corresponding to the back-electron transfer to each of the two donor groups. **Chart 31**.

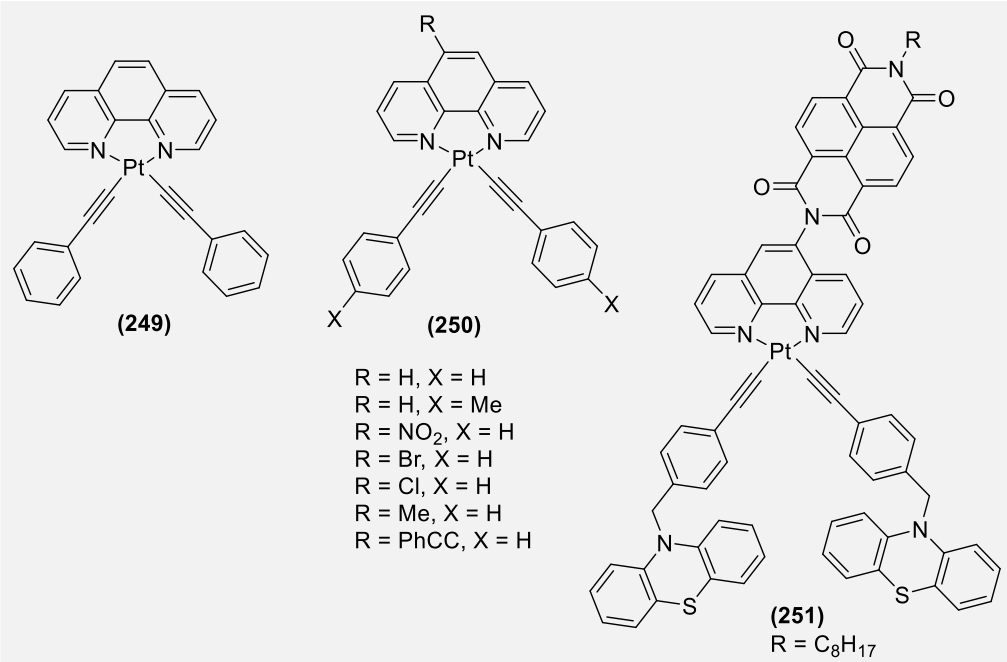

Following the remarkable work of Yam and co-workers[490] on cationic Pt(II) terpyridyl (Tpy) acetylide complexes **252** (Chart 32), several research groups synthesized and assessed photo-physical properties and application of Tpy-based Pt(II) alkynyl complexes.[462] The preparation, spectroscopy, photo-chemistry, and photophysics of Pt(II) chromophores bearing Bpy or Tpy has already been reviewed by Castellano and co-workers.[491] Using Bpy and Tpy auxiliaries, acetylide based ligand-localized triplet states can be sensitized to visible light.[481,492] As in other systems, substituents on the terpyridyl and acetylide ligands dramatically affect the excited state energetics of the complexes. In Tpy-based Pt(II) acetylide complexes, the LUMOs are localized on the Tpy unit while the HOMOs are dominated by the d(Pt) and the π(C≡CR) components. The lowest singlet excited state is generally regarded as a ^{1}MLCT/^{1}LLCT state and ^{3}MLCT is considered as emitting state.[493] Yam and co-workers[490] reported that for Pt(II) Tpy acetylide complexes with different auxiliary substituents on the phenylacetylide ligand, electron-donating substituents cause red shift

in their ^{1}MLCT/^{1}LLCT absorption band and ^{3}MLCT emission band, while an electron-withdrawing substituent induces blue shifts. Wu and Tung et al.[494] also discovered that in the 4'-tolylTpy Pt(II) acetylide complexes, one with the pentynyl ligand possesses a LE absorption band at about 441 nm, and the emission appears at 580 nm in DCM. In contrast, the ^{1}MLCT/^{1}LLCT transition was much broader for the complex with the phenylacetylide ligand ($\lambda_{max.}^{abs.}$ = 433 nm alonwith a shoulder at 482 nm), and the emission was observed at 619 nm. Shikova et al.[495] synthesized and compared the PL properties of Pt(II) Tpy acetylide complexes **253a-d** (Chart 32). They demonstrated that the nature of transition (mixed to pure MLCT or pure LLCT) is significantly determined by the σ-donacity of the substituents and the extent of conjugation. For example, the LE absorption band of complex **253a** having *t*butyl group attached to acetylenic unit was red-shifted compared to **253b** bearing triethylsilyl (TES) group. Similarly, emission maxima of **253c** & **253d** were red-shifted compared to **253a** & **253b**, while chlorinated analogue was non-luminescent. Complexes **253a-d** exhibited broad structureless PL in the range of 475-800 nm with quantum yield between 0.03 to 0.17, and a lifetime between 1-3 µS. In addition, the value of k_{nr} was enhanced by a factor of 2.2 compared to Bpy analogues[483,485] attributed to electronic coupling of acetylide ligand with metal. The replacement of phenyl from **253c**[495] by a Bpy unit **253e**[496] enhances the lifetime (5.8 µs at RT) and quantum yield (0.22). The values of k_r and k_{nr} for **253e** and **253c** were quantitatively same and larger than bis-phosphine complex, indicating ^{3}CT-based parentage of the emitting excited state. The excited state lifetimes of Tpy-based complexes (at 77 K) were lower than phosphine counterpart. Castellano and co-workers[497] investigated the photo-physics of peryleneacetylide Pt(II) CT complexes bearing Bpy/ Tpy cores and compared them with their analogous CT (**253c** and **245** (R = H)) and ^{3}IL (Bpy and dppe decorated) model chromophores. Comparison of the absorption spectra of **253f** and **253c** shows that the attachment of the peryleneacetylide chromophore substantially affects the position of the CT transitions (the CT transitions are red shifted by several thousand wavenumbers) relative to the corresponding phenylacetylide structure. Like others, the lowest energy excited state in these complexes was triplet in nature. However, unlike ^{3}CT photo-physics of Pt(II) Tpy and Bpy acetylide chromophores, these complexes exhibited ^{3}IL excited state localized on the peryleneacetylide(s). The complexes in this study are unique in that long-lived excited states are produced without generating any corresponding PL, which may be desirable under certain circumstances.

Chart 32.

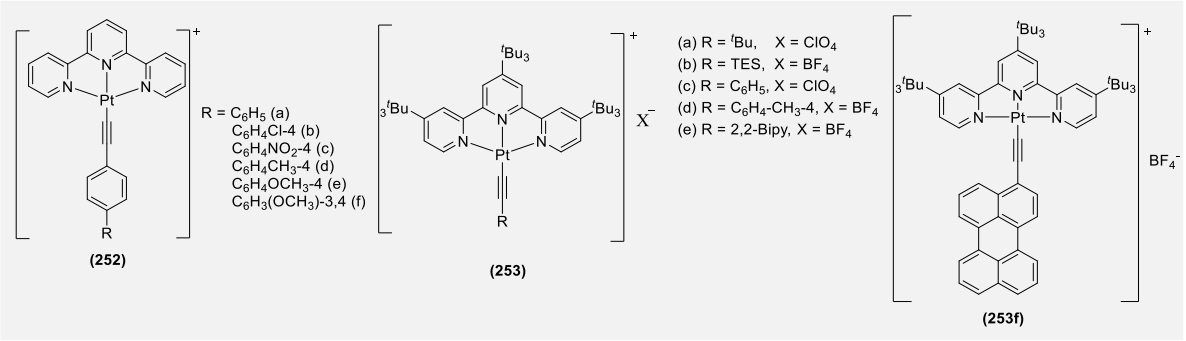

3.2.6.2.2. Complexes bearing bidentate (C^N or C^C) and tridentate (C^N^N, N^C^N or C^C^N) auxiliaries

Square planar cyclometalated Pt(II) complexes bearing bi- and tridentate cyclometalating and arylacetylide ligands have drawn great attention owing to their rich PL properties and multi-dimensional applications.[223,274,465,492,498-509] These complexes, depending on the type of cyclometalating ligands[510] used, are divided into (a) bidentate *(viz* C^N or C^C*)* and (b) tridentate *(*C^N^N, N^C^N, C^C^N, C^N^C etc.*)* cyclometalated complexes. Due to some inherent features associated with these ligands, they endow the complexes with unique properties and applications. For example, a C^C chelate backbone presents a strong ligand field to the Pt(II) center, raises the energy of non-radiative d-d excited states, reduces the possibility of non-radiative d-d transition and thermal quenching.[511] On the other hand, N^N motifs have been associated with achieving high efficiency green light emission at ambient temperature.[512] Similarly, C^N^N ligand is a stronger σ-donor and a better π acceptor.[513] The PL properties and CT transition bands in such complexes can be modulated by the smart functionalization of cyclometalating ligand.

As reported in the literature,[514] the quantum yield of a non-alkynylated (C^N^N)PtCl complex is 2.5%, which increases slightly (4%) upon the replacement of chloride with a phenylacetylide.[492] Seneclauze et al.[515] synthesized various phosphorescent ethynylfluorene or ethynylcarbazole-linked cyclometallated C^N^N complexes and found that the solubility and extent of delocalization could be tuned by the ethynyl segment.[515] Absorption studies in DCM showed admixture of MLCT and LLCT (alkynyl-to- C^N^N ligand-to-ligand charge transfer) peaks at ~ 445 nm in fluorene derivatives (**254a** and **254e,** Chart 33) which was red shifted (~ 479 nm) in the case of carbazole analogues (**254d** and **254f**). A large shift in this band for their dinuclear analogues (**255** and **256**, Chart 33) indicated enhanced electron delocalization between the termini. Despite the fact that fluorene analogues **254a, 254e** and **255** showed red phosphorescence in fluid solution (Φ = 0.1% to 1%, t = 1.5-39 ns), carbazole derivatives were found to have inefficient emission profile, attributed to intra-molecular electron transfer involving the tertiary amine of the carbazole subunit. Furthermore, the increase in charge density was responsible for the decrease in excited state lifetimes due to the occurrence of non-radiative deactivation pathways.

Chart 33.

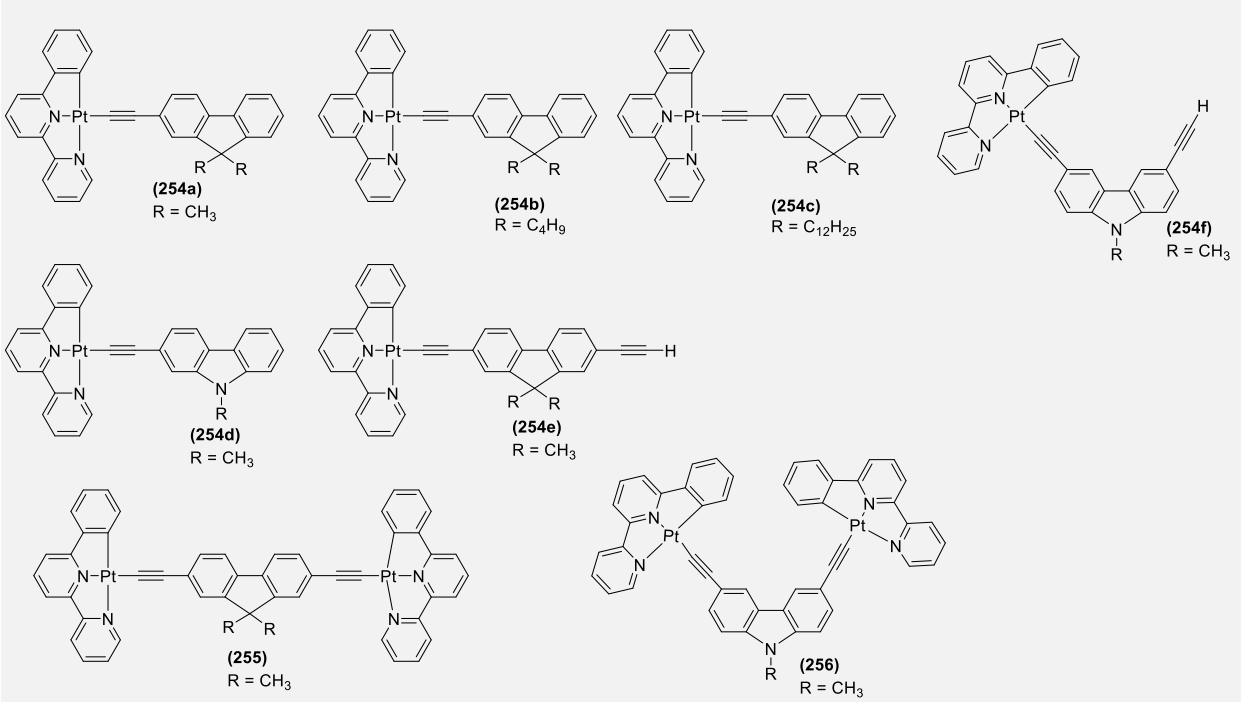

Unlike Tpy based complexes, there is no substantial contribution of the acetylide unit in the excited state properties of C^N^N based complexes (except for the enhancement in the HE region assigned to $^1\pi-\pi^*$ transitions).[493,512] However, it enhances the PL efficiency. Sun and co-workers[516] showed that the introduction of 9,9-dihexylfluoren-2-yl substituent to the 4-position of a C^N^N ligand **(257-258**, Chart 34) introduces ILCT with some ^{3}MLCT character into the lowest excited states of the complexes with longer triplet excited-state lifetimes and higher quantum yields. In addition, the introduction of electron donating fluorenyl unit was also reported to enhance the excited-state absorption cross-section, a highly important parameter for NLO devices. The reported complexes exhibit strong $^1\pi,\pi^*$ absorption bands in the UV region, and a broad, structureless CT band in the visible region, which further broadened and shifted to the red upon alkynylation.

Chart 34.

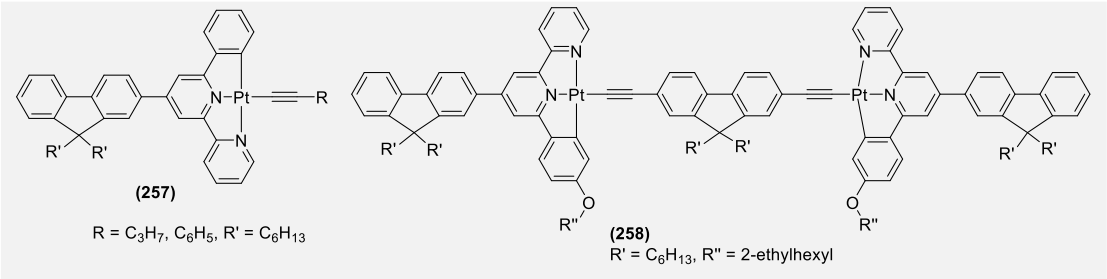

Replacing the fluorenyl by phenyl at position 4 and introducing alkoxy substituent on phenyl ring at position 2 connected to central pyridinyl of a C^N^N cyclometalating ligand improve the solubility and PL properties.[492,493] The introduction of an electron donor group enriches the electron density of the 6-phenyl

ring, leading to the occurrence of admixture of the ILCT character into the lowest excited states. Notably, complexes **259-260** (Chart 35) showed a very high emission quantum yields in DCM (Φ_{em} = 0.15-0.21). Despite the beneficial consequence of the alkoxyl substitution, Sun and co-workers[493] claimed that it would be unnecessary to convert the chloride ligand into acetylide ligand for NLO application as the ancillary acetylide ligand did not influence the triplet excited-state characteristics profoundly.

Chart 35.

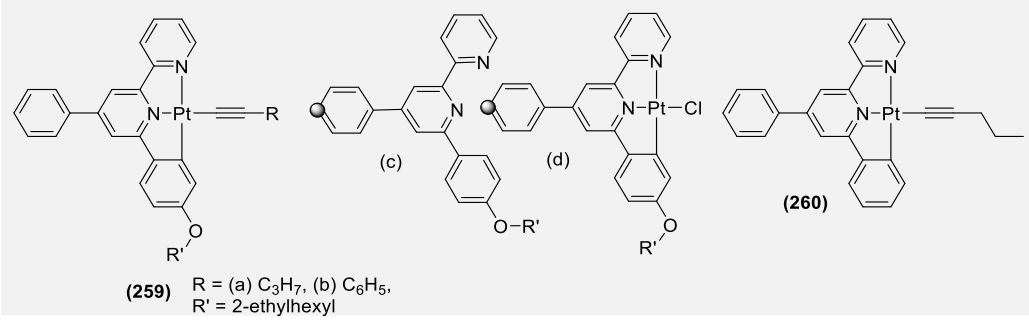

(259) R = (a) C_3H_7, (b) C_6H_5, R' = 2-ethylhexyl

To achieve phosphorescent Pt(II) complexes, one strategy is to replace one of the pyridines of an N^C^N ligand (6-phenyl-2,2'-bipyridine, **261**) by an azole-based donor (**262**, Chart 36). This modification significantly modifies the charge, intermolecular interactions and excited state characteristics of the resulting complex.[517] Not only the azole introduction in C^N^N complexes improves the PL yield, but also the replacement of conventional C^N^N ligand (with fused five-five-membered chelation) by C^N*N ligand (fused five-six-membered) leads to a remarkable improvement in phosphorescence efficiency. Huo and co-workers[518] reported cyclometalated Pt(II) complexes **(263-265)** (C^N*N)PtL (L = acetylide) (Chart 36) with geometry close to ideal square planar. Even though this geometric variation did not increase the rigidity of the molecule, the complex with acetylenic unit demonstrated remarkable emission profile at RT. Compared to performance of **262** (Φ = 4%)[492], an exponential rise has been noted in complex **263** (Φ = 56%). This remarkable enhancement in the performance was attributed to stronger field effect exerted by C^N*N ligand. Furthermore, it has also been proposed that the absence of Pt−Pt or π−π interactions, which is the main cause of ACQ, (due to perpendicular *N*-phenyl ring and the twisted acetylide groups) might have also contributed to enhanced quantum efficiency. Following this work, the same group reported that fused five-five-membered C^N^N metallacycle can also produce high PL efficiency. Despite the fact that pyrazoles are weak acceptor than pyridyl unit, they demonstrated that Pt(II)-acetylide complexes based on *N*,*N*-diphenyl-6-(1H-pyrazol-1-yl)pyridin-2-amine **266** (C*N^N)- and 2-phenyl-6-(1H-pyrazol-1-yl)pyridine **267** (C^N^N) ligands (Chart 36) shows intriguing structure and improved emission profile.[512] Like previous example, C*N^N-coordinated Pt(II) complexes adopted closer to a square planar geometry while the C^N^N-coordinated complexes adopted a nearly perfect planar geometry. Interestingly, absorption study of **267** in DCM showed unique ^{3}LC peak at 497 nm, which otherwise were absent in other chlorinated and acetylenic complex **266**. Similarly, **267** emitted a strong green light at RT and possess PL characteristics (τ_o < 5.2 μs, Φ = 62%) better than related acetylenic complex **266** (τ_o < 8.6 μs, Φ = 43%) and other complexes. This enhancement in the efficiency was attributed to the more rigid fused five–five-membered metallacycle and

minimal geometric distortion of the triplet state. Using experimental and theoretical tools, it was found that the lowest singlet and triplet excited states were admixture of one or more CT transitions (ILCT, MLCT, and LLCT).

Chart 36.

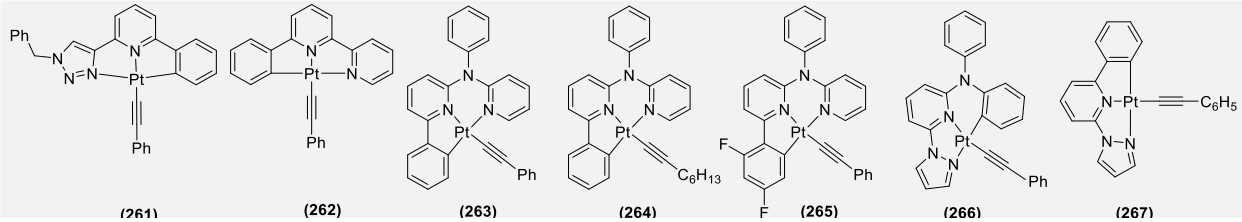

In the previous example, it has been shown that the lack of Pt−Pt or π−π interactions endows materials with high PL efficiency. However, in some cases, the scenario is different. For example, Che et al.[519] reported that (N^C^N) based cycloplatinated complexes **268(a-h)** (Chart 37) form photoresponsive supramolecular organometallic nanosheets due to Pt(II)···Pt(II) and CH···π(C-C) interactions. The resulting self-assembled quasi-2D nanostructures display NIR phosphorescence and light-modulated conductivity. The reported complex, depending upon the combinations of D-A moieties showed a range of colors in the solid-state (Figure 29). H-bond induced 2D or 3D architectures supramolecular assembly have also formed in anionic complexes $(NBu_4)[Pt(C^N^C)X]$ (HC^N^CH) 2,6-diphenyl pyridine) **269** (Chart 37) containing acetylide (X) C≡CR) R = Bu, Ph, Tol, Ph-4-OMe).[520] The electronic absorption spectra of **a-d** were dominated by IL ππ* and MLCT transitions. However, these complexes were emissive (concentration-dependent) only at low temperature. The emissions at 77 K are sensitive to solvent concentration. In dilute glassy solutions, complexes exhibit highly structured bands, assigned to a metal-perturbed ^{3}ππ* excited state. In addition to this, other N^C^N based cycloplatinated complexes have also been investigated and reported with NIR emission profile.[521]

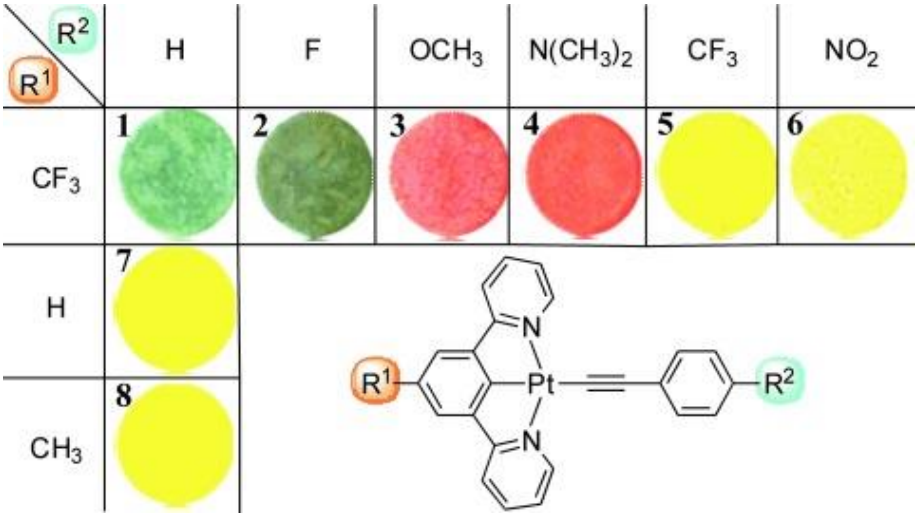

Figure 29. Solid state colors of complex **268**. Reprinted with permission from ref [519]. Copyright 2009 John Wiley and Sons.

Chart 37.

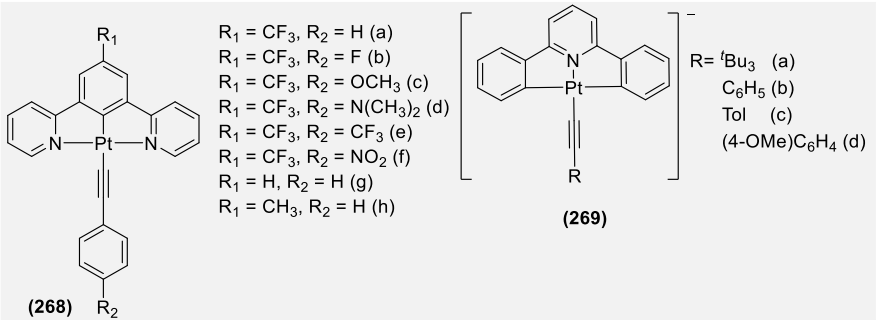

3.2.6.2.3. Complexes bearing *N*-heterocyclic carbene (NHC) auxiliaries

Pt(II) acetylide complexes bearing mono- and bidentate NHC auxiliaries in both the *cis*- and *trans*-dispositions are available in the literature. Venkatesan and co-workers[522] reported the first examples of *cis- and trans*-NHC Pt(II) acetylides **270**-**271** (Chart 38).[522] The *cis*-complex **270** was the kinetically favored, while the *trans*-counterpart (**271**, Chart 38) was thermodynamically favored product. The properties of the NHC-bearing Pt(II) acetylide complexes are very different from those of the non-emissive phosphine and the green-emitting diimine bearing complexes. The authors functionalized NHC core by alkyl group to enhance the solubility. The resuting complexes exhibit phosphorescence in solution and in the solid state at RT as well as in frozen glass at 77 K. The emission in the NHC bearing complexes were found to be a mixture of metal-perturbed ^{3}IL with a small contribution from ^{3}MLCT. The emission wavelength and quantum yields were highly tunable as a function of the alkynyl ligand. Interestingly, a spin-coated film (10 wt% in PMMA) of one of the complexes **271b** exhibited a high Φ_P value (80%), which is highest among Pt(II)-based deep-blue emitters.[522] Schanze and co-workers[523] demonstrated that although both *trans*-Pt(II) complexes bearing phosphine/NHC auxiliaries have similar optical profiles, the extent of SOC in the carbene complexes **272** (Chart 38) was less than the phosphine counterparts. The X-ray structure data suggested that there is a slightly greater interaction between the metal center and the alkynyl ligand in the phosphine complexes relative to the carbene congeners.[523] However, carbene complexes have had higher Φ_F, τ_P and Φ_P.

Chart 38.

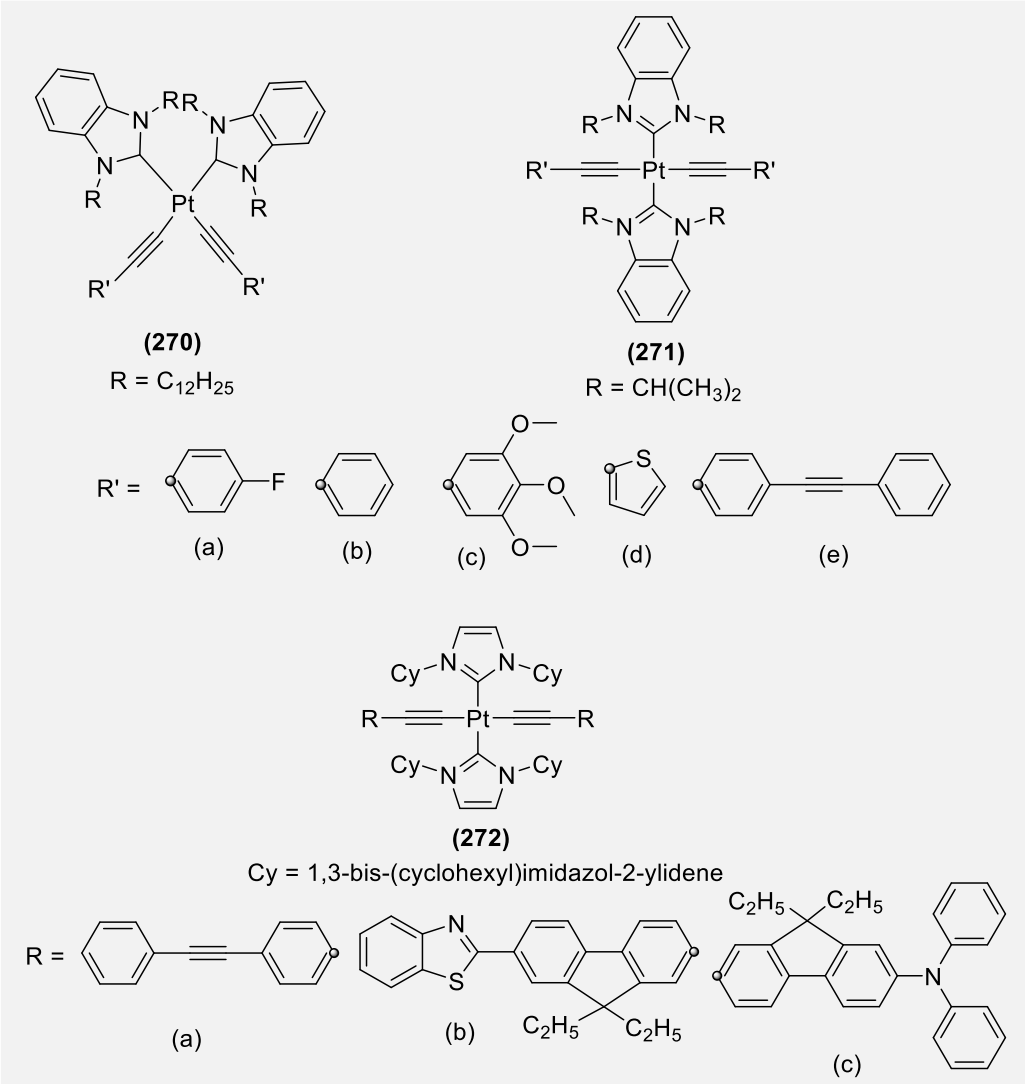

Recently, Zhang et al.[278] demonstrated that NHC as well as alkynyl ligand exert a major effect on the excited states of the complexes. Using a series of acetylide ligands with different electronic structures, the phosphorescence emission efficiencies and resulting emission profiles were tuned. (deep blue emission in the solid state). They found a moderate electronic influence of the *bis* NHC ligands on the emission quantum yields and a strong influence exerted by the pyridyl NHC ligand. Due to change in the CT character of the T-manifold, the quantum efficiencies of complexes **273** and **274** (Chart 39) were significantly lower compared to **275**, attributed to change in the CT character of the triplet manifold. The emission was ascribed to metal perturbed ^{3}LLCT(πalk → π*alk) in the case of *bis* NHC complexes and an admixture of metal perturbed ^{3}LLCT(πalk → π*alk) and ^{3}MLCT (Pt → π*alk) in complexes bearing pyridyl-NHC ligands. Prior to this work, Schnaze and co-workers[370] reported a series of square planar bis-*N*-heterocyclic carbene Pt(II) bis-arylacetylide complexes **275** (Chart 39) exhibiting ^{3}IL based phosphorescence with MLCT characters.

Chart 39.

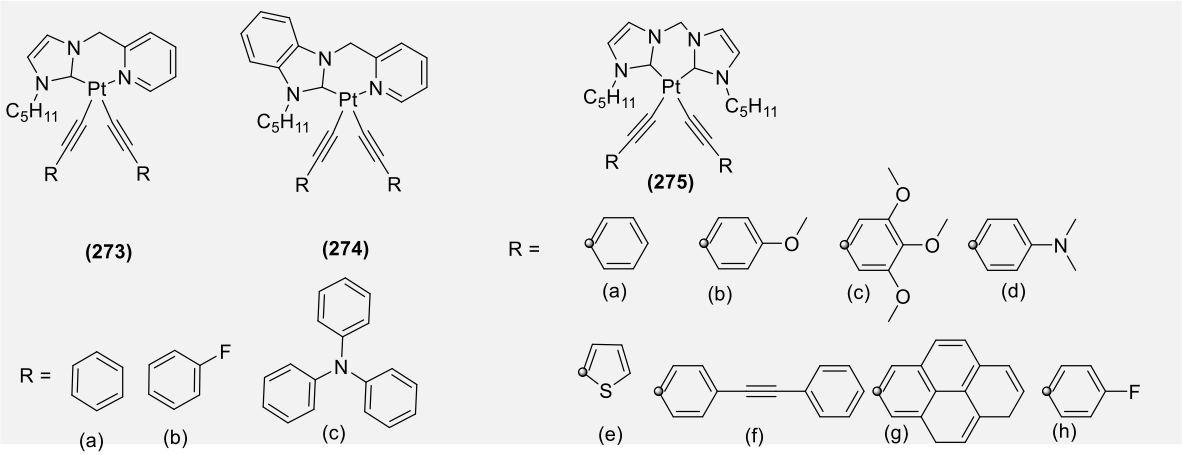

In another recent work, Venkatesan and co-workers[275] combined the strong σ-donor property of the NHC ligands with intermolecular interactions property Pt(II) to achieve single molecule white light triplet emitter. They reported the first Pt(II) *bis*-alkynyl complexes **(276a-d)** (Chart 40) ligated to C^N ligand (pyridine NHC ligands) having ability to emit white light with high purity. The complexes displayed a strong band at wavelengths below 300 nm and a moderate intense absorption band at 320−420 nm, which shifted depending on the substituents attached to alkynyl ligand. Yam and coworkers[524] reported the cyclometalated *bis*(carbene) Pt(II) complexes **277** (Chart 40) bearing functionalized alkynyl ligands. These complexes exhibited alkynyl-dependent emission energy with strong phosphorescence (^{3}MLCT/^{3}LLCT) in degassed MeCN. Furthermore, the incorporation of these alkynyl groups was thought to play an important role in the luminescence enhancement.[524]

Chart 40.

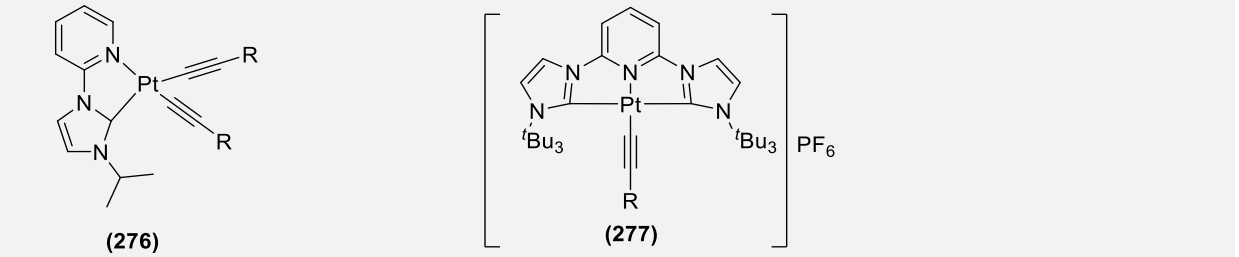

3.2.7. Group 11 metalla-ynes

d^{10} Metal-alkynyls constitute an interesting class of molecules with diverse applications in the area of catalysis, sensing, electronics and drug discovery.[525-531] d^{10} Metals (Cu, Ag and Au) feature metallophilicity and flexible binding modes, which are not so common among metals of other groups. Several homo- and hetero-metallic cationic and alkynyl clusters based on group 11 metals have been reported in the past and are still being explored,[532-537] but literature on σ-acetylide complexes containing Cu(I) and Ag(I) is

limited.[538,539] This is, in part, due to the instability of the compounds, which hampers the handling, characterization and application of the materials in devices. Cu(I) and Ag(I) acetylides are heat/shock sensitive explosive materials. Several groups have synthesized and investigated the properties of Au(I) σ-acetylide polymers but faced difficulties during handling due to their low solubility in organic solvents.[540-545] Despite these challenges, researchers continue to explore new synthetic methodologies and techniques to stabilize these materials under ambient condition. For example, Seifert et al.[546] reported the synthesis and structural characterization of bis(acetylide) metallates(I) of the coinage metals with the general formula $[K(THF)_n(18\text{-crown-6})][R\text{-}C{\equiv}C\text{-}M\text{-}C{\equiv}C\text{-}R]$ (M = Cu, Ag, Au) with varying substituents R (R = Fc, Ph, ^{t}Bu). (Chart 41, Figure 30a-c, **278**) Prior to this, Wu and-co-workers[547] noticed the unprecedented formation of Ag-incorporated oligo-ynes on an Ag(100) surface. However, none of them reported photo-physical properties of the synthesized materials. In a recent work, Belyaev et al.[548] found that reaction of a phosphine $(2\text{-}PPh_2C_6H_4)_3P$ with polymeric Cu(I)phenylacetylide $(CuC_2Ph)_n$ in 1:1 molar ratio produces the yellow mononuclear complex **279** (Chart 41) in high yield. At RT, the solution of complex **279** was non-luminescent; however, in the solid state (Figure 30d), it displayed a broad emissive band of low intensity (Φ = 0.03) in the orange-red region (635 nm).

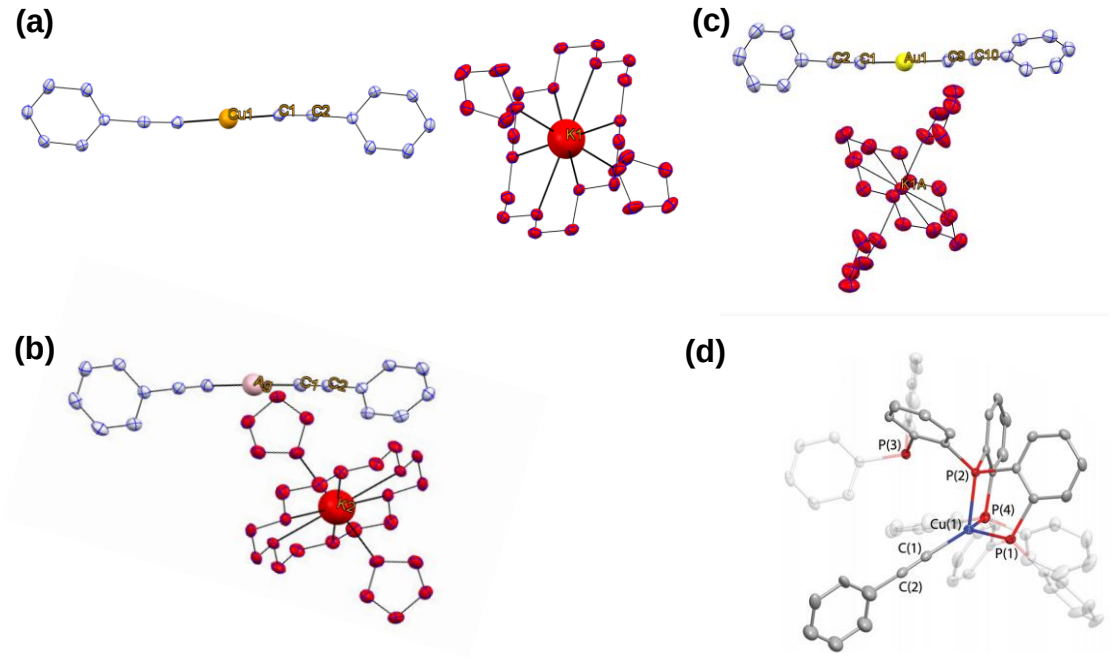

Figure 30. Solid state structures of **278** M = Cu (a), Ag (b), Au-alkynyls complexes. Reproduced with permission from ref [546]. Copyright 2017 Elsevier Ltd. Solid state structure of **279**. Reprinted with permission from ref [548]. Copyright 2016 American Chemical Society.

Chart 41.

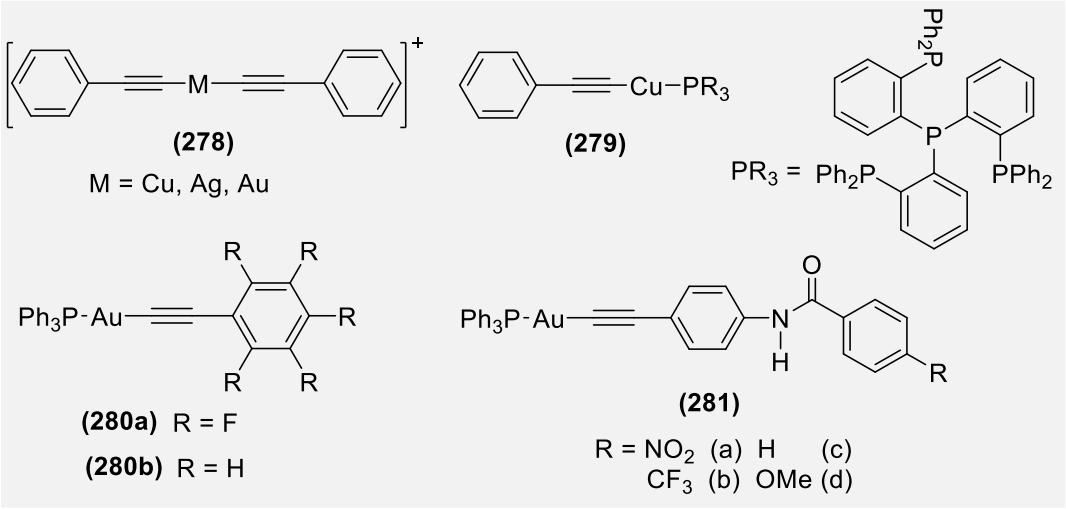

In the case of Au(I) σ-acetylides, aurophilicity is the main role-player which largely controls the morphology of molecular assembly and PL properties.[549] Research on Au(I) alkynyl complexes started back in 1960s with the synthesis of Au(I)-oligomers and polymers $[Au(C{\equiv}C^tBu)]_n$, an analogue of Cu(I) acetylide $[Cu(C{\equiv}C^tBu)]$.[550] In this very initial study, authors suggested the tetrameric structure for the complexes. However, Mingos and co-workers[551] demonstrated highly unusual catenate structure of $[Au(C{\equiv}C^tBu)]_n$ with intriguing aurophilicity. In 1967 Corfield and Shearer[552] reported the first structurally characterized Au(I) σ-acetylide complex (^{i}PrNH$_2$)AuC≡CPh. The complexes formed by phenylethynyl Au(I) with amines tend to be sparingly soluble in inert solvents. Following this, several other reports also emerged on the synthesis and structural characterization of Au(I) acetylides. For example Au(I) acetylide complexes bearing simple aryl phosphine (**280a-b** Chart 41) and bulky phosphines were investigated.[553-555] Tunik and co-workers[556] found that in NHC-supported mono and bisalkynyl Au(I) complexes, the morphology of the crystals are controlled by intermolecular interaction. Furthermore, an inverse relationship between the Au···Au distance and emission energy was also observed (the shorter the aurophilic contact, the higher the emission energy). Chao et al.[528] reported mononuclear Au(I) acetylide complexes having substituted (4-benzamidophenyl) moiety (**281a-d**) (Chart 41). Complexes (**281b-d**) (Chart 41) shared almost similar absorption spectra with one shoulder (ca. 296 nm) and three additional bands (*ca*. 268, 277 and 312 nm). The introduction of electron withdrawing substituent (**281a)** caused only a minor shift of the bands with emergence of an extra low energy CT band at 330 nm. Except **281a**, all complexes exhibited luminescence in the solid state and in degassed THF solutions in the visible region at 298 K with an Φ_{em} between 0.0042-0.0102 (THF). The emission in the complexes was attributed to the $^3\pi\pi^*$ excited state of the acetylide ligand. Yam et al.[527] reported the presence of alkynyl core sensitive vibronically structured absorption bands in Au(I) complex bearing 1,5-diethynylnaphthalene ligand (**282**, Chart 42). The bands were attributed to the IL [π→π* (C≡C)] or [σ(Au-P)→π*(C≡C)] transitions. The emission profile of the complex **282** exhibits intense emission bands at 563-568 nm and 571-595 nm in solution and in the solid state, respectively. As expected, both the

absorption and emission bands in these 1,5-diethynylnaphthalene complexes were shifted to the red compared to their phenylene counterparts.[525]

The impact of molecular topology on PL properties was investigated by Che and co-workers.[557] Using different oligo(*o*-PE or *m*-PE) **(283-287**, Chart 42**)**, they demonstrated that except **284** and **286** (n = 1), which showed phosphorescence only, all complexes exhibit ligand-centered dual emissions. The attachment of a metal fragment $[Au(PCy_3)]^+$ induced the *heavy atom effect* and "*switched-on*" the $^3\pi\pi^*$ emission of the PE ligands. Besides, they also found that both the prompt fluorescence (PF) and delayed fluorescence (DF) contribute to the emissions. Furthermore, the efficiency of a triplet-triplet annihilation (TTA) was affected by both the topology and the extension of the OPE length. In a recent study, Chang et al.[558] carried out extensive PL studies on OPE bridged Au(I) complexes (**288-289**, Chart 42**)** to establish the relationship between the chromophore-metal distance and their emission properties. They systematically synthesized Au(I) complexes (**288-289**, Chart 42**)** and showed that the value of the $S_1 \rightarrow T_1$ ISC rate constant (k_{isc}) decreases with increase in effective distance between Au(I) and the center of the emitting ππ* chromophore. Furthermore, they also showed that the phosphorescence in these systems could be harvested following an alternate mechanism[559,560] and bypassing the slow $S_1 \rightarrow T_1$ ISC pathway. Overall, the results of this study was well complemented by the results of Ma et al.[561] who found an inverse relationship between the k_{ISC} and conjugation length in Au(I) complexes (~ 2 orders decrease in k_{ISC} with increasing π-conjugation).

Chart 42.

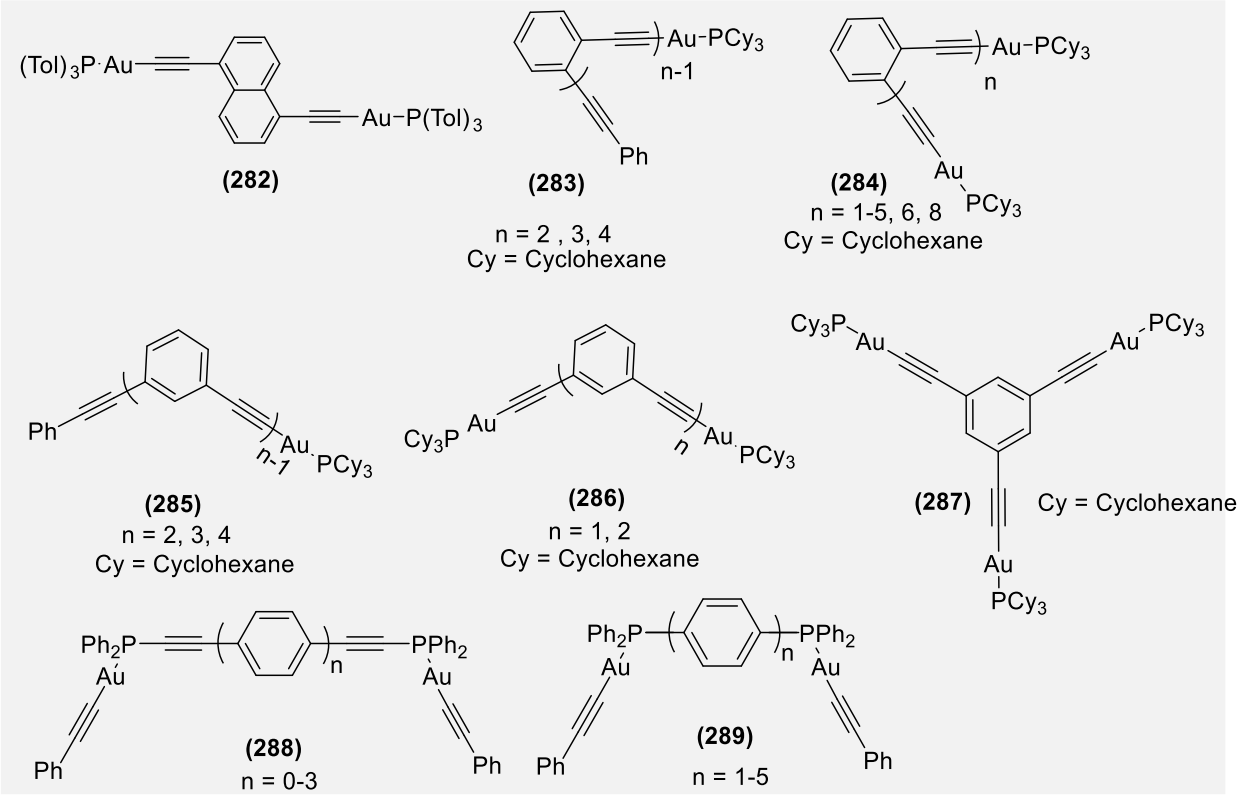

Rodríguez et al.[562] investigated the correlation between the Au(I)···Au(I) distance and the emission quantum yields and decay times in complex **290a** (Chart 43**)**. These complexes showed the same relationship between the metal centers and PL properties. The radiative rate constant as well as emission quantum yield varies inversely with Au(I)···Au(I) distance. The emission color, behavior and molecular arrangement of the metal complex largely depend on the ligands as well as position of the ligand attached to the metal. In a recent work, Yao et al.[563] reported PL properties of anthracene-based binuclear Au(I)-diphosphine acetylide complexes **290b** (Chart 43**)**. These binuclear complexes were achieved *via* depolymerization of the corresponding polymeric Au(I) acetylides $(C_{14}H_9C{\equiv}CAu)_n$ ($C_{14}H_9C{\equiv}CH$ = 9-ethynyl anthracence) with diphosphine ligands of different length. Though complexes in DCM solution showed only fluorescence, both phosphorescence and fluorescence emissions were observed in the solid state. The absence of phosphorescence in solution was attributed to, other than oxygen, the presence of flexible linkers connecting two metal fragments. Solid state structural studies show that the complex with shortest linker length formed 1-D zigzag chain through Au···Au interaction. However, when two Au(I) units are attached to the 9,10- positions of anthracene moiety (**291a,** Chart 43), it exhibited rare non-covalent intermolecular Au···H−C interactions, leading to the formation of a supramolecular 2D network.[564] On the other hand, their counterparts **291b** and **291c** (Chart 43) form 1D-polymeric chain *via* C−H···π and π···π interactions and intramolecular Au···H−C interactions, respectively. Furthermore, complex **291a** exhibited high fluorescence together with high quantum yield compared to weakly fluorescent **291b** and **291c**, attributed to more perturbation of Au(I) on π system. The perturbation by the metal as well as by the substituents is also reported in the tetracene-based binuclear Au(I) complexes **292** (Chart 43).[565] Compared to anthracene, the attachment of a metal fragment to the tetracene through acetylide shows a pronounced effect on the structure and PL properties. For instance, a significant red shift in the absorption/emission of binuclear complexes **292** were observed compared to its TMS-protected ligand (Figure 31a). In addition, emission studies also indicated that the presence of two metallated ethynyl groups exerts more perturbation than a single metal. Comparatively, the extent of perturbation was lower in Au(I) complexes compared to the Pt(II) counterparts. The crystal structure analysis of Au(I) complex having methyl group at the termini showed aurophilic attraction leading to the formation of honeycomb like structure (Figure 31b). Jin et al.[566] showed that the phosphorescence in Au(I) acetylide **293** (Chart 43) can be controlled by tuning aurophilicity and molecular rotation. Using state-of-the-art methods, they showed that green emitting complexes exhibit reversible luminescent color changes between 298 to 193 K. In a recent study, Patra et al.[567] demonstrated that the PL properties of the Au(I)-systems can also be modulated by varying electronic property of the central aromatic core. They showed that the insertion of an electron-withdrawing unit (*viz* BTD) as the central spacer in fluorene-based complexes **294(a-c)** (Chart 43**)** moves the absorption and emission towards the red, evidently due to the creation of the D-A system. Interestingly, one of the reported complexes **294c** and its corresponding ligand emit in the yellow, thus opening a class gate of emissive small molecules. As expected, solutions of these complexes showed phosphorescence at low temperature only (**Table 9**).

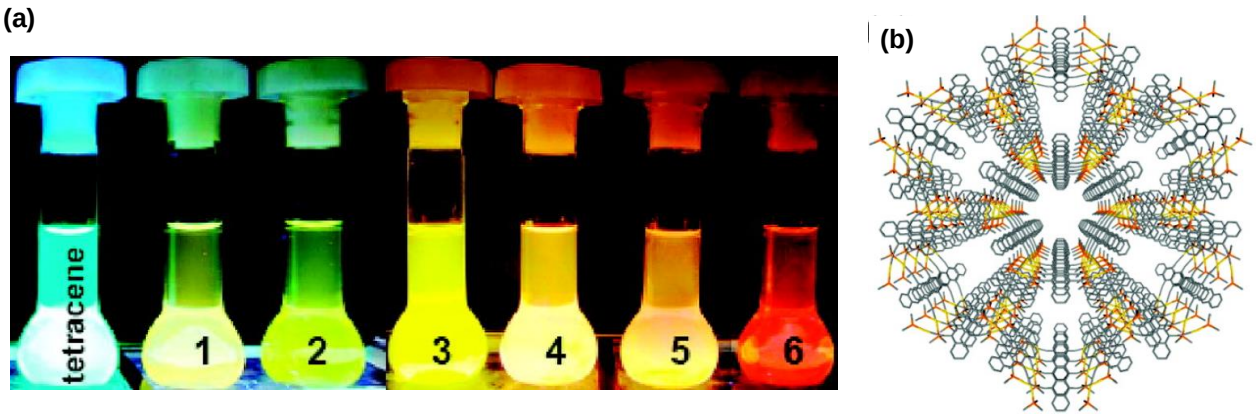

Figure 31. (a) Image showing shift of emission colors of the metallated tetracene and diethynyl tetracene. Photograph labelled as **1** and **2** shows solutions of metallated tetracene (bearing $Pt(Et_3)_2Br$ and $AuPPh_3$ fragments without alkynyl moiety). Photograph labelled as **3**-**6** shows tetracenyldiacetylide complex **292** (**3**: R = TIPS; **4**: R $AuPPh_3$; **5**: R = $AuPMe_3$; **6**: R = $Pt(Et_3)_2I$). (b) Honeycomb-like framework formed by complex **292** (R = PMe_3) showing the open channels. The network is supported by aurophilic interactions. Reprinted with permission from ref [565]. Copyright 2010 American Chemical Society.

Table 9. Lifetime values for Au(I) acetylide complex **294a-c.** Reproduced with permission from ref [567].

Compound	Fluorescence lifetime (ns)			Phosphorescence lifetime (μs)
	τ (A_1)	τ (A_2)	τ_{av}[a]	
294a	0.42 (98%)	0.99 (2%)	0.43	766
294b	0.73 (70%)	1.05 (30%)	0.83	1211
294c	0.85 (19%)	3.12 (81%)	2.69	1931

[a]The average lifetime (τ_{av}) was calculated using the equation, $\tau_{av} = (A_1/(A_1 + A_2))\ \tau_1 + (A_1/(A_1 + A_2))\ \tau_2$, where A_1 and A_2 are the contribution from each component.

Chart 43:

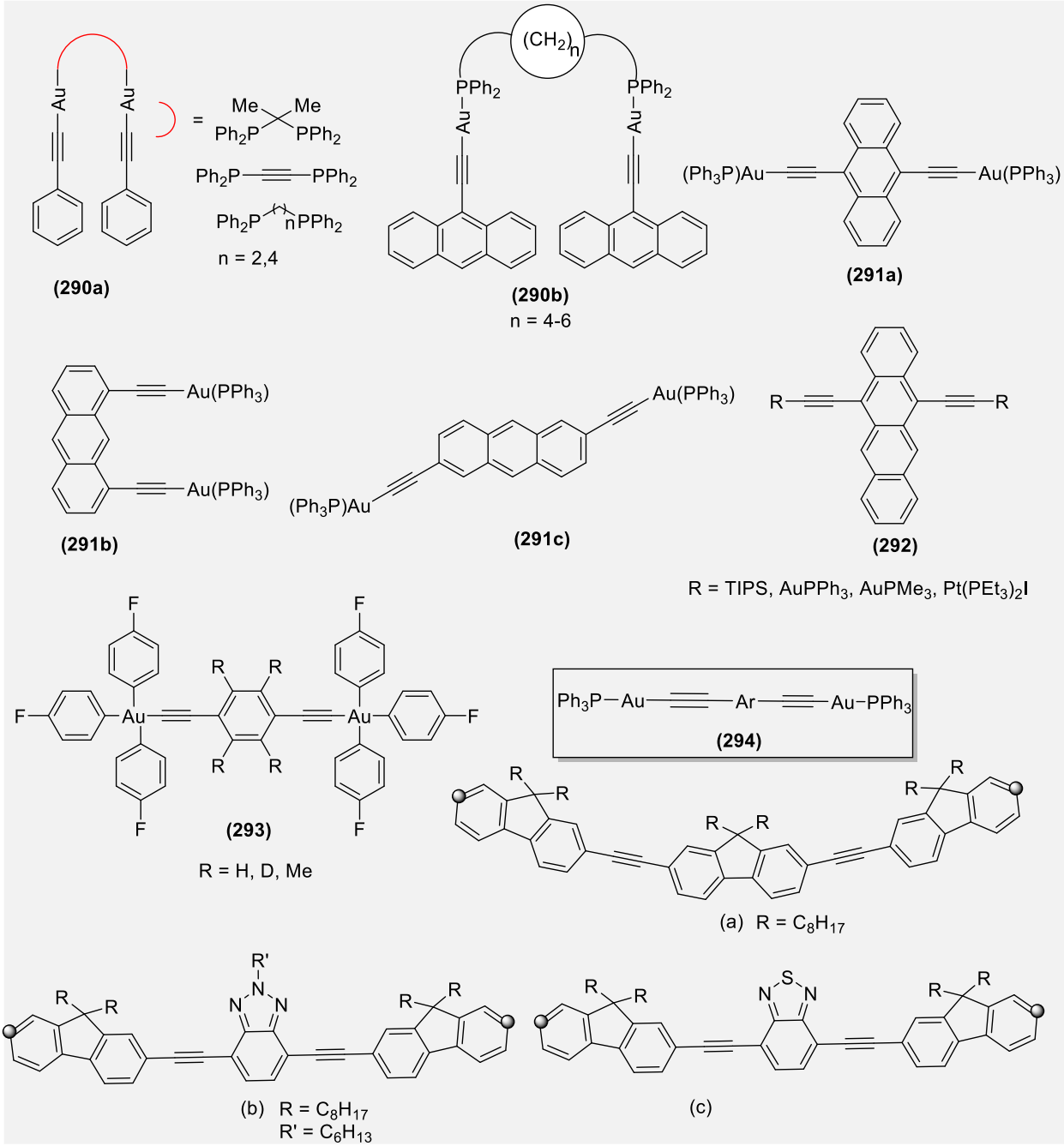

4. Applications

From the above discussion, it follows that organic oligo- and poly-ynes as well as poly(metalla-ynes) constitute a family of compounds where the conjugation and photo-physical properties can be modified by smart selection of end groups, spacers, number of π-linkages and the type of metal ions. These features render ‘‘*control over*’’ and improvement of the O-E properties of the materials.[568] Moreover, light weight,

flexibility and low cost are extra assets which make them suitable as new generation materials for applications in various domains of science. In the following subsections, we shall review some recent progress in the application of oligo-ynes, poly-ynes and poly(metalla-ynes) in O-Es (such as PVs, LEDs, FETs, molecular wires, molecular magnets, memory devices, NLOs), sensing, catalysis, drug discovery, multiplexing imaging and others.

4.1. Optoelectronics (O-Es)

4.1.1. Photovoltaics (PVs)

π-Conjugated polymers offer great technological potential for light to electricity conversion and are considered as one of the most promising materials for next generation PVs.[569-571] A typical PV device is comprised of electrodes, interfacial layers, and active materials/dye composed of small, medium or large sized π-conjugated organic or organometallic materials as donor/acceptor/sensitizer. All of these components contribute to the overall efficiency of a device[7], but from a chemist's point of view, most of the studies aimed to develop novel active materials/sensitizer.[572-574] In the quest for new materials, alkynyl-based organic and organometallic systems have emerged as interesting class of materials due to their good absorption profile, easy processability, low cost and high flexibility.[440,442,575-582] Furthermore, the introduction of alkynyl unit in a D-A architecture has been associated with improved PV performance.[583]

4.1.1.1. Dye sensitized solar cells (DSSCs)

One of the important components of a dye-sensitized solar cell (DSSC) or Grätzel cell is its dye/sensitizer which injects electron to the semiconductor (TiO_2) upon light irradiation.[584,585] A plethora of research has been undertaken to develop organic, inorganic and hybrid dyes leading to the development of Ru(III)/Co(II)/Zn(II)-based dyes with excellent efficiencies.[584-587] However, in the quest for green alternative and cheap dyes, researchers are actively pursuing new organic or organic-inorganic hybrid dyes. Since alkynyl unit has electron withdrawing nature and its incorporation into an organic backbone imparts molecular rigidity along with altered frontier molecular orbitals energy levels, and improve PV performance,[568] several studies have been carried on the development of mono, di- or oligo-ethynyl linker-based dyes.[588,589] In a recent study, Chou et al.[590] demonstrated that using an alkynyl-based dye, an efficiency of ~ 15.8% could be achieved, which is much higher than many standard electrolytes. Prior to this report, several organic dyes have been developed with moderate to high efficiency. Donor triphenylamine (TPA) and acceptors fluorene or cyanoacrylic acid based materials (**295-297**, Chart 44) have been found to generate a power conversion efficiency (PCE) up to 3.50%.[591] In such oligomers, PCE was found to be inversely related to the length of the bridge between the donor moiety and the anchoring group (**295 > 297 > 296**). Interestingly, all dyes have had close values for the open circuit voltage (V_{OC}) with the highest current density (J_{SC}) for **295**, attributed to its broader absorption spectrum.[591] Moreover, the performance of Pt(II)-metalla-yne based dye was also found similar to those of organic counterparts (PCE = 2%).

Chart 44.

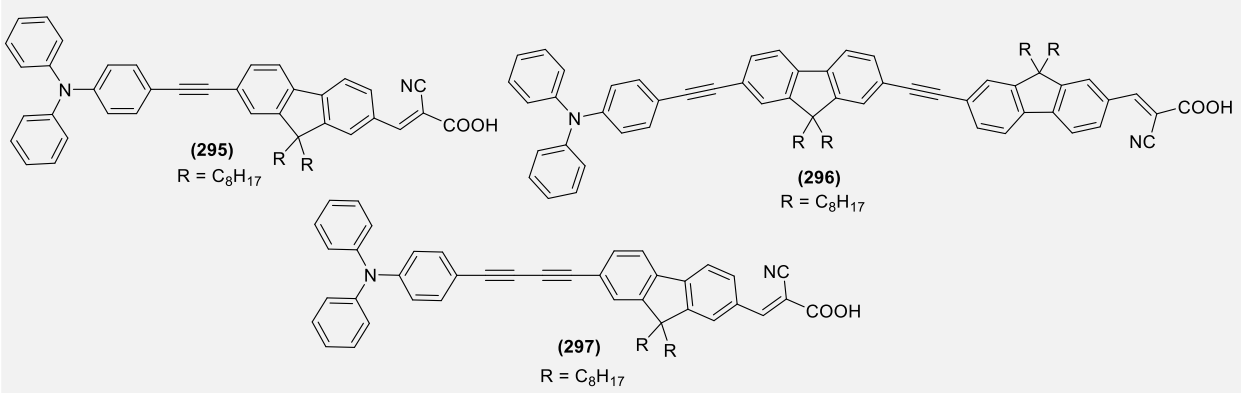

Not only the length, but also the position of ethynyl linker affect the device performance. It is reported that when an ethynyl unit is inserted in a benzothiadiazole-indole system **298a** (Chart 45) and **299a** (Chart 46), it improves the optical and PV performance.[592] The insertion of ethynyl fragment to the side of the anchoring group gave a high Ɛ with a red shift in the absorption band (compared to its non-alkynylated analogues). Due to the longer electron lifetime and slower charge recombination, **298a** exhibited high *V*oc (786 mV), PCE (7.13%) and FF (0.675) values compared to **299a** (PCE = 6.28%, *V*oc = 0.69, FF = 0.683) and to its non-alkynylated counterpart (PCE = 6.12%, *V*oc = 0.72 mV, FF = 0.667). A further improvement in efficiency (9.83%) was achieved *via* a co-sensitization strategy with a long-wavelength-responsive dye WS-2 in the iodine electrolyte. Wang and co-workers[593] compared the efficiency of structural analogue **298b-d** (Chart 45). Under optimized conditions, PCE between 8-13.0% and *V*oc = 0.73-0.81 mV was reported. Especially, the NIR photosensitizing dye **298d** exhibits over 80% external quntaum efficiency (EQE) and a PCE as high as 13.0%. On the other hand, phenanthrocarbazole based dyes **299b-e** (Chart 46) showed PCE between 7.6%-10.7%.[594] Further improvement in the performance (PCE = 12.5%) was noted upon rigidification of the donor core (**299f**, Chart 46).[595]

Chart 45.

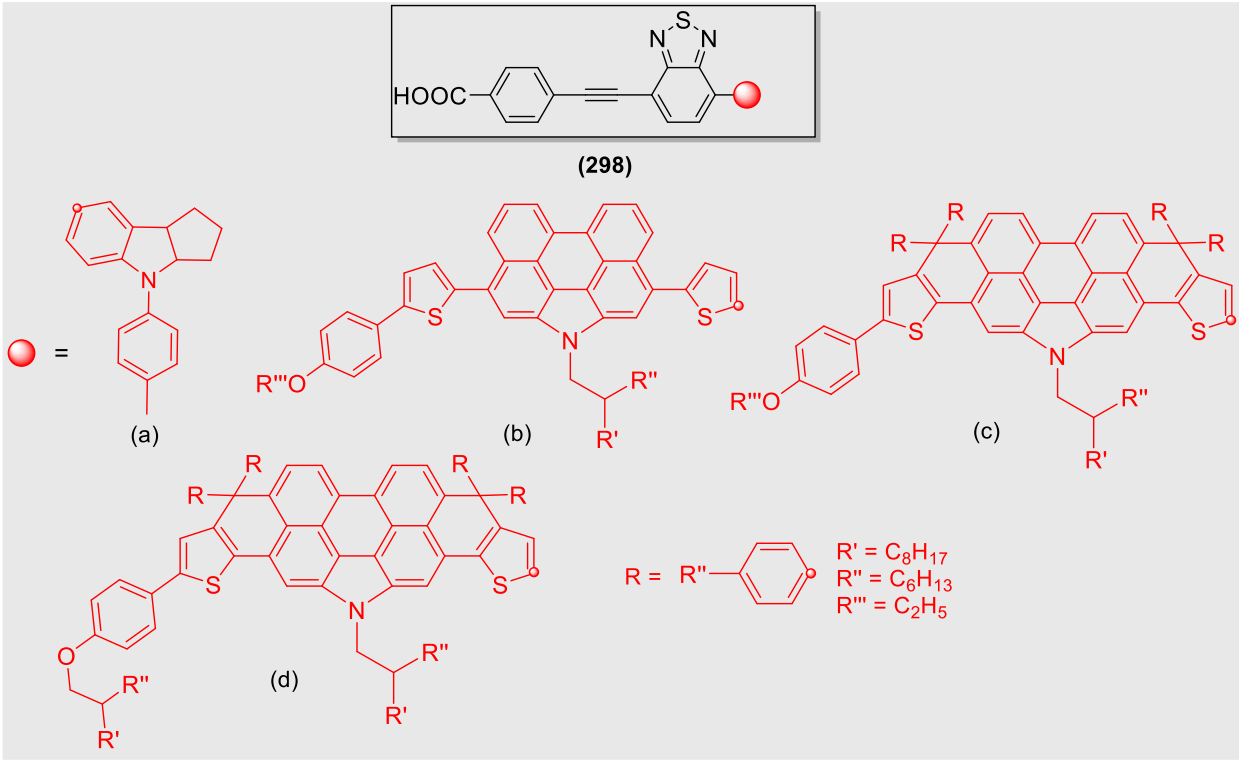

Chart 46.

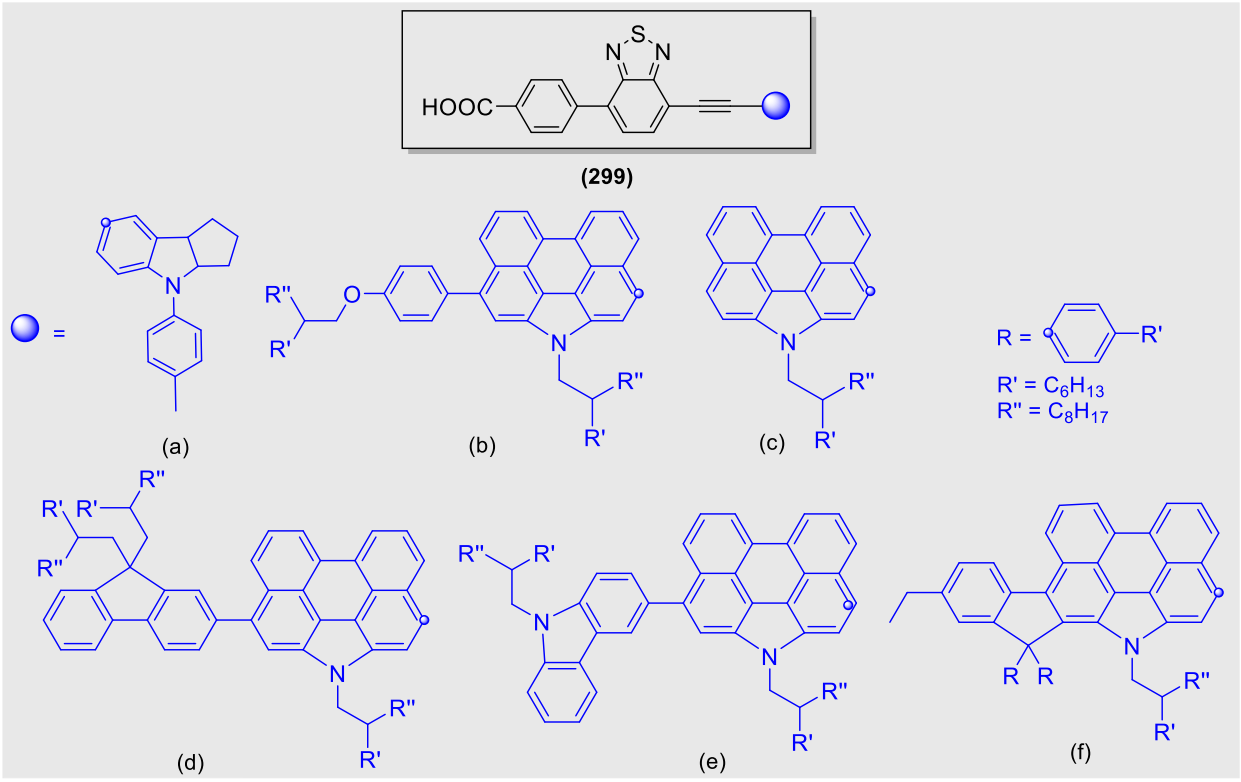

Polycyclic cores such as anthracene and anthanthrene are potential starting material for achieveing high perfomance electronic devices.[596-600] Anthracene-based molecular materials have unique photophysical properties with thermal stability and are known for potential application in OLEDs and PVs.[596] Despite the fact that the strength of electronic communication in aromatic systems varies in the order benzene > naphthalene > anthracene, the introduction of an alkynyl moiety mediates and enhances the electronic coupling between the redox centers, thus playing the role of a “molecular wire” allowing efficient charge transfer. Considering this fact, Mai et al.[601] reported acetylene-bridged 9,10-conjugated anthracene D-π-A system **300a** (Chart 47). The DSSC based on **300a** has shown a respectable cell performance of 5.44% and a high *Voc* (0.86 V). An enhancement in the PV performance was also reported for **300a** *via* structural optimization (changing alkyl to alkoxy chain and incorporation of electron-deficient moieties **300b-d**, Chart 47).[602] Among the reported dye, **300d** exhibited the best efficiency of 8.08% (under 1 sun, AM 1.5G), 28.56% (under T5 fluorescent illumination of 6000 lux) and 20.72% under same illuminance from a commercial LED light source, thus taking it one step closer towards commercialization.

Chart 47.

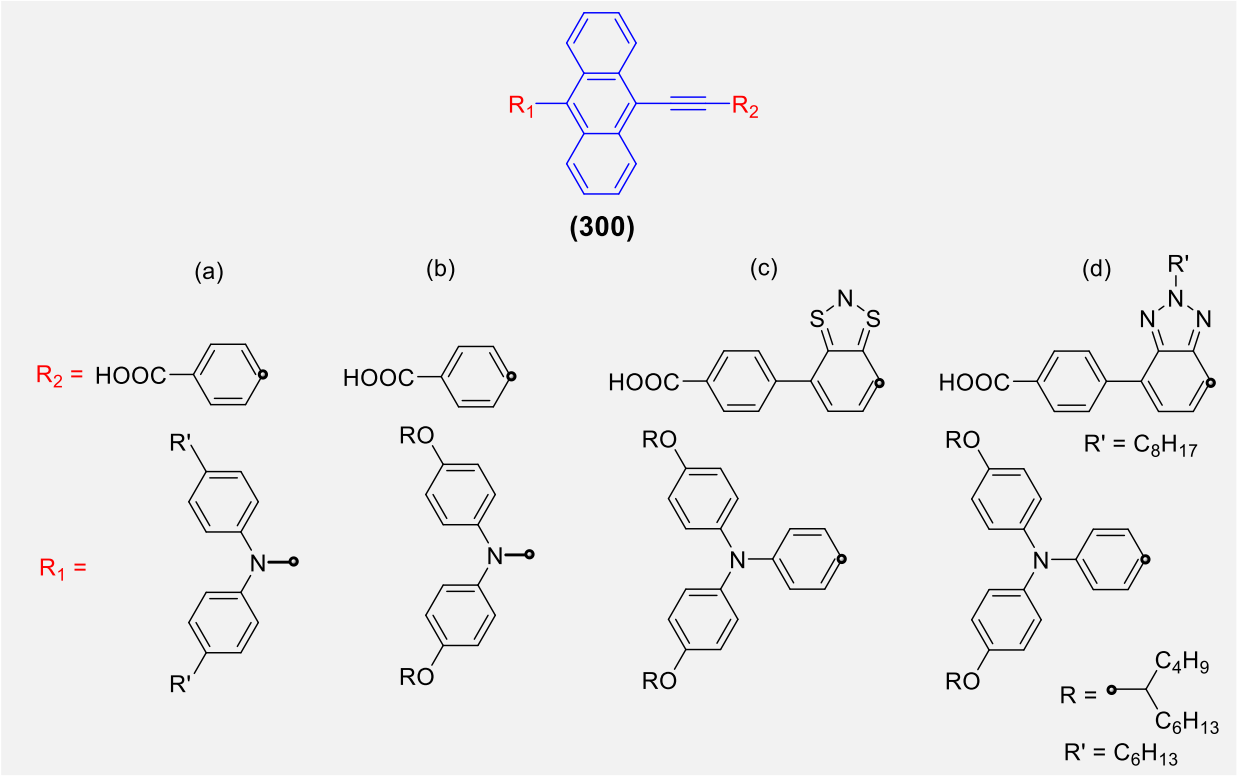

Upon replacing anthracene by a perylene moiety in the central fragment, five new dyes **301a-e** (Chart 48) were reported which showed PCE between 4.48-6.00%.[590] Other than the performance, one other important feature of these dyes is cost effectiveness (due to shorter synthetic route). One of the dyes **301e** containing benzothiadiazole-benzoic acid showed the best PCE of 6.16% with *Voc* of 0.70 V and *Jsc* of 11.88 mA/cm^2 using a liquid iodide-based electrolyte. It also shows high performance in converting light with a PCE of 15.79%. Interestingly, the benzoic-containing dye **301a** with a simple molecular structure has

comparable performance in generating power output of 0.26 mW/cm^2 (PCE = 15.01%) under the same conditions and is potentially viable for future application. These results strongly indicate potential indoor applications of DSSCs using alkynyl based perylene dyes, especially for the more cost-efficient benzothiadiazole-free dye **301a**. Almost similar efficiency of the device was found for DSSCs based on D-π-A dye **302a-e** (Chart 48).[603] Particularly **302b** showed a PCE ~ 5.90% under AM 1.5 irradiation (100 mW/cm^2) while under a dim light condition, it exhibited a PCE of 5.45% (comparable with that of the reference cell). Long-term stability studies showed the overall efficiency of the **302b** based cell dropped by only 3% after 2000 h, showcasing its potential for indoor applications.

Chart 48.

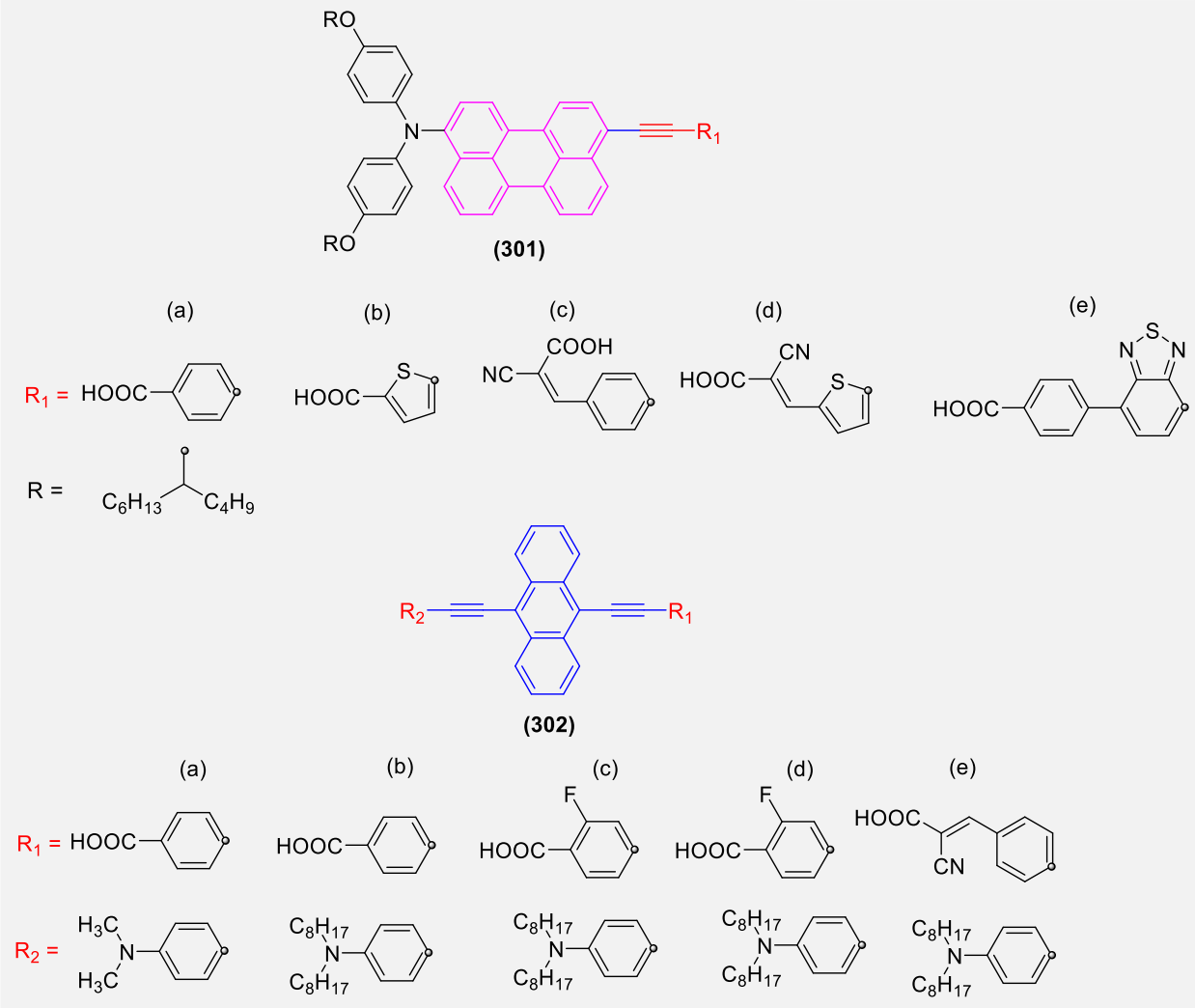

Alongside the small organic oligo-yne sensitizer, metalla-yne based dyes have also been assessed. In general, metalla-ynes shows lower efficiency compared to pure organic dye, despite the fact that the presence of metal provides extra sites for chemical and physico-chemical modification.[591] For example, spacer dependent PV performance was reported in Pt(II) di-ynes **303-306** (Chart 49) flanked by different spacers (fluorene, thiophene, bithiophene, phenothiazine etc.).[591,604,605] An enhanced PCE and *Jsc* values

were observed when the 9,9-disubstituted fluorene spacer in **303** (Chart 49)[591] was replaced by thiophene and bithiophene spacers.[606] DSSC composed of sensitizer **304b** (Chart 49) generated a PCE of 4.21% and enhanced V_{OC} (0.65 mV). However, the rigidification of TPA unit (i.e. carbazole) and replacement of $Pt(Et_3)_2$ by a Ru(II)-dppe unit led to further enhancement in device performance (J_{SC} = 15.56 mA/cm^2, V_{OC} = 680 mV, and FF = 69.2 %, PCE = 7.3%).[605] DSSCs composed of sensitizers **305**(a-c) (Chart 49) having both carbocyclic (electron-donating arylacetylide) and heterocyclic (phenothiazine) spacers around Pt(II) produces V_{OC} between 0.69-0.73 V, J_{SC} = 8.75-10.98 mA/cm^2 and PCE between 4.34-5.78%.[607] Particularly, the complex **305a** exhibited attractive PV performance (PCE = 5.78 %, J_{SC} = 10.98 mA/cm^2, V_{OC} = 0.73 V, FF = 0.713) values. Higher PCE was attributed to high resistance to the recombination of electrons (R_{rec} = 159-478 Ω). Since these values were either comparable or better than the conventionally used Ru-based sensitizer (N719, PCE = 7.91%, J_{SC} = 15.84 mA/cm^2, V_{OC} = 0.70 mV, FF = 0.713 and R_{rec} = 93.53 Ω), these Pt(II)-acetylide sensitizers have great potential as promising photosensitizers in DSSC applications. Gauthier and co-workers[608] reported DSSCs based on dyes **306** (Chart 49) Devices based on these Pt(II) acetylide complexes showed overall efficiency between 1.70-4.69%, which can be considered high for DSSC applications. Like the previous example, the best performance was shown by device fabricated using terthiophene-based dye **306e**. However, limited light harvesting efficiency (LHE) is one of the major concerns with reported Pt(II)-based dyes. A comparatively similar sensitization effect of metalloporphyrin-linked alkynyl Pt(II) polypyridine complexes has also been reported.[609] Under optimized condition, an efficiency between 1-3.4% was achieved. However, there are some ethynyl incorporated "*push–pull*" type porphyrin dyes having performance superior to currently employed dyes. Grätzel et al.[574] reported two ethynyl-containing porphyrin sensitizers with a record efficiency (up to 13%). Oligo-yne based porphyrin sensitizers, along with a co-sensitization strategy to achieve a high efficiency of 10.45% in an iodine electrolyte has already been reported.[610] In addition to the examples discussed above, a number of ethynyl decorated porphyrin-based sensitizers with PCE between 4.7-13% has also been reported.[574,595,610-626]

Chart 49.

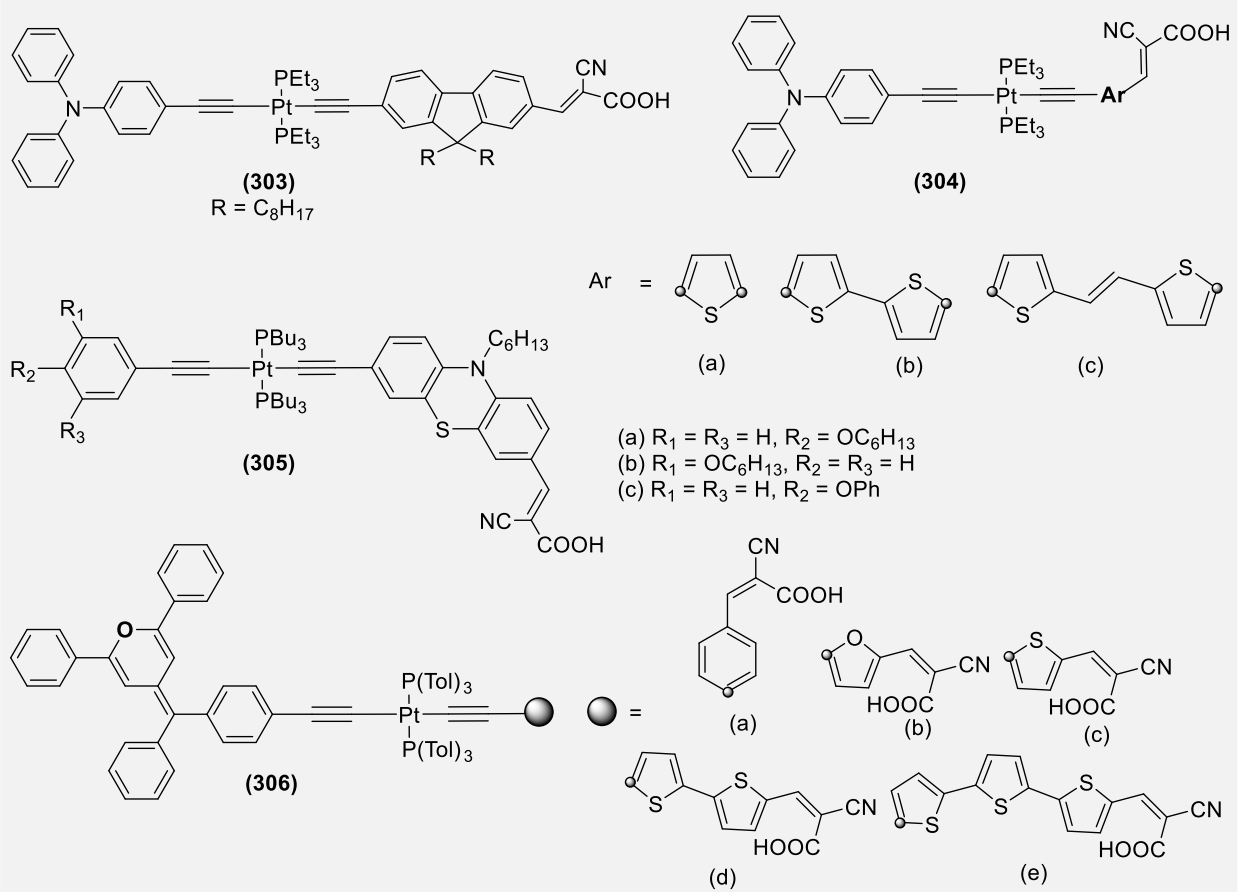

4.1.1.2. Bulk heterojunction (BHJ) cells

The interest in the development of ethynyl-based active layers for bulk heterojunction (BHJ) cells started more than two decades ago.[627] Since then, numerous organic and organometallic small-molecule donor based materials have been tested.[628,629] Similar to DSSCs, researchers employed combination of D-A, D-π-A, D-A-A-π-A, etc. based small, medium and large organic and organometallic acetylenic compounds as active materials.[630] Recently, Gautam et al.[631] employed the concept of D-A-A-π-A and synthesized benzothiadiazole-based small molecule **307** (Chart 50). This low E_g small molecule showed a respectable PCE (4.61%). An appreciable efficiency was also reported for **308-309** (Chart 50) with peak PCE of 3.21%.[632] In a recent study, it has been demonstrated that monodispersed compounds **310-311** (Chart 50) are better donor materials than their polymeric counterpart, signifying the importance of material homogeneity in the device performance.[633] The PCE value (1.3%) obtained with **310** ranks among the highest reported for non-polymeric small molecule-based BHJ solar cells constructed without the use of additives or annealing processes, demonstrating that ethynylene-containing electron-rich systems are promising donors for organic solar cells (OSCs). Compared to this, similar or high PCE were also reported for porphyrin-based donors for small molecule surrounded by ethynyl spacers.[634-636] Inverted BHJ fabricated

using BODIPY based small donors **312** and **313** (Chart 50) produced PCE of 2.46% and 3.22 %,[637] which is interestingly higher than earlier reported BODIPY polymers based BHJ (2%).[638]

Among various building blocks, the dithienyldiketopyrrolo pyrrole (TDPP) unit remains potentially attractive candidate due to its high planarity, strong electron-withdrawing nature, easy chemical modification and intense absorption in the visible range, as well as facile availability.[639] The planar and polar TDPP core is thought to enhance both intra-molecular and intermolecular charge transport in polymer semiconductors. Due to these intriguing features, alkynyl incorporated TDPP-based small-molecules have already been reported with impressive PCE of 2.06-5.94%.[630] Zhu and co-workers[640] reported an oligo-yne **314a** (Chart 51) in which TDPP was symmetrically connected through a 9,10-anthracenyl unit to 3-alkylthiophene *via* an ethynyl linkage. BHJ based on this visible light absorbing materials (650 nm with a shoulder at 737 nm, tailing until ca. 800 nm) as cast active layer without a processing additive or solvent vapor annealing generated a PCE of ~ 4.0 % (V_{OC} = 0.77 V, J_{SC} = 10.0 mA/cm^2, and FF = 52 %). An improvement in performance (PCE ~ 4.4 %) was observed upon thermal annealing at mild temperature (50 °C). However, annealing at higher temperature (> 70 °C) led to decrease in PCE, attributed to the large domain size morphology. A considerable change in the performance of the device was also reported upon minor changes, i.e. lengthening of the alkyl group and the introduction of 1,4-phenylene unit.[641] Device based on **314b** (Chart 51) showed a PCE of 3.56% which enhanced to 3.86 % upon thermal annealing. Interestingly, phenylene embedded analogue **314c** showed a PCE of 4.86 % which rose to 5.07% upon thermal annealing. Compared to the parent oligo-yne **314a**, device based on these two oligo-ynes possess enhanced FF values (64.59 and 63% for **314b** and **314c**, respectively after annealing). Related analogues **314d** and **314e** (Chart 51) having high tendency to form amorphous film have also been reported with lower efficiency.[642] Due to the electron donating nature of ferrocene and acceptor nature of TDPP, strong CT interaction has been reported in D–π–A–π–D type small molecule consisting of thiophene flanked TDPP as a core and an end-capping ferrocene donor linked by an ethynyl bridge (**314f**, Chart 51).[643] BHJ based on this small molecule showed high Voc (980 mV) and a PCE of 2.55%, but low values of J_{sc} (6.35 mA/cm^2) and FF (0.41). A significant improvement in the PCE was observed upon the modification of film morphology.

Chart 50.

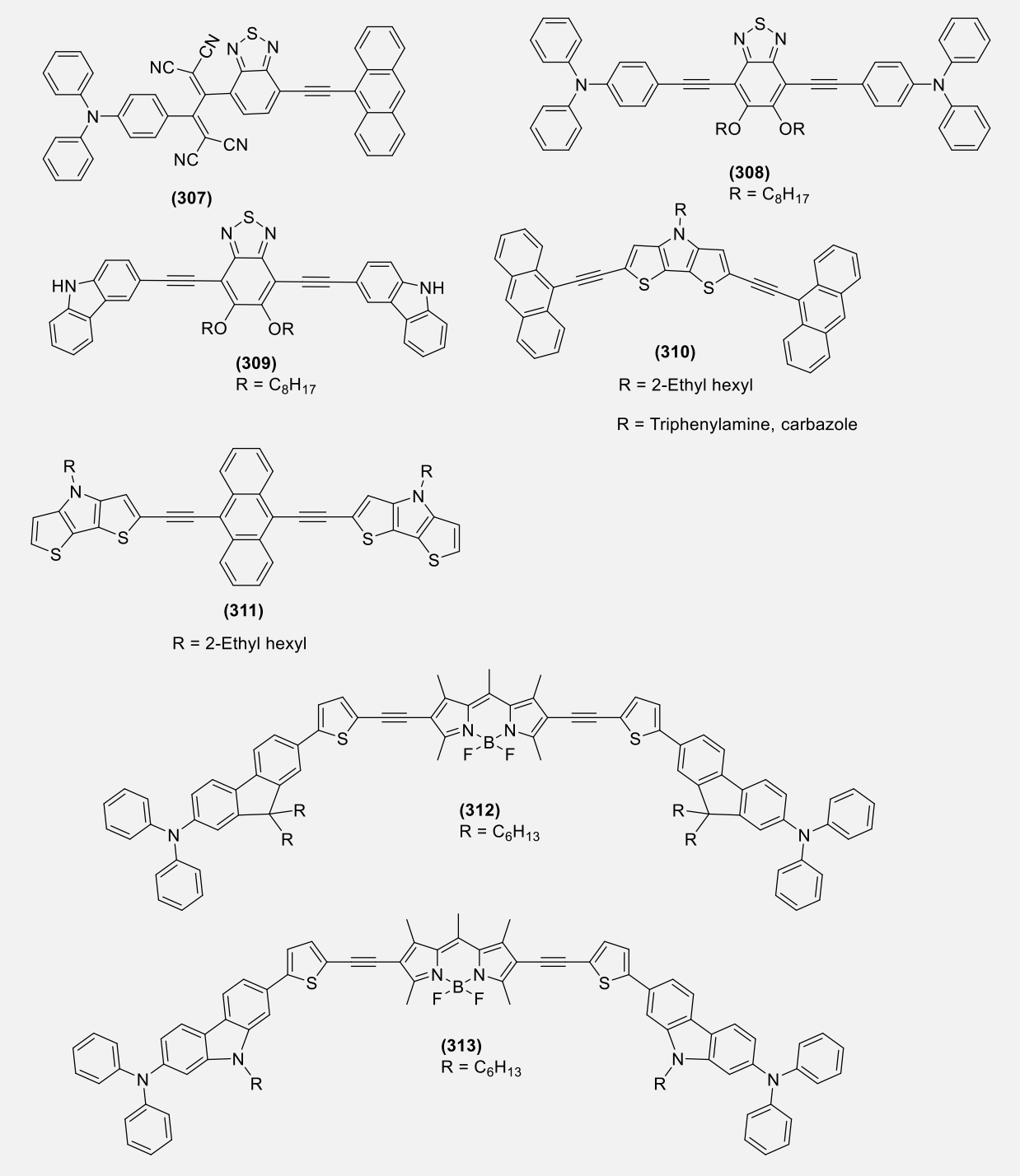

Li and co-workers[568] reported that BHJ device based on a small molecule (5,6-bis-(octyloxy)benzo[c] [1,2,5]thiadiazole as acceptor and TPA as donor connected through ethynylbenzene π-linkage **315**, Chart 51) produces *V*oc (1.03 V) higher than its non-alknyl counterparts. Under optimizied conditions, the device of configuration **315**/$PC_{61}BM$ showed J_{sc} of 6.56 mA/cm^2, FF of 0.30 and PCE of 2.03%. It was suggested that electron-withdrawing nature and high rigidity offered by ethnylbenzene were the main reasons behind

this high performnace. Later, the same group proposed that if the TPA units are replaced by carbazole-based donors (weak electron-donating capacity), it might further improve the performance.[632] To confirm this proposition, they designed and synthesized a small donor molecule **316** Chart 51).[632] Surprisingly, a solution processed with configuration of ITO/PEDOT:PSS/**316**:$PC_{61}BM$/Al showed performance (*V*oc = 1.06 V, J_{sc} = 6.68 mA/cm^2, FF = 0.30 and PCE = 2.10%) better than the device based on **315**. Contrary to this, when the central acceptor unit (5,6-bis-(octyloxy)benzo[c] [1,2,5]thiadiazole from **316** was replaced by TDPP unit **317** Chart 51), a slight drop in the performance (*V*oc = 0.84 V, J_{sc} = 7.67 mA/cm^2, FF = 0.31, and PCE = 1.99%) was noted.[644] However, a structural analog of **317** in which carbzole side-arms were replaced by fluorene units showed much better ad higher performance (*V*oc = 0.98 V, J_{sc} = 9.04 mA/cm^2, FF = 0.35, and PCE = 3.10%).[644]

Chart 51.

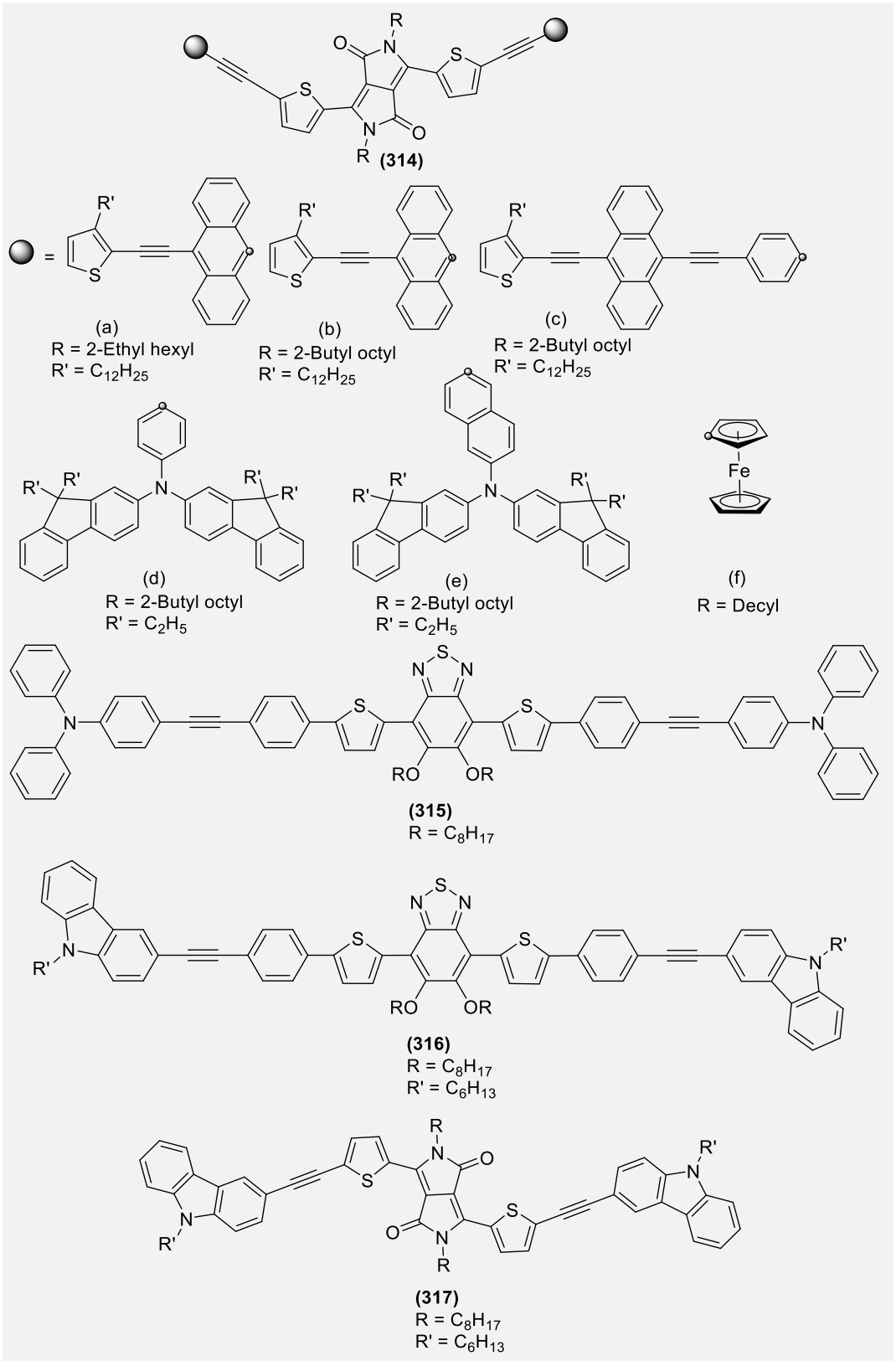
(314)
(a)
R = 2-Ethyl hexyl
R' = $C_{12}H_{25}$
(b)
R = 2-Butyl octyl
R' = $C_{12}H_{25}$
(c)
R = 2-Butyl octyl
R' = $C_{12}H_{25}$
(d)
R = 2-Butyl octyl
R' = C_2H_5
(e)
R = 2-Butyl octyl
R' = C_2H_5
(f)
R = Decyl
(315)
R = C_8H_{17}
(316)
R = C_8H_{17}
R' = C_6H_{13}
(317)
R = C_8H_{17}
R' = C_6H_{13}

Despite the fact that π-conjugated oligo-ynes and poly-ynes incorporating mono- or mixed heterocyclic core have excellent photo-chemical and photo-physical properties[645], their PV performance remains limited. According to Guo and co-workers[646], one of the reasons for poor performance of conjugated spacer bearing polymeric material is the steric hindrance arising due to alkyl chains present over the chain. To circumvent this issue and to realize polymers with high backbone planarity, several strategies are being adopted.[646] For example, some incorporate non-alkylated π-spacers while some prefer conformation locking *via* covalent or noncovalent interactions (Figure 32a).

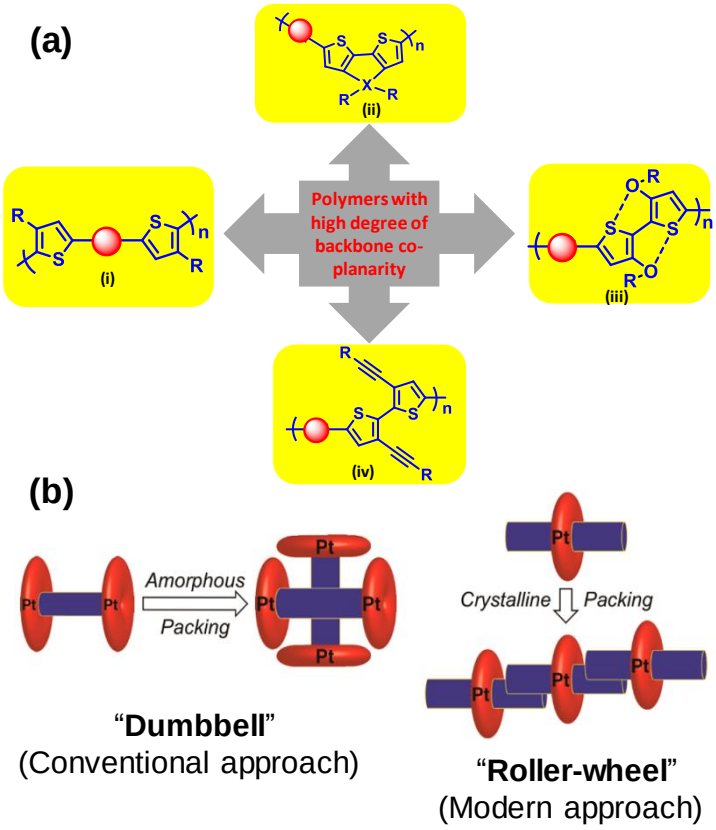

Figure 32. Strategies for achieving high efficiency organic and organometallic semiconductors. (a) In organic polymer, high degrees of backbone coplanarity can be achieved by (i) inserting non-alkylated π-spacers, (ii) conformation locking through covalent bonds; (iii) conformation locking through intramolecular noncovalent interactions and (iv) introducing alkynyl side chains. Reprinted with permission from ref [646] Copyright 2017 American Chemical Society. (b) The "roller-wheel" approach in Pt(II)-polymers give efficient π-π overlap *via* slip stacking leading to improved PL and PV performance. Reprinted with permission from ref [647]. Copyright 2017 American Chemical Society.

Recently, Guo and co-workers[646] proposed that the replacement of alkyl chains with less sterically demanding alkynyl chains should reduce the steric hindrance and thus improve the performance. To test this hypothesis, they synthesized and assessed the efficiency of a 3,3′-dialkynyl-2,2′-bithiophene donor based low band gap (1.6 eV) polymer **318** (Chart 52). The polymer showed hole mobility up to 0.13 cm^2

$V^{-1}\,s^{-1}$ and PCE of ~ 8% with remarkable V_{oc} values (0.91−1.04 V, Table 10) The high efficiency of the cell was attributed to the low-lying polymer HOMOs (−5.5 to −5.7 eV) enabled by the electron-withdrawing alkynyl substituents and absence of the typical electron-rich π-spacers. In contrast to ethynylene-containing moieties, the 1,3-butadiynyl (diacetylene) group has been barely studied. Recently a very first work on the O-E applications (PV and OFETs) of 1,3-butadiyne based co-polymers has been reported.[648] The co-poly-yne was obtained by conjugating alkyl-substituted 1,4-di(thiophen-2-yl)buta-1,3-diyne (R-DTB) donor and TDPP acceptor (**319a-d**, Chart 52).[648] Whereas polymers **319a** and **319b** showed low solubility (due to severe aggregation), polymers **319c** and **319d** with longer solubilizing chains exhibit excellent solution processablity. Under optimized condition, **319c** and **319d** showed a PCE of 2.69 and 3.70%, respectively, which is the highest value for any alkyne-containing organic polymer. The high performance was attributed to the enhanced J_{sc} and FF values, which were linked to the solvent dependent blend film morphology. Overall, this study paved a way for reassessment of organic and organometallic polymers which were reported before with moderate efficiency.

Table 10. BHJ SC performance of 3,3′-dialkynyl-2,2′-bithiophene donor based low band gap polymers (**318**).[646]

Poly-yne	***V*oc (V)**	***J*sc (mA/cm^{-2})**	***FF* (%)**	**PCE (%)**
X = O	1.04	6.56	49.0	3.35
X = S	0.91	14.13	`59.88	7.69

Chart 52.

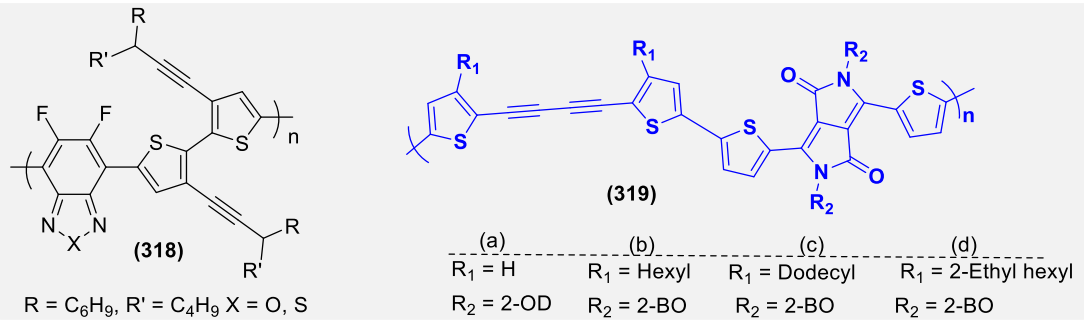

Since the discovery of PV effect in Pt(II) poly-ynes,[649] several attempts have been made to develop metalla-yne based BHJ active layers.[7] Other than Pt(II), researchers have also investigated the PV performance of Ru(III), Hg(II), etc. based di-, oligo- and poly-ynes.[650-653] The introduction of a metal ion in an organic framework is likely to show synergistic effect on the PV performance, mainly through the intermixing of orbitals and the delocalization of excitons. A metal ion also provides redox-active site that generates species for charge transport and the auxiliary ligand imparts solubility that helps in the device fabrication.[24] Despite these advantages, one major issue with most of the metalla-ynes is their absorption profile; especially platina-ynes, which absorb in the UV-region and remain transparent in the visible region of light. To circumvent this issue, researcher uses D-A strategy, in which a D-A organic chromophore is linked to the metal *via* σ-linkage. The linkage significantly modifies the photo-physical properties of the materials

(*viz*. absorption in the visible region and reduced E_g).[23] Based on this idea, several metal-based di-, oligo- and poly-ynes have been designed, synthesized and assessed. For example, Pt(II) alkynyl oligomers containing BDT as central core and different number of thiophenes at termini (**320**, Chart 53) show broad absorption profile with excellent solubility. These oligo-ynes possess low E_g (~ 1.9 eV) and the BHJ device based on these materials showed appreciable performance (PCE upto 3.0%).[568,576] In spite of varying number of oligothiophene units, their HOMO level remains localized on the core unit as indicated by similar V_{oc} (0.71-0.82 V). Notably, the performance of the device significantly depended on the type of acceptor used ($PC_{71}BM$ gave better performance than $PC_{61}BM$). Somewhat similar performance was reported for **321** and **322** (Chart 53).[654,655]

Chart 53.

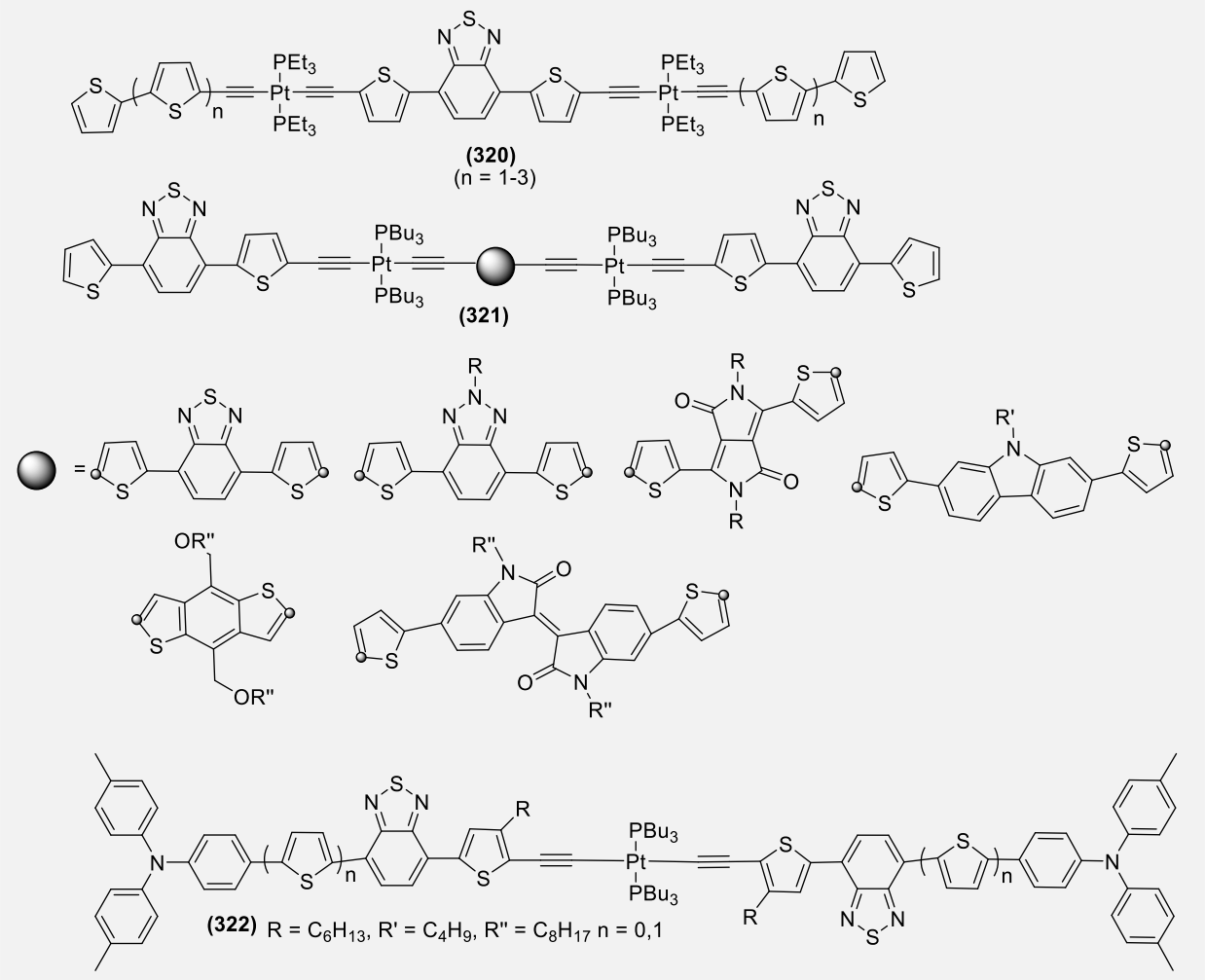

However, the concept of D-A is not a "*rule of thumb"*, there are several exceptions to it. For example, BHJ device fabricated using low E_g Pt(II) diynes **323 and 324** (Chart 54) showed a solvent additive dependent PV performances.[656] The BHJ cell fabricated using **323** showed an overall efficiency of 0.9% (*J*sc = 3.11 mA/cm^2, V_{oc} = 0.78 V, and FF = 36.7%) which rose to 1.4% (*J*sc = 4.14 mA/cm^2, V_{oc} = 0.75 V, and FF 45.4%) upon the addition of 1,8-diiodooctane (0.3 vol%) as a solvent additive. Contrary to this, a decrease

in performance was reported in the case of **324**. The difference in performance was attributed to the different crystallization and morphology behaviour of blends. In addition, the possibility of inappropriate molecular geometry of the oligomers cannot be ruled out. Traditionally, an oligo- or poly-yne incorporating Pt(II) ion in the main chain adopts a dumbbell geometry in which molecules are cross-stacked over each other (Figure 32b).[647,657] This cross stacking led to inefficient π-π overlap, and hence most of the small to large molecules are amorphous and show low to moderate performance. In a recent work, the group led by Qin showed that if the molecules are arranged in *roller-wheel* way, it would enhance the π-π overlap *via* slip stacking.[647,657] Using this proof-of-concept, the group synthesised a number of Pt(II) acetylides **325-327** that showed excellent performance over their cross stacked counterparts. **325-326** (Chart 54) showed PCE between 3.9-5.9%, outperforming all existing Pt(II) di-, oligo- and poly-ynes. While high crystallinity and charge mobility were the main reasons behind high performance of **325-326**, very low performance of the device based on **327** (Chart 54) was attributed to the lack of π−π interactions between organic chromophores.

Chart 54.

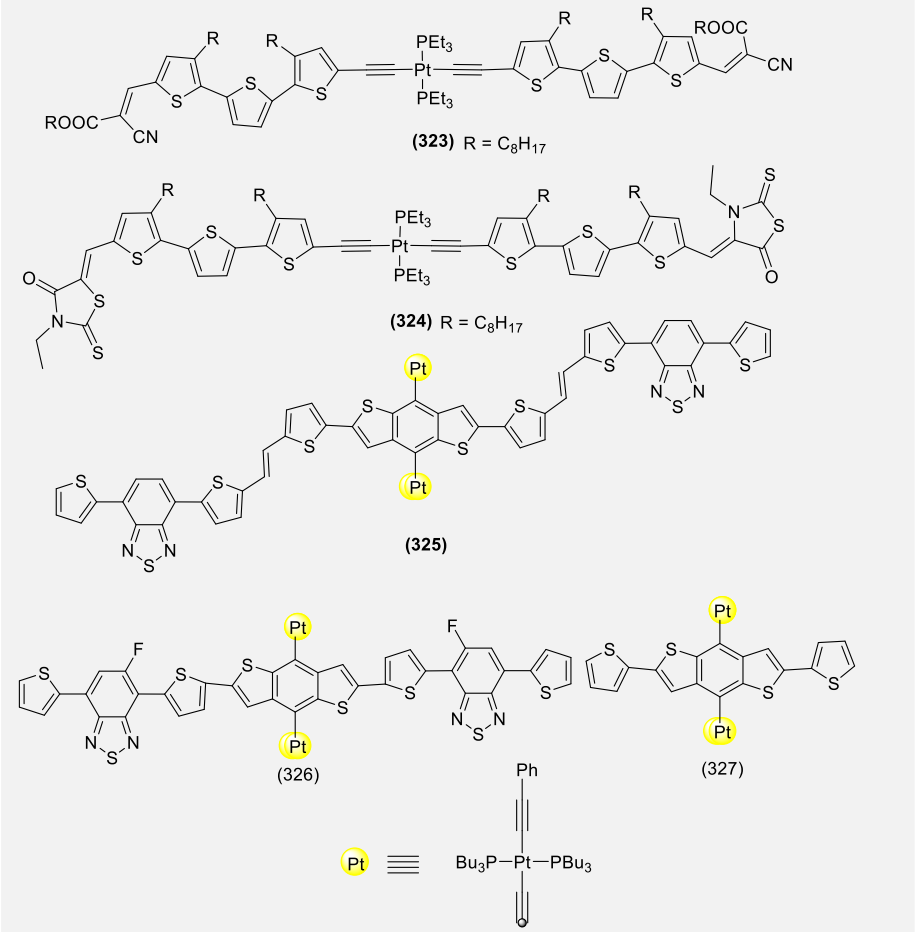

In addition to above-discussed Pt(II) oligo-ynes, several other poly-ynes have also been reported with low to moderate efficiency. For example, poly-ynes (**328-329**, Chart 55) with alternating donor and acceptor units linked *via* ethynylene possess absorption in the visible region (up to ~670 nm) and low E_g (~ 1.46-

1.72 eV).[658] BHJ device based on these polymers shows PCE between 1.34-1.74%. On the other hand, polymers based on alkoxy-substituted benzo[1,2-b:4,5-b']dithiophene (**330a**, Chart 55) and thiazolothiazole (**330b**, Chart 55), showed absorption in visible region and produces PCE of 0.85 and 2.40%, respectively.[659] Compared to these, device based on Pt(II) poly-ynes incorporating thiophene or thieno[3,2-*b*]thiophene (**331a-c**, Chart 55) and 2,1,3-benzothiodiazole spacers have been reported to show excellent performance.[660] Device fabricated using **331c** produces V_{oc} =0.79, J_{sc} = 10.12 mA/cm^2, FF 51.4%, and a PCE as high as 4.13%. In 2007, Wong et al. reported a remarkably high efficiency (4.93%) of the device fabricated using benzodithiazole-thienyl spacer based Pt(II) poly-yne (**240ag**).[440] Contrarily, Schanze and co-workers[661] found that the same polymer is able to generate a maximum PCE of 1.1-1.4%. Enhancing the absorption coefficient of the band by increasing the polymer conjugation chain length with additional thienyl rings is an effective way to improve the cell performance.[446] An enhanced light-harvesting ability and solar cell efficiency was reported upon the incorporation of additional thiophene rings in the polymer (**240ap**, Chart 28).[446] A PCE of 1.61% has been reported with poly-yne having two thiophene rings compared to the PCE of 1.09% for poly-yne with only one thiophene. Wong's group developed a series of solution processable polymers containing bithiazole-oligothienyl rings (**240an**, Chart 28) with strong visible-light absorption.[444] The PCE as well as optical and charge-transport properties of the polymers were found to be tunable by the number of thienyl rings (m). The same group reported Pt(II) poly-yne analogous to **240an** in which the thiazole moiety was replaced by electron donor phenothiazine.[662] Such combination, (oligothiophene(A)-phenothiazine(D) with higher E_g (> 1.5 eV), led to the overall PCE of 1.3% with $PC_{61}BM$ with a corresponding peak external quantum efficiency of 63% . Blending of poly-ynes and poly(metalla-ynes) often results in enhanced PCE of the SCs. An excellent class of strongly visible-absorbing low E_g poly(metalla-ynes) was reported with PCE over 4% without annealing or using the tandem structures (**240m** and **240q**, Chart 28). Upon varying the number of thienyl rings, the absorption features and charge carrier mobilities of the resulting metallopolymers were also enhanced. Similaryly, other low-performing Pt(II)-based poly-ynes PCE varying between 0.3-1% have also been[448,663441,443,660,664] For example, BHJ made up of low Eg (1.7 eV) Pt(II)-poly-ynes **332** with BODIPY spacer (Chart 55) gave high open circuit voltages up to 0.92 V and PCE close to 1%.[663] Not only the Pt(II), but other transition metal based metalla-ynes are know with impressive results. For example, an inverted polymer solar cells based on amino-functionalized conjugated metallopolymer **333** (Chart 55) gave a PCE of > 9%.[650] In addition, the outstanding performaces produced by alknyl- based small molecule organic solar cells [651-653] are also noteworthy.

Chart 55.

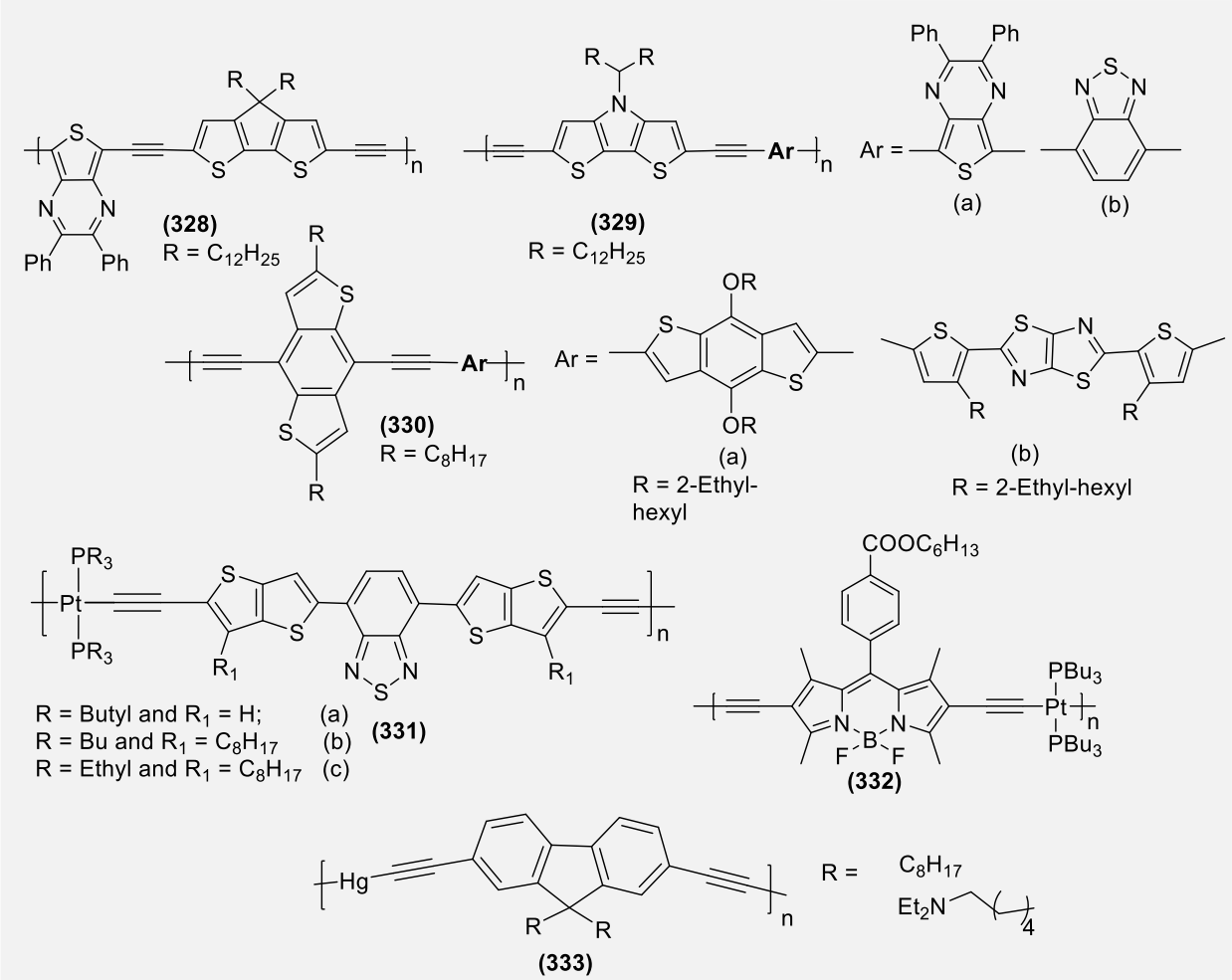

4.1.2. Non-linear optics (NLOs)

Optical power limiters (OPL) are specially designed devices used to filter out radiations of unwanted frequencies. These devices are made in such a way that their spectral response matches the operating waveband of the device/sensor/organ which is intended to protect.[665] These limiters have found application in various domains of science and technology such as LASER, medicine, sensor, optical data storage, etc. OPL possesses the property of NLA, in which the absorption of the light by the material depends on the intensity of waves passing through it. It has been reported that a material may show NLO either through multiphoton absorption (e.g., two- or three-photon absorption) or excited state absorption (also known as reverse saturable absorption) mechanism.[665] To be used as OPL material, properties like high optical transparencies, good optical nonlinearity, excellent solubility, high transmission zone (around 532 nm) and a quick response speed are highly desirable. To serve this purpose, a number of organic and organometallic materials including nanomaterials have been reported[666-670]. However, poor solubility and the deep color of most of the reported materials limited device processing and fabrication.[191] Therefore, highly soluble and optically transparent material is always welcome and desperately desired. The linear structure and π-electron delocalization of oligo-/poly-ynes endowed this class of materials with great potential for NLO

applications. The NLO properties of oligo-/poly-ynes is known since early 1990s.[671] They remain a very interesting family of compounds from the NLO viewpoint, especially as small molecules (< MW 500 g mol^{-1}) exhibit quite large values of the NLO response. It has been well established that the NLO parameters of oligo-/poly-ynes could be modulated through various means: extending conjugation length, incorporating D-A groups, increasing the content of transition metal ions, metallic end-capping, etc.[88,332,672-674] In addition to the linear Pt(II) oligo- and poly-ynes, several other metalla-ynes *viz*. cross-conjugated, branched, triangular Pt(II) acetylide complexes etc.[675-678] have been reported with excellent OPL properties. Recently, Li et al.[679] reviewed the efficiency of several organic hyperbranched polymers (HBPs) including poly-ynes as LEDs, sensors, NLO materials, solar cells and others. According to the authors, HBPs as second-order NLO materials, efficiently decreases the dipole-dipole interactions among the chromophore moieties having D-π-A structure and enhances their NLO coefficients. The size of groups in the periphery can also affect the NLO effect to a large degree; for 2PA materials, the activity of functional groups in the periphery could adjust the push-pull electronic structures.[680-682] It has also been reported that the NLO responses of the organic material enhances up to a limit with the conjugation length and then it saturates. However, this flaw of organic material can be avoided by using a metal ion. The efficiency of group 8-12 metals as NLO materials have been reviewed by Humphrey et al.[680] and Zhou and Wong.[682] They reported that the magnitude of the NLO response of alkynyl complexes could be modulated by changing the parameters like metals and length of conjugation. They stress that the metal complexes are better NLO materials than their organic counterparts.

As discussed in the synthesis section, the presence of bulky substituents at termini stabilizes the highly reactive oligo-ynes. For example, adamantyl substituted oligo-ynes show better stability than other analogues (**334a**, Chart 56). Not only they are stable, they also show chain length dependent NLO properties.[683,684] It was found that the γ_{vib} values as a function of length are of the same order of magnitude as those arising from the electronic contribution to the molecular second hyperpolarizability (γ), as reported for triisopropylsilyl poly-yne TIPS[n]. The nonlinear response for Ad[n] poly-ynes, supported by the analogous response for TIPS[n] poly-ynes, confirms that linear sp-carbon molecules have large second hyperpolarizabilities that show a power-law increase in γ_{vib}-values versus length that is larger than other known π-conjugated systems, such as polyenes. In the case of TIPS protected oligo-ynes, a moderate value of second hyperpolarizabilities was reported for shorter poly-ynes (n < 6), while it was large for the long poly-ynes.[684] (**334b**, Chart 56).

End-capping of tetra-ynes with electron-withdrawing aryl group (**335**, Chart 56) resulted strong nonlinear absorption and nonlinear refraction properties in visible-NIR region.[685] f-Scan (modified Z-scan) studies of the oligo-ynes indicated strong negative third-order nonlinear refraction (3NR) in the 540–580 nm spectral range, with peak values of Re(γ) in the order of -5 and -4 x 10^{-33} esu in compounds **335a** and **335b**, respectively and -1.4 x10^{-32} esu in compound **335c**. This phenomenon was followed by two-photon absorption (2PA) with the maximum cross-section $\sigma^{(2)}$ varying from ~ 100 GM in **335b** up to ~ 200 GM in **335a** and **335c**, corresponding to Im(γ) between 2.5 and 4.5 x 10^{-34} esu. At longer wavelength the samples

exhibited complex nonlinear absorption behaviour, involving various multiphoton phenomena, with three-photon absorption being a dominant process in the range of 640–825 nm, showing the maximum cross-section $\sigma^{(3)}$ at 640 nm in the order of 5 x 10^{-79} cm^6 s^2 in **335b**, and up to 1 x 10^{-78} cm^6 s^2 in **335a** and **335c**. The third-order optical non-linearities could be improved by increasing the electron acceptor strength of terminal groups.[192] Recently, a series of soluble push-pull chromophores **126** (n= 0-5) with alkyne spacers of varying length between aniline donor ring and the TCBD (1,1,4,4-tetracyanobuta-1,3-diene) acceptor has been reported.[192] This work also shed light on the influence of the ethynyl spacer length on their third-order optical non-linearities. In these systems, the E_g decreased with increasing length of the poly-yne chain spacer up to six carbon atoms and then it saturated. This trend was also observed in the NLO studies. The rotational average of the third-order polarizability γ_{rot} for **126** (n = 0-5) ranged from 2-80 x 10^{-48} m^5V^{-2}. Here a lowering of the specific off-resonant third-order polarizability for chromophores with four and five triple-bond spacers was found. In terms of nonlinear optical response, the optimal conjugation length was provided by the two- and three triple bond spacers, which featured a remarkably high, non-resonantly enhanced third-order optical nonlinearity. In poly(thienylene ethynylene)s (PTEs), the OPL effect was found to be better than C_{60}[686] (**336-338**, Chart 56**)** Furthermore, it has been observed that the OPL effect was maximum in a member having highest conjugation length (**338**). The D-A interaction in PTE was found to enhance the π-stacking interactions and thus their self-assembly. This assembly ultimately affected the NLO absorption behaviour. Thus, the optical nonlinear absorption behaviours of PHTE can be tuned easily by changing the strength of the interaction between the PHTE molecules.[687] In another system of PAEs containing thiophene rings (**339a-c**, Chart 56), a synergistic effect on the optical limiting property was found upon the inclusion of an aromatic ring.[688] The optical limiting results for these systems indicated the role of conjugation length and D-A architectures. The optical response (**339c** > **339b** > **339a**) of these polymers clearly indicated the role of these two factors.

Chart 56.

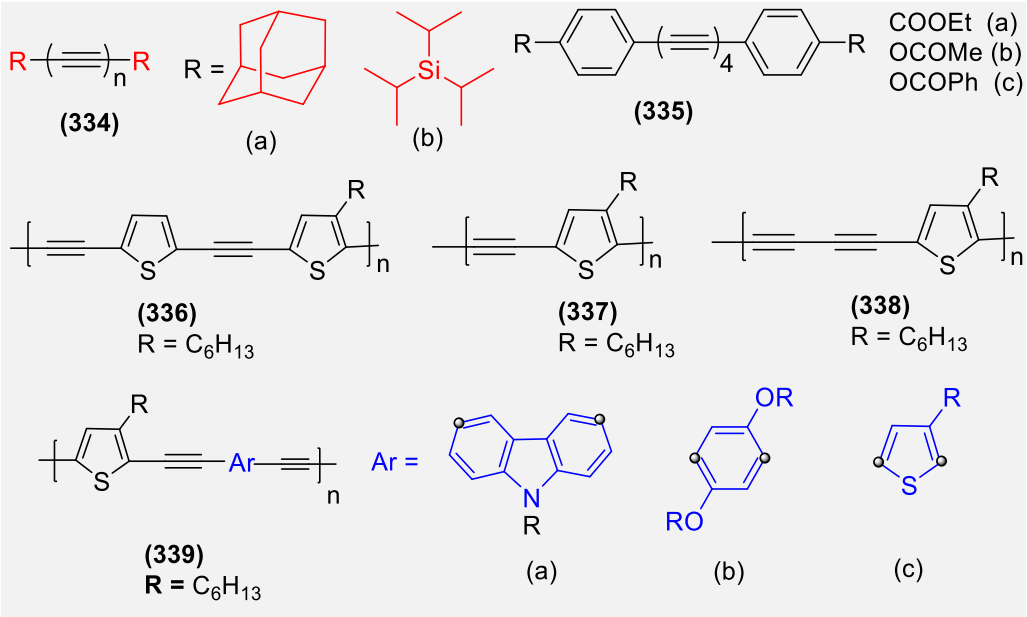

Most of the OPL measurements are conducted in solution where the nonlinear absorbent is dissolved in a suitable solvent. However, for real-life applications, solid state materials are preferred. The unique NLO properties of Pt(II) oligo- and poly-ynes is well-established. The spacers as well as auxiliaries in *trans* position verily fine tune the OPL properties of such materials. Pt(II) di-ynes containing 4-(diphenylamino)-fluorene (**340a**, Chart 57) and 4-(benzothiazole)fluorene (**340b**, Chart 57) moities in PMMA based host material exhibited a moderately large TPA cross-section in the 600-800 nm region and efficient NLA response to nanosecond pulses *via* the TPA/ESA mechanism.[689] The absorption spectra of the monomers as well as polymers were similar in solution, film, and monoliths. At 600 nm excitation wavelength, the response trend of the polymeric chromophores was in the order: **341** (PMMA) ~ **340b**(PMMA) < **340a**(PMMA) (Figure 33). The comparatively weaker NLA response of the **341**(PMMA) and **342**(PMMA) materials were attributed to the lower TPA cross-sections of **341** and **340b** chromophores compared to **340a**.[690] Despite promising results, the main obstacle was the chromophore loading. A maximum loading of organic guest (~ 10-12%) into the PMMA host was achieved, which was less than that reported earlier using the same host (PMMA).[691] However, in a recent report, it has been claimed that the silica based host materials offer better result than the PMMA based host, as the former has higher T_g and % loading capacity of the guest molecule and can be cut-polished to give desired shape.[677,692] Chateau et al.[692] reported a monolithic MTEO (methyltriethoxysilane)-based hybrid materials **342**-**344** (Chart 57) highly doped (up to 400 mM, equivalent to 30% by weight) by various Pt(II) di-ynes. The optical limiting response for silica glasses doped with 50 mM of chromophores indicated that there was positive impact on the nonlinear response and material damage threshold of increased conjugation length of the chromophore system (Figure 33). Furthermore, a sudden drop in transmitted energy indicated that the material damage threshold increases with an increased chromophore conjugation length.

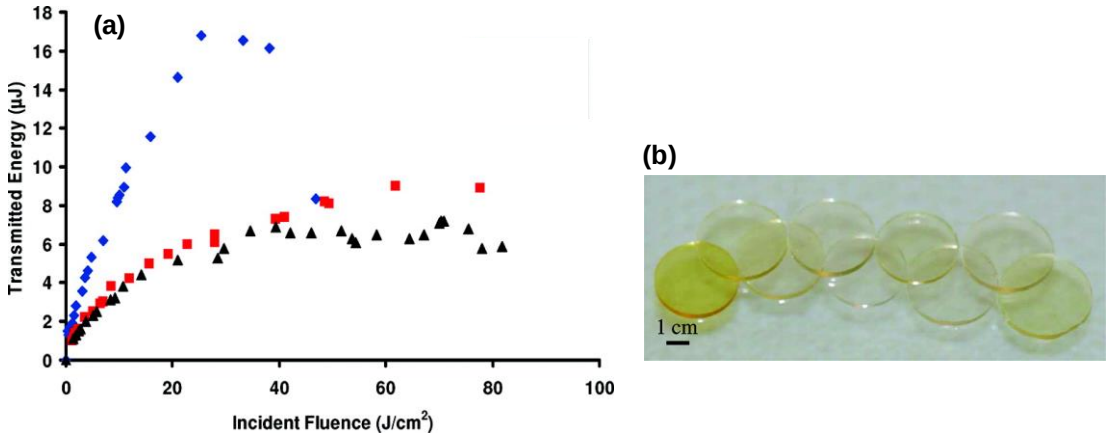

Figure 33. (a) Incident fluence *vs* transmitted energy at 532 nm, 5 ns laser pulses, for 1 mm thick MTEOS glasses doped with 50 mM of chromophores **342-343**, with linear transmission of 88, 87, and 85% respectively. (Blue = **342**, Red = **343** and Black = **344**). (b) Cut and polished monolithic hybrid silica glasses of approximately 2.5 cm diameter and a thickness of 1 mm. Reprinted with permission from ref [692]. Copyright 2012 American Chemical Society.

Durand et al.[505] compared the NLO properties of push-pull chromophores incorporating a Pt(II) center in the π-conjugated core and their organic counterpart. They noted that the second-order NLO responses of the chromophores enhance upon the metalation as well as methylation of pyridine unit. They claimed that the complex **345** (Chart 57) bearing a *tert*-butyl group on the pyranylidene flanked on the other side by N-methylated vinyl-pyrimidium fragment is characterized by a huge μβ values and is among one of the best reported to date for alkynyl metal complexes.

Chart 57.

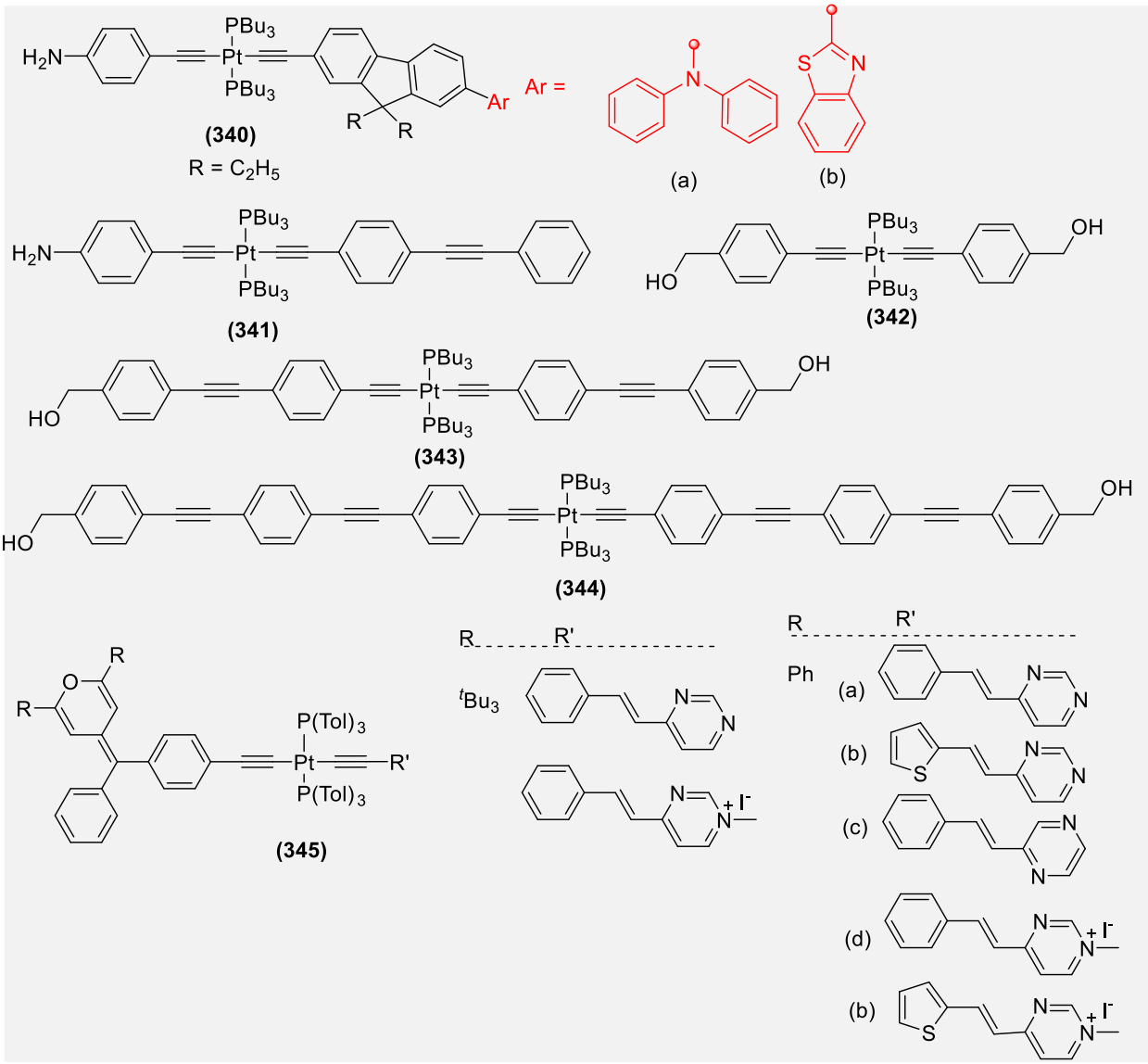

Cooper et al.[693] carried out an extensive 2PA studies of fluorene based Pt(II) oligo-ynes (**346**, Chart 58) and their model complexes. A nominally quasi-centrosymmetric spacer *trans*-*bis*(tributylphosphine)-*bis*-(4-((9,9-diethyl-7-ethynyl-9H-fluoren-2-yl)ethynyl) decorated with a range of electron donor and acceptor groups were reported (**346a-h**, Chart 58). Both model complexes, which differ only by the size of the peripheral groups, possessed nearly identical linear extinction spectra and a 2PA peak near 560 nm with

the maximum value σ_2 = 35-40 GM. They also found that peak 2PA cross-sections of neutral and electron donating group substituted Pt(II) complexes increases with increase in donor group strength and was maximum ($\sigma_2 \approx$ 300 GM for R = NPh_2). Pt(II) oligo-ynes incorporating spacers like phenylene (a), thiophene (b), bithiophene (c), EDOT (d), benzo[c][1,2,5]thiadiazole (e), and 4,7-di(thiophen-2-yl)benzo[c][1,2,5] thiadiazole (f) as core spacers and diphenylamino-2,7-fluorenylene (DPAF) as termini (**347a-f**, Chart 58) displayed a marked nonlinear response.[694] Oligo-ynes of this class displayed a decrease in transmittance with increase in input pulse energy (>100 μJ). Among different spacers, the non-linear response varies in the order **347a** < **347b** ≈ **347d** < **347c**, with the latter displaying a markedly stronger nonlinear response at higher pulse energies (> 1 mJ). These complexes featured a TPA absorption band in the NIR region (λ ≈ 700-750 nm) with a cross-section σ_2 = 50-200 GM. The σ_2 values for the Pt(II) oligo-ynes were two or more times greater than the cross-section of the reference compounds that contain only one DPAF moiety. The efficient nonlinear absorption of nanosecond pulses in the NIR region (600-800 nm) was more efficient in the chromophores in which the TPA cross-section maxima coincides spectrally with the excited T-state absorption. Oligo-yne **348** (Chart 58) with two branches containing three phenylacetylene units separated by a Pt(II) centre showed complete transparency in the visible region. It has been reported that in oligo-yne **348**, the S-state is localized over the whole molecule.[695] However, no experimental or theoretical data about the spectral behavior and magnitude of the 2PA cross-section was available until the reports by Vivas and co-workers.[696] They reported the relationship between the molecular properties and the strong 2PA capability of **348**. They showed that 2PA cross-section from tens to thousands of GM units, observed along the nonlinear spectrum, is due to pure S-S transitions. The 2PA spectrum in DCM for such system exhibited three distinct regions with reasonable (120 GM at 760 nm), high (680 GM at 610 nm), and sizable (>1000 GM between 460 and 500 nm) cross-sections. The first region, with reasonable 2PA cross-section (120 GM) around 760 nm, was attributed to presence of the non-centrosymmetric conformations of **348**. The second spectral region, with high 2PA cross-section (680 GM), located around 610 nm was ascribed to the 1^1Ag-like → 3^1Ag-like transition, which is associated with the strong intra-molecular interaction between the branches due to the presence of Pt atom. The strong 2PA cross-section observed between 460 and 500 nm (>1000 GM) was assigned to the double resonance effect and spectral coincidence of the final state in the transition induced by 2PA with the intense peak singlet ESA, which contributes to an effective intermediate state resonance. Recently, a comparative quantitative structure-property relationships for photophysical and NLO properties have been reported for Au(I) and Pt(II) acetylide complexes **349** (Chart 58) containing π-conjugated donor-acceptor-donor (D-A-D) chromophore.[697,698] Au(I) complexes featured larger fluorescence quantum yields and longer emission lifetimes compared to Pt(II) acetylide. The Pt(II) complexes exhibit enhanced triplet−triplet absorption, reduced triplet-state lifetimes, and larger singlet oxygen quantum yields, consistent with more efficient ISC compared to the Au(I) complexes. When excited by 100 fs laser pulses, all of the D-A-D chromophores exhibit moderate two-photon absorption in the NIR between 700 and 900 nm. The 2PA cross-section for the Au(I) complexes is almost the same as the unmetalated D-A-D chromophore (~100 GM). The Pt(II) complexes exhibit significantly enhanced 2PA

compared to the other chromophores, reaching 1000 GM at 750 nm. Taken together, the results indicate that the Pt(II) centre is considerably more effective in inducing S-T ISC and in enhancing the 2PA cross section. Compared to Au(I) complexes, high quantum yield and efficiency were found in Pt(II) complexes. This result reveals the greater promise for Pt(II) acetylides in chromophores for temporal and frequency agile nonlinear absorption. A similar observation has been made by Schanze and co-workers[698] (**350,** Chart 58) that the Pt(II) di-ynes have better NLO property than Pt(II) poly-ynes or the Au(I) complexes. A large second-order NLO response has also been reported for D-π-A systems in which fullerene unit (acceptor) connected through a cyclopropane ring to an ethynyl thienyl fragment (bridge) which binds a trimethylsilyl or Pt(II) alkynyl fragment (donor).[699] Substitution of the thienyl fragment by a terthiophene leads to an increase of the NLO performance by using trimethylsilyl as a donor group, whereas no effect is observed in the case of Pt(II) derivatives. Remarkably, fullerene Pt(II) alkynyl complexes can be dispersed in PMMA or PS, affording NLO-active polymer films. This work has confirmed the great potential of fullerene as an acceptor group in the design of second-order NLO-phores.

Chart 58.

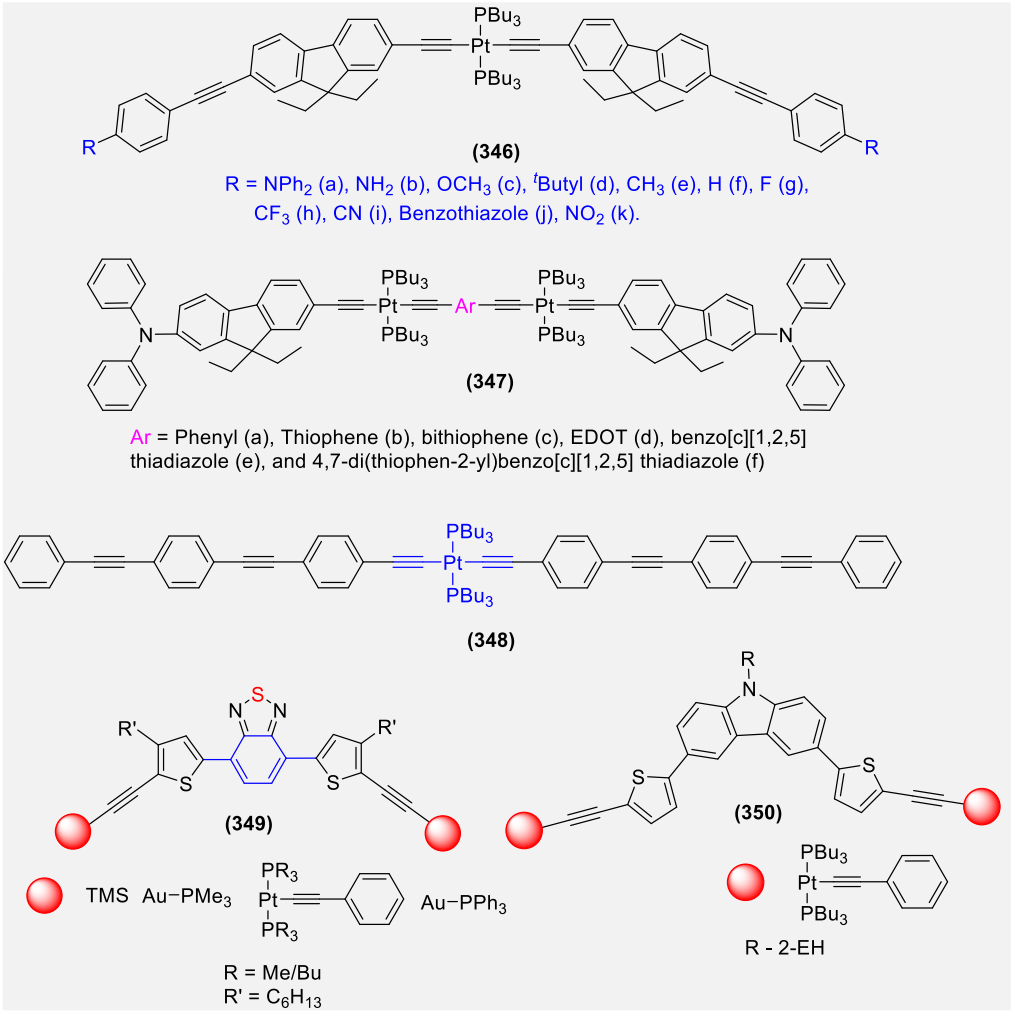

In addition to Pt(II) oligo- and poly-ynes, other transition metals viz. Fe(II), Ru(II), Ni(II), etc. based homo- and hetero-metallic systems with NLO properties have also been reported.[700,701] Silva et al.[702] reported the first hyperpolarizability of mono(η^5-cyclopentadienyl)metal(II) complexes (metal = Fe, Ru and Ni) with nitro-substituted thienyl ethynyl ligands (**351-353**, Chart 59). They found that the LE-MLCT bands were the key for second order NLO properties. These optical properties were mainly dependent upon the metal and acetylide chromophore chain length and, to a lesser extent, on the different auxiliary ligands on Ru complexes (**301**). Surprisingly a high quadratic hyperpolarizability for **353** (n = 1) was obtained compared to **351** (n = 1), **352** (n = 1, L = dppe) and **352** (n = 1, L = PPh_3) in spite of the better donor properties of Fe and Ru organometallic moieties. This phenomenon indicated the presence of some other electronic transitions (in addition to the main MLCT) which controlled the effectiveness of second-order NLO properties in these push-pull systems. Chain lengthening of the acetylide chromophores, with the introduction of one thiophene ring, led to the higher quadratic hyperpolarizabilities for all these complexes. Overall, for short-length ethynyl chromophores an enhanced effect on the magnitude of quadratic hyperpolarizability was caused by Ni organometallics, whereas organo iron and ruthenium compounds were effective for long-length chromophores NLO application. Thus, Fe and Ru complexes were more sensitive to the extension of the aromatic system than the Ni analogues. Complex **352** (n = 2, L = PPh_3) showed a better value of the corrected hyperpolarizability (224×10^{-30} esu) which places this complex at the top in the literature available so far. These results are well complemented by a recent study in which bis-alkynyl **354** (Chart 59) was found more active than monoalkynyl analogue and exhibits TPA around 860–1050 nm with TPA cross-sections above 350 GM.[703] The NLO properties of Ru(II) dialkynyl complexes were found to be easily modified by nature of the alkynyl substituents.[704] Complexes **355** bearing a 2,1,3-benzothiadiazole flanked on either side by 2,5-thienyl units, showed a negative value of $\mu\beta_{1.907\ EFISH}$ when determined by electric-field-induced second harmonic generation (EFISH) technique (DCM solution at 1907 nm). Similarly, high values for homobimetallic symmetrical complexes **356-358** (Chart 59) carrying Ru and Pt metal fragments and 2,1,3-benzothiadiazole as central spacer have been reported in the literature.[705] These values are some of the best reported values for organometallic complexes for the preparation of second harmonic generation active polymeric films.

Chart 59.

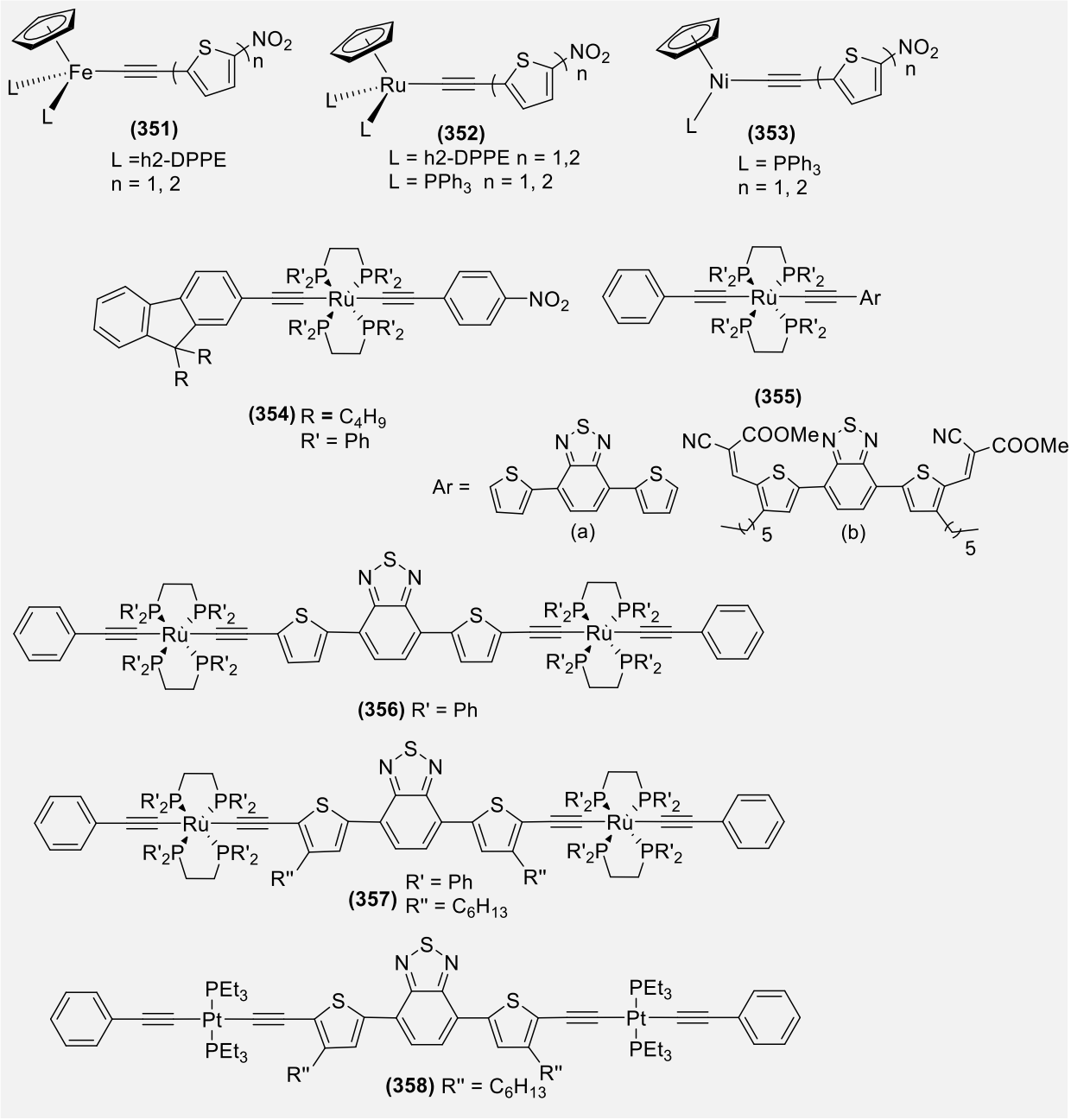

4.1.3. Organic light emitting diodes (OLEDs)

Recently, there has been increased interest in organic light emitting diodes (OLEDs) made from small organic and organometallic compounds as well as polymers due to their potential low cost and applications in solid-state lighting and flat-panel displays. OLEDs are considered as more versatile than conventional inorganic LEDs due to their flexible nature, low cost and energy efficient technology.[706] Additionally, they also offer the distinct advantages of high luminous efficiency, a full-colour range, and low manufacturing cost.[707-710] Ethynyl compounds bearing conjugated spacers and metals have achieved a good reputation

as both the emitters and dopants with high brightness and efficient electroluminescence (EL).[275,711,712] The alkynyl moiety present between the metal and ligand significantly enhances the PL quantum efficiency. It is to be noted that most of the OLEDs reported with high efficiency are based on tridentate cyclometalated and NHC ligands attached to Pt(II) or Au(III) through ethynyl linkages.[275,713-720] Other materials such as cross-linked polymers and nanoclusters will not be discussed here due to the limitation of the scope. For a detailed discussion on the light-emitting conjugated poly(arylene ethynylene)s, interested readers are referred to the reviews by Grimsdale et al.[721] and Ho et al.[5]

In the previous sections, we discussed the intriguing photo-physical properties of acenes and their heterocyclic analogues, *viz*. azaacenes. The optical properties and crystallization behaviour of the acenes, which are governing factors for O-E application, are greatly influenced by the number of rings, presence/absence of heteroatoms, the connectivity of the rings, etc. Due to the excellent emitting properties, several acenes/heteroacenes have been reported for the fabrication of OLEDs as emitting layers as well as dopants.[392] Several LEDs based on ethynylated tetracene with orange to red electroluminescence (EL) have been reported in the past.[722,723] OLEDs based on **360** (Chart 60) showed improved device performance[724] compared to the previously reported structurally similar tetracenes.[722] (Figure 34) In these molecules, the length of the acene backbone and the position of the TIPS-ethynyl substituents affect the solid-state structure and optical properties. For example, **359** was found as crystalline solid while **360** and **361** (Chart 60) were amorphous solids.

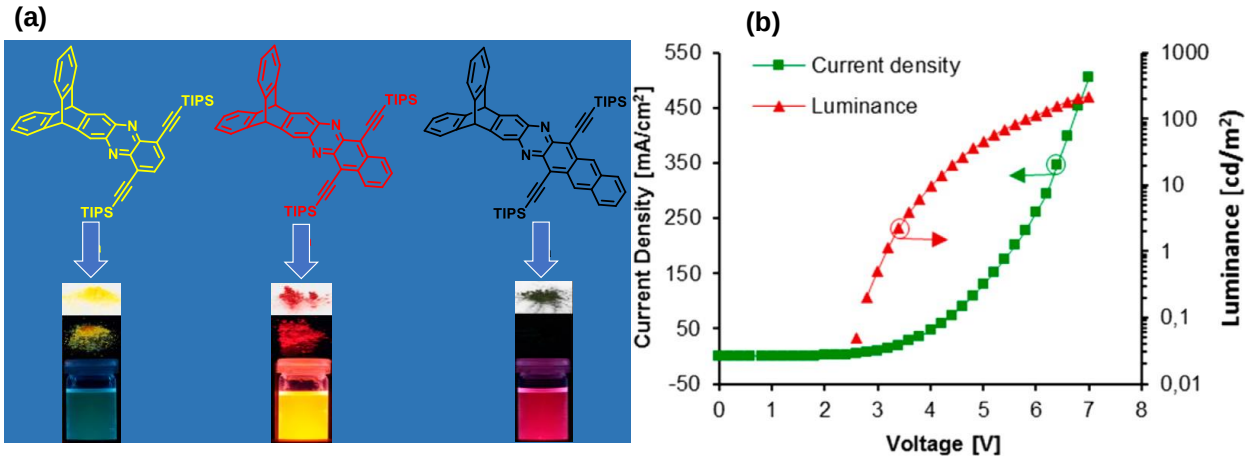

Figure 34. (a) Chemical Structure of compounds **359-361**, (b) The luminance-voltage (red) and current density-voltage (green) plots of an OLED with **360** as the emitter. Reprinted with permission from ref [724]. Copyright 2015 American Chemical Society

Chart 60.

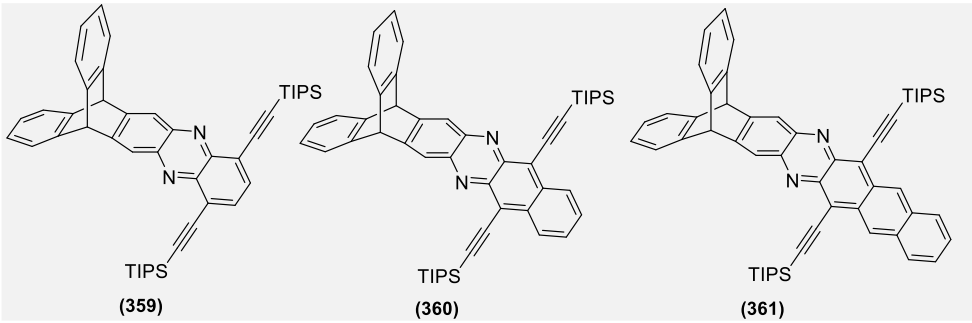

Small ISC rate constant and larger fluorescence emission are some of the important criteria to obtain white-OLEDs (WOLEDs).[711] A white light emission has been reported in D-A type phenyl butadi-yne chromophore. The intensities of the LE and exciplex emissions of the push−pull diphenylbutadiyne are suitably balanced in CH_3CN to generate the pure white light emitting with a good CIE value (0.33, 0.32) (Figure 35a) through control of the fluorophore concentration (4 μM).[712] Recently, Maji and co-workers[725] reported bola-amphiphile (gels) based on **362** (Chart 61) that showed gelation behaviour with vesicular morphology (Figure 35b). Upon *in-situ* loading of a suitable dye and redox-active molecule, pure white light emitting and CT-gels, respectively were realized. This work could pave the way towards realizing the immense potential of opto-electronically active organic bola-amphiphilic OPE systems by transforming them into solution processable soft hybrids.

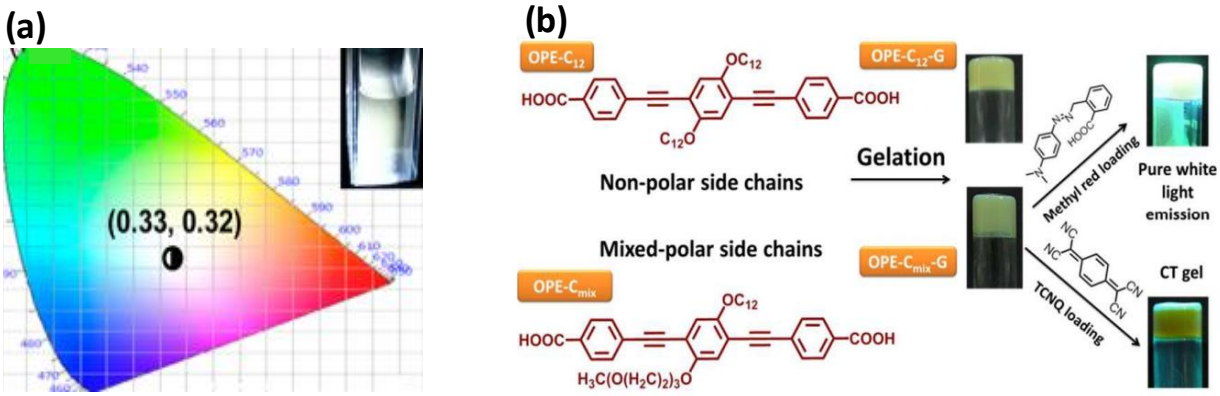

Figure 35. (a) The luminance-voltage (red) and current density-voltage (green) plots of an OLED with **362(a)** as the emitter. Reprinted with permission from ref [712]. Copyright 2016 American Chemical Society. (b) The gelation of two bola-amphiphilic chromophores **362b**, utilized for pure white light emission and CT gel formation. μM). Reprinted with permission from ref [725]. Copyright 2017 Royal Society of Chemistry.

Due to the far separated dual emissions (fluorescence and phosphorescence), complex **289** (n = 3, Chart 42)[558] was assessed as dopant for WOLEDs. Although preliminary, device fabricated using this complex showed some promising results. A device with configuration ITO/PEDOT:PSS (30 nm)/**289**(50 nm)/TPBI (50 nm)/LiF (0.5 nm)/Al (100 nm) showed maximum EQE of 0.22% with current 0.31 cd A^{-1} and power efficiency equal to 0.25 lm/W^1. In combination with hole transporting material TCTA, the EL spectra of the

device exhibited whole visible region with high color-rendering index (CRI = 89.2−92.2). WOLEDs have also been reported using Pt(II) oligo-ynes incorporating diethynyl benzene spacer (n = 1-3).[711] Pt(II) Poly-ynes (**363**, Chart 61) incorporating alternating oxadiazole and 9-substituted fluorene showed HOMO at -3.63 eV and LUMO at around -6.5 eV. This combination of poly-ynes displayed a good potential as LED and single-dopant for white PLEDs.[726] Device doped with 1% of **363** (Chart 61) gave the best performance with maximum external quantum efficiency (η_{ext}) of 0.15%, a luminance efficiency (ηL) of 0.58 cdA^{-1}, a power efficiency of 0.58 cdA^{-1}, and a power efficiency (ηp) of 0.16 lmW^{-1}. A decrease in η_{ext} above 1% was attributed to the concentration quenching effect. To act as a WOLED, the x and y coordinates of CIE chromaticity should be equal to (0.33, 0.33). Here, in this case, the device based on **311** was very close to the coordinates closely approaching the white light using a single dopant. LED based on bithiazole containing polymer **240ao** (Chart 28, n = 9) showed some promising results.[445] The EL of the device and PL spectra of the poly-yne in thin film as well as in solution showed a similar behavior indicating the absence of aggregation or π-stacking and hence both processes arise from the same excited state or the same type of exciton. A device based on **240ao** showed emitted green light with a prominent EL maximum at 500 nm with a shoulder at 522 nm and the CIE chromaticity coordinates lie at x = 0.26, and y = 0.58 at 8 V. The EL was almost invariant of the driving voltage under the operating conditions and has a stable color. The PLED had a turn-on voltage for light emission at a brightness of 1 cdm^{-2} of 8.8 V and the luminance reached 37 cdm^{-2} at 16 V. The high driving voltages relative to other typical vacuum evaporated devices may be a result of the thicker emissive layer used and the large hole barrier at the PEDOT:PSS/Polymer (n = 9) interface (HOMOs of polymer (n = 9) 5.7 eV *vs* PEDOT 5.0 eV). With an increase in applied voltage, the current began to increase rapidly, accompanied by a rapid increase in luminance. The maximum luminance efficiency of the device is moderate at 0.11 cdA^{-1} at 9.0 V, which compares well to the performance of organic devices from some fluorene-based alternating organic copolymers that contain bithiazole units as reported by Lee and co-workers.[727]

When Re-complexes **155** (Chart 14) were used as electrophosphorescent emitters or dopants for the fabrication of multi-layer OLEDs, a maximum luminance of 2577 cdm^{-2} at 16 V, 2735 cdm^{-2} at 18 V, 2130 cdm^{-2} at 17 V and 2438 cdm^{-2} at 19 V were obtained.[320] The maximum current efficiencies obtained were 1.97, 1.89, 1.55 and 1.83 cdA^{-1}, respectively. On the other hand, two different metal centres showed synergistic effect in governing the photo-physical behaviour of hetero-metallic oligo(metalla-ynes). In a thermally stable hetero-bimetallic oligo(metalla-ynes) having Ir(III) 2-phenylpyridine complex with a square planar Pt(II) unit (**364-365**, Chart 61), it was found that the emissive species involved in these oligo(metalla-ynes) were mainly arising from the Ir(III)-centred building block with added benefits endowed by the Pt(II) component.[728] A device made up of these heterobimetallic complexes gives a maximum brightness of 3356 cdm^{-2} (or 2708 cdm^{-2}), EQE of 0.50% (or 0.67%), luminance efficiency of 1.59 cdA^{-1} (or 1.55 cdA^{-1}), and power efficiency of 0.60 LmW^{-1} (or 0.55 LmW^{-1}) for the yellow (or orange) PHOLEDs. In a recent report, Chen and co-workers showed that OLED fabricated using $PtAg_2$ hetero-trinuclear complexes produces 67.4 cdA^{-1} of peak current efficiency and 17.4% of external quantum efficiency.[729]

Chart 61.

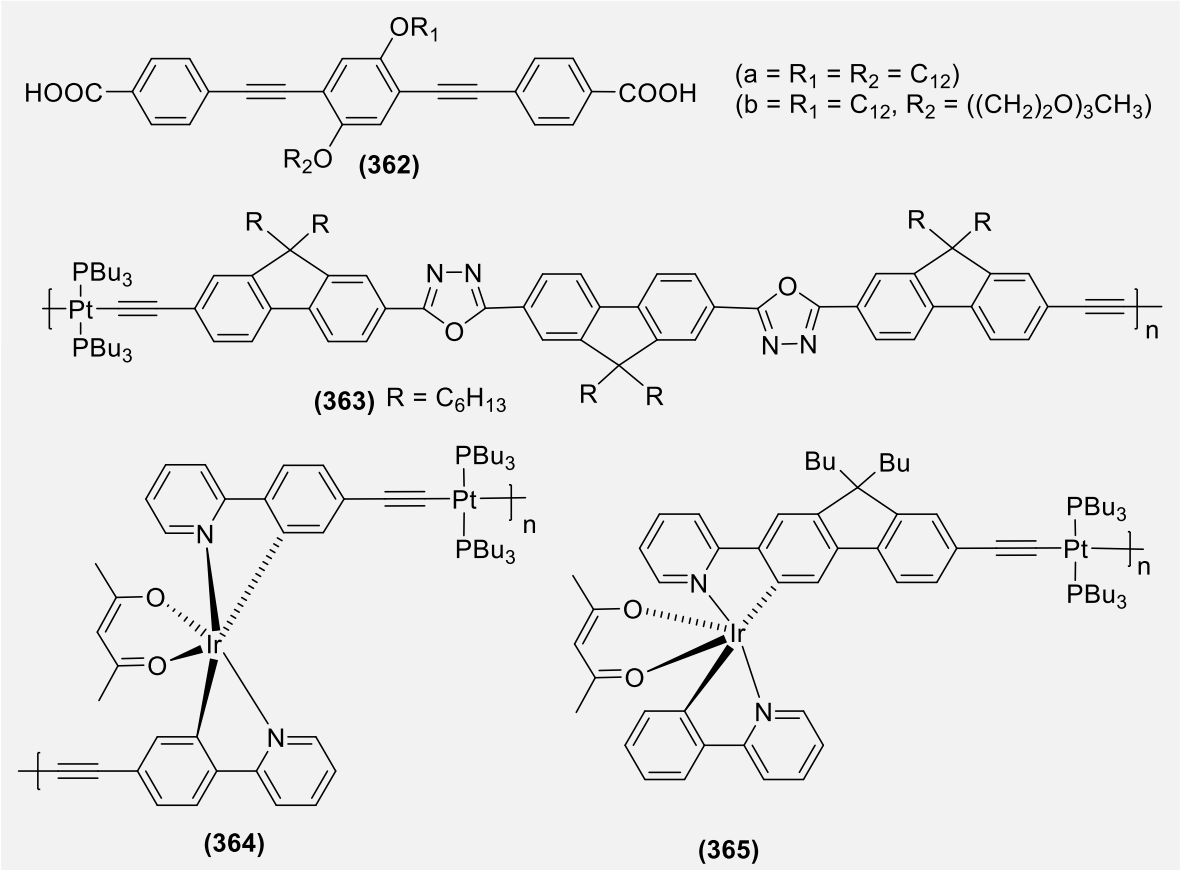

4.1.4. Organic field-effect transistors (OFETs)

Organic field-effect transistors (OFETs) have attracted immense research interest due to their possible use in the fabrication of new generation electronic devices. OFET has a switching device configuration and is composed of source, drain and gate electrodes, and an active layer of organic semiconductor. In between the gate electrode and semiconductor, an insulator layer, such as SiO_2, also exists. Due to the high mobility, low cost, flexibility, easy processing and light weight, several conjugated organic semiconductors (n-type as well as p-type) have been reported.[730,731] The semiconducting property of an organic systems depends on various factors: molecular structure, molecular packing, electronic structure, energy alignment, purity, etc.[730-732] In general, an OFET device is considered good if it shows high mobility, large on/off ratio and low threshold voltage under ambient condition (*i.e*. stable in air).[732] In this context, oligo-ynes and metalla-ynes are considered excellent candidates as they have rigid-rod structure with significant π-conjugation, steric and conformational advantages for orbital delocalization, high solubility and offers structure tunability.[733] Since the frontier orbitals of ethynyl containing materials can be easily tuned, both n-type (molecules with low HOMO or electron acceptor) and p-type (molecules with high HOMO or electron donor) organic materials have been reported.[732] As discussed before, molecular structure of the organic semiconductor has significant impact on carrier mobility as the structure with π-stacking has high carrier mobility due to the strong intermolecular interaction. Therefore, construction of π-stacking structures would give materials

with high mobilities. Among several strategies, one way to achive π-stacking structures is the introduction of bulky substituents. Based on this notion, several, diethynylacenes based OFETs have been reported with low to high carrier mobility. Furthermore, it has also been reported that the increment in the bulkiness of ethynyl moiety enhances the solubility and mobility of the material.[734-737] The introduction of ethynyl core not only enhances the carrier mobilities *via* efficient molecular packaging, but also imparts stability to the organic backbone.[645,736] For example, solution-deposited films of pentacene derivatives **367** (Chart 62) and anthradithiophene derivatives **368** (Chart 62) gave device processing independent (solution/thermal) mobility values of 1.5 $cm^2/V.s$ and 1.0 $cm^2/V.s$, respectively.[736] This high value was attributed to efficient molecular packaging (2-D π-stacked arrangement). Swartz and co-workers found that the charge carrier mobility of electron deficient pentacene derivatives (**366**, Chart 62) varies with the number of fluorine atoms.[738] Furthermore, addition of fluorine was found to increase the solubility and stability and lower the reduction potential. Ostoja et al.[739] compared OFET device performance of unsubstituted and modified quinquethiophenes including **369**. (Chart 62) XRD results of vacuum deposited thin film showed the formation of highly ordered and crystalline thin films at different temperatures (30, 90 and 140 °C). All compounds including **369** (Chart 62) showed temperature dependent carrier mobility and current on/off ratio. Compared to the parent quinquethiophenes and its methylated derivative, **369** showed very low carrier mobility (4×10^{-6} to 8×10^{-4} $cm^2/V.s$). Kim et al.[740] used D-A-D strategy to develop organic semiconductors **370** (Chart 62). A top-contact/bottom-gate solution processed device fabricated with **370** gave a carrier mobility up to 1×10^{-4} $cm^2/V.s$ with I_{on}/I_{off} ratios of $> 10^5$. Despite the fact that di-ynes has high stability (5% loss at > 237 °C) with moderate band-gap (2.54 eV), poor performance could be attributed to the poor film texture. Similar values were reported for anthracene based oligo-yne **371-373**. (Chart 62 and 63)[645] One of the systems, **372** (n = 1) has shown excellent performance (0.01 $cm^2/V.s$).

Chart 62.

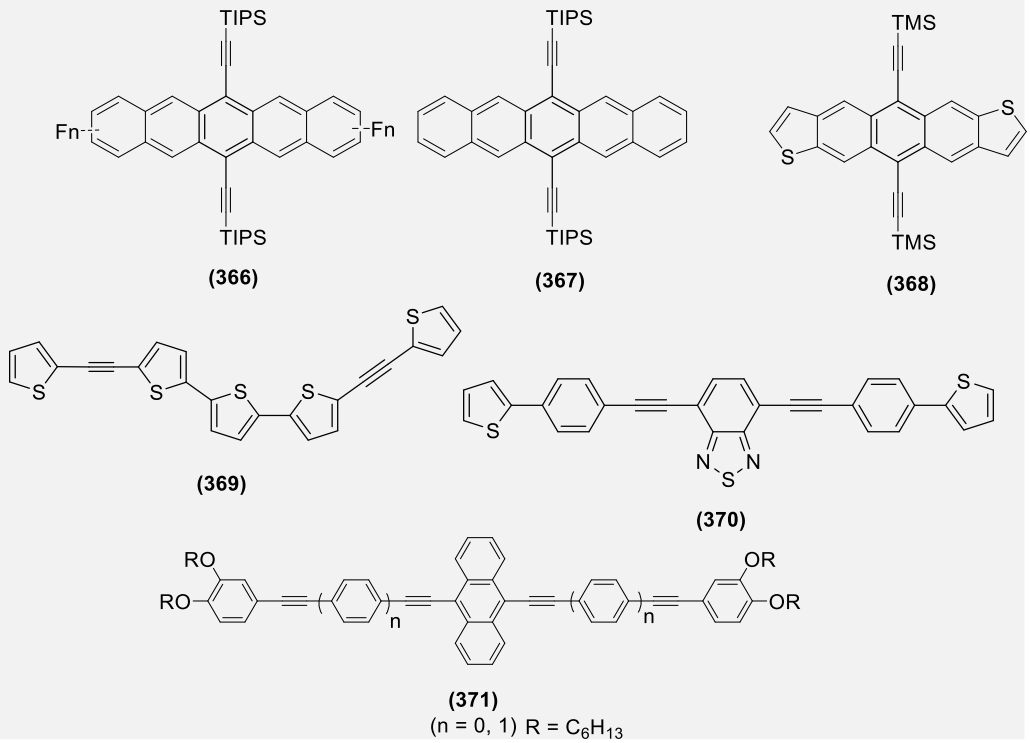

As discussed before in PV section, an improvement in OFET's performance is observed when an alkyl chain is replaced by less sterically demanding alkynyl chains. OFET device fabricated using polymer **318** (X = S, Chart 52) of top-gate/bottom-contact (TG/BC) architecture showed a very high hole mobility (μ_h = up to 0.13 $cm^2/V.s$) and I_{on}/I_{off} ratios > 10^4. Interestingly, changing the device structure from TG/BC to BG/TC (bottom-gate/top-contact) led to the inversion of charge carrier polarity, i.e. OFET device with moderate electron mobility (μ_e = 0.057 $cm^2/V.s$) with I_{on}/I_{off} ratio 10^3. Annealed materials-based devices showed higher performance than non-annealed counterpart, a synergistic effect on the performance. Bodreault et al.[741] reported electron-rich building block, 2,2′-ethyne-1,2-diylbis[3-(alk-1-yn-1-yl) thiophene flanked by the 2-ethylhexyl substituted TDPP π-acceptor unit based three low band gap materials. **374** Based semi-conductors (Chart 63) showed very high hole mobilities. BG/TC OTFT device performance indicated hole mobilities as high as 0.17 $cm^2/V.s$ for compound **374** with I_{on}/I_{off} ratios greater than 10^4 under ambient conditions. In 2015, Giguère, Sariciftci and Morin reported three cruciform anthanthrene scaffold with different pendant groups-based semiconductors **375-377** (Chart 63).[597] A bottom-gate/bottom-contact (BC/BG) device with **377** as semiconductor showed mobility as high as 0.078 $cm^2/V.s$ with I_{on}/I_{off} ratios of > 10^6, and a low threshold voltage of -6 V. All compounds showed an improvement in the performance upon solvent annealing due to the formation of J-aggregates.

Chart 63.

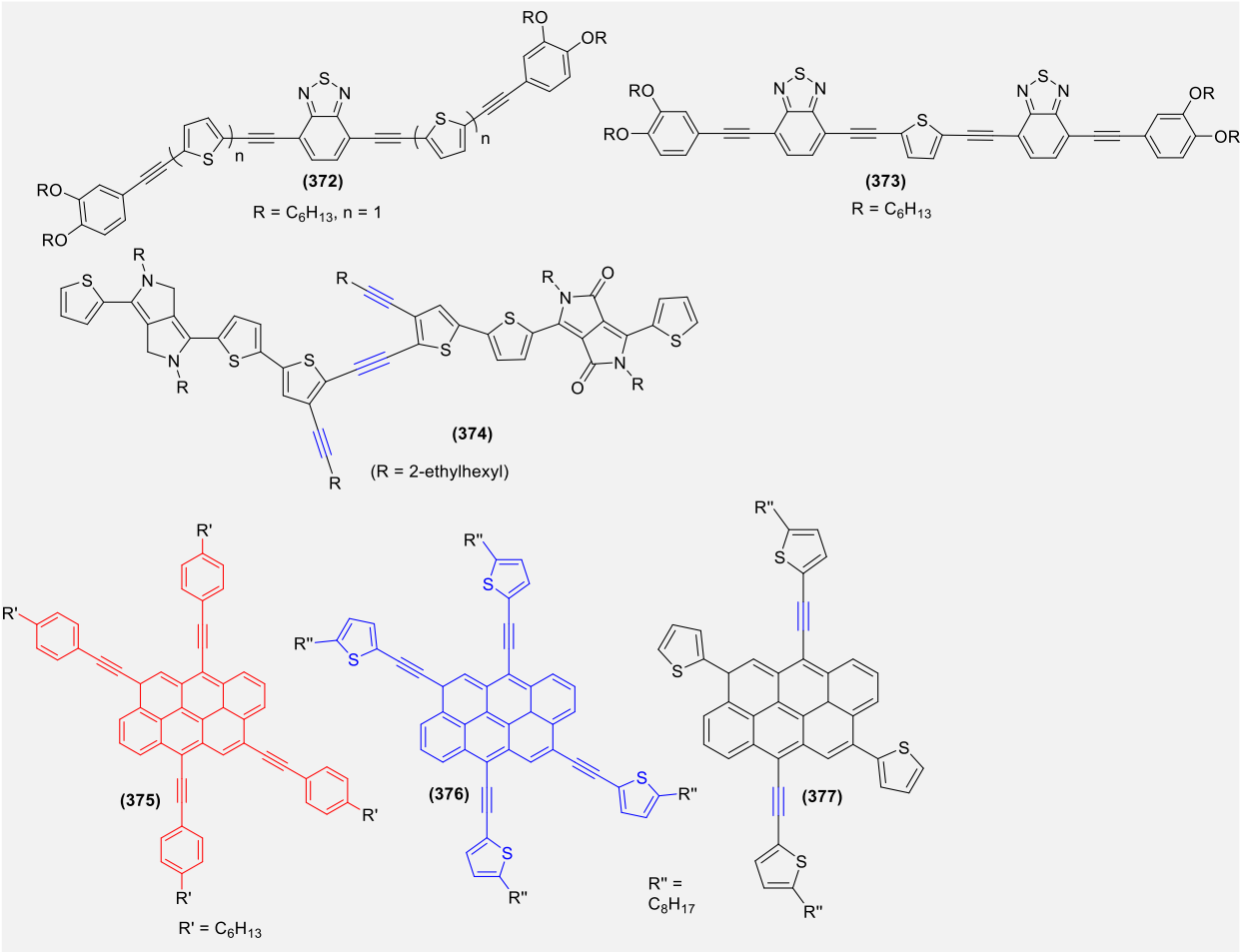

Other than the small oligo-ynes discussed above, several other poly-ynes (**378-387,** Chart 64) and poly-(metalla-ynes) (**388-392**, Chart 65) have also been assessed as OFET materials (Table 11). Among organic systems, those based on TDPPs are particularly attractive candidates.[730] In 2012, Lee et al.[737] demonstrated that the co-poly-ynes based on TDPP and anthracene (**386** and **387**) can produce highest charge mobility (0.12 $cm^2/V.s$) depending on how TDPP and anthracene are connected. Three years ago, Yun et al.[733] reported ambipolar behaviour of 1,4-di(thiophen-2-yl)buta-1,3-diyne (DTB) donor and TDPP as acceptor separated by an acetylide (n = 1) **385** (Chart 64) polymer with a high electron mobility (0.38 $cm^2/(V.s)$, high hole mobility (2.19 $cm^2/V.s$) and ambipolarity (μ_e/μ_h = 0.26). Contrary to this, its vinyl analogue showed unipolar characteristics only. The μe/μh ratios was low for the vinylene based FETs (~0.008), whereas those based on alkynyls showed almost 30 times higher performance (~0.26), indicating that alkynyl-based device forms both hole- and electron-accumulated channels with high mobilities. This behaviour strongly suggested the presence of ethynyl core, which effectively promotes overlap of the electron wave functions of the DPP units along the main chain (Figure 36). However, in a recent study, Eckstein et al.[648] found that further extension of alkynyl unit (n = 2) in polymer **385** endows only unipolar behaviour with hole mobility as high as 0.1 $cm^2/V.s$ with threshold voltage of -8.3 V and I_{on}/I_{off} ratios of >

10^5. The authors noted significant impact of the alkyl functionality on the performance. High solubility of the polymers allows fabrication of BG/TC OFETs devices. Similar to the previous example, annealing of the polymers greatly affected the performance of device (μ = 0.017 (unannealed)/0.062 (annealed) and 0.049 (unannealed)/0.077(annealed) $cm^2/V.s$.

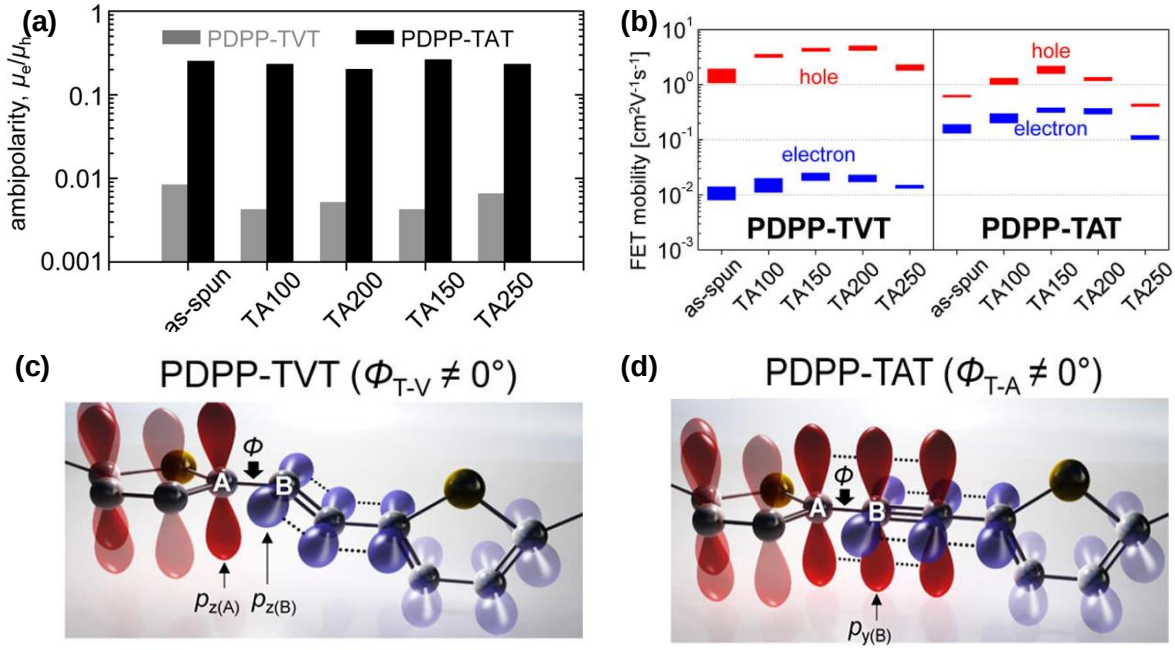

Figure 36. (a) The range of electron and hole mobilities of vinylene (PDPP-TVT, gray) and acetylenic polymers (PDPP-TAT FETs according to the thermal annealing (TA) temperature (100, 150, 200, and 250 °C). (b) The average electron/hole mobility ratio (μe/μh) of PDPP-TVT) and PDPP-TAT FETs. p-orbitals of the carbon atoms in (c) PDPP-TVT and (d) PDPP-TAT when ϕ ≠ 0°. Reprinted with permission from ref [733]. Copyright 2014 American Chemical Society.

Chart 64.

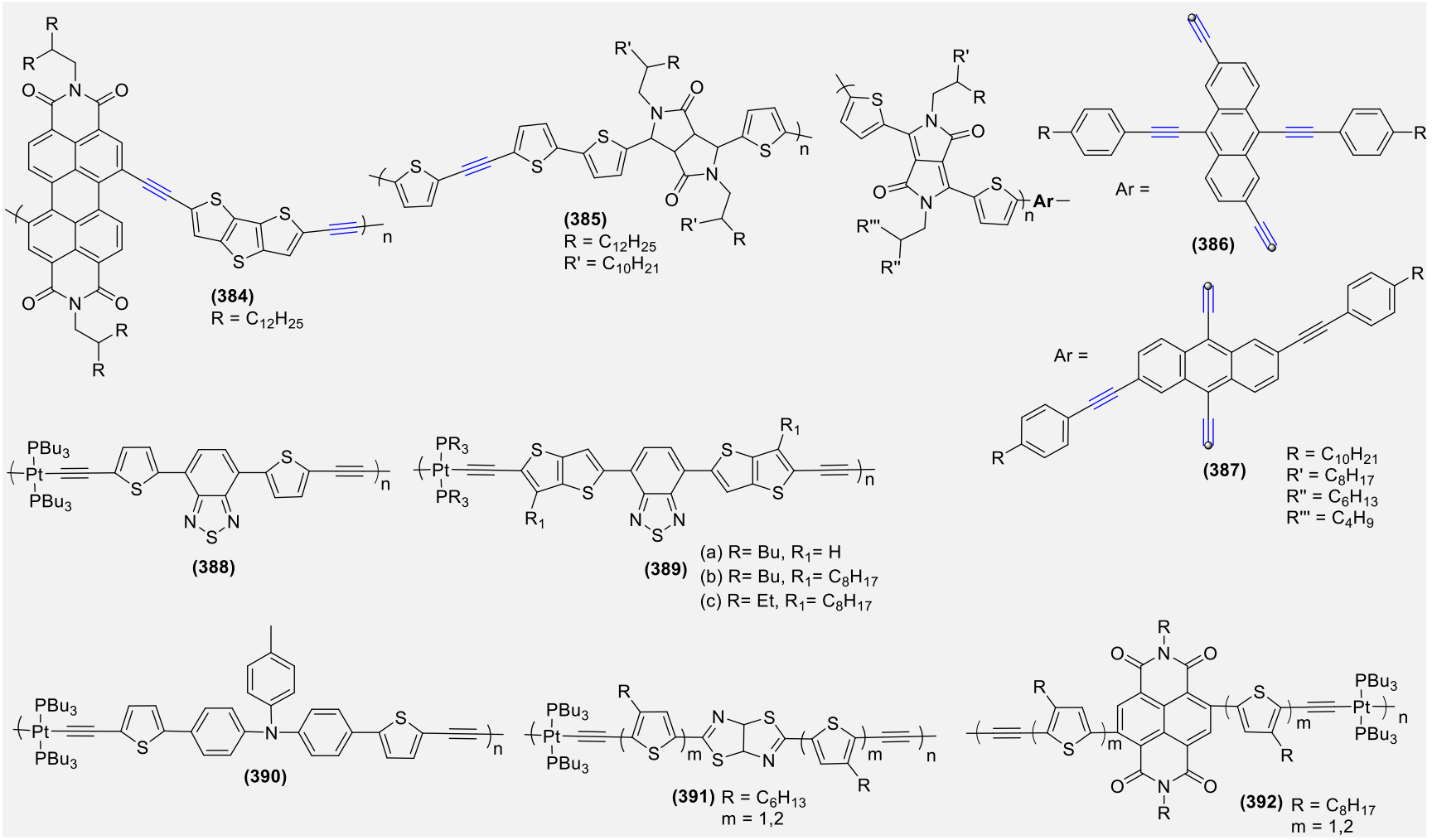
(384)
R = C12H25
(385)
R = C12H25
R' = C10H21
Ar =
(386)
Ar =
(387)
R = C10H21
R' = C8H17
R'' = C6H13
R''' = C4H9
(388)
(389)
(a) R= Bu, R1= H
(b) R= Bu, R1= C8H17
(c) R= Et, R1= C8H17
(390)
(391) R = C6H13
m = 1,2
(392) R = C8H17
m = 1,2

Table 11 summarizes mobility, I_{on}/I_{off} ratio and threshold voltage of a range of organic and organometallic poly-ynes. Similarly, Pt(II) poly-ynes have also been reported with low to moderate performances.[442,575,742] For example, in 2008, Baek and co-workers[575] reported OFET performance of 4,7-di-2′-thienyl-2,1,3-benzothiadiazole **388** (Chart 65) and 4,7-di-2′-thieno[3,2-*b*]thiophene-2,1,3-benzothiadiazole **389** (Chart 65) based Pt(II)-polymers. OFET devices of BG/TC configuration showed low mobility (0.006×10^{-2} $cm^2/(V.s)$ with I_{on}/I_{off} ratio of 4.8×10^2 in case of polymer **388**, while a significant improvement in performance was observed for polymer **389** ($0.15\text{-}0.89 \times 10^{-2}$ $cm^2/V.s$), despite its amorphous nature. They found that the alkylation of rigid-core (thieno[3,2-*b*]thiophene) improves the performance of device, attributed to the enhanced packing of polymer chains *via* face-to-face stacking. Furthermore, shortening of the phosphine chain length led to the enhancement in mobility, possibly due to the reduced steric hindrance between two adjacent alkyl side-chains present over metals. One of the recognized factors for low OFET device performance is '*chain folding*' which limits the charge carrier mobility. One way to circumvent this issue is to incorporate rigid unit to the polymer backbone. Based on this notion, an improved performance was noted for Pt(II) poly-ynes **391** (Chart 65) bearing rigid thiazolothiazole spacer.[743] These polymers had higher Eg than **389**, (Chart 65) but they showed enhanced hole mobility ($2.1\text{–}2.8 \times 10^{-2}$ $cm^2/V.s$) with an I_{on}/I_{off} ratios of $\sim 10^5$. On performing structure-property relationship, a direct relationship between hole mobility and the conjugation length was found. To control the chain folding issue, polymer **392** (Chart 65) has also been reported recently. Unlike other NDI-incorporated polymers which shows electron-mobility, **392** showed hole mobility with $\mu \sim \times 10^{-4}$ $cm^2/V.s$, attributed to the introduction of metal centre. In a recent investigation, Huang et al.[744] reported some novel D–A type organic multifunctional semiconductors. They synthesized one carbazole-fluorene copolymer and four other co-polymers composed of carbazole-fluorene as donor and (2,1,3-benzothiadiazole, 4,7-bis(2-thienyl)-2,1,3-benzothiadiazole, 5,6-difluoro-2,1,3-difluorobenzothiadiazole, and 5,6-difluoro-4,7-bis(4-hexyl-2-thienyl)-2,1,3-benzothiadiazole as acceptors. Due to the presence of uracil functionality at the donor core, the resulting polymers formed extensive chain of H-bonds leading to the formation of cross-linked structure and supra molecular assembly films with excellent electron transport properties. Among donors (carbazole and fluorene), polymer with fluorene exhibited much smaller threshold voltages (3.5-4.6 V) and higher electron mobilities ($1.87\text{-}3.55 \times 10^{-4}$ $cm^2/V.s$) than *tris*(8-hydroxyquinolinato) aluminium (Alq_3). (6.2 V; $1.21 \times 10 -5$ $cm^2/V.s$).

Table 11. OFETs parameters of some organic and organometallic di-, oligo- and poly-ynes based semiconductors.

Semiconductors	V_{th} (V)	I_{on}/I_{off}	E_g^{opt}	μ ($cm^2/V.s$)	Ref.
378 (R = n-doceyl)	-8.3	5.6	1.51*	$1.7 \times 10^{-2*}$	648
378 (R = 2-Ethylhexyl)	-27.9	5.7	1.54*	$4.9 \times 10^{-2*}$	
379	-30	8.2×10^3	1.57	3.70×10^{-4}	745
380	-23	9.3	1.28	4.42×10^{-9}	746
381	42	5.79×10^3	1.42	3.10×10^{-7c}	746
382	-15	5.91×10^3	1.67	2.99×10^{-6}	746
383	55	10^3	2.57	2.00×10^{-4}	747
384	4	$\approx 10^5$	1.98	6.0×10^{-2}	748
385	-	-	1.5	0.38[a] 2.19	733
388	-	4.8×10^2	1.85	6×10^{-5}	575
3894a	-	5.2×10^4	1.84	1.5×10^{-3}	575
389b	-	1.5×10^6	1.82	5.7×10^{-3}	575
389c	-	1.5×10^6	1.81	8.9×10^{-3}	575
390	-	-	2.72	1.9×10^{-5}	742
391a (m = 1)	-	$\approx 10^5$	2.15	1.5×10^{-2}	743
391b (m = 1)	-	$\approx 8 \times 10^4$	2.05	2.2×10^{-2}	
392a (m = 2)	-25	3.3×10^3	1.55	3.84×10^{-4}	749
392b (m = 2)	-21	2.5×10^2	1.45	2.89×10^{-4}	

Chart 65.

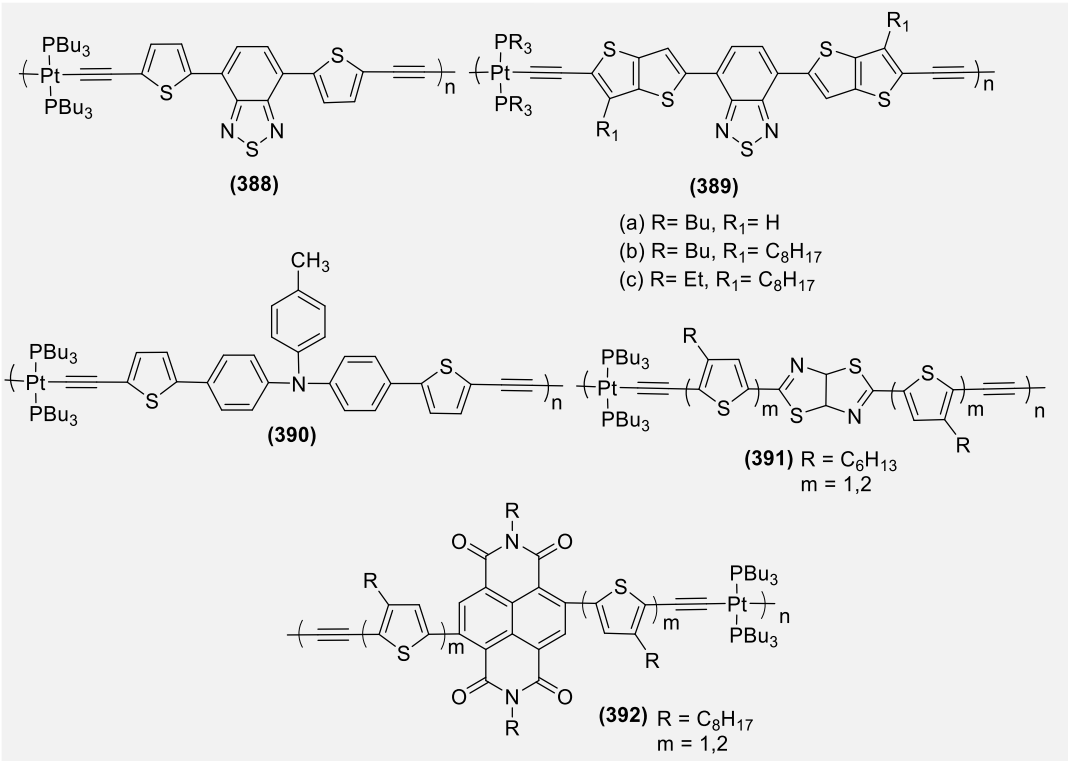

4.1.5. Molecular wires

In the quest for new materials for single-molecule electronics, organic and organometallic oligo-ynes have attracted huge interest. This can be attributed to the advantages offered by this class of molecules: high thermal stability and long-range conductivity at single molecular level.[4,21] Furthermore, they offer an additional feature of electronic properties modulation *via* molecular architecture or molecular engineering. For example, π-conjugated molecular wires strapped by cyclic π-conjugated side-chains have been reported for possible use in molecular electronics.[225] Similarly, the possibility of decorating termini with different end groups (*viz*. thiol, azide etc.) further equips researchers with the ability to anchor the molecular wires to the metallic and graphene based electrodes through the thiol or azide linkers. The group led by Moreno-Garcia[750,751] performed comparative electrical conductance studies of tetra-yne bearing electron-rich and electron-deficient aromatic rings **(393a-j**, Chart 66). They found that the presence of an electron withdrawing group at the termini produces more stable oligo-ynes (**a** and **f**) than electron donor functionalities (**b-e**). The electrical conductance studies indicated that **393e** has the highest probability of junction formation (junction formation probability, JFP ≈ 100%) and the conductance values are higher than the other reported molecular wires of similar length.[599] They also found that the oligo-yne **393e** bearing benzothiophene had superior anchoring ability compared to the traditional anchors. Prompted by these results, Sadeghi et al.[752] carried out an investigation of comparative phonon and electron transport properties of unsaturated (oligo-ynes) and saturated (alkane) benzothiophene-based wires **393e** of varying lengths (n =1, 2, 4, 8). Unexpectedly, they noticed that oligo-ynes had lower phonon thermal conductance than the corresponding alkanes and showed an inverse relationship with the chain length, which was attributed to the rigid-rod nature of the C≡C-containing systems. However, low thermal conductance combined with higher thermopower and higher electrical conductance led to a maximum thermoelectric figure of merit of ZT = 1.4, which is several orders of magnitude higher than that of alkanes. Almost similar result has been reported for benzothiazole oligomers in which the conductance lowered with increasing chain length.[750] Zhao et al.[47] carried out the first study on length dependent conductance properties of pyridyl end capped oligo-ynes **(394-396**, Chart 66**)**.[47] Due to the varying length of the wires (~ 2-6 nm), some unique charge transport properties were noted. For instance, in short molecules, a coherent transport mechanism was dominant while in the longer ones, incoherent hopping mechanism was favored. This transition occurred at a molecular length ~ 3.0 nm and conductance below 10-6.5 G_0. The probability for a molecular junction was found to be inversely related to the molecular length and this was attributed to the larger number of molecular conformations and the increased number of side-chains. Prior to this, the same group developed a novel method for conductance measurements at the nanoscale.[753] They showed that TMS protected arylethynyl **397** (Chart 66) can be cleaved *in-situ* and attached to the electrode (Au) to form a mechanically stable and directional Au−C σ-bond. Single-molecular conductance studies using mechanically controllable break junction (MCBJ) technique demonstrated high conductivity of the resulting molecular junctions, even than their dithiol analogues. In summary, the reported strategy paved a new way to integrate functional molecules to electrodes to realize nano-electronics constructs.

Chart 66.

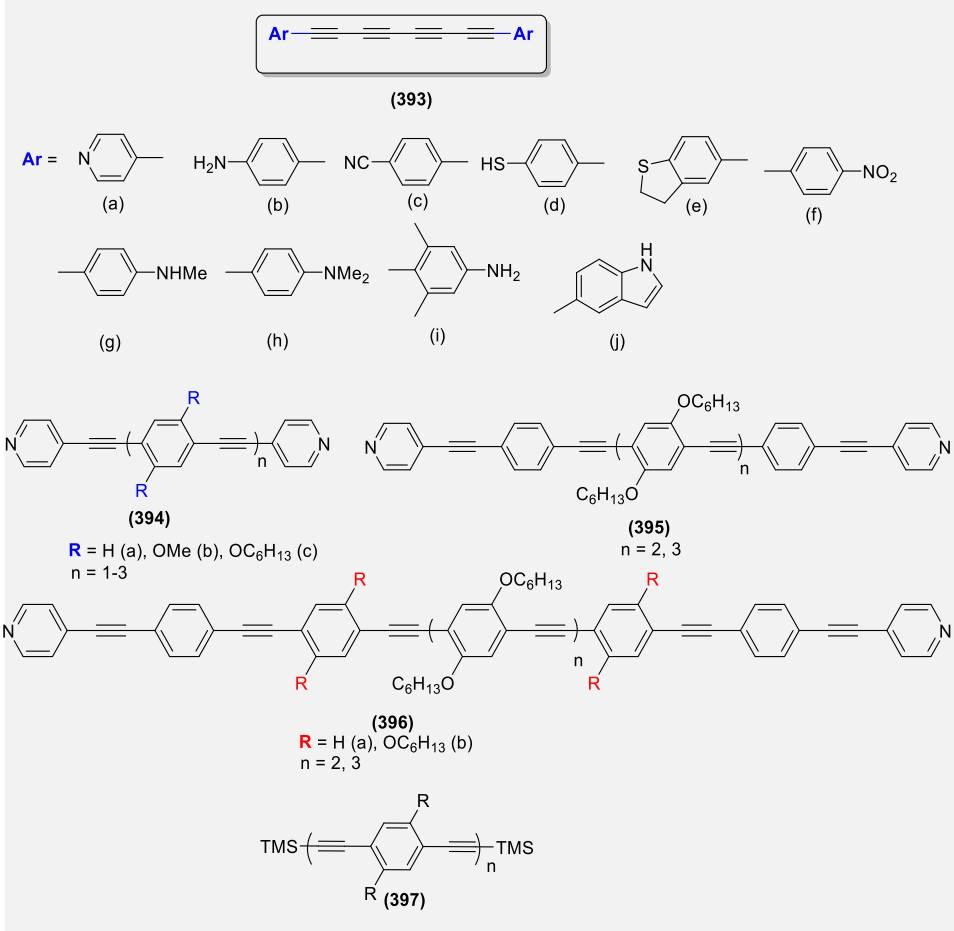

In general, the introduction of metal ion significantly improves the electronic properties of the materials. Cea and co-workers[264,754-758] assessed the conductivity of di-ynes **398-402** (Chart 67) and found a synergistic role of metal in the backbone of the OPEs. Besides, an end-capped dependent variation in the conductivity was also noted (Figure 37a). It was found that the conductance of the molecular wire significantly depends on the termini employed and it rises when a metal is incorporated (Figure 37b). Almost similar result has been reported for benzothiazole oligomers **403** (Chart 67) in which the conductance lowered with increasing chain length.[750] In a recent report, Akita and co-workers[759] showed that the single molecule conductance performance of monometallic Ru-molecular wires with pyridine termini **404-406** (Chart 67) is better than their organic counterparts despite the longer molecular dimension of the complexes (Figure 37c). Although the auxiliary ligands have some impact on the M-C backbone, almost negligible impact on molecular conductance has been reported.[264]

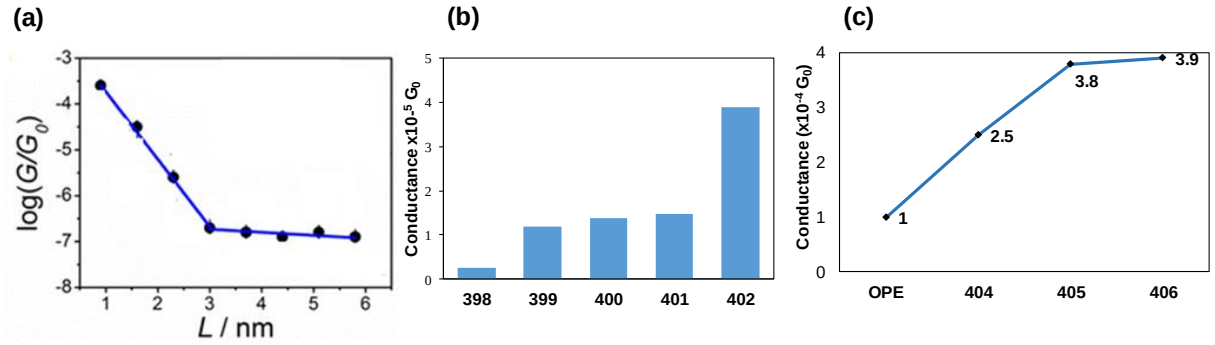

Figure 37. (a) Length dependent conductance in **394-396**. Reprinted with permission from ref [47]. Copyright 2013 American Chemical Society. (b) Molecular conductance of **398-402**, and (c) for **404-406** compared to organic counterpart (OPE).

Chart 67.

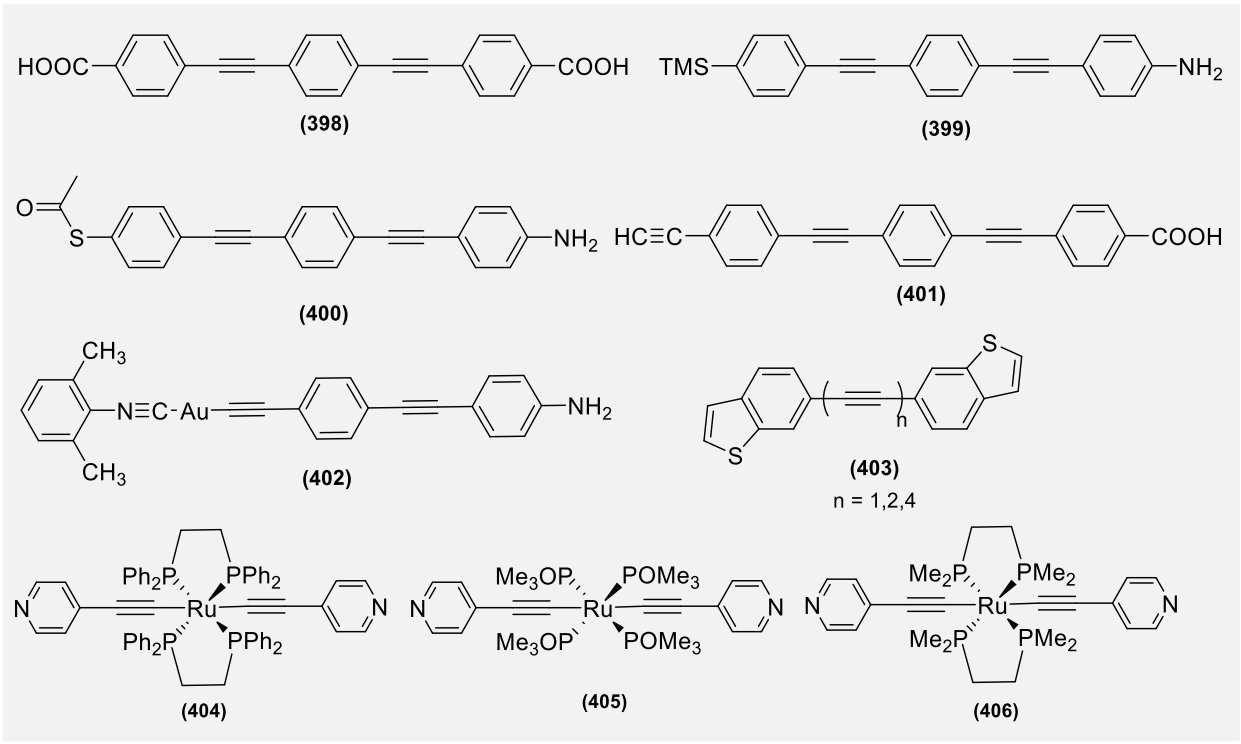

4.2. Sensors

High and distinct luminescence characteristics, long-range exciton migration and conductivity make oligo- and poly-ynes based materials ideal candidates for chemical/optical sensors.[760] Furthermore, the unique reactivity of acetylene moieties toward volatile nucleophiles like ammonia, hydrazine, hydrogen sulfide, and carbonyl compounds render diacetylene-based suitable active layer materials for next generation sensors.[761-763] Materials based on poly-ynes and poly(metalla-ynes) are known to detect chemical species selectively from different biological and environmental sources at low concentration and exhibit multiple changes in their absorption and luminescence spectra.[125,764] For example an acetylide-thiourea based single-molecular system **407** (Chart 68) was found to show an excellent response (variation in spectral features) for CO in the concentration range of 10-30 ppm at RT.[765,766] In general, the response of the

sensors depends on the nature of substituent present. For example, at lower concentration (10 ppm), sensing ability of acetylides follows the order **407 (**H) > **407 (**CN) > **407 (**CH_3), while at higher concentration (30 ppm), a reverse trend was noted. Butadiyne **108c** shows reversible fluorescence switching upon the application of mechanical/thermal change (Figure 38).

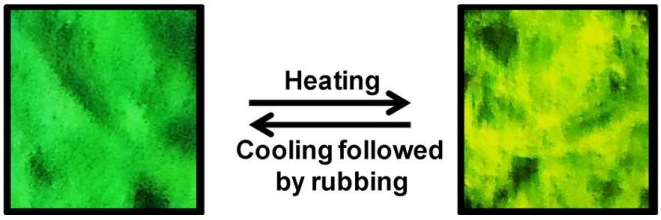

Figure 38. Fluorescently coloured images of the solid powder of **108c**. Pasted on a quartz plate upon heating and subsequent cooling followed by rubbing. Reprinted with permission from ref [174]. Copyright 2015 American Chemical Society.

Core-substituted naphthalene diimide (c-NDI) absorbs in the visible region, has unique fluorescence properties and the changes are visible to the naked eye. Buckland et al.[767] reported c-NDI bearing TMSA moiety **408** (Chart 68) for colorimetric and fluorescent chemodosimeter for anions. The detection which was carried out by desilylation of the detector, showed significant and rapid changes within tens of seconds to minutes. This type of detector showed a naked eye detection of F^- anion. A new naphthalimide-based fluorescent probe **409** (Chart 68) for detection of nitric oxide (NO) has been reported.[768] **409** Responds to NO quickly and shows a 25-fold fluorescence enhancement within 10 seconds, which is the fastest detection rate for NO based on an *o*-phenylenediamine receptor. Moreover, **409** can detect NO quantitatively in aqueous solution with an estimated detection limit of 0.87×10^{-8} M (Figure 39a,b). Prior to this work, Qu and co-workers[769] used a hyperbranched poly-yne **410** (Chart 68) decorated with naphthalimide at the periphery for specific and selective Hg(II) ion sensing ability.[769] The hyperbranched poly-yne **410** (Chart 68) composed of poly *tris*(4-ethynyl phenyl)amine (PTEPA) as the core and benzoyl thiourea naphthalimide (NAP) as Hg(II) detecting unit, showed a blue-shift in λ_{em}. along with increase in fluorescence intensity upon the addition of Hg(II) ion. Huang et al.[770] reported mono- and bis-ethynyl based pyrene-containing compounds which exhibited selective fluorescence behavior towards Zn(II) in aqueous solution (Figure 39c). Interestingly, 1,8-bis-substituted compound **411** (Chart 68) displayed stable and fluorescent gel-forming properties, which undergoes gel-to-sol transition upon heating or the addition of Zn(II). Similar reversible stimuli-responsive gel–sol transition behavior was reported for Pt(II) acetylide in the presence of fluoride anions.[771] Polymeric films made up of poly-(bistributylphosphine-platinum-diethynylbiphenyl, poly-2,5-dioctylyoxy ethynyl benzene and poly-2,5-dibutoxyethynylbenzene (**412**, Chart 68) efficiently detected different gases (NO_2, SO_2, CO, CH_4, NH_3, H_2S, NO), humidity and organic vapours at ppm level.[772] Although these poly-ynes showed high sensitivity, they lacked selectivity. Surprisingly, these materials possessed better sensing activity against relative humidity, which was competitive with commercial hygrometers.

Chart 68.

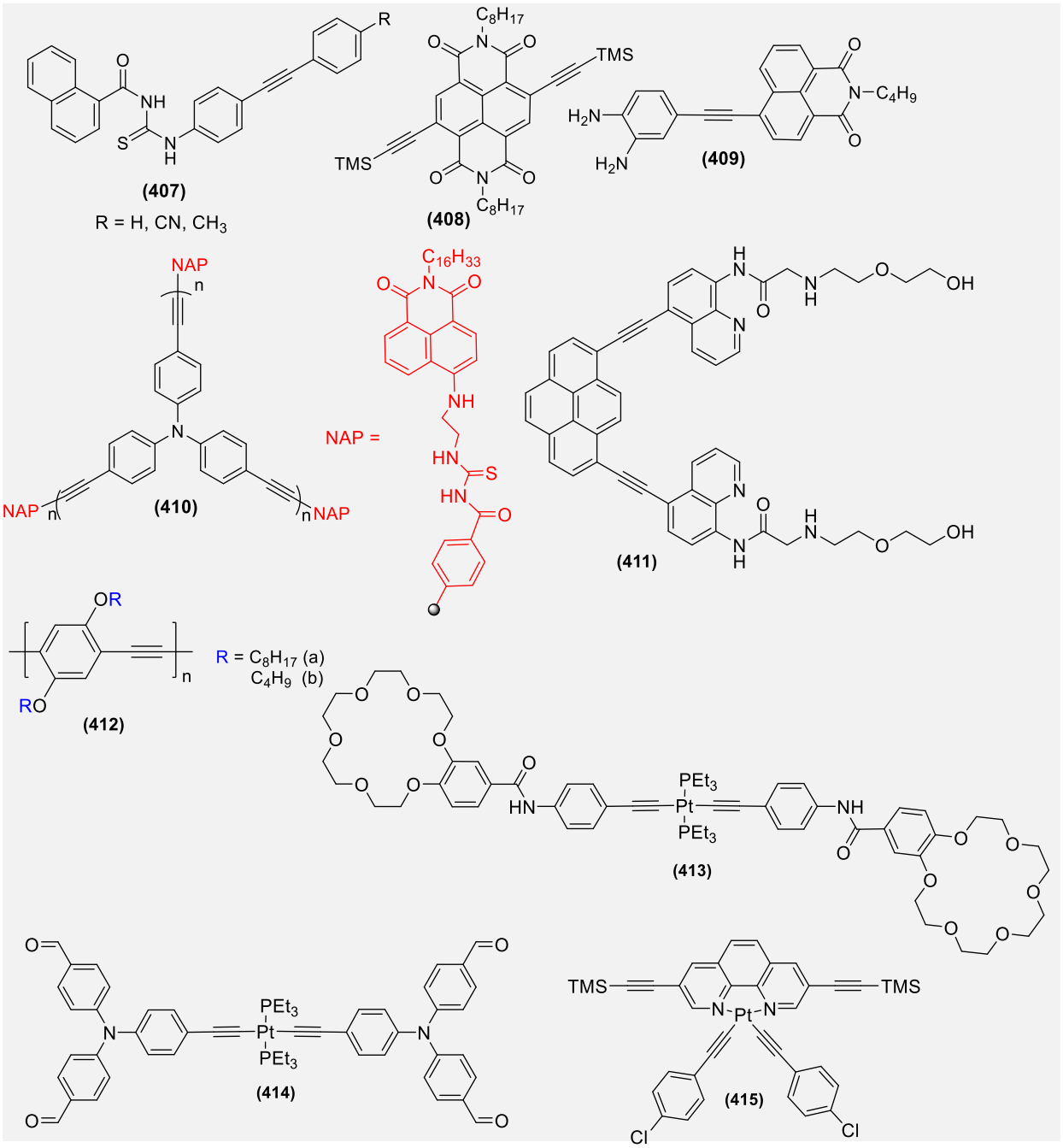

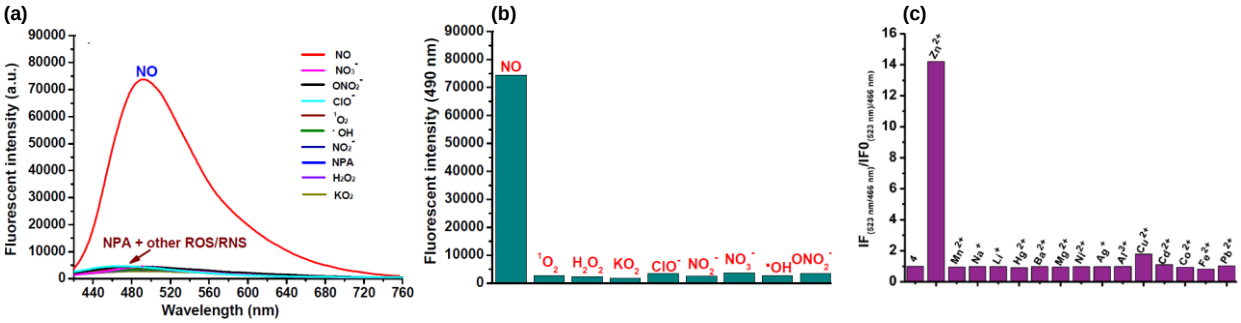

Figure 39. (a) The fluorescence spectra and (b) fluorescent intensity at 490 nm of **409** (100 μM) in the presence of 2.5 equivalents NO and 100 equivalents of other ROS/RNS in sodium phosphate buffer (50 mM, ethanol–water, 1:1, pH 7.4) (λex = 400 nm) Reprinted with permission from ref [768]. Copyright 2015 Royal Society of Chemistry. (c) Fluorescence intensity ratio of **410** (10 μM) at 523 and 466 nm in the presence of 4 equiv. various metal ions to free **410** (10 μM) at 523 and 466 nm in acetone–water (1:1, v/v, 10 mM Tris–HCl, pH 7.2). Reprinted with permission from ref [770]. Copyright 2014 Royal Society of Chemistry.

In a recent example of a morphological transition in response to additives, Pt(II) acetylide-based bolaamphiphile **413** equipped with two peripheral benzo-18-crown-6-ether moieties (Chart 68) has been reported.[773] This bolaamphiphile exhibited a strong tendency to form spherical aggregates in the presence of L-alanine ester salt, in a polar methanol/chloroform (3/1,v/v) solution. It has been proposed that amino acid additives influence the aggregation of the bolaamphiphile significantly in polar medium leading to the morphological transition from nanospherical to disordered structures. This type of intelligent materials opened a new door of application in controlled release, biosensing, and optical resolution. Complex **210** (Chart 24) having pentiptycene as backbone shield showed an excellent "on-off" optical response to oxygen concentration.[399] The long and green phosphorescence intensity was found to be highly sensitive to molecular oxygen. In addition to this, the emission color depends on the concentration of oxygen as well as complex. Using the complex, oxygen in the range of 1− 5% air volume could be detected (Figure 40a), thus making it useful for the ratiometric probes. The group led by Mukherjee[774] reported organic solvent vapour and cysteine detection ability of Pt(II) acetylide complex **414** and its organic counterparts. When 3,8-*bis*(trimethylsilylethynyl)-Phen was coordinated to Pt(II) bisacetylide, **415** (Chart 68), it showed a strong, selective, naked-eye perceivable, sensitive, reversible, reproducible vapochromism and vapoluminescese upon exposure to benzene.[775] This vaporchromic behavior was reversible and the complex could be recovered by exposing DCM vapors. When a quartz slide deposited with **415** was exposed to different VOCs, it showed a sensitivity towards benzene compounds (including benzene, toluene, chlorobenzene, nitrobenzene, xylene, *p*-xylene and *o*-xylene). The change in chromatic behavior was attributed to the presence of dual recognition site. The π-π stacking site situated above the Phen rings stabilises benzene and its compounds while H-bond site located between two phenylacetylene auxiliaies stabilizes DCM. The compound presents red color and red luminescence under ambient light and UV light (365 nm), respectively (Figure 40b).

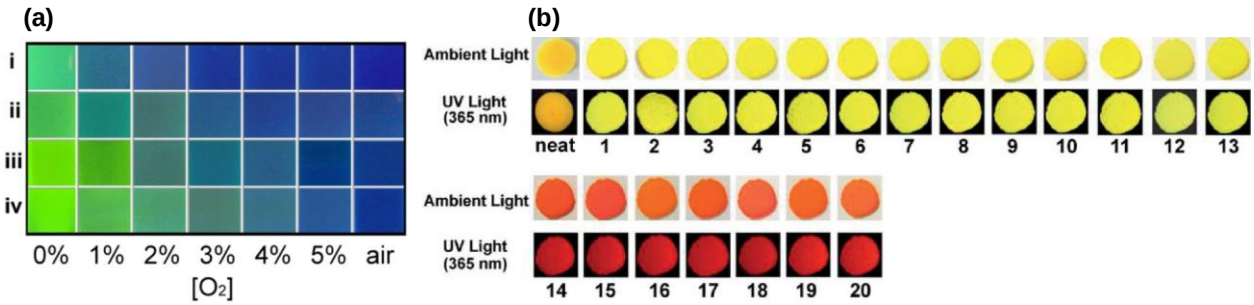

Figure 40. The color of emission of **210b** in the concentration of (i) 3×10^{-6} M, (ii) 9×10^{-5} M, (iii) 1.8×10^{-4} M, and (iv) 3.6×10^{-4} M at different volumetric ratio of molecular oxygen (O_2) in the mixture of O_2 and N_2. Reprinted with permission from ref [399]. Copyright 2014 American Chemical Society. (b) Photographic images of **415** deposited on quartz slide upon exposure to various VOC (1-20) vapors under ambient light and UV light irradiation (365 nm). For the details of VOC, please see the reference. Reprinted with permission from ref [775] Copyright 2015 Royal Society of Chemistry.

Polymers **416-421** (Chart 69) consisting of different combinations of D-A have been employed for the detection of VOC sensing.[776] These visible absorbing polymers showed selective and reproducible detection of volatile organic solvents, such as toluene and benzene. For the polymers **417** and **421**, the selectivity of sensing decreases in the following order: toluene>benzene>acetone>methanol>water. The higher selectivity towards aromatic solvent vapors could be due to strong π-π interactions between polymers and aromatic solvent molecules. In particular, polymers **417** and **421** showed higher toluene adsorption than other polymers. This could be caused by stronger π-interactions from electron-deficient DPP and triazolo quinoxaline with aromatic solvents, which is consistent with absorption studies that showed the largest redshifts of I_{max} for **417** and **421** from toluene.

Table 12. Versatile sensing ability of organic and organometallic oligo-ynes and poly-ynes.

Entry	Sensing analytes	Ref
422-423, 426-427, 439	Metal Ions	[777] [778]
424, 427, 438	Nitroaromatic explosives (2,4,6-trinitrotoluene TNT, 2,4-dinitrotoluene DNT, picric acid PA) and 4-nitrotoluene NT)	[779] [780]
425-434, 436-437	Organic acids (Mono-, di- and tricarboxylic acids)	[781] [782]
435	Thirteen white wines	[783]
428-429	Non-steroidal anti-inflammatory drugs (NSAIDs)	[784]

Chart 69.

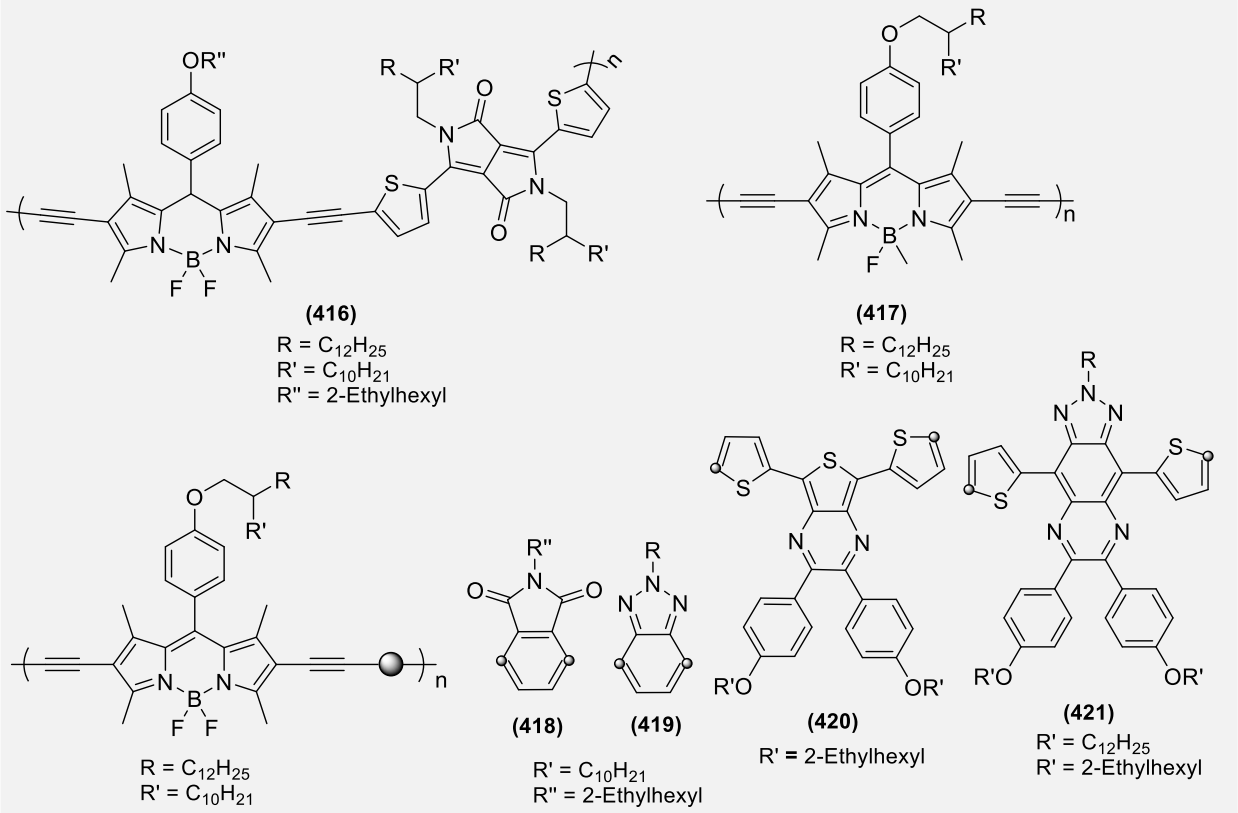

Similarly, other polymers **422**-**439** (Chart 70) have been reported for different sensing applications. (Table 12) Detection of chemical explosives such as dinitrotoluene (DNT), trinitrotoluene (TNT) and picric acid (PA) by chemical sensor is a challenging task. These are commonly buried in the landmines and also used for industrial and military purposes.[785,786] As the nitroaromatic explosives are electron deficient in nature, it is worthwhile to use an electron-rich species for the detection of these explosives.[785] In this quest, ruthenium-based multicomponent H-bonded supramolecular system has been recently reported, of which the fluorescence undergoes drastically changed after binding to 2,4-dinitrotoluene (DNT) in DCM solution.[786]

Chart 70.

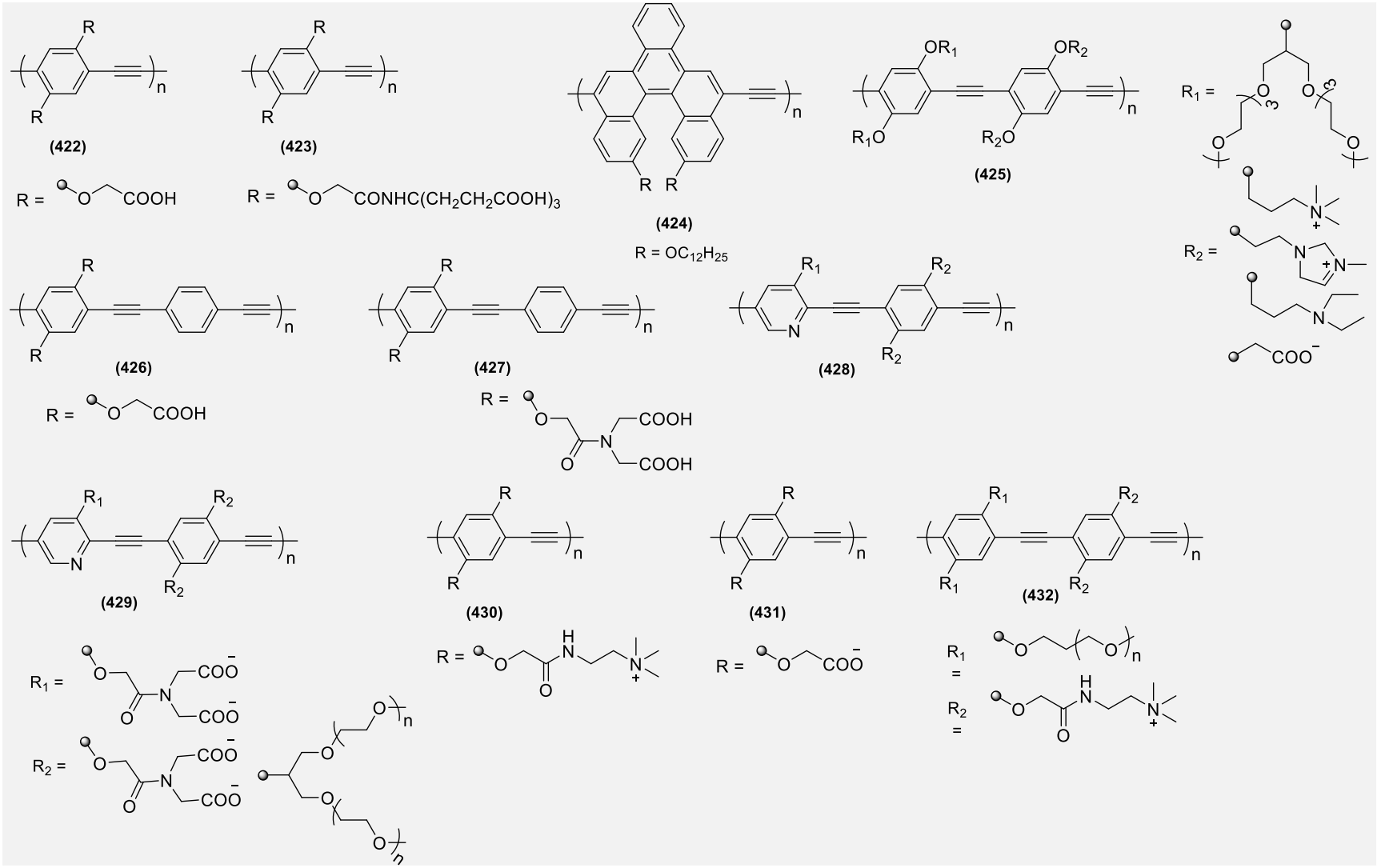

continue...

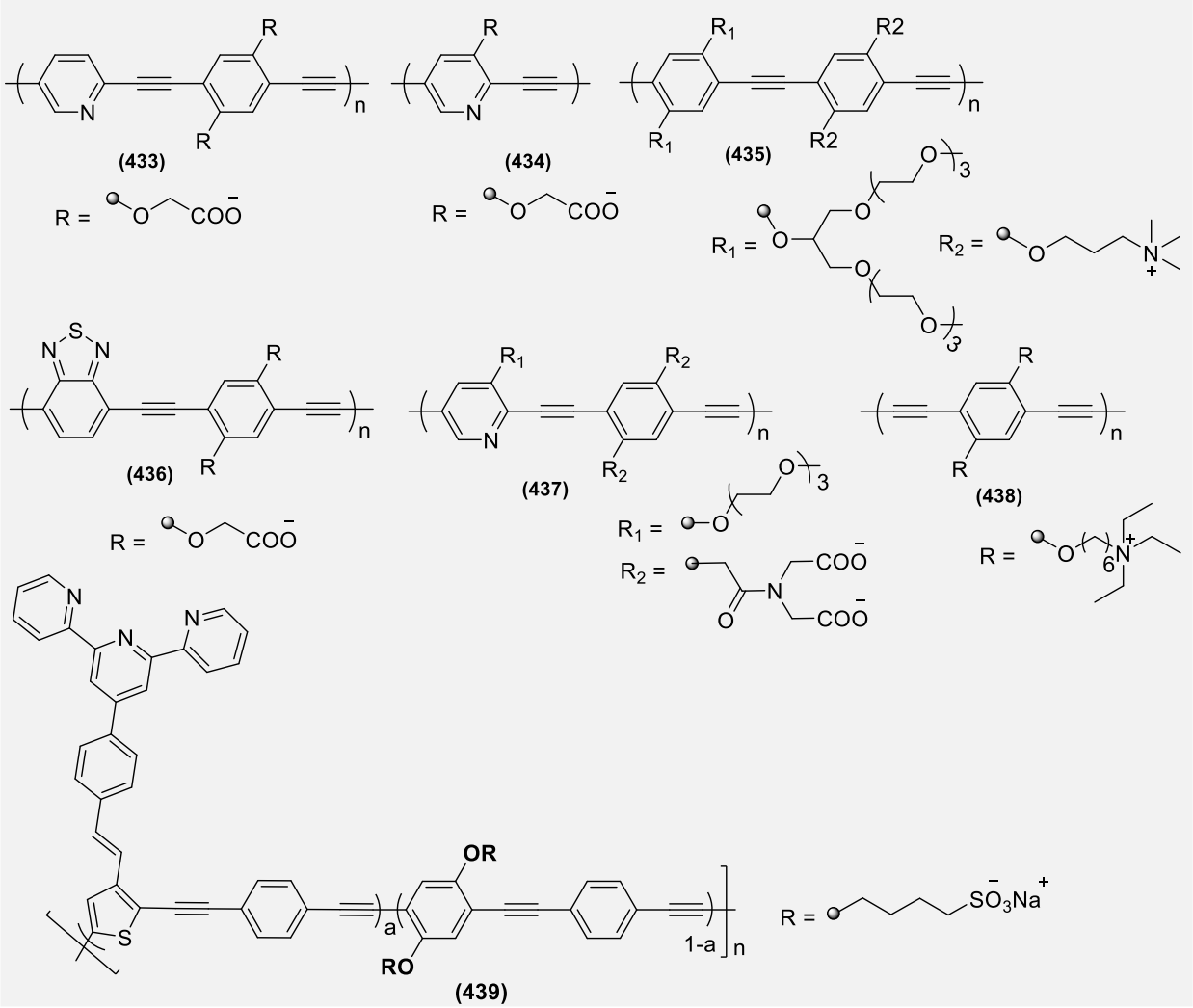

On the other hand, when a similar poly-yne poly-(bistriethylphosphine)-platinum-diethynylbenzene (Pt-DEB) (**440**, Chart 71) based quartz crystal microbalance (QCM) was used for chloroform, tetrahydrofuran, acetone, isopropyl alcohol, ethanol and methanol, it showed a good reversibility, reproducibility and linear sensitivity to organic vapours at RT.[787] Unlike earlier examples, sensor specifically showed maximum sensitivity to $CHCl_3$ and high molecular weight alcohols. Furthermore, it gave a stable performance up to a period of 30 days with detection limits ranging from 1.0 to 3.56 ppm for the organic vapors. In summary, poly-ynes are likely to get a market for environmental and industrial applications. When the triethyl phosphine auxiliary was replaced by a triphenyl phosphine and aromatic spacer was substituted with 1,4-dihexadecyloxy moiety (**441**, Chart 71), it showed a good sensitivity to relative humidity.[788] It could respond even to very low (< 10% RH) humidity conditions at RT with high reproducibility, repeatability and stability.[788] Schanze et al.[789] reported red and hypsochromic shift of absorbance band and quenching of phosphorescence in Pt(II) acetylide co-polymer upon interaction with transition metal ions (Fe(III), Co(II), Ni(II), Cu(II) and Pd(II). They reported that these metal ions bind to the Bpy units (**442**, Chart 71) of the co-

polymer. Among these metals, Ni(II) and Cu(II) showed "*amplified quenching effect*" upon interaction with polymer.

Alkali and alkaline earth metals are extensively present in biological to environmental samples. Though some are classified as essential constituents for life, some are highly toxic. Due to this fact, their detection is an important issue. Au complexes within supramolecular assemblies of different size and shape can be employed as sensors for the detection of a range of alkali and alkaline metal cations and other anions.[790] Formation of the complex with receptors including crown ethers, calix[4]arenes, oligoether pendants and dipicolylamines of different sizes showed a selective binding mode.[790] A number of Au(I) acetylides bearing tethering ligand such as amide have been reported for the sensing of anions (especially F^-).[528,530] Using these complexes, naked eye detection of analytes is possible. Complex **443** (Chart 71) showed a promotive and differentiating effect on the binding constant (log*K*) in THF compared to DMSO. In such complexes, the binding constant (log*K*) with the same anion in THF depends on the substituent R on the acetylide ligand. The same research group reported similar anion binding properties by Au(I) alkynyl complexes **281** (Chart 41) which exhibits the highest binding affinity towards anions due to the strongest electron-withdrawing ability of the NO_2 group.[528] Complexes **444-446** (Chart 71) are different types of Au(I/II) and Pt(II)-based ethynyl complexes, which have shown their selective/preferential binding against a range of essential metal ions and minerals.[791-801] In addition to this, π-extended tetrathiafulvalene analogues (ex-TTFs) and shape-persistent macrocycles, which possess redox-switchable behavior in the Vis-NIR region offer unique supramolecular host for metal ions and aromatic molecular guests and gases.[802] For a range of sensors, readers are encouraged to read a recent review by Yam et al.[801] In addition to the sensors discussed above, other sensors utilizing alkyne moiety have also been reported for heavy metal ions.[803]

Chart 71.

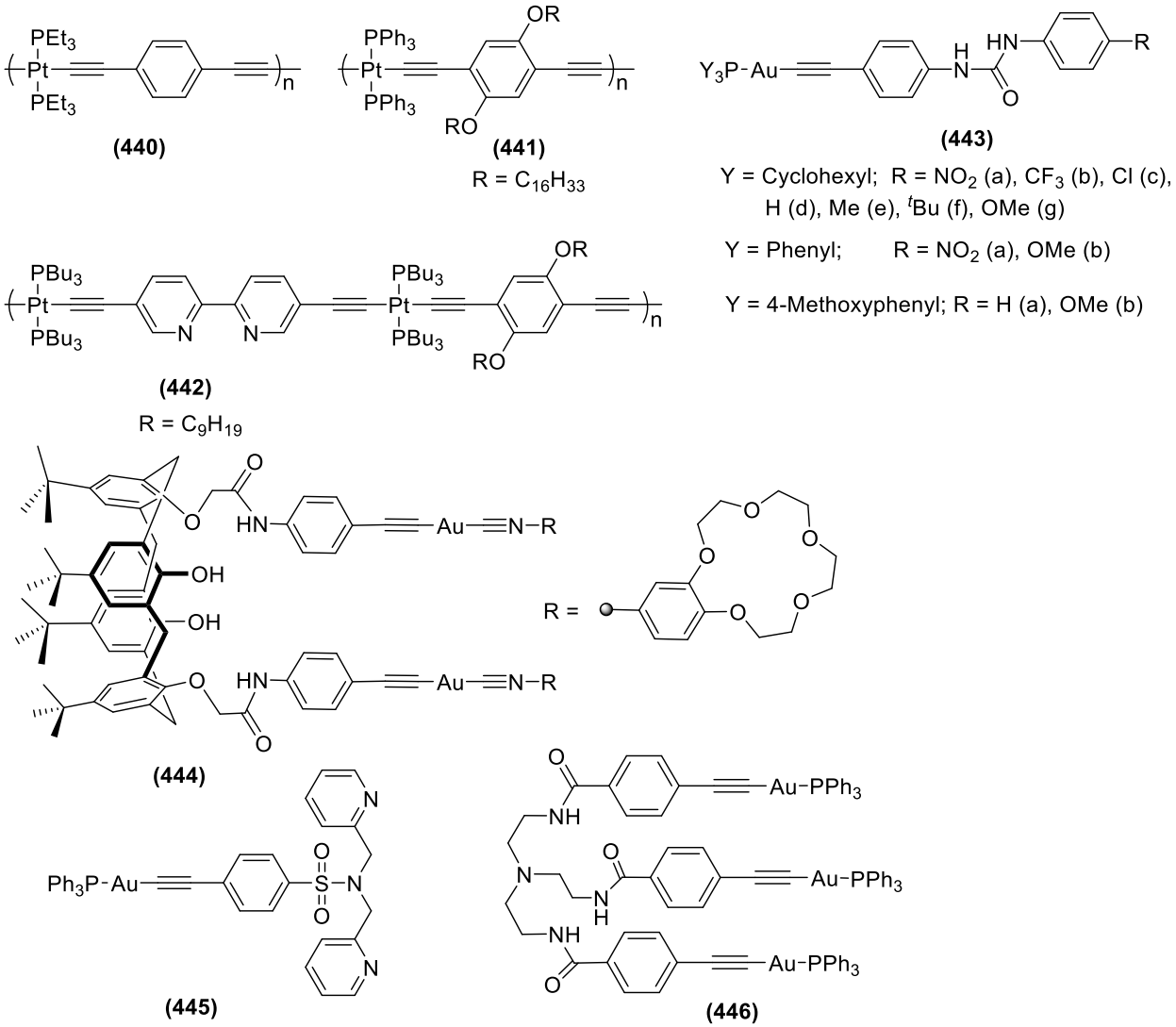

4.3. Molecular magnets

Molecular magnets, a term used to define discrete molecular entities exhibiting magnetic phenomena under certain conditions, have garnered a great deal of interest due to their light weight, transparency and magneto-optical properties.[804,805] Following the report on the magnetic properties of [(Me$_3$tacn)Cr(CCH)$_3$],[296] several studies have been undertaken to delineate the magnetism in transition metal acetylide complexes[301,310,806-808] as they have potential to be used as component for nano-scale information storage.[458,459]The magnetic property of such complexes depends on several factors: the type of ligand, the type and orientation of metal centre, counterions, position of alkynyl linkage and nature of the conjugated spacer, etc. When a transition metal is ligated to a redox-active planar ligand separated by an ethynyl moiety, it shows unique magnetic properties. This is attributed to the "*π-d interaction*" between π-spin (*S* = 1/2) of a ligand with the d-spin of transition metal assisted by ethynyl group and strengthened by inter-ligand π–π stacking.[806,809,810] In the majority of molecular magnets, Cr(III) is used as it has large magnetic

moment (*S*= 3/2) and produces a strong intermolecular exchange interaction leading to magnetic transition. This fact is well-exemplified by recent interest in chromium-acetylide based magnetic materials. In 2009, Nishijo et al.[301] reported very first examples of a ferrimagnet and weak-ferromagnet containing Cr(III) acetylides **147(a&i)** (Chart 12). These phenylene or thiophene containing complexes with paramagnetic $[Ni(mdt)_2]^-$ (mdt = 1,3-dithiole-4,5-dithiolate) counterion produce ferrimagnetic chains of alternately stacked $[CrCyclam(C\equiv C\text{-}R)]^+$ cations and $[Ni(mdt)_2]^-$ anions.[301] For **147a**, the intra-chain exchange interactions of 2J = -5.7 K was found while for **147l**, it was 2J = -6.1 K. Contrarily, naphthyl substituted complex formed one dimensional uniform ferrimagnetic chains of $[Cr\text{-}Cyclam(C\equiv C\text{-}6\text{-}methoxynaphthalene)_2]^+$ and $(TCNQ)_n^-$ (TCNQ =7,7,8,8-tetra cyanoquinodimethane).[810] The π-π stacking between the cations and anions mediated intermolecular exchange interactions, leading to intra-chain exchange interactions ranging between 2J/kB = -19.5 to - 4.6 K. The same group observed that the substitution of phenylene/thiophene/ anthracene by redox-active ligand like tetrathiafulvalene (TTF) moiety greatly modifies the magnetic properties. Considering this, a number of $[Cr(III)Cyclam(C\equiv C\text{-}TTF)_2]^{n+}$ complexes have been synthesized and assessed. Nishijo et al.[806] found a strong inter- and intra-molecular π-d interaction in Cr(III) complex **447a** (Chart 72) with spin-spin exchange interaction (2J/kB) upto 30 K in the crystal. The molar magnetic susceptibility (χ) for **447a** obeys the Curie-Weiss law with a Curie constant of 1.89 emu $Kmol^{-}1$, very small Weiss temperature (-0.1 K) and lack of magnetic transition below 1.8 K. However, the electrochemical oxidation of **447a** in electrolyte **(**$[ClO_4]^-$ or $[BF_4]^-$) in a mixture of acetonitrile–chlorobenzene resulted in weak ferromagnet [**447a**][anion]$_2(PhCl)_2$ (MeCN). To underpin the exact reason behind this observation, extensive solvent- and anion-dependent magnetism was carried out by Nishojo and Enomoto.[811] They found that due to the overlap of TTF-type ligands, the complex $[357a]^+$ forms ferrimagnetic chains and the extent of interchain interaction significantly depends on the nature of the solvent as well as the anion. Although materials exhibit weak ferromagnetism at low temperature, transition temperature (Tc) and the remanent magnetization values (Mrem) vary significantly. For example, the value of Tc increases from 14.5 to 26.0 K with decreasing interchain distance, while the Mrem at 2 K decreases from 0.0215 to 0.0079 μ_B.

Chart 72.

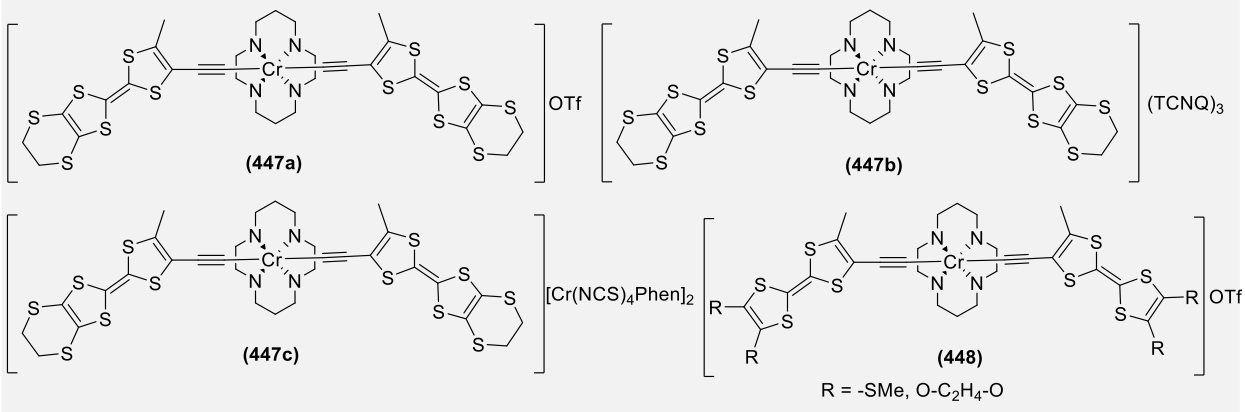

Considering the promising magnetic response of Cr-TTF cations, one of them further assessed the potential of molecular magnets composed of [**447**]$^{n+}$, *i.e*. **447b and c** (Chart 72), bearing magnetic anions TCNQ

and $[Cr(NCS)_4Phen]_2$ $(acetone)_2(toluene)$.[807] Similar to **447a**, **447b** also obeys the Curie-Weiss law (Curie constant = 2.25 emu $Kmol^{-1}$), but with a small positive Weiss temperature (0.3 K). In the complex **447b**, TCNQ and TTF fragments were stacked and showed weak ferromagnetic interaction between the two units. On the other hand, the crystals of **447c** showed ferrimagnetic to ferromagnetic transition below 5 K. A similar type of observation, i.e. strong interaction between the spin on the dimer and metal through the ethynyl group was found in analogues complex **448** (Chart 72), having thiomethyl or ethylenedioxy substituted TTFs.[808] These functionalities also imparted high solubility to the complexes in organic solvents. Due to the rigid structure and ability to arrange diamagnetic transition metals around C_6H_3 core, 1,3,5-triethynylbenzene is considered as a promising scaffold which can impart strong magnetic exchange coupling and endow magneto-optical activity to the materials.[805,812-814] Veugels et al.[805] found that organic thin film materials based on CF_3-terminated phenylacetylenes with varying symmetry possess high MO-activity. The activity was found to depend on the geometry of the molecule (*viz*. octopolar, wedge/de-symmetrized, and linear). Prior to this, a similar observation, i.e. geometric-guided magnetism has been made for [(dppe)(Cp*)Fe(III)]-containing acetylide complexes (Cp* = η^5 -C^5Me^5).[815] However, Shores and co-workers[816] found that the magnetism in Fe(III) ethynylbenzene complexes **449-453** (Chart 73) is governed by combination of alkynyl ligand electronics and the topology. For example, antiferromagnetic coupling in **449** (J = -134 cm^{-1}) and ferromagnetic coupling in **452** (J = +37 cm^{-1} and J' = +5 cm^{-1}) and **453** (J = +11 cm^{-1}) were found, which are different in their topologies. The same group carried out the magnetic studies of mono-, di-, and trinuclear U(IV) aryl acetylide complexes (**454a-d,** Chart 72).[817] In these complexes too, geometry and nuclearity dependent coupling was observed. For example, *meta*-linked **454b** exhibited a J value double that of *para*-counterpart **454c**. Furthermore, increasing the number of U centers led to fall in coupling constant value. The lack of significant intermolecular and intramolecular interaction/contacts in **454a-d** (except weak van der Waals interactions) suggested residual magnetism in these complexes is perhaps due to the intramolecular communication between the U-centers.

Chart 73.

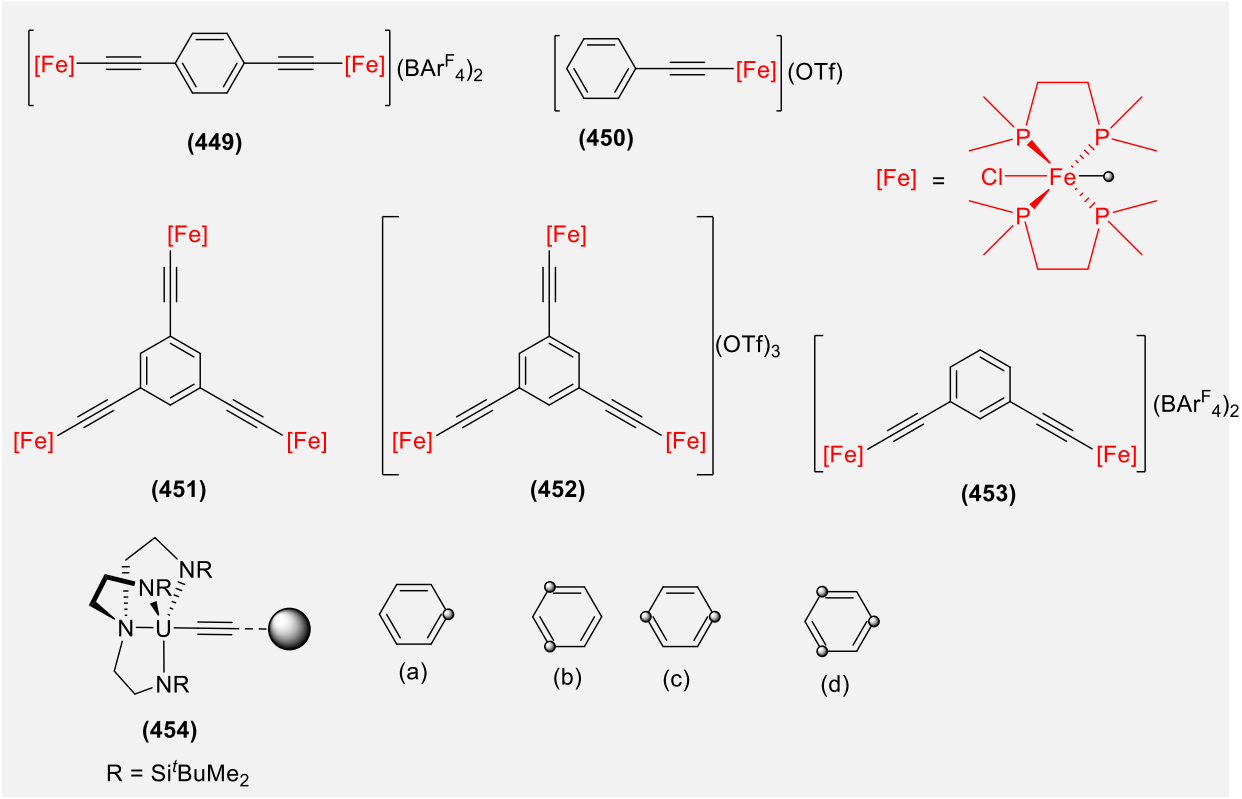

4.4. Memory devices

A sharp rise in the demand for state-of-the-art technologies in the information communication sector and the limitation presented by existing materials in the semiconductor industry have motivated researchers to develop new, cheap and efficient memory-switching devices. This demand is further strengthened by physical and economic constraints posed by inorganic semiconductor-based memory devices. These factors led to the development of several new classes of electro-active materials with volatile and non-volatile memory characteristics. This included devices based on small organic molecules.[818], polymers[819], and complexes of nitrogen-donor ligands Ag(I),[820] Ni(II), Au(I/III), Co(II),[821] Cu(II), Ru(II),[822] Ir(III),[823] Ln(IIII)[824] etc. as well as hybrid materials.[825-827] Among these, organic material electronics have gained tremendous interest due to good scalability, flexibility, low cost, ease of processing, 3D-stacking capability, and large capacity for data storage. Despite the fact that a number of conjugated polymers have been tested as component for memory devices,[819,827] literature on the use of conjugated di-ynes and poly-ynes is relatively scarce. It has already been demonstrated that the insertion of a linear π-spacer bridge induces a critical change in molecular organization and electron density distribution in the conjugated backbone.[828,829] This led to a remarkable variation of memory performance. For example, Wang and co-worker[828,829] showed that the introduction of acetylenic linkage led to a remarkable variation of memory performance of the device. They found that when hydrazone linkage is replaced by a linear π-spacer bridging a carbazole donor and a naphthalimide acceptor (**455**, Chart 74), the performance of the device changed from DRAM to “write-once read-many times” (WORM) memory. The memory devices based on

small molecular compounds have poor stability, low device yield and short retention time, while polymeric materials exhibit promising application prospects in information storage devices.[830] Sun and co-workers[831] reported a transparent and flexible non-volatile memory device fabricated using composite based on reduced graphene oxide **456** (Chart 74). The device exhibited typical storage performance of rewritable memory that can be electrically erased and reprogrammed, with turn-on and turn-off voltages of 1.55 and -1.80 V, and an ON/OFF current ratio exceeding 10^5. The memory behavior of the flexible device were almost unchanged under the bending test (Figure 41).

Chart 74.

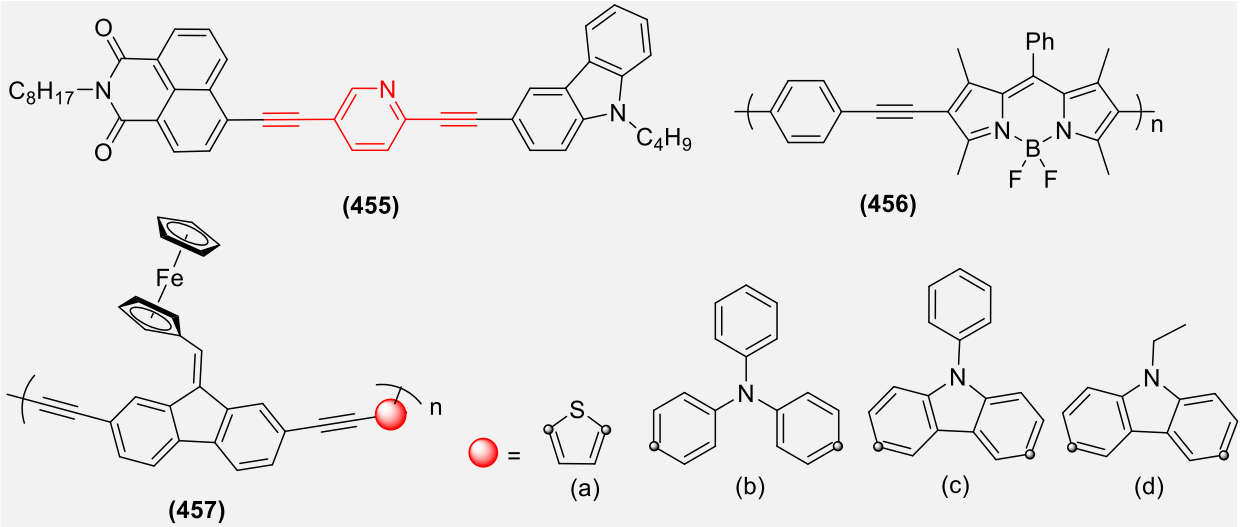

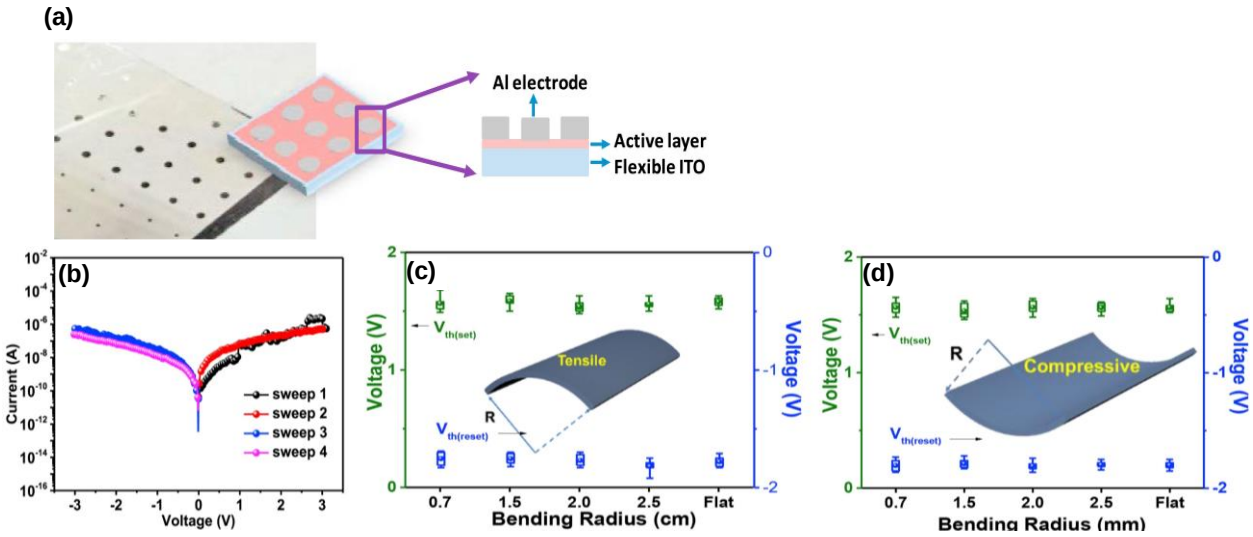

Figure 41. (a) Configuration of the transparent and flexible memory devices; (b) current-voltage characteristics of an Al/**456**-g-RGO/ITO-coated PET device; experimental and fitted data of I–V characteristics for the device in the OFF state. (c, d) Vset and Vreset threshold voltages as a function of the bending condition. Reproduced with permission from ref[831]. Copyright 2017 Elsevier Ltd.

It has been reported that the non-volatile memory effect of conjugated co-polymer also depends on the spacer used. A two terminal single layer device (ITO/polymer/Al) having active layer composed of ferrocene-containing poly(fluorenylethynylene)s exhibited flash memory behaviours when the carbazole or triphenylamine was used as spacer while it exhibited the (WORM) memory effect with thiophene as spacer.[832] The triphenylamine-based polymer **457** (Chart 74) achieved the best result with a high ON/OFF ratio of 10^3 to 10^4 and a long reliable retention time (3000 s), which provides great potential for further memory application (Figure 42). These results would provide a new series of ferrocene-containing conjugated polymers with further opportunities for memory applications.

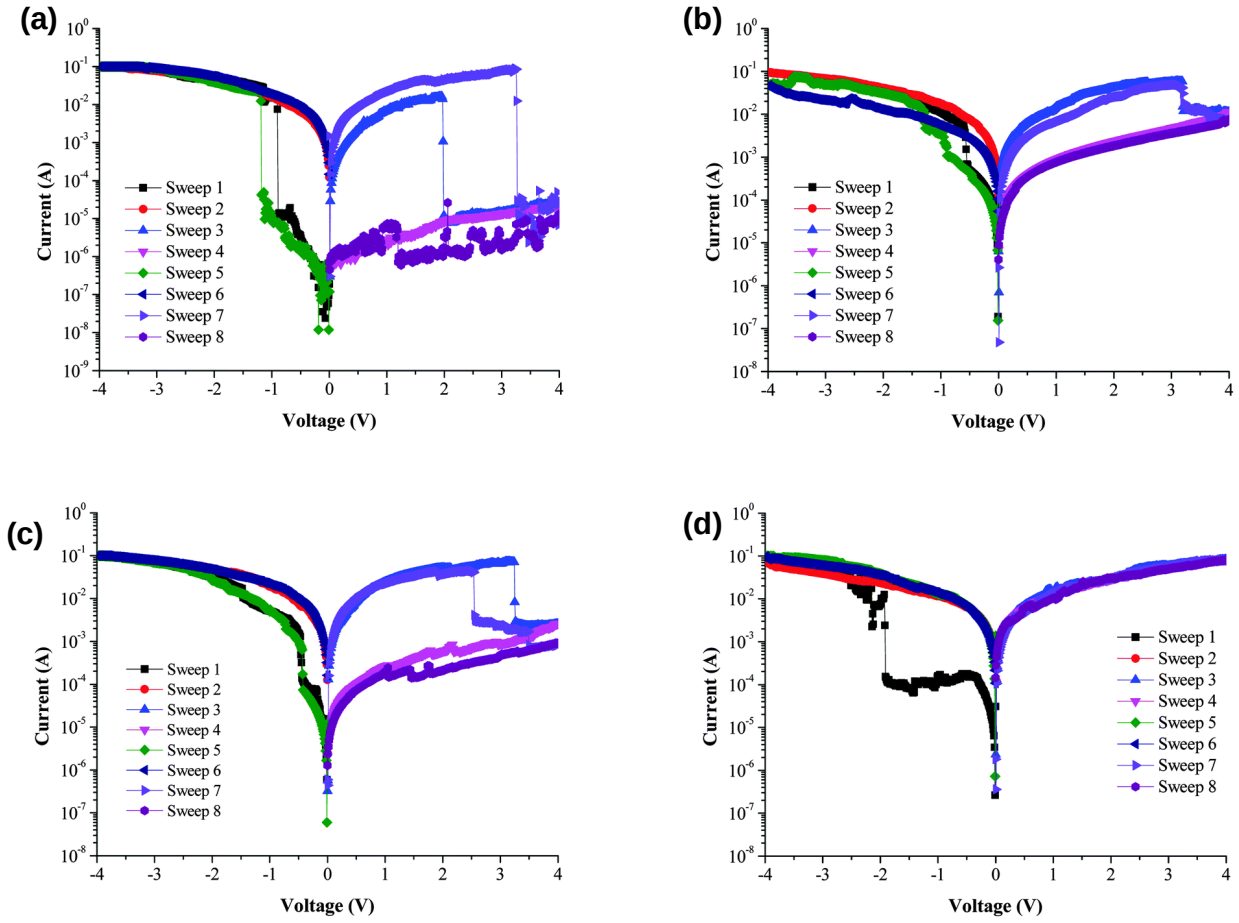

Figure 42. Typical *I*–*V* characteristics of the ITO/polymer/Al memory devices: (a) (**457b**); (b) **457c**; (c) **457d**; (d) **457a**. Reprinted with permission from ref [832]. Copyright 2015 Royal Society of Chemistry.

Research on memory devices based on alkynyl Au(I/III) materials has started to attract the interest of researchers. This is attributed to the electron-rich and rigid nature of alkynyl moiety and the favourable properties endowed by d^8 or d^{10} configuration metal Au(I/III) such as chemical stability, non-toxic nature, environmental benignancy and favorable PL. Both WORM type and Flash-type devices have been reported in the very short span of time.[833,834] We present here some representative examples of acetylide cyclometallated complexes having potential for multilevel memory devices. Metal complexes with tridentate

cyclometalated ligands in C^N^N and N^C^N coordination modes exhibit intense luminescence and versatile emissive excited states, including not only intra-ligand (IL) (π−π*) excited states but also the excimeric excited states.[835] For the fabrication of memory devices, synthetic versatility, high thermal stability and resistance to atmospheric oxidation, good film forming property and homogeneous film of high optical transparency are some of the important pre-requisites for the materials to be used. Considering the criteria, Yam and co-workers[833] tested and found that the visible light absorbing bis-cyclometalated Au(III) complex, [Au(^{t}BuC^N^C^{t}Bu)(C≡C−C_6H_4N (C_6H_5)$_2$-*p*)] (**458a**) (Chart 75) is an excellent candidate for the fabrication of organic memory device. In fact, it is the first example of organic memory device based on small-molecule organometallic complexes. Key features of the memory device include operation with low voltages (2.2−2.8 V), high ON/OFF ratios (10^5), long retention times (10^4 s) and good stability and reliability. An enhancement in the performance of the device, i.e. ternary memory performances with distinct and low switching threshold voltages, high OFF/ON1/ON2 current ratio of 1/10^3/10^7, and a long retention time for the three states was observed upon the replacement of triphenylamine of **458a** by phosphole oxide **458b** (Chart 75), which provides extra charge-trapping site to the system.[836] The complex-based device could work under both positive and negative voltage bias. Moreover, the presence of weak π−π stacking and ordered molecular packing make device active layer very smooth, which is believed to be beneficial in governing an efficient charge transport and the resultant low threshold voltage. The replacement of phosphole with a coumarin unit and substituted phenyl rings (present at 2,6-position of pyridine) by benzimidazole moieties **459** (Chart 75) showed an interesting modulation of electronic properties and applications. In fact, using complex **459**, a very first example of the flash-type organic memory devices based on alkynyl Au(III) complex has been realized.[834] The complex possesses stable rewritable behaviour under a lower compliance current of 10^{-6} A. The devices based on complex **459** showed a different switching characteristic from Flash-type binary resistance switching (Icc ≤10-3 A) to WORM-type ternary resistance switching (Icc = 10^{-2} A), which is the first example. Recently, the same group[837] fabricated resistive memory devices with an active layer based on isocyanide and NHC supported trinuclear alkynyl Au(I) complexes bearing *N*-alkyl substituted triindole ligands **460** (Chart 75). All complexes showed high thermal stability (T_d = 242-356 ºC). Interestingly, compared to ligand, complexes showed good film forming properties and gave a homogeneous film of high optical transparency under ambient conditions (Figure 43). Since both isocyanide and NHC terminated ligand-based complexes exhibited similar memory performance, it has been suggested that the triindole moieties of the complexes serve as charge traps which impede the mobility of charge carriers and give rise to the electrical bistability. Overall, promising binary memory performances with low switching threshold voltages of ca. 1.5 V, high ON/OFF current ratio of up to 10^5, long retention time of over 10^4 s, were some of the important and noteworthy features displayed by the materials. In addition to Au(I/III) complexes as promising candidates, Pt(II)-based cyclometalated N^C^N complexes have also shown interesting results. Pt(II) complexes bearing 2,6-bis(benzimidazol-2-yl)pyridines exhibit solid-state polymorphism and interesting photophysical properties, mainly arising from MLCT and MMLCT excited states.[835] Recently, some N^C^N Pt(II) carbazolyl and alkynyl complexes have been reported which showed their suitability as

OLED and memory material.[835] Organic memory devices based on di(thienyl)bithiazole exhibited binary memory performances with low operating voltages, high ON/OFF ratios of over 10^5 and long retention times of over 10^4 s.

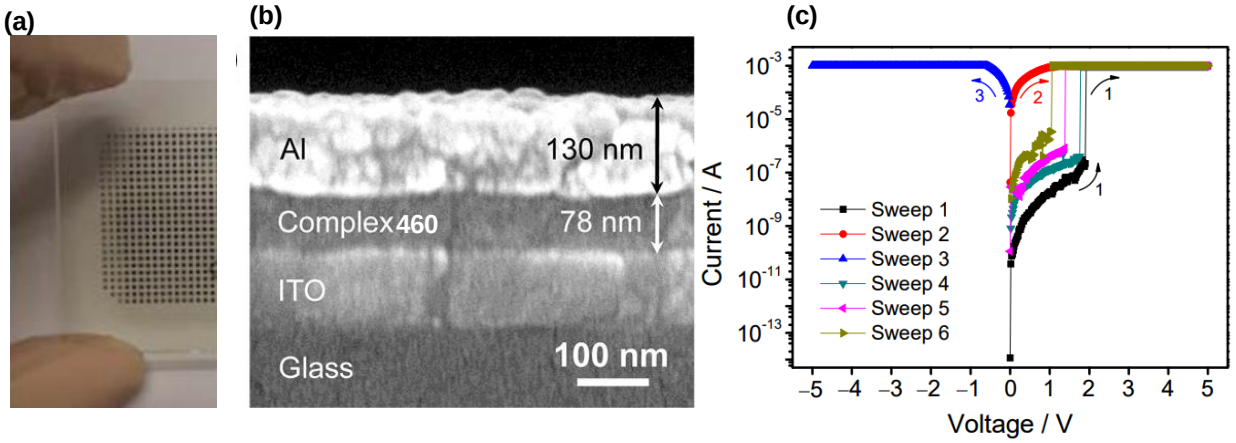

Figure 43. (a) Optical image of a transparent memory device, (b) SEM image of the cross sections of the device, (c) *I-V* characteristics of the memory devices fabricated with **460** (n =14, Ar = $C_{14}H_{29}$). Reprinted with permission from ref [837]. Copyright 2017 American Chemical Society.

Chart 75.

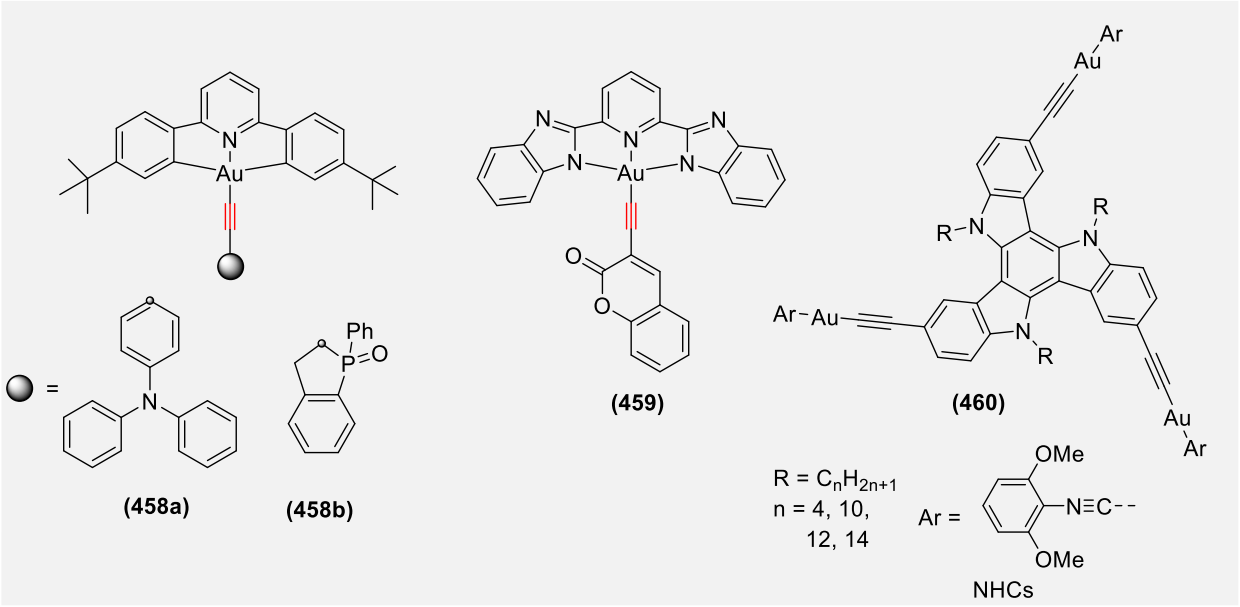

4.5. Catalysis

The use of transition metal acetylides as catalysts for polymerization started in late twentieth century and work is still on the rise. One of the examples of acetylide catalysts is Cu(I)-acetylide used in petrochemical sector. There are a number of possible industrial applications for metal acetylides (M = Co, Ni, Pd, Pt, Rh) and some of the most promising examples are listed in Table 13.[262,838-850] The number of well-defined homogeneous alkyne metathesis catalysts that are capable of efficiently promoting the reversible cleavage and formation of carbon–carbon triple bonds has steadily grown over the past decade. For the

polymerization of non-polar alkynes and polar substituted acetylenes, both Group 9 (Co(II) and Group 10 metal acetylides (Ni(II), Pd(II), Pt(II) carrying phosphines as co-ligands are capable. Interestingly, contrary to the O-E application, the catalytic activity of the metal decreases down the group (Ni(II) >> Pd(II) > Pt(II). For example, a comparative study on the catalytic efficiency of Group 9 (Co(II)) and 10 (Ni(II), Pd(II), Pt(II) acetylide complexes for the polymerization of *p*-diethynylbenzene (*p*-DEB) indicated that Co(II) acetylide is the best catalyst followed by Ni(II) > Pd(II) > Pt(II)-acetylides in terms of yield and molecular weight of the polymers (**461**, Chart 76). Overall, the yield of the polymer diminishes with heaviness of the metal. In fact, Pd(II) and Pt(II) acetylides were unable to polymerise *p*-DEB efficiently. This report is in line with the earlier works in which a low degree of polymerization of ethynylfluorenol, ethynyltrimethylsilane, phenylacetylene and *N*-benzylpropargylamine has been reported even at elevated temperature and at longer time when Pt(II) acetylide bearing PPh_3 auxiliary was used as catalyst.[844,851-853] This variation in the catalytic potential was attributed to the electronic configuration of the metals. Prior to this work, the catalytic activity of metal acetylide as a function of polarity, steric hindrance and electron-donating ability of ligands attached to metal atom has also been assessed.[262]. Li and Yang[841] studied the effect of different PPh_3 bearing Pd(II) acetylide complexes ($Pd(PPh_3)_2(C{\equiv}CR)_2$ (R = $C(CH_3)_2OH$, CH_2OCOCH_3, CH_2OH, p-$C_6H_4C{\equiv}CH$, C_6H_5) for copolymerization between polar and non-polar alkynes (propargyl alcohol (OHP) with p-DEB). They showed that the complexes containing polar alkynyl ligands show higher activity than corresponding complexes containing non-polar ligands. A similar observation has been made for the polymerization of (dimethylamino)ethyl methylate (DMAEMA) using Pd(II) catalysts.[854] Sun and co-workers[855] reported that the Ni(II) acetylide complexes in conjunction with organic halide ($BrCCl_3$/$Ni(C{\equiv}CPh)_2(PBu_3)_2$) are better in catalytic activity than Ni(II) halides and Ni(0) complexes for the polymerization of methyl methacrylate (MMA). In a recent work, Xu and co-workers[856] demonstrated that a Pt(II)-based polymer **462** (Mn = 69 kDa, Chart 76) can be used as latent catalyst under mechanical stimulus for the hydrosilylation of 1-octene by $(Me_3SiO)_2MeSiH$. The mechanically induced chain scission was demonstrated to be able to release catalytically active platinum species which could catalyse the olefin hydrosilylation process. They showed that the chain scission and catalytic reaction originated from the ultrasound-induced dissociation of Pt(II) acetylide complex.

Chart 76.

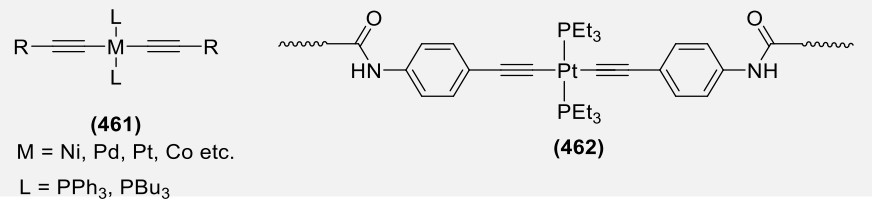

In addition of σ-acetylide oligo- and poly-mers, some recent works also demonstrated that cyclometallated complexes are also potential candidate as catalysts. Tung and co-workers[857] reported a visible light-induced **463**-catalyzed dehydrogenation of Hantzsch esters (Chart 77). In a rare work, Yu et al.[858] reported neutral cyclometalated Au(III) complexes **464-465** (Chart 77) as photosensitizer for the photocatalyzed production of hydrogen from water. In addition to the above-discussed examples of catalysts, organic conjugated

polymers as photo-catalysts for visible light mediated oxidation of thioanisole,[859,860] conversion of α-terpinene into ascaridole,[861] splitting of water[862] have also been reported. Several examples of Pt(II) acetylide cyclometalated complexes have been reported for light-driven generation of H_2 from water.[503,508,509] For example, when **466** (Chart 77) is used as a molecular catalyst/sensitizer in multiple component systems (such as methyl viologen + triethanolamine + colloidal platinum in aqueous media), it produces modest to high quantity of H_2, thus offering a new avenue for alternative energy.

Chart 77.

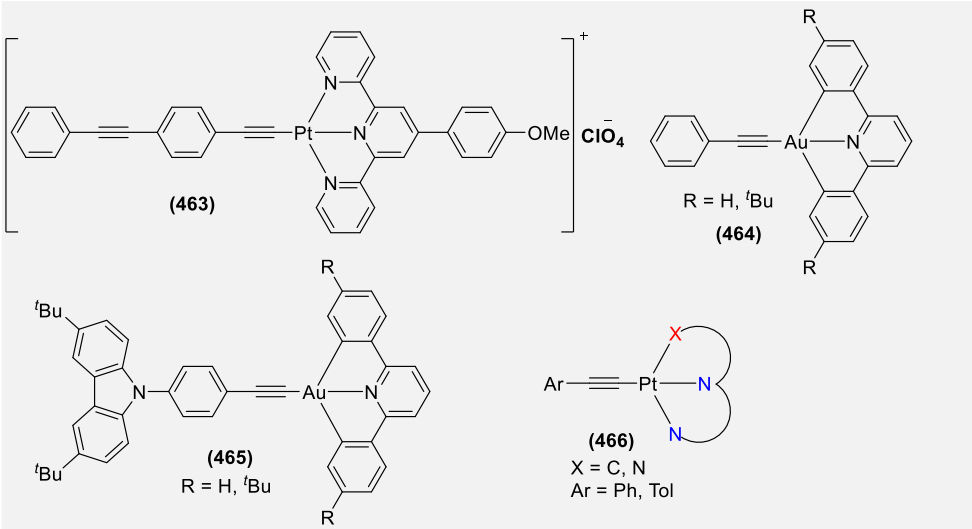

Table 13. Transition metal acetylides as catalysts

Entry	Metal (M)	Auxiliary ligand (L)	Main ligand (R)	Polymerized product	Reaction condition	Yield (Mw/Mn)	Ref
461a	Co	PPh_3	Phenyl	*p*-DEB	Dioxane/Toluene (1:1), 25 °C, 3h	82 (2.2)	[842]
461b	Co	PBu_3	Phenyl	*p*-DEB	DMSO, 25 °C, 9h	84.7 (2.4)	[842]
461c	Pt	PPh_3	Phenyl	*p*-DEB	Pyridine, 60 °C, 24h	0 (-)	[842]
461d	Pt	PBu_3	Phenyl	*p*-DEB	Pyridine, 60 °C, 48h	0 (-)	[842]
461e	Ni	PPh_3	Phenyl	*p*-DEB	Dioxane/toluene (1:1), 25 °C,	71.5 (2.3)	[842]
461e	Ni	PPh_3	Phenyl	*p*-PA	THF, 60 °C, 48 h	11.5(1.8)	[863]
461f	Ni	PPh_3	Phenylacetylene	*p*-DEB	DMSO, 30 °C, 3.5h	81.2 (2.3)	[262]
461f	Ni	PPh_3	Phenylacetylene	*p*-PA	THF, 60 °C, 48 h	13.5 (1.6)	[863]
461g	Ni	PPh_3	CH_2OCOCH_3	*p*-PA	THF, 60 °C, 48 h	11.8 (1.4)	[863]
461h	Ni	PPh_3	Cl	*p*-DEB	DMSO, 30 °C, 3.5h	71.2 (1.7)	[262]
461i	Ni	PBu_3	Phenyl	*p*-DEB	DMSO, 60 °C, 9h,	90.4 (2.6)	[842]
461j	Ni	PBu_3	Phenylacetylene	*p*-PA	THF, 60 °C, 48 h	4.6 (1.7)	[863]
461k	Ni	PBu_3	Phenyl	*p*-PA	THF, 60 °C, 48 h	3.5(2.4)	[863]
461l	Ni	PBu_3	CH_2OCOCH_3	*p*-PA	THF, 60 °C, 48 h	5.7 (2.1)	[863]
461m	Pd	PPh_3	Phenyl	*p*-DEB	Pyridine, 60 °C, 18h	75.7 (2.9)	[842]
461m	Pd	PPh_3	Phenyl	*p*-(DMAEMA-co-MMA	$CHCl_3$, 60 °C, 12 h,	98 (-)	[864]
461m	Pd	PPh_3	Phenyl	*p*-PA	$CHCl_3$/MeOH (3:1), 60 °C, 24 h	57.4 (1.6)	[863]
461n	Pd	PPh_3	CH_2OH	DEB-co-PA	$CHCl_3$/MeOH (3:1), 60 °C, 16 h	60.5 (1.7)	[841]
461n	Pd	PPh_3	CH_2OH	*p*-PA	Toluene, 55°C, 24h	98 (1.4)	[843]
461n	Pd	PPh_3	CH_2OH	*p*-PA	$CHCl_3$/MeOH =3:1, 60 °C, 24 h	58.2 (1.4)	[863]
461o	Pd	PPh_3	Phenylacetylene	*p*-DEB	Pyridine, 60 °C, 18h	79.9 (3.8)	[840]
461o	Pd	PPh_3	Phenylacetylene	*p*-PA	$CHCl_3$/MeOH (3:1), °C, 24 h	66.4 (1.8)	[863]
461p	Pd	PPh_3	H	*p*-DEB	Pyridine, 60 °C, 18h	55.5 (3.0)	[840]
461p	Pd	PPh_3	H	*p*-PA	$CHCl_3$/MeOH (3:1), 60 °C , 24 h	53.8(2.2)	[863]
461q	Pd	PPh_3	$CH_2OCOC_6H_4OH$-o	*p*-DEB	Pyridine, 60°C, 18h	84.1 (3.0)	[840]
461q	Pd	PPh_3	$CH_2OCOC_6H_4OH$-o	*p*-PA	$CHCl_3$/MeOH =3:1, 60°C, 24 h	79.1 (2.2)	[863]
461r	Pd	PPh_3	$CH_2OCOC_6H_4$	*p*-DEB	Pyridine, 60 °C, 18h	79.1 (2.8)	[840]
461r	Pd	PPh_3	$CH_2OCOC_6H_4$	*p*-PA	$CHCl_3$/MeOH =3:1, 60 °C, 24 h	71.0 (2.0)	[863]
461s	Pd	PPh_3	CH_2OCOCH_3	*p*-DEB	Pyridine, 60 °C, 18h	70.9 (2.6)	[840]
461s	Pd	PPh_3	CH_2OCOCH_3	*p*-PA	$CHCl_3$/MeOH =3:1, 60 °C, 24 h	67.2 (1.9)	[863]
461t	Pd	PPh_3	$CH_2N(CH_3)_2$	*p*-PA	Toluene, 55 °C, 24h	52 (3.0)	[843]
461u	Pd	PPh_3	$Si(CH_3)_3$	TMSE	$HNEt_2$,50 °C, 24h	69.7	[844]
461v	Pd	PBu_3	Phenyl	*p*-DEB/	Pyridine, 60 °C, 18h,	0 (-)	[842]
461w	Pd	PBu_3	CH_2OH	*p*-DEB	Pyridine, 60 °C, 18h	0(-)	[840]
461w	Pd	PBu_3	CH_2OH	*p*-PA	$CHCl_3$/MeOH =3:1, 60 °C, 24 h	45.9 (2.3)	[863]
461x	Pd	PBu_3	Phenylacetylene	*p*-DEB	Pyridine, 60 °C, 18h	0(-)	[840]
461x	Pd	PBu_3	Phenylacetylene	*p*-PA	$CHCl_3$/MeOH (3:1), 60 °C, 24 h	21.2 (2.5)	[863]
461y	Rh	PBu_3	Phenylacetylene	*p*-DEB	DMSO, 60 °C, 9h	95.1 (3.2)	[262]

p-DEB = Poly(diethnylbenzene), *p*-PA = poly(propargyl alcohol); p(DEB-co-PA) = Poly(dietnylbenzene-co-propargyl alcohol); TMSE = ethynyltrimethylsilane
p-(DMAEMA-co-MMA = poly[2-(dimethylamino)ethyl-co- methyl methacrylate methacrylate)

4.6. Biologically active natural and synthetic oligo-ynes

In addition to the O-E and other applications, oligo-ynes are also known for their biological activity and are found in flora and fauna.[11,12,865] Despite the fact that all natural products harbour an alkynyl core with 1-4 C≡C units, natural product chemists and other researchers often use the term "*polyacetylenes*" for describing acetylenic compounds, which is technically inappropriate.[866] Therefore, in the present section, we will use the same nomenclature that we used in previous sections and sub-sections (mono, di-, tri-, tetra-, penta- or so on etc.). Historically, the first report on the isolation of oligo-ynes from natural source appeared in the early ninetieth century.[866] Since then, more than 1000 acetylenic natural products have been isolated from organisms such as plants, mosses and lichens, fungi, bacteria, insects, algae, sponges, and tunicates with a variety of biological activities *viz*. anti-inflammatory, antimicrobial, antitumor, antiviral, neurotrophic, phytotoxic properties etc.[11,12,865] Inspired by nature and enormous biological applications of acetylene moiety containing scaffolds, several synthetic or semi-synthetic analogues or derivatives have been prepared.[867-873] The interesting and diverse activity of these compounds have been directly related to their linear rod like conjugated structure.[872,874] Chart 78 shows some of the prominent and biologically active acetylenic compounds found in nature (kingdom plantae and animalia both) as well as recently reported synthetic and semi-synthetic acetylenic compounds. Acetylenic compounds found in higher plants can be classified into seven families, with the majority being isolated from the botanically related apiaceae, araliaceae and asteraceae families. Acetylenes found in these family of plants are structurally diverse: ranging from aliphatic to aromatic, carbocyclic to heterocyclic, alkamides, lactones, spiroketals, glycosides, etc. These oligo-ynes possess unique bioactivity such as anti-diabetic, antifungal, cytotoxic, T-proliferative, angiogenesis and apoptotic activity.[875-878] For example, cytopiloyne and its aglycone are tetra-ynes found in *Bidens pilosa*, which is itself an anti-diabetic asteraceae plant. Biavatti and co-workers isolated eight tri-ynes (**467**) from the leaves of *V. scorpioides*.[879] The isolated compounds showed no inhibitory effect against cancer cells, but presented a mild non-selective *in-vitro* antiviral activity, although their corresponding glycosides were inactive. Gymnasterkoreayne B, E and G (**468a**, Chart 78) are diacetylenic compounds found in Gymnaster koraiensis (NAKAI) KITAMURA (Compositae), an edible wild vegetable. These three compounds exhibit good *in-vitro* and *in-vivo* quinone reductase (QR) induction activity, relatively low cytotoxicity, elicit anticancer and hepatoprotective effects.[880-882] In addition to these, glycosides, gymnasterkoreasides A and B, have also been reported.[883] Recently, a new eighteen-membered immunosuppressive macrolide Ivorenolide A **469** (Chart 78) has been reported to be present in the stem bark of *Khaya ivorensis* A. Chev. (Meliaceae), the well-known African mahogany.[884] Yue and co-workers[884] recently reported total synthesis of enantiomer of **469a**, which like the original molecule, exhibited remarkable inhibition of ConA-induced T-cell proliferation and LPS induced B-cell proliferation. They obtained the target enantiomer **469b** *via* Cadiot−Chodkiewicz coupling and Sonogashira cross-coupling of terminal acetylenes. Both **469a** and **b** showed comparable or more selectivity indexes (SI) than those of the positive controls cyclosporine A (CsA) and periplocoside A (PSA). Motivated by the QR induction activity and biological results of Gymnasterkoreayne B, E and G, Lee and Shin[874] carried out an extensive SAR of

a series of compounds based on 1-phenylhexa-2,4-diyne-1,6-diol scaffold **470a**. The study indicated that the biological activity of the compound was significantly affected by the length of alkyl group present over terminal phenyl group. In particular, 4-fluorophenyl, 3-chlorophenyl, and 3,4-dioxolophenyl derivatives showed the best profiles in terms of QR induction, cytotoxicity, and CI. Further investigation of the structure–activity relationship for alkyl substituents on the opposite side of the phenyl group **470b** revealed that employment of a relatively short chain maintained high CI values, while the introduction of longer or bulkier groups increased cytotoxicity.

Bacterial infection poses a major threat to developing and under-developed countries. Diseases like tuberculosis, meningitis, cholera, pneumonia, etc. cause significant damage to the human population. The main problem with bacteria is their tendency to develop drug resistance. For example, the development of antibiotic resistance in Gram-negative uropathogens is a major global concern, especially in the Asian countries.[885] To curb this challenge, researchers are exploring new inhibitors that can target essential enzyme/other biomolecules. Zn-dependent UDP-3-O-(acyl)-N-acetyl glucosamine deacetylase (LpxC) is one of the essential enzymes in the lipid A biosynthetic pathway which does not show homology to any mammalian protein, it is thus regarded as a promising target for the treatment of Gram-negative bacterial infections. Diphenyl-acetylene compound (**471**) is the first known molecule that effectively killed both *E. coli* and *P. aeruginosa in-vitro*.[886] However, the possibility of rapid evolution of antibiotic resistance for **471** sensitive strains (as evidenced by less effectiveness against LpxC orthologs from the *Rhizobiaceae* family than against *E. coli*) prompted researchers to investigate and develop new compounds like **472-473**.[887] Inspired by the biological activity of diphenyl-acetylene compounds and in order to improve the solubility of LPC-009 in aqueous solution as well as to probe the stereochemical requirement of the threonyl group, Toone and co-workers[887] reported the synthesis and antibiotic profiles of **472** derivatives diphenyl-diacetylene (1,4-diphenyl-1,3-butadiyne) threonyl hydroxamate scaffold. They found that the functionality and its position (amino group present over distal phenyl ring) affects water solubility as well as the bioactivity. Interestingly, they found that stereochemistry of threonyl does not have much effect on the bioactivity.

For example, compounds with either *S*- or *R*-configurations at the C3 position of threonyl shows similar antibiotic activities. Using scaffold-hopping approach, Kurasaki and co-workers[888] recently reported threonine-based and oxazolidinone-based inhibitors. The most active compound **474** showed excellent activity in nanomolar range against different strains of bacteria. Young and co-workers[889] reported the antibacterial efficiency of several semi-synthetic oligo-ynes **475-476**. The acetylenic compounds which were synthesized *via* solid supported Glaser Hay coupling showed moderate antibacterial potential. The same group reported novel Cadiot–Chodkiewicz bioconjugation strategy for the preparation of bio-conjugates with minimal protein oxidation.[890,891]

Chart 78.

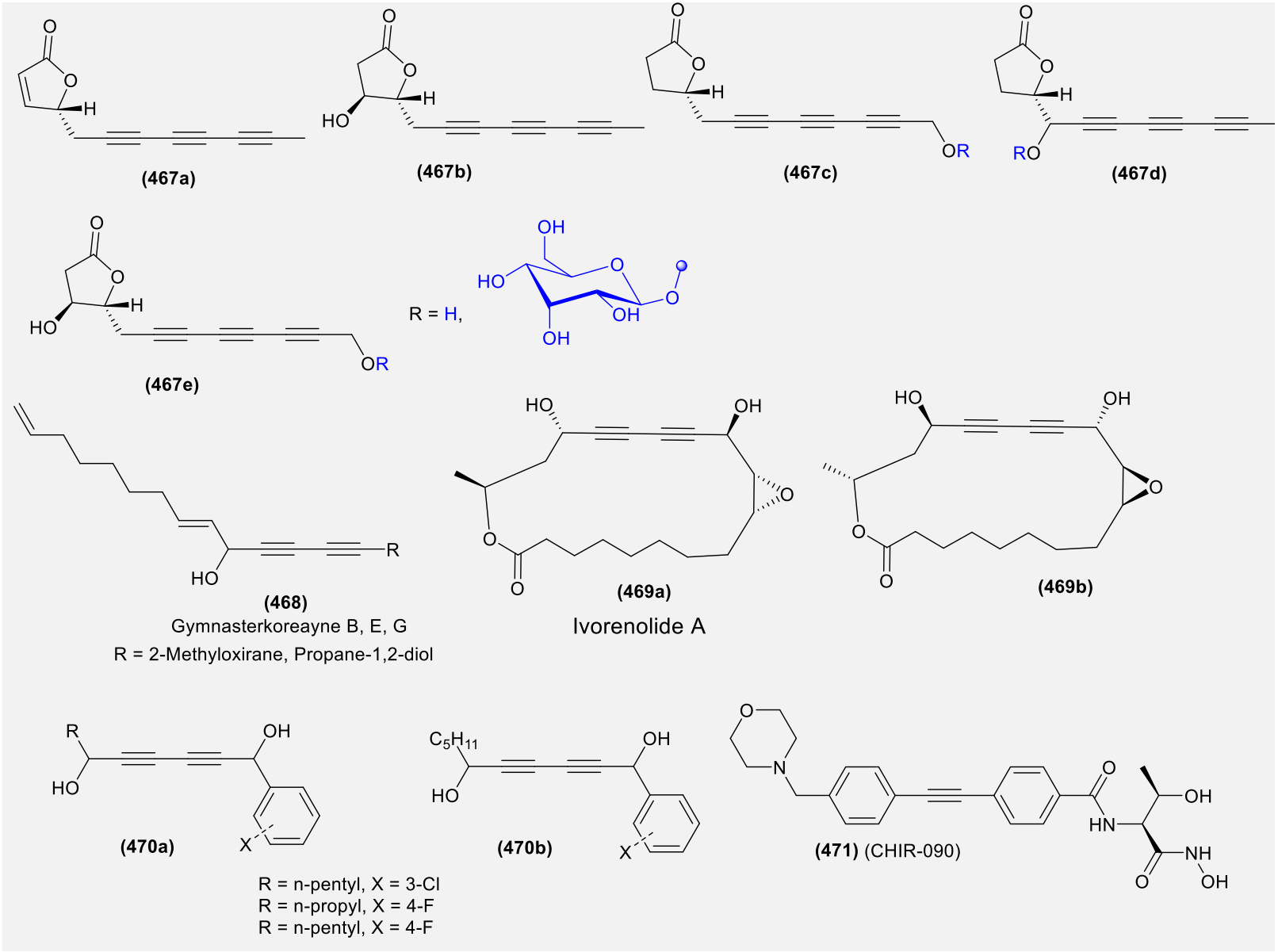
(467a)
(467b)
(467c)
(467d)
(467e)
R = H,
(468)
Gymnasterkoreayne B, E, G
R = 2-Methyloxirane, Propane-1,2-diol
(469a)
Ivorenolide A
(469b)
(470a)
(470b)
R = n-pentyl, X = 3-Cl
R = n-propyl, X = 4-F
R = n-pentyl, X = 4-F
(471) (CHIR-090)

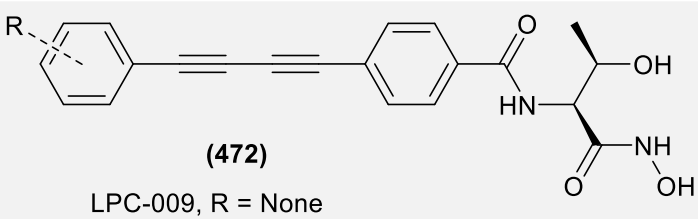

(472)

LPC-009, R = None

LPC-012, R= 3-NH_2)

LPC-011, R = 4-NH_2)

LPC-013, R = 2-NH_2)

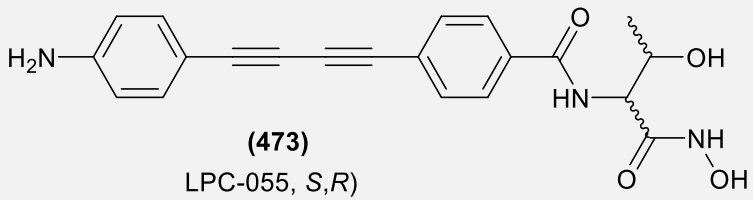

(473)

LPC-055, *S*,*R*)

LPC-054, *R*,*R*)

LPC-053, *S*,*S*)

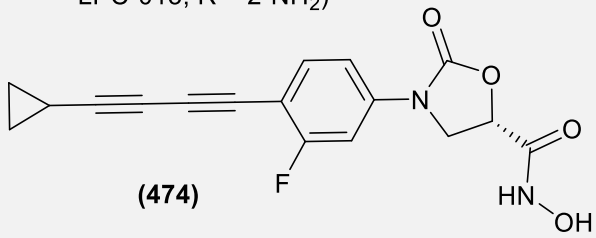

(474)

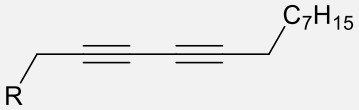

(475)

(R = OH)

(R = OCH_2COOH)

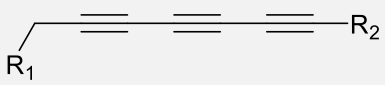

(476)

(R_1 = OH, R_2 = Me)

(R_1 = OCOMe, R_2 = Ph)

Imaging technology, especially using fluorescent labels has seen a tremendous growth in the last few decades.[892] Different classes of materials *viz*. organic (rhodamine, BODIPY, squaraine, porphyrin, phthalocyanine etc.), inorganic (transition and lanthanide complexes) and nano materials (quantum dots, nanocubes, nanotubes, etc.) able to emit/absorb in the NIR region are used to image dysfunction and deformities at the supramolecular level as in this region biological molecule has minimum perturbation.[892-895] [rashid Ilmi]The importance of acetylenic moieties is well appreciated by bioorganic and medicinal chemists due their rigidity, tunable conjugated structure, spectroscopic features, exogenous (nearly non-existent inside cells) and bioorthogonal (inert to reactions with endogenous biomolecules) nature. Carroll and co-workers[891,892] demonstrated the effectiveness of alkyne-based chemical probes for selective profiling of cellular protein S-sulfenylation (an oxidized form of cysteine thiol), which plays a crucial role in protein functioning and is considered as a potential biomarker. In a recent work, Kim and co-workers[896] reported that the introduction of triyne fragment to the core of 7-nitrobenz-2-oxa-1,3-diazol-4-yl (NBD)-labeled-sphingosine **477** not only imposed rigidity to the backbone and make it highly fluorescent, but also led to enhanced antiproliferative activity against human colon carcinoma cell line (**Figure 44**). The triyne compound was selectively accumulated within the cytoplasm. Similarly, Barattucci and co-workers[166] reported glucoside tagged tetra-yne that selectively accumulated in the cytoplasmic vesicles of epidermoid carcinoma larynx cells.

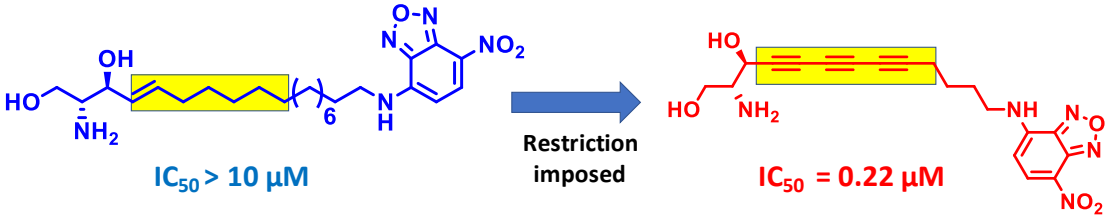

Figure 44. Impact of triyne incorporation to sphingosine.

One exceptional property that makes acetylenic moieties unique is its Raman band.[897] Compared to other conjugated polymeric counterparts, alkyne-based systems shows a distinct Raman band in biologicaly silent region (~ 2000-2200 cm^{-1}, Figure 45a).[897,898] Therefore, Raman band of acetylenic moieties do not interferes/overlap with any endogenous bio-molecule.[897] Based on this notion, several tags and barcodes bearing C≡C moieties have been developed (known as alkyne-tag Raman imaging, ATRI) for visualizing non-immobilized receptors *viz* protein, nucleus, cytoplasm, cellular compartments, etc. in live cells (Figure 45b,c).[232,897,899-904] However, one challenge associated with Raman microscopy is its weak signal leading to prolonged imaging time. To circumvent this issue, Sodeoka and co-workers[904] simply increased the conjugation length of the tags, which possess strong Raman signals. They performed an extensive structure-Raman shift/intensity relationship of various probes labeled with Raman tags (alkynes, nitrile, azide and deuterium) and reported some important information. For example, the conjugation of alkyne to an aromatic ring greatly increases the Raman intensity, di-ynes are suitable sensitive tag for non-aromatic compounds such as lipids etc. and alkynes are the best tag compared to nitrile, azide and deuterium.

Overall, they usefully demonstrated the application of ATRI in imaging using alkyne based small molecules in living cells.

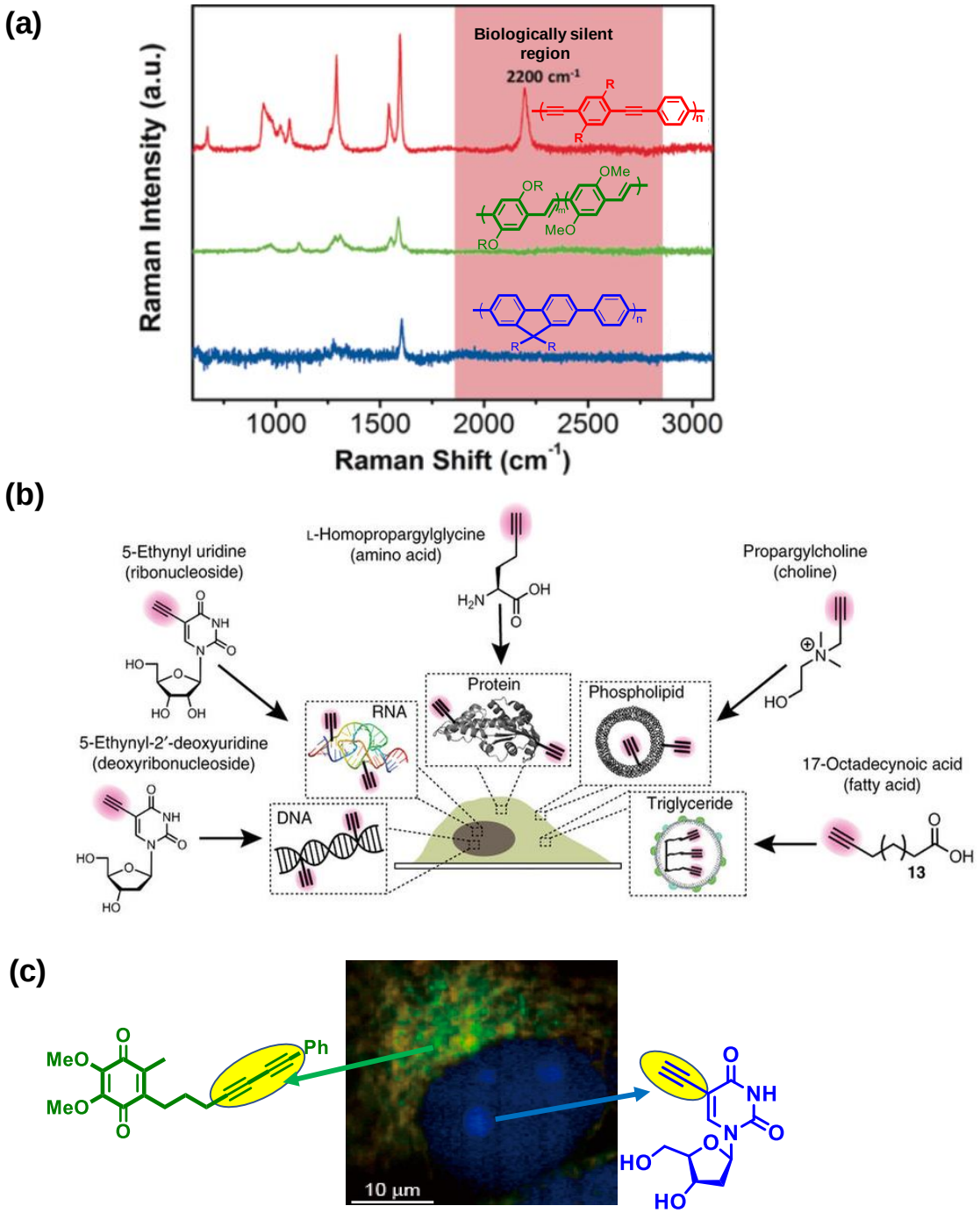

Figure 45. (a) Raman shifts of cationic conjugated polymers. Reprinted with permission from ref [903]. Copyright 2017 John Wiley and Sons. (b) Metabolic incorporation scheme for a broad spectrum of alkyne-tagged small precursors, Reprinted with permission from ref [897]. Copyright 2014 Nature Publishing Group (c) Multi-color alkyne tag Raman imaging of a live cell. Reprinted with permission from ref [904]. Copyright 2012 American Chemical Society.

Not only the small molecule based acetylenic systems are a promising scaffold for Raman imaging, but large size poly-ynes have also shown promising results. Recently, Schanze and co-workers[903] utilized poly(phenylene ethynylene) based conjugated cationic polymers **478-483** (Chart 79) and their corresponding nanomaterials as probes for living cell imaging. Compared to corresponding poly(phenylene vinylene) and PPE polymers, the reported polymers showed strong signal. Introduction of anionic groups to conjugated polymers significantly enhances water solubility of the conjugated glycopolymers by preventing the π–π stacking interactions of polymer backbones through charge repulsion. Due to the integration of multiple alkyne groups into the rigid backbone and the delocalized π-conjugation, the system showed a synergistic-enhancement effect of alkyne vibrations. Tang and co-workers[206] fabricated a **128**-cetuximab conjugate for the imaging of lung cancer cells. The mAb-AIE dots exhibit excellent specificity to HCC 827 lung cancer cells with overexpressed epidermal growth factor receptor (EGFR), high photostability and good biocompatibility. The cellular uptake process was also elucidated as receptor mediated endocytosis.

Chart 79.

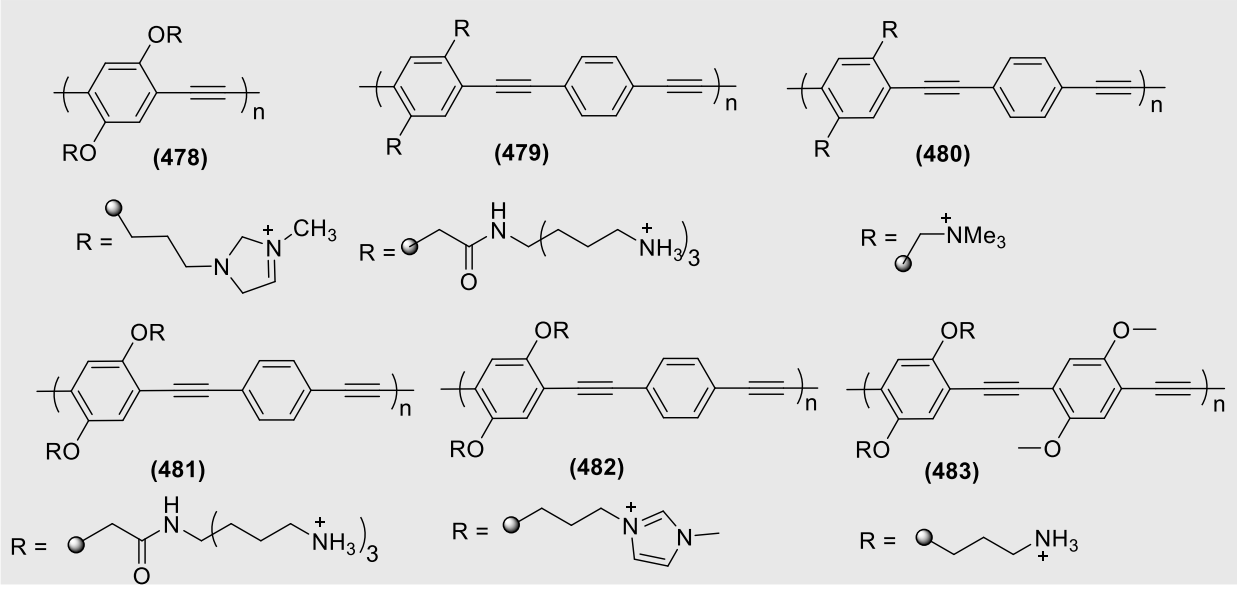

In addition to the organic, a number of fluorescent organometallic systems have been reported to be localized intracellularly and utilized in imaging applications. Wang and co-workers[905] integrated an electron-deficient benzothiadiazole unit between the dinuclear platinum metals to prepare D-A type dinuclear Pt(II) acetylide bolaamphiphile **484**, which formed fluorescent nano-sphere in protic condition (Figure 46). Good biocompatibility, sufficient stability and interesting bio-imaging behaviours were some of the unique features of the reported system. In a recent work, Bian et al.[906] assessed the NIR imaging efficiency of nano-probes based on Pt/Pd-containing metallopolymers. Due to the favourable probe size, they showed good biocompatibility and specificity to HeLa cancer cells.

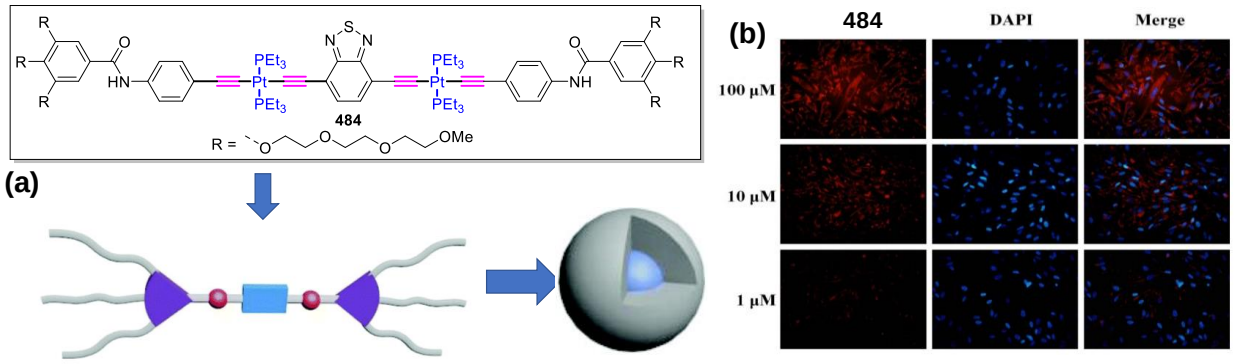

Figure 46. (a) Chemical structure of dinuclear platinum acetylide **484** and schematic representation of supramolecular nanoparticles formation (b) Fluorescent microscopy images of 1 in 35 A549 cells; middle, nuclear staining image with DAPI; and right, merged image from 24 h to 72 h post incubation. Reprinted with permission from ref [905]. Copyright 2015 Royal Society of Chemistry.

Au(I)-based therapeutics have a long tradition in medicine lasting from ancient times through alchemy to modern ages. Au(I)-alkynyl complexes have good potential for developing biologically active Au(I) complexes.[531] A number of Au(I)-appended alkynyl complexes have been investigated as anticancer, thioredoxin reductase (TrxR) inhibitor, antibacterial and antimalarial agents.[907] An extensive review on the photo-physical properties and application of Au(I) acetylide system has already been published.[531,908]. Herein, some recent examples are discussed. Rodriguez and co-workers[909] investigated enzymatic inhibition and tumour cell proliferation potential of dinuclear Au(I) alkynyl complexes bearing different phosphine ligands and methylene centres. Inhibition of the enzyme thioredoxin reductase (TrxR) was confirmed for the gold derivatives containing dppm and dppb bridging ligands and indicated a preference for the shorter bridging ligand. Compared to the free ligands, the Au(I) complexes showed excellent antiproliferative effects in MCF-7 and HT-29 cells. Despite the interesting activity profile, the solubility of the materials in biological media was a major concern. Their application in biological assays was hampered by solubility problems, which are most probably the consequence of the large lipophilic residues at the phosphines. It was expected that by improving the solubility in aqueous media, the bioactivity could have enhanced. Considering this fact, the same group synthesized and assessed water soluble 4-pyridylethynyl and propargyloxycoumarin based Au(I) complexes.[910] The complexes showed very low effects against tumour cell growth but an inhibitory potency against thioredoxin reductase (TrxR). The low cytotoxic effects were attributed to the low bioavailability, which ultimately is related to Au-P bond strength.[911] It has been recently demonstrated that an alkynyl Au(I) derivative [Au(C≡CPh)(PTA)] (PTA = 1,3,5-triaza-7-phosphaadamantane), a lipophilic drug, induce high antiproliferative activity. The complex was found to induce apoptosis in colorectal carcinoma tumour cells (Caco-2) without affecting normal enterocytes and was found to act *via* multiple pathways.[912]. Replacing phenyl by 2-pyridine, i.e. [Au(C≡C-NC_5H_4)(PTA)]) also produced excellent anticancer agent that alters the mitochondrial function and increases the level of ROS.[913] This complex is the first report of an alkynyl Au(I) complex able to induce necroptosis in cancer cells. Since these complexes showed high activity at very low concentration and does not target nucleic

acid, they have promising future as a chemotherapeutic agent for carcinoma and are potential alternative to platinum-based drugs, which have strong side effects. When Au(I) alkynyl complexes were functionalized with naphthalimide units, it produced highly fluorescent and cytotoxic fluorophores compatible with fluorescence microscopy.[914] The complexes showed some clear intracellular localization patterns that are dependent upon the specific nature of the naphthalimide substituent. The complexes showed the best cytotoxicity on MCF-7 and HEK cell lines. In a recent study, good antiproliferative ability of Au(I) complexes was coupled with excellent photo-physical properties of Re complexes to generate hybrid probes with new properties and application.[915] Other than these examples, several organic and organometallic complexes endowed with anticancer[916], antibacterial[917], antifungal[918] and for cellular component or protein imaging[914,919-921], photodynamic therapy[922], are available.

4.7. Miscellaneous

In addition to the above-discussed wide-ranging applications of organic and organometallic di-, oligo- and poly-ynes, some other new and emerging uses of these materials have been reported (Figure 47). For example, due to the free rotatable feature of the acetylene axis, oligo-ynes are often employed as an axle for molecular rotors.[923] Jiang et al.[*211*] prepared an ethynylene-based MOF that could be used to probe viscosity. In 2015, Wong and co-workers[924] demonstrated that poly(fluorenyl ethynylene)s with ferrocene could be used as cathode materials coin cells. They showed that poly-yne based electrode retained over 90% of the initial capacity after 100 cycles and exhibited a stable discharge capacity of 73 mAh g^{-1} at 1 C, which is close to the theoretical value (82.3 mAh g^{-1}). In a recent study, Zhou et al.[925] reported alkyne-rich 2,2,6,6-tetramethylpiperidine-1-oxy (TEMPO) built-in porous organic frameworks (POFs) as cathode materials for lithium-sulphur (Li-S) batteries. The polymers, synthesized *via* bottom-up strategy exhibited cycling capacity of up to 470 mAh g^{-1} after 200 cycles. Carbon nano-tubes based on conjugated polymers has also been assessed for Li-storage.[926] Shen et al.[927] demonstrated that Ru(II) complexes with DTE as ligand shows photochromic and electrochromic properties, and thus have a strong potential to serve as NOR/OR logic gates. Zhou et al.[928] synthesized 1,3,5,7-octatetrayne-linked bis(fullerene) and used it for the preparation of carbon-rich, fullerene-containing nanoparticles. One of the interesting and a vital application of conjugated polymer is the purification of water in treatment plants. In a recent work, Wang et al.[*929*] has disclosed that conjugated microporous polymer (CMPs) has excellent potential of killing bacteria present in the water. A dispersion of 100 µg/mL was found to completely inhibit the bacterial activity in two hours. This is one the first examples based on acetylenic materials. On the other hand, Choi and co-workers[930] reported an OPE based wettable and compressible polymer that can remove both methylene blue and methylene orange dyes. However, due to the presence of carboxylate functionality over the polymeric chain, cationic dye was found to be adsorbed preferentially over the anionic ones. Since C≡C bonds and aromatic spacers have strong affinity for molecular iodine, a number of research work has been undertaken on the preparation of alkyne-rich porous aromatic frameworks (PAFs), covalent organic frameworks (COFs) and conjugated porous polymers (CPPs) for iodine adsorption and other applications.[931,932] In 2016, the group led by Trabolsi[933] prepared an alkyne rich covalent calix[4]arene-

based polymer and harnessed it for water purification. The adsorbent showed excellent sorption capacity for a range of organic solvents, oils, and toxic dyes. Very recently, the same group reported some lithiated polycalix[4]arenes which was prepared by lithiation of hyper-cross-linked π-bond-rich porous covalent polycalix[4]arenes. The lithiated polymers were successfully used as iodine adsorbent from both the solution and vapor phases.[934] Prior to this work, Yan et al.[935] reported charged PAFs that showed excellent sorption abilities to iodine molecules from the solution. Due to the presence of charged sites, aromatic spacers and π-bonds, the reported polymers showed adsorption *via* multiple interaction mechanism and possess loading capacity higher than all porous materials (zeolites, MOFs, and POFs). From the notion that hydrogens present at 2,6-position of BODIPY undergo rapid halogenation, Zhu et al.[936] prepared BODIPY-based CPPs as iodine adsorbent. The reported adsorbent showed high capacity for iodine (2230-2830 mg g^{-1}) with high thermal stability and reusability. Similarly, Ren et al.[937] reported a honeycomb-like porous spheres with ultrahigh absorption feature. The reported thiophene-based conjugated polymers show iodine vapor uptake up to 345 wt.%. Besides, poly-ynes have also been reported to capture molecular species such as methane, carbon dioxide, benzene, toluene, nitrogen, hydrogen etc. In a recent work, Xu et al.[938] synthesized triphenylphosphine-based microporous poly-ynes that have affinity towards CO_2, N_2 and CH_4. Among studied gases, the polymers showed highest affinity, strong binding and adsorption capacity for CO_2. BODIPY-based polymers were also reported for the CO_2 and H_2 adsorption.[860] High CO_2 uptake (201.6 cm^3g^{-1} at 196 K, under 1 atm) and sorption ability for acetone (upto 5%) has also been demonstrated by molecular rotors.[939,940] High selectivity and adsorption efficiency of these rotors and poly-ynes dictates that they might find application in gas storage and separation. Sen et al.[941] found that BODIPY-based polymers are excellent materials for the adsorption of benzene and toluene. (order of sensitivity: toluene > benzene). A number of other beautiful supramolecular nano architecture with diverse applications can also be obtained.[6,218,942] Recently, Castagnolo and co-workers[943] reviewed the synthesis and application of propargylamines and transformations of propargylamines into heterocyclic compounds such as pyrroles, pyridines, thiazoles, and oxazoles, as well as other relevant organic derivatives.

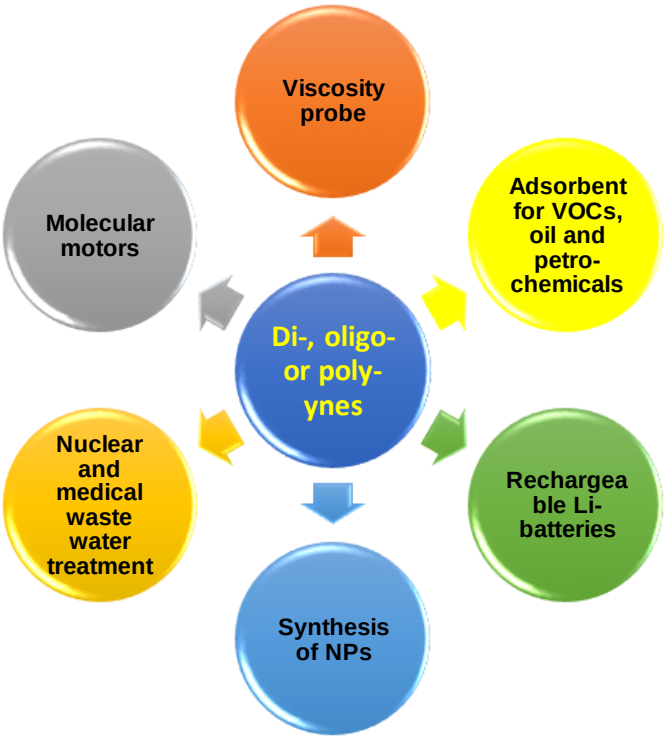

Figure 47. Other emerging applications of di-, oligo- and poly-ynes.

5. Future perspectives and suggestions

The study of organic and organometallic poly-ynes continues to be an immensely popular and active field of research due to their intriguing photophysical properties and versatile applications. The introduction of ethynyl unit(s) into an organic or organometallic framework improves the performance of materials in several ways: *via* introducing rigidity, enhancing conjugation, facilitating *π-d* interaction, etc. The past few decades have witnessed a tremendous growth in the development of organic and organometallic acetylenic materials due to their rapidly developing OEs and other interesting applications. Thanks to the development in new synthetic methodologies, a variety of functional materials with predictable shape and symmetry can now be realized. Other than the traditional transition-metal catalysed cross-coupling reactions, several new catalysts are available for C_{sp}–C_{sp}, C_{sp}–C_{sp^2} or C_{sp}–C_{sp^3} bond formation. Custom designed and synthesized small to medium organic and organometallic acetylides offer unique properties, stability and use in real-world applications. Not only the acetylenic compounds are unique, but also serve as starting materials for several value-added products such as biologically active molecules, catalysts, and other functional materials.[69] The extensive research and development conducted in organic and organometallic di-, oligo- and poly-ynes have delineated several important hidden treasures about these materials including new and interesting applications. From several examples, it has been exemplified here that the incorporation of ethynyl core drastically modifies and improves the O-E properties of the new functional materials. Moreover, acetylenic polymers have strong affinity and uptake for molecular species like iodine, carbon dioxide, methane, organic VOCs etc. meaning materials based on these polymers can be used for chemical/ medical/nuclear waste management, fuel storage and gas separation. Furthermore, the Raman active

nature of ethynyl core is being exploited to develop imaging probes to detect deformation at molecular level. Advantage of using Raman probes is that most of the biological entities are silent in the region.

Despite the bright prospect of these materials, some challenges still remain to be addressed through further studies. This would require an array of interdisciplinary researchers from the domains of chemistry, biology and physics. For example, most of the reactions, with few exceptions, employ multi-step processes utilizing costly, corrosive and toxic solvents in combination with a high load of costly catalysts. Therefore, there is an urgent need to develop more efficient, selective, inexpensive, and eco-friendly methods and processes. In addition, many synthesized organic and organometallic materials possess low stability in the presence of air/oxygen or water, hampering their real-life applications. Also, several examples of varying performance of the same material are reported in the literature.[439,440,816] Materials inhomogeneity is blamed in some cases while in others minor impurity in the synthesized materials is the culprit. On the other hand, studies also demonstrated that the device performance depends not only on chemical composition of the materials but also on the device structure and fabrication technique. Thus, there is a need to reassess the materials which were found to be stable and had excellent O-E properties, but low to moderate O-E performance. Wherever materials stability is an issue, alternative methods (by introducing molecular shielding around the chain (*via* iptycene or network of H-bond forming side chain functionalities) should be employed to stabilize oligomeric and polymeric chain. In the domain of biological applications, it would be interesting and useful to study the immune response of the system along with extensive genotoxicity and cytotoxicity on animal model. Since most of the research work reviewed in this article is concerned with acetylenic materials dealing with real-life applications, their safety profile including biodegradability of the materials should be studied in detail. Otherwise, the materials are likely to pose the same risks, damage and challenges to the flora and fauna as plastic-based materials.

6. Conclusion

This review has outlined custom-designed syntheses of organic and organometallic oligo- and poly-ynes that offer fascinating structure, properties and applications. Several classical and modern synthetic methodologies affording a variety of functional acetylenic molecules have been described. A critical evaluation of the structure-property relationship with respect to spacers, metals and conjugation length in these materials has been discussed. We have shown how each component of this class of materials affects their properties and application. Due to the diverse range of photo-physical, photo-chemical and structural properties, their application in various domains of science have been delineated. As described through several examples, both organic and organometallic oligo- and poly-yne materials have potential to be used as active materials/layers for energy generation from sun/electricity. They can be derivatized with specific functionality/receptor to sense analyte of interest from air/moisture/aqueous/organic vapor samples. A number of organic and organometallic poly-ynes have been developed featuring chirality (due to hydrophobic exterior and hydrophilic interior), which makes the new materials potential candidates for the chiral separation of pharmaceuticals and organic pollutants. Due to high memory retention ability and flexibility, they are being explored as materials for next generation memory/magnetic devices. Among

several unique applications, catalysis is another interesting area of research. They have shown potential for catalytic conversion of precursors into industrially useful polymers as well photocatalysis of water to produce hydrogen. Last, but not the least, bright luminescence and Raman-active nature of such materials are attracting researchers to employ them as imaging probes. In addition, we have also shown that this class of molecules is getting attention for other emerging applications, such as viscosity probes, adsorbent for industrial and medical effluents, battery component, etc. It has also been observed that there are some areas (such as materials homogeneity, presence of impurities, etc) which need careful attention of the researchers. To the best of our knowledge and experience, we strongly feel that the future of this family of organic and organometallic di-, oligo- and poly-ynes is quite bright.

Acknowledgements

The literature review leading to this review article was conducted with funding from His Majesty's Trust Fund for Strategic Research (SR/SCI/CHEM/16/02). AH acknowledges The Research Council (TRC), Oman TRC for a Postdoctoral fellowship. RAB acknowledges TRC for a Research Assistantship and SQU for a PhD scholarship. IJAB acknowledges the Ministry of Education, Oman for a PhD scholarship. PRR is grateful to the EPSRC for continued funding (EP/K004956/1).

LIST OF SYMBOLS

ε	Molar absorptivity
μ_h	Hole mobility
I_{on}/I_{off}	Current on/off ratio
K_c	Equilibrium constant
k_{isc}	Intersystem crossing rate constant.
k_{nr}	Non-Radiative decay rate constant.
k_r	Radiative decay rate constant
E_g^{ec}	Electrochemical band-gap
E_g^{op}	Optical band-gap
$\lambda_{max.}^{abs.}$	Absorption maxima
$\lambda_{max.}^{em.}$	Emission maxima
J_{sc}	Current density
k_{isc}	Intersystem crossing rate constant
k_{nr}	Non-radiative decay rate constant
k_r	Radiative decay rate constant
S_n	Singlet state
T_n	Triplet state
V_{oc}	Open-circuit potential
τ_F	Fluorescence lifetime
τ_P	Phosphorescence lifetime
Φ_F	Fluorescence quantum yield
Φ_P	Phosphorescence quantum yield
Φ_{ISC}	Intersystem crossing quantum yield
η_{ext}	External quantum efficiency.
Φ_{EnT}	Energy transfer quantum yield
R_{rec}	Resistance to the recombination of electrons

LIST OF ABBREVIATIONS

2-MeTHF	2-methyl tetrahydrofuran
2PA	Two-photon absorption
^{1}LLCT	Singlet ligand-to-ligand charge transfer
^{3}LLCT	Triplet ligand-to-ligand charge transfer
^{1}MLCT	Singlet metal-to-ligand charge transfer
^{3}MLCT	Triplet metal-to-ligand charge transfer
AIE	Aggregation induced emission
AIEgens	AIE luminogens
Ar	Aromatic spacer
ATRI	Alkyne-tag Raman imaging
Aπ	Effective conjugation length
BG/TC	Bottom-gate/top-contact
BHJ	Bulk heterojunction cells
BINOL	1,1'-Bi-2-naphthol
BODIPY	Boron-dipyrromethene
Bpy	2,2-bipyridyl
BTD	Benzothiadiazole
CD	Circular dichroism
CMPs	Conjugated microporous polymer
COFs	Covalent organic frameworks
CPL	Circularly polarized luminescence
CPL	Circularly polarized luminescence
CPPs	Conjugated porous polymers
CS	Charged separated

CT	Charge transfer
D-A	Donor-Accepter
DAPI	4',6-Diamidino-2-phenylindole.
DCM	Dichloromethane
DF	Delayed fluorescence
DFBT	5,6-Difluoro-2,1,3-difluorobenzothiadiazole
DFDBT	5,6-Difluoro-4,7-bis(4-hexyl-2-thienyl) 2,1,3-benzothiadiazole
DFT	Density functional theory
DHA	N,N-dihexylanilino
DHBT	2,3-Dihydrobenzo[b]thiophene
DMA	N,N-dimethylanilino
DMAEMA	Dimethylamino)ethyl methylate
DMF	Dimethylformamide
dmpe	1,2-Bis(dimethylphosphinoethane)
DNT	Dinitrotoluene
DP	Degree of polymerization.
DPAF	Diphenylamino-2,7-fluorenylene.
DPP	Diketopyrrolopyrrole
dppb	1,4-bis(diphenylphosphino)butane
Dppe	1,2-Bis(diphenylphosphino) ethane
Dppe	1,2-bis(diphenylphosphino)ethane
dppp	1,3-bis(diphenylphosphino)propane
DRAM	Dynamic random-access memory
DSSCs	Dye-sensitized solar cells.
DTE	Dithienylethene
DTE	Dithienylethene
DWCNTs	Double wall carbon nanotubes
EBXs	Ethynylbenziodoxolones
EDOT	3,4-Ethylenedioxythiophene
E_{FISH}	Electric-field-induced second harmonic
Eg	Optical band gap.
EL	Electroluminescence.
EQE	External quntaum efficiency.
ESA	Excited state absorption.
FETs	Field effect transistors
FF	Fill factor
fs	Femtosecond
GM	Göppert-Mayer units
HBA	Hydrogen bond acceptor
HBD	Hydrogen bond donor
HBPs	Hyperbranched polymers
HE	High energy
HOMO	Highest occupied molecular orbital
HOMO	Highest occupied molecular orbital.
HS	High-spin
ICT	Intramolecular charge transfer.
ICT	Intramolecular charge transfer
IDC	Iterative divergent/convergent
IFV	Internal free volume
IL	Intraligand
ISC	Intersystem crossing
JFP	Junction formation probability.
L	Auxiliary ligand
LDA	Lithium diisopropylamide
LE	Low energy
LE	Low energy (LE)
LEDs	Light emitting diodes
LHE	Light harvesting efficiency
Li-S	Lithium-Sulphur
LLC	Lyotropic liquid crystals
LMCT	Ligand to metal charge transfer.
LMCT	Ligand to metal charge transfer
LUMO	Lowest occupied molecular orbital
LUMO	Lowest occupied molecular orbital.
M	Metal
MCBJ	Mechanically controllable break junction
MeCN	Acetonitrile
MV	Mixed-valence
MLCT	Metal-ligand charge transfer
MMCT	Metal-to-metal-charge transfer
MOF	Metal organic framework
MTEOS	Methyltriethoxysilane
MV	Mixed- valence
NAP	Benzoyl thiourea naphthalimide
NBD	7-Nitrobenz-2-oxa-1,3-diazol-4-yl
NDI	1,4,5,8-Naphthalene diimide
NHC	N-heterocyclic carbene
NIR	Near-infrared
NLA	Non-linear absorption
NLO	Nonlinear optics
NO	Nitric oxide
O-E	Opto-electronic
OLED	Organic light emitting diode
o-PE	Ortho-Phenyleneethynylene
OPEs	Oligo(p-phenyleneethynylene)s
OPL	Optical power limiters
OPVs	Oligo(p-phenylene vinylene)s
OSC	Organic solar cell
OTF	Trifluoromethanesulfonate
OTFTs	Organic thin film transistors
PA	Picric acid
PAEs	Poly(aryleneethynylenes)
PAFs	Porous aromatic frameworks
PC	Phenanthrocarbazole
$PC_{61}BM$	[6,6]-phenyl-C61-butyric acid methyl ester
$PC_{71}BM$	[6,6]-Phenyl C71 butyric acid methyl ester
PCE	Power conversion efficiency
p-DEB	para-diethynylbenzene
PDI	Perylenediimides
PES	Photo electron spectroscopy
PF	Prompt fluorescence
Phen	Phenanthroline
PHOLEDs	Phosphorescent organic light emitting diodes
PHTE	Poly(3-hexyl-2,5-thienylene diethynylene)

PL	Photoluminescence
PLEDs	Polymer light emitting diodes
PM α-CD	Permethylated α-cyclodextrin
PMMA	Poly(methyl methacrylate).
POFs	Porous organic frameworks.
ps	Picoseconds
PS	Polystyrene
PTEPA	Poly tris(4-ethynyl phenyl)amine
PVs	Photovoltaic devices
QCM	Quartz crystal microbalance
RET	Resonance energy transfe
S → T	Singlet → Triplet
SEM	Scan electron microscope.
SOC	Spin-orbit coupling
SOC	Spin orbit coupling
T→ T	Triplet → Triplet
TBAB	Tetrabutyl ammonium butyl bromide
TBET	Through-bond energy-transfer
TCBD	1,1,4,4-Tetracyanobuta-1,3-diene
TNT	Trinitrotoluene
TPA	Triphenylamine
Tpy	Terpyridyl
TrxR	Thioredoxin reductase
TTA	Triplet-triplet annihilation
TTF	Tetrathiafulvalene
TTF	Tetrathiafulvalene
UPE	Ultraviolet photoelectron
VOC	Volatile organic content
WOLEDs	White organic light emitting diodes.
WORM	Write-once read-many times
WRFs	Whole-rainbow fluorophores
XRD	X-ray diffraction.
ΔE_{S1-T1}	Singlet-triplet splitting energy
TCNQ	7,7,8,8-Tetracyanoquinodi methane
TCTA:	Tris(4-carbazoyl-9-ylphenyl)amine
TDPP	Dithienyldiketopyrrolopyrrole.
TEA	Triethylamine
TEMPO	2,2,6,6-Tetramethylpiperidine-1-oxy
TFA	Trifluroacetic acid
TG/BC	Top-gate/bottom-contact
THF	Tetrahydrofuran
TICT	Twisted intramolecular charge transfer
TIPS	Triisopropylsilyl
TMC	Tetramethyl-1,4,8,11-tetraaza cyclotetradecane
TMEDA	N^1,N^1,N^2,N^2-tetramethylethylene diamine, TMEDA
TMS	Trimethysilyl
TMSA	Trimethysilyl acetylene

References

(1) Astumian, R. How Molecular Motors Work–Insights From The Molecular Machinist's Toolbox: The Nobel Prize In Chemistry. *Chem. Sci.* **2017**, *8*, 840-845.

(2) Ostroverkhova, O. Organic Optoelectronic Materials: Mechanisms and Applications. *Chem. Rev.* **2016**, *116*, 13279-13412.

(3) Chen, Q.; De Marco, N.; Yang, Y. M.; Song, T.-B.; Chen, C.-C.; Zhao, H.; Hong, Z.; Zhou, H.; Yang, Y. Under the Spotlight: The Organic–Inorganic Hybrid Halide Perovskite for Optoelectronic Applications. *Nano Today* **2015**, *10*, 355-396.

(4) Bunz, U. H. Poly(aryleneethynylene)s: Syntheses, Properties, Structures, and Applications. *Chem. Rev.* **2000**, *100*, 1605-1644.

(5) Ho, C. L.; Yu, Z. Q.; Wong, W. Y. Multifunctional Polymetallaynes: Properties, Functions and Applications. *Chem. Soc. Rev.* **2016**, *45*, 5264-5295.

(6) Tahir, N.; Nyayachavadi, A.; Morin, J.-F.; Rondeau-Gagné, S. Recent Progress in the Stabilization of Supramolecular Assemblies with Functional Polydiacetylenes. *Polym. Chem.* **2018**, *9*, 3019-3028.

(7) Khan, M. S.; Al-Suti, M. K.; Maharaja, J.; Haque, A.; Al-Balushi, R.; Raithby, P. R. Conjugated Poly-ynes and Poly (metalla-ynes) Incorporating Thiophene-based Spacers for Solar Cell (SC) Applications. *J. Organomet. Chem.* **2016**, *812*, 13-33.

(8) Bizzarri, C.; Spuling, E.; Knoll, D. M.; Volz, D.; Bräse, S. Sustainable Metal Complexes for Organic Light-Emitting Diodes (OLEDs). *Coord. Chem. Rev.* **2017**, DOI:10.1016/j.ccr.2017.09.011.

(9) Broggi, A.; Tomasi, I.; Bianchi, L.; Marrocchi, A.; Vaccaro, L. Small Molecular Aryl Acetylenes: Chemically Tailoring High-Efficiency Organic Semiconductors for Solar Cells and Field-Effect Transistors. *ChemPlusChem* **2014**, *79*, 486-507.

(10) Harvey, P. D. Organometallic and Coordination Polymers, and Linear and Star Oligomers Using the trans-Pt $(PR_3)_2$ $(C{\equiv}C)_2$ Linker. *J. Inorg. Organomet. Polym. Mater.* **2017**, *27*, 3-38.

(11) Zhou, Z. F.; Menna, M.; Cai, Y. S.; Guo, Y. W. Polyacetylenes of Marine Origin: Chemistry and Bioactivity. *Chem. Rev.* **2015**, *115*, 1543-1596.

(12) Negri, R. Polyacetylenes from Terrestrial Plants and Fungi: Recent Phytochemical and Biological Advances. *Fitoterapia* **2015**, *106*, 92-109.

(13) Gu, X.; Kim, Y. S.; Kaiser, R. I.; Mebel, A. M.; Liang, M. C.; Yung, Y. L. Chemical Dynamics of Triacetylene Formation and Implications to The Synthesis of Polyynes in Titan's Atmosphere. *Proc. Natl. Acad. Sci. U. S. A.* **2009**, *106*, 16078-16083.

(14) Casari, C.; Tommasini, M.; Tykwinski, R.; Milani, A. Carbon-atom Wires: 1-D Systems with Tunable Properties. *Nanoscale* **2016**, *8*, 4414-4435.

(15) Marsden, J. A.; Haley, M. M. Carbon Networks Based on Dehydrobenzoannulenes. 5. Extension of Two-Dimensional Conjugation in Graphdiyne Nanoarchitectures. *J. Org. Chem.* **2005**, *70*, 10213-10226.

(16) Hirsch, A. The Era of Carbon Allotropes. *Nat. Mater.* **2010**, *9*, 868.

(17) Varkey, E. C.; Hutter, J. r.; Limacher, P. A.; Lüthi, H. P. Impact of Donor–Acceptor Functionalization on the Properties of Linearly π-Conjugated Oligomers: Establishing Quantitative Relationships for the Substituent and Substituent Cooperative Effect Based on Quantum Chemical Calculations. *J. Org. Chem.* **2013**, *78*, 12681-12689.

(18) Lapprand, A.; Khiri, N.; Fortin, D.; Juge, S.; Harvey, P. D. Organometallic Oligomers Based on Bis(arylacetylide)bis(P-chirogenic phosphine)Platinum (II) Complexes: Synthesis and Photonic Properties. *Inorg. Chem.* **2013**, *52*, 2361-2371.

(19) Zhao, G. J.; Yu, F.; Zhang, M. X.; Northrop, B. H.; Yang, H.; Han, K. L.; Stang, P. J. Substituent Effects on the Intramolecular Charge Transfer and Fluorescence of Bimetallic Platinum Complexes. *J. Phys. Chem. A* **2011**, *115*, 6390-6393.

(20) Köhler, A.; Wilson, J. S.; Friend, R. H. Fluorescence and Phosphorescence in Organic Materials. *Adv. Mater.* **2002**, *14*, 701-707.

(21) Tour, J. M. Molecular Electronics. Synthesis and Testing of Components. *Acc. Chem. Res.* **2000**, *33*, 791-804.

(22) Xu, L.; Yang, H. B. Our Expedition in Linear Neutral Platinum- Acetylide Complexes: The Preparation of Micro/nanostructure Materials, Complicated Topologies, and Dye- Sensitized Solar Cells. *Chem. Rec.* **2016**, *16*, 1274-1297.

(23) Nguyen, P.; Gomez-Elipe, P.; Manners, I. Organometallic Polymers with Transition Metals in the Main Chain. *Chem. Rev.* **1999**, *99*, 1515-1548.
(24) Wong, W.-Y.; Ho, C.-L. Organometallic Photovoltaics: A New and Versatile Approach for Harvesting Solar Energy Using Conjugated Polymetallaynes. *Acc. Chem. Res.* **2010**, *43*, 1246-1256.
(25) Long, N. J.; Williams, C. K. Metal Alkynyl σ-Complexes: Synthesis and Materials. *Angew. Chem. Int. Ed. Engl.* **2003**, *42*, 2586-2617.
(26) Liu, J.; Lam, J. W.; Tang, B. Z. Acetylenic Polymers: Syntheses, Structures, and Functions. *Chem. Rev.* **2009**, *109*, 5799-5867.
(27) Cheng, Y. J.; Yang, S. H.; Hsu, C. S. Synthesis of Conjugated Polymers for Organic Solar Cell Applications. *Chem. Rev.* **2009**, *109*, 5868-5923.
(28) Glaser, C. Beiträge zur Kenntniss des Acetenylbenzols. *Berichte der deutschen chemischen Gesellschaft* **1869**, *2*, 422-424.
(29) Shi, W.; Lei, A. 1, 3-Diyne Chemistry: Synthesis and Derivations. *Tetrahedron Lett.* **2014**, *55*, 2763-2772.
(30) Sindhu, K.; Anilkumar, G. Recent Advances and Applications of Glaser Coupling Employing Greener Protocols. *RSC Adv*. **2014**, *4*, 27867-27887.
(31) Sindhu, K. S.; Thankachan, A. P.; Sajitha, P.; Anilkumar, G. Recent Developments and Applications of the Cadiot–Chodkiewicz Reaction. *Org. Biomol. Chem.* **2015**, *13*, 6891-6905.
(32) Liu, C.; Yuan, J.; Gao, M.; Tang, S.; Li, W.; Shi, R.; Lei, A. Oxidative Coupling Between Two Hydrocarbons: An Update of Recent C–H Functionalizations. *Chem. Rev.* **2015**, *115*, 12138-12204.
(33) Hay, A. Communications- Oxidative Coupling of Acetylenes. *J. Org. Chem* **1960**, *25*, 1275-1276.
(34) Hay, A. S. Oxidative Coupling of Acetylenes. II[1]. *J. Org. Chem* **1962**, *27*, 3320-3321.
(35) Eglinton, G.; Galbraith, A. R. 182. Macrocyclic Acetylenic Compounds. Part I. Cyclotetradeca-1 :3-diyne and Related Compounds. *J. Chem. Soc.* **1959**, 889-896.
(36) Sonogashira, K.; Tohda, Y.; Hagihara, N. A Convenient Synthesis of Acetylenes: Catalytic Substitutions of Acetylenic Hydrogen with Bromoalkenes, Iodoarenes and Bromopyridines. *Tetrahedron Lett.* **1975**, *16*, 4467-4470.
(37) Cummins, C. H. Synthesis of Symmetrical Diarylalkynes by Double Stille Coupling of Bis (tributylstannyl) Acetylene. *Tetrahedron Lett.* **1994**, *35*, 857-860.
(38) Negishi, E. Palladium- or Nickel-Catalyzed Cross Coupling. A New Selective Method for Carbon-Carbon Bond Formation. *Acc. Chem. Res.* **2002**, *15*, 340-348.
(39) Yang, L. M.; Huang, L. F.; Luh, T. Y. Kumada-Corriu Reactions of Alkyl Halides With Alkynyl Nucleophiles. *Org. Lett.* **2004**, *6*, 1461-1463.
(40) Knappke, C. E.; von Wangelin, A. J. 35 Years of Palladium-Catalyzed Cross-Coupling With Grignard Reagents: How Far Have We Come? *Chem. Soc. Rev.* **2011**, *40*, 4948-4962.
(41) Jahnke, E.; Tykwinski, R. R. The Fritsch–Buttenberg–Wiechell Rearrangement: Modern Applications For an Old Reaction. *Chem. Commun.* **2010**, *46*, 3235-3249.
(42) Crowley, J. D.; Goldup, S. M.; Gowans, N. D.; Leigh, D. A.; Ronaldson, V. E.; Slawin, A. M. An Unusual Nickel-Copper-Mediated Alkyne Homocoupling Reaction For The Active-Template Synthesis of [2]Rotaxanes. *J. Am. Chem. Soc.* **2010**, *132*, 6243-6248.
(43) Gulia, N.; Osowska, K.; Pigulski, B.; Lis, T.; Galewski, Z.; Szafert, S. Mori-Hiyama Versus Hay Coupling for Higher Polyynes. *Eur. J. Org. Chem.* **2012**, *2012*, 4819-4830.
(44) Lampkowski, J. S.; Maza, J. C.; Verma, S.; Young, D. D. Optimization of Solid-Supported Glaser-Hay Reactions in the Microwave. *Molecules* **2015**, *20*, 5276-5285.
(45) Kuhn, P.; Alix, A.; Kumarraja, M.; Louis, B.; Pale, P.; Sommer, J. Copper-Zeolites as Catalysts for the Coupling of Terminal Alkynes: An Efficient Synthesis of Diynes. *Eur. J. Org. Chem.* **2009**, *2009*, 423-429.
(46) Lampkowski, J. S.; Durham, C. E.; Padilla, M. S.; Young, D. D. Preparation of Asymmetrical Polyynes by A Solid-Supported Glaser–Hay Reaction. *Org. Biomol. Chem.* **2015**, *13*, 424-427.
(47) Zhao, X.; Huang, C.; Gulcur, M.; Batsanov, A. S.; Baghernejad, M.; Hong, W.; Bryce, M. R.; Wandlowski, T. Oligo(aryleneethynylene)s with Terminal Pyridyl Groups: Synthesis and Length Dependence of the Tunneling-to-Hopping Transition of Single-Molecule Conductances. *Chem. Mater.* **2013**, *25*, 4340-4347.
(48) Tripp, V. T.; Lampkowski, J. S.; Tyler, R.; Young, D. D. Development of Solid-Supported Glaser-Hay Couplings. *ACS Comb. Sci.* **2014**, *16*, 164-167.

(49) Sarmah, M.; Dewan, A.; Thakur, A. J.; Bora, U. Urea as Mild and Efficient Additive for Palladium Catalyzed Sonogashira Cross Coupling Reaction. *Tetrahedron Lett.* **2016**, *57*, 914-916.
(50) Sheng, W.-B.; Chen, T.-Q.; Zhang, M.-Z.; Tian, M.; Jiang, G.-F.; Guo, C.-C. Copper Porphyrin-Catalyzed Aerobic Oxidative Coupling of Terminal Alkynes with High TON. *Tetrahedron Lett.* **2016**, *57*, 1641-1643.
(51) Chinta, B. S.; Baire, B. A Systematic Study on the Cadiot–Chodkiewicz Cross Coupling Reaction for the Selective and Efficient Synthesis of Hetero-Diynes. *RSC Adv*. **2016**, *6*, 54449-54455.
(52) Sagadevan, A.; Charpe, V. P.; Hwang, K. C. Copper (I) Chloride Catalysed Room Temperature C sp–C sp Homocoupling of Terminal Alkynes Mediated by Visible Light. *Catal. Sci. Technol.* **2016**, *6*, 7688-7692.
(53) Li, X.; Li, D.; Bai, Y.; Zhang, C.; Chang, H.; Gao, W.; Wei, W. Homocoupling Reactions of Terminal Alkynes and Arylboronic Compounds Catalyzed by in situ Formed Al $(OH)_3$-Supported Palladium Nanoparticles. *Tetrahedron* **2016**, *72*, 6996-7002.
(54) Liu, W.; Li, L.; Li, C.-J. Empowering a Transition-Metal-Free Coupling Between Alkyne and Alkyl Iodide with Light in Water. *Nat. Commun.* **2015**, *6*, 6526.
(55) Matsuyama, N.; Kitahara, M.; Hirano, K.; Satoh, T.; Miura, M. Nickel-and Copper-Catalyzed Direct Alkynylation of Azoles and Polyfluoroarenes with Terminal Alkynes under O_2 or Atmospheric Conditions. *Org. Lett.* **2010**, *12*, 2358-2361.
(56) Negishi, E.; Anastasia, L. Palladium-Catalyzed Alkynylation. *Chem. Rev.* **2003**, *103*, 1979-2017.
(57) Kamikawa, T.; Hayashi, T. Dichloro [(2-dimethylamino)propyldiphenylphosphine] Palladium (II)($PdCl_2$ (alaphos)): An Efficient Catalyst for Cross-Coupling of Aryl Triflates with Alkynyl Grignard Reagents1. *J. Org. Chem.* **1998**, *63*, 8922-8925.
(58) Ahammed, S.; Kundu, D.; Ranu, B. C. Cu-Catalyzed Fe-Driven C_{sp}–C_{sp} and C_{sp}–C_{sp2} Cross-Coupling: An Access to 1, 3-Diynes and 1, 3-Enynes. *J. Org. Chem.* **2014**, *79*, 7391-7398.
(59) Mišicák, R.; Stříteský, S.; Vala, M.; Weiter, M.; Cigáň, M.; Gmucová, K.; Végsö, K.; Weis, M.; Kožíšek, J.; Pavúk, M. Effect of The Ethynylene Linker on The Properties and Carrier Mobility of Naphthalene Derivatives with Hexylbithienyl Arms. *Synth. Met.* **2016**, *217*, 156-171.
(60) Gong, Y.; Liu, J. Sequential Sonogashira and Glaser Coupling Reactions: Facile Access to 1, 4-Disubstituted 1, 3-Butadiynes from Arylbromide. *Tetrahedron Lett.* **2016**, *57*, 2143-2146.
(61) Peng, H.; Xi, Y.; Ronaghi, N.; Dong, B.; Akhmedov, N. G.; Shi, X. Gold-Catalyzed Oxidative Cross-Coupling of Terminal Alkynes: Selective Synthesis of Unsymmetrical 1,3-Diynes. *J. Am. Chem. Soc.* **2014**, *136*, 13174-13177.
(62) Qian, L. W.; Sun, M.; Dong, J.; Xu, Q.; Zhou, Y.; Yin, S. F. Palladium-Catalyzed Desulfitative Cross-Coupling of Arylsulfonyl Hydrazides with Terminal Alkynes: A General Approach toward Functionalized Internal Alkynes. *J. Org. Chem.* **2017**, *82*, 6764-6769.
(63) García Ruano, J. L.; Alemán, J.; Marzo, L.; Alvarado, C.; Tortosa, M.; Díaz- Tendero, S.; Fraile, A. Expanding the Scope of Arylsulfonylacetylenes as Alkynylating Reagents and Mechanistic Insights in the Formation of C_{sp2}-C_{sp} and C_{sp3}-C_{sp} Bonds from Organolithiums. *Chem. Eur. J.* **2012**, *18*, 8414-8422.
(64) Esteban, F.; Boughani, L.; Garcia Ruano, J. L.; Fraile, A.; Aleman, J. Anti-Michael Addition" of Grignard Reagents to Sulfonylacetylenes: Synthesis of Alkynes. *Org. Biomol. Chem.* **2017**, *15*, 3901-3908.
(65) Marzo, L.; Pérez, I.; Yuste, F.; Alemán, J.; Ruano, J. L. G. A Straightforward Alkynylation of Li and Mg Metalated Heterocycles with Sulfonylacetylenes. *Chem. Commun.* **2015**, *51*, 346-349.
(66) Ye, F.; Orita, A.; Doumoto, A.; Otera, J. Double Elimination Protocol for Access to Unsymmetrically Substituted Aromatic Polyynes Starting from Sulfones and Aldehydes. *Tetrahedron* **2003**, *59*, 5635-5643.
(67) Chinchilla, R.; Nájera, C. The Sonogashira Reaction: A Booming Methodology in Synthetic Organic Chemistry. *Chem. Rev.* **2007**, *107*, 874-922.
(68) Sagadevan, A.; Hwang, K. C. Photo- Induced Sonogashira C-C Coupling Reaction Catalyzed by Simple Copper (I) Chloride Salt at Room Temperature. *Adv. Synth. Catal.* **2012**, *354*, 3421-3427.
(69) Lei, J.; Su, L.; Zeng, K.; Chen, T.; Qiu, R.; Zhou, Y.; Au, C.-T.; Yin, S.-F. Recent Advances of Catalytic Processes on the Transformation of Alkynes into Functional Compounds. *Chem. Eng. Sci.* **2017**, *171*, 404-425.

(70) Shi, W.; Liu, C.; Lei, A. Transition-Metal Catalyzed Oxidative Cross-Coupling Reactions to form C–C Bonds Involving Organometallic Reagents as Nucleophiles. *Chem. Soc. Rev.* **2011**, *40*, 2761-2776.
(71) Su, L.; Dong, J.; Liu, L.; Sun, M.; Qiu, R.; Zhou, Y.; Yin, S. F. Copper Catalysis for Selective Heterocoupling of Terminal Alkynes. *J. Am. Chem. Soc.* **2016**, *138*, 12348-12351.
(72) Yin, W.; He, C.; Chen, M.; Zhang, H.; Lei, A. Nickel-Catalyzed Oxidative Coupling Reactions of Two Different Terminal Alkynes Using O_2 as the Oxidant at Room Temperature: Facile Syntheses of Unsymmetric 1, 3-Diynes. *Org. Lett.* **2008**, *11*, 709-712.
(73) Vilhanová, B.; Václavík, J. i.; Artiglia, L.; Ranocchiari, M.; Togni, A.; van Bokhoven, J. A. Subnanometer Gold Clusters on Amino-Functionalized Silica: An Efficient Catalyst for the Synthesis of 1, 3-Diynes by Oxidative Alkyne Coupling. *ACS Catal.* **2017**, *7*, 3414-3418.
(74) Banerjee, S.; Patil, N. T. Exploiting the Dual Role of Ethynylbenziodoxolones in Gold-Catalyzed C(sp)-C(sp) Cross-Coupling Reactions. *Chem. Commun. (Camb)* **2017**, *53*, 7937-7940.
(75) Mohanty, A.; Roy, S. Glaser–Hay Hetero-Coupling in a Bimetallic Regime: a Ni (ii)/Ag (i) Assisted Base, Ligand and Additive Free Route to Selective Unsymmetrical 1, 3-Diynes. *Chem. Commun.* **2017**, *53*, 10796-10799.
(76) Li, X.; Xie, X.; Sun, N.; Liu, Y. Gold- Catalyzed Cadiot–Chodkiewicz- Type Cross- Coupling of Terminal Alkynes with Alkynyl Hypervalent Iodine Reagents: Highly Selective Synthesis of Unsymmetrical 1, 3- Diynes. *Angew. Chem.* **2017**, *129*, 7098-7102.
(77) Krishnan, K. K.; Ujwaldev, S.; Thankachan, A. P.; Harry, N. A.; Gopinathan, A. A Novel Zinc-catalyzed Cadiot-Chodkiewicz cross-coupling Reaction of Terminal Alkynes with 1-Bromoalkynes in Ethanol Solvent. *Mol. Catal.* **2017**, *440*, 140-147.
(78) Hattori, T.; Kijima, M.; Shirakawa, H. Oxidative Polycondensation of Acetylene by Iodine in the Presence of a Palladium-Copper Catalyst. *Synth. Met.* **1997**, *84*, 357-358.
(79) Cataldo, F.; Ursini, O.; Angelini, G.; Tommasini, M.; Casari, C. Simple Synthesis of α, ω-Diarylpolyynes Part 1: Diphenylpolyynes. *J. Macromol. Sci. Part A Pure Appl. Chem* **2010**, *47*, 739-746.
(80) Cataldo, F.; Ravagnan, L.; Cinquanta, E.; Castelli, I. E.; Manini, N.; Onida, G.; Milani, P. Synthesis, Characterization, and Modeling of Naphthyl-Terminated sp Carbon Chains: Dinaphthylpolyynes. *J. Phys. Chem. B* **2010**, *114*, 14834-14841.
(81) Cataldo, F.; Ursini, O.; Milani, A.; Casari, C. S. One-Pot Synthesis and Characterization of Polyynes End-Capped by Biphenyl Groups (α, ω-Biphenylpolyynes). *Carbon* **2017**, *126*, 232-240.
(82) Tripp, V. T.; Lampkowski, J. S.; Tyler, R.; Young, D. D. Development of Solid-Supported Glaser–Hay Couplings. *ACS Comb. Sci.* **2014**, *16*, 164-167.
(83) DeCicco, R. C.; Black, A.; Li, L.; Goroff, N. S. An Iterative Method for the Synthesis of Symmetric Polyynes. *Eur. J. Org. Chem.* **2012**, *2012*, 4699-4704.
(84) Alonso, F.; Beletskaya, I. P.; Yus, M. Transition-Metal-Catalyzed Addition of Heteroatom−Hydrogen Bonds to Alkynes. *Chem. Rev.* **2004**, *104*, 3079-3160.
(85) Toutov, A. A.; Betz, K. N.; Schuman, D. P.; Liu, W. B.; Fedorov, A.; Stoltz, B. M.; Grubbs, R. H. Alkali Metal-Hydroxide-Catalyzed C(sp)-H Bond Silylation. *J. Am. Chem. Soc.* **2017**, *139*, 1668-1674.
(86) Eisler, S.; Tykwinski, R. R. Migrating Alkynes in Vinylidene Carbenoids: An Unprecedented Route to Polyynes. *J. Am. Chem. Soc.* **2000**, *122*, 10736-10737.
(87) Luu, T.; Morisaki, Y.; Cunningham, N.; Tykwinski, R. R. One-Pot Formation and Derivatization of Di- and Triynes Based on the Fritsch-Buttenberg-Wiechell Rearrangement. *J. Org. Chem.* **2007**, *72*, 9622-9629.
(88) Luu, T.; Elliott, E.; Slepkov, A. D.; Eisler, S.; McDonald, R.; Hegmann, F. A.; Tykwinski, R. R. Synthesis, Structure, and Nonlinear Optical Properties of Diarylpolyynes. *Org. Lett.* **2005**, *7*, 51-54.
(89) Morisaki, Y.; Luu, T.; Tykwinski, R. R. A One-Pot Synthesis and Functionalization of Polyynes. *Org. Lett.* **2006**, *8*, 689-692.
(90) Lewis, J.; Lin, B.; Khan, M. S.; Al-Mandhary, M. R.; Raithby, P. R. Synthesis and Structural Characterization of Cobalt Complexes Derived from Conjugated Tetraynes. *J. Organomet. Chem.* **1994**, *484*, 161-167.
(91) Shvo, Y.; Hazum, E. A Simple Method for the Disengagement of Organic Ligands from Iron Complexes. *J. Chem. Soc., Chem. Commun.* **1974**, 336-337.

(92) Cetini, G.; Gambino, O.; Rossetti, R.; Sappa, E. Acetylenic Derivatives of Metal Carbonyls I. Substitution Reactions of CO_2 $(CO)_6C_2RR'$ Complexes. *J. Organomet. Chem.* **1967**, *8*, 149-154.
(93) Allison, N. T.; Fritch, J. R.; Vollhardt, K. P. C.; Walborsky, E. C. An Unprecedented Bis (carbyne) Cluster Rearrangement Involving Simultaneous Coupling and Decoupling of Carbyne Fragments: A New Homogeneous Model for Carbon-Carbon Bond Forming and Bond Breaking on Surfaces. *J. Am. Chem. Soc.* **1983**, *105*, 1384-1386.
(94) Kohn, D. R.; Gawel, P.; Xiong, Y.; Christensen, K. E.; Anderson, H. L. Synthesis of Polyynes Using Dicobalt Masking Groups. *J. Org. Chem.* **2018**, *83*, 2077-2086.
(95) Chalifoux, W. A.; Tykwinski, R. R. Synthesis of Polyynes to Model the sp-Carbon Allotrope Carbyne. *Nat Chem* **2010**, *2*, 967-971.
(96) Prenzel, D.; Kirschbaum, R. W.; Chalifoux, W. A.; McDonald, R.; Ferguson, M. J.; Drewello, T.; Tykwinski, R. R. Polymerization of Acetylene: Polyynes, but not Carbyne. *Org. Chem. Front.* **2017**, *4*, 668-674.
(97) Wu, W.; Jiang, H. Haloalkynes: A Powerful and Versatile Building Block in Organic Synthesis. *Acc. Chem. Res.* **2014**, *47*, 2483-2504.
(98) Srujana, K.; Swamy, P.; Naresh, M.; Durgaiah, C.; Rammurthy, B.; Sai, G. K.; Sony, T.; Narender, N. A Quaternary Ammonium Salt Promoted Regioselective Iodination of Terminal Alkynes: A Convenient Access to 1- Iodoalkynes in Aqueous Media. *ChemistrySelect* **2017**, *2*, 748-752.
(99) Pigulski, B.; Gulia, N.; Szafert, S. Synthesis of Long, Palladium End- Capped Polyynes through the Use of Asymmetric 1- Iodopolyynes. *Chem. Eur. J.* **2015**, *21*, 17769-17778.
(100) Pigulski, B.; Arendt, A.; Tomilin, D. N.; Sobenina, L. N.; Trofimov, B. A.; Szafert, S. Transition-Metal Free Mechanochemical Approach to Polyyne Substituted Pyrroles. *J. Org. Chem.* **2016**, *81*, 9188-9198.
(101) Tomilin, D. N.; Pigulski, B.; Gulia, N.; Arendt, A.; Sobenina, L. N.; Al'bina, I. M.; Szafert, S.; Trofimov, B. A. Direct Synthesis of Butadiynyl-Substituted Pyrroles under Solvent-and Transition Metal-Free Conditions. *RSC Adv.* **2015**, *5*, 73241-73248.
(102) Pigulski, B.; Męcik, P.; Cichos, J.; Szafert, S. Use of Stable Amine-Capped Polyynes in the Regioselective Synthesis of Push–Pull Thiophenes. *J. Org. Chem.* **2017**, *82*, 1487-1498.
(103) Gilbert, M.; Albinsson, B. Photoinduced Charge and Energy Transfer in Molecular Wires. *Chem. Soc. Rev.* **2015**, *44*, 845-862.
(104) Schubert, C.; Margraf, J. T.; Clark, T.; Guldi, D. M. Molecular Wires-Impact of π-Conjugation and Implementation of Molecular Bottlenecks. *Chem. Soc. Rev.* **2015**, *44*, 988-998.
(105) Schumm, J. S.; Pearson, D. L.; Tour, J. M. Iterative Divergent/Convergent Approach to Linear Conjugated Oligomers by Successive Doubling of the Molecular Length: A Rapid Route to a 128Å-Long Potential Molecular Wire. *Angew. Chem. Int. Ed.* **1994**, *33*, 1360-1363.
(106) Pearson, D. L.; Schumm, J. S.; Tour, J. M. Iterative Divergent/Convergent Approach to Conjugated Oligomers by a Doubling of Molecular Length at Each Iteration. A Rapid Route to Potential Molecular Wires. *Macromolecules* **1994**, *27*, 2348-2350.
(107) Pearson, D. L.; Tour, J. M. Rapid Syntheses of Oligo(2,5-thiophene ethynylene)s with Thioester Termini: Potential Molecular Scale Wires with Alligator Clips. *J. Org. Chem.* **1997**, *62*, 1376-1387.
(108) Tour, J. M. Conjugated Macromolecules of Precise Length and Constitution. Organic Synthesis for the Construction of Nanoarchitectures. *Chem. Rev.* **1996**, *96*, 537-554.
(109) Li, G.; Wang, X.; Li, J.; Zhao, X.; Wang, F. Rapid Solution and Solid Phase Synthesis of Monodisperse Oligo[(1,4-phenyleneethynylene)-alt-(2,5-thiopheneethynylene)]s. *Tetrahedron* **2006**, *62*, 2576-2582.
(110) Binauld, S.; Damiron, D.; Connal, L. A.; Hawker, C. J.; Drockenmuller, E. Precise Synthesis of Molecularly Defined Oligomers and Polymers by Orthogonal Iterative Divergent/convergent Approaches. *Macromol. Rapid Commun.* **2011**, *32*, 147-168.
(111) Xue, C.; Luo, F.-T. Rapid Syntheses of Oligo(p-phenyleneethynylene)s via Iterative Convergent Approach. *Tetrahedron* **2004**, *60*, 6285-6294.
(112) Huang, S.; Tour, J. M. Rapid Solid-Phase Synthesis of Oligo(1,4-phenylene ethynylene)s by a Divergent/Convergent Tripling Strategy. *J. Am. Chem. Soc.* **1999**, *121*, 4908-4909.
(113) Huang, S.; Tour, J. M. Rapid Bi-Directional Synthesis of Oligo(1,4-phenyleneethynylene)s. *Tetrahedron Lett.* **1999**, *40*, 3447-3450.

(114) Arias, E.; Moggio, I.; Torres, R.; Ziolo, R. F.; Maldonado, J. L.; Green, K.; Cooper, T. M.; Wicks, G.; Rebane, A.; Drobizhev, M. Direct Synthesis of 2, 5- Bis(dodecanoxy)phenyleneethynylene-Butadiynes by Sonogashira Coupling Reaction. *Eur. J. Org. Chem.* **2013**, *2013*, 5341-5352.
(115) Castruita, G.; Arias, E.; Moggio, I.; Pérez, F.; Medellín, D.; Torres, R.; Ziolo, R.; Olivas, A.; Giorgetti, E.; Muniz-Miranda, M. Synthesis, Optical Properties and Supramolecular Order of π-Conjugated 2,5-di(alcoxy)Phenyleneethynylene Oligomers. *J. Mol. Struct.* **2009**, *936*, 177-186.
(116) Jones, L.; Schumm, J. S.; Tour, J. M. Rapid Solution and Solid Phase Syntheses of Oligo(1,4-phenylene ethynylene)s with Thioester Termini: Molecular Scale Wires with Alligator Clips. Derivation of Iterative Reaction Efficiencies on a Polymer Support. *J. Org. Chem.* **1997**, *62*, 1388-1410.
(117) Darkwa, J. Palladium Catalyzed Phenylacetylene Polymerization to Low Molecular Weight cis-Transoidal and trans-Cisoidal Poly (phenylacetylene) s: A Perspective. *Polym. Rev.* **2017**, *57*, 52-64.
(118) Shiotsuki, M.; Sanda, F.; Masuda, T. Polymerization of Substituted Acetylenes and Features of the Formed Polymers. *Polym. Chem.* **2011**, *2*, 1044-1058.
(119) Choi, S. K.; Gal, Y. S.; Jin, S. H.; Kim, H. K. Poly(1,6-heptadiyne)-Based Materials by Metathesis Polymerization. *Chem. Rev.* **2000**, *100*, 1645-1682.
(120) Guo, M.; Chen, B.; Lv, M.; Zhou, X.; Wen, Y.; Shen, X. The Homocoupling Reaction of Aromatic Terminal Alkynes by a Highly Active Palladium(II)/$AgNO_3$ Cocatalyst in Aqueous Media Under Aerobic Conditions. *Molecules* **2016**, *21*, 606-613.
(121) Asiri, A. M.; Hashmi, A. S. Gold-Catalysed Reactions of Diynes. *Chem. Soc. Rev.* **2016**, *45*, 4471-4503.
(122) Sagadevan, A.; Lyu, P.-C.; Hwang, K. C. Visible-Light-Activated Copper (I) Catalyzed Oxidative C sp–Csp Cross-Coupling Reaction: Efficient Synthesis of Unsymmetrical Conjugated Diynes without Ligands and Base. *Green Chem.* **2016**, *18*, 4526-4530.
(123) Xu, Y. L.; Pan, Y. M.; Liu, P.; Wang, H. S.; Tian, X. Y.; Su, G. F. Indium(III) Chloride Catalyzed Conjugate Addition Reaction of Alkynylsilanes to Acrylate Esters. *J. Org. Chem.* **2012**, *77*, 3557-3562.
(124) Dhakshinamoorthy, A.; Asiri, A. M.; Garcia, H. Metal–Organic Frameworks Catalyzed C–C and C–Heteroatom Coupling Reactions. *Chem. Soc. Rev.* **2015**, *44*, 1922-1947.
(125) Pigulski, B.; Cichos, J.; Szafert, S. Polyynes as Precursors of Photoluminescent Solvent Polarity Probes. *ACS Sustainable Chem. Eng.* **2017**, *5*, 7077-7085.
(126) Tanaka, T.; Osuka, A. Conjugated Porphyrin Arrays: Synthesis, Properties and Applications for Functional Materials. *Chem. Soc. Rev.* **2015**, *44*, 943-969.
(127) Zhang, Y. Q.; Kepcija, N.; Kleinschrodt, M.; Diller, K.; Fischer, S.; Papageorgiou, A. C.; Allegretti, F.; Bjork, J.; Klyatskaya, S.; Klappenberger, F.; et al. Homo-Coupling of Terminal Alkynes on a Noble Metal Surface. *Nat. Commun.* **2012**, *3*, 1286-1293.
(128) Cirera, B.; Zhang, Y. Q.; Bjork, J.; Klyatskaya, S.; Chen, Z.; Ruben, M.; Barth, J. V.; Klappenberger, F. Synthesis of Extended Graphdiyne Wires by Vicinal Surface Templating. *Nano Lett.* **2014**, *14*, 1891-1897.
(129) Colazzo, L.; Sedona, F.; Moretto, A.; Casarin, M.; Sambi, M. Metal-Free on-Surface Photochemical Homocoupling of Terminal Alkynes. *J. Am. Chem. Soc.* **2016**, *138*, 10151-10156.
(130) Taguchi, Y.; Endo, H.; Kodama, T.; Achiba, Y.; Shiromaru, H.; Wakabayashi, T.; Wales, B.; Sanderson, J. Polyyne Formation by ns and fs Laser Induced Breakdown in Hydrocarbon Gas Flow. *Carbon* **2017**, *115*, 169-174.
(131) Tsuji, M.; Kuboyama, S.; Matsuzaki, T.; Tsuji, T. Formation of Hydrogen-capped Polyynes by Laser Ablation of C 60 Particles Suspended in Solution. *Carbon* **2003**, *41*, 2141-2148.
(132) Zhao, C.; Kitaura, R.; Hara, H.; Irle, S.; Shinohara, H. Growth of Linear Carbon Chains Inside Thin Double-Wall Carbon Nanotubes. *J. Phys. Chem. C* **2011**, *115*, 13166-13170.
(133) Williams, K. A.; Boydston, A. J.; Bielawski, C. W. Main-Chain Organometallic Polymers: Synthetic Strategies, Applications, and Perspectives. *Chem. Soc. Rev.* **2007**, *36*, 729-744.
(134) Sonogashira, K.; Fujikura, Y.; Yatake, T.; Toyoshima, N.; Takahashi, S.; Hagihara, N. Syntheses and Properties of cis- and trans-Dialkynyl Complexes of Platinum(II). *J. Organomet. Chem.* **1978**, *145*, 101-108.
(135) Takahashi, S.; Morimoto, H.; Murata, E.; Kataoka, S.; Sonogashira, K.; Hagihara, N. Studies on Polyyne Polymers Containing Transition Metals in the Main Chain. VII. Synthesis and

Characterization of Palladium-Polyyne Polymers. *J. Polym. Sci. Part A Polym. Chem.* **1982**, *20*, 565-573.
(136) Sonogashira, K.; Ohga, K.; Takahashi, S.; Hagihara, N. Studies of Poly-yne Polymers Containing Transition Metals in the Main Chain. *J. Organomet. Chem.* **1980**, *188*, 237-243.
(137) Ananikov, V. P.; Musaev, D. G.; Morokuma, K. Theoretical Insight into the C− C Coupling Reactions of the Vinyl, Phenyl, Ethynyl, and Methyl Complexes of Palladium and Platinum. *Organometallics* **2005**, *24*, 715-723.
(138) Kim, P.; Masai, H.; Sonogashira, K.; Hagihara, N. Preparations of α, ω-Bis-Nickel-Polyacetylenes. *Inorg. Nucl. Chem. Lett.* **1970**, *6*, 181-185.
(139) Cardin, C. J.; Cardin, D. J.; Lappert, M. F. Unsaturated σ-Hydrocarbyl Transition-Metal Complexes. Part 2. Synthesis and Reactions of Vinylplatinum Complexes and a Comparison with Analogous Fluorovinyl and Alkynyl Complexes. *J. Chem. Soc., Dalton Trans.* **1977**, 767-779.
(140) Cetinkaya, B.; Lappert, M.; McMeeking, J.; Palmer, D. Reactions of Trialkyltin Acetylides with some Low Oxidation State Transition Metal Complexes: Oxidative Addition, Oxidative Cleavage, and Alkynylation. *J. Organomet. Chem.* **1972**, *34*, C37-C40.
(141) Davies, S. J.; Johnson, B. F. G.; Khan, M. S.; Lewis, J. Synthesis of Monomeric and Oligomeric Bis(Acetylide) Complexes of Platinum and Rhodium. *J. Chem. Soc., Chem. Commun.* **1991**, doi: 10.1039/c39910000187.
(142) Brown, A. W.; Verschoyle, R. D.; Street, B. W.; Aldridge, W. N.; Grindley, H. The Neurotoxicity of Trimethyltin Chloride in Hamsters, Gerbils and Marmosets. *J. Appl. Toxicol.* **1984**, *4*, 12-21.
(143) Koch, M.; Garg, J. A.; Blacque, O.; Venkatesan, K. trans Bis-N-Heterocyclic Carbene Bis-Acetylide Palladium (II) Complexes. *J. Organomet. Chem.* **2012**, *700*, 154-159.
(144) Fyfe, H. B.; Mlekuz, M.; Zargarian, D.; Taylor, N. J.; Marder, T. B. Synthesis of Mononuclear, Dinuctear and Oligomeric Rigid-Rod Acetylide Complexes of Rhodium, and the Molecular Structure of $[Rh(PMe_3)_4(C{\equiv}C–p\text{-}C_6H_4–C{\equiv}C)Rh(PMe_3)_4]$ *J. Chem. Soc., Chem. Commun.* **1991**, doi :10.1039/c39910000188, 188-190.
(145) Haquette, P.; Pirio, N.; Touchard, D.; Toupet, L.; Dixneuf, P. H. Activation of Terminal Alkynes with *cis*-$[RuCl_2(Ph_2PCH_2PPH_2)_2]$: New Vinylidene–and Acetylide–Ruthenium Complexes and Crystal Structures of $[(Ph_2PCH_2PPH_2)_2(Cl)Ru{=}C{=}CH_2]PF_6$ and $[(Ph_2PCH_2PPH_2)_2(Cl)RuC{\equiv}CH]$ *J. Chem. Soc., Chem. Commun.* **1993**, doi :10.1039/c39930000163, 163-165.
(146) Field, L. D.; George, A. V. The Use of High Reaction Pressures in the Synthesis of Acetylide Complexes of Iron. *J. Organomet. Chem.* **1993**, *454*, 217-219.
(147) Hackenberg, J. D.; Kundu, S.; Emge, T. J.; Krogh-Jespersen, K.; Goldman, A. S. Acid-Catalyzed Oxidative Addition of a C–H Bond to a Square Planar d^8 Iridium Complex. *J. Am. Chem. Soc.* **2014**, *136*, 8891-8894.
(148) Kumar, A.; Feller, M.; Ben-David, Y.; Diskin-Posner, Y.; Milstein, D. Formal Oxidative Addition of a CH Bond by a 16e Iridium (I) Complex involves Metal-Ligand Cooperation. *Chem. Commun.* **2018**, *54*, 5365-5368
(149) Mazzacano, T. J.; Leon, N. J.; Waldhart, G. W.; Mankad, N. P. Fundamental Organometallic Chemistry under Bimetallic Influence: Driving β-Hydride Elimination and Diverting Migratory Insertion at Cu and Ni. *Dalton Trans.* **2017**, *46*, 5518-5521.
(150) Wilson, G. L.; Abraha, M.; Krause, J. A.; Guan, H. Reactions of Phenylacetylene with Nickel POCOP-Pincer Hydride Complexes Resulting in Different Outcomes from their Palladium Analogues. *Dalton Trans.* **2015**, *44*, 12128-12136.
(151) Younus, M.; Long, N. J.; Raithby, P. R.; Lewis, J.; Page, N. A.; White, A. J. P.; Williams, D. J.; Colbert, M. C. B.; Hodge, A. J.; Khan, M. S.; et al. Synthesis and Characterisation of Mono-Acetylide and Unsymmetrical Bis-Acetylide Complexes of Ruthenium and Osmium: X-ray Structure Determinations on $[(dppe)_2Ru(Cl)(C{\equiv}C–C_6H_4\text{-}p\text{-}NO_2)]$, $[(dppe)_2Ru(Cl)(C{\equiv}C–C_6H_3\text{-}o\text{-}CH_3\text{-}p\text{-}NO_2)]$ and $[(dppm)_2Os(C{\equiv}C–C_6H_4\text{-}p\text{-}CH_3)(C{\equiv}C–C_6H_4\text{-}p\text{-}NO_2)]$. *J. Organomet. Chem.* **1999**, *578*, 198-209.
(152) Eaves, S. G.; Yufit, D. S.; Skelton, B. W.; Lynam, J. M.; Low, P. J. Reactions of Alkynes with cis-$RuCl_2(dppm)_2$: Exploring the Interplay of Vinylidene, Alkynyl and η_3-Butenynyl Complexes. *Dalton Trans.* **2015**, *44*, 21016-21024.
(153) Natoli, S. N.; Zeller, M.; Ren, T. An Aerobic Synthetic Approach toward Bis-Alkynyl Cobalt(III) Compounds. *Inorg. Chem.* **2017**, *56*, 10021-10031.

(154) Cook, T. D.; Natoli, S. N.; Fanwick, P. E.; Ren, T. Co^{III}(cyclam) Oligoynyls: Monomeric Oligoynyl Complexes and Dimeric Complexes with an Oligoyn-diyl Bridge. *Organometallics* **2016**, *35*, 1329-1338.
(155) Cook, T. D.; Natoli, S. N.; Fanwick, P. E.; Ren, T. Dimeric Complexes of Co^{III}(cyclam) with a Polyynediyl Bridge. *Organometallics* **2015**, *34*, 686-689.
(156) Field, L. D.; Magill, A. M.; Shearer, T. K.; Colbran, S. B.; Lee, S. T.; Dalgarno, S. J.; Bhadbhade, M. M. Controlled Synthesis of Dinuclear Acetylide-Bridged Ruthenium Complexes. *Organometallics* **2010**, *29*, 957-965.
(157) Field, L. D.; George, A. V.; Hambley, T. W.; Malouf, E. Y.; Young, D. J. Formation of Metal Acetylides via Complexes of Molecular Hydrogen. *J. Chem. Soc., Chem. Commun.* **1990**, 931-933.
(158) Oerthel, M.-C.; Yufit, D. S.; Fox, M. A.; Bryce, M. R.; Low, P. J. Syntheses and Structures of Buta-1, 3-Diynyl Complexes from *"on Complex*" Cross-Coupling Reactions. *Organometallics* **2015**, *34*, 2395-2405.
(159) Gulia, N.; Pigulski, B.; Szafert, S. Palladium End-Capped Polyynes via Oxidative Addition of 1-Haloalkynes to $Pd(PPh_3)_4$. *Organometallics* **2015**, *34*, 673-682.
(160) Gulia, N.; Pigulski, B.; Charewicz, M.; Szafert, S. A Versatile and Highly Efficient Method for 1-Chlorination of Terminal and Trialkylsilyl-Protected Alkynes. *Chemistry* **2014**, *20*, 2746-2749.
(161) de Quadras, L.; Bauer, E. B.; Mohr, W.; Bohling, J. C.; Peters, T. B.; Martín-Alvarez, J. M.; Hampel, F.; Gladysz, J. A. sp Carbon Chains Surrounded by sp^3 Carbon Double Helices: Directed Syntheses of Wirelike $Pt(C{\equiv}C)_n$ Pt Moieties That Are Spanned by Two $P(CH_2)_mP$ Linkages via Alkene Metathesis. *J. Am. Chem. Soc.* **2007**, *129*, 8296-8309.
(162) Liu, Y.; Jiang, S.; Glusac, K.; Powell, D. H.; Anderson, D. F.; Schanze, K. S. Photophysics of Monodisperse Platinum-Acetylide Oligomers: Delocalization in the Singlet and Triplet Excited States. *J. Am. Chem. Soc.* **2002**, *124*, 12412-12413.
(163) Zheng, Q.; Gladysz, J. A Synthetic Breakthrough into an Unanticipated Stability Regime: Readily Isolable Complexes in which C16−C28 Polyynediyl Chains Span Two Platinum Atoms. *J. Am. Chem. Soc.* **2005**, *127*, 10508-10509.
(164) Zheng, Q.; Bohling, J. C.; Peters, T. B.; Frisch, A. C.; Hampel, F.; Gladysz, J. A Synthetic Breakthrough into an Unanticipated Stability Regime: A Series of Isolable Complexes in which C_6, C_8, C_{10}, C_{12}, C_{16}, C_{20}, C_{24}, and C_{28} Polyynediyl Chains Span two Platinum Atoms. *Chem. Eur. J.* **2006**, *12*, 6486-6505.
(165) Kraft, A.; Grimsdale, A. C.; Holmes, A. B. Electroluminescent Conjugated Polymers-Seeing Polymers in a New Light. *Angew. Chem. Int. End Engl* **1998**, *37*, 402-428.
(166) Barattucci, A.; Deni, E.; Bonaccorsi, P.; Ceraolo, M. G.; Papalia, T.; Santoro, A.; Sciortino, M. T.; Puntoriero, F. Oligo (phenyleneethynylene) Glucosides: Modulation of Cellular Uptake Capacity Preserving Light ON. *J. Org. Chem.* **2014**, *79*, 5113-5120.
(167) Yamaguchi, Y.; Matsubara, Y.; Ochi, T.; Wakamiya, T.; Yoshida, Z.-i. How the π-Conjugation Length Affects the Fluorescence Emission Efficiency. *J. Am. Chem. Soc.* **2008**, *130*, 13867-13869.
(168) Yamaguchi, Y.; Ochi, T.; Matsubara, Y.; Yoshida, Z. Highly Emissive Whole Rainbow Fluorophores Consisting of 1,4-Bis(2-phenylethynyl)benzene Core Skeleton: Design, Synthesis, and Light-Emitting Characteristics. *J. Phys. Chem. A* **2015**, *119*, 8630-8642.
(169) Humbert-Droz, M.; Piguet, C.; Wesolowski, T. A. Fluorescence Quantum Yield Rationalized by the Magnitude of the Charge Transfer in π -Conjugated Terpyridine Derivatives. *Phys. Chem. Chem. Phys.* **2016**, *18*, 29387-29394.
(170) Khan, M. S.; Al-Mandhary, M. R. A.; Al-Suti, M. K.; Corcoran, T. C.; Al-Mahrooqi, Y.; Attfield, J. P.; Feeder, N.; David, W. I. F.; Shankland, K.; Friend, R. H.; et al. Synthesis and Optical Characterisation of Platinum(II) Poly-yne Polymers Incorporating Substituted 1, 4-Diethynylbenzene Derivatives and an Investigation of the Intermolecular Interactions in the Diethynylbenzene Molecular Precursors. *New J. Chem.* **2003**, *27*, 140-149.
(171) Fasina, T. M.; Collings, J. C.; Burke, J. M.; Batsanov, A. S.; Ward, R. M.; Albesa-Jové, D.; Porrès, L.; Beeby, A.; Howard, J. A.; Scott, A. J. Synthesis, Optical Properties, Crystal Structures and Phase Behaviour of Symmetric, Conjugated Ethynylarene-Based Rigid Rods with Terminal Carboxylate Groups. *J. Mater. Chem.* **2005**, *15*, 690-697.
(172) Nguyen, P.; Todd, S.; Van den Biggelaar, D.; Taylor, N. J.; Marder, T. B.; Wittmann, F.; Friend, R. H. Facile Route to Highly Fluorescent 9, 10-bis (pr-phenylethynyl) Anthracene Chromophores via Palladium-Copper Catalyzed Cross-Coupling. *Synlett* **1994**, 299-301.

(173) Siddle, J. S.; Ward, R. M.; Collings, J. C.; Rutter, S. R.; Porres, L.; Applegarth, L.; Beeby, A.; Batsanov, A. S.; Thompson, A. L.; Howard, J. A. Synthesis, Photophysics and Molecular Structures of Luminescent 2, 5-Bis (phenylethynyl) Thiophenes (BPETs). *New J. Chem.* **2007**, *31*, 841-851.
(174) Pati, A. K.; Gharpure, S. J.; Mishra, A. K. Contrasting Solid-State Fluorescence of Diynes with Small and Large Aryl Substituents: Crystal Packing Dependence and Stimuli-Responsive Fluorescence Switching. *J. Phys. Chem. A* **2015**, *119*, 10481-10493.
(175) Xu, F.; Nishida, T.; Shinohara, K.; Peng, L.; Takezaki, M.; Kamada, T.; Akashi, H.; Nakamura, H.; Sugiyama, K.; Ohta, K.; et al. Trimethylsilyl Group Assisted Stimuli Response: Self-Assembly of 1,3,6,8-Tetrakis((trimethysilyl)ethynyl)pyrene. *Organometallics* **2017**, *36*, 556-563.
(176) Nguyen, P.; Yuan, Z.; Agocs, L.; Lesley, G.; Marder, T. B. Synthesis of Symmetric and Unsymmetric 1, 4-Bis (p-R-phenylethynyl) Benzenes via Palladium/Copper Catalyzed Cross-Coupling and Comments on the Coupling of Aryl Halides with Terminal Alkynes. *Inorg. Chim. Acta* **1994**, *220*, 289-296.
(177) Cacioppa, G.; Carlotti, B.; Elisei, F.; Gentili, P.; Marrocchi, A.; Spalletti, A. Unexpected Multiple Activated Steps in the Excited State Decay of Some Bis (phenylethynyl)-Fluorenes and-Anthracenes. *Phys. Chem. Chem. Phys.* **2016**, *18*, 285-294.
(178) Fasina, T. M.; Collings, J. C.; Lydon, D. P.; Albesa-Jove, D.; Batsanov, A. S.; Howard, J. A.; Nguyen, P.; Bruce, M.; Scott, A. J.; Clegg, W. Synthesis, Optical Properties, Crystal Structures and Phase Behaviour of Selectively Fluorinated 1, 4-Bis (4′-pyridylethynyl) Benzenes, 4-(phenylethynyl) Pyridines and 9, 10-Bis (4′-pyridylethynyl) Anthracene, and a Zn $(NO_3)_2$ Coordination Polymer. *J. Mater. Chem.* **2004**, *14*, 2395-2404.
(179) Pawle, R.; Haas, T.; Müller, P.; Thomas III, S. Twisting and Piezochromism of Phenylene-Ethynylenes with Aromatic Interactions Between Side Chains and Main Chains. *Chem. Sci.* **2014**, *5*, 4184-4188.
(180) Sharber, S. A.; Baral, R. N.; Frausto, F.; Haas, T. E.; Müller, P.; Thomas III, S. W. Substituent Effects that Control Conjugated Oligomer Conformation through Non-Covalent Interactions. *J. Am. Chem. Soc.* **2017**, *139*, 5164-5174.
(181) Wautelet, P.; Moroni, M.; Oswald, L.; Le Moigne, J.; Pham, A.; Bigot, J. Y.; Luzzati, S. Rigid Rod Conjugated Polymers for Nonlinear Optics. 2. Synthesis and Characterization of Phenylene−Ethynylene Oligomers. *Macromolecules* **1996**, *29*, 446-455.
(182) Pawle, R. H.; Agarwal, A.; Malveira, S.; Smith, Z. C.; Thomas III, S. W. Bandgap Engineering of Conjugated Materials with Nonconjugated Side Chains. *Macromolecules* **2014**, *47*, 2250-2256.
(183) Tang, Y.; Zhou, Z.; Ogawa, K.; Lopez, G. P.; Schanze, K. S.; Whitten, D. G. Photophysics and Self-Assembly of Symmetrical and Unsymmetrical Cationic Oligophenylene Ethynylenes. *J. Photochem. Photobiol., A* **2009**, *207*, 4-6.
(184) Tang, Y.; Zhou, Z.; Ogawa, K.; Lopez, G. P.; Schanze, K. S.; Whitten, D. G. Synthesis, Self-Assembly, and Photophysical Behavior of Oligo Phenylene Ethynylenes: from Molecular to Supramolecular Properties. *Langmuir* **2009**, *25*, 21-25.
(185) Mei, J.; Leung, N. L.; Kwok, R. T.; Lam, J. W.; Tang, B. Z. Aggregation-Induced Emission: Together We Shine, United We Soar! *Chem. Rev.* **2015**, *115*, 11718-11940.
(186) Jiu, T.; Li, Y.; Liu, H.; Ye, J.; Liu, X.; Jiang, L.; Yuan, M.; Li, J.; Li, C.; Wang, S. Brightly Full-Color Emissions of Oligo (p-phenylenevinylene)s: Substituent Effects on Photophysical Properties. *Tetrahedron* **2007**, *63*, 3168-3172.
(187) Shimizu, M.; Takeda, Y.; Higashi, M.; Hiyama, T. 1,4-Bis(alkenyl)-2,5-Dipiperidinobenzenes: Minimal Fluorophores Exhibiting Highly Efficient Emission in the Solid State. *Angew. Chem. Int. Ed. Engl.* **2009**, *48*, 3653-3656.
(188) Yamaguchi, Y.; Shimoi, Y.; Ochi, T.; Wakamiya, T.; Matsubara, Y.; Yoshida, Z.-i. Photophysical Properties of Oligophenylene Ethynylenes Modified by Donor and/or Acceptor Groups. *J. Phys. Chem. A* **2008**, *112*, 5074-5084.
(189) Yamaguchi, Y.; Tanaka, T.; Kobayashi, S.; Wakamiya, T.; Matsubara, Y.; Yoshida, Z.-i. Light-Emitting Efficiency Tuning of Rod-Shaped π-Conjugated Systems by Donor and Acceptor Groups. *J. Am. Chem. Soc.* **2005**, *127*, 9332-9333.
(190) Yamaguchi, Y.; Ochi, T.; Wakamiya, T.; Matsubara, Y.; Yoshida, Z.-i. New Fluorophores with Rod-Shaped Polycyano π-Conjugated Structures: Synthesis and Photophysical Properties. *Org. Lett.* **2006**, *8*, 717-720.

(191) Frank, B. B.; Laporta, P. R.; Breiten, B.; Kuzyk, M. C.; Jarowski, P. D.; Schweizer, W. B.; Seiler, P.; Biaggio, I.; Boudon, C.; Gisselbrecht, J.-P.; et al. Comparison of CC Triple and Double Bonds as Spacers in Push-Pull Chromophores. *Eur. J. Org. Chem.* **2011**, *2011*, 4307-4317.
(192) Stefko, M.; Tzirakis, M. D.; Breiten, B.; Ebert, M. O.; Dumele, O.; Schweizer, W. B.; Gisselbrecht, J. P.; Boudon, C.; Beels, M. T.; Biaggio, I.; et al. Donor-Acceptor (D-A)-Substituted Polyyne Chromophores: Modulation of Their Optoelectronic Properties by Varying the Length of the Acetylene Spacer. *Chemistry* **2013**, *19*, 12693-12704.
(193) Liu, X.; McCormack, M. P.; Waters, S. P. *Org. Lett*. **2010**, *12*, 692.
(194) Klymchenko, A. S. Solvatochromic and Fluorogenic Dyes as Environment-Sensitive Probes: Design and Biological Applications. *Acc. Chem. Res.* **2017**, *50*, 366-375.
(195) Hu, R.; Leung, N. L.; Tang, B. Z. AIE Macromolecules: Syntheses, Structures and Functionalities. *Chem. Soc. Rev.* **2014**, *43*, 4494-4562.
(196) Qin, A.; Lam, J. W.; Tang, B. Z. Luminogenic Polymers with Aggregation-Induced Emission Characteristics. *Prog. Polym. Sci.* **2012**, *37*, 182-209.
(197) Hong, Y.; Lam, J. W.; Tang, B. Z. Aggregation-Induced Emission. *Chem. Soc. Rev.* **2011**, *40*, 5361-5388.
(198) Li, K.; Liu, B. Polymer-Encapsulated Organic Nanoparticles for Fluorescence and Photoacoustic Imaging. *Chem. Soc. Rev.* **2014**, *43*, 6570-6597.
(199) Li, Q.; Li, Z. The Strong Light- Emission Materials in the Aggregated State: What Happens from a Single Molecule to the Collective Group. *Adv. Sci.* **2017**, *4*, 1600484-1600498.
(200) Gu, X.; Kwok, R. T. K.; Lam, J. W. Y.; Tang, B. Z. AIEgens for Biological Process Monitoring and Disease Theranostics. *Biomaterials* **2017**, *146*, 115-135.
(201) Hong, Y.; Lam, J. W.; Tang, B. Z. Aggregation-Induced Emission: Phenomenon, Mechanism and Applications. *Chem. Commun. (Camb)* **2009**, doi :10.1039/b904665h 10, 4332-4353.
(202) Qin, A.; Jim, C. K.; Tang, Y.; Lam, J. W.; Liu, J.; Mahtab, F.; Gao, P.; Tang, B. Z. Aggregation-Enhanced Emissions of Intramolecular Excimers in Disubstituted Polyacetylenes. *J. Phys. Chem. B* **2008**, *112*, 9281-9288.
(203) Yuan, W. Z.; Zhao, H.; Shen, X. Y.; Mahtab, F.; Lam, J. W.; Sun, J. Z.; Tang, B. Z. Luminogenic Polyacetylenes and Conjugated Polyelectrolytes: Synthesis, Hybridization with Carbon Nanotubes, Aggregation-Induced Emission, Superamplification in Emission Quenching by Explosives, and Fluorescent assay for Protein Quantitation. *Macromolecules* **2009**, *42*, 9400-9411.
(204) Ishi-i, T.; Ikeda, K.; Ogawa, M.; Kusakaki, Y. Light-Emitting Properties of Donor–Acceptor and Donor–Acceptor–Donor Dyes in Solution, Solid, and Aggregated States: Structure–Property Relationship of Emission Behavior. *RSC Adv.* **2015**, *5*, 89171-89187.
(205) Desroches, M.; Morin, J.-F. o. Anthanthrene as a Super-Extended Tetraphenylethylene for Aggregation-Induced Emission. *Org. Lett.* **2018**, *20*, 2797-2801.
(206) Zhao, Z.; Su, H.; Zhang, P.; Cai, Y.; Kwok, R. T.; Chen, Y.; He, Z.; Gu, X.; He, X.; Sung, H. H. Polyyne Bridged AIE Luminogens with Red Emission: Design, Synthesis, Properties and Applications. *J. Mater. Chem. B* **2017**, *5*, 1650-1657.
(207) Zhang, P.; Zhao, Z.; Li, C.; Su, H.; Wu, Y.; Kwok, R. T.; Lam, J. W.; Gong, P.; Cai, L.; Tang, B. Z. Aptamer-Decorated Self-Assembled AIE Organic Dots for Cancer Cell Targeting and Imaging. *Anal. Chem.* **2017**, *90*, 1063-1067.
(208) Jiang, Y.; Chen, C. F. Recent Developments in Synthesis and Applications of Triptycene and Pentiptycene Derivatives. *Eur. J. Org. Chem.* **2011**, *2011*, 6377-6403.
(209) Lin, C. J.; Kundu, S. K.; Lin, C. K.; Yang, J. S. Conformational Control of Oligo(p-phenyleneethynylene)s with Intrinsic Substituent Electronic Effects: Origin of the Twist in Pentiptycene-Containing Systems. *Chemistry* **2014**, *20*, 14826-14833.
(210) Long, T. M.; Swager, T. M. Using “Internal Free Volume” to Increase Chromophore Alignment. *J. Am. Chem. Soc.* **2002**, *124*, 3826-3827.
(211) Jiang, X.; Duan, H.-B.; Khan, S. I.; Garcia-Garibay, M. A. Diffusion-Controlled Rotation of Triptycene in a Metal–Organic Framework (MOF) Sheds Light on the Viscosity of MOF-Confined Solvent. *ACS Cent. Sci.* **2016**, *2*, 608-613.
(212) Zhang, C.; Chen, C. F. Synthesis and Structure of a Triptycene-Based Nanosized Molecular Cage. *J. Org. Chem.* **2007**, *72*, 9339-9341.

(213) Goldsmith, R. H.; Vura-Weis, J.; Scott, A. M.; Borkar, S.; Sen, A.; Ratner, M. A.; Wasielewski, M. R. Unexpectedly Similar Charge Transfer Rates Through Benzo-Annulated Bicyclo [2.2.2] Octanes. *J. Am. Chem. Soc.* **2008**, *130*, 7659-7669.
(214) Matsunaga, Y.; Yang, J. S. Multicolor Fluorescence Writing Based on Host–Guest Interactions and Force- Induced Fluorescence- Color Memory. *Angew. Chem. Int. Ed.* **2015**, *54*, 7985-7989.
(215) Mazrad, Z. A. I.; Lee, K.; Chae, A.; In, I.; Lee, H.; Park, S. Y. Progress in Internal/External Stimuli Responsive Fluorescent Carbon Nanoparticles for Theranostic and Sensing Applications. *J. Mater. Chem.* **2018**, *6*, 1149-1178.
(216) Karimi, M.; Ghasemi, A.; Sahandi Zangabad, P.; Rahighi, R.; Moosavi Basri, S. M.; Mirshekari, H.; Amiri, M.; Shafaei Pishabad, Z.; Aslani, A.; Bozorgomid, M.; et al. Smart Micro/Nanoparticles in Stimulus-Responsive Drug/Gene Delivery Systems. *Chem. Soc. Rev.* **2016**, *45*, 1457-14501.
(217) Sharker, S. M.; Jeong, C. J.; Kim, S. M.; Lee, J. E.; Jeong, J. H.; In, I.; Lee, H.; Park, S. Y. Photo- and pH- Tunable Multicolor Fluorescent Nanoparticle- Based Spiropyran- and BODIPY- Conjugated Polymer with Graphene Oxide. *Chem. Asian J.* **2014**, *9*, 2921-2927.
(218) Aliprandi, A.; Genovese, D.; Mauro, M.; De Cola, L. Recent Advances in Phosphorescent Pt(II) Complexes Featuring Metallophilic Interactions: Properties and Applications. *Chem. Lett.* **2015**, *44*, 1152-1169.
(219) Zhang, X.-P.; Zhang, D.-S.; Qi, X.-W.; Zhu, L.-H.; Wang, X.-H.; Sun, W.; Shi, Z.-F.; Lin, Q. Luminescent Mechanochromism of Chiral Alkynylplatinum(II) Bipyridine Complexes Functionalized with Pinene Groups. *Inorg. Chim. Acta* **2017**, *467*, 99-105.
(220) Carrara, S.; Aliprandi, A.; Hogan, C. F.; De Cola, L. Aggregation-Induced Electrochemiluminescence of Platinum(II) Complexes. *J. Am. Chem. Soc.* **2017**, *139*, 14605-14610.
(221) Kang, E. B.; Choi, C. A.; Mazrad, Z. A. I.; Kim, S. H.; In, I.; Park, S. Y. Determination of Cancer Cell-Based pH-Sensitive Fluorescent Carbon Nanoparticles of Cross-Linked Polydopamine by Fluorescence Sensing of Alkaline Phosphatase Activity on Coated Surfaces and Aqueous Solution. *Anal. Chem.* **2017**, *89*, 13508-13517.
(222) Ni, J.; Wang, Y. G.; Wang, H. H.; Xu, L.; Zhao, Y. Q.; Pan, Y. Z.; Zhang, J. J. Thermo- and Mechanical-Grinding-Triggered Color and Luminescence Switches of the Diimine-Platinum (II) Complex with 4-Bromo-2,2'-Bipyridine. *Dalton Trans.* **2014**, *43*, 352-360.
(223) Lin, C.-J.; Liu, Y.-H.; Peng, S.-M.; Shinmyozu, T.; Yang, J.-S. Excimer–Monomer Photoluminescence Mechanochromism and Vapochromism of Pentiptycene-Containing Cyclometalated Platinum (II) Complexes. *Inorg. Chem.* **2017**, *56*, 4978-4989.
(224) Koo, B.; Swager, T. M. Interfacial Pressure/Area Sensing: Dual-Fluorescence of Amphiphilic Conjugated Polymers at Water Interfaces. *ACS Macro Lett.* **2017**, *6*, 134-138.
(225) Terao, J.; Ohsawa, M.; Masai, H.; Kurashige, Y.; Fujihara, T.; Tsuji, Y. Synthesis of Molecular Wires Strapped by pi-Conjugated Side Chains: Integration of Dehydrobenzo[20]annulene Units. *J. Org. Chem.* **2015**, *80*, 8874-8880.
(226) Hu, W.; Yan, Q.; Zhao, D. Oligo(p-phenylene-ethynylene)s with Backbone Conformation Controlled by Competitive Intramolecular Hydrogen Bonds. *Chemistry* **2011**, *17*, 7087-7094.
(227) Khan, M. S.; Kakkar, A. K.; Long, N. J.; Lewis, J.; Raithby, P.; Nguyen, P.; Marder, T. B.; Wittmann, F.; Friend, R. H. Synthesis and Optical Spectroscopy of Linear Long-Chain Di-Terminal Alkynes and Their Pt–σ-Acetylide Polymeric Complexes. *J. Mater. Chem.* **1994**, *4*, 1227-1232.
(228) Li, J.; Terec, A.; Wang, Y.; Joshi, H.; Lu, Y.; Sun, H.; Stuparu, M. C. π-Conjugated Discrete Oligomers Containing Planar and Nonplanar Aromatic Motifs. *J. Am. Chem. Soc.* **2017**, *139*, 3089-3094.
(229) Kendall, J.; McDonald, R.; Ferguson, M. J.; Tykwinski, R. R. Synthesis and Solid-State Structure of Perfluorophenyl End-Capped Polyynes. *Org. Lett.* **2008**, *10*, 2163-2166.
(230) Chen, G.; Mahmud, I.; Dawe, L. N.; Daniels, L. M.; Zhao, Y. Synthesis and Properties of Conjugated Oligoyne-Centered π-Extended Tetrathiafulvalene Analogues and Related Macromolecular Systems. *J. Org. Chem.* **2011**, *76*, 2701-2715.
(231) Wang, C.; Batsanov, A. S.; Bryce, M. R.; Martin, S.; Nichols, R. J.; Higgins, S. J.; Garcia-Suarez, V. M.; Lambert, C. J. Oligoyne Single Molecule Wires. *J. Am. Chem. Soc.* **2009**, *131*, 15647-15654.
(232) Hu, F.; Zeng, C.; Long, R.; Miao, Y.; Wei, L.; Xu, Q.; Min, W. Supermultiplexed Optical Imaging and Barcoding with Engineered Polyynes. *Nat. methods* **2018**, *15*, 194-200.

(233) Nelson, J. C.; Saven, J. G.; Moore, J. S.; Wolynes, P. G. Solvophobically Driven Folding of Nonbiological Oligomers. *Science* **1997**, *277*, 1793-1796.
(234) Nagai, K.; Masuda, T.; Nakagawa, T.; Freeman, B. D.; Pinnau, I. Poly[1-(trimethylsilyl)-1-propyne] and Related Polymers: Synthesis, Properties and Functions. *Prog. Polym. Sci.* **2001**, *26*, 721-798.
(235) McQuade, D. T.; Pullen, A. E.; Swager, T. M. Conjugated Polymer-Based Chemical Sensors. *Chem. Rev.* **2000**, *100*, 2537-2574.
(236) Sogawa, H.; Miyagi, Y.; Shiotsuki, M.; Sanda, F. Synthesis of Novel Optically Active Poly(phenyleneethynylene–aryleneethynylene)s Bearing Hydroxy Groups. Examination of the Chiroptical Properties and Conjugation Length. *Macromolecules* **2013**, *46*, 8896-8904.
(237) Sogawa, H.; Shiotsuki, M.; Hirao, T.; Haino, T.; Sanda, F. Synthesis of Optically Active Poly (m-phenyleneethynylene–aryleneethynylene)s Bearing Hydroxy Groups and Examination of the Higher Order Structures. *Macromolecules* **2013**, *46*, 8161-8170.
(238) Meng, F.; Li, Y.; Zhang, W.; Li, S.; Quan, Y.; Cheng, Y. Circularly Polarized Luminescence Based Chirality Transfer of the Chiral BINOL Moiety via Rigid π-Conjugation Chain Backbone Structures. *Polym. Chem.* **2017**, *8*, 1555-1561.
(239) Ikai, T.; Shimizu, S.; Awata, S.; Shinohara, K.-i. Chiral Amplification in π-Conjugated Helical Polymers with Circularly Polarized Luminescence. *Macromolecules* **2018**, *51*, 2328-2334.
(240) Miyagi, Y.; Ishida, T.; Marumoto, M.; Sano, N.; Yajima, T.; Sanda, F. Ligand Exchange Reaction for Controlling the Conformation of Platinum-Containing Polymers. *Macromolecules* **2018**, *51*, 815-824.
(241) Nast, R. Coordination Chemistry of Metal Alkynyl Compounds. *Coord. Chem. Rev.* **1982**, *47*, 89-124.
(242) Szafert, S.; Gladysz, J. A. Carbon in One Dimension: Structural Analysis of the Higher Conjugated Polyynes. *Chem. Rev.* **2003**, *103*, 4175-4205.
(243) Liu, Y.; Li, Y.; Schanze, K. S. Photophysics of π-Conjugated Oligomers and Polymers that Contain Transition Metal Complexes. *J. Photochem. Photobiol., C* **2002**, *3*, 1-23.
(244) Kokado, K.; Tokoro, Y.; Chujo, Y. Luminescent m-Carborane-Based π-Conjugated Polymer. *Macromolecules* **2009**, *42*, 2925-2930.
(245) Mishra, A.; Ma, C. Q.; Bauerle, P. Functional Oligothiophenes: Molecular Design for Multidimensional Nanoarchitectures and their Applications. *Chem. Rev.* **2009**, *109*, 1141-1276.
(246) Friend, R. H.; Gymer, R. W.; Holmes, A. B.; Burroughes, J. H.; Marks, R. N.; Taliani, C.; Bradley, D. D. C.; Dos Santos, D. A.; Bredas, J. L.; Logdlund, M.; et al. Electroluminescence in Conjugated Polymers. *Nature* **1999**, *397*, 121-128.
(247) Wilson, J. S.; Köhler, A.; Friend, R. H.; Al-Suti, M. K.; Al-Mandhary, M. R. A.; Khan, M. S.; Raithby, P. R. Triplet States in a Series of Pt-Containing Ethynylenes. *J. Chem. Phys.* **2000**, *113*, 7627-7634.
(248) Wilson, J. S.; Chawdhury, N.; Al-Mandhary, M. R.; Younus, M.; Khan, M. S.; Raithby, P. R.; Kohler, A.; Friend, R. H. The Energy Gap Law for Triplet States in Pt-Containing Conjugated Polymers and Monomers. *J. Am. Chem. Soc.* **2001**, *123*, 9412-9417.
(249) Beljonne, D.; Wittmann, H. F.; Köhler, A.; Graham, S.; Younus, M.; Lewis, J.; Raithby, P. R.; Khan, M. S.; Friend, R. H.; Brédas, J. L. Spatial Extent of the Singlet and Triplet Excitons in Transition Metal- Containing Poly- ynes. *J. Chem. Phys.* **1996**, *105*, 3868-3877.
(250) Wittmann, H. F.; Friend, R. H.; Khan, M. S.; Lewis, J. Optical Spectroscopy of Platinum and Palladium Containing Poly-ynes. *J. Chem. Phys.* **1994**, *101*, 2693-2698.
(251) Lepetit, C.; Maraval, V.; Canac, Y.; Chauvin, R. On the Nature of the Dative Bond: Coordination to Metals and Beyond. The Carbon Case. *Coord. Chem. Rev.* **2016**, *308*, 59-75.
(252) McGarrah, J. E.; Eisenberg, R. Dyads for Photoinduced Charge Separation Based on Platinum Diimine Bis(acetylide) Chromophores: Synthesis, Luminescence and Transient Absorption Studies. *Inorg. Chem.* **2003**, *42*, 4355-4365.
(253) Hissler, M.; McGarrah, J. E.; Connick, W. B.; Geiger, D. K.; Cummings, S. D.; Eisenberg, R. Platinum Diimine Complexes: Towards a Molecular Photochemical Device. *Coord. Chem. Rev.* **2000**, *208*, 115-137.
(254) Muro, M. L.; Rachford, A. A.; Wang, X.; Castellano, F. N. Platinum(II) Acetylide Photophysics. In *Photophysics of Organometallics*, Springer, New York, 2009; pp 1-35.
(255) Kostic, N. M.; Fenske, R. F. Molecular Orbital Study of Bonding, Conformations, and Reactivity of Transition-Metal Complexes Containing Unsaturated Organic Ligands. Electrophilic and

Nucleophilic Additions to Acetylide, Vinylidene, Vinyl, and Carbene ligands. *Organometallics* **1982**, *1*, 974-982.

(256) Lichtenberger, D. L.; Renshaw, S. K.; Wong, A.; Tagge, C. D. Investigation of Metal-dπ-butadiynyl-π Interactions in (η^5-C_5H_5)$(CO)_2$FeC≡CC≡CCH Using Photoelectron Spectroscopy. *Organometallics* **1993**, *12*, 3522-3526.

(257) Lichtenberger, D. L.; Renshaw, S. K.; Bullock, R. M. Metal-Acetylide Bonding in (η^5-C_5H_5)$Fe(CO)_2$ C≡CR Compounds. Measures of Metal-dπ-acetylide-π Interactions from Photoelectron Spectroscopy. *J. Am. Chem. Soc.* **1993**, *115*, 3276-3285.

(258) Lhost, O.; Toussaint, J. M.; Bredas, J. L.; Wittmann, H. F.; Fuhrmann, K.; Friend, R. H.; Khan, M. S.; Lewis, J. Electronic Structure of Platinum-Containing Polyynes. *Synth. Met.* **1993**, *57*, 4525-4530.

(259) Frapper, G.; Kertesz, M. Metal Oligo-yne Polymers: Electronic Structures of [-(L)nMC≡CRC≡C-]x Polymers. *Inorg. Chem.* **1993**, *32*, 732-740.

(260) Head, A. R.; Renshaw, S. K.; Uplinger, A. B.; Lomprey, J. R.; Selegue, J. P.; Lichtenberger, D. L. Experimental Measure of Metal–Alkynyl Electronic Structure Interactions by Photoelectron Spectroscopy:(η^5-C_5H_5)$Ru(CO)_2$C≡CMe and [(η^5-C_5H_5)$Ru(CO)_2$]$_2$(μ-C≡C). *Polyhedron* **2015**, *86*, 141-150.

(261) Vacher, A.; Barrière, F.; Camerel, F.; Bergamini, J.-F.; Roisnel, T.; Lorcy, D. Cis and trans-bis(tetrathiafulvalene-acetylide) Platinum (II) Complexes: Syntheses, Crystal Structures, and Influence of the Ancillary Ligands on Their Electronic Properties. *Dalton Trans.* **2013**, *42*, 383-394.

(262) Zhan, X.; Yang, M. Transition Metal Acetylide Catalysts for Polymerization of Alkynes: 1. Effect of Ligands on Catalytic Activity of Nickel Complexes. *J. Mol. Catal. A: Chem.* **2001**, *169*, 27-31.

(263) Khan, M. S.; Kakkar, A. K.; Ingham, S. L.; Raithby, P. R.; Lewis, J.; Spencer, B.; Wittmann, F.; Friend, R. H. Synthesis and Electronic Structure of Rigid Rod Octahedral Ru-σ-Acetylide Complexes. *J. Organomet. Chem.* **1994**, *472*, 247-255.

(264) Schull, T. L.; Kushmerick, J. G.; Patterson, C. H.; George, C.; Moore, M. H.; Pollack, S. K.; Shashidhar, R. Ligand Effects on Charge Transport in Platinum (II) Acetylides. *J. Am. Chem. Soc.* **2003**, *125*, 3202-3203.

(265) Long, N. J.; White, A. J.; Williams, D. J.; Younus, M. Synthesis and Characterisation of New Platinum Ethynyl Dimers and Polymers with Pendant Ferrocenyl Groups. *J. Organomet. Chem.* **2002**, *649*, 94-99.

(266) Miesel, D.; Hildebrandt, A.; Rüffer, T.; Schaarschmidt, D.; Lang, H. Electron- Transfer Studies of trans- Platinum Bis(acetylide) Complexes. *Eur. J. Inorg. Chem.* **2014**, *2014*, 5541-5553.

(267) Lara, R.; Lalinde, E.; Moreno, M. T. Phosphorescent Platinum (II) Alkynyls End-Capped with Benzothiazole Units. *Dalton Trans.* **2017**, *46*, 4628-4641.

(268) Berenguer, J. R.; Fernandez, J.; Lalinde, E.; Sanchez, S. New Trans-Configured Acetylide-Cyanide Platinum(II) Anions: Spectroscopic and Optical Studies. *Organometallics* **2013**, *32*, 835-845.

(269) Sun, W.; Zhang, B.; Li, Y.; Pritchett, T. M.; Li, Z.; Haley, J. E. Broadband Nonlinear Absorbing Platinum 2, 2′-Bipyridine Complex Bearing 2-(Benzothiazol-2′-yl)-9, 9-diethyl-7-ethynylfluorene Ligands. *Chem. Mater.* **2010**, *22*, 6384-6392.

(270) Qu, L.; Dong, X.; Zhong, C.; Liu, Z.; Qin, J. Synthesis and Photophysical Properties of Two Platinum (II) Diimine Diacetylides–A New Approach for Fluorescent Two-Photon Absorption Materials from Organometallics. *Chem. Phys. Lett.* **2011**, *513*, 103-107.

(271) Hissler, M.; Connick, W. B.; Geiger, D. K.; McGarrah, J. E.; Lipa, D.; Lachicotte, R. J.; Eisenberg, R. Platinum diimine bis(acetylide) complexes: synthesis, characterization, and luminescence properties. *Inorg. Chem.* **2000**, *39*, 447-457.

(272) Lalinde, E.; Moreno, M. T.; Ruiz, S.; Sanchez, S. Synthesis, Structural, and Photophysical Studies of Phenylquinoline and Phenylquinolinyl Alkynyl Based Pt (II) Complexes. *Organometallics* **2014**, *33*, 3078-3090.

(273) Muro, M. L.; Castellano, F. N. Room Temperature Photoluminescence from [Pt (4′-C≡CR-tpy) Cl]$^+$ Complexes. *Dalton Trans.* **2007**, 4659-4665.

(274) Bullock, J. D.; Salehi, A.; Zeman IV, C. J.; Abboud, K. A.; So, F.; Schanze, K. S. In Search of Deeper Blues: Trans-N-Heterocyclic Carbene Platinum Phenylacetylide as a Dopant for Phosphorescent OLEDs. *ACS Appl. Mater. Interfaces* **2017**, *9*, 41111-41114.

(275) Bachmann, M.; Suter, D.; Blacque, O.; Venkatesan, K. Tunable and Efficient White Light Phosphorescent Emission Based on Single Component N-Heterocyclic Carbene Platinum(II) Complexes. *Inorg. Chem.* **2016**, *55*, 4733-4745.

(276) Chung, L. H.; Chan, S. C.; Lee, W. C.; Wong, C. Y. Emissive Osmium (II) Complexes Supported by N-Heterocyclic Carbene-Based C^C^C-Pincer Ligands and Aromatic Diimines. *Inorg. Chem.* **2012**, *51*, 8693-8703.

(277) Rogers, J. E.; Hall, B. C.; Hufnagle, D. C.; Slagle, J. E.; Ault, A. P.; McLean, D. G.; Fleitz, P. A.; Cooper, T. M. Effect of Platinum on the Photophysical Properties of a Series of Phenyl-Ethynyl Oligomers. *J. Chem. Phys.* **2005**, *122*, 214708- 214713.

(278) Zhang, Y.; Clavadetscher, J.; Bachmann, M.; Blacque, O.; Venkatesan, K. Tuning the Luminescent Properties of Pt(II) Acetylide Complexes through Varying the Electronic Properties of N-Heterocyclic Carbene Ligands. *Inorg. Chem.* **2014**, *53*, 756-771.

(279) Guo, H.; Muro-Small, M. L.; Ji, S.; Zhao, J.; Castellano, F. N. Naphthalimide Phosphorescence Finally Exposed in a Platinum(II) Diimine Complex. *Inorg. Chem.* **2010**, *49*, 6802-6804.

(280) Zhang, Y.; Hauke, C. E.; Crawley, M. R.; Schurr, B. E.; Fulong, C. R. P.; Cook, T. R. Increasing Phosphorescent Quantum Yields and Lifetimes of Platinum-Alkynyl Complexes with Extended Conjugation. *Dalton Trans.* **2017**, *46*, 9794-9800.

(281) Razuvaev, G.; Domrachev, G.; Sharutin, V.; Suvorova, O. Ferrocenyl Derivatives of Dicyclopentadienyl-Titanium,-Zirconium and-Hafnium. *J. Organomet. Chem.* **1977**, *141*, 313-317.

(282) Hayashi, Y.; Osawa, M.; Kobayashi, K.; Wakatsuki, Y. Reductive Elimination by Remote Electron Transfer Activation in C 4-Bridged Titanocene-Ferrocenyl Complexes. *Chem. Commun.* **1996**, 1617-1618.

(283) Hayashi, Y.; Osawa, M.; Wakatsuki, Y. Reductive Coupling Reaction Induced by Remote-Site Oxidation in Titanocene Bis (metallocenylacetylide), Where Metallocenyl= Ferrocenyl or Ruthenocenyl: a Novel Route to C_n (n = 4, 6, and 8) Wire with the Metallocenyl Groups at both Terminals. *J. Organomet. Chem.* **1997**, *542*, 241-246.

(284) Back, S.; Rheinwald, G.; Lang, H. Synthesis, Electrochemistry and Electronic Spectra of Tetranuclear Bis (η^2-alkynyl) Transition-Metal Complexes. The Molecular Structure of [(η^5-C_5H_4 $SiMe_3$)$_2$ Ti (C≡CFc)$_2$]CuBr. *J. Organomet. Chem.* **2000**, *601*, 93-99.

(285) Back, S.; Gossage, R. A.; Rheinwald, G.; del Río, I.; Lang, H.; van Koten, G. Titanium σ-Acetylides as Building Blocks for Heterobimetallic Transition Metal Complexes: Synthesis and Redox Behaviour of π-Conjugated Organometallic Systems. *J. Organomet. Chem.* **1999**, *582*, 126-138.

(286) Sahoo, P. K.; Swain, S. K. Synthesis of Zirconocene- Acetylene and Zirconocene- Diacetylene Polymer. *J. Polym. Sci., Part A: Polym. Chem.* **1999**, *37*, 3899-3902.

(287) Turlington, M. D.; Pienkos, J. A.; Carlton, E. S.; Wroblewski, K. N.; Myers, A. R.; Trindle, C. O.; Altun, Z.; Rack, J. J.; Wagenknecht, P. S. Complexes with Tunable Intramolecular Ferrocene to TiIV Electronic Transitions: Models for Solid State Fe (II) to Ti (IV) Charge Transfer. *Inorg. Chem.* **2016**, *55*, 2200-2211.

(288) Pienkos, J. A.; Agakidou, A. D.; Trindle, C. O.; Herwald, D. W.; Altun, Z.; Wagenknecht, P. S. Titanocene as a New Acceptor (A) for Arylamine Donors (D) in D−π–A Chromophores. *Organometallics* **2016**, *35*, 2575-2578.

(289) Ng, K.-H.; Ng, F.-N.; Yu, W.-Y. A Convenient Synthesis of Anthranilic Acids by Pd-Catalyzed Direct Intermolecular ortho-C–H Amidation of Benzoic Acids. *Chem. Commun.* **2012**, *48*, 11680-11682.

(290) Roberts, H. N.; Brown, N. J.; Edge, R.; Fitzgerald, E. C.; Ta, Y. T.; Collison, D.; Low, P. J.; Whiteley, M. W. Synthesis, Redox Chemistry, and Electronic Structure of the Butadiynyl and Hexatriynyl Complexes [Mo {(C≡C)$_n$C≡CR}(L2)(η-C_7H_7)]$^{z+}$(n = 1, 2; z = 0, 1; R= $SiMe_3$, H; L2= 2, 2′-bipyridine, $Ph_2PCH_2CH_2PPh_2$). *Organometallics* **2012**, *31*, 6322-6335.

(291) Brown, N. J.; Collison, D.; Edge, R.; Fitzgerald, E. C.; Helliwell, M.; Howard, J. A. K.; Lancashire, H. N.; Low, P. J.; McDouall, J. J. W.; Raftery, J.; et al. Spectroscopic Properties and Electronic Structure of the Cycloheptatrienyl Molybdenum Alkynyl Complexes [Mo(C≡CR)($Ph_2PCH_2CH_2PPh_2$) (η-C_7H_7)]$^{n+}$(n= 0 or 1; R =Bu^t, Fc, CO_2Me, or C_6H_4-4-X, X = NH_2, OMe, Me, H, CHO, CO_2Me). *Organometallics* **2010**, *29*, 1261-1276.

(292) Adams, J. S.; Bitcon, C.; Brown, J. R.; Collison, D.; Cunningham, M.; Whiteley, M. W. The Chemistry of Cycloheptatrienyl Complexes of Molybdenum and Tungsten: the Synthesis and Reactions of some Vinylidene and Alkynyl Derivatives. *J. Chem. Soc., Dalton Trans.* **1987**, doi :10.1039/dt9870003049.

(293) O'Hanlon, D. C.; Cohen, B. W.; Moravec, D. B.; Dallinger, R. F.; Hopkins, M. D. Electronic, Redox, and Photophysical Consequences of Metal-for-Carbon Substitution in Oligo-Phenylene-Ethynylenes. *J. Am. Chem. Soc.* **2014**, *136*, 3127-3136.
(294) Bittner, C.; Ehrhorn, H.; Bockfeld, D.; Brandhorst, K.; Tamm, M. Tuning the Catalytic Alkyne Metathesis Activity of Molybdenum and Tungsten 2, 4, 6-Trimethylbenzylidyne Complexes with Fluoroalkoxide Ligands OC $(CF_3)_n Me_{3-n}$ (n= 0–3). *Organometallics* **2017**, *36*, 3398-3406.
(295) Yee, G. M.; Kowolik, K.; Manabe, S.; Fettinger, J. C.; Berben, L. A. Simple Routes to Bulky Silyl-Substituted Acetylide Ligands and Examples of V(III), Fe(II), and Mn(II) Complexes. *Chem. Commun.* **2011**, *47*, 11680-11682.
(296) Berben, L. A.; Long, J. R. Synthesis and Alkali Metal Ion-Binding Properties of a Chromium(III) Triacetylide Complex. *J. Am. Chem. Soc.* **2002**, *124*, 11588-11589.
(297) Astruc, D. From Organotransition-Metal Chemistry Toward Molecular Electronics: Electronic Communication Between Ligand-Bridged Metals. *Acc. Chem. Res.* **1997**, *30*, 383-391.
(298) Semenov, S. N.; Taghipourian, S. F.; Blacque, O.; Fox, T.; Venkatesan, K.; Berke, H. An Iron-Capped Metal−Organic Polyyne: {[Fe]$(C\equiv C)_2$[W]≡CC≡CC≡[W]$(C\equiv C)_2$[Fe]}. *J. Am. Chem. Soc.* **2010**, *132*, 7584-7585.
(299) John, K.; Hopkins, M. Synthesis and Reactions of Netallo-Diethynylbenzenes: Building Blocks for Redox-Active Poly (phenyleneethynylene)s. *Chem. Commun.* **1999**, 589-590.
(300) Sun, C.; Turlington, C. R.; Thomas, W. W.; Wade, J. H.; Stout, W. M.; Grisenti, D. L.; Forrest, W. P.; VanDerveer, D. G.; Wagenknecht, P. S. Synthesis of cis and trans Bis-Alkynyl Complexes of Cr(III) and Rh(III) Supported by a Tetradentate Macrocyclic Amine: a Spectroscopic Investigation of the M(III)-Alkynyl Interaction. *Inorg. Chem.* **2011**, *50*, 9354-9364.
(301) Nishijo, J.; Judai, K.; Numao, S.; Nishi, N. Chromium Acetylide Complex Based Ferrimagnet and Weak Ferromagnet. *Inorg. Chem.* **2009**, *48*, 9402-9408.
(302) Berben, L. A.; Kozimor, S. A. Dinitrogen and Acetylide Complexes of Low-Valent Chromium. *Inorg. Chem.* **2008**, *47*, 4639-4467.
(303) Tyler, S.; Zeller, M.; Fanwick, P.; Ren, T. Synthesis and Investigation of Macrocyclic Cr(III) Bis-Alkynyl Complexes: Structural and Spectroscopic Properties. *Eur. J. Inorg. Chem.* **2017**, *2017*, 4068-4076.
(304) Venkatesan, K.; Fox, T.; Schmalle, H. W.; Berke, H. Synthesis and Characterization of Redox-Active C_4-Bridged Rigid-Rod Complexes with Acetylide-Substituted Manganese End Groups. *Organometallics* **2005**, *24*, 2834-2847.
(305) Fritz, T.; Schmalle, H. W.; Blacque, O.; Venkatesan, K.; Berke, H. Synthesis and Characterization of Mononuclear and Dinuclear Manganese Bis- acetylide Complexes. *Z. Anorg. Allg. Chem.* **2009**, *635*, 1391-1401.
(306) Fernandez, F. J.; Venkatesan, K.; Blacque, O.; Alfonso, M.; Schmalle, H. W.; Berke, H. Generation and Coupling of [Mn$(dmpe)_2$(C≡CR)(C≡C)]* Radicals Producing Redox-Active C_4-Bridged Rigid-Rod Complexes. *Chemistry* **2003**, *9*, 6192-6206.
(307) Unseld, D.; Krivykh, V. V.; Heinze, K.; Wild, F.; Artus, G.; Schmalle, H.; Berke, H. Versatile Routes to Mono-and Bis (alkynyl) Manganese (II) and Manganese (III) Complexes via Manganocenes. *Organometallics* **1999**, *18*, 1525-1541.
(308) Kheradmandan, S.; Heinze, K.; Schmalle, H. W.; Berke, H. Electronic Communication in C_4-Bridged Binuclear Complexes with Paramagnetic Bisphosphane Manganese End Groups. *Angew. Chem. Int. Ed.* **1999**, *38*, 2270-2273.
(309) Fernández, F. J.; Alfonso, M.; Schmalle, H. W.; Berke, H. Utilization of Redox and Acid/Base Chemistry for the Deprotection of a Mn $(dmpe)_2$ $(C\equiv CSiMe_3)_2$ Complex. *Organometallics* **2001**, *20*, 3122-3131.
(310) Krivykh, V. V.; Eremenko, I. L.; Veghini, D.; Petrunenko, I. A.; Pountney, D. L.; Unseld, D.; Berke, H. Stable Paramagnetic Bis(alkynyl) Manganese Complexes. *J. Organomet. Chem.* **1996**, *511*, 111-114.
(311) Venkatesan, K.; Blacque, O.; Berke, H. Organometallic Manganese Complexes as Scaffolds for Potential Molecular Wires. *Dalton Trans.* **2007**, 1091-1100.
(312) Wong, K. M.; Lam, S. C.; Ko, C. C.; Zhu, N.; Yam, V. W.; Roue, S.; Lapinte, C.; Fathallah, S.; Costuas, K.; Kahlal, S.; et al. Electroswitchable Photoluminescence Activity: Synthesis, Spectroscopy, Electrochemistry, Photophysics, and X-ray Crystal and Electronic Structures of

[Re(bpy)(CO)$_3$(C≡C-C$_6$H$_4$-C≡C)Fe(C$_5$Me$_5$)(dppe)][PF$_6$]$_{(n)}$ (n = 0, 1). *Inorg. Chem.* **2003**, *42*, 7086-7097.

(313) Bruce, M.; Harbourne, D.; Waugh, F.; Stone, F. Some Transition-Metal Acetylides. *J. Chem. Soc. A* **1968**, 356-359.

(314) Weng, W.; Bartik, T.; Brady, M.; Bartik, B.; Ramsden, J. A.; Arif, A. M.; Gladysz, J. Synthesis, Structure, and Redox Chemistry of Heteropolymetallic Carbon Complexes with MC2M', MC4M', and MC4M'C4M Linkages. Transmetalations of Lithiocarbon Complexes (5-C$_5$Me$_5$)Re (NO)(PPh$_3$)(C≡CLi) and (η^5-C$_5$Me$_5$) Re(NO)(PPh$_3$)(C≡CC≡CLi). *J. Am. Chem. Soc.* **1995**, *117*, 11922-11931.

(315) Dembinski, R.; Lis, T.; Szafert, S.; Mayne, C. L.; Bartik, T.; Gladysz, J. Appreciably Bent sp Carbon Chains: Synthesis, Structure, and Protonation of Organometallic 1, 3, 5-Triynes and 1, 3, 5, 7-Tetraynes of the Formula (η^5-C$_5$Me$_5$)Re(NO)(PPh $_3$)((C≡C) n-p-C$_6$H$_4$Me). *J. Organomet. Chem.* **1999**, *578*, 229-246.

(316) Yam, V. W.-W.; Lo, K. K.-W.; Wong, K. M.-C. Luminescent Polynuclear Metal Acetylides. *J. Organomet. Chem.* **1999**, *578*, 3-30.

(317) Dembinski, R.; Bartik, T.; Bartik, B.; Jaeger, M.; Gladysz, J. Toward Metal-Capped One-Dimensional Carbon Allotropes: Wirelike C6-C20 Polyynediyl Chains That Span Two Redox-Active (η^5-C$_5$Me$_5$) Re(NO)(PPh$_3$) Endgroups. *J. Am. Chem. Soc.* **2000**, *122*, 810-822.

(318) Lam, S.-T.; Zhu, N.; Au, V. K.-M.; Yam, V. W.-W. Synthesis, Characterization, Electrochemistry and Photophysical Studies of Rhenium(I) Tricarbonyl Diimine Complexes with Carboxaldehyde Alkynyl Ligands. *Polyhedron* **2015**, *86*, 10-16.

(319) Lam, S.-T.; Kwok, E. C.-H.; Ko, V. C.-C.; Chan, M.-Y.; Yam, V. W.-W. Synthesis and Characterization of Alkynylrhenium (I) Tricarbonyl Diimine Complexes with Fused Thiophene and Cyanoacrylic Acid Moiety. *Polyhedron* **2016**, *116*, 144-152.

(320) Chung, W. K.; Wong, K. M. C.; Lam, W. H.; Zhu, X. L.; Zhu, N. Y.; Kwok, H. S.; Yam, V. W. W. Syntheses, Photophysical, Electroluminescence and Computational Studies of Rhenium(I) Diimine Triarylamine-Containing Alkynyl Complexes. *New J. Chem.* **2013**, *37*, 1753-1767.

(321) Colbert, M. C. B.; Lewis, J.; Long, N. J.; Raithby, P. R.; Younus, M.; White, A. J. P.; Williams, D. J.; Payne, N. N.; Yellowlees, L.; Beljonne, D.; et al. Synthesis and Characterization of Dinuclear Metal σ-Acetylides and Mononuclear Metal σ-Allenylidenes. *Organometallics* **1998**, *17*, 3034-3043.

(322) Wong, W.-Y.; Ho, C.-L. Di-, Oligo-and Polymetallaynes: Syntheses, Photophysics, Structures and Applications. *Coord. Chem. Rev.* **2006**, *250*, 2627-2690.

(323) Green, K.; Gauthier, N.; Sahnoune, H.; Argouarch, G.; Toupet, L.; Costuas, K.; Bondon, A.; Fabre, B.; Halet, J.-F. o.; Paul, F. d. r. Synthesis and Characterization of Redox-Active Mononuclear Fe (κ^2-dppe)(η^5-C$_5$Me$_5$)-Terminated π-Conjugated Wires. *Organometallics* **2013**, *32*, 4366-4381.

(324) Wang, X.-Z.; Wong, W.-Y. Metallopolyyne Polymers as New Functional Materials for Solar Cell Applications. *Polymer Prepr* **2009**, *50*, 307-308.

(325) Tohmé, A.; Grelaud, G.; Argouarch, G.; Roisnel, T.; Labouille, S.; Carmichael, D.; Paul, F. Redox-Induced Reversible P-P Bond Formation to Generate an Organometallic σ^{4}λ^4-1,2- Biphosphane Dication. *Angew. Chem. Int. Ed.* **2013**, *52*, 4445-4448.

(326) Tohmé, A.; Hagen, C. T.; Essafi, S.; Bondon, A.; Roisnel, T.; Carmichael, D.; Paul, F. Easy and Quantitative Access to Fe (II) and Fe (III) Di (aryl) Alkynylphosphine Oxides Featuring [Fe (dppe) Cp*] Endgroups: Terminal P=O Functionality Blocks the Dimerisation of the Fe (III) Derivatives. *Chem. Commun.* **2015**, *51*, 1316-1319.

(327) Cao, Z.; Forrest, W. P.; Gao, Y.; Fanwick, P. E.; Zhang, Y.; Ren, T. New Iron (III) Bis(acetylide) Compounds Based on the Iron Cyclam Motif. *Inorg. Chem.* **2011**, *50*, 7364-7366.

(328) Cao, Z.; Forrest, W. P.; Gao, Y.; Fanwick, P. E.; Ren, T. trans-[Fe (cyclam)(C$_2$R) $_2$]$^+$: A New Family of Iron (III) Bis-Alkynyl Compounds. *Organometallics* **2012**, *31*, 6199-6206.

(329) Lissel, F.; Blacque, O.; Venkatesan, K.; Berke, H. Structural and Electronic Variations of sp/sp^2 Carbon-Based Bridges in Di-and Trinuclear Redox-Active Iron Complexes Bearing Fe (diphosphine)$_2$X (X= I, NCS) Moieties. *Organometallics* **2015**, *34*, 408-418.

(330) Lissel, F.; Fox, T.; Blacque, O.; Polit, W.; Winter, R. F.; Venkatesan, K.; Berke, H. Stepwise Construction of an Iron-Substituted Rigid-Rod Molecular Wire: Targeting a Tetraferra-Tetracosa-Decayne. *J. Am. Chem. Soc.* **2013**, *135*, 4051-4060.

(331) Makhoul, R.; Sahnoune, H.; Dorcet, V.; Halet, J.-F.; Hamon, J.-R.; Lapinte, C. 1, 2-Diethynylbenzene-Bridged [Cp*(dppe) Fe]$^{n+}$ Units: Effect of Steric Hindrance on the Chemical and Physical Properties. *Organometallics* **2015**, *34*, 3314-3326.
(332) Malvolti, F.; Rouxel, C. d.; Triadon, A. d. e.; Grelaud, G.; Richy, N.; Mongin, O.; Blanchard-Desce, M.; Toupet, L.; Razak, F. I. A.; Stranger, R. 2, 7-Fluorenediyl-Bridged Complexes Containing Electroactive "Fe (η^5-C_5Me_5)(κ^2-dppe) C≡C–" End Groups: Molecular Wires and Remarkable Nonlinear Electrochromes. *Organometallics* **2015**, *34*, 5418-5437.
(333) Pfaff, U.; Hildebrandt, A.; Korb, M.; Schaarschmidt, D.; Rosenkranz, M.; Popov, A.; Lang, H. Five-Membered Heterocycles as Linking Units in Strongly Coupled Homobimetallic Group 8 Metal Half-Sandwich Complexes. *Organometallics* **2015**, *34*, 2826-2840.
(334) Burgun, A.; Gendron, F.; Sumby, C. J.; Roisnel, T.; Cador, O.; Costuas, K.; Halet, J.-F.; Bruce, M. I.; Lapinte, C. Hexatriynediyl Chain Spanning Two Cp*(dppe) M Termini (M= Fe, Ru): Evidence for the Dependence of Electronic and Magnetic Couplings on the Relative Orientation of the Termini. *Organometallics* **2014**, *33*, 2613-2627.
(335) Lohan, M.; Justaud, F. d. r.; Lang, H.; Lapinte, C. Synthesis, Spectroelectrochemical, and EPR Spectroscopic Studies of Mixed Bis (alkynyl) biferrocenes of the Type ($L_nMC{\equiv}C$)($L_nM'C{\equiv}C$)bfc. *Organometallics* **2012**, *31*, 3565-3574.
(336) Zhang, D. B.; Wang, J. Y.; Wen, H. M.; Chen, Z. N. Electrochemical, Spectroscopic, and Theoretical Studies on Diethynyl Ligand Bridged Ruthenium Complexes with 1,3-Bis(2-pyridylimino) isoindolate. *Organometallics* **2014**, *33*, 4738-4746.
(337) Zhang, J.; Zhang, M.-X.; Sun, C.-F.; Xu, M.; Hartl, F. e.; Yin, J.; Yu, G.-A.; Rao, L.; Liu, S. H. Diruthenium Complexes with Bridging Diethynyl Polyaromatic Ligands: Synthesis, Spectroelectrochemistry, and Theoretical Calculations. *Organometallics* **2015**, *34*, 3967-3978.
(338) Ou, Y.-P.; Zhang, J.; Zhang, F.; Kuang, D.; Hartl, F.; Rao, L.; Liu, S. H. Notable Differences between Oxidized Diruthenium Complexes Bridged by four Isomeric Diethynyl Benzodithiophene Ligands. *Dalton Trans.* **2016**, *45*, 6503-6516.
(339) Wang, X.; You, X.; Shang, Z.-P.; Xia, J. Synthesis, Crystal structure and Electronic Properties of 3.3 Metaparacyclophane-Bridged Bimetallic Ruthenium Alkynyl Complexes. *J. Organomet. Chem.* **2016**, *803*, 111-118.
(340) Savchenko, J.; Cao, Z.; Natoli, S. N.; Cummings, S. P.; Prentice, B. M.; Fanwick, P. E.; Ren, T. New Diruthenium Bis-alkynyl Compounds as Potential Ditopic Linkers. *Organometallics* **2013**, *32*, 6461-6467.
(341) Cai, X.-M.; Zhang, X.-Y.; Savchenko, J.; Cao, Z.; Ren, T.; Zuo, J.-L. New Linear π-Conjugated Diruthenium Compounds Containing Axial Tetrathiafulvalene-acetylide Ligands. *Organometallics* **2012**, *31*, 8591-8597.
(342) Cao, Z.; Xi, B.; Jodoin, D. S.; Zhang, L.; Cummings, S. P.; Gao, Y.; Tyler, S. F.; Fanwick, P. E.; Crutchley, R. J.; Ren, T. Diruthenium–Polyyn-diyl–Diruthenium Wires: Electronic Coupling in the Long Distance Regime. *J. Am. Chem. Soc.* **2014**, *136*, 12174-12183.
(343) Khan, M. S.; Davies, S. J.; Kakkar, A. K.; Schwartz, D.; Lin, B.; Johnson, B. F. G.; Lewis, J. Synthesis of Monomeric, Oligomeric and Polymeric σ-Acetylide Complexes of Platinum, Palladium, Nickel and Rhodium. *J. Organomet. Chem.* **1992**, *424*, 87-97.
(344) Khan, M. S.; Pasha, N. A.; Kakkar, A. K.; Raithby, P. R.; Lewis, J.; Fuhrmann, K.; Friend, R. H. Synthesis and Optical Spectroscopy of Monomeric and Polymeric Cobalt σ-Acetylide Complexes. *J. Mater. Chem.* **1992**, *2*, 759-760.
(345) Steffen, A.; Ward, R. M.; Tay, M. G.; Edkins, R. M.; Seeler, F.; van Leeuwen, M.; Palsson, L. O.; Beeby, A.; Batsanov, A. S.; Howard, J. A.; et al. Regiospecific Formation and Unusual Optical Properties of 2,5-Bis(arylethynyl)rhodacyclopentadienes: A New Class of Luminescent Organometallics. *Chemistry* **2014**, *20*, 3652-3666.
(346) Cook, T. D.; Fanwick, P. E.; Ren, T. Unsymmetric Mononuclear and Bridged Dinuclear CoIII(cyclam) Acetylides. *Organometallics* **2014**, *33*, 4621-4626.
(347) Banziger, S. D.; Cook, T. D.; Natoli, S. N.; Fanwick, P. E.; Ren, T. Synthetic and Structural Studies of Mono-Acetylide and Unsymmetric Bis-acetylide Complexes Based on Co III-cyclam. *J. Organomet. Chem.* **2015**, *799*, 1-6.
(348) Cook, T. D.; Natoli, S. N.; Fanwick, P. E.; Ren, T. Dimeric Complexes of Co^{III}(cyclam) with a Polyynediyl Bridge. *Organometallics* **2015**, *34*, 686-689.

(349) Cook, T. D.; Natoli, S. N.; Fanwick, P. E.; Ren, T. Co^{III}(cyclam) Oligoynyls: Monomeric Oligoynyl Complexes and Dimeric Complexes with an Oligoyn-diyl Bridge. *Organometallics* **2016**, *35*, 1329-1338.
(350) Hoffert, W. A.; Kabir, M. K.; Hill, E. A.; Mueller, S. M.; Shores, M. P. Stepwise Acetylide Ligand Substitution for the Assembly of Ethynylbenzene-linked Co(III) Complexes. *Inorg. Chim. Acta* **2012**, *380*, 174-180.
(351) Thakker, P. U.; Aru, R. G.; Sun, C.; Pennington, W. T.; Siegfried, A. M.; Marder, E. C.; Wagenknecht, P. S. Synthesis of trans Bis-Alkynyl Complexes of Co (III) Supported by a Tetradentate Macrocyclic Amine: A Spectroscopic, Structural, and Electrochemical Analysis of π-Interactions and Electronic Communication in the C≡C-M-C≡C structural unit. *Inorg. Chim. Acta* **2014**, *411*, 158-164.
(352) Sun, C.; Thakker, P. U.; Khulordava, L.; Tobben, D. J.; Greenstein, S. M.; Grisenti, D. L.; Kantor, A. G.; Wagenknecht, P. S. Trifluoropropynyl as a Surrogate for the Cyano Ligand and Intense, Room-Temperature, Metal-Centered Emission from Its Rh(III) Complex. *Inorg. Chem.* **2012**, *51*, 10477-10479.
(353) Steffen, A.; Tay, M. G.; Batsanov, A. S.; Howard, J. A. K.; Beeby, A.; Vuong, K. Q.; Sun, X. Z.; George, M. W.; Marder, T. B. 2,5-Bis(p-R-arylethynyl)rhodacyclopentadienes Show Intense Fluorescence: Denying the Presence of a Heavy Atom. *Angew. Chem. Int. Ed.* **2010**, *49*, 2349-2353.
(354) Sieck, C.; Tay, M. G.; Thibault, M. H.; Edkins, R. M.; Costuas, K.; Halet, J. F.; Batsanov, A. S.; Haehnel, M.; Edkins, K.; Lorbach, A. Reductive Coupling of Diynes at Rhodium Gives Fluorescent Rhodacyclopentadienes or Phosphorescent Rhodium 2,2'-Biphenyl Complexes. *Chem. Eur. J.* **2016**, *22*, 10523-10532.
(355) Steffen, A.; Costuas, K.; Boucekkine, A.; Thibault, M. H.; Beeby, A.; Batsanov, A. S.; Charaf-Eddin, A.; Jacquemin, D.; Halet, J. F.; Marder, T. B. Fluorescence in Rhoda- and Iridacyclopentadienes Neglecting the Spin-Orbit Coupling of the Heavy Atom: the Ligand Dominates. *Inorg. Chem.* **2014**, *53*, 7055-7069.
(356) Tong, G. S. M.; Chow, P. K.; Che, C. M. Where is the Heavy- Atom Effect? Role of the Central Ligand in Tetragold (I) Ethynyl Complexes. *Angew. Chem. Int. Ed.* **2010**, *49*, 9206-9209.
(357) Fernández-Cestau, J.; Giménez, N.; Lalinde, E.; Montaño, P.; Moreno, M. T.; Sánchez, S. Synthesis, Characterization, and Properties of Doubly Alkynyl Bridging Dinuclear Cyclometalated Iridium(III) Complexes. *Organometallics* **2015**, *34*, 1766-1778.
(358) Fernández-Cestau, J.; Giménez, N.; Lalinde, E.; Montaño, P.; Moreno, M. T.; Sánchez, S.; Weber, M. D.; Costa, R. D. Alkynyl bridged cyclometalated Ir_2M_2 clusters: impact of the heterometal in the photo-and electro-luminescence properties. *Dalton Trans.* **2016**, *45*, 3251-3255.
(359) Obara, S.; Itabashi, M.; Okuda, F.; Tamaki, S.; Tanabe, Y.; Ishii, Y.; Nozaki, K.; Haga, M.-a. Highly Phosphorescent Iridium Complexes Containing both Tridentate Bis (benzimidazolyl)-Benzene or-Pyridine and Bidentate Phenylpyridine: Synthesis, Photophysical Properties, and Theoretical Study of Ir-Bis (benzimidazolyl) Benzene Complex. *Inorg. Chem.* **2006**, *45*, 8907-8921.
(360) Fu, J.-Z.; Zhang, X.; Wang, J.-Y.; Zhang, L.-Y.; Chen, Z.-N. Syntheses and Photophysical Properties of Cyclometallated Iridium(III) Acetylide Complexes. *Inorg. Chem. Commun.* **2012**, *22*, 123-125.
(361) Wang, Y.-M.; Teng, F.; Gan, L.-h.; Liu, H.-M.; Zhang, X.-H.; Fu, W.-F.; Wang, Y.-S.; Xu, X.-R. Blue Light-Emitting Bisorthometalated Ir(III) Complex: Origin of Blue Emission and Application in Electrophosphorescent Devices. *J. Phys. Chem. C* **2008**, *112*, 4743-4747.
(362) del Rio, M. P.; Lopez, J. A.; Ciriano, M. A.; Tejel, C. Connecting C Identical with C Bonds to Tetrairidium Chains. *Chemistry* **2013**, *19*, 4707-4711.
(363) Mauro, M.; Aliprandi, A.; Septiadi, D.; Kehr, N. S.; De Cola, L. When Self-Assembly Meets Biology: Luminescent Platinum Complexes for Imaging Applications. *Chem. Soc. Rev.* **2014**, *43*, 4144-4166.
(364) Yam, V. W. Behind Platinum's Sparkle. *Nat. Chem.* **2010**, *2*, 790.
(365) La Groia, A.; Ricci, A.; Bassetti, M.; Masi, D.; Bianchini, C.; Sterzo, C. L. Preparation of Models and Oligomers of Metal Alkynyls: NMR, GPC and X-ray Structural Characterization of Building Blocks for the Construction of Molecular Devices. *J. Organomet. Chem.* **2003**, *683*, 406-420.

(366) Masai, H.; Sonogashira, K.; Hagihara, N. Electronic Spectra of Square-Planar Bis (tertiary phosphine) Dialkynyl Complexes of Nickel(II), Palladium(II), and Platinum(II). *Bull. Chem. Soc. Jpn.* **1971**, *44*, 2226-2230.
(367) Ogawa, H.; Onitsuka, K.; Joh, T.; Takahashi, S.; Yamamoto, Y.; Yamazaki, H. Synthesis, Characterization, and Molecular Structure of. mu.-ethynediyl Complexes [X(PR_3)MC. ident. CM (PR_3) 2X](M= Pd, Pt; R= Me, Et, n-Bu; X= Cl, I). *Organometallics* **1988**, *7*, 2257-2260.
(368) Haas, T.; Kaspar, K.; Forner, K.; Drexler, M.; Fischer, H. Nickel Alkynyl and Allenylidene Complexes: Synthesis and Properties. *J. Organomet. Chem.* **2011**, *696*, 946-955.
(369) Tyler, S. F.; Natoli, S. N.; Vlaisavljevich, B.; Fanwick, P. E.; Ren, T. Turning a New Leaf on Metal-TMC Chemistry: Ni^{II}(TMC) Acetylides. *Inorg. Chem.* **2015**, *54*, 10058-10064.
(370) Zhang, Y.; Garg, J. A.; Michelin, C.; Fox, T.; Blacque, O.; Venkatesan, K. Synthesis and Luminescent Properties of cis bis-N-Heterocyclic Carbene Platinum(II) Bis-arylacetylide Complexes. *Inorg. Chem.* **2011**, *50*, 1220-1228.
(371) Braddock-Wilking, J.; Acharya, S.; Rath, N. P. Bis (alkynyl) PTA and DAPTA complexes of Pt(II) and Pd(II). *Polyhedron* **2015**, *87*, 55-62.
(372) Smeyanov, A.; Namyslo, J. C.; Hübner, E.; Nieger, M.; Schmidt, A. Synthesis, Characterization and Palladium Complex Formation of Pyridinium- and Quinolinium-3-Acetylides: Mesomeric Betaines or Betaine-Stabilized Carbenes? *Tetrahedron* **2015**, *71*, 6665-6671.
(373) Asay, M.; Donnadieu, B.; Schoeller, W. W.; Bertrand, G. Synthesis of Allenylidene Lithium and Silver Complexes, and Subsequent Transmetalation Reactions. *Angew. Chem. Int. Ed. Engl.* **2009**, *48*, 4796-4799.
(374) Figueira, J.; Czardybon, W.; Mesquita, J. C.; Rodrigues, J.; Lahoz, F.; Russo, L.; Valkonen, A.; Rissanen, K. Synthesis, Characterization and Solid-State Photoluminescence Studies of Six Alkoxy Phenylene Ethynylene Dinuclear Palladium(II) Rods. *Dalton Trans.* **2015**, *44*, 4003-4015.
(375) Tao, C.-H.; Zhu, N.; Yam, V. W.-W. Synthesis, Characterisation and Luminescence Properties of Carbazole-Containing Platinum(II) and Palladium(II) Alkynyl Complexes. *J. Photochem. Photobiol., A* **2009**, *207*, 94-101.
(376) Ho, C.-L.; Wong, W.-Y. Synthesis, Structures and Photoluminescence Behavior of Some Group 10 Metal Alkynyl Complexes Derived from 3-(N-carbazolyl)-1-propyne. *J. Organomet. Chem.* **2006**, *691*, 395-402.
(377) Wing-WahYam, V.; Zhang, L.; Tao, C.-H.; Man-Chung Wong, K.; Cheung, K.-K. Synthesis and Structural Characterisation of Luminescent Di-and Tri-nuclear Palladium(II) Acetylide Complexes as Building Blocks for Metallodendrimers. *J. Chem. Soc., Dalton Trans.* **2001**, 1111-1116.
(378) Yam, V. W.-W.; Tao, C.-H.; Zhang, L.; Wong, K. M.-C.; Cheung, K.-K. Synthesis, Structural Characterization, and Luminescence Properties of Branched Palladium(II) and Platinum(II) Acetylide Complexes. *Organometallics* **2001**, *20*, 453-459.
(379) D'Amato, R.; Fratoddi, I.; Cappotto, A.; Altamura, P.; Delfini, M.; Bianchetti, C.; Bolasco, A.; Polzonetti, G.; Russo, M. V. Organometallic Platinum(II) and Palladium(II) Polymers Containing 2, 6-Diethynyl-4-nitroaniline Bridging Spacer and Related Dinuclear Model Complexes. *Organometallics* **2004**, *23*, 2860-2869.
(380) Chong, S. H.-F.; Lam, S. C.-F.; Yam, V. W.-W.; Zhu, N.; Cheung, K.-K.; Fathallah, S.; Costuas, K.; Halet, J.-F. Luminescent Heterometallic Branched Alkynyl Complexes of Rhenium(I)−Palladium(II): Potential Building Blocks for Heterometallic Metallodendrimers. *Organometallics* **2004**, *23*, 4924-4933.
(381) Li, Y.; Winkel, R. W.; Weisbach, N.; Gladysz, J. A.; Schanze, K. S. Photophysics of Platinum Tetrayne Oligomers: Delocalization of Triplet Exciton. *J. Phys. Chem. A* **2014**, *118*, 10333-10339.
(382) Farley, R. T.; Zheng, Q.; Gladysz, J. A.; Schanze, K. S. Photophysics of Diplatinum Polyynediyl Oligomers: Chain Length Dependence of the Triplet State in sp Carbon Chains. *Inorg. Chem.* **2008**, *47*, 2955-2963.
(383) Keller, J. M.; Schanze, K. S. Synthesis of Monodisperse Platinum Acetylide Oligomers End-Capped with Naphthalene Diimide Units. *Organometallics* **2009**, *28*, 4210-4216.
(384) Khan, M. S.; Al-Mandhary, M. R.; Al-Suti, M. K.; Al-Battashi, F. R.; Al-Saadi, S.; Ahrens, B.; Bjernemose, J. K.; Mahon, M. F.; Raithby, P. R.; Younus, M.; et al. Synthesis, Characterisation and Optical Spectroscopy of Platinum(II) Di-ynes and Poly-ynes Incorporating Condensed Aromatic Spacers in the Backbone. *Dalton Trans.* **2004**, doi :10.1039/B405070C, 2377-2385.

(385) Köhler, A.; Younus, M.; Al-Mandhary, M. R. A.; Raithby, P. R.; Khan, M. S.; Friend, R. H. Donor-Acceptor Interactions in Organometallic and Organic poly-ynes. *Synth. Met.* **1999**, *101*, 246-247.
(386) Khan, M. S.; Al-Suti, M. K.; Al-Mandhary, M. R. A.; Ahrens, B.; Bjernemose, J. K.; Mahon, M. F.; Male, L.; Raithby, P. R.; Friend, R. H.; Köhler, A. Synthesis and Characterisation of New Acetylide-Functionalised Aromatic and Hetero-aromatic Ligands and Their Dinuclear Platinum Complexes. *Dalton Trans.* **2003**, 1, 65-73.
(387) Wilson, J. S.; Dhoot, A. S.; Seeley, A. J.; Khan, M. S.; Kohler, A.; Friend, R. H. Spin-Dependent Exciton Formation in π-Conjugated Compounds. *Nature* **2001**, *413*, 828-831.
(388) Miyagi, Y.; Shibutani, Y.; Otaki, Y.; Sanda, F. Synthesis of Platinum-containing Poly (phenyleneethynylene) s having Various Chromophores: Aggregation and Optical Properties. *Polym. Chem.* **2016**, 7, 1070-1078.
(389) Li, Y.; Kose, M. E.; Schanze, K. S. Intramolecular Triplet Energy Transfer in Anthracene-Based Platinum Acetylide Oligomers. *J. Phys. Chem. B* **2013**, *117*, 9025-9033.
(390) Cekli, S.; Winkel, R. W.; Alarousu, E.; Mohammed, O. F.; Schanze, K. S. Triplet Excited State Properties in Variable Gap π-Conjugated Donor–Acceptor–Donor Chromophores. *Chem. Sci.* **2016**, *7*, 3621-3631.
(391) Cekli, S.; Winkel, R. W.; Schanze, K. S. Effect of Oligomer Length on Photophysical Properties of Platinum Acetylide Donor-Acceptor-Donor Oligomers. *J. Phys. Chem. A* **2016**, *120*, 5512-5521.
(392) Li, J.; Zhang, Q. Linearly Fused Azaacenes: Novel Approaches and New Applications Beyond Field-Effect Transistors (FETs). *ACS Appl. Mater. Interfaces* **2015**, *7*, 28049-28062.
(393) Nguyen, M.-H.; Nguyen, V. H.; Yip, J. H. Sequence-Specific Synthesis of Platinum-Conjugated Trichromophoric Energy Cascades of Anthracene, Tetracene, and Pentacene and Fluorescent "Black Chromophores". *Organometallics* **2013**, *32*, 7283-7291.
(394) Fudickar, W.; Linker, T. Why Triple Bonds Protect Acenes from Oxidation and Decomposition. *J. Am. Chem. Soc.* **2012**, *134*, 15071-15082.
(395) Biegger, P.; Tverskoy, O.; Rominger, F.; Bunz, U. H. Synthesis of Triptycene-Substituted Azapentacene and Azahexacene Derivatives. *Chemistry* **2016**, *22*, 16315-16322.
(396) Hahn, S.; Geyer, F. L.; Koser, S.; Tverskoy, O.; Rominger, F.; Bunz, U. H. Bent N-Heteroarenes. *J. Org. Chem.* **2016**, *81*, 8485-8494.
(397) Nguyen, M.-H.; Wong, C.-Y.; Yip, J. H. Ligand Perturbations on Fluorescence of Dinuclear Platinum Complexes of 5, 12-Diethynyltetracene: A Spectroscopic and Computational Study. *Organometallics* **2013**, *32*, 1620-1629.
(398) Nguyen, M.-H.; Yip, J. H. K. Pushing Pentacene-Based Fluorescence to the Near-Infrared Region by Platination. *Organometallics* **2011**, *30*, 6383-6392.
(399) Lin, C.-J.; Chen, C.-Y.; Kundu, S. K.; Yang, J.-S. Unichromophoric Platinum-Acetylides that Contain Pentiptycene Scaffolds: Torsion-Induced Dual Emission and Steric Shielding of Dynamic Quenching. *Inorg. Chem.* **2014**, *53*, 737-745.
(400) Al-Balushi, R. A.; Haque, A.; Jayapal, M.; Al-Suti, M. K.; Husband, J.; Khan, M. S.; Koentjoro, O. F.; Molloy, K. C.; Skelton, J. M.; Raithby, P. R. Experimental and Theoretical Investigation for the Level of Conjugation in Carbazole-Based Precursors and Their Mono-, Di-, and Polynuclear Pt(II) Complexes. *Inorg. Chem.* **2016**, *55*, 6465-6480.
(401) Miyagi, Y.; Shibutani, Y.; Otaki, Y.; Sanda, F. Synthesis of Platinum-containing Poly(phenylene ethynylene)s Having Various Chromophores: Aggregation and Optical properties. *Polym. Chem.* **2016**, *7*, 1070-1078.
(402) Roncali, J. Conjugated Poly(thiophenes): Synthesis, Functionalization, and Applications. *Chem. Rev.* **1992**, *92*, 711-738.
(403) Cinar, M. E.; Ozturk, T. Thienothiophenes, Dithienothiophenes, and Thienoacenes: Syntheses, Oligomers, Polymers, and Properties. *Chem. Rev.* **2015**, *115*, 3036-3140.
(404) Wong, H. L.; Tao, C. H.; Zhu, N.; Yam, V. W. Photochromic Alkynes as Versatile Building Blocks for Metal Alkynyl Systems: Design, Synthesis, and Photochromic Studies of Diarylethene-containing Platinum(II) Phosphine Alkynyl Complexes. *Inorg. Chem.* **2011**, *50*, 471-481.
(405) Li, B.; Wen, H.-M.; Wang, J.-Y.; Shi, L.-X.; Chen, Z.-N. Multistate and Multicolor Photochromism through Selective Cycloreversion in Asymmetric Platinum(II) Complexes with Two Different Dithienylethene–Acetylides. *Inorg. Chem.* **2015**, *54*, 11511-11519.
(406) Brayshaw, S. K.; Schiffers, S.; Stevenson, A. J.; Teat, S. J.; Warren, M. R.; Bennett, R. D.; Sazanovich, I. V.; Buckley, A. R.; Weinstein, J. A.; Raithby, P. R. Highly Efficient Visible- Light

Driven Photochromism: Developments towards a Solid- State Molecular Switch Operating through a Triplet- Sensitised Pathway. *Chem. Eur. J.* **2011**, *17*, 4385-4395.
(407) Al-Balushi, R. A.; Haque, A.; Jayapal, M.; Al-Suti, M. K.; Husband, J.; Khan, M. S.; Skelton, J. M.; Molloy, K. C.; Raithby, P. R. Impact of the Alkyne Substitution Pattern and Metalation on the Photoisomerization of Azobenzene-Based Platinum(II) Diynes and Polyynes. *Inorg. Chem.* **2016**, *55*, 10955-10967.
(408) Xu, X. D.; Zhang, J.; Chen, L. J.; Zhao, X. L.; Wang, D. X.; Yang, H. B. Large- Scale Honeycomb Microstructures Constructed by Platinum–Acetylide Gelators through Supramolecular Self-Assembly. *Chem. Eur. J.* **2012**, *18*, 1659-1667.
(409) Haskins-Glusac, K.; Ghiviriga, I.; Abboud, K. A.; Schanze, K. S. Photophysics and Photochemistry of Stilbene-containing Platinum Acetylides. *J. Phys. Chem. B* **2004**, *108*, 4969-4978.
(410) Jia, H.; Küçüköz, B.; Xing, Y.; Majumdar, P.; Zhang, C.; Karatay, A.; Yaglioglu, G.; Elmali, A.; Zhao, J.; Hayvali, M. trans-Bis(alkylphosphine) Platinum(II)-Alkynyl Complexes Showing Broadband Visible Light Absorption and Long-lived Triplet Excited States. *J. Mater. Chem. C* **2014**, *2*, 9720-9736.
(411) Yang, W.; Karatay, A.; Zhao, J.; Song, J.; Zhao, L.; Xing, Y.; Zhang, C.; He, C.; Yaglioglu, H. G.; Hayvali, M.; et al. Near-IR Broadband-Absorbing trans-Bisphosphine Pt(II) Bisacetylide Complexes: Preparation and Study of the Photophysics. *Inorg. Chem.* **2015**, *54*, 7492-7505.
(412) Zhong, F.; Karatay, A.; Zhao, L.; Zhao, J.; He, C.; Zhang, C.; Yaglioglu, H. G.; Elmali, A.; Kucukoz, B.; Hayvali, M. Broad-Band N^N Pt(II) Bisacetylide Visible Light Harvesting Complex with Heteroleptic Bodipy Acetylide Ligands. *Inorg. Chem.* **2015**, *54*, 7803-7817.
(413) Geist, F.; Jackel, A.; Irmler, P.; Linseis, M.; Malzkuhn, S.; Kuss-Petermann, M.; Wenger, O. S.; Winter, R. F. Directing Energy Transfer in Panchromatic Platinum Complexes for Dual Vis–Near-IR or Dual Visible Emission from σ-Bonded BODIPY Dyes. *Inorg. Chem.* **2016**, *56*, 914-930.
(414) Zhan, X.; Facchetti, A.; Barlow, S.; Marks, T. J.; Ratner, M. A.; Wasielewski, M. R.; Marder, S. R. Rylene and Related Diimides for Organic Electronics. *Adv. Mater.* **2011**, *23*, 268-284.
(415) Mishra, A.; Bauerle, P. Small Molecule Organic Semiconductors on the Move: Promises for Future Solar Energy Technology. *Angew. Chem. Int. Ed. Engl.* **2012**, *51*, 2020-2067.
(416) Llewellyn, B. A.; Slater, A. G.; Goretzki, G.; Easun, T. L.; Sun, X. Z.; Davies, E. S.; Argent, S. P.; Lewis, W.; Beeby, A.; George, M. W.; et al. Photophysics and Electrochemistry of a Platinum-Acetylide Disubstituted Perylenediimide. *Dalton Trans.* **2014**, *43*, 85-94.
(417) Lee, S.-H.; Chan, C. T.-L.; Wong, K. M.-C.; Lam, W. H.; Kwok, W.-M.; Yam, V. W.-W. Synthesis and Photoinduced Electron Transfer in Platinum(II) Bis (N-(4-Ethynylphenyl) Carbazole) Bipyridine Fullerene Complexes. *Dalton Trans.* **2014**, *43*, 17624-17634.
(418) Zhang, R.-L.; Yang, Y.; Yang, S.-Q.; Neti, V. S. P. K.; Sepehrpour, H.; Stang, P. J.; Han, K.-L. Direct Observation of a Triplet-State Absorption-Emission Conversion in a Fullerene-Functionalized Pt (II) Metallacycle. *J. Phys. Chem. C* **2017**, *121*, 14975-14980.
(419) Fratoddi, I.; Battocchio, C.; Furlani, A.; Mataloni, P.; Polzonetti, G.; Russo, M. V. Study of Chemical Structure and Conjugation Length in Organometallic Pt(II) Oligomers and Polymers Containing 1,4-Diethynylbenzene Derivatives as Bridging Units. *J. Organomet. Chem.* **2003**, *674*, 10-23.
(420) Aly, S. M.; Ho, C.-L.; Wong, W.-Y.; Fortin, D.; Harvey, P. D. Intrachain Electron and Energy Transfers in Metal Diynes and Polyynes of Group 10− 11 Transition Elements Containing Various Carbazole and Fluorene Hybrids. *Macromolecules* **2009**, *42*, 6902-6916.
(421) Khan, M. S.; Al-Mandhary, M. R. A.; Al-Suti, M. K.; Ahrens, B.; Mahon, M. F.; Male, L.; Raithby, P. R.; Boothby, C. E.; Köhler, A. Synthesis, Characterisation and Optical Spectroscopy of Diynes and Poly-ynes Containing Derivatised Fluorenes in the Backbone. *Dalton Trans.* **2003**, *0*, 74-84.
(422) Liu, L.; Wong, W.-Y.; Poon, S.-Y.; Shi, J.-X.; Cheah, K.-W.; Lin, Z. Effect of Acetylenic Chain Length on the Tuning of Functional Properties in Fluorene-Bridged Polymetallaynes and Their Molecular Model Compounds. *Chem. Mater.* **2006**, *18*, 1369-1378.
(423) Wong, W.-Y.; Liu, L.; Poon, S.-Y.; Choi, K.-H.; Cheah, K.-W.; Shi, J.-X. Harvesting of Organic Triplet Emissions in Metal Diynes and Polyynes of Group 10-12 Transition Elements Containing the Conjugation-interrupting Diphenylfluorene Unit. *Macromolecules* **2004**, *37*, 4496-4504.
(424) Zhang, N.; Hayer, A.; Al-Suti, M. K.; Al-Belushi, R. A.; Khan, M. S.; Kohler, A. The Effect of Delocalization on the exchange Energy in Meta- and Para-linked Pt-containing Carbazole Polymers and Monomers. *J. Chem. Phys.* **2006**, *124*, 244701-244710.

(425) Aly, S. M.; Ho, C. L.; Fortin, D.; Wong, W. Y.; Abd-El-Aziz, A. S.; Harvey, P. D. Intrachain Electron and Energy Transfer in Conjugated Organometallic Oligomers and Polymers. *Chemistry* **2008**, *14*, 8341-8352.
(426) Ho, C.-L.; Poon, S.-Y.; Lo, P.-K.; Wong, M.-S.; Wong, W.-Y. Synthesis, Characterization and Photophysical Properties of Metallopolyynes and Metallodiynes of Platinum(II) with Dibenzothiophene Derivatives. *J. Inorg. Organomet. Polym Mater.* **2013**, *23*, 206-215.
(427) Köhler, A.; Wilson, J. S.; Friend, R. H.; Al-Suti, M. K.; Khan, M. S.; Gerhard, A.; Bässler, H. The Singlet–triplet Energy Gap in Organic and Pt-containing Phenylene Ethynylene Polymers and Monomers. *J. Chem. Phys.* **2002**, *116*, 9457-9463.
(428) Chawdhury, N.; Kohler, A.; Friend, R. H.; Wong, W. Y.; Lewis, J.; Younus, M.; Raithby, P. R.; Corcoran, T. C.; Al-Mandhary, M. R. A.; Khan, M. S. Evolution of Lowest Singlet and Triplet Excited States with Number of Thienyl Rings in Platinum Poly-ynes. *J. Chem. Phys.* **1999**, *110*, 4963-4970.
(429) Mahrok, A. K.; Carrera, E. I.; Tilley, A. J.; Ye, S.; Seferos, D. S. Synthesis and Photophysical Properties of Platinum-Acetylide Copolymers with Thiophene, Selenophene and Tellurophene. *Chem. Commun. (Camb)* **2015**, *51*, 5475-5478.
(430) Liang, T.; Xiao, L.; Liu, C.; Gao, K.; Qin, H.; Cao, Y.; Peng, X. Porphyrin Small Molecules Containing Furan- and Selenophene-substituted Diketopyrrolopyrrole for Bulk Heterojunction Organic Solar Cells. *Org. Electron.* **2016**, *29*, 127-134.
(431) Sudha Devi, L.; Al-Suti, M. K.; Zhang, N.; Teat, S. J.; Male, L.; Sparkes, H. A.; Raithby, P. R.; Khan, M. S.; Koʇˆhler, A. Synthesis and Comparison of the Optical Properties of Platinum(II) Poly-ynes with Fused and Non-Fused Oligothiophenes. *Macromolecules* **2009**, *42*, 1131-1141.
(432) Li, P.; Ahrens, B.; Feeder, N.; Raithby, P. R.; Teat, S. J.; Khan, M. S. Luminescent Digold Ethynyl Thienothiophene and Dithienothiophene Complexes; Their Synthesis and Structural Characterisation. *Dalton Trans.* **2005**, doi:10.1039/b415965a.
(433) Lewis, J.; Long, N. J.; Raithby, P. R.; Shields, G. P.; Wong, W.-Y.; Younus, M. Synthesis and Characterisation of New Acetylide-functionalised Oligothiophenes and Their Dinuclear Platinum Complexes. *J. Chem. Soc., Dalton Trans.* **1997**, 4283-4288.
(434) Khan, M. S.; Al-Suti, M. K.; Shah, H. H.; Al-Humaimi, S.; Al-Battashi, F. R.; Bjernemose, J. K.; Male, L.; Raithby, P. R.; Zhang, N.; Kohler, A.; et al. Synthesis and Characterization of Platinum(II) Di-ynes and Poly-ynes Incorporating Ethylenedioxythiophene (EDOT) Spacers in the Backbone. *Dalton Trans.* **2011**, *40*, 10174-10183.
(435) Khan, M. S.; Al-Mandhary, M. R. A.; Al-Suti, M. K.; Hisahm, A. K.; Raithby, P. R.; Ahrens, B.; Mahon, M. F.; Male, L.; Marseglia, E. A.; Tedesco, E. Structural Characterisation of a Series of Acetylide-functionalised Oligopyridines and the Synthesis, Characterisation and Optical Spectroscopy of Platinum Di-ynes and Poly-ynes Containing Oligopyridyl Linker Groups in the Backbone. *J. Chem. Soc., Dalton Trans.* **2002**, *0*, 1358-1368
(436) Chawdhury, N.; Kohler, A.; Friend, R. H.; Younus, M.; Long, N. J.; Raithby, P. R.; Lewis, J. Synthesis and Electronic Structure of Platinum-containing Poly-ynes with Aromatic and Heteroaromatic Rings. *Macromolecules* **1998**, *31*, 722-727.
(437) Khan, M. S.; Al-Mandhary, M. R.; Al-Suti, M. K.; Feeder, N.; Nahar, S.; Köhler, A.; Friend, R. H.; Wilson, P. J.; Raithby, P. R. Synthesis, Characterisation and Electronic Properties of a Series of Platinum (II) Poly-ynes Containing Novel Thienyl-pyridine Linker Groups. *J. Chem. Soc., Dalton Trans.* **2002**, 2441-2448.
(438) Younus, M.; Kohler, A.; Cron, S.; Chawdhury, N.; Al-Mandhary, M. R. A.; Khan, M. S.; Lewis, J.; Long, N. J.; Friend, R. H.; Raithby, P. R. Synthesis, Electrochemistry, and Spectroscopy of Blue Platinum(II) Polyynes and Diynes. *Angew. Chem. Int. Ed. Engl.* **1998**, *37*, 3036-3039.
(439) Mei, J.; Ogawa, K.; Kim, Y.-G.; Heston, N. C.; Arenas, D. J.; Nasrollahi, Z.; McCarley, T. D.; Tanner, D. B.; Reynolds, J. R.; Schanze, K. S. Low-band-gap Platinum Acetylide Polymers as Active Materials for Organic Solar Cells. *ACS Appl. Mater. Interfaces* **2009**, *1*, 150-161.
(440) Wong, W.-Y.; Wang, X.-Z.; He, Z.; Djurišić, A. B.; Yip, C.-T.; Cheung, K.-Y.; Wang, H.; Mak, C. S.; Chan, W.-K. Metallated Conjugated Polymers as a New Avenue Towards High-efficiency Polymer Solar Cells. *Nat. Mater.* **2007**, *6*, 521-527.
(441) Wong, W.-Y.; Wang, X.; Zhang, H.-L.; Cheung, K.-Y.; Fung, M.-K.; Djurišić, A. B.; Chan, W.-K. Synthesis, Characterization and Photovoltaic Properties of a Low-Bandgap Platinum (II) Polyyne Functionalized with a 3, 4-Ethylenedioxythiophene-Benzothiadiazole Hybrid Spacer. *J. Organomet. Chem.* **2008**, *693*, 3603-3612.

(442) Wu, P.-T.; Bull, T.; Kim, F. S.; Luscombe, C. K.; Jenekhe, S. A. Organometallic Donor− Acceptor Conjugated Polymer Semiconductors: Tunable Optical, Electrochemical, Charge Transport, and Photovoltaic Properties. *Macromolecules* **2009**, *42*, 671-681.
(443) Zhan, H.; Wong, W.-Y.; Ng, A.; Djurišić, A. B.; Chan, W.-K. Synthesis, Characterization and Photovoltaic Properties of Platinum-containing Poly (aryleneethynylene) Polymers with Phenanthrenyl-imidazole Moiety. *J. Organomet. Chem.* **2011**, *696*, 4112-4120.
(444) Wong, W. Y.; Wang, X. Z.; He, Z.; Chan, K. K.; Djurisic, A. B.; Cheung, K. Y.; Yip, C. T.; Ng, A. M.; Xi, Y. Y.; Mak, C. S.; et al. Tuning the Absorption, Charge Transport Properties, and Solar Cell Efficiency with the Number of Thienyl Rings in Platinum-containing Poly(aryleneethynylene)s. *J. Am. Chem. Soc.* **2007**, *129*, 14372-14380.
(445) Wong, W. Y.; Zhou, G. J.; He, Z.; Cheung, K. Y.; Ng, A. M. C.; Djurišić, A. B.; Chan, W. K. Organometallic Polymer Light-Emitting Diodes Derived from a Platinum (II) Polyyne Containing the Bithiazole Ring. *Macromol. Chem. Phys.* **2008**, *209*, 1319-1332.
(446) Wang, Q.; Wong, W.-Y. New Low-bandgap Polymetallaynes of Platinum Functionalized with a Triphenylamine-benzothiadiazole Donor–Acceptor unit for Solar Cell Applications. *Polym. Chem.* **2011**, *2*, 432-440.
(447) Liu, L.; Ho, C. L.; Wong, W. Y.; Cheung, K. Y.; Fung, M. K.; Lam, W. T.; Djurišić, A. B.; Chan, W. K. Effect of Oligothienyl Chain Length on Tuning the Solar Cell Performance in Fluorene-Based Polyplatinynes. *Adv. Funct. Mater.* **2008**, *18*, 2824-2833.
(448) Qin, C.; Fu, Y.; Chui, C. H.; Kan, C. W.; Xie, Z.; Wang, L.; Wong, W. Y. Tuning the Donor–Acceptor Strength of Low-Bandgap Platinum-Acetylide Polymers for Near-Infrared Photovoltaic Applications. *Macromol. Rapid Commun.* **2011**, *32*, 1472-1477.
(449) Masai, H.; Terao, J.; Makuta, S.; Tachibana, Y.; Fujihara, T.; Tsuji, Y. Enhancement of Phosphorescence and Unimolecular Behavior in the Solid State by Perfect Insulation of Platinum-Acetylide Polymers. *J. Am. Chem. Soc.* **2014**, *136*, 14714-14717.
(450) Hosomi, T.; Masai, H.; Fujihara, T.; Tsuji, Y.; Terao, J. A Typical Metal-Ion-Responsive Color-Tunable Emitting Insulated pi-Conjugated Polymer Film. *Angew. Chem. Int. Ed. Engl.* **2016**, *55*, 13427-13431.
(451) Wong, W.-Y.; Liu, L.; Poon, S.-Y.; Choi, K.-H.; Cheah, K.-W.; Shi, J.-X. Harvesting of Organic Triplet Emissions in Metal Diynes and Polyynes of Group 10−12 Transition Elements Containing the Conjugation-Interrupting Diphenylfluorene Unit. *Macromolecules* **2004**, *37*, 4496-4504.
(452) Liu, L.; Wong, W.-Y.; Shi, J.-X.; Cheah, K.-W.; Lee, T.-H.; Leung, L. M. Synthesis, Spectroscopy, Structures and Photophysics of Metal Alkynyl Complexes and Polymers Containing Functionalized Carbazole Spacers. *J. Organomet. Chem.* **2006**, *691*, 4028-4041.
(453) Chawdhury, N.; Köhler, A.; Friend, R.; Wong, W.-Y.; Lewis, J.; Younus, M.; Raithby, P.; Corcoran, T.; Al-Mandhary, M.; Khan, M. Evolution of Lowest Singlet and Triplet Excited States with Number of Thienyl Rings in Platinum Poly-ynes. *J. Chem. Phys.* **1999**, *110*, 4963-4970.
(454) Sudha Devi, L.; Al-Suti, M. K.; Zhang, N.; Teat, S. J.; Male, L.; Sparkes, H. A.; Raithby, P. R.; Khan, M. S.; Köhler, A. Synthesis and Comparison of the Optical Properties of Platinum (II) Poly-ynes with Fused and Non-Fused Oligothiophenes. *Macromolecules* **2009**, *42*, 1131-1141.
(455) Khan, M. S.; Al-Mandhary, M. R. A.; Al-Suti, M. K.; Hisahm, A. K.; Raithby, P. R.; Ahrens, B.; Mahon, M. F.; Male, L.; Marseglia, E. A.; Tedesco, E.; et al. Structural Characterisation of a Series of Acetylide-functionalised Oligopyridines and the Synthesis, Characterisation and Optical Spectroscopy of Platinum Di-ynes and Poly-ynes Containing Oligopyridyl Linker Groups in the Backbone. *J. Chem. Soc., Dalton Trans.* **2002**, *0*, 1358-1368.
(456) Wong, W.-Y.; Wang, X.-Z.; He, Z.; Chan, K.-K.; Djurišić, A. B.; Cheung, K.-Y.; Yip, C.-T.; Ng, A. M.-C.; Xi, Y. Y.; Mak, C. S. Tuning the absorption, charge transport properties, and solar cell efficiency with the number of thienyl rings in platinum-containing poly (aryleneethynylene) s. *J. Am. Chem. Soc.***2007**, *129*, 14372-14380.
(457) Goeb, S.; Prusakova, V.; Wang, X.; Vezinat, A.; Salle, M.; Castellano, F. N. Phosphorescent Self-assembled Pt(II) Tetranuclear Metallocycles. *Chem. Commun. (Camb)* **2011**, *47*, 4397-4399.
(458) Liu, K.; Ho, C. L.; Aouba, S.; Zhao, Y. Q.; Lu, Z. H.; Petrov, S.; Coombs, N.; Dube, P.; Ruda, H. E.; Wong, W. Y. Synthesis and Lithographic Patterning of FePt Nanoparticles Using a Bimetallic Metallopolyyne Precursor. *Angew. Chem. Int. Ed.* **2008**, *47*, 1255-1259.

(459) Dong, Q.; Li, G.; Ho, C. L.; Faisal, M.; Leung, C. W.; Pong, P. W. T.; Liu, K.; Tang, B. Z.; Manners, I.; Wong, W. Y. A Polyferroplatinyne Precursor for the Rapid Fabrication of L10-FePt-type Bit Patterned Media by Nanoimprint Lithography. *Adv. Mater.* **2012**, *24*, 1034-1040.
(460) Kwok, E. C. H.; Chan, M. Y.; Wong, K. M. C.; Lam, W. H.; Yam, V. W. W. Functionalized Alkynylplatinum(II) Polypyridyl Complexes for Use as Sensitizers in Dye-Sensitized Solar Cells. *Chem. Eur. J.* **2010**, *16*, 12244-12254.
(461) Haque, A.; Ilmi, R.; Al-Busaidi, I. J.; Khan, M. S. Coordination Chemistry and Application of Mono- and Oligopyridine-based Macrocycles. *Coord. Chem. Rev.* **2017**, *350*, 320-339.
(462) Wong, K. M.-C.; Yam, V. W.-W. Luminescence Platinum (II) Terpyridyl Complexes—from Fundamental Studies to Sensory Functions. *Coord. Chem. Rev.* **2007**, *251*, 2477-2488.
(463) Adams, C. J.; James, S. L.; Raithby, P. R. Novel Pyridyl-stabilised Rigid-rod Organometallic Polymers and Their Monomeric Precursors. *Chem. Commun.* **1997**, DOI:DOI 10.1039/a706586h DOI 10.1039/a706586h, 2155-2156.
(464) Ho, P. Y.; Zheng, B.; Mark, D.; Wong, W. Y.; McCamant, D. W.; Eisenberg, R. Chromophoric Dyads for the Light-Driven Generation of Hydrogen: Investigation of Factors in the Design of Multicomponent Photosensitizers for Proton Reduction. *Inorg. Chem.* **2016**, *55*, 8348-8358.
(465) Chan, S. C.; Chan, M. C.; Wang, Y.; Che, C. M.; Cheung, K. K.; Zhu, N. Organic Light-emitting Materials Based on Bis(arylacetylide)platinum(II) Complexes Bearing Substituted Bipyridine and Phenanthroline Ligands: Photo- and Electroluminescence from ^{3}MLCT Excited States. *Chemistry* **2001**, *7*, 4180-4190.
(466) Hissler, M.; Connick, W. B.; Geiger, D. K.; McGarrah, J. E.; Lipa, D.; Lachicotte, R. J.; Eisenberg, R. Platinum Diimine Bis(acetylide) Complexes: Synthesis, Characterization, and Luminescence Properties. *Inorg. Chem.* **2000**, *39*, 447-457.
(467) Hua, F.; Kinayyigit, S.; Cable, J. R.; Castellano, F. N. Platinum(II) Diimine Diacetylides: Metallacyclization Enhances Photophysical Properties. *Inorg. Chem.* **2006**, *45*, 4304-4306.
(468) Li, Q.; Guo, H.; Ma, L.; Wu, W.; Liu, Y.; Zhao, J. Tuning the Photophysical Properties of N^N Pt(II) Bisacetylide Complexes with Fluorene Moiety and its Applications for Triplet–Triplet-Annihilation Based Upconversion. *J. Mater. Chem.* **2012**, *22*, 5319-5329.
(469) Zhang, X.-P.; Wu, T.; Liu, J.; Zhang, J.-X.; Li, C.-H.; You, X.-Z. Vapor-induced Chiroptical Switching in Chiral Cyclometalated Platinum (II) Complexes with Pinene Functionalized C^N^N Ligands. *J. Mater. Chem. C* **2014**, *2*, 184-194.
(470) Ni, J.; Zhang, L. Y.; Wen, H. M.; Chen, Z. N. Luminescence Vapochromic Properties of a Platinum (II) Complex with 5,5'-Bis(trimethylsilylethynyl)-2,2'-bipyridine. *Chem. Commun. (Camb)* **2009**, doi :10.1039/b901248f, 3801-3803.
(471) Ni, J.; Wang, Y.-G.; Wang, J.-Y.; Zhao, Y.-Q.; Pan, Y.-Z.; Wang, H.-H.; Zhang, X.; Zhang, J.-J.; Chen, Z.-N. A New Sensor for Detection of CH 3 CN and ClCH 2 CN Vapors Based on Vapoluminescent Platinum(II) Complex. *Dalton Trans.* **2013**, *42*, 13092-13100.
(472) Ni, J.; Wang, Y. G.; Wang, H. H.; Xu, L.; Zhao, Y. Q.; Pan, Y. Z.; Zhang, J. J. Thermo- and Mechanical-Grinding-Triggered Color and Luminescence Switches of the Diimine-Platinum(II) Complex with 4-Bromo-2,2'-Bipyridine. *Dalton Trans.* **2014**, *43*, 352-360.
(473) Ni, J.; Zhang, X.; Qiu, N.; Wu, Y. H.; Zhang, L. Y.; Zhang, J.; Chen, Z. N. Mechanochromic Luminescence Switch of Platinum(II) Complexes with 5-Trimethylsilylethynyl-2,2'-bipyridine. *Inorg. Chem.* **2011**, *50*, 9090-9096.
(474) Ni, J.; Zhang, X.; Wu, Y. H.; Zhang, L. Y.; Chen, Z. N. Vapor-and Mechanical-Grinding-Triggered Color and Luminescence Switches for Bis (σ-fluorophenylacetylide) Platinum(II) Complexes. *Chem. Eur. J.* **2011**, *17*, 1171-1183.
(475) Zhang, X.; Wang, J. Y.; Ni, J.; Zhang, L. Y.; Chen, Z. N. Vapochromic and Mechanochromic Phosphorescence Materials Based on a Platinum(II) Complex with 4-Trifluoromethyl phenylacetylide. *Inorg. Chem.* **2012**, *51*, 5569-5579.
(476) McGarrah, J. E.; Hupp, J. T.; Smirnov, S. N. Electron Transfer in Platinum(II) Diimine-centered Triads: Mechanistic Insights from Photoinduced Transient Displacement Current Measurements. *J. Phys. Chem. A* **2009**, *113*, 6430-6436.
(477) James, S. L.; Younus, M.; Raithby, P. R.; Lewis, J. Platinum Bis-acetylide Complexes with the 4, 4′-Dimethyl-2, 2′-bipyridyl Ligand. *J. Organomet. Chem.* **1997**, *543*, 233-235.

(478) Adams, C. J.; James, S. L.; Liu, X.; Raithby, P. R.; Yellowlees, L. J. Synthesis and Characterisation of New Platinum–Acetylide Complexes Containing Diimine Ligands. *J. Chem. Soc., Dalton Trans.* **2000**, 63-67.
(479) Hua, F.; Kinayyigit, S.; Cable, J. R.; Castellano, F. N. Green Photoluminescence from Platinum(II) Complexes Bearing Silylacetylide Ligands. *Inorg. Chem.* **2005**, *44*, 471-473.
(480) Hua, F.; Kinayyigit, S.; Rachford, A. A.; Shikhova, E. A.; Goeb, S.; Cable, J. R.; Adams, C. J.; Kirschbaum, K.; Pinkerton, A. A.; Castellano, F. N. Luminescent Charge-transfer Platinum(II) Metallacycle. *Inorg. Chem.* **2007**, *46*, 8771-8783.
(481) Pomestchenko, I. E.; Luman, C. R.; Hissler, M.; Ziessel, R.; Castellano, F. N. Room Temperature Phosphorescence from a Platinum(II) Diimine Bis(pyrenylacetylide) Complex. *Inorg. Chem.* **2003**, *42*, 1394-1396.
(482) Stengel, I.; Strassert, C. A.; De Cola, L.; Bäuerle, P. Tracking Intramolecular Interactions in Flexibly Linked Binuclear Platinum(II) Complexes. *Organometallics* **2014**, *33*, 1345-1355.
(483) Pomestchenko, I. E.; Castellano, F. N. Solvent Switching Between Charge Transfer and Intraligand Excited States in a Multichromophoric Platinum(II) Complex. *J. Phys. Chem. A* **2004**, *108*, 3485-3492.
(484) Connick, W. B.; Geiger, D.; Eisenberg, R. Excited-State Self-Quenching Reactions of Square Planar Platinum (II) Diimine Complexes in Room-Temperature Fluid Solution. *Inorg. Chem.* **1999**, *38*, 3264-3265.
(485) Whittle, C. E.; Weinstein, J. A.; George, M. W.; Schanze, K. S. Photophysics of Diimine Platinum (II) Bis-acetylide Complexes. *Inorg. Chem.* **2001**, *40*, 4053-4062.
(486) Chan, C.-W.; Cheng, L.-K.; Che, C.-M. Luminescent Donor-Acceptor Platinum(II) Complexes. *Coord. Chem. Rev.* **1994**, *132*, 87-97.
(487) Sazanovich, I. V.; Alamiry, M. A.; Best, J.; Bennett, R. D.; Bouganov, O. V.; Davies, E. S.; Grivin, V. P.; Meijer, A. J.; Plyusnin, V. F.; Ronayne, K. L.; et al. Excited State Dynamics of a Pt(II) Diimine Complex Bearing a Naphthalene-diimide Electron Acceptor. *Inorg. Chem.* **2008**, *47*, 10432-10445.
(488) McGarrah, J. E.; Kim, Y. J.; Hissler, M.; Eisenberg, R. Toward a Molecular Photochemical Device: a Triad for Photoinduced Charge Separation Based on a Platinum Diimine bis(acetylide) Chromophore. *Inorg. Chem.* **2001**, *40*, 4510-4511.
(489) Sazanovich, I. V.; Best, J.; Scattergood, P. A.; Towrie, M.; Tikhomirov, S. A.; Bouganov, O. V.; Meijer, A. J.; Weinstein, J. A. Ultrafast Photoinduced Charge Transport in Pt(II) Donor–Acceptor Assembly Bearing Naphthalimide Electron Acceptor and Phenothiazine Electron Donor. *PCCP* **2014**, *16*, 25775-25788.
(490) Yam, V. W.-W.; Tang, R. P.-L.; Wong, K. M.-C.; Cheung, K.-K. Synthesis, Luminescence, Electrochemistry, and Ion-binding Studies of Platinum(II) Terpyridyl Acetylide Complexes. *Organometallics* **2001**, *20*, 4476-4482.
(491) Castellano, F. N.; Pomestchenko, I. E.; Shikhova, E.; Hua, F.; Muro, M. L.; Rajapakse, N. Photophysics in Bipyridyl and Terpyridyl Platinum(II) Acetylides. *Coord. Chem. Rev.* **2006**, *250*, 1819-1828.
(492) Lu, W.; Mi, B. X.; Chan, M. C.; Hui, Z.; Che, C. M.; Zhu, N.; Lee, S. T. Light-Emitting Tridentate Cyclometalated Platinum(II) Complexes Containing Sigma-alkynyl Auxiliaries: Tuning of Photo- and Electrophosphorescence. *J. Am. Chem. Soc.* **2004**, *126*, 4958-4971.
(493) Shao, P.; Li, Y.; Azenkeng, A.; Hoffmann, M. R.; Sun, W. Influence of Alkoxyl Substituent on 4,6-Diphenyl-2,2'-bipyridine Ligand on Photophysics of Cyclometalated Platinum(II) Complexes: Admixing Intraligand Charge Transfer Character in Low-lying Excited States. *Inorg. Chem.* **2009**, *48*, 2407-2419.
(494) Yang, Q. Z.; Wu, L. Z.; Wu, Z. X.; Zhang, L. P.; Tung, C. H. Long-lived Emission from Platinum(II) Terpyridyl Acetylide Complexes. *Inorg. Chem.* **2002**, *41*, 5653-5655.
(495) Shikhova, E.; Danilov, E. O.; Kinayyigit, S.; Pomestchenko, I. E.; Tregubov, A. D.; Camerel, F.; Retailleau, P.; Ziessel, R.; Castellano, F. N. Excited-state Absorption Properties of Platinum(II) Terpyridyl Acetylides. *Inorg. Chem.* **2007**, *46*, 3038-3048.
(496) Muro, M. L.; Diring, S.; Wang, X.; Ziessel, R.; Castellano, F. N. Photophysics in Platinum(II) Bipyridylacetylides. *Inorg. Chem.* **2009**, *48*, 11533-11542.
(497) Rachford, A. A.; Goeb, S.; Ziessel, R.; Castellano, F. N. Ligand Localized Triplet Excited States in Platinum(II) Bipyridyl and Terpyridyl Peryleneacetylides. *Inorg. Chem.* **2008**, *47*, 4348-4355.

(498) Yang, Q. Z.; Wu, L. Z.; Zhang, H.; Chen, B.; Wu, Z. X.; Zhang, L. P.; Tung, C. H. A Luminescent Chemosensor with Specific Response for Mg^{2+}. *Inorg. Chem.* **2004**, *43*, 5195-5197.
(499) Liu, R.; Hu, J.; Zhu, S.; Lu, J.; Zhu, H. Synergistically Enhanced Optical Limiting Property of Graphene Oxide Hybrid Materials Functionalized with Pt Complexes. *ACS Appl. Mater. Interfaces* **2017**, *9*, 33029-33040.
(500) Díez, Á.; Lalinde, E.; Moreno, M. T. Heteropolynuclear Cycloplatinated Complexes: Structural and Photophysical Properties. *Coord. Chem. Rev.* **2011**, *255*, 2426-2447.
(501) Siu, P. K.; Lai, S. W.; Lu, W.; Zhu, N.; Che, C. M. A Diiminoplatinum(II) Complex of 4-Ethynylbenzo-15-crown-5 as a Luminescent Sensor for Divalent Metal Ions. *Eur. J. Inorg. Chem.* **2003**, *2003*, 2749-2752.
(502) Lanoe, P.-H.; Fillaut, J.-L.; Toupet, L.; Williams, J. G.; Le Bozec, H.; Guerchais, V. Cyclometallated Platinum (II) Complexes Incorporating Ethynyl–flavone Ligands: Switching Between Triplet and Singlet Emission Induced by Selective Binding of Pb^{2+} Ions. *Chem. Commun.* **2008**, 4333-4335.
(503) Schneider, J.; Du, P.; Jarosz, P.; Lazarides, T.; Wang, X.; Brennessel, W. W.; Eisenberg, R. Cyclometalated 6-phenyl-2,2'-bipyridyl (CNN) Platinum(II) Acetylide Complexes: Structure, eElectrochemistry, Photophysics, and Oxidative- and Reductive-quenching Studies. *Inorg. Chem.* **2009**, *48*, 4306-4316.
(504) Law, A. S.; Yeung, M. C.; Yam, V. W. Arginine-Rich Peptide-Induced Supramolecular Self-Assembly of Water-Soluble Anionic Alkynylplatinum(II) Complexes: A Continuous and Label-Free Luminescence Assay for Trypsin and Inhibitor Screening. *ACS Appl. Mater. Interfaces* **2017**, *9*, 41143-41150.
(505) Durand, R. J.; Gauthier, S.; Achelle, S.; Kahlal, S.; Saillard, J.-Y.; Barsella, A.; Wojcik, L.; Le Poul, N.; Robin-Le Guen, F. Incorporation of a Platinum Center in the π-Conjugated Core of Push–Pull Chromophores for Nonlinear Optics (NLO). *Dalton Trans.* **2017**, *46*, 3059-3069.
(506) Lee, C. H.; Tang, M. C.; Wong, Y. C.; Chan, M. Y.; Yam, V. W. Sky-Blue-Emitting Dendritic Alkynylgold(III) Complexes for Solution-Processable Organic Light-Emitting Devices. *J. Am. Chem. Soc.* **2017**, *139*, 10539-10550.
(507) Rossi, E.; Colombo, A.; Dragonetti, C.; Roberto, D.; Ugo, R.; Valore, A.; Falciola, L.; Brulatti, P.; Cocchi, M.; Williams, J. G. Novel N^C^N-cyclometallated Platinum Complexes with Acetylide Co-ligands as Efficient Phosphors for OLEDs. *J. Mater. Chem.* **2012**, *22*, 10650-10655.
(508) Du, P.; Schneider, J.; Jarosz, P.; Eisenberg, R. Photocatalytic Generation of Hydrogen from Water Using a Platinum (II) Terpyridyl Acetylide Chromophore. *J. Am. Chem. Soc.* **2006**, *128*, 7726-7727.
(509) Du, P.; Schneider, J.; Jarosz, P.; Zhang, J.; Brennessel, W. W.; Eisenberg, R. Photoinduced Electron Transfer in Platinum(II) Terpyridyl Acetylide Chromophores: Reductive and Oxidative Quenching and Hydrogen Production. *J. Phys. Chem. B* **2007**, *111*, 6887-6894.
(510) Vezzu, D. A.; Deaton, J. C.; Jones, J. S.; Bartolotti, L.; Harris, C. F.; Marchetti, A. P.; Kondakova, M.; Pike, R. D.; Huo, S. Highly Luminescent Tetradentate Bis-cyclometalated Platinum Complexes: Design, Synthesis, Structure, Photophysics, and Electroluminescence Application. *Inorg. Chem.* **2010**, *49*, 5107-5119.
(511) Hudson, Z. M.; Sun, C.; Helander, M. G.; Chang, Y. L.; Lu, Z. H.; Wang, S. Highly Efficient Blue Phosphorescence from Triarylboron-functionalized Platinum(II) Complexes of N-heterocyclic Carbenes. *J. Am. Chem. Soc.* **2012**, *134*, 13930-13933.
(512) Harris, C. F.; Vezzu, D. A.; Bartolotti, L.; Boyle, P. D.; Huo, S. Synthesis, Structure, Photophysics, and a DFT Study of Phosphorescent C* N^ N-and C^ N^ N-Coordinated Platinum Complexes. *Inorg. Chem.* **2013**, *52*, 11711-11722.
(513) Lu, W.; Chan, M. C.; Zhu, N.; Che, C. M.; Li, C.; Hui, Z. Structural and Spectroscopic Studies on Pt--Pt and π-π Interactions in Luminescent Multinuclear Cyclometalated Platinum(II) Homologues Tethered by Oligophosphine Auxiliaries. *J. Am. Chem. Soc.* **2004**, *126*, 7639-7651.
(514) Lai, S.-W.; Chan, M. C.-W.; Cheung, T.-C.; Peng, S.-M.; Che, C.-M. Probing d8− d8 Interactions in Luminescent Mono-and Binuclear Cyclometalated Platinum (II) Complexes of 6-Phenyl-2, 2 '-bipyridines. *Inorg. Chem.* **1999**, *38*, 4046-4055.
(515) Seneclauze, J. B.; Retailleau, P.; Ziessel, R. Design and Preparation of Neutral Substituted Fluorene-and Carbazole-based Platinum(II)–Acetylide Complexes. *New J. Chem.* **2007**, *31*, 1412-1416.

(516) Shao, P.; Li, Y.; Yi, J.; Pritchett, T. M.; Sun, W. Cyclometalated Platinum(II) 6-phenyl-4-(9,9-dihexylfluoren-2-yl)-2,2'-bipyridine Complexes: Synthesis, Photophysics, and Nonlinear Absorption. *Inorg. Chem.* **2010**, *49*, 4507-4517.
(517) Hebenbrock, M.; Stegemann, L.; Kosters, J.; Doltsinis, N. L.; Muller, J.; Strassert, C. A. Phosphorescent Pt(II) Complexes Bearing a Monoanionic C^N^N Luminophore and Tunable Ancillary Ligands. *Dalton Trans.* **2017**, *46*, 3160-3169.
(518) Ravindranathan, D.; Vezzu, D. A.; Bartolotti, L.; Boyle, P. D.; Huo, S. Improvement in Phosphorescence Efficiency Through Tuning of Coordination Geometry of Tridentate Cyclometalated Platinum(II) Complexes. *Inorg. Chem.* **2010**, *49*, 8922-8928.
(519) Chen, Y.; Li, K.; Lu, W.; Chui, S. S. Y.; Ma, C. W.; Che, C. M. Photoresponsive Supramolecular Organometallic Nanosheets Induced by Pt(II)---Pt(II) and C-H---π Interactions. *Angew. Chem. Int. Ed.* **2009**, *48*, 9909-9913.
(520) Berenguer, J. R.; Lalinde, E.; Torroba, J. Synthesis, Characterization and Photophysics of a New Series of Anionic C,N,C Cyclometalated Platinum Complexes. *Inorg. Chem.* **2007**, *46*, 9919-9930.
(521) Wu, W.; Zhao, J.; Guo, H.; Sun, J.; Ji, S.; Wang, Z. Long-Lived Room-Temperature Near-IR Phosphorescence of BODIPY in a Visible-Light-Harvesting N^ C^ N Pt(II)–Acetylide Complex with a Directly Metalated BODIPY Chromophore. *Chem. Eur. J.* **2012**, *18*, 1961-1968.
(522) Zhang, Y.; Blacque, O.; Venkatesan, K. Highly Efficient Deep-Blue Emitters Based on cis and trans N-Heterocyclic Carbene PtII Acetylide Complexes: Synthesis, Photophysical Properties, and Mechanistic Studies. *Chem. Eur. J.* **2013**, *19*, 15689-15701.
(523) Winkel, R. W.; Dubinina, G. G.; Abboud, K. A.; Schanze, K. S. Photophysical Properties of trans-Platinum Acetylide Complexes Featuring N-heterocyclic Carbene Ligands. *Dalton Trans.* **2014**, *43*, 17712-17720.
(524) Leung, S. Y.; Lam, E. S.; Lam, W. H.; Wong, K. M.; Wong, W. T.; Yam, V. W. Luminescent Cyclometalated Alkynylplatinum(II) Complexes with a Tridentate Pyridine-based N-Heterocyclic Carbene Ligand: Synthesis, Characterization, Electrochemistry, Photophysics, and Computational Studies. *Chemistry* **2013**, *19*, 10360-10369.
(525) Yam, V. W.-W.; Choi, S. W.-K. Synthesis, Photophysics and Photochemistry of Alkynylgold (I) Phosphine Complexes. *J. Chem. Soc., Dalton Trans.* **1996**, 4227-4232.
(526) McDonagh, A. M.; Lucas, N. T.; Cifuentes, M. P.; Humphrey, M. G.; Houbrechts, S.; Persoons, A. Organometallic Complexes for Nonlinear Optics: Part 20. Syntheses and Molecular Quadratic Hyperpolarizabilities of Alkynyl Complexes Derived from (E)-4, 4′-$HC{\equiv}CC_6H_4N{=}NC_6H_4NO_2$. *J. Organomet. Chem.* **2000**, *605*, 193-201.
(527) Lo, H.-S.; Zhu, N.; Au, V. K.-M.; Yam, V. W.-W. Synthesis, Characterization, Photophysics and Electrochemistry of Polynuclear Copper(I) and Gold(I) Alkynyl Phosphine Complexes. *Polyhedron* **2014**, *83*, 178-184.
(528) Shi, H.-Y.; Qi, J.; Zhao, Z.-Z.; Feng, W.-J.; Li, Y.-H.; Sun, L.; Lin, Z.-J.; Chao, H.-Y. Synthesis, Characterization, Photophysics, and Anion Binding Properties of Gold(I) Acetylide Complexes with Amide Groups. *New J. Chem.* **2014**, *38*, 6168-6175.
(529) Zhou, Y. P.; Liu, E. B.; Wang, J.; Chao, H. Y. Highly Ag^+ Selective Tripodal Gold(I) Acetylide-based "off-on" Luminescence Chemosensors Based on $^3(\pi\pi^*)$ Emission Switching. *Inorg. Chem.* **2013**, *52*, 8629-8637.
(530) Zhou, Y. P.; Zhang, M.; Li, Y. H.; Guan, Q. R.; Wang, F.; Lin, Z. J.; Lam, C. K.; Feng, X. L.; Chao, H. Y. Mononuclear Gold(I) Acetylide Complexes with Urea Group: Synthesis, Characterization, Photophysics, and Anion Sensing Properties. *Inorg. Chem.* **2012**, *51*, 5099-5109.
(531) Lima, J. C.; Rodriguez, L. Applications of Gold(I) Alkynyl Systems: A Growing Field to Explore. *Chem. Soc. Rev.* **2011**, *40*, 5442-5456.
(532) Stephens, R.; Castro, C. The Substitution of Aryl Iodides with Cuprous Acetylides. A Synthesis of Tolanes and Heterocyclics1. *J. Org. Chem.* **1963**, *28*, 3313-3315.
(533) Bruce, M. I.; Halet, J.-F.; Le Guennic, B.; Skelton, B. W.; Sobolev, A. N.; Sumby, C. J.; White, A. H. Structural Systematics of some Trinuclear Alkynyl and Diynyl Group 11 Complexes Containing dppm [dppm= $CH_2(PPh_2)_2$]. *Coord. Chem. Rev.* **2017**, doi : 10.1016/j.ccr.2017.09.021.
(534) Lei, Z.; Wan, X.-K.; Yuan, S.-F.; Wang, J.-Q.; Wang, Q.-M. Alkynyl-protected Gold and Gold–Silver Nanoclusters. *Dalton Trans.* **2017**, *46*, 3427-3434.
(535) Mathur, P.; Chatterjee, S.; Avasare, V. D. Mixed Metal Acetylide Complexes. *Adv. Organomet. Chem.* **2007**, *55*, 201-277.

(536) Wei, Q.-H.; Zhang, L.-Y.; Shi, L.-X.; Chen, Z.-N. Octahedral Hexanuclear Silver (I) and Copper (I) Ferrocenylacetylide Complexes. *Inorg. Chem. Commun.* **2004**, *7*, 286-288.
(537) Koshevoy, I. O.; Koskinen, L.; Haukka, M.; Tunik, S. P.; Serdobintsev, P. Y.; Melnikov, A. S.; Pakkanen, T. A. Self-Assembly of Supramolecular Luminescent Au(I)–Cu(I) Complexes: "Wrapping" an Au_6Cu_6 Cluster in a $[Au_3(diphosphine)_3]^{3+}$ "Belt". *Angew. Chem.* **2008**, *120*, 4006-4009.
(538) Judai, K.; Nishijo, J.; Nishi, N. Self-Assembly of Copper Acetylide Molecules into Extremely Thin Nanowires and Nanocables. *Adv. Mater.* **2006**, *18*, 2842-2846.
(539) Halbes-Letinois, U.; Weibel, J.-M.; Pale, P. The Organic Chemistry of Silver Acetylides. *Chem. Soc. Rev.* **2007**, *36*, 759-769.
(540) Irwin, M. J.; Vittal, J. J.; Puddephatt, R. J. Luminescent Gold(I) Acetylides: From Model Compounds to Polymers. *Organometallics* **1997**, *16*, 3541-3547.
(541) Irwin, M. J.; Jia, G.; Payne, N. C.; Puddephatt, R. J. Rigid-rod Polymers and Model Compounds with Gold (I) Centers Bridged by Diisocyanides and Diacetylides. *Organometallics* **1996**, *15*, 51-57.
(542) Vicente, J.; Chicote, M. a. T.; Abrisqueta, M. a. D.; Alvarez-Falcón, M. M. The First Anionic Arenediethynylgold (I) Complexes. *J. Organomet. Chem.* **2002**, *663*, 40-45.
(543) Vicente, J.; Chicote, M.-T.; Alvarez-Falcón, M. M.; Bautista, D. The First Metal Complexes Derived from 3, 5-Diethynylpyridine. X-ray Crystal Structure of $[(AuPTo_3)_2\{\mu\text{-}(C{\equiv}C)_2Py\}](Py=$ Pyridine-3, 5-diyl; To= p-Tolyl). *Organometallics* **2004**, *23*, 5707-5712.
(544) Vicente, J.; Chicote, M.-T.; Alvarez-Falcón, M. M.; Jones, P. G. Platinum(II) and Mixed Platinum(II)/ gold(I) σ-Alkynyl Complexes. The first Anionic σ-Alkynyl Metal Polymers. *Organometallics* **2005**, *24*, 2764-2772.
(545) Vicente, J.; Chicote, M.-T.; Alvarez-Falcón, M. M.; Fox, M. A.; Bautista, D. Alkynyl Gold (I) Rigid-Rod Molecules from 1, 12-Bis (ethynyl)-1, 12-dicarba-c loso-dodecaborane (12). *Organometallics* **2003**, *22*, 4792-4797.
(546) Seifert, T. P.; Boukis, A. C.; Feuerstein, T. J.; Roesky, P. W. A Straightforward Synthetic Route to Symmetric Bis (acetylide) Metallates of the Coinage Metals. *J. Organomet. Chem.* **2018**, *867*, 92-97.
(547) Liu, J.; Chen, Q.; Xiao, L.; Shang, J.; Zhou, X.; Zhang, Y.; Wang, Y.; Shao, X.; Li, J.; Chen, W.; et al. Lattice-Directed Formation of Covalent and Organometallic Molecular Wires by Terminal Alkynes on Ag Surfaces. *ACS Nano* **2015**, *9*, 6305-6314.
(548) Belyaev, A.; Dau, T. M.; Jänis, J.; Grachova, E. V.; Tunik, S. P.; Koshevoy, I. O. Low-nuclearity Alkynyl d^{10} Clusters Supported by Chelating Multidentate Phosphines. *Organometallics* **2016**, *35*, 3763-3774.
(549) Li, P.; Ahrens, B.; Choi, K. H.; Khan, M. S.; Raithby, P. R.; Wilson, P. J.; Wong, W. Y. Metal-metal and Ligand-ligand Interactions in Gold Poly-yne Systems. *CrystEngComm* **2002**, *4*, 405-412.
(550) Coates, G.; Parkin, C. 621. Gold(I) Alkynyls and Their Co-ordination Complexes. *J. Chem. Soc.* **1962**, 3220-3226.
(551) Mingos, D. M. P.; Yau, J.; Menzer, S.; Williams, D. J. A gold(I) [2]Catene. *Angew. Chem. Int. Ed.* **1995**, *34*, 1894-1895.
(552) Corfield, P. W. R.; Shearer, H. The Crystal Structure of Phenylethynyl(isopropylamine) Gold(I). *Acta Crystallographica* **1967**, *23*, 156-162.
(553) Müller, T. E.; Choi, S. W.-K.; Mingos, D. M. P.; Murphy, D.; Williams, D. J.; Yam, V. W.-W. Synthesis, Structural Characterization and Photophysical Properties of Ethyne-gold(I) Complexes. *J. Organomet. Chem.* **1994**, *484*, 209-224.
(554) Bruce, M.; Horn, E.; Matisons, J.; Snow, M. Chemistry of the Group 1B metals. XVII. Preparation of some Gold(I) Acetylide Complexes Containing Group 5 Donor Ligands: Crystal and Molecular Structures of Au $(C_2C_6F_5)(PPh_3)$. *Aust. J. Chem.* **1984**, *37*, 1163-1170.
(555) Bruce, M.; Duffy, D. Chemistry of the Group-1B Metals. XIX. Crystal and Molecular-Structures of (2-Phenylethynyl)(Triphenylphosphine) Gold (I), Au (C= CPh)(PPh_3). *Aust. J. Chem.* **1986**, *39*, 1697-1701.
(556) Penney, A. A.; Starova, G. L.; Grachova, E. V.; Sizov, V. V.; Kinzhalov, M. A.; Tunik, S. P. Gold (I) Alkynyls Supported by Mono-and Bidentate NHC Ligands: Luminescence and Isolation of Unprecedented Ionic Complexes. *Inorganic chemistry* **2017**, 56, 14771-14787.
(557) Lu, W.; Kwok, W.-M.; Ma, C.; Chan, C. T.-L.; Zhu, M.-X.; Che, C.-M. Organic Triplet Excited States of Gold (I) Complexes with Oligo (*o*-or *m*-phenyleneethynylene) Ligands: Conjunction of Steady-

state and Time-resolved Spectroscopic Studies on Exciton Delocalization and Emission Pathways. *J. Am. Chem. Soc.* **2011**, *133*, 14120-14135.

(558) Chang, Y.-C.; Tang, K.-C.; Pan, H.-A.; Liu, S.-H.; Koshevoy, I. O.; Karttunen, A. J.; Hung, W.-Y.; Cheng, M.-H.; Chou, P.-T. Harnessing Fluorescence versus Phosphorescence Branching Ratio in (Phenyl) n-Bridged (n= 0–5) Bimetallic Au (I) Complexes. *J. Phys. Chem. C* **2013**, *117*, 9623-9632.

(559) Chang, Y.-C.; Tang, K.-C.; Pan, H.-A.; Koshevoy, I. O.; Karttunen, A. J.; Chou, P.-T. Harvesting Fluorescence from Efficient T k→ S j (j, k> 1) Reverse Intersystem Crossing for ππ* Emissive Transition-Metal Complexes. *J. Phys. Chem. C* **2013**, *117*, 20494-20499.

(560) Hsu, C. C.; Lin, C. C.; Chou, P. T.; Lai, C. H.; Hsu, C. W.; Lin, C. H.; Chi, Y. Harvesting Highly Electronically Excited Energy to Triplet Manifolds: State-dependent Intersystem Crossing Rate in Os(II) and Ag(I) Complexes. *J. Am. Chem. Soc.* **2012**, *134*, 7715-7724.

(561) Ma, C.; Chan, C. T.-L.; Kwok, W.-M.; Che, C.-M. Ligand π-Conjugation Dictated Intersystem Crossing in Phenyleneethynylene Gold(I) Complexes. *Chem. Sci.* **2012**, *3*, 1883-1892.

(562) Rodríguez, L.; Ferrer, M.; Crehuet, R.; Anglada, J.; Lima, J. o. C. Correlation Between Photophysical Parameters and Gold–gold Distances in Gold(I)(4-Pyridyl) Ethynyl Complexes. *Inorg. Chem.* **2012**, *51*, 7636-7641.

(563) Yao, X.-X.; Guo, Y.-M.; Chen, J.; Huang, M.-M.; Shi, Y.; Li, X.-L. Synthesis, Structure and Luminescent Properties of Three Organogold (I)-9-ethynyl-anthracence-Diphosphine Complexes. *J. Organomet. Chem.* **2017**, *834*, 58-63.

(564) Mishra, V.; Raghuvanshi, A.; Saini, A. K.; Mobin, S. M. Anthracene Derived Dinuclear Gold(I) Diacetylide Complexes: Synthesis, Photophysical Properties and Supramolecular Interactions. *J. Organomet. Chem.* **2016**, *813*, 103-109.

(565) Nguyen, M.-H.; Yip, J. H. Gold(I) and Platinum(II) Tetracenes and Tetracenyldiacetylides: Structural and Fluorescence Color Changes Induced by σ-Metalation. *Organometallics* **2010**, *29*, 2422-2429.

(566) Jin, M.; Chung, T. S.; Seki, T.; Ito, H.; Garcia-Garibay, M. A. Phosphorescence Control Mediated by Molecular Rotation and Aurophilic Interactions in Amphidynamic Crystals of 1,4-Bis[tri-(p-fluorophenyl)phosphane-gold(I)-ethynyl]benzene. *J. Am. Chem. Soc.* **2017**, *139*, 18115-18121.

(567) Islam, S. N.; Sil, A.; Patra, S. K. Achieving Yellow Emission by Varying the Donor/Acceptor Units in Rod-shaped Fluorenyl-alkynyl Based π-Conjugated Oligomers and Their Binuclear Gold(I) Alkynyl Complexes. *Dalton Trans.* **2017**, *46*, 5918-5929.

(568) Wang, L.; Yin, L.; Ji, C.; Zhang, Y.; Gao, H.; Li, Y. High Open-circuit Voltage of the Solution-processed Organic Solar Cells Based on Benzothiadiazole–triphenylamine Small Molecules Incorporating π-Linkage. *Org. Electron.* **2014**, *15*, 1138-1148.

(569) Brabec, C. J.; Sariciftci, N. S.; Hummelen, J. C. Plastic Solar Cells. *Adv. Funct. Mater.* **2001**, *11*, 15-26.

(570) Brabec, C. J. Organic Photovoltaics: Technology and Market. *Sol. Energy Mater. Sol. Cells* **2004**, *83*, 273-292.

(571) Coakley, K. M.; McGehee, M. D. Conjugated Polymer Photovoltaic Cells. *Chem. Mater.* **2004**, *16*, 4533-4542.

(572) Gratzel, M. Solar Energy Conversion by Dye-Sensitized Photovoltaic Cells. *Inorg. Chem.* **2005**, *44*, 6841-6851.

(573) Gratzel, M. Recent Advances in Sensitized Mesoscopic Solar Cells. *Acc. Chem. Res.* **2009**, *42*, 1788-1798.

(574) Mathew, S.; Yella, A.; Gao, P.; Humphry-Baker, R.; Curchod, B. F.; Ashari-Astani, N.; Tavernelli, I.; Rothlisberger, U.; Nazeeruddin, M. K.; Grätzel, M. Dye-Sensitized Solar Cells with 13% Efficiency Achieved Through the Molecular Engineering of Porphyrin Sensitizers. *Nat. Chem.* **2014**, *6*, 242-247.

(575) Baek, N. S.; Hau, S. K.; Yip, H.-L.; Acton, O.; Chen, K.-S.; Jen, A. K.-Y. High Performance Amorphous Metallated π-Conjugated Polymers for Field-Effect Transistors and Polymer Solar Cells. *Chem. Mater.* **2008**, *20*, 5734-5736.

(576) Zhao, X.; Piliego, C.; Kim, B.; Poulsen, D. A.; Ma, B.; Unruh, D. A.; Fréchet, J. M. Solution-Processable Crystalline Platinum-Acetylide oligomers with Broadband Absorption for Photovoltaic Cells. *Chem. Mater.* **2010**, *22*, 2325-2332.

(577) Whittell, G. R.; Hager, M. D.; Schubert, U. S.; Manners, I. Functional Soft Materials from Metallopolymers and Metallosupramolecular Polymers. *Nat. Mater* **2011**, *10*, 176-188.

(578) Ho, C.-L.; Wong, W.-Y. Metal-containing Polymers: Facile Tuning of Photophysical Traits and Emerging Applications in Organic Electronics and Photonics. *Coord. Chem. Rev.* **2011**, *255*, 2469-2502.
(579) Köhler, A.; Wittmann, H.; Friend, R.; Khan, M.; Lewis, J. The Photovoltaic Effect in a Platinum Poly-yne. *Synth. Met.* **1994**, *67*, 245-249.
(580) Köhler, A.; Wittmann, H.; Friend, R.; Khan, M.; Lewis, J. Enhanced Photocurrent Response in Photocells made with Platinum-poly-yne/C_{60} Blends by Photoinduced Electron Transfer. *Synth. Met.* **1996**, *77*, 147-150.
(581) Tore, N.; Parlak, E. A.; Tumay, T. A.; Kavak, P.; Sarıoğlan, Ş.; Bozar, S.; Günes, S.; Ulbricht, C.; Egbe, D. A. M. Improvement in Photovoltaic Performance of Anthracene-containing PPE–PPV Polymer-based Bulk Heterojunction Solar Cells with Silver Nanoparticles. *J. Nanopart. Res.* **2014**, *16*, 1-8.
(582) Xu, L.; Ho, C.-L.; Liu, L.; Wong, W.-Y. Molecular/polymeric metallaynes and related molecules: Solar cell materials and devices. *Coord. Chem. Rev.* **2017**.
(583) Wu, R.; Yin, L.; Li, Y. π-Linkage Effect of Push-Pull-Structure Organic Small Molecules for Photovoltaic Application. *Sci China Chem* **2016**, *59*, 371-388.
(584) Pashaei, B.; Shahroosvand, H.; Graetzel, M.; Nazeeruddin, M. K. Influence of ancillary ligands in dye-sensitized solar cells. *Chem. Rev.* **2016**, *116*, 9485-9564.
(585) Lee, C.-P.; Lin, R. Y.-Y.; Lin, L.-Y.; Li, C.-T.; Chu, T.-C.; Sun, S.-S.; Lin, J. T.; Ho, K.-C. Recent Progress in Organic Sensitizers for Dye-Sensitized Solar Cells. *RSC Adv.* **2015**, *5*, 23810-23825.
(586) Mohd-Nasir, S.; Sulaiman, M.; Ahmad-Ludin, N.; Ibrahim, M. A.; Sopian, K.; Mat-Teridi, M. Review of polymer, dye-sensitized, and hybrid solar cells. *Int. J. Photoenergy* **2014**, doi: 10.1155/2014/370160.
(587) Shalini, S.; Balasundaraprabhu, R.; Kumar, T. S.; Prabavathy, N.; Senthilarasu, S.; Prasanna, S. Status and Outlook of Sensitizers/Dyes used in Dye Sensitized Solar Cells (DSSC): a review. *Int. J. Energy Res.* **2016**, *40*, 1303-1320.
(588) Zhang, L.; Cole, J. M. Anchoring Groups for Dye-Sensitized Solar Cells. *ACS Appl. Mater. Interfaces* **2015**, *7*, 3427-3455.
(589) Chaurasia, S.; Liang, C.-J.; Yen, Y.-S.; Lin, J. T. Sensitizers with Rigidified-Aromatics as the Conjugated Spacers for Dye-Sensitized Solar Cells. *J. Mater. Chem. C* **2015**, *3*, 9765-9780.
(590) Chou, H.-H.; Liu, Y.-C.; Fang, G.; Cao, Q.-K.; Wei, T.-C.; Yeh, C.-Y. Structurally Simple and Easily Accessible Perylenes for Dye-Sensitized Solar Cells Applicable to Both 1 Sun and Dim-Light Environments. *ACS Appl. Mater. Interfaces* **2017**, *9*, 37786-37796.
(591) Tigreros, A.; Dhas, V.; Ortiz, A.; Insuasty, B.; Martín, N.; Echegoyen, L. Influence of Acetylene-linked π-Spacers on Triphenylamine-fluorene Dye Sensitized Solar Cells Performance. *Sol. Energy Mater. Sol. Cells* **2014**, *121*, 61-68.
(592) Song, X.; Zhang, W.; Li, X.; Jiang, H.; Shen, C.; Zhu, W.-H. Influence of Ethynyl Position on Benzothiadiazole Based D–A–π–A Dye-Sensitized Solar Cells: Spectral Response and Photovoltage Performance. *J. Mater. Chem. C* **2016**, *4*, 9203-9211.
(593) Yao, Z.; Wu, H.; Li, Y.; Wang, J.; Zhang, J.; Zhang, M.; Guo, Y.; Wang, P. Dithienopicenocarbazole as the Kernel Module of Low-energy-gap Organic Dyes for Efficient Conversion of Sunlight to Electricity. *Energy Environ. Sci.* **2015**, *8*, 3192-3197.
(594) Wu, H.; Yang, L.; Li, Y.; Zhang, M.; Zhang, J.; Guo, Y.; Wang, P. Unlocking the Effects of Ancillary Electron-donors on Light Absorption and Charge Recombination in Phenanthrocarbazole Dye-Sensitized Solar Cells. *J. Mater. Chem. A* **2016**, *4*, 519-528.
(595) Yao, Z.; Zhang, M.; Wu, H.; Yang, L.; Li, R.; Wang, P. Donor/Acceptor Indenoperylene Dye for Highly Efficient Organic Dye-Sensitized Solar Cells. *J. Am. Chem. Soc.* **2015**, *137*, 3799-3802.
(596) Ostroverkhova, O. Organic Optoelectronic Materials: Mechanisms and Applications. *Chem. Rev.* **2016**, *116*, 13279-13412.
(597) Giguère, J.-B.; Sariciftci, N. S.; Morin, J.-F. Polycyclic Anthanthrene Small Molecules: Semiconductors for Organic Field-Effect Transistors and Solar Cells Applications. *J. Mater. Chem. C* **2015**, *3*, 601-606.
(598) Wu, C.-L.; Chang, C.-H.; Chang, Y.-T.; Chen, C.-T.; Chen, C.-T.; Su, C.-J. High Efficiency Non-Dopant Blue Organic Light-Emitting Diodes Based on Anthracene-Based Fluorophores with Molecular Design of Charge Transport and Red-Shifted Emission Proof. *J. Mater. Chem. C* **2014**, *2*, 7188-7200.

(599) Shah, B. K.; Neckers, D. C.; Shi, J.; Forsythe, E. W.; Morton, D. Anthanthrene Derivatives asBlue Emitting Materials for Organic Light-Emitting Diode Applications. *Chem. Mater.* **2006**, *18*, 603-608.
(600) Lafleur-Lambert, A.; Giguère, J.-B.; Morin, J.-F. Anthanthrene as a large PAH building block for the synthesis of conjugated polymers. *Polym. Chem.* **2015**, *6*, 4859-4863.
(601) Mai, C.-L.; Moehl, T.; Kim, Y.; Ho, F.-Y.; Comte, P.; Su, P.-C.; Hsu, C.-W.; Giordano, F.; Yella, A.; Zakeeruddin, S. M. Acetylene-bridged Dyes with High Open Circuit Potential for Dye-Sensitized Solar Cells. *RSC Adv.* **2014**, *4*, 35251-35257.
(602) Tingare, Y. S.; Vinh, N. S. n.; Chou, H. H.; Liu, Y. C.; Long, Y. S.; Wu, T. C.; Wei, T. C.; Yeh, C. Y. New Acetylene-Bridged 9, 10-Conjugated Anthracene Sensitizers: Application in Outdoor and Indoor Dye-Sensitized Solar Cells. *Adv. Energy Mater.* **2017**, *7*, 1700032-1700042.
(603) Wang, C.-L.; Lin, P.-T.; Wang, Y.-F.; Chang, C.-W.; Lin, B.-Z.; Kuo, H.-H.; Hsu, C.-W.; Tu, S.-H.; Lin, C.-Y. Cost-effective Anthryl Dyes for Dye-Sensitized Cells under One Sun and Dim Light. *J. Phys. Chem. C* **2015**, *119*, 24282-24289.
(604) Wu, W.; Xu, X.; Yang, H.; Hua, J.; Zhang, X.; Zhang, L.; Long, Y.; Tian, H. D–π–M–π–A Structured Platinum Acetylide Sensitizer for Dye-Sensitized Solar Cells. *J. Mater. Chem.* **2011**, *21*, 10666-10671.
(605) De Sousa, S.; Ducasse, L.; Kauffmann, B.; Toupance, T.; Olivier, C. Functionalization of a Ruthenium–Diacetylide Organometallic Complex as a Next-Generation Push–Pull Chromophore. *Chem. Eur. J.* **2014**, *20*, 7017-7024.
(606) Wu, W.; Zhang, J.; Yang, H.; Jin, B.; Hu, Y.; Hua, J.; Jing, C.; Long, Y.; Tian, H. Narrowing Band Gap of Platinum Acetylide Dye-Sensitized Solar Cell Sensitizers with Thiophene π-Bridges. *J. Mater. Chem.* **2012**, *22*, 5382-5389.
(607) Siu, C. H.; Lee, L. T.; Yiu, S. C.; Ho, P. Y.; Zhou, P.; Ho, C. L.; Chen, T.; Liu, J.; Han, K.; Wong, W. Y. Synthesis and Characterization of Phenothiazine-Based Platinum(II)-Acetylide Photosensitizers for Efficient Dye-Sensitized Solar Cells. *Chemistry* **2016**, *22*, 3750-3757.
(608) Gauthier, S.; Caro, B.; Robin-Le Guen, F.; Bhuvanesh, N.; Gladysz, J. A.; Wojcik, L.; Le Poul, N.; Planchat, A.; Pellegrin, Y.; Blart, E. Synthesis, Photovoltaic Performances and TD-DFT Modeling of Push-Pull Diacetylide Platinum Complexes in TiO_2 Based Dye-Sensitized Solar Cells. *Dalton Trans.* **2014**, *43*, 11233-11242.
(609) Kwok, E. C. H.; Chan, M. Y.; Wong, K. M. C.; Yam, V. W. W. Molecular Dyads Comprising Metalloporphyrin and Alkynylplatinum(II) Polypyridine Terminal Groups for Use as a Sensitizer in Dye-Sensitized Solar Cells. *Chem. Eur. J.* **2014**, *20*, 3142-3153.
(610) Wang, Y.; Chen, B.; Wu, W.; Li, X.; Zhu, W.; Tian, H.; Xie, Y. Efficient Solar Cells Sensitized by Porphyrins with an Extended Conjugation Framework and a Carbazole Donor: from Molecular Design to Cosensitization. *Angew. Chem. Int. Ed. Engl.* **2014**, *53*, 10779-10783.
(611) Higashino, T.; Nimura, S.; Sugiura, K.; Kurumisawa, Y.; Tsuji, Y.; Imahori, H. Photovoltaic Properties and Long-Term Durability of Porphyrin-Sensitized Solar Cells with Silicon-Based Anchoring Groups. *ACS Omega* **2017**, *2*, 6958-6967.
(612) Yella, A.; Lee, H. W.; Tsao, H. N.; Yi, C.; Chandiran, A. K.; Nazeeruddin, M. K.; Diau, E. W.; Yeh, C. Y.; Zakeeruddin, S. M.; Gratzel, M. Porphyrin-Sensitized Solar Cells with Cobalt(II/III)-based Redox Electrolyte Exceed 12% Efficiency. *Science* **2011**, *334*, 629-634.
(613) Chou, C. C.; Hu, F. C.; Yeh, H. H.; Wu, H. P.; Chi, Y.; Clifford, J. N.; Palomares, E.; Liu, S. H.; Chou, P. T.; Lee, G. H. Highly Efficient Dye-Sensitized Solar Cells Based on Panchromatic Ruthenium Sensitizers with Quinolinylbipyridine Anchors. *Angew. Chem. Int. Ed. Engl.* **2014**, *53*, 178-183.
(614) Yella, A.; Mai, C.-L.; Zakeeruddin, S. M.; Chang, S.-N.; Hsieh, C.-H.; Yeh, C.-Y.; Grätzel, M. Molecular Engineering of Push-Pull Porphyrin Dyes for Highly Efficient Dye-Sensitized Solar Cells: The Role of Benzene Spacers. *Angew. Chem.* **2014**, *126*, 3017-3021.
(615) Xie, Y.; Tang, Y.; Wu, W.; Wang, Y.; Liu, J.; Li, X.; Tian, H.; Zhu, W. H. Porphyrin Cosensitization for a Photovoltaic Efficiency of 11.5%: a Record for Non-Ruthenium Solar Cells Based on Iodine Electrolyte. *J. Am. Chem. Soc.* **2015**, *137*, 14055-14058.
(616) Wang, C.-L.; Hu, J.-Y.; Wu, C.-H.; Kuo, H.-H.; Chang, Y.-C.; Lan, Z.-J.; Wu, H.-P.; Wei-Guang Diau, E.; Lin, C.-Y. Highly Efficient Porphyrin-Sensitized Solar Cells with Enhanced Light Harvesting Ability Beyond 800 nm and Efficiency Exceeding 10%. *Energy Environ. Sci.* **2014**, *7*, 1392-1396

(617) Luo, J.; Xu, M.; Li, R.; Huang, K. W.; Jiang, C.; Qi, Q.; Zeng, W.; Zhang, J.; Chi, C.; Wang, P.; et al. N-annulated Perylene as an Efficient Electron Donor for Porphyrin-based Dyes: Enhanced Light-Harvesting Ability and High-Efficiency Co(II/III)-based Dye-Sensitized Solar Cells. *J. Am. Chem. Soc.* **2014**, *136*, 265-272.
(618) Qi, Q.; Wang, X.; Fan, L.; Zheng, B.; Zeng, W.; Luo, J.; Huang, K. W.; Wang, Q.; Wu, J. N-annulated Perylene-based Push-Pull-type Sensitizers. *Org. Lett.* **2015**, *17*, 724-727.
(619) Pellejà, L.; Kumar, C. V.; Clifford, J. N.; Palomares, E. D-π-A Porphyrin Employing an Indoline Donor Group for High Efficiency Dye-Sensitized Solar Cells. *J. Phys. Chem. C* **2014**, *118*, 16504-16509.
(620) Hsieh, C.-P.; Lu, H.-P.; Chiu, C.-L.; Lee, C.-W.; Chuang, S.-H.; Mai, C.-L.; Yen, W.-N.; Hsu, S.-J.; Diau, E. W.-G.; Yeh, C.-Y. Synthesis and Characterization of Porphyrin Sensitizers with Various Electron-donating Substituents for Highly Efficient Dye-Sensitized Solar Cells. *J. Mater. Chem.* **2010**, *20*, 1127-1134.
(621) Shiu, J.-W.; Chang, Y.-C.; Chan, C.-Y.; Wu, H.-P.; Hsu, H.-Y.; Wang, C.-L.; Lin, C.-Y.; Diau, E. W.-G. Panchromatic Co-sensitization of Porphyrin-Sensitized Solar Cells to Harvest Near-Infrared Light Beyond 900 nm. *J. Mater. Chem. A* **2015**, *3*, 1417-1420.
(622) Wei, T.; Sun, X.; Li, X.; Agren, H.; Xie, Y. Systematic Investigations on the Roles of the Electron Acceptor and Neighboring Ethynylene Moiety in Porphyrins for Dye-Sensitized Solar Cells. *ACS Appl. Mater. Interfaces* **2015**, *7*, 21956-21965.
(623) Yang, G.; Tang, Y.; Li, X.; Agren, H.; Xie, Y. Efficient Solar Cells Based on Porphyrin Dyes with Flexible Chains Attached to the Auxiliary Benzothiadiazole Acceptor: Suppression of Dye Aggregation and the Effect of Distortion. *ACS Appl. Mater. Interfaces* **2017**, *9*, 36875-36885.
(624) Chou, H. H.; Reddy, K. S.; Wu, H. P.; Guo, B. C.; Lee, H. W.; Diau, E. W.; Hsu, C. P.; Yeh, C. Y. Influence of Phenylethynylene of Push-Pull Zinc Porphyrins on the Photovoltaic Performance. *ACS Appl. Mater. Interfaces* **2016**, *8*, 3418-3427.
(625) Tang, Y.; Wang, Y.; Li, X.; Agren, H.; Zhu, W. H.; Xie, Y. Porphyrins Containing a Triphenylamine Donor and up to Eight Alkoxy Chains for Dye-Sensitized Solar Cells: A High Efficiency of 10.9%. *ACS Appl. Mater. Interfaces* **2015**, *7*, 27976-27985.
(626) Hu, Y.; Yellappa, S.; Thomas, M. B.; Jinadasa, R. G. W.; Matus, A.; Shulman, M.; D'Souza, F.; Wang, H.β-Functionalized Push-Pull opp-Dibenzoporphyrins as Sensitizers for Dye-Sensitized Solar Cells. *Chem. Asian. J.* **2017**, *12*, 2749-2762.
(627) Bunz, U. H. Poly(aryleneethynylene)s. *Macromol. Rapid Commun.* **2009**, *30*, 772-805.
(628) Ilmi, R.; Haque, A.; Khan, M. High Efficiency Small Molecule-based Donor Materials for Organic Solar Cells. *Org. Electron.* **2018**, 58, 53-62.
(629) Yuan, Y.; Michinobu, T.; Oguma, J.; Kato, T.; Miyake, K. Attempted Inversion of Semiconducting Features of Platinum Polyyne Polymers: A New Approach for All-Polymer Solar Cells. *Macromol. Chem. Phys.* **2013**, *214*, 1465-1472.
(630) Gao, H.; Li, Y.; Wang, L.; Ji, C.; Wang, Y.; Tian, W.; Yang, X.; Yin, L. High Performance Asymmetrical Push–Pull Small Molecules End-Capped with Cyanophenyl for Solution-Processed Solar Cells. *Chem. Commun.* **2014**, *50*, 10251-10254.
(631) Gautam, P.; Misra, R.; Siddiqui, S. A.; Sharma, G. D. Unsymmetrical Donor-Acceptor-Acceptor-pi-Donor Type Benzothiadiazole-Based Small Molecule for a Solution Processed Bulk Heterojunction Organic Solar Cell. *ACS Appl. Mater. Interfaces* **2015**, *7*, 10283-10292.
(632) Wang, L.; Yin, L.; Wang, L.; Xie, B.; Ji, C.; Li, Y. Tuning Photovoltaic Performance of DOBT-based Dyes via Molecular Design with Ethynyl-linker and Terminal Electron-donating Segment. *Dyes and Pigments* **2017**, *140*, 203-211.
(633) Grisorio, R.; Allegretta, G.; Suranna, G. P.; Mastrorilli, P.; Loiudice, A.; Rizzo, A.; Mazzeo, M.; Gigli, G. Monodispersed vs. Polydispersed Systems for Bulk Heterojunction Solar Cells: the Case of Dithienopyrrole/Anthracene Based Materials. *J. Mater. Chem.* **2012**, *22*, 19752-19760.
(634) Hatano, J.; Obata, N.; Yamaguchi, S.; Yasuda, T.; Matsuo, Y. Soluble Porphyrin Donors for Small Molecule Bulk Heterojunction Solar Cells. *J. Mater. Chem.* **2012**, *22*, 19258-19263.
(635) Hsu, F.-C.; Hsieh, M.-K.; Kashi, C.; Yeh, C.-Y.; Lin, T.-Y.; Chen, Y.-F. Porphyrin Dimers as Donors for Solution-Processed Bulk Heterojunction Organic Solar Cells. *RSC Adv.* **2016**, *6*, 60626-60632.
(636) Nakagawa, T.; Hatano, J.; Matsuo, Y. Influence of Additives in Bulk Heterojunction Solar Cells Using Magnesium Tetraethynylporphyrin with Triisopropylsilyl and Anthryl Substituents. *J. Porphyrins Phthalocyanines* **2014**, *18*, 735-740.

(637) Lin, H.-Y.; Huang, W.-C.; Chen, Y.-C.; Chou, H.-H.; Hsu, C.-Y.; Lin, J. T.; Lin, H.-W. BODIPY Dyes with β-Conjugation and Their Applications for High-Efficiency Inverted Small Molecule Solar Cells. *Chem. Commun.* **2012**, *48*, 8913-8915.
(638) Kim, B.; Ma, B.; Donuru, V. R.; Liu, H.; Frechet, J. M. Bodipy-backboned Polymers as Electron Donor in Bulk Heterojunction Solar Cells. *Chem. Commun.* **2010**, *46*, 4148-4150.
(639) Li, W.; Hendriks, K. H.; Wienk, M. M.; Janssen, R. A. Diketopyrrolopyrrole Polymers for Organic Solar Cells. *Acc. Chem. Res.* **2015**, *49*, 78-85.
(640) Wang, L. P.; Xia, Y.; Luo, G. P.; Zhang, C. H.; Liu, Q.; Tan, W. Y.; Zhu, X. H.; Wu, H. B.; Peng, J.; Cao, Y. A Solution-Processable Dithienyldiketopyrrolopyrrole Dye Molecule with Acetylene as a π-Linkage for Organic Solar Cells. *Asian J. Org. Chem.* **2015**, *4*, 470-476.
(641) Zhang, C.-H.; Wang, L.-P.; Tan, W.-Y.; Wu, S.-P.; Liu, X.-P.; Yu, P.-P.; Huang, J.; Zhu, X.-H.; Wu, H.-B.; Zhao, C.-Y. Effective Modulation of an Aryl Acetylenic Molecular System Based on Dithienyldiketopyrrolopyrrole for Organic Solar Cells. *J. Mater. Chem. C* **2016**, *4*, 3757-3764.
(642) Xia, Y.; Tan, W.-Y.; Wang, L.-P.; Zhang, C.-H.; Peng, L.; Zhu, X.-H.; Peng, J.; Cao, Y. Soluble Acetylenic Molecular Glasses Based on Dithienyldiketopyrrolopyrrole for Organic Solar Cells. *Dyes and Pigments* **2016**, *126*, 96-103.
(643) Patil, Y.; Misra, R.; Singh, M. K.; Sharma, G. D. Ferrocene-diketopyrrolopyrrole Based Small Molecule Donors for Bulk Heterojunction Solar Cells. *Phys. Chem. Chem. Phys.* **2017**, *19*, 7262-7269.
(644) Ji, C.; Yin, L.; Li, K.; Wang, L.; Jiang, X.; Sun, Y.; Li, Y. D–π–A–π–D-type Low Band Gap Diketopyrrolopyrrole Based Small Molecules Containing an Ethynyl-Linkage: Synthesis and Photovoltaic Properties. *RSC Adv.* **2015**, *5*, 31606-31614.
(645) Silvestri, F.; Marrocchi, A.; Seri, M.; Kim, C.; Marks, T. J.; Facchetti, A.; Taticchi, A. Solution-processable Low-molecular Weight Extended Arylacetylenes: Versatile p-type Semiconductors for Field-effect Transistors and Bulk Heterojunction Solar Cells. *J. Am. Chem. Soc.* **2010**, *132*, 6108-6123.
(646) Wang, Y.; Liao, Q.; Wang, G.; Guo, H.; Zhang, X.; Uddin, M. A.; Shi, S.; Su, H.; Dai, J.; Cheng, X. Alkynyl-Functionalized Head-to-Head Linkage Containing Bithiophene as a Weak Donor Unit for High-Performance Polymer Semiconductors. *Chem. Mater.* **2017**, *29*, 4109-4121.
(647) He, W.; Livshits, M. Y.; Dickie, D. A.; Zhang, Z.; Mejiaortega, L. E.; Rack, J. J.; Wu, Q.; Qin, Y. "Roller-Wheel"-Type Pt-Containing Small Molecules and the Impact of "Rollers" on Material Crystallinity, Electronic Properties, and Solar Cell Performance. *J. Am. Chem. Soc.* **2017**, *139*, 14109-14119.
(648) Eckstein, B. J.; Melkonyan, F. S.; Zhou, N.; Manley, E. F.; Smith, J.; Timalsina, A.; Chang, R. P.; Chen, L. X.; Facchetti, A.; Marks, T. J. Buta-1, 3-diyne-based π-Conjugated Polymers for Organic Transistors and Solar Cells. *Macromolecules* **2017**, *50*, 1430-1441.
(649) Köhler, A.; Wittmann, H.; Friend, R.; Khan, M.; Lewis, J. Enhanced Photocurrent Response in Photocells made with Platinum-poly-yne/C_{60} Blends by Photoinduced Electron Transfer. *Synth. Met.* **1996**, *77*, 147-150.
(650) Liu, S.; Zhang, K.; Lu, J.; Zhang, J.; Yip, H.-L.; Huang, F.; Cao, Y. High-efficiency Polymer Solar Cells via the Incorporation of an Amino-functionalized Conjugated Metallopolymer as a Cathode Interlayer. *J. Am. Chem. Soc.* **2013**, *135*, 15326-15329.
(651) Montcada, N. F.; Arrechea, S.; Molina-Ontoria, A.; Aljarilla, A. I.; de la Cruz, P.; Echegoyen, L.; Palomares, E.; Langa, F. High Photo-current in Solution Processed Organic Solar Cells based on a Porphyrin Core A-π-D-π-A as Electron Donor Material. *Org. Electron.* **2016**, *38*, 330-336.
(652) Vartanian, M.; Singhal, R.; de la Cruz, P.; Biswas, S.; Sharma, G. D.; Langa, F. Low Energy Loss of 0.57 eV and High Efficiency of 8.80% in Porphyrin-Based BHJ Solar Cells. *ACS Appl. Energy Mater.* **2018**, *1*, 1304-1315.
(653) Vartanian, M.; de la Cruz, P.; Biswas, S.; Sharma, G. D.; Langa, F. Panchromatic Ternary Organic Solar Cells with 9.44% Efficiency Incorporating Porphyrin-based Donors. *Nanoscale* **2018**, doi: 10.1039/C8NR02856G.
(654) Liu, Q.; Zhu, N.; Ho, C.-L.; Fu, Y.; Lau, W.-S.; Xie, Z.; Wang, L.; Wong, W.-Y. Synthesis, Characterization, Photophysical and Photovoltaic Properties of New Donor–Acceptor Platinum(II) Acetylide Complexes. *J. Organomet. Chem.* **2016**, *812*, 2-12.

(655) Zhan, H.; Liu, Q.; Dai, F.; Ho, C.-L.; Fu, Y.; Li, L.; Zhao, L.; Li, H.; Xie, Z.; Wong, W.-Y. Organic Donor Materials Based on Bis(arylene ethynylene)s for Bulk Heterojunction Organic Solar Cells with High Voc Values. *Chem. Asian. J.* **2015**, *10*, 1017-1024.
(656) Wang, H.; Chen, M.; Jiang, B.; Tong, W.; Qian, Q.; Lin, K.; Liu, F. Solution-Processable Platinum-Acetylide-based Small Molecular Bulk Heterojunction Solar Cells. *Chin. J. Chem .* **2015**, *33*, 917-924.
(657) He, W.; Livshits, M. Y.; Dickie, D. A.; Yang, J.; Quinnett, R.; Rack, J. J.; Wu, Q.; Qin, Y. A "roller-wheel" Pt-containing Small Molecule that Outperforms its Polymer Analogs in Organic Solar Cells. *Chem. Sci.* **2016**, *7*, 5798-5804.
(658) Ashraf, R. S.; Gilot, J.; Janssen, R. A. J. Fused Ring Thiophene-based Poly(heteroarylene ethynylene)s for Organic Solar Cells. *Sol. Energy Mater. Sol. Cells* **2010**, *94*, 1759-1766.
(659) Wen, S.; Bao, X.; Shen, W.; Gu, C.; Du, Z.; Han, L.; Zhu, D.; Yang, R. Benzodithiophene-based Poly (aryleneethynylene) s: Synthesis, Optical Properties, and Applications in Organic Solar Cells. *J. Polym. Sci., Part A: Polym. Chem.* **2014**, *52*, 208-215.
(660) Wang, X. Z.; Wang, Q.; Yan, L.; Wong, W. Y.; Cheung, K. Y.; Ng, A.; Djurisic, A. B.; Chan, W. K. Very-low-bandgap Metallopolyynes of Platinum with a Cyclopentadithiophenone Ring for Organic Solar Cells Absorbing down to the Near-infrared Spectral Region. *Macromol. Rapid Commun.* **2010**, *31*, 861-867.
(661) Mei, J.; Ogawa, K.; Kim, Y.-G.; Heston, N. C.; Arenas, D. J.; Nasrollahi, Z.; McCarley, T. D.; Tanner, D. B.; Reynolds, J. R.; Schanze, K. S. Low-Band-Gap Platinum Acetylide Polymers as Active Materials for Organic Solar Cells. *ACS Appl. Mat. Science Inter.* **2009**, *1*, 150-161.
(662) Wong, W.-Y.; Chow, W.-C.; Cheung, K.-Y.; Fung, M.-K.; Djurišić, A. B.; Chan, W.-K. Harvesting Solar Energy Using Conjugated Metallopolyyne Donors Containing Electron-rich Phenothiazine–oligothiophene Moieties. *J. Organomet. Chem.* **2009**, *694*, 2717-2726.
(663) He, W.; Jiang, Y.; Qin, Y. Synthesis and Photovoltaic Properties of a Low Bandgap BODIPY–Pt Conjugated Polymer. *Polym. Chem.* **2014**, *5*, 1298-1304.
(664) Wang, X.-Z.; Ho, C.-L.; Yan, L.; Chen, X.; Chen, X.; Cheung, K.-Y.; Wong, W.-Y. Synthesis, Characterization and Photovoltaic Behavior of a Very Narrow-Bandgap Metallopolyyne of Platinum: Solar Cells with Photocurrent Extended to Near-Infrared Wavelength. *J. Inorg. Organomet. Poly. Mat.* **2010**, *20*, 478-487.
(665) McKay, T.; Staromlynska, J.; Wilson, P.; Davy, J. Nonlinear Luminescence Spectroscopy in a Pt: Ethynyl Compound. *J. Appl. Phys.* **1999**, *85*, 1337-1341.
(666) Abd-El-Aziz, A. S.; Strohm, E. A. Transition Metal-containing Macromolecules: En Route to New Functional Materials. *Polymer* **2012**, *53*, 4879-4921.
(667) McLean, D.; Fleitz, P.; Pottenger, T.; Sutherland, R.; Brant, M.; Brandelik, D. Nonlinear Absorption study of a C60/ Toluene Solution. *Opt. Lett.* **1993**, *18*, 858-860.
(668) de la Torre, G.; Bottari, G.; Sekita, M.; Hausmann, A.; Guldi, D. M.; Torres, T. A Voyage into the Synthesis and Photophysics of Homo-and Heterobinuclear Ensembles of Phthalocyanines and Porphyrins. *Chem. Soc. Rev.* **2013**, *42*, 8049-8105.
(669) Perry, J.; Mansour, K.; Lee, I.-Y.; Wu, X.-L.; Bedworth, P.; Chen, C.-T.; Ng, D.; Marder, S.; Miles, P.; Wada, T. Organic Optical Limiter with a Strong Nonlinear Absorptive Response. *Science* **1996**, *273*, 1533-1536.
(670) Tang, B. Z.; Xu, H. Preparation, Alignment, and Optical Properties of Soluble Poly (phenylacetylene)-wrapped Carbon nanotubes. *Macromolecules* **1999**, *32*, 2569-2576.
(671) McKay, T.; Bolger, J.; Staromlynska, J.; Davy, J. Linear and Nonlinear Optical Properties of Platinum-Ethynyl. *J. Chem. Phys.* **1998**, *108*, 5537-5541.
(672) Eisler, S.; Slepkov, A. D.; Elliott, E.; Luu, T.; McDonald, R.; Hegmann, F. A.; Tykwinski, R. R. Polyynes as a Model for Carbyne: Synthesis, Physical Properties, and Nonlinear Optical Response. *J. Am. Chem. Soc.* **2005**, *127*, 2666-2676.
(673) Lan, Y.-Z.; Gao, Y.-E.; Kang, H.-L. A Large Enhancement of (hyper)polarizabilities of Polyyne Capped by Cu. *Chem. Phys. Lett.* **2014**, *608*, 308-313.
(674) Liu, R.; Azenkeng, A.; Zhou, D.; Li, Y.; Glusac, K. D.; Sun, W. Tuning Photophysical Properties and Improving Nonlinear Absorption of Pt(II) Diimine Complexes with Extended π-Conjugation in the Acetylide Ligands. *J. Phys. Chem. A* **2013**, *117*, 1907-1917.

(675) Dubinina, G. G.; Price, R. S.; Abboud, K. A.; Wicks, G.; Wnuk, P.; Stepanenko, Y.; Drobizhev, M.; Rebane, A.; Schanze, K. S. Phenylene Vinylene Platinum(II) Acetylides with Prodigious Two-Photon Absorption. *J. Am. Chem. Soc.* **2012**, *134*, 19346-19349.
(676) Chan, C. K.; Tao, C. H.; Li, K. F.; Wong, K. M.; Zhu, N.; Cheah, K. W.; Yam, V. W. Design, Synthesis, Characterization, Luminescence and Non-linear Optical (NLO) Properties of Multinuclear Platinum(II) Alkynyl Complexes. *Dalton Trans.* **2011**, *40*, 10670-10685.
(677) Price, R. S.; Dubinina, G.; Wicks, G.; Drobizhev, M.; Rebane, A.; Schanze, K. S. Polymer Monoliths Containing Two-Photon Absorbing Phenylenevinylene Platinum(II) Acetylide Chromophores for Optical Power Limiting. *ACS Appl. Mater. Interfaces* **2015**, *7*, 10795-10805.
(678) Yao, C.; Tian, Z.; Jin, D.; Zhao, F.; Sun, Y.; Yang, X.; Zhou, G.; Wong, W.-Y. Platinum(II) Acetylide Complexes with Star-and V-shaped Configurations Possessing Good Trade-off Between Optical Transparency and Optical Power Limiting Performance. *J. Mater. Chem. C* **2017**, *5*, 11672-11682.
(679) Wu, W.; Tang, R.; Li, Q.; Li, Z. Functional Hyperbranched Polymers with Advanced Optical, Electrical and Magnetic Properties. *Chem. Soc. Rev.* **2015**, *44*, 3997-4022.
(680) Grelaud, G.; Cifuentes, M. P.; Paul, F.; Humphrey, M. G. Group 8 Metal Akynyl Complexes for Nonlinear Optics. *J. Organomet. Chem.* **2014**, *751*, 181-200.
(681) Green, K. A.; Cifuentes, M. P.; Samoc, M.; Humphrey, M. G. Syntheses and NLO Properties of Metal Alkynyl Dendrimers. *Coord. Chem. Rev.* **2011**, *255*, 2025-2038.
(682) Zhou, G.-J.; Wong, W.-Y. Organometallic Acetylides of Pt (II), Au (I) and Hg (II) as New Generation Optical Power Limiting Materials. *Chem. Soc. Rev.* **2011**, *40*, 2541-2566.
(683) Lucotti, A.; Tommasini, M.; Fazzi, D.; Del Zoppo, M.; Chalifoux, W.; Tykwinski, R.; Zerbi, G. Absolute Raman Intensity Measurements and Determination of the Vibrational Second Hyperpolarizability of Adamantyl Endcapped Polyynes. *J. Raman Spectrosc.* **2012**, *43*, 1293-1298.
(684) Slepkov, A. D.; Hegmann, F. A.; Eisler, S.; Elliott, E.; Tykwinski, R. R. The Surprising Nonlinear Optical Properties of Conjugated Polyyne Oligomers. *J. Chem. Phys.* **2004**, *120*, 6807-6810.
(685) Arendt, A.; Kolkowski, R.; Samoc, M.; Szafert, S. Spectral Dependence of Nonlinear Optical Properties of Symmetrical Octatetraynes with p-Substituted Phenyl End-groups. *Phys. Chem. Chem. Phys.* **2015**, *17*, 13680-13688.
(686) Zhou, G.; Zhang, S.; Wu, P.; Ye, C. Optical Limiting Properties of Soluble Poly (thienyleneethynylene) s. *Chem. Phys. Lett.* **2002**, *363*, 610-614.
(687) Zhou, G. J.; Zhang, S.; Ye, C. The Effect of Self-Assembly on the Optical Nonlinear Absorption of Poly (3-hexyl-2, 5-thienylenediethynylene). *J. Phys. Chem. B* **2004**, *108*, 3985-3988.
(688) Zhou, G.; Liu, Y.; Ye, C. Optical-limiting Properties of Poly(arylene ethynylenes) Containing Thiophene Ring. *J. Appl. Polym. Sci.* **2004**, *93*, 131-135.
(689) Shelton, A. H.; Price, R. S.; Brokmann, L.; Dettlaff, B.; Schanze, K. S. High Efficiency Platinum Acetylide Nonlinear Absorption Chromophores Covalently Linked to Poly(methyl methacrylate). *ACS Appl Mater Interfaces* **2013**, *5*, 7867-7874.
(690) Liao, C.; Shelton, A. H.; Kim, K. Y.; Schanze, K. S. Organoplatinum Chromophores for Application in High-Performance Nonlinear Absorption Materials. *ACS Appl. Mater. Interfaces* **2011**, *3*, 3225-3238.
(691) Westlund, R.; Malmström, E.; Lopes, C.; Öhgren, J.; Rodgers, T.; Saito, Y.; Kawata, S.; Glimsdal, E.; Lindgren, M. Efficient Nonlinear Absorbing Platinum (II) Acetylide Chromophores in Solid PMMA Matrices. *Adv. Funct. Mater.* **2008**, *18*, 1939-1948.
(692) Chateau, D.; Chaput, F.; Lopes, C.; Lindgren, M.; Brannlund, C.; Ohgren, J.; Djourelov, N.; Nedelec, P.; Desroches, C.; Eliasson, B.; et al. Silica Hybrid Sol-Gel Materials with Unusually High Concentration of Pt-Organic Molecular Guests: Studies of Luminescence and Nonlinear Absorption of Light. *ACS Appl. Mater. Interfaces* **2012**, *4*, 2369-2377.
(693) Rebane, A.; Drobizhev, M.; Makarov, N. S.; Wicks, G.; Wnuk, P.; Stepanenko, Y.; Haley, J. E.; Krein, D. M.; Fore, J. L.; Burke, A. R.; et al. Symmetry Breaking in Platinum Acetylide Chromophores Studied by Femtosecond Two-Photon Absorption Spectroscopy. *J. Phys. Chem. A* **2014**, *118*, 3749-3759.
(694) Kim, K. Y.; Shelton, A. H.; Drobizhev, M.; Makarov, N.; Rebane, A.; Schanze, K. S. Optimizing Simultaneous Two-Photon Absorption and Transient Triplet-Triplet Absorption in Platinum Acetylide Chromophores. *J. Phys. Chem. A* **2010**, *114*, 7003-7013.

(695) Cooper, T. M.; Krein, D. M.; Burke, A. R.; McLean, D. G.; Rogers, J. E.; Slagle, J. E.; Fleitz, P. A. Spectroscopic Characterization of a Series of Platinum Acetylide Complexes having a Localized Triplet Exciton. *J. Phys. Chem. A* **2006**, *110*, 4369-4375.

(696) Vivas, M. G.; De Boni, L.; Cooper, T. M.; Mendonca, C. R. Interpreting Strong Two-Photon Absorption of PE3 Platinum Acetylide Complex: Double Resonance and Excited State Absorption. *ACS Photonics* **2014**, *1*, 106-113.

(697) Goswami, S.; Winkel, R. W.; Schanze, K. S. Photophysics and Nonlinear Absorption of Gold(I) and Platinum(II) Donor-Acceptor-Donor Chromophores. *Inorg. Chem.* **2015**, *54*, 10007-10014.

(698) Goswami, S.; Wicks, G.; Rebane, A.; Schanze, K. S. Photophysics and Non-linear Absorption of Au (I) and Pt (II) Acetylide Complexes of a Thienyl-Carbazole Chromophore. *Dalton Trans.* **2014**, *43*, 17721-17728.

(699) Dragonetti, C.; Colombo, A.; Fontani, M.; Marinotto, D.; Nisic, F.; Righetto, S.; Roberto, D.; Tintori, F.; Fantacci, S. Novel Fullerene Platinum Alkynyl Complexes with High Second-Order Nonlinear Optical Properties as a Springboard for NLO-Active Polymer Films. *Organometallics* **2016**, *35*, 1015–1021.

(700) Dalton, G. T.; Cifuentes, M. P.; Watson, L. A.; Petrie, S.; Stranger, R.; Samoc, M.; Humphrey, M. G. Organometallic Complexes for Nonlinear Optics. 42. Syntheses, Linear, and Nonlinear Optical Properties of Ligated Metal-functionalized Oligo(p-phenyleneethynylene)s. *Inorg. Chem.* **2009**, *48*, 6534-6547.

(701) Merhi, A.; Grelaud, G.; Ripoche, N.; Barlow, A.; Cifuentes, M. P.; Humphrey, M. G.; Paul, F.; Paul-Roth, C. O. A zinc(II) Tetraphenylporphyrin Peripherally Functionalized with Redox-active "trans-[(η^5-C_5H_5) Fe (η^5-C_5H_4)C≡C](κ^2-dppe)$_2$ Ru (C≡C)-" Substituents: Linear Electrochromism and Third-order Nonlinear optics. *Polyhedron* **2015**, *86*, 64-70.

(702) Silva, T. J. L.; Mendes, P. J.; Santos, A. M.; Garcia, M. H.; Robalo, M. P.; Ramalho, J. P. P.; Carvalho, A. J. P.; Büchert, M.; Wittenburg, C.; Heck, J. Mono(η^5-cyclopentadienyl)metal(II) Complexes with Thienyl Acetylide Chromophores: Synthesis, Electrochemical Studies, and First Hyperpolarizabilities. *Organometallics* **2014**, *33*, 4655-4671.

(703) Malvolti, F.; Rouxel, C.; Grelaud, G.; Toupet, L.; Roisnel, T.; Barlow, A.; Yang, X.; Wang, G.; Razak, A.; Fazira, I. Iron and Ruthenium Alkynyl Complexes with 2-Fluorenyl Groups: Some Linear and Nonlinear Optical Absorption Properties. *Eur. J. Inorg. Chem.* **2016**, *2016*, 3868-3882.

(704) Nisic, F.; Colombo, A.; Dragonetti, C.; Garoni, E.; Marinotto, D.; Righetto, S.; De Angelis, F.; Lobello, M. G.; Salvatori, P.; Biagini, P. Functionalized Ruthenium Dialkynyl Complexes with High Second-Order Nonlinear Optical Properties and Good Potential as Dye Sensitizers for Solar Cells. *Organometallics* **2014**, *34*, 94-104.

(705) Colombo, A.; Nisic, F.; Dragonetti, C.; Marinotto, D.; Oliveri, I. P.; Righetto, S.; Lobello, M. G.; De Angelis, F. Unexpectedly high second-order nonlinear optical properties of simple Ru and Pt alkynyl complexes as an analytical springboard for NLO-active polymer films. *Chem. Commun.* **2014**, *50*, 7986-7989.

(706) Wong, W.-Y. Challenges in Organometallic Research–Great Opportunity for Solar Cells and OLEDs. *J. Organomet. Chem.* **2009**, *694*, 2644-2647.

(707) Lam, E. S. H.; Tsang, D. P. K.; Lam, W. H.; Tam, A. Y. Y.; Chan, M. Y.; Wong, W. T.; Yam, V. W. W. Luminescent Platinum (II) Complexes of 1, 3-Bis (N-alkylbenzimidazol-2′-yl) benzene-Type Ligands with Potential Applications in Efficient Organic Light-Emitting Diodes. *Chem. Eur. J.* **2013**, *19*, 6385-6397.

(708) Forrest, S. R. The Path to Ubiquitous and Low-cost Organic Electronic Appliances on Plastic. *Nature* **2004**, *428*, 911-918.

(709) D'Andrade, B. W.; Forrest, S. R. White Organic Light-Emitting Devices for Solid-State Lighting. *Adv. Mater.* **2004**, *16*, 1585-1595.

(710) D'Andrade, B. Lighting: White Phosphorescent LEDs Offer Efficient Answer. *Nat. Photonics* **2007**, *1*, 33-34.

(711) Sheng, C. X.; Singh, S.; Gambetta, A.; Drori, T.; Tong, M.; Tretiak, S.; Vardeny, Z. V. Ultrafast Intersystem-crossing in Platinum Containing π-Conjugated Polymers with Tunable Spin-Orbit Coupling. *Sci. Rep.* **2013**, *3*, 2653-2660.

(712) Pati, A. K.; Jana, R.; Gharpure, S. J.; Mishra, A. K. Photophysics of Diphenylbutadiynes in Water, Acetonitrile–Water, and Acetonitrile Solvent Systems: Application to Single Component White Light Emission. *J. Phys. Chem. A* **2016**, *120*, 5826-5837.

(713) Tang, M. C.; Chan, A. K.; Chan, M. Y.; Yam, V. W. Platinum and Gold Complexes for OLEDs. *Top Curr Chem (Cham)* **2016**, *374*, 46-89.
(714) Tang, M. C.; Tsang, D. P.; Chan, M. M.; Wong, K. M.; Yam, V. W. Dendritic Luminescent Gold(III) Complexes for Highly Efficient Solution-Processable Organic Light-Emitting Devices. *Angew. Chem. Int. Ed. Engl.* **2013**, *52*, 446-449.
(715) Au, V. K.; Wong, K. M.; Tsang, D. P.; Chan, M. Y.; Zhu, N.; Yam, V. W. High-Efficiency Green organic Light-Emitting Devices Utilizing Phosphorescent Bis-cyclometalated Alkynylgold (III) Complexes. *J. Am. Chem. Soc.* **2010**, *132*, 14273-14278.
(716) Wong, K. M.; Zhu, X.; Hung, L. L.; Zhu, N.; Yam, V. W.; Kwok, H. S. A Novel Class of Phosphorescent Gold(III) Alkynyl-based Organic Light-Emitting Devices with Tunable Colour. *Chem. Commun. (Camb)* **2005**, DOI:10.1039/b503315b, 2906-2908.
(717) Wong, K. M.; Hung, L. L.; Lam, W. H.; Zhu, N.; Yam, V. W. A Class of Luminescent Cyclometalated Alkynylgold (III) Complexes: Synthesis, Characterization, and Electrochemical, Photophysical, and Computational Studies of [Au(C^N^C)(C≡C-R)] (C^N^C=κ^3C,N,C bis-cyclometalated 2,6-diphenyl pyridyl). *J. Am. Chem. Soc.* **2007**, *129*, 4350-4365.
(718) Yam, V. W.; Wong, K. M.; Hung, L. L.; Zhu, N. Luminescent Gold (III)Alkynyl Complexes: Synthesis, Structural Characterization, and Luminescence Properties. *Angew. Chem. Int. Ed. Engl.* **2005**, *44*, 3107-3110.
(719) Au, V. K.; Wong, K. M.; Zhu, N.; Yam, V. W. Luminescent Cyclometalated Dialkynylgold(III) Complexes of 2-Phenylpyridine-type Derivatives with readily Tunable Emission Properties. *Chemistry* **2011**, *17*, 130-142.
(720) Au, V. K.; Lam, W. H.; Wong, W. T.; Yam, V. W. Luminescent Cyclometalated Alkynylgold (III) Complexes with 6-Phenyl-2,2'-bipyridine Derivatives: Synthesis, Characterization, Electrochemistry, Photophysics, and Computational Studies. *Inorg. Chem.* **2012**, *51*, 7537-7545.
(721) Grimsdale, A. C.; Chan, K. L.; Martin, R. E.; Jokisz, P. G.; Holmes, A. B. Synthesis of Light-Emitting Conjugated Polymers for Applications in Electroluminescent Devices. *Chem. Rev.* **2009**, *109*, 897-1091.
(722) Odom, S. A.; Parkin, S. R.; Anthony, J. E. Tetracene Derivatives as Potential Red Emitters for Organic LEDs. *Org. Lett.* **2003**, *5*, 4245-4248.
(723) Wolak, M. A.; Melinger, J. S.; Lane, P. A.; Palilis, L. C.; Landis, C. A.; Delcamp, J.; Anthony, J. E.; Kafafi, Z. H. Photophysical Properties of Dioxolane-Substituted Pentacene Derivatives Dispersed in Tris(quinolin-8-olato)aluminum(III). *J. Phys. Chem. B* **2006**, *110*, 7928-7937.
(724) Biegger, P.; Stolz, S.; Intorp, S. N.; Zhang, Y.; Engelhart, J. U.; Rominger, F.; Hardcastle, K. I.; Lemmer, U.; Qian, X.; Hamburger, M.; et al. Soluble Diazaiptycenes: Materials for Solution-Processed Organic Electronics. *J. Org. Chem.* **2015**, *80*, 582-589.
(725) Roy, S.; Samanta, D.; Kumar, P.; Maji, T. K. Pure White Light Emission and Charge transfer in Organogels of Symmetrical and Unsymmetrical π-Chromophoric Oligo-p-(phenyleneethynylene) Bola-amphiphiles. *Chem. Commun. (Camb)* **2018**, *54*, 275-278.
(726) Goudreault, T.; He, Z.; Guo, Y.; Ho, C.-L.; Zhan, H.; Wang, Q.; Ho, K. Y.-F.; Wong, K.-L.; Fortin, D.; Yao, B. Synthesis, Light-Emitting, and Two-Photon Absorption Properties of Platinum-Containing Poly (arylene-ethynylene) s Linked by 1, 3, 4-Oxadiazole Units. *Macromolecules* **2010**, *43*, 7936-7949.
(727) Lee, J.; Jung, B. J.; Lee, S. K.; Lee, J. I.; Cho, H. J.; Shim, H. K. Fluorene-based aAternating Polymers Containing Electron-Withdrawing Bithiazole Units: Preparation and Device Applications. *J. Polym. Sci., Part A: Polym. Chem.* **2005**, *43*, 1845-1857.
(728) Zhou, G.; He, Y.; Yao, B.; Dang, J.; Wong, W. Y.; Xie, Z.; Zhao, X.; Wang, L. Electrophosphorescent Heterobimetallic Oligometallaynes and Their Applications in Solution-Processed Organic Light-Emitting Devices. *Chem. Asian J.* **2010**, *5*, 2405-2414.
(729) Li, Y.-P.; Fan, X.-X.; Wu, Y.; Zeng, X.-C.; Wang, J.-Y.; Wei, Q.-H.; Chen, Z.-N. High-Efficiency Organic Light-Emitting Diodes of Phosphorescent $PtAg_2$ Heterotrinuclear Acetylide Complexes Supported by Triphosphine. *J. Mater. Chem. C* **2017**, *5*, 3072-3078.
(730) Nielsen, C. B.; Turbiez, M.; McCulloch, I. Recent Advances in the Development of Semiconducting DPP-Containing Polymers for Transistor Applications. *Adv. Mater.* **2013**, *25*, 1859-1880.
(731) Murphy, A. R.; Frechet, J. M. Organic Semiconducting Oligomers for use in Thin Film Transistors. *Chem. Rev.* **2007**, *107*, 1066-1096.

(732) Yamashita, Y. Organic Semiconductors for Organic Field-Effect Transistors. *Sci. Technol. Adv. Mater.* **2009**, *10*, 024313-024322.
(733) Yun, H.-J.; Choi, H. H.; Kwon, S.-K.; Kim, Y.-H.; Cho, K. Conformation-insensitive Ambipolar Charge Transport in a Diketopyrrolopyrrole-based Co-polymer Containing Acetylene Linkages. *Chem. Mater.* **2014**, *26*, 3928-3937.
(734) Anthony, J. E.; Brooks, J. S.; Eaton, D. L.; Parkin, S. R. Functionalized Pentacene: Improved Electronic Properties from Control of Solid-State Order. *J. Am. Chem. Soc.* **2001**, *123*, 9482-9483.
(735) Sheraw, C. D.; Jackson, T. N.; Eaton, D. L.; Anthony, J. E. Functionalized Pentacene Active Layer Organic Thin-Film Transistors. *Adv. Mater.* **2003**, *15*, 2009-2011.
(736) Payne, M. M.; Parkin, S. R.; Anthony, J. E.; Kuo, C.-C.; Jackson, T. N. Organic Field-Effect Transistors from Solution-Deposited Functionalized Acenes with Mobilities as High as 1 cm^2/V.s. *J. Am. Chem. Soc.* **2005**, *127*, 4986-4987.
(737) Lee, J. B.; Kim, K. H.; Hong, C. S.; Choi, D. H. High-Performance Amorphous Donor–Acceptor Conjugated Polymers Containing X-shaped Anthracene-based Monomer and 2, 5-Bis (2-octyldodecyl) pyrrolo [3, 4-c] pyrrole-1, 4 (2H, 5H)-dione for Organic Thin-Film Transistors. *J. Polym. Sci., Part A: Polym. Chem.* **2012**, *50*, 2809-2818.
(738) Swartz, C. R.; Parkin, S. R.; Bullock, J. E.; Anthony, J. E.; Mayer, A. C.; Malliaras, G. G. Synthesis and Characterization of Electron-Deficient Pentacenes. *Org. Lett.* **2005**, *7*, 3163-3166.
(739) Ostoja, P.; Maccagnani, P.; Gazzano, M.; Cavallini, M.; Kengne, J.; Kshirsagar, R.; Biscarini, F.; Melucci, M.; Zambianchi, M.; Barbarella, G. FET Device Performance, Morphology and X-ray Thin Film Structure of Unsubstituted and Modified Quinquethiophenes. *Synth. Met.* **2004**, *146*, 243-250.
(740) Kim, H.; Reddy, M. R.; Kwon, G.; Choi, D.; Kim, C.; Seo, S. Synthesis and Characterization of Arylacetylene Derivative as Solution Processable Organic Semiconductors for Organic Thin-Film Transistors. *J. Nanosci. Nanotechnol.* **2016**, *16*, 10331-10336.
(741) Boudreault, P.-L. T.; Hennek, J. W.; Loser, S.; Ortiz, R. P.; Eckstein, B. J.; Facchetti, A.; Marks, T. J. New Semiconductors Based on 2, 2′-Ethyne-1, 2-diylbis [3-(alk-1-yn-1-yl) thiophene] for Organic Opto-Electronics. *Chem. Mater.* **2012**, *24*, 2929-2942.
(742) Wang, Q.; He, Z.; Wild, A.; Wu, H.; Cao, Y.; S Schubert, U.; Chui, C. H.; Wong, W. Y. Platinum–Acetylide Polymers with Higher Dimensionality for Organic Solar Cells. *Chem. Asian J.* **2011**, *6*, 1766-1777.
(743) Yan, L.; Zhao, Y.; Wang, X.; Wang, X. Z.; Wong, W. Y.; Liu, Y.; Wu, W.; Xiao, Q.; Wang, G.; Zhou, X.; et al. Platinum-based Poly(aryleneethynylene) Polymers Containing Thiazolothiazole Group with High Hole Mobilities for Field-Effect Transistor Applications. *Macromol. Rapid Commun.* **2012**, *33*, 603-609.
(744) Huang, J.; Peng, B.; Wang, W.; Ji, H.; Li, L.; Xi, K.; Lai, W.; Zhang, X.; Jia, X. Architecture of Conjugated Donor–Acceptor (D–A)-Type Polymer Films with Cross-Linked Structures. *Adv. Funct. Mater.* **2016**, *26*, 1646-1655.
(745) Debnath, S.; Singh, S.; Bedi, A.; Krishnamoorthy, K.; Zade, S. S. Synthesis, Optoelectronic, and Transistor Properties of BODIPY-and Cyclopenta [c] thiophene-Containing π-Conjugated Copolymers. *J. Phys. Chem. C* **2015**, *119*, 15859-15867.
(746) Debnath, S.; Singh, S.; Bedi, A.; Krishnamoorthy, K.; Zade, S. S. Site-Selective Synthesis and Characterization of BODIPY-Acetylene Copolymers and Their Transistor Properties. *J. Polym. Sci., Part A: Polym. Chem.* **2016**, *54*, 1978-1986.
(747) Kola, S.; Kim, J. H.; Ireland, R.; Yeh, M.-L.; Smith, K.; Guo, W.; Katz, H. E. Pyromellitic Diimide–Ethynylene-Based Homopolymer Film as an N-Channel Organic Field-Effect Transistor Semiconductor. *ACS Macro Lett.* **2013**, *2*, 664-669.
(748) Zhao, X.; Ma, L.; Zhang, L.; Wen, Y.; Chen, J.; Shuai, Z.; Liu, Y.; Zhan, X. An Acetylene-Containing Perylene Diimide Copolymer for High Mobility n-Channel Transistor in Air. *Macromolecules* **2013**, *46*, 2152-2158.
(749) Yan, L.; Li, C.; Cai, L.; Shi, K.; Tang, W.; Qu, W.; Ho, C.-L.; Yu, G.; Li, J.; Wang, X. Metallopolyyne Polymers Containing Naphthalene Diimide-Oligothiophene Moieties and Their Applications in Organic Field-Effect Transistors. *J. Organomet. Chem.* **2017**, *846*, 269-276.
(750) Moreno-Garcia, P.; Gulcur, M.; Manrique, D. Z.; Pope, T.; Hong, W.; Kaliginedi, V.; Huang, C.; Batsanov, A. S.; Bryce, M. R.; Lambert, C.; et al. Single-Molecule Conductance of Functionalized Oligoynes: Length Dependence and Junction Evolution. *J. Am. Chem. Soc.* **2013**, *135*, 12228-12240.

(751) Gulcur, M.; Moreno-García, P.; Zhao, X.; Baghernejad, M.; Batsanov, A. S.; Hong, W.; Bryce, M. R.; Wandlowski, T. The Synthesis of Functionalised Diaryltetraynes and Their Transport Properties in Single-Molecule Junctions. *Chem. Eur. J.* **2014**, *20*, 4653-4660.
(752) Sadeghi, H.; Sangtarash, S.; Lambert, C. J. Oligoyne Molecular Junctions for Efficient Room Temperature Thermoelectric Power Generation. *Nano Lett.* **2015**, *15*, 7467-7472.
(753) Hong, W.; Li, H.; Liu, S.-X.; Fu, Y.; Li, J.; Kaliginedi, V.; Decurtins, S.; Wandlowski, T. Trimethylsilyl-Terminated Oligo (phenylene ethynylene) s: an Approach to Single-Molecule Junctions with Covalent Au–C σ-Bonds. *J. Am. Chem. Soc.* **2012**, *134*, 19425-19431.
(754) Ballesteros, L. M.; Martín, S.; Marqués-González, S.; López, M. C.; Higgins, S. J.; Nichols, R. J.; Low, P. J.; Cea, P. Single Gold Atom Containing Oligo (phenylene) Ethynylene: Assembly into Lb Films and Electrical Characterization. *J. Phys. Chem. C* **2014**, *119*, 784-793.
(755) Ballesteros, L. M.; Martín, S.; Momblona, C.; Marqués-González, S.; López, M. C.; Nichols, R. J.; Low, P. J.; Cea, P. Acetylene used as a New Linker for Molecular Junctions in Phenylene–Ethynylene Oligomer Langmuir–Blodgett Films. *J. Phys. Chem. C* **2012**, *116*, 9142-9150.
(756) Ballesteros, L. M.; Martín, S.; Cortés, J.; Marqués-González, S.; Higgins, S. J.; Nichols, R. J.; Low, P. J.; Cea, P. Controlling the Structural and Electrical Properties of Diacid Oligo (Phenylene Ethynylene) Langmuir–Blodgett Films. *Chem. Eur. J.* **2013**, *19*, 5352-5363.
(757) Pera, G.; Martín, S.; Ballesteros, L. M.; Hope, A. J.; Low, P. J.; Nichols, R. J.; Cea, P. Metal–Molecule–Metal Junctions in Langmuir–Blodgett Films Using a New Linker: Trimethylsilane. *Chem. Eur. J.* **2010**, *16*, 13398-13405.
(758) Ballesteros, L. M.; Martin, S.; Pera, G.; Schauer, P. A.; Kay, N. J.; Lopez, M. C.; Low, P. J.; Nichols, R. J.; Cea, P. Directionally Oriented LB Films of an OPE Derivative: Assembly, Characterization, and Electrical Properties. *Langmuir* **2011**, *27*, 3600-3610.
(759) Sugimoto, K.; Tanaka, Y.; Fujii, S.; Tada, T.; Kiguchi, M.; Akita, M. Organometallic Molecular Wires as Versatile Modules for Energy-Level Alignment of the Metal–Molecule–Metal Junction. *Chem. Commun.* **2016**, *52*, 5796-5799.
(760) Bruce, M. I. Organometallic Chemistry of Vinylidene and Related Unsaturated Carbenes. *Chem. Rev.* **1991**, *91*, 197-257.
(761) Maretina, I. A.; Trofimov, B. A. Diacetylene: A Candidate for Industrially Important Reactions. *Russ. Chem. Rev.* **2000**, *69*, 591-608.
(762) Zhang, C.; Chen, P.; Hu, W. Organic Field-Effect Transistor-based Gas Sensors. *Chem. Soc. Rev.* **2015**, *44*, 2087-2107.
(763) Zang, Y.; Huang, D.; Di, C. A.; Zhu, D. Device Engineered Organic Transistors for Flexible Sensing Applications. *Adv. Mater.* **2016**, *28*, 4549-4555.
(764) Swager, T. M. The Molecular Wire Approach to Sensory Signal Amplification. *Acc. Chem. Res.* **1998**, *31*, 201-207.
(765) Daud, A. I.; Khairul, W. M.; Zuki, H. M.; Kubulat, K. Aerobic Synthetic Approach and Characterisation of some Acetylide–Thiourea Derivatives for the Detection of Carbon Monoxide (CO) Gas. *J. Mol. Struct.* **2015**, *1093*, 172-178.
(766) Daud, A. I.; Khairul, W. M.; Mohamed Zuki, H.; KuBulat, K. Synthesis and Characterization of N-(4-Aminophenylethynylbenzonitrile)-N′-(1-naphthoyl) Thiourea as Single Molecular Chemosensor for Carbon Monoxide Sensing. *J. Sulfur Chem.* **2014**, *35*, 691-699.
(767) Buckland, D.; Bhosale, S. V.; Langford, S. J. A Chemodosimer Based on a Core-substituted Naphthalene Diimide for Fluoride Ion Detection. *Tetrahedron Lett.* **2011**, *52*, 1990-1992.
(768) Huang, C.-B.; Huang, J.; Xu, L. A Highly Selective Fluorescent Probe for Fast Detection of Nitric Oxide in Aqueous Solution. *RSC Adv.* **2015**, *5*, 13307-13310.
(769) Qu, Y.; Jiang, Y.; Hua, J. Hyperbranched Polyyne Containing Naphthalimide Moiety as a Fluorescent Chemosensor for Mercury Ion. *Front. Chem. Chin.* **2010**, *5*, 226-233.
(770) Huang, C.-B.; Chen, L.-J.; Huang, J.; Xu, L. A Novel Pyrene-Containing Fluorescent Organogel Derived from a Quinoline-based Fluorescent Porbe: Synthesis, Sensing Properties, and its Aggregation Behavior. *RSC Adv.* **2014**, *4*, 19538-19549.
(771) Ren, Y. Y.; Wu, N. W.; Huang, J.; Xu, Z.; Sun, D. D.; Wang, C. H.; Xu, L. A Neutral Branched Platinum-Acetylide Complex Possessing a Tetraphenylethylene Core: Preparation of a Luminescent Organometallic Gelator and its Unexpected Spectroscopic Behaviour during Sol-to-Gel Transition. *Chem. Commun. (Camb)* **2015**, *51*, 15153-15156.

(772) Penza, M.; Cassano, G.; Sergi, A.; Lo Sterzo, C.; Russo, M. V. SAW Chemical Sensing using Polyynes and Organometallic Polymer Films. *Sens. Actuators, B* **2001**, *81*, 88-98.
(773) Tian, Y. J.; Shi, E. T.; Tian, Y. K.; Yao, R. S.; Wang, F. Cooperative Complexation of Amino Acid Derivatives to Platinum Acetylide-Based Bolaamphiphile. *Org. Lett.* **2014**, *16*, 3180-3183.
(774) Chowdhury, A.; Howlader, P.; Mukherjee, P. S. Mechano-fluorochromic Pt(II) Luminogen and Its Cysteine Recognition. *Chem. Eur. J.* **2016**, *22*, 1424-1434.
(775) Ni, J.; Kang, J.-J.; Wang, H.-H.; Gai, X.-Q.; Zhang, X.-X.; Jia, T.; Xu, L.; Pan, Y.-Z.; Zhang, J.-J. A Colorimetric/Luminescent Benzene Compound Sensor Based on a Bis (σ-acetylide) Platinum(II) Complex: Enhancing Selectivity and Reversibility Through Dual-Recognition Sites Strategy. *RSC Adv.* **2015**, *5*, 65613-65617.
(776) Sen, C. P.; Shrestha, R. G.; Shrestha, L. K.; Ariga, K.; Valiyaveettil, S. Low-Band-Gap BODIPY Conjugated Copolymers for Sensing Volatile Organic Compounds. *Chemistry* **2015**, *21*, 17344-17354.
(777) Wu, Y.; Tan, Y.; Wu, J.; Chen, S.; Chen, Y. Z.; Zhou, X.; Jiang, Y.; Tan, C. Fluorescence Array-based Sensing of Metal Ions using Conjugated Polyelectrolytes. *ACS Appl. Mater. Interfaces* **2015**, *7*, 6882-6888.
(778) Wu, W.; Chen, A.; Tong, L.; Qing, Z.; Langone, K. P.; Bernier, W. E.; Jones, W. E., Jr. Facile Synthesis of Fluorescent Conjugated Polyelectrolytes Using Polydentate Sulfonate as Highly Selective and Sensitive Copper(II) Sensors. *ACS Sens.* **2017**, *2*, 1337-1344.
(779) Zhou, L.-L.; Li, M.; Lu, H.-Y.; Chen, C.-F. Benzo [5] Helicene-based Conjugated Polymers: Synthesis, Photophysical Properties, and Application for the Detection of Nitroaromatic Explosives. *Polym. Chem.* **2016**, *7*, 310-318.
(780) Wu, J.; Tan, C.; Chen, Z.; Chen, Y. Z.; Tan, Y.; Jiang, Y. Fluorescence Array-based Sensing of Nitroaromatics using Conjugated Polyelectrolytes. *Analyst* **2016**, *141*, 3242-3245.
(781) Han, J.; Wang, B.; Bender, M.; Seehafer, K.; Bunz, U. H. Water-Soluble Poly(p-aryleneethynylene)s: A Sensor Array Discriminates Aromatic Carboxylic Acids. *ACS Appl. Mater. Interfaces* **2016**, *8*, 20415-20421.
(782) Han, J.; Bender, M.; Hahn, S.; Seehafer, K.; Bunz, U. H. Polyelectrolyte Complexes Formed from Conjugated Polymers: Array-Based Sensing of Organic Acids. *Chemistry* **2016**, *22*, 3230-3233.
(783) Han, J.; Bender, M.; Seehafer, K.; Bunz, U. H. Identification of White Wines by using Two Oppositely Charged Poly(p-phenyleneethynylene)s Individually and in Complex. *Angew. Chem. Int. Ed. Engl.* **2016**, *55*, 7689-7692.
(784) Han, J.; Wang, B.; Bender, M.; Kushida, S.; Seehafer, K.; Bunz, U. H. Poly(aryleneethynylene) Tongue That Identifies Nonsteroidal Anti-Inflammatory Drugs in Water: A Test Case for Combating Counterfeit Drugs. *ACS Appl. Mater. Interfaces* **2017**, *9*, 790-797.
(785) Shanmugaraju, S.; Joshi, S. A.; Mukherjee, P. S. Self-assembly of Metallamacrocycles using a Dinuclear Organometallic Acceptor: Synthesis, Characterization, and Sensing Study. *Inorg. Chem.* **2011**, *50*, 11736-11745.
(786) Gatri, R.; Ouerfelli, I.; Efrit, M. L.; Serein-Spirau, F. o.; Lère-Porte, J.-P.; Valvin, P.; Roisnel, T.; Bivaud, S. b.; Akdas-Kilig, H.; Fillaut, J.-L. Supramolecular Ruthenium–Alkynyl Multicomponent Architectures: Engineering, Photophysical Properties, and Responsiveness to Nitroaromatics. *Organometallics* **2014**, *33*, 665-676.
(787) Sun, P.; Jiang, Y.; Xie, G.; Yu, J.; Du, X.; Hu, J. Synthesis and Sensitive Properties of Poly-(bistriethylphosphine)-platinum-diethynylbenzene for Organic Vapor Detection. *J. Appl. Polym. Sci.* **2010**, *116*, 562-567.
(788) Caliendo, C.; Fratoddi, I.; Russo, M. V. Sensitivity of a Platinum-polyyne-based Sensor to Low Relative Humidity and Chemical Vapors. *Appl. Phys. Lett.* **2002**, *80*, 4849-4851.
(789) Ogawa, K.; Guo, F.; Schanze, K. S. Phosphorescence Quenching of a Platinum Acetylide Polymer by Transition Metal Ions. *J. Photochem. Photobiol., A* **2009**, *207*, 79-85.
(790) Lu, X. X.; Li, C. K.; Cheng, E. C.; Zhu, N.; Yam, V. W. Syntheses, Structural Characterization, and Host-guest Chemistry of Ethynylcrown Ether Containing Polynuclear Gold(I) Complexes. *Inorg. Chem.* **2004**, *43*, 2225-2227.
(791) Zhou, Y.-P.; Liu, E.-B.; Wang, J.; Chao, H.-Y. Highly Ag^+ Selective Tripodal Gold(I) Acetylide-based "Off–On" Luminescence Chemosensors based on $^3(\pi\pi^*)$ Emission Switching. *Inorg. Chem.* **2013**, *52*, 8629-8637.

(792) Yam, V. W.-W.; Cheung, K.-L.; Yuan, L.-H.; Wong, K. M.-C.; Cheung, K.-K. Synthesis, Structural Characterization and Binding Studies of a Novel Dinuclear Gold(I) Calix[4]Crown Acetylide Complex. *Chem. Commun.* **2000**, 1513-1514.
(793) Yam, V. W.-W.; Yip, S.-K.; Yuan, L.-H.; Cheung, K.-L.; Zhu, N.; Cheung, K.-K. Synthesis, Structure, and Ion-Binding Properties of Luminescent Gold(I) Alkynylcalix[4]Crown-5 Complexes. *Organometallics* **2003**, *22*, 2630-2637.
(794) He, X.; Lam, W. H.; Zhu, N.; Yam, V. W. W. Design and Synthesis of Calixarene-Based Bis-alkynyl-Bridged Dinuclear AuI Isonitrile Complexes as Luminescent Ion Probes by the Modulation of Au··· Au Interactions. *Chem. Eur. J.* **2009**, *15*, 8842-8851.
(795) He, X.; Cheng, E. C.-C.; Zhu, N.; Yam, V. W.-W. Selective Ion Probe for Mg^{2+} Based on Au(I)··· Au(I) Interactions in a Tripodal Alkynylgold(I) Complex with Oligoether Pendants. *Chem. Commun.* **2009**, 4016-4018.
(796) He, X.; Zhu, N.; Yam, V. W.-W. Synthesis, Characterization, Structure, and Selective Cu^{2+} Sensing Studies of an Alkynylgold(I) Complex Containing the Dipicolylamine Receptor. *Organometallics* **2009**, *28*, 3621-3624.
(797) He, X.; Yam, V. W. A Highly Selective Bifunctional Luminescence Probe for Potassium and Fluoride Ions. *Org. Lett.* **2011**, *13*, 2172-2175.
(798) Ghosh, S.; Chakrabarty, R.; Mukherjee, P. S. Design, Synthesis, and Characterizations of a Series of Pt4 Macrocycles and Fluorescent Sensing of Fe^{3+}/Cu^{2+}/Ni^{2+} Through Metal Coordination. *Inorg. Chem.* **2008**, *48*, 549-556.
(799) Shanmugaraju, S.; Bar, A. K.; Chi, K.-W.; Mukherjee, P. S. Coordination-Driven Self-Assembly of Metallamacrocycles via a New Pt^{II}_2 Organometallic Building Block with 90° Geometry and Optical Sensing of Anions. *Organometallics* **2010**, *29*, 2971-2980.
(800) Liu, B.; Yu, W.-L.; Pei, J.; Liu, S.-Y.; Lai, Y.-H.; Huang, W. Design and Synthesis of Bipyridyl-containing Conjugated Polymers: Effects of Polymer Rigidity on Metal Ion Sensing. *Macromolecules* **2001**, *34*, 7932-7940.
(801) He, X.; Yam, V. W.-W. Luminescent Gold(I) Complexes for Chemosensing. *Coord. Chem. Rev.* **2011**, *255*, 2111-2123.
(802) Chen, G.; Mahmud, I.; Dawe, L. N.; Daniels, L. M.; Zhao, Y. Synthesis and Properties of Conjugated Oligoyne-centered π-Extended Tetrathiafulvalene Analogues and Related Macromolecular Systems. *J. Org. Chem.* **2011**, *76*, 2701-2715.
(803) Zeng, Y.; Ren, J. Q.; Shen, A. G.; Hu, J. M. Field and Pretreatment-free Detection of Heavy Metal Ions in Organic Polluted Water through Alkyne-coded SERS Test Kit. *ACS Appl. Mater. Interfaces* **2016**, *8*, 27772-27778.
(804) Sekine, Y.; Kosaka, W.; Taniguchi, K.; Miyasaka, H. Conductive Molecular Magnets. In *Molecular Magnetic Materials: Concepts and Applications;* Wiley-VCH Verlag GmbH & Co. KGaA:Weinheim, Germany, **2016**; pp 369-404.
(805) Vleugels, R.; de Vega, L.; Brullot, W.; Verbiest, T.; Gómez-Lor, B.; Gutierrez-Puebla, E.; Hennrich, G. Magneto-Optical Activity in Organic Thin Film Materials. *Smart Mater. Struct.* **2016**, *25*, 12LT01-12LT08.
(806) Nishijo, J.; Judai, K.; Nishi, N. Weak Ferromagnetism and Strong Spin-Spin Interaction Mediated by the Mixed-valence Ethynyltetrathiafulvalene-type Ligand. *Inorg. Chem.* **2011**, *50*, 3464-3470.
(807) Nishijo, J. Chromium-ethynyltetrathiafulvalene Complex Based Magnetic Materials. *Polyhedron* **2013**, *66*, 43-47.
(808) Nishijo, J.; Shima, Y.; Enomoto, M. Synthesis, Crystal Structures and Magnetic Properties of New Chromium(III)–acetylide–TTF type Complexes. *Polyhedron* **2017**, *136*, 35-41.
(809) Vacher, A.; Barrière, F.; Roisnel, T.; Lorcy, D. Electronic Communication Between Metal–organic Electrophores in an Organometallic Ruthenium–acetylide–tetrathiafulvalene Complex. *Chem. Commun.* **2009**, 7200-7202.
(810) Nishijo, J.; Enomoto, M. Synthesis, Structure and Magnetic Properties of [CrCyclam(C≡C-6-methoxynaphthalene)$_2$](TCNQ)$_n$ (1,2-dichloroethane) (*n = 1, 2*). *Inorg. Chim. Acta* **2015**, *437*, 59-63.
(811) Nishijo, J.; Enomoto, M. A Series of Weak Ferromagnets Based on a Chromium-acetylide-TTF type Complex: Correlation of the Structures and Magnetic Properties and Origin of the Weak Ferromagnetism. *Inorg. Chem.* **2013**, *52*, 13263-13268.

(812) Onitsuka, K.; Fujimoto, M.; Kitajima, H.; Ohshiro, N.; Takei, F.; Takahashi, S. Convergent Synthesis of Platinum–acetylide Dendrimers. *Chem. Eur. J.* **2004**, *10*, 6433-6446.
(813) Onitsuka, K.; Fujimoto, M.; Ohshiro, N.; Takahashi, S. Convergent Route to Organometallic Dendrimers Composed of Platinum–Acetylide Units. *Angew. Chem. Int. Ed.* **1999**, *38*, 689-692.
(814) McDonagh, A. M.; Powell, C. E.; Morrall, J. P.; Cifuentes, M. P.; Humphrey, M. G. Convergent Synthesis of Alkynylbis (bidentate phosphine) ruthenium Dendrimers. *Organometallics* **2003**, *22*, 1402-1413.
(815) Weyland, T.; Costuas, K.; Mari, A.; Halet, J.-F.; Lapinte, C. [(Cp*)(dppe) Fe(III)−]$^{+}$ Units Bridged through 1, 3-Diethynylbenzene and 1, 3, 5-Triethynylbenzene Spacers: Ferromagnetic Metal−Metal Exchange Interaction. *Organometallics* **1998**, *17*, 5569-5579.
(816) Hoffert, W. A.; Rappe, A. K.; Shores, M. P. Topological and Electronic Influences on Magnetic Exchange Coupling in Fe(III) Ethynylbenzene Dendritic Building Blocks. *J. Am. Chem. Soc.* **2011**, *133*, 20823-20836.
(817) Newell, B. S.; Rappe, A. K.; Shores, M. P. Experimental Evidence for Magnetic Exchange in Di- and Trinuclear Uranium(IV) Ethynylbenzene Complexes. *Inorg. Chem.* **2010**, *49*, 1595-1606.
(818) Poon, C. T.; Wu, D.; Lam, W. H.; Yam, V. W. W. A Solution-Processable Donor–Acceptor Compound Containing Boron(III) Centers for Small-Molecule-Based High-Performance Ternary Electronic Memory Devices. *Angew. Chem. Int. Ed.* **2015**, *54*, 10569-10573.
(819) Yen, H.-J.; Shan, C.; Wang, L.; Xu, P.; Zhou, M.; Wang, H.-L. Development of Conjugated Polymers for Memory Device Applications. *Polymers* **2017**, *9*, 25-40.
(820) Mukherjee, B.; Mukherjee, M.; Park, J.-e.; Pyo, S. High-Performance Molecular Memory Device Using Ag−TCNQ Crystals Grown by Solution Process. *J. Phys. Chem. C* **2009**, *114*, 567-571.
(821) Bakkar, A.; Cobo, S.; Lafolet, F.; Roldan, D.; Saint-Aman, E.; Royal, G. A Redox-and Photo-responsive Quadri-state Switch based on Dimethyldihydropyrene-appended Cobalt Complexes. *J. Mater. Chem. C* **2016**, *4*, 1139-1143.
(822) Pradhan, B.; Das, S. Role of New Bis (2,2′-bipyridyl)(triazolopyridyl) ruthenium(II) Complex in the Organic Bistable Memory Application. *Chem. Mater.* **2008**, *20*, 1209-1211.
(823) Goswami, S.; Sengupta, D.; Paul, N. D.; Mondal, T. K.; Goswami, S. Redox Non-Innocence of Coordinated 2-(Arylazo) Pyridines in Iridium Complexes: Characterization of Redox Series and an Insight into Voltage-Induced Current Characteristics. *Chem. Eur. J.* **2014**, *20*, 6103-6111.
(824) Fang, J.; You, H.; Chen, J.; Lin, J.; Ma, D. Memory Devices Based on Lanthanide (Sm3+, Eu3+, Gd3+) Complexes. *Inorg. Chem.* **2006**, *45*, 3701-3704.
(825) Chan, H.; Lee, S. H.; Poon, C. T.; Ng, M.; Yam, V. W. W. Manipulation of Push–Pull System by Functionalization of Porphyrin at β-Position for High-Performance Solution-Processable Ternary Resistive Memory Devices. *ChemNanoMat* **2017**, *3*, 164-167.
(826) Leung, M. Y.; Leung, S. Y. L.; Wu, D.; Yu, T.; Yam, V. W. W. Synthesis, Electrochemistry, and Photophysical Studies of Ruthenium(II) Polypyridine Complexes with D–π–A–π–D Type Ligands and Their Application Studies as Organic Memories. *Chem. Eur. J.* **2016**, *22*, 14013-14021.
(827) Cheng, X. F.; Shi, E. B.; Hou, X.; Shu, J.; He, J. H.; Li, H.; Xu, Q. F.; Li, N. J.; Chen, D. Y.; Lu, J. M. 1D π-d Conjugated Coordination Polymers for Multilevel Memory of Long-Term and High-Temperature Stability. *Adv. Electron. Mater.* **2017**, *3*, 1700107-1700115.
(828) Wang, G.; Miao, S.; Zhang, Q.; Liu, H.; Li, H.; Li, N.; Xu, Q.; Lu, J.; Wang, L. Effect of a π-Spacer Between a Donor and an Acceptor on Small Molecule-based Data-Storage Device Performance. *Chem. Commun.* **2013**, *49*, 9470-9472.
(829) Li, H.; Jin, Z.; Li, N.; Xu, Q.; Gu, H.; Lu, J.; Xia, X.; Wang, L. A Small-molecule-based Device for Data Storage and Electro-optical Switch Applications. *J. Mater. Chem.* **2011**, *21*, 5860-5862.
(830) Jin, C.; Lee, J.; Lee, E.; Hwang, E.; Lee, H. Nonvolatile Resistive Memory of Ferrocene Covalently Bonded to Reduced Graphene Oxide. *Chem. Commun. (Camb)* **2012**, *48*, 4235-4237.
(831) Sun, S.; Zhuang, X.; Wang, L.; Liu, B.; Zhang, B.; Chen, Y. BODIPY-based Conjugated Polymer Covalently Grafted Reduced Graphene Oxide for Flexible Nonvolatile Memory Devices. *Carbon* **2017**, *116*, 713-721.
(832) Xiang, J.; Wang, T.-K.; Zhao, Q.; Huang, W.; Ho, C.-L.; Wong, W.-Y. Ferrocene-containing Poly(fluorenylethynylene)s for Nonvolatile Resistive Memory Devices. *J. Mater. Chem. C* **2016**, *4*, 921-928.
(833) Au, V. K.; Wu, D.; Yam, V. W. Organic Memory Devices based on a Bis-cyclometalated Alkynylgold(III) Complex. *J. Am. Chem. Soc.* **2015**, *137*, 4654-4657.

(834) Wang, P.; Fang, Y.; Jiang, J.; Ji, Y.; Li, Y.; Zheng, J.; Xu, Q.; Lu, J. Resistance Controllability in Alkynylgold(III) Complex-Based Resistive Memory for Flash-Type Storage Applications. *Chem. Asian. J.* **2017**, *12*, 1790-1795.
(835) Chan, A. K.-W.; Ng, M.; Wong, Y.-C.; Chan, M.-Y.; Wong, W.-T.; Yam, V. W.-W. Synthesis and Characterization of Luminescent Cyclometalated Platinum(II) Complexes with Tunable Emissive Colors and Studies of Their Application in Organic Memories and Organic Light-Emitting Devices. *J. Am. Chem. Soc.* **2017**, *139*, 10750-10761.
(836) Hong, E. Y.; Poon, C. T.; Yam, V. W. A Phosphole Oxide-Containing Organogold(III) Complex for Solution-Processable Resistive Memory Devices with Ternary Memory Performances. *J. Am. Chem. Soc.* **2016**, *138*, 6368-6371.
(837) Hong, E. Y.; Yam, V. W. Triindole-Tris-Alkynyl-Bridged Trinuclear Gold(I) Complexes for Cooperative Supramolecular Self-Assembly and Small-Molecule Solution-Processable Resistive Memories. *ACS Appl. Mater. Interfaces* **2017**, *9*, 2616-2624.
(838) Zhan, X.; Yang, M.; Sun, H. Transition Metal Acetylide Catalysts for Polymerization of Polar Alkynes. *Catal. Lett.* **2000**, *70*, 79-82.
(839) Kishimoto, Y.; Eckerle, P.; Miyatake, T.; Ikariya, T.; Noyori, R. Living Polymerization of Phenylacetylenes Initiated by Rh ($C{\equiv}CC_6H_5$)(2,5-norbornadiene)[$P(C_6H_5)_3$]$_2$. *J. Am. Chem. Soc.* **1994**, *116*, 12131-12132.
(840) Zhan, X.; Yang, M.; Sun, H. Transition Metal Acetylide Catalysts for Polymerization of Alkynes. *J. Mol. Catal. A: Chem.* **2001**, *169*, 63-66.
(841) Li, Y.; Yang, M. Transition Metal Acetylide Catalysts for Polymerization of Alkynes. *J. Mol. Catal. A: Chem.* **2002**, *184*, 161-165.
(842) Zhan, X.; Yang, M.; Lei, Z. Transition Metal Acetylide Catalysts for Polymerization of p-Diethynylbenzene 4. *J. Mol. Catal. A: Chem.* **2002**, *184*, 139-145.
(843) Russo, M. V.; Furlani, A.; Altamura, P.; Fratoddi, I.; Polzonetti, G. Synthesis and X.p.s. Characterization of Organometallic Pd Containing Polymers from Monosubstituted Acetylenes. *Polymer* **1997**, *38*, 3677-3690.
(844) Russo, M. V.; Furlani, A.; Cuccu, M.; Polzonetti, G. Synthesis and Characterization of Poly(ethynyltrimethylsilane) Containing Pd(II) Coordination Sites. *Polymer* **1996**, *37*, 1715-1722.
(845) Bolasco, A.; Chimenti, F.; Frezza, A.; Furlani, A.; Infante, G.; Muraglia, E.; Ortaggi, G.; Polzonetti, G.; Russo, M.; Sleiter, G. Polymerization of p-Diethynylbiphenyl via Oxidative or Catalytic Reactions. *Polymer* **1992**, *33*, 3049-3054.
(846) Kishimoto, Y.; Miyatake, T.; Ikariya, T.; Noyori, R. An Efficient Rhodium(I) Initiator for Stereospecific Living Polymerization of Phenylacetylenes. *Macromolecules* **1996**, *29*, 5054-5055.
(847) Yang, M.; Zheng, M.; Furlani, A.; Russo, M. V. A Novel Palladium Catalyst for the Polymerization of Propargyl Alcohol. *J. Polym. Sci., Part A: Polym. Chem.* **1994**, *32*, 2709-2713.
(848) Zhan, X.; Yang, M. Polymerization of p-Diethynylbenzene and its Derivatives with Nickelocene Acetylide Catalysts Containing Different Phosphine and Alkynyl Ligands. *Macromol. Rapid Commun.* **2000**, *21*, 1263-1266.
(849) Zhan, X.; Yang, M. Polymerization of p-Diethynylbenzene Catalyzed by (π-C_5H_5)(PPh_3)Ni ($C{\equiv}CC_6H_4C{\equiv}CH$). *Eur. Polym. J.* **2001**, *37*, 1649-1654.
(850) Zhan, X.; Yang, M.; Sun, H. Polymerization of Substituted Acetylenes Carrying Non-Polar and Polar Groups with Transition Metal Acetylide Catalysts. *Macromol. Rapid Commun.* **2001**, *22*, 530-534.
(851) Furlani, A.; Collamati, I.; Sartori, G. Linear Polymerization of Phenylacetylene using some (triphenylphosphine) Platinum Complexes. *J. Organomet. Chem.* **1969**, *17*, 463-468.
(852) Russo, M.; Iucci, G.; Polzonetti, G.; Furlani, A. Organic Conducting Polymers: Synthesis, Characterization and Conductivity of Polyethynylfluorenol. *Polymer* **1992**, *33*, 4401-4409.
(853) Furlani, A.; Paolesse, R.; Russo, M.; Camus, A.; Marsich, N. Polymerization of N-benzylpropargylamine in the Presence of Ionic Rhodium(I) Complexes. A New Functionalized Polyacetylene: Investigation of its Conducting Properties. *Polymer* **1987**, *28*, 1221-1226.
(854) Hongmei, S.; Xinan, P.; Mansheng, C.; Qi, S. Neutral Pd(II) and Ni(II) Acetylide Initiators for Polymerization of (dimethylamino) Ethyl Methacrylate. *Catal. Lett.* **2003**, *90*, 85-89.
(855) Shao, Q.; Sun, H.; Pang, X.; Shen, Q. A Neutral Ni(II) Acetylide-mediated Radical Polymerization of Methyl Methacrylate using the Atom Transfer Radical Polymerization Method. *Eur. Polym. J.* **2004**, *40*, 97-102.

(856) Wei, K.; Gao, Z.; Liu, H.; Wu, X.; Wang, F.; Xu, H. Mechanical Activation of Platinum–Acetylide Complex for Olefin Hydrosilylation. *ACS Macro Lett.* **2017**, *6*, 1146-1150.
(857) Zhang, D.; Wu, L. Z.; Zhou, L.; Han, X.; Yang, Q. Z.; Zhang, L. P.; Tung, C. H. Photocatalytic Hydrogen Production from Hantzsch 1,4-Dihydropyridines by Platinum(II) Terpyridyl Complexes in Homogeneous Solution. *J. Am. Chem. Soc.* **2004**, *126*, 3440-3441.
(858) Yu, Z. T.; Liu, X. L.; Yuan, Y. J.; Li, Y. H.; Chen, G. H.; Zou, Z. G. Evaluation of Bis-Cyclometalated Alkynylgold(III) Sensitizers for Water Photoreduction to Hydrogen. *Dalton Trans.* **2016**, *45*, 17223-17232.
(859) Liras, M.; Iglesias, M.; Sánchez, F. l. Conjugated Microporous Polymers Incorporating BODIPY Moieties as Light-Emitting Materials and Recyclable Visible-Light Photocatalysts. *Macromolecules* **2016**, *49*, 1666-1673.
(860) Bandyopadhyay, S.; Anil, A. G.; James, A.; Patra, A. Multifunctional Porous Organic Polymers: Tuning of Porosity, CO2 and H2 Storage and Visible-Light-Driven Photocatalysis. *ACS Appl. Mater. Interfaces* **2016**, *8*, 27669-27678.
(861) Zhang, K.; Kopetzki, D.; Seeberger, P. H.; Antonietti, M.; Vilela, F. Surface Area Control and Photocatalytic Activity of Conjugated Microporous Poly(benzothiadiazole) Networks. *Angew. Chem. Int. Ed. Engl.* **2013**, *52*, 1432-1436.
(862) Jayanthi, S.; Muthu, D.; Jayaraman, N.; Sampath, S.; Sood, A. Semiconducting Conjugated Microporous Polymer: An Electrode Material for Photoelectrochemical Water Splitting and Oxygen Reduction. *ChemistrySelect* **2017**, *2*, 4522-4532.
(863) Zhan, X.; Yang, M.; Sun, H. Transition Metal Acetylide Catalysts for Polymerization of Polar Alkynes. *Catal. Lett.* **2000**, *70*, 79-82.
(864) Pang, X. A.; Sun, H. M.; Shen, Q. Copolymerizations of 2-(dimethylamino)ethyl Methacrylate with (methyl)acrylates Initiated by a Neutral Pd (II)-based Complex. *Polymer* **2004**, *45*, 4029-4035.
(865) Ross, C.; Scherlach, K.; Kloss, F.; Hertweck, C. The Molecular Basis of Conjugated Polyyne Biosynthesis in Phytopathogenic Bacteria. *Angew. Chem. Int. Ed. Engl.* **2014**, *53*, 7794-7798.
(866) Minto, R. E.; Blacklock, B. J. Biosynthesis and Function of Polyacetylenes and Allied Natural Products. *Prog. Lipid Res.* **2008**, *47*, 233-306.
(867) Schmidt, B.; Audorsch, S. Stereoselective Total Synthesis of Atractylodemayne A, a Conjugated 2(E),8(Z),10(E)-Triene-4,6-diyne. *Org. Lett.* **2016**, *18*, 1162-1165.
(868) Gung, B. W.; Kumi, G. Total Synthesis of (S)-(-)-(E)-15,16-Dihydrominquartynoic Acid: A Highly Potent Anticancer Agent. *J. Org. Chem.* **2004**, *69*, 3488-3492.
(869) Gangadhar, P.; Reddy, A. S.; Srihari, P. A Facile Approach for the Total Synthesis of Neurotrophic Diyne Tetraol Petrosiol A and Petrosiol E. *Tetrahedron* **2016**, *72*, 5807-5817.
(870) Yadav, J.; Boyapelly, K.; Alugubelli, S. R.; Pabbaraja, S.; Vangala, J. R.; Kalivendi, S. V. Stereoselective Total Synthesis of (+)-oploxyne A,(−)-oploxyne B, and Their C-10 Epimers and Structure Revision of Natural Oploxyne B. *J. Org. Chem.* **2011**, *76*, 2568-2576.
(871) Srihari, P.; Reddy, A. S.; Yadav, J.; Yedlapudi, D.; Kalivendi, S. V. First total Synthesis and Structure Confirmation of Diacetylenic Polyol (+)-Oploxyne B. *Tetrahedron Lett.* **2013**, *54*, 5616-5618.
(872) Kanikarapu, S.; Marumudi, K.; Kunwar, A. C.; Yadav, J. S.; Mohapatra, D. K. Total Synthesis and Stereochemical Revision of 4,8-Dihydroxy-3,4-dihydrovernoniyne. *Org. Lett.* **2017**, *19*, 4167-4170.
(873) Dembitsky, V. M. Anticancer Activity of Natural and Synthetic Acetylenic Lipids. *Lipids* **2006**, *41*, 883-924.
(874) Lee, C.-Y.; Shin, D. Systemic Structure–activity Relationship Study of Phenyl Polyyne Diols as Potential Chemopreventive agents. *Bioorg. Med. Chem. Lett.* **2016**, *26*, 4907-4910.
(875) Wu, L.-W.; Chiang, Y.-M.; Chuang, H.-C.; Wang, S.-Y.; Yang, G.-W.; Chen, Y.-H.; Lai, L.-Y.; Shyur, L.-F. Polyacetylenes Function as Anti-Angiogenic Agents. *Pharm. Res.* **2004**, *21*, 2112-2119.
(876) Chiang, Y. M.; Chang, C. L.; Chang, S. L.; Yang, W. C.; Shyur, L. F. Cytopiloyne, a Novel Polyacetylenic Glucoside from Bidens Pilosa, Functions as a T Helper Cell modulator. *J. Ethnopharmacol.* **2007**, *110*, 532-538.
(877) Chang, C. L.; Chang, S. L.; Lee, Y. M.; Chiang, Y. M.; Chuang, D. Y.; Kuo, H. K.; Yang, W. C. Cytopiloyne, a Polyacetylenic Glucoside, Prevents Type 1 Diabetes in Nonobese Diabetic Mice. *J Immunol.* **2007**, *178*, 6984-6993.

(878) Chung, C.-Y.; Yang, W.-C.; Liang, C.-L.; Liu, H.-Y.; Lai, S.-K.; Chang, C. L.-T. Cytopiloyne, a Polyacetylenic Glucoside from Bidens Pilosa, acts as a Novel Anticandidal Agent via Regulation of Macrophages. *J. Ethnopharmacol.* **2016**, *184*, 72-80.
(879) Pollo, L. A.; Bosi, C. F.; Leite, A. S.; Rigotto, C.; Kratz, J.; Simoes, C. M.; Fonseca, D. E.; Coimbra, D.; Caramori, G.; Nepel, A.; et al. Polyacetylenes from the leaves of Vernonia Scorpioides (Asteraceae) and Their Antiproliferative and Antiherpetic Activities. *Phytochemistry* **2013**, *95*, 375-383.
(880) Jung, H.-J.; Min, B.-S.; Park, J.-Y.; Kim, Y.-H.; Lee, H.-K.; Bae, K.-H. Gymnasterkoreaynes A− F, Cytotoxic Polyacetylenes from Gymnaster k oraiensis. *J. Nat. Prod.* **2002**, *65*, 897-901.
(881) Lee, S. B.; Kang, K.; Oidovsambuu, S.; Jho, E. H.; Yun, J. H.; Yoo, J. H.; Lee, E. H.; Pan, C. H.; Lee, J. K.; Jung, S. H.; et al. A Polyacetylene from Gymnaster Koraiensis Exerts Hepatoprotective Effects in vivo and in vitro. *Food Chem. Toxicol.* **2010**, *48*, 3035-4301.
(882) Lee, S. B.; Kim, C. Y.; Lee, H. J.; Yun, J. H.; Nho, C. W. Induction of the Phase II Detoxification Enzyme NQO1 in Hepatocarcinoma Cells by Lignans from the Fruit of Schisandra Chinensis Through Nuclear Accumulation of Nrf2. *Planta Med.* **2009**, *75*, 1314-1318.
(883) Park, J.; Min, B.; Jung, H.; Kim, Y.; Lee, H.; Bae, K. Polyacetylene Glycosides from Gymnaster Koraiensis. *Chem. Pharm. Bull. (Tokyo)* **2002**, *50*, 685-687.
(884) Zhang, B.; Wang, Y.; Yang, S. P.; Zhou, Y.; Wu, W. B.; Tang, W.; Zuo, J. P.; Li, Y.; Yue, J. M. Ivorenolide A, an Unprecedented Immunosuppressive Macrolide from Khaya Ivorensis: Structural Elucidation and Bioinspired Total Synthesis. *J. Am. Chem. Soc.* **2012**, *134*, 20605-20608.
(885) Zowawi, H. M.; Harris, P. N.; Roberts, M. J.; Tambyah, P. A.; Schembri, M. A.; Pezzani, M. D.; Williamson, D. A.; Paterson, D. L. The Emerging Threat of Multidrug-resistant Gram-negative Bacteria in Urology. *Nat. Rev. Urol.* **2015**, *12*, 570-584.
(886) McClerren, A. L.; Endsley, S.; Bowman, J. L.; Andersen, N. H.; Guan, Z.; Rudolph, J.; Raetz, C. R. A Slow, Tight-binding Inhibitor of the Zinc-dependent Deacetylase LpxC of Lipid A Biosynthesis with Antibiotic Activity Comparable to Ciprofloxacin. *Biochemistry* **2005**, *44*, 16574-16583.
(887) Liang, X.; Lee, C. J.; Chen, X.; Chung, H. S.; Zeng, D.; Raetz, C. R.; Li, Y.; Zhou, P.; Toone, E. J. Syntheses, Structures and Antibiotic Activities of LpxC Inhibitors Based on the Diacetylene Scaffold. *Bioorg. Med. Chem.* **2011**, *19*, 852-860.
(888) Kurasaki, H.; Tsuda, K.; Shinoyama, M.; Takaya, N.; Yamaguchi, Y.; Kishii, R.; Iwase, K.; Ando, N.; Nomura, M.; Kohno, Y. LpxC inhibitors: Design, Synthesis, and Biological Evaluation of Oxazolidinones as Gram-negative Antibacterial Agents. *ACS Med. Chem. Lett.* **2016**, *7*, 623-628.
(889) Lampkowski, J. S.; Uthappa, D. M.; Halonski, J. F.; Maza, J. C.; Young, D. D. Application of the Solid-Supported Glaser–Hay Reaction to Natural Product Synthesis. *J. Org. Chem.* **2016**, *81*, 12520-12524.
(890) Maza, J. C.; Nimmo, Z. M.; Young, D. D. Expanding the Scope of Alkyne-mediated Bioconjugations Utilizing Unnatural Amino Acids. *Chem. Commun. (Camb)* **2016**, *52*, 88-91.
(891) Lampkowski, J. S.; Villa, J. K.; Young, T. S.; Young, D. D. Development and Optimization of Glaser–Hay Bioconjugations. *Angew. Chem. Int. Ed.* **2015**, *54*, 9343-9346.
(892) Haque, A.; Faizi, M. S. H.; Rather, J. A.; Khan, M. S. Next Generation NIR Fluorophores for Tumor Imaging and Fluorescence-guided Surgery: A review. *Bioorg. Med. Chem.* **2017**, *25*, 2017-2034.
(893) Ilmi, R.; Hasan, N.; Liu, J.; Mara, D.; Van Deun, R.; Iftikhar, K. Effect of 2,4,6-Tri(2-pyridyl)-1,3,5-triazine on Visible and NIR Luminescence of Lanthanide Tris(trifluoroacetylacetonates). *J. Photochem. Photobiol., A* **2017**, *347*, 116-129.
(894) Yi, X.; Wang, F.; Qin, W.; Yang, X.; Yuan, J. Near-Infrared Fluorescent Probes in Cancer Imaging and Therapy: An Emerging Field. *Int. J. Nanomed.* **2014**, *9*, 1347-1365.
(895) Xie, J.; Lee, S.; Chen, X. Nanoparticle-based Theranostic Agents. *Adv. Drug. Deliv. Rev.* **2010**, *62*, 1064-1079.
(896) Lee, Y. M.; Lim, C.; Lee, H. S.; Shin, Y. K.; Shin, K.-O.; Lee, Y.-M.; Kim, S. Synthesis and Biological Evaluation of a Polyyne-Containing Sphingoid Base Probe as a Chemical Tool. *Bioconjugate chemistry* **2013**, *24*, 1324-1331.
(897) Wei, L.; Hu, F.; Shen, Y.; Chen, Z.; Yu, Y.; Lin, C. C.; Wang, M. C.; Min, W. Live-cell Imaging of Alkyne-Tagged Small Biomolecules by Stimulated Raman Scattering. *Nat. Methods* **2014**, *11*, 410-412.

(898) Lucotti, A.; Tommasini, M.; Fazzi, D.; Del Zoppo, M.; Chalifoux, W. A.; Tykwinski, R. R.; Zerbi, G. Absolute Raman Intensity Measurements and Determination of the Vibrational Second Hyperpolarizability of Adamantyl Endcapped Polyynes. *J. Raman Spectrosc.* **2012**, *43*, 1293-1298.
(899) Palonpon, A. F.; Ando, J.; Yamakoshi, H.; Dodo, K.; Sodeoka, M.; Kawata, S.; Fujita, K. Raman and SERS Microscopy for Molecular Imaging of Live Cells. *Nat. Protoc* **2013**, *8*, 677-692.
(900) Ando, J.; Asanuma, M.; Dodo, K.; Yamakoshi, H.; Kawata, S.; Fujita, K.; Sodeoka, M. Alkyne-tag SERS Screening and Identification of Small-molecule-binding Sites in Protein. *J. Am. Chem. Soc.* **2016**, *138*, 13901-13910.
(901) Chen, Z.; Paley, D. W.; Wei, L.; Weisman, A. L.; Friesner, R. A.; Nuckolls, C.; Min, W. Multicolor Live-cell Chemical Imaging by Isotopically Edited Alkyne Vibrational Palette. *J. Am. Chem. Soc.* **2014**, *136*, 8027-8033.
(902) Wei, L.; Hu, F.; Chen, Z.; Shen, Y.; Zhang, L.; Min, W. Live-Cell Bioorthogonal Chemical Imaging: Stimulated Raman Scattering Microscopy of Vibrational Probes. *Acc. Chem. Res.* **2016**, *49*, 1494-1502.
(903) Li, S.; Chen, T.; Wang, Y.; Liu, L.; Lv, F.; Li, Z.; Huang, Y.; Schanze, K. S.; Wang, S. Conjugated Polymer with Intrinsic Alkyne Units for Synergistically Enhanced Raman Imaging in Living Cells. *Angew. Chem. Int. Ed. Engl.* **2017**, *56*, 13455-13458.
(904) Yamakoshi, H.; Dodo, K.; Palonpon, A.; Ando, J.; Fujita, K.; Kawata, S.; Sodeoka, M. Alkyne-tag Raman Imaging for Visualization of Mobile Small Molecules in Live Cells. *J. Am. Chem. Soc.* **2012**, *134*, 20681-20689.
(905) Shi, E.; Gao, Z.; Yuan, M.; Wang, X.; Wang, F. Self-assembly of Benzothiadiazole-functionalized Dinuclear Platinum Acetylide Bolaamphiphiles for Bio-imaging Application. *Polym. Chem.* **2015**, *6*, 5575-5579.
(906) Bian, W.; Lian, H.; Zhang, Y.; Tai, F.; Wang, H.; Dong, Q.; Yu, B.; Wei, X.; Zhao, Q. Porphyrin-based Pt/Pd-containing Metallopolymers: Synthesis, Characterization, Optical Property and Potential Application in Bioimaging. *J. Organomet. Chem.* **2017**, *835*, 25-30.
(907) Sun, R. W.-Y.; Ma, D.-L.; Wong, E. L.-M.; Che, C.-M. Some uses of Transition Metal Complexes as Anti-cancer and Anti-HIV Agents. *Dalton Trans.* **2007**, 4884-4892.
(908) Yam, V. W.; Au, V. K.; Leung, S. Y. Light-Emitting Self-Assembled Materials Based on d^8 and d^{10} Transition Metal Complexes. *Chem. Rev.* **2015**, *115*, 7589-7728.
(909) Meyer, A.; Gutiérrez, A.; Ott, I.; Rodríguez, L. Phosphine-bridged Dinuclear Gold(I) Alkynyl Complexes: Thioredoxin Reductase Inhibition and Cytotoxicity. *Inorg. Chim. Acta* **2013**, *398*, 72-76.
(910) Gavara, R.; Aguiló, E.; Schur, J.; Llorca, J.; Ott, I.; Rodríguez, L. Study of the Effect of the Chromophore and Nuclearity on the Aggregation and Potential Biological Activity of Gold(I) Alkynyl Complexes. *Inorg. Chim. Acta* **2016**, *446*, 189-197.
(911) Andermark, V.; Göke, K.; Kokoschka, M.; el Maaty, M. A. A.; Lum, C. T.; Zou, T.; Sun, R. W.-Y.; Aguiló, E.; Oehninger, L.; Rodríguez, L. Alkynyl Gold(I) Phosphane Complexes: Evaluation of Structure–activity-relationships for the Phosphane Ligands, Effects on Key Signaling Proteins and Preliminary in-vivo Studies with a Nanoformulated Complex. *J. Inorg. Biochem.* **2016**, *160*, 140-148.
(912) Sanchez-de-Diego, C.; Marmol, I.; Perez, R.; Gascon, S.; Rodriguez-Yoldi, M. J.; Cerrada, E. The Anticancer Effect Related to Disturbances in Redox Balance on Caco-2 Cells Caused by an Alkynyl Gold (I) cCmplex. *J. Inorg. Biochem.* **2017**, *166*, 108-121.
(913) Marmol, I.; Virumbrales-Munoz, M.; Quero, J.; Sanchez-de-Diego, C.; Fernandez, L.; Ochoa, I.; Cerrada, E.; Yoldi, M. J. R. Alkynyl Gold(I) Complex Triggers Necroptosis via ROS Generation in Colorectal Carcinoma Cells. *J. Inorg. Biochem.* **2017**, *176*, 123-133.
(914) Langdon-Jones, E. E.; Lloyd, D.; Hayes, A. J.; Wainwright, S. D.; Mottram, H. J.; Coles, S. J.; Horton, P. N.; Pope, S. J. Alkynyl-naphthalimide Fluorophores: Gold Coordination Chemistry and Cellular Imaging Applications. *Inorg. Chem.* **2015**, *54*, 6606-6615.
(915) Fernández-Moreira, V.; Marzo, I.; Gimeno, M. C. Luminescent Re(I) and Re(I)/Au(I) Complexes as Cooperative Partners in Cell Imaging and Cancer Therapy. *Chem. Sci.* **2014**, *5*, 4434-4446.
(916) Bhowmick, S.; Jana, A.; Marri, S. R.; Gupta, P.; Behera, J.; Mandal, B. B.; Das, N. Pyrazine based Pt (II) bis-alkynyl organometallic complexes: Synthesis, characterization, and cytotoxic effect on A549 human lung carcinoma cells. *Appl. Organomet. Chem.* **2017**, *31*, e3824.

(917) Zhao, Q.; Li, J.; Zhang, X.; Li, Z.; Tang, Y. Cationic Oligo(thiophene ethynylene) with Broad-Spectrum and High Antibacterial Efficiency under White Light and Specific Biocidal Activity against S. aureus in Dark. *ACS Appl. Mater. Interfaces* **2016**, *8*, 1019-1024.
(918) Pappas, H. C.; Sylejmani, R.; Graus, M. S.; Donabedian, P. L.; Whitten, D. G.; Neumann, A. K. Antifungal Properties of Cationic Phenylene Ethynylenes and Their Impact on β-Glucan Exposure. *Antimicrob. Agents Chemother.* **2016**, *60*, 4519-4529.
(919) Wang, L.; Fang, G.; Cao, D. Synthesis of a Cationic BODIPY-Containing Conjugated Polymer for Detection of DNA and Cellular Imaging. *J Fluoresc* **2016**, *26*, 427-437.
(920) Chen, Z.; Wu, P.; Cong, R.; Xu, N.; Tan, Y.; Tan, C.; Jiang, Y. Sensitive Conjugated-Polymer-Based Fluorescent ATP Probes and Their Application in Cell Imaging. *ACS Appl. Mater. Interfaces* **2016**, *8*, 3567-3574.
(921) Wang, S.; Li, Z.; Liu, X.; Phan, S.; Lv, F.; Belfield, K. D.; Wang, S.; Schanze, K. S. Two-Photon Absorption of Cationic Conjugated Polyelectrolytes: Effects of Aggregation and Application to 2-Photon-Sensitized Fluorescence from Green Fluorescent Protein. *Chem. Mater.* **2017**, *29*, 3295-3303.
(922) Donabedian, P. L.; Creyer, M. N.; Monge, F. A.; Schanze, K. S.; Chi, E. Y.; Whitten, D. G. Detergent-induced Self-assembly and Controllable Photosensitizer Activity of Diester Phenylene ethynylenes. *Proc. Natl. Acad. Sci. U. S .A* **2017**, *114*, 7278-7282.
(923) Kaleta, J.; Kaletová, E.; Cisarova, I.; Teat, S. J.; Michl, J. Synthesis of Triptycene-Based Molecular Rotors for Langmuir–Blodgett Monolayers. *J. Org. Chem.* **2015**, *80*, 10134-10150.
(924) Xiang, J.; Burges, R.; Häupler, B.; Wild, A.; Schubert, U. S.; Ho, C.-L.; Wong, W.-Y. Synthesis, Characterization and Charge–discharge Studies of Ferrocene-containing Poly(fluorenylethynylene) Derivatives as Organic Cathode Materials. *Polymer* **2015**, *68*, 328-334.
(925) Zhou, B.; Hu, X.; Zeng, G.; Li, S.; Wen, Z.; Chen, L. Bottom-Up Construction of Porous Organic Frameworks with Built-In TEMPO as a Cathode for Lithium–Sulfur Batteries. *ChemSusChem* **2017**, *10*, 2955-2961.
(926) Zhang, Q.; Dai, Q.; Li, M.; Wang, X.; Li, A. Incorporation of MnO Nanoparticles Inside Porous Carbon Nanotubes Originated from Conjugated Microporous Polymers for Lithium Storage. *J. Mater. Chem. A* **2016**, *4*, 19132-19139.
(927) Shen, C.; He, X.; Toupet, L.; Norel, L.; Rigaut, S.; Crassous, J. Dual Redox And Optical Control Of Chiroptical Activity In Photochromic Dithienylethenes Decorated with Hexahelicene and Bis-Ethynyl-Ruthenium Units. *Organometallics* **2017**, *37*, 697-705.
(928) Zhou, N.; Merschrod, S. E.; Zhao, Y. Preparation of Fullerene-polyyne Nanospheres via Thermally Induced Solid-state Polymerization. *J. Am. Chem. Soc.* **2005**, *127*, 14154-14155.
(929) Wang, F.; Ren, F.; Ma, D.; Mu, P.; Wei, H.; Xiao, C.; Zhu, Z.; Sun, H.; Liang, W.; Chen, J. Particle and Nanofiber Shaped Conjugated Microporous Polymers Bearing Hydantoin-substitution with High Antibacterial Activity for Water Cleanness. *J. Mater. Chem. A* **2018**, *6*, 266-274.
(930) Choi, T. J.; Chang, J. Y. Water Wettable, Compressible, and Hierarchically Porous Polymer Composite. *Microporous Mesoporous Mater.* **2017**, *242*, 82-89.
(931) Xu, D.; Guo, J.; Yan, F. Porous ionic polymers: Design, synthesis, and applications. *Prog. Polym. Sci.* **2017**, *79*, 121-143.
(932) Chaoui, N.; Trunk, M.; Dawson, R.; Schmidt, J.; Thomas, A. Trends and Challenges for Microporous Polymers. *Chem. Soc. Rev.* **2017**, *46*, 3302-3321.
(933) Shetty, D.; Jahovic, I.; Raya, J.; Ravaux, F.; Jouiad, M.; Olsen, J. C.; Trabolsi, A. An Ultra-absorbent Alkyne-rich Porous Covalent Polycalix[4]arene for Water Purification. *J. Mater. Chem. A* **2017**, *5*, 62-66.
(934) Shetty, D.; Raya, J.; Han, D. S.; Asfari, Z.; Olsen, J.-C.; Trabolsi, A. Lithiated Polycalix [4] arenes for Efficient Adsorption of Iodine from Solution and Vapor Phases. *Chem. Mater.* **2017**, *29*, 8968-8972.
(935) Yan, Z.; Yuan, Y.; Tian, Y.; Zhang, D.; Zhu, G. Highly Efficient Enrichment of Volatile Iodine by Charged Porous Aromatic Frameworks with Three Sorption Sites. *Angew. Chem. Int. Ed.* **2015**, *54*, 12733-12737.
(936) Zhu, Y.; Ji, Y.-J.; Wang, D.-G.; Zhang, Y.; Tang, H.; Jia, X.-R.; Song, M.; Yu, G.; Kuang, G.-C. BODIPY-based Conjugated Porous Polymers for Highly Efficient Volatile Iodine Capture. *J. Mater. Chem. A* **2017**, *5*, 6622-6629.

(937) Ren, F.; Zhu, Z.; Qian, X.; Liang, W.; Mu, P.; Sun, H.; Liu, J.; Li, A. Novel Thiophene-bearing Conjugated Microporous Polymer Honeycomb-like Porous Spheres with Ultrahigh Iodine Uptake. *Chem. Commun. (Camb)* **2016**, *52*, 9797-9800.
(938) Xu, J.; Zhang, C.; Qiu, Z.; Lei, Z.; Chen, B.; Jiang, J. X.; Wang, F. Synthesis and Characterization of Functional Triphenylphosphine-Containing Microporous Organic Polymers for Gas Storage and Separation. *Macromol. Chem. Phys.* **2017**, *218*, 1700275-1700282.
(939) Aguilar-Granda, A.; Perez-Estrada, S.; Sanchez-Gonzalez, E.; Alvarez, J. R.; Rodriguez-Hernandez, J.; Rodriguez, M.; Roa, A. E.; Hernandez-Ortega, S.; Ibarra, I. A.; Rodriguez-Molina, B. Transient Porosity in Densely Packed Crystalline Carbazole-(p-Diethynylphenylene)-Carbazole Rotors: CO2 and Acetone Sorption Properties. *J. Am. Chem. Soc.* **2017**, *139*, 7549-7557.
(940) Bracco, S.; Castiglioni, F.; Comotti, A.; Galli, S.; Negroni, M.; Maspero, A.; Sozzani, P. Ultrafast Molecular Rotors and Their CO_2 Tuning in MOFs with Rod-Like Ligands. *Chem. Eur. J.* **2017**, *23*, 11210-11215.
(941) Sen, C. P.; Goud, V. D.; Shrestha, R. G.; Shrestha, L. K.; Ariga, K.; Valiyaveettil, S. BODIPY based Hyperbranched Conjugated Polymers for Detecting Organic Vapors. *Polym. Chem.* **2016**, *7*, 4213-4225.
(942) Au-Yeung, H. L.; Leung, S. Y.; Tam, A. Y.; Yam, V. W. Transformable Nanostructures of Platinum-containing Organosilane Hybrids: Non-covalent Self-assembly of Polyhedral Oligomeric Silsesquioxanes Assisted by Pt--Pt and π-π Stacking Interactions of Alkynylplatinum (II) Terpyridine Moieties. *J. Am. Chem. Soc.* **2014**, *136*, 17910-17913.
(943) Lauder, K.; Toscani, A.; Scalacci, N.; Castagnolo, D. Synthesis and Reactivity of Propargylamines in Organic Chemistry. *Chem. Rev.* **2017**, *117*, 14091-14200.

Author Biography

Ashanul Haque completed his B.Sc. in Chemistry (2006) from Jamia Millia Islamia, India and M.Sc. in Chemistry (2008) from Jamia Hamdard, India. He obtained his PhD in Chemistry from Jamia Millia Islamia, India (2014) under the supervision of Prof. Imran Ali and Prof. Kishwar Saleem. During his PhD, he was the recipient of two major national research fellowships: Basic Science Junior Research Fellowship for meritorious students (BSR-JRF) and Senior Research Fellowship (SRF) in Organic Chemistry awarded by the University Grant's Commission (UGC) and Council of Scientific and Industrial Research (CSIR), New Delhi, India respectively. Since September 2014, he has been working as a postdoctoral fellow with Prof. Muhammad S. Khan at Sultan Qaboos University, Oman. His present research interests are centered on design and development of organic and organometallic compounds for biological and opto-electronics applications. Dr. Haque has an *h*-index of 13, an i10-index of 14 and 596 citations for his 39 published papers.

Rayya A. Al Balushi was born and brought up in A'Sharqiyah, Oman. She received her MSc degree in Chemistry from Sultan Qaboos University, Oman (2006). She received Ph.D from the same University in 2016 under the supervision of Professor Muhammad S. Khan. Her PhD project focused on the Design, Synthesis and Characterization of Some Novel Metalla-yne and Poly(metalla-yne) Materials. Dr. Al-Balushi received the Best PhD Thesis award from Sultan Qaboos University in 2017. Dr. Al-Balushi is currently an Assistant Professor in the College of Applied and Health Sciences, A'Sharqiyah University (ASU), Oman. Her research interests include designing conjugated polymers for photo-switch, photo-voltaic and LED applications.

Idris J. Al-Busaidi earned a B.Sc. degree from Sultan Qaboos University, Oman in 2004. He received his M.Sc. degree from the same university in 2016. He was a recipient of the best M.Sc. Thesis Award from Sultan Qaboos University in 2017. He joined Prof. Muhammad S. Khan in the department of Chemistry at Sultan Qaboos University in 2017 for his Ph.D. His doctoral research focuses on conjugated poly-ynes and poly(metalla-ynes), structure-luminescent properties relationships of lanthanide β-diketonate and bipyridine-based chromophores and lanthanide(III) complexes for OLED applications.

Muhammad S. Khan received his Ph.D. (1983) from the Department of Chemistry, University of Cambridge, UK. He was a Research Fellow at Cambridge (1987-1994). Currently he is a Professor of Chemistry at Sultan Qaboos University, Oman, prior to which he was a faculty member at the Department of Chemistry, University of Dhaka, Bangladesh for 16 years. He has received many scholarships and awards; notably, the H.P. Ray Gold Medal of Dhaka University (1987), the Junior Gold Medal in Physical Sciences of the Bangladesh Academy of Sciences (1994), the Best Researcher Award of the College of Science, Sultan Qaboos University (2005, 2017) and the Best Research Paper Award of the College of Science, Sultan

Qaboos University (2016). His research interests include the design and development of novel synthetic protocol for conjugated organic, organometallic and coordination polymers for opto-electronic applications. With 120 strong papers to his credit, Prof. Khan is the highest cited scientist in the Sultanate of Oman and the highest cited materials chemist among the 57 members Organization of Islamic Countries (OIC).

Paul Raithby is Professor of Inorganic Chemistry at the University of Bath, prior to which he was a faculty member of the Department of at the University of Cambridge for 25 years. He has been awarded the RSC Corday Morgan Medal and Prize (1988) and the RSC Prize for Structural Chemistry (2008), and was President of the British Crystallographic Association between 2006-2009. He has over 840 publications covering the research themes of chemical crystallography, organometallic polymer chemistry and carbonyl cluster chemistry.